

AD _____

Award Number: DAMD17-02-C-0001

TITLE: Protein Receptor (s) of Botulinum Neurotoxin

PRINCIPAL INVESTIGATOR: Bal Ram Singh, Ph.D.

CONTRACTING ORGANIZATION: University of Massachusetts Dartmouth
North Dartmouth, MA 02747-2300

REPORT DATE: January 2005

TYPE OF REPORT: Final

PREPARED FOR: U.S. Army Medical Research and Materiel Command
Fort Detrick, Maryland 21702-5012

DISTRIBUTION STATEMENT: Approved for Public Release;
Distribution Unlimited

The views, opinions and/or findings contained in this report are those of the author(s) and should not be construed as an official Department of the Army position, policy or decision unless so designated by other documentation.

20050916 159

REPORT DOCUMENTATION PAGE

Form Approved
OMB No. 0704-0188

Public reporting burden for this collection of information is estimated to average 1 hour per response, including the time for reviewing instructions, searching existing data sources, gathering and maintaining the data needed, and completing and reviewing this collection of information. Send comments regarding this burden estimate or any other aspect of this collection of information, including suggestions for reducing this burden to Department of Defense, Washington Headquarters Services, Directorate for Information Operations and Reports (0704-0188), 1215 Jefferson Davis Highway, Suite 1204, Arlington, VA 22202-4302. Respondents should be aware that notwithstanding any other provision of law, no person shall be subject to any penalty for failing to comply with a collection of information if it does not display a currently valid OMB control number. **PLEASE DO NOT RETURN YOUR FORM TO THE ABOVE ADDRESS.**

1. REPORT DATE 01-01-2005			2. REPORT TYPE Final		3. DATES COVERED 19 Dec 01 - 18 Dec 04	
4. TITLE AND SUBTITLE Protein Receptor (s) of Botulinum Neurotoxin					5a. CONTRACT NUMBER DAMD17-02-C-0001	
					5b. GRANT NUMBER	
					5c. PROGRAM ELEMENT NUMBER	
6. AUTHOR(S) Bal Ram Singh, Ph.D.					5d. PROJECT NUMBER	
					5e. TASK NUMBER	
					5f. WORK UNIT NUMBER	
7. PERFORMING ORGANIZATION NAME(S) AND ADDRESS(ES) University of Massachusetts Dartmouth North Dartmouth, MA 02747-2300					8. PERFORMING ORGANIZATION REPORT NUMBER	
9. SPONSORING / MONITORING AGENCY NAME(S) AND ADDRESS(ES) U.S. Army Medical Research and Materiel Command Fort Detrick, Maryland 21702-5012					10. SPONSOR/MONITOR'S ACRONYM(S)	
					11. SPONSOR/MONITOR'S REPORT NUMBER(S)	
12. DISTRIBUTION / AVAILABILITY STATEMENT Approved for Public Release; Distribution Unlimited						
13. SUPPLEMENTARY NOTES Original contains color plates: ALL DTIC reproductions will be in black and white						
14. ABSTRACT - SEE ATTACHED PAGE						
15. SUBJECT TERMS NOT PROVIDED						
16. SECURITY CLASSIFICATION OF:				17. LIMITATION OF ABSTRACT	18. NUMBER OF PAGES	19a. NAME OF RESPONSIBLE PERSON
a. REPORT U	b. ABSTRACT U	c. THIS PAGE U	19b. TELEPHONE NUMBER (include area code)			
				UU	361	

Abstract

Seven serotypes of botulinum neurotoxin (BoNT) are a group of water-soluble large proteins that act on the presynaptic nerve cells of the neuro-muscular junctions. BoNTs act intracellularly to block acetylcholine neurotransmitter release leading to the flaccid muscle paralysis in the dreaded botulism disease. In order to enter the neuronal cells, BoNTs bind to as yet to be clearly identified protein receptor(s), which could be targeted to develop proper antidotes.

The aim of this research has been to identify protein receptor(s) of BoNTs by purifying them from neuronal tissues, and characterize its binding mechanism with the neurotoxin, including the effects of low pH and membrane lipid interactions. During the past three years, we have made major strides in discovering the domain of receptor that binds to the BoNT/A and /E, a novel form of BoNT/E, interaction of native and purified BoNTs to the a potential receptor protein, GT1b-induced structural changes in purified BoNT/E and its light chain, role of receptor in the translocation of the toxin, differential binding of the identified receptor with different serotypes of BoNT, identification of a component within BoNT complex that effectively binds to nerve membrane, and a surprise survival of quahogs with exposure to heavy doses of BoNT. In addition, we have improved methodologies to examine structural changes in BoNT proteins. These results have been communicated through 8 published article, 2 pending publications, and over 35 conference presentations.

Table of Contents

Cover.....	1
SF 298.....	2
Table of Contents.....	3
Introduction.....	4
Body.....	5
Key Research Accomplishments.....	172
Reportable Outcomes.....	174
Conclusions.....	177
References.....	
Appendices.....	178

Introduction

Clostridium botulinum is responsible for the deadly food poisoning disease botulism in humans and animals. The bacteria produce the most toxic protein known to humankind, the botulinum neurotoxin (BoNT) which is known to cause flaccid muscle paralysis after blocking the release of acetylcholine at the neuromuscular junctions. BoNTs are produced by the bacteria after their growth in improperly stored foods that can sustain anaerobic conditions. Ingestion of the intoxicated food causes flaccid muscle paralysis in patients leading to dreaded botulism disease. Seven different serotypes (A-G) of BoNT are produced by various strains of *C. botulinum*.

Because of the extreme toxicity of BoNTs, and also in view of their robust stability under adverse environmental conditions such as high temperature, BoNTs are on the top of the list of biological warfare threats (1-4). The mode of action botulism involves three steps; binding, internalization and translocation, and intracellular enzymatic activity. An understanding of the mode of action of BoNT is key to the development of any antidotes against botulism, in general, and against biothreats of botulism in particular.

In order to take preventive measures to provide protection against botulism, and to develop proper antidotes, a comprehensive knowledge of the BoNT receptor(s) is warranted. We proposed the following specific plans to address the issue of botulinum receptor:

- (1) Isolation, purification and characterization of BoNT receptor from neuronal tissues.
- (2) Analysis of binding between the purified receptor and BoNT.

Our efforts in the past three years have involved mostly the confirmation of a potential BoNT receptor (synaptotagmin), analysis of the role of receptor(s) or other proteins in the translocation of BoNT's light chain, role of BoNT associated proteins in the binding, translocation, and endopeptidase activity of BoNT, and binding of BoNT complex, purified BoNT and its light chain with gangliosides. Our results (**Annual Report 1**) suggests that synaptotagmin can bind to more than one BoNT types,

BoNT/A associated protein also bind to synaptotagmin, one of the neurotoxin associated proteins (NAPs), known as Hn-33 specifically binds to the synaptotagmin, Hn-33 also enhances the endopeptidase activity of BoNT/A and BoNT/E, and gangliosides bind to BoNT/E as well as its L chain, which results in substantial polypeptide folding changes.

In addition, we have discovered a new native form of BoNT/E consisting of BoNT and five other associated proteins, which stabilize BoNT/E against proteases and heat, and enhance its endopeptidase activity. In an effort to understand the role of receptor in the translocation of BoNT L chain, we have compared membrane channel activity of BoNT/A and /E, which suggests that the channel activity of the two toxins is same in liposomes. This result in combination with a recent report from Keller et al. (2004) suggests that receptor or other proteins present in nerve membrane play a major role in the translocation of the BoNT L chain.

Project A (Unpublished data)

Binding of BoNT/E, BoNT/E Complex, and BoNT/A Complex with the N-terminal fragment of synaptotagmin

Abstract

Isothermal Calorimetry was used to demonstrate the 1:1 binding interaction between the type E Botulinum neurotoxin (BoNT/E), BoNT/E complex, or BoNT/A complex, and the 20-mer N-terminal segment of the membrane protein Synaptotagmin I. The titration of 25 μ M of the 20-mer Syn I peptide with 0.02mM BoNT/E, 0.03 mM BoNT/E complex, 0.02 mM BoNT/A complex, each in 0.1M phosphate buffer, pH 7.6, at a temperature of 28 °C showed 1:1 binding for BoNT/E and BoNT/E complex, but 1.5:1 (Syn:BoNT) binding for the BoNT/A complex. Association constant of Syn I peptide binding to BoNT/A complex was over 2.5 fold higher than that of its binding with BoNT/E complex, which in turn was about 25% higher than that of its binding with purified BoNT/E.

Synaptotagmin has been demonstrated to bind BoNT/A, /B, and /E (5-7). It is well known that only the N-terminal domain of synaptotagmin is actually available for binding with any protein, including the botulinum neurotoxin. In our previous efforts, we were able to only get a small quantity of synaptotagmin with our isolation protocols. Such amount is generally not sufficient for structural and binding analysis. We therefore designed an approach in which synthetic peptide corresponding to the N-terminal domain of the synaptotagmin was used to test its binding with purified BoNT/E, BoNT/E complex, and BoNT/A complex.

Methods

The 20-mer N-terminus of the Synaptotagmin I protein was synthesized to >98% purity as determined by HPLC. The sequence of the peptide is as follows MVSASHPEAL AAPVTTVATL. A 25 μ M solution of the peptide in 0.1M phosphate buffer (pH 7.6) was prepared as was a 0.02 mM, 0.03 mM, and 0.02 mM solution of the BoNT/E, BoNT/E complex, and BoNT/A complex, respectively in the same buffer. The titration parameters for the ITC experiment were as follows: 1st injection time = 200 seconds; time between injections 200 seconds; injection size = 5 μ L; number of injections = 30

Results

The results of the isothermal calorimetry experiment for the titration of Syn I (1-20) and BoNT/E are illustrated in **Figure 1**. The background-subtracted, integrated, and normalized data from the titration experiment was plotted and a best-fit line was extrapolated through the points to generate the graph illustrated in **Figure 2**.

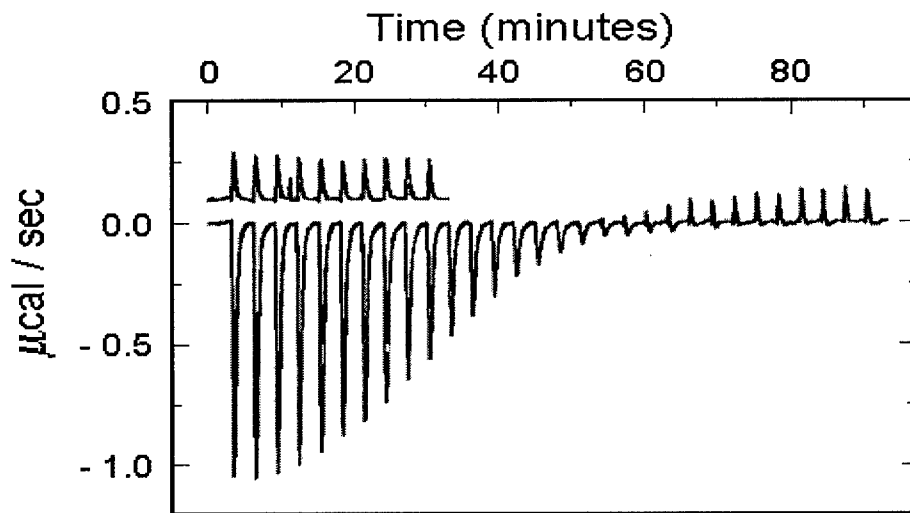


Figure 1. Plot of isothermal calorimetry results for the titration of 25 micromolar solution of Syn I peptide (1-20) in 0.1M phosphate buffer with 0.02 millimolar solution of BoNT/E in 0.1M phosphate buffer. The top trace is the negative control trace for the titration of ten (10) injections of 5 μ L of the Syn I peptide solution into buffer only. The lower trace depicts the thirty (30) injections of 5 μ L of 25 μ M Syn I peptide solution into 0.02 mM of BoNT/E solution.

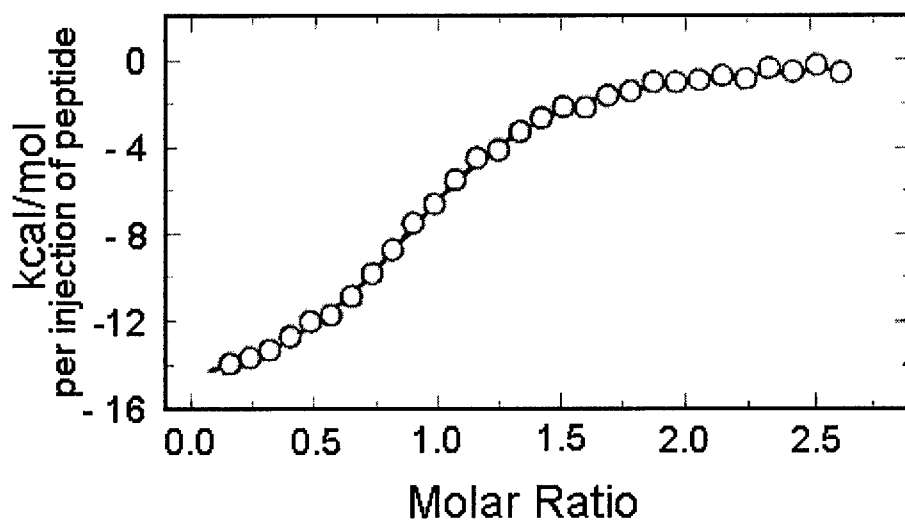


Figure 2. Plot of integrated data from above experiment. The data is plotted as a function of energy change (kcal/mol) for each sequential addition of the Syn I peptide aliquot versus the molar ratio for the substrate-ligand binding.

From the resulting data it was determined that the binding molar ratio for the Syn I peptide (1-20) and the BoNT/E protein was $\sim 1:1$ ($n=1.14$). The thermodynamic data from the ITC experiments resulted in an enthalpy value of ~ 13 kcal/mol. The Gibbs free energy change was also found to be ~ -7.5 kcal/mol. A similar analysis of isothermal calorimetric data for the

binding of Syn I with BoNT/E complex and BoNT/A complex showed 1:1 binding for the former whereas 1:1.5 stoichiometry for BoNT/A complex (**Table 1**).

Table 1. Binding parameters of Syn I with BoNT/E, BoNT/E complex, and BoNT/A complex

BoNT	n (binding sites)	K _a (association const) x 10 ⁻⁵ M ⁻¹	ΔH (kcal/mol)
BoNT/E	1.14	2.8	-12.8
BoNT/E complex	0.98	3.4	-13.7
BoNT/A complex	1.45	8.8	-16.4

Binding data suggest that synaptotagmin binds to both BoNT/A and BoNT/E, consistent with our earlier findings (**Li and Singh, 1998**). Interestingly, the complex binds better than the purified toxin. This is possible either if the complex form (native) of the toxin has a more suitable conformation for binding, or if other components of the complex bind to the synaptotagmin. The second possibility is unlikely since there seems to be only one binding site. BoNT/A complex was most effective over 2.5 fold higher binding constant), but we need to examine the binding of purified BoNT/A before any conclusive explanation can be offered. However, binding of the complex with the potential receptor augers well for the possible effective use of the complex in its therapeutic use. Also, it would suggest that if an antidote is designed based on synaptotagmin receptor, it would be effective not against the purified toxin but also against the toxin in its native complex.

References (Project A)

1. Steffen, R., Mellin, J., Woodall, J P., Rollin, P. E., Lang, R. H., Luthy, R. and Waldvogel, A. (1997) *J. Infect.* 34, 127-132.
2. Franz, D. R., Jahrling, P. B., Fiedlander, A. M., McClain, D. J., Hoover, D. L., Bryne, W. R., Pavlin, J. A., Christopher, G. W. and Eitzen, Jr., E. M. (1997) *J. Am. Med. Assoc.* 278. 399-411.
3. Zilinskas, R. A. (1997) *J. Am. Med. Assoc.* 278, 418-424.

4. Altas, R. M. (1998) *Crit. Rev. Microbiol.* 24, 157-168.
5. Nishiki, T. Kamata, Y., Nemoto, Y., Omori, Y., Ito, T., Takahashi, M. and Kozaki, S. (1994) *J. Biol. Chem.* 269, 10498-10503.
6. Li, L. and Singh, B. R. (1998) *J. Natural Toxins* 7, 215-226.
7. Schengrund, C. -L. (1999) *J. Toxicol.* 18, 35-44.

Project B (published in Biophysical Chemistry 99, 17-29, 2002)

Spectroscopic Analysis of Low pH and Lipid induced structural changes in Type A Botulinum Neurotoxin Relevant to Membrane Channel Formation and Translocation

Abstract

We have examined the membrane channel activity of type A BoNT (BoNT/A) and its heavy (H) chain in planar lipid membrane under various pH conditions to understand the possible role of the channel activity in the translocation of BoNT/A's light (L) chain under physiological conditions. Only BoNT/A H chain, and not the BoNT/A, exhibited membrane channel activity for translocation of ions. The H chain-induced increase in conductance did not require a pH gradient across the lipid membrane, though it was enhanced by a pH gradient. To understand the molecular basis of the membrane channel activity and the translocation of the L chain, secondary structure of BoNT/A and its H and L chains were analyzed using circular dichroism (CD) and Fourier transform infrared (FT-IR) spectroscopy at different pHs. BoNT/A showed no structural alternation upon acidifying the buffer pH. However, an increase in β -sheet content of BoNT/A H chain at low pH is noticed when examined by FT-IR. The L chain structure changed significantly with decrease in the pH, and the change was mostly reversible. Additionally, the neurotoxin and its subunit chains induced a partially reversible aggregation of liposomes at low pH, which indicated their integration into the lipid

bilayer. Temperature-induced denaturation studies of BoNT/A H chain indicated major structural reorganization upon its interaction with membrane, especially at low pH.

Botulinum neurotoxins (BoNTs) are the most toxic substances known to mankind with strong potential as biological warfare agents, and they are lethal to animals within 30 minutes. Seven serotypes of BoNT are produced by different strains of *Clostridium botulinum* in the form of a single polypeptide chain. The single chain is nicked endogenously or exogenously by proteases into a 50 kDa light (L) chain and a 100 kDa heavy (H) chain linked through a disulfide bond (see 8,9).

The mode of BoNT action is not well understood at the molecular level especially in terms of its internalization by endocytosis, and translocation across the endosomal membrane into the cytoplasm. Based on some experimental evidence and analogies with other dichain toxins such as diphtheria, cholera and *Pseudomonas* exotoxin A, a working model has been proposed (9,10). According to this model, the C-terminus half of the BoNT H chain binds to the presynaptic membrane presumably through *gangliosides* and a protein receptor. Upon binding, BoNT is internalized into the neuronal cell through endocytosis (8,11,12). Inside the cell, the pH of the endosome is lowered to 5-6, which leads to the formation of a membrane transporter by the N-terminal half of the H chain. This transporter helps translocate the whole or a part of BoNT into the cytoplasm. At least the 50-kDa BoNT L chain is transported into the cytoplasm from acidic endocytotic vesicles. Although the transporter is often referred to as the "H chain channel", we will refer to the H-chain based structure which facilitates the L chain transport as the L-chain transporter (LCT), and reserve the term "channel" for experimentally detected ion channels. The induction of other small molecule permeability will be referred to as (small molecule such as calcein) transport.

An understanding of the molecular mechanism of membrane channel or small molecule transport activity of the neurotoxin could provide knowledge of the translocation process of the neurotoxin and its toxic subunit into the cell. Membrane channel formation by a water-soluble protein is an intriguing phenomenon, because for water solubility, hydrophilic domains are needed on the surface of a protein whereas for membrane channel formation, adequate hydrophobic segments will be required for the interaction with a non-polar membrane bilayer. Sequence analysis has revealed a 23-residue stretch in the N-terminal domain of BoNT H chain which would have a propensity to form an amphipathic helix bundle in a hydrophobic environment (13) and the synthetic peptide of the same sequence has been shown to form channels in phospholipid bilayers (14). However, the diameter of such channels is about 2.5 Å, definitely not sufficient for the translocation of a 50-kDa L chain.

Hydrophobicity calculations of BoNT/A have revealed two adjacent peptide segments (H-183-201 and H-205-240; where H refers to the H chain), with strong hydrophobicity compatible for interaction with lipid bilayer (15). But again, 1-2 hydrophobic segments of limited length, would not be adequate for the membrane channel formation (14). To explain adequate interaction of BoNT with lipid bilayers, hydrophobic moment characteristics of BoNT/A were analyzed (16-18). Several polypeptide segments were amphiphilic and could form integral membrane segments or surface segments in conjunction with lipid bilayers. Surface and/or membrane segments were identified in both L and H chains of the neurotoxin. However, it is not clearly understood how these segments are organized to form membrane channels nor whether there is a any relationship between ion channels observed in lipid membranes and the light chain translocation mechanism.

There have been several reports of interactions of clostridial neurotoxins with artificial membranes that lead to the formation of ion-conducting pores, which generally is an acid-dependent process (13,19-22). These studies were either accomplished with planar lipid

bilayers for channel conductance measurement, or were carried out with lipid vesicles for ion permeability. The acid dependence of neurotoxin translocation in intact cells has been inferred from studies where agents which neutralize or dissipate pH gradients in acidic compartments and block the acidification of the endosomes have been shown to block neurotoxin action (23-26).

Low pH is required for the strong channel formation activity of BoNT and its H chains (19,27). A pH of 5.0 or lower induces the channel formation. Low pH is likely to affect not only the surface charges of the neurotoxin, but also its conformation (8). Extensive research work has been carried out with diphtheria toxin to examine low pH-induced structural changes to correlate its membrane channel activity and translocation. However, no information is available on the structural response of BoNT or its subunits to low pH.

In this article, we describe the membrane channel activity of BoNT/A and its H chain in planar lipid membrane under various pH conditions to elicit the quantitative difference in the channel forming activities of these proteins. Only BoNT/A H chain, and not the BoNT/A, exhibited ion transport activity (channel). The H chain-induced increase in conductance did not require a pH gradient across the lipid membrane, though it was enhanced by a pH gradient. Secondary structure of BoNT/A and its H and L chains was analyzed using circular dichroism (CD) and Fourier transform infrared (FT-IR) spectroscopy at different pHs. BoNT/A showed no structural alternation upon acidifying the buffer pH. However, an increase in β -sheet content of BoNT/A H chain is noticed at low pH using FT-IR. The L chain structure changed significantly with decrease in the pH, and such a change was mostly reversible. Additionally, the neurotoxin and its subunit chains induced a partially reversible aggregation of liposomes at low pH, which indicated their integration into the lipid bilayer.

Material and methods

Preparation of BoNT/A and its L and H chains:

BoNT/A was isolated following the method described in detail in Fu et al (28). In order to obtain L and H chains, the pure neurotoxin was applied to a QAE-Sephadex A-50 column (2.5 × 40 cm) for the chain separation (29). Following an overnight incubation with 0.1 M DTT and 2 M urea containing borate buffer (pH 8.4), the L chain was first eluted with 0.01 M DTT and 2 M urea containing borate buffer and the H chain was then eluted with the same buffer (0.01 M DTT, 2 M urea) containing 0.2 M NaCl. Both L and H chains are pooled after analyzing the fractions on the SDS-PAGE for their purity.

Membrane channel activity in planar lipid bilayer experiments:

Diphytanoylphosphatidylcholine (DPhPC, from Avanti Polar Lipids, Birmingham, AL) was first dissolved in HPLC grade chloroform and was dried under nitrogen stream to a thin lipid film which was resuspended in squalene (Sigma Chemical Co. St Louis, MO) to a final concentration of 20 mg/ml. Planar lipid bilayers were formed by painting the lipid solution across the orifice, ~100 μm in diameter of a 250 μl polyethylene pipette tip (30). The membrane bilayers formed from the DPhPC were found to be more stable for our experiments than those from typical diacylphosphatidyl choline. The salt solution, containing 1 M KCl, 5 mM CaCl₂ and 0.1 mM EDTA, was buffered at pH 4.7 with 5 mM dimethylglutaric acid (DMG, Sigma Chemical Co. St Louis, MO) or with HEPES buffer, pH 7.4. The 100 mV square wave potential was applied across the bilayer and the current relayed to a digitizing oscilloscope (Nicolet, Madison, WI) and then to a strip chart recorder. The sign of the potential was recorded according to the potential applied to the *trans* compartment. The bilayer was considered optimally thinned when its resistance approached 50 GΩ and its capacitance, 250 pF. After the membrane was stabilized, heavy chain was added to the front compartment (*cis* side) and mixed into the solution. The *trans* compartment was alkalinized (pH > 7.5) by the addition of 0.85% volume of 1 M KOH.

Effect of BoNT/A and its L and H chains on liposomes aggregation:

In this set of experiments, the liposomes were prepared as described previously (31). In order to monitor the degree of liposome aggregation, the optical density (OD) of liposome suspension was monitored at 465 nm, a wavelength that is away from the protein absorption spectral region (320- 240 nm). The OD was expected to increase upon aggregation of liposomes because large particles scatter more light. The OD was recorded using a UV/Vis spectrophotometer (Uvikon Model 9410, Kontron Instruments, San Diego, CA) at room temperature (25 °C). One milliliter liposome suspension with OD of approximately 0.05 at 465 nm was used for each experiment. The liposome suspension was taken in a 1 cm-pathlength quartz cuvette and OD was recorded for 4 min. The solution was then acidified using 2 M HCl (12-15 μ l) to pH 4.0 and the OD signal was recorded for another 4 min. The suspension was again titrated with 2 M NaOH (14-17 μ l) back to pH 7.5 and the OD recording was continued for 4 additional min. The OD after every 4 min incubation period was considered to be the steady state signal and was used to obtain data for histograms. For investigating the effect of BoNT/A and its H/L subunits on the liposome aggregation, 0.1 μ M of each protein was premixed separately with liposomes before recording the low pH-induced light scattering changes.

Circular dichroism spectroscopy:

The structures of BoNT/A and its L and H chains were analyzed with CD spectroscopy using Jasco model J-715 spectropolarimeter equipped with Peltier temperature controller (Model PTC-348W). Samples for CD recording in the far UV spectral region were prepared in 50 mM citrate (pH 4.0) or 50 mM citrate-phosphate (pH 7.0) buffer to a final concentration of 0.5-1.0 mg/ml. CD spectra were recorded at room temperature (~25 °C) using a 0.1 mm pathlength quartz cell at a spectral resolution of 0.1 nm. Five spectral scans were averaged to obtain spectrum for each sample. The scan speed was set at 20 nm/min with 8 second

response time. To obtain the actual spectrum of a protein sample, the spectrum recorded for the buffer used for protein solution was mathematically subtracted, and the resulting spectrum was smoothed using a 7 point, 3rd order smoothing algorithm.

Near UV CD spectra were recorded between 250 and 320 nm on a JASCO J500 upgrade instrument using 1 cm pathlength quartz cuvette at a 0.2 nm spectral resolution with ~0.6-1.0 mg/ml protein solution either in 50 mM citrate-phosphate buffer, pH 7.0 or in 50 mM citrate buffer, pH 4.0. The recording speed used was 20 nm/min with a time constant of 4 second. The spectral bandwidth was set at 1 nm, and 5 scans were recorded at room temperature (25 °C), averaged and smoothed. Actual protein spectra were obtained by subtracting CD signals of buffers used for protein solutions.

FT-IR spectroscopy:

The secondary structure of the heavy chain was also examined by FT-IR spectroscopy using a Nicolet 8210 FT-IR spectrometer with a zinc selenide ATR (attenuated total reflectance) accessory. The spectral recording conditions were similar to those described in Fu et al. (32,33). The H chain (~0.5 mg/ml) in different pH buffers (pH 4.0 or 7.0) was introduced to the ATR compartment and the spectra were immediately recorded. The protein spectra at pH 4.0 and 7.0 were obtained by subtracting the respective buffer (pH 4.0 or 7.0) spectra. The secondary structure estimation was carried out by curve-fitting analysis after identifying spectral band positions with Fourier self deconvolution and second order derivatization, as described in Fu et al. (32,33).

Results

Effect of pH on the channel formation of the BoNT/A and its subunits:

In order to investigate the pH effect on the channel activity of BoNT/A, reduced BoNT/A (10 µg/ml), or its H chain (5 µg/ml) was added the front of two chambers divided by a 100 µm

diameter thin lipid bilayer. pH conditions on two sides of the bilayer was varied and a measurement of the conductance across the lipid bilayer was carried out as an index of the channel activity of the neurotoxin and its H chain subunit. The L chain of BoNT does not exhibit voltage-gated membrane channel activity (19).

Addition of BoNT/A H chain to one side of the DPhPC membrane separating solutions at a symmetric pH of 7.4 did not induce any significant channel activity except for a few single-channels that open and close within seconds (**Fig. 1**). The membrane conductance (G) at a given time was obtained from the relation $G = I/V$, where V is the voltage applied to the *cis* compartment and I is the resulting current. The single channel conductance of the BoNT/A H chain was estimated to be ~ 5 picoSiemens (pS) under this symmetric neutral pH (7.4) condition.

At a symmetric pH of 4.7, shortly (1.6 min) after the H chain addition, active single-channel activity began (indicated by the noisy trace) (**Fig. 2**), which was not observed under symmetric pH 7.4 conditions (**Fig. 1**). Following this initial channel opening, more channels opened simultaneously (indicated by an abrupt drop within the negative half cycle), which then led to a steady rise of the macroscopic membrane conductance (indicated by the downward trace in the negative potential half cycles) (**Fig. 2**). From the initial opening to the macro-opening, the rate of increase in channel activity (to reflect the rate of peptide integration in the membrane) is estimated as 7.5 pS/sec.

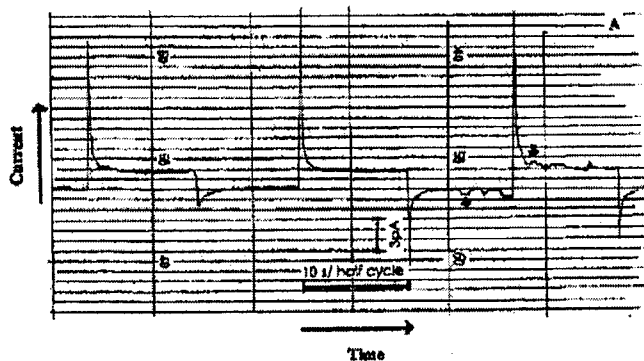


Fig. 1. Single channel currents in a planar lipid bilayer caused by addition of BoNT/A H chain (final concentration 5 $\mu\text{g/ml}$) at pH 7.4. A 100-mV square-wave potential was applied to a thin DPhPC/squalene bilayer in 0.1 M KCl, 5 mM CaCl_2 , 0.1 mM EDTA at room temperature (25 $^\circ\text{C}$). The arrow indicates single channel activity; 3-pA and 10-s bars indicate the current and time scales, respectively.

When H chain was placed in an asymmetric pH condition (*cis* side 4.7, *trans* alkaline), a rapid increase in the macroscopic membrane conductance was observed following a short time lag after H chain addition (Fig. 3). A rate of increase in channel activity was estimated as 51 pS/sec within the first 10 seconds.

In Figures 2 and 3, active channel activity was also observed within the positive half cycles. However, the channel closing frequency appears to be greater than the opening frequency at the positive potential. Such observations are illustrated more clearly in Fig. 3 as indicated by the asymmetric trace. This phenomena indicates the voltage-gated channel property of BoNT/A H chain channels, which has also been reported by other researchers previously (19). In our membrane bilayer system, membrane conductance was increased when the low pH side was made electrically positive.

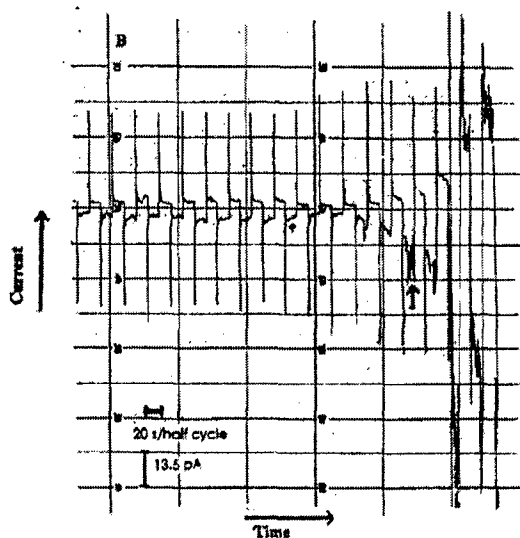


Fig. 2. Channel conductance of a thin DPhPC/squalene bilayer in the presence of 5 $\mu\text{g}/\text{ml}$ of H chain with symmetric pH of 4.7. The short arrow indicates the time of H chain addition, and the long arrow indicates the region of the trace with active channel activity. All other experimental conditions were the same as in Fig. 1.

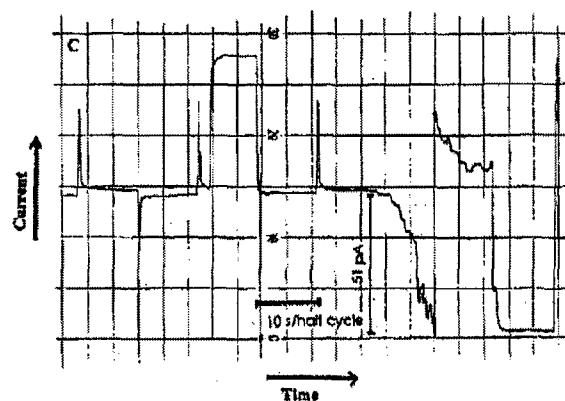


Fig. 3. Channel conductance of DPhPC/squalene bilayer in the presence of 5 $\mu\text{g}/\text{ml}$ H chain at an asymmetric (*cis* 4.7/*trans* alkalized) pH condition. The sample was added before the chart shown here, and other experimental conditions were the same as in Fig. 1.

The reduced form of BoNT/A was also tested for its channel activity. At symmetric low pH (4.7) condition, 10 $\mu\text{g}/\text{ml}$ reduced BoNT/A (treated with 15 mM DTT) either did not exhibit any channel activity or at the maximum evoked 7.5 pS of conductance over a twenty-five minute period (data not shown). When attempts were made to induce the asymmetric conditions, a higher channel activity was triggered but the membrane bilayer collapsed repeatedly, suggesting that the reduced protein might destabilize the membrane. A similar observation was made earlier by Blaustein et al. (27) who reported that the membrane channel conductance was noisy when the holo-neurotoxin (reduced) rather than H chain was used. Whether or not this observation could be due to a possible interference with the membrane channel activity by the presence of the L chain in the holo-neurotoxin needs to be further investigated.

Effect of pH on structure of BoNT/A, H and L chains:

The conformations of BoNT/A and its subunits were examined with far and near UV CD spectroscopy to derive structural information both at secondary and tertiary structural levels under low and neutral pH conditions to address the question of molecular responses of these proteins to pH which could provide a molecular basis for their membrane channel activity and translocation.

Alternation in the secondary structure of H and L chains upon acidification:

It has been suggested and observed from the functional activity assays that low pH triggers the membrane channel activity (*vide supra*) which might be responsible for the translocation of the light chain into the cytosol. The effect of pH on the secondary structure of dichain BoNT/A and its subunits was monitored using far UV CD. The spectrum recorded for BoNT/A at pH 7.4 (*spectrum not shown*) showed maximum negative signals at 210 ($-11443 \text{ deg} \cdot \text{cm}^2/\text{dmol}$) and 218 ($-11220 \text{ deg} \cdot \text{cm}^2/\text{dmol}$) nm, and a large positive signal at 193 ($16761 \text{ deg} \cdot \text{cm}^2/\text{dmol}$), indicating a relatively high α -helical content. Applying a secondary structure estimation method which employs the least squares combination of standard protein spectra (27) revealed $36.6 \pm 1.6\%$ α -helix, $24.9 \pm 2.6\%$ β -sheet, $12.4 \pm 1.1\%$ turns and $26.2 \pm 0.7\%$ random coil of BoNT/A (**Table 1**). Changing the pH to 4.0 did not seem to alter the secondary structure significantly, except for a slight increase in the β -sheet content (**Table 1**) which was within the experimental error of estimation.

The far UV CD spectra were also recorded for the BoNT/A H chain under the same conditions as for BoNT/A. A double minimum signal at 210 and 218 nm ($-10074 \text{ deg} \cdot \text{cm}^2/\text{dmol}$, and $-10218 \text{ deg} \cdot \text{cm}^2/\text{dmol}$, respectively, *spectrum not shown*) was also present in the H chain spectrum at neutral pH. A positive spectral band was observed at ~ 193 nm ($12947 \text{ deg} \cdot \text{cm}^2/\text{dmol}$). Similar to the BoNT/A, the CD spectral shape of BoNT/A H chain

basically remained unaltered upon lowering of the pH (spectrum not shown). Application of the spectral analysis program (27) revealed no structural difference in BoNT/A H chain at two pHs (pH 7.4 and 4.0; **Table 1**).

In contrast to insignificant structural alternations observed in BoNT/A and H chain with lowering of pH, the far UV CD spectrum of the L chain appeared to indicate drastic structural differences under the two different pH conditions (**Fig. 4**). The double-well spectral feature of BoNT/A L chain with minima at 218 and 210 nm observed at pH 7.4 changed dramatically to a single minimum centered at 225 nm. The intensity of the CD signal also decreased substantially (33%, 57% and 51% change at 218, 210 and 193 nm, respectively). Changing the pH of BoNT/A L chain, which was previously exposed to pH 4.0 buffer, back to the pH 7.4 buffer fully restored the far UV CD spectrum to the original BoNT/A L chain spectrum recorded under pH 7.4 buffer conditions (**Fig. 4**). The double minimum spectral feature of BoNT/A L chain similar to BoNT/A and H chain suggested that L chain was also rich in α -helical polypeptide folding.

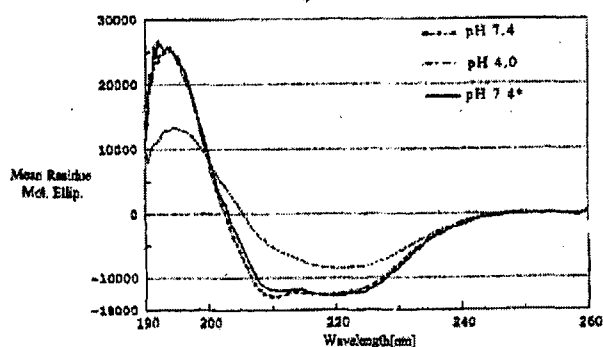


Fig. 4. Far-UV CD spectra of BoNT/A L chain were recorded under different pH conditions: 0.5–1 mg/ml of BoNT/A in a 0.1-mm-pathlength cuvette was scanned from 180 to 260 nm at a scan speed set at 20 nm/min with 8-s response time at room temperature. The spectra presented are the average spectrum from five scans, and the spectral resolution was 0.1 nm.

Upon exposure to the acidic condition, the changes in the spectral shape as well as intensity of BoNT/A L chain CD signal suggested a significant decrease in the α -helical

content. However, the remnant positive signal between 190-200 nm ($\sim 13000 \text{ deg} \cdot \text{cm}^2/\text{dmol}$ at the peak), indicated the presence of substantial amount of the ordered structure under the low pH condition. Secondary structure estimation of BoNT/A L chain at pH 4.0 revealed $31.2 \pm 3.1\%$ α -helix, $32.8 \pm 8\%$ β -sheets, $18.8 \pm 10.1\%$ β -turns and $23.8 \pm 5.3\%$ random coils. (**Table 1**). Analysis of the reversibility of the low pH-induced structural changes in the L chain revealed a very high degree of secondary structure restoration (44.7 ± 3.1 vs. 47.2 ± 4.7 α -helix, 22.1 ± 5.2 vs. 21.1 ± 7.1 β -sheet, 11.8 ± 1.8 vs. 15 ± 2.1 turns, 21.3 ± 1.8 vs. 18.2 ± 0.3 random coils; Table 1).

The effect of pH on the secondary structure of the H chain was also investigated using the FT-IR/ATR technique. **Fig. 5** shows the IR spectra of the H chain in the amide III spectral region under two pH conditions. At pH 7.0, two major peaks featured at ~ 1235 and 1315 cm^{-1} representing bands corresponding to β -sheets and α -helix, respectively. The small shoulder at $\sim 1280 \text{ cm}^{-1}$ corresponds to unordered structure (32). When the H chain was exposed to acidic solution, the band at 1235 cm^{-1} maintained similar intensity, although it was shifted slightly. A shoulder at $\sim 1260 \text{ cm}^{-1}$ appeared, and a general decrease in spectral intensity was observed above 1265 cm^{-1} . Most strikingly, the band at 1324 cm^{-1} corresponding to the α -helical structure of H chain was drastically reduced under the low pH conditions. Estimation of secondary structure by curve-fitting analysis (32,33) revealed a decrease in α -helical content (32% vs. 23 %) and increase in β -sheets (32% vs. 45 %) after the acid exposure of the BoNT/A H chain. The content of other structures (β -turns and random coils) posted only relatively small changes (36% vs. 32%).

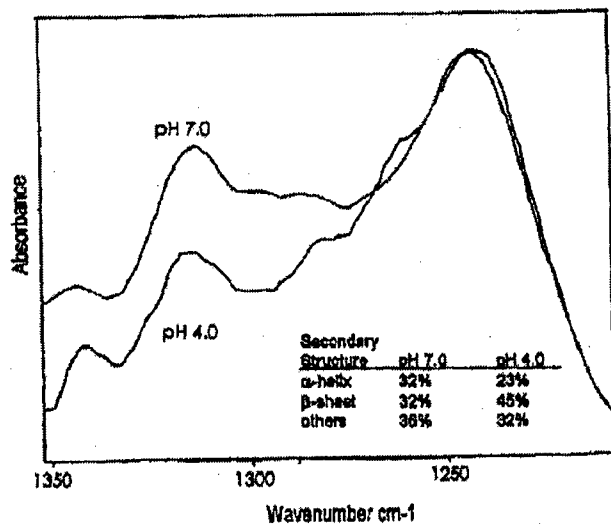


Fig. 5. FT-IR spectrum of BoNTA H chain in the amide III spectral region under neutral and acidic conditions: 0.5 mg/ml of H chain was applied to a 60° horizontal zinc selenide ATR crystal and 256 scans at 2-cm⁻¹ resolution were collected at room temperature (25 °C). The average was smoothed and the buffer background was subtracted.

Low pH effects on the Tyr topography of BoNT/A H chain:

Near UV CD signal of aromatic amino acid residues are sensitive to topographical and environmental changes in their vicinity (35-38). At pH 7.0, the H chain spectrum showed two distinctive bands at 295 nm and 285 nm (Fig. 6), which could be assigned to the ¹L_b vibronic state of tryptophan and the ¹L_a state of tyrosine, respectively (36). A relatively featureless spectrum was observed from 280-255 nm with a small shoulder at 270 nm. Upon exposure of the H chain to acidic environment (pH 4.0), the overall optical activity increased (~35-50 %) at 285 nm and 280 nm, whereas the band at 295 nm remained unchanged (Fig. 6). Relatively more prominent bands at 264 and 270 nm, known to arise from Phe residues, were observed under pH 4.0 conditions (Fig. 6).

Heavy chain induces the liposome aggregation at low pH

An attempt was made to investigate the impact of liposomes on the folding pattern of the BoNT/A H chain, especially under acidic conditions. However, addition of the H chain to liposome suspension under acidic conditions resulted in turbid solution that was unsuitable for

CD spectral recording for secondary structure analysis. Temperature-induced unfolding of BoNT/A H chain was investigated by monitoring CD signal changes at 222 nm in the presence and absence of liposomes at pH 7.4 and 4.0. The H chain in the absence of the liposomes showed clear optical activity under both acidic and neutral conditions (*vide supra*). Heating of the H chain at pH 7.4 appeared to precipitate it quickly once the temperature reached about 50 °C (**Fig. 7**). Under low pH conditions, temperature-induced unfolding exhibited a relatively prolonged transition, which appeared to have at least one intermediate state during the transition (**Fig. 7**). Temperature-induced unfolding of the H chain, when mixed with liposomes under pH 7.4 conditions, exhibited initiation of the unfolding transition at 30 °C which reaches a steady state plateau at 45 °C, with clear steady state intermediates at 37-39 °C and 41-42 °C. When the pH of the H chain/liposomes mixture was decreased, it resulted in a turbid solution with a total loss of the CD signal. The H chain-mediated enhancement of aggregation (turbidity) was specifically observed only under low pH conditions, which appeared to correlate well with its functional as well as structural responses analyzed in this study.

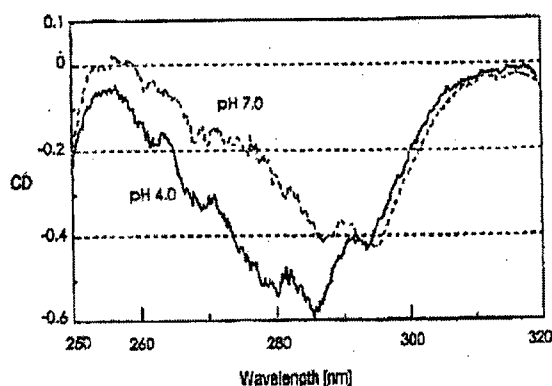


Fig. 6. Near-UV CD spectra of BoNT/A H chain at pH 7.0 and 4.0. Spectra were recorded between 250 and 320 nm at 0.2-nm spectral resolution with a scan speed of 20 nm/min and time constant of 4 s.

In order to further investigate the H chain-induced aggregation of liposomes under different conditions, change in the turbidity was monitored by recording changes in OD, as a measure of light scattering, using a UV/VIS spectrophotometer. Steady state changes in light

scattering of liposome solution either without or with added protein were monitored at 465 nm for 4 min at three pH levels, and final OD readings are plotted in Fig. 8.

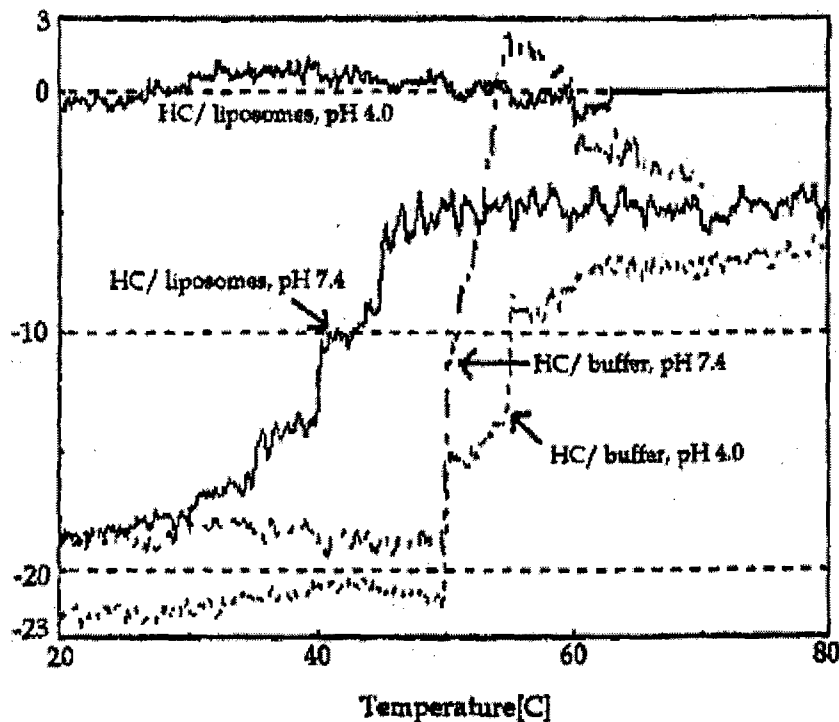


Fig. 7. Temperature-induced unfolding of the BoNT/A H chain (HC) in the presence and absence of liposomes under neutral and acidic pH values: 0.26 mg/ml of the HC was dissolved in pH 7.4 buffer, which was subsequently acidified by adding 3.4 μ l of 2 M HCl to pH 4.0. The same concentration of the HC was mixed with liposome suspension ($OD_{465} = 0.185$) for the liposome effect experiments, and the pH was adjusted by adding 3.4 μ l of 2 M HCl.

As shown in Fig. 8, the OD of the liposome suspension in the absence of any added protein was not affected by lowering the pH from 7.4 to 4.0 (the OD only increased from 0.03 to 0.045) (Table 2; Fig. 8), indicating that alteration of the external pH in the absence of BoNT/A or its L and H chains did not induce liposome aggregation. Addition of H chain to the pH 7.4 solution containing liposomes did not induce any change in the OD (Fig. 8). However, a drastic increase in OD occurred after acidifying the solution (OD increased from 0.058 to 0.50). Titration of the low pH sample back to pH 7.4 partially reduced the OD to 0.39 (a 22%

reduction; **Table 2**). When a similar experiment was performed with BoNT/A L chain, lowering of the pH evoked OD increase from 0.044 to 0.19, and the back titration to pH 7.4 resulted in the reduction of the OD to 0.137, showing a reversibility of 27% (**Fig. 8; Table 2**). Lowering the pH of BoNT/A in the presence of liposomes resulted in the largest increase in OD (from 0.039 to 0.56). Back titration of BoNT/A/liposome mixture reduced the light scattering by about 41% (**Fig. 8; Table 2**).

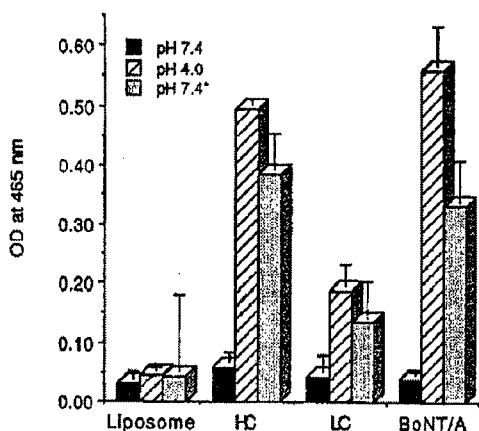


Fig. 8. Degree of liposome aggregation induced by BoNT/A, H chain (HC) and L chain (LC), as measured by optical density (OD) at 465 nm. pH* denotes that the pH has been readjusted from 4.0 back to 7.4 using 2 M NaOH.

Discussion

Translocation of the BoNT or its L chain across endosomal membrane to the cytosol is a critical step in the mode of BoNT action. Because BoNT is a water-soluble protein, its passage through a non-polar lipid bilayer membrane must require structural adaptation so that peptide segments within the protein having membrane interactive properties (amphiphilic and hydrophobic) could rearrange themselves for integration in the endosomal membrane. One major factor which is known to trigger such structural responses is the low pH occurring physiologically during the endocytosis process. The response of BoNT and its active subunits to low pH and the subsequent behavior of the proteins with planar lipid bilayers and liposomes have been analyzed in this study.

The BoNT/A H chain ion-conducting channel in the planar lipid bilayer (Figs. 1-3): (1) is voltage-gated, (2) has low conductance, 5 picoSiemens (pS), at near neutral pHs, and (3) has increased propensity of formation under low pH conditions. Based on these observations, low pH seems to stimulate H chain channel activity, and may be playing a role in inducing the H chain insertion into the lipid bilayer. The role of pH gradient in the membrane channel activity is not very clear as yet. However, in view of the "voltage-gated" nature of the channel, the pH gradient might play the role of a "driving force". In this model, while the applied voltage could trigger a specific structure of H chain membrane channel to an open state, the pH gradient could provide an ionic gradient allowing stabilization to the open channel state. Such a situation could sustain a deeper opening of the channel resulting in a faster ionic conduction indicated by higher conductance in our experiments (Fig. 3). It is possible that the deepened opening of the membrane channel could be responsible for the translocation of L chain. Hoch et al. (19) demonstrated that under similar conditions BoNT/B H chain membrane channels could translocate cations with the size as large as 12-16 Å. However, in previous studies symmetric low pH condition was not examined for ion channel activity of BoNT H chain. Our experimental results under symmetric low pH conditions (**Fig. 2**) suggest that structural changes in BoNT/A H chain introduced by the low pH are not sufficient to induce substantial ion transport. These results therefore suggest the possibility of new role of the low pH on the cis side of the membrane.

Others have also shown that low pH is required for the strong channel formation activity of BoNT and its H chains (19,39). A pH of 5.0 or lower induces the channel formation. Two possible effects of a low pH are (i) neutralization of negative charges of the protein, and/or (ii) conformational changes in the polypeptide folding due to modulation of backbone hydrogen bonds, either of which could allow exposure of hydrophobic domains and integration of the neurotoxin into the membrane bilayer. It has been observed that low pH increases the surface

hydrophobicity of tetanus neurotoxin (TeNT) as demonstrated by labeled Triton-X-100 binding (39). Similar observations were made for other dichain toxins such as *Pseudomonas* exotoxin A (40).

The L chain of BoNT, which is the pharmacologically active subunit, is translocated from the endosome to the cytosol to exhibit the toxic activity. How the L chain after adaptation to low pH and translocation across the membrane retains its biological activity is not clearly understood. Based on the observation of the ion-conducting channels formed by BoNT/A and other similar toxins at low pH (13,19-21), it is hypothesized that the L chain undergoes total unfolding and directly traverses the membrane through this ion-pore (19) into the cytosol.

The unfolding hypothesis is necessary to explain how a protein the size of the L chain can pass through a pore that has been demonstrated to be only 12-16 Å in diameter (19). Our experimental results clearly indicate low pH-induced structural changes in BoNT/A L chain as monitored by CD spectroscopy (**Fig. 4**). The structure reflects a refolded state at pH 4.0. Although our results do not match with results obtained with TeNT L chain (41) where no secondary structure change was observed at pH 5.0, the β -sheets structure promoted below pH 3.0 is similar to our observations at pH 4.0 (**Table 1**). Most significantly, we have observed that the structural change induced by the low pH in BoNT/A L chain is almost totally reversible, a finding that will explain retention of its biological activity as a zinc protease against SNAP-25 at near neutral pH under both *in vivo* and *in vitro* conditions (42). It has also been reported that the zinc protease activity of BoNT/A L chain pre-exposed to pH 4.7 is identical to the L chain maintained at pH 7.0 (43).

Because the L chain is not unfolded; *it is rather refolded* under low pH conditions, it is reasonable to consider an alternative mechanism for the L chain transport through the H chain ion channel. The L chain might undergo a structural change at low pH leading to a partially unfolded state, where part of the L chain can interact with the H chain and another part with

the lipid bilayer. Such a L/H/lipid multimeric transient complex may only exist at low luminal pH. Once the L chain reaches the cytoplasmic face of the membrane, the complex disassembles in response to the change in pH (back to physiological) where the L chain regains its natural conformation. The fact that L chain is actually capable of interacting with lipid membrane as observed in liposome permeability experiments (44,45) affords an evidence in support of such a proposed mechanism. Furthermore, low pH is known to increase L chain interaction with lipids (46) and its surface hydrophobicity (43).

In contrast to the L chain, the secondary structure of H chain as monitored by CD does not change with pH. However, a decrease in the α -helix content is detected by FT-IR/ATR technique. The discrepancy in results from the two techniques could be either due to higher sensitivity of the FT-IR technique in the amide III region or due to the differential interaction of the protein at two pH values with the ATR crystal. FT-IR spectroscopy is known to be relatively more sensitive to structural change (47, 48). We therefore believe that irrespective of the cause of sensitivity of the FT-IR, this technique is more likely to elucidate differences in BoNT/A H chain at two different pHs. Results from X-ray crystallographic data is at quite variance from the estimation of secondary structure of BoNT/A in solution with optical spectroscopy (49). Therefore, it is not possible to have a reliable independent method to verify estimation of secondary structure. However, it has been reported recently that the hydrophobic transmembrane segment (650-681) which is predicted to be the channel forming segment (14,16) is actually a 95 Å straight α -helix according to x-ray crystallography (50). Taking the thickness of the lipid bilayer (32 Å) into consideration, it is reasonable to predict that this fragment undergoes a conformational change to prevent exposing itself to the hydrophilic (endoplasmic or cytosolic) environment and to accommodate itself within the lipid bilayer. Whether such a change could be triggered by low pH or a lipid environment remains to be elucidated. Our Near UV CD data clearly show a change in the aromatic side chain

arrangement of H chain under acidic (pH 4.0) conditions. A substantial increase in the CD intensity at 285 nm and 280 nm, possibly arising from Tyr residues, suggests that the microenvironment around Tyr residues becomes more asymmetric or that the domain containing Tyr residues becomes more rigid under low pH conditions. There are 49 Tyr residues in the H chain and six of them are distributed in the hydrophobic region of H chain. Y636, Y648 and Y684 are located in the vicinity of the channel forming region of the BoNT/A H chain, and therefore likely to be sensitive to any conformational change induced at low pH.

Liposome aggregation experiments reveal that BoNT/A and its individual subunits can induce vesicle aggregation at low pH. Low pH does not cause any significant aggregation of liposomes in the absence of BoNT proteins, suggesting a critical role for proteins in this process. Protein-induced aggregation of lipid vesicles could occur either through a charge screening of lipid head groups by the protein or through the association of bound proteins. Proteins could also induce fusion of lipid vesicles by the same mechanisms leading to larger vesicles which scatter more light. Aggregation of vesicles either through charge screening or through protein association could be reversible, whereas lipid bilayer fusion would probably not be reversible. BoNT/A was the most effective reagent in inducing aggregation and nearly half was reversible, suggesting that the aggregation mediated by the holotoxin does not involve membrane fusion to a large extent. The H chain is nearly as effective in inducing liposome aggregation as the holotoxin whereas the L chain was only 38% as effective as the H chain (Fig. 8). The sizes of these proteins differ, which is likely to account for some of the differences in their ability to induce liposome aggregation. Reversibility of both L and H chain mediated aggregation is 22-26%, which is quite significant but considerably less than the reversibility of holotoxin induced aggregation.

A significant portion of the aggregation reversibility with pH can be explained if we assume that at least part of the aggregation is directly mediated by the oligomeric association

of the proteins. Perhaps the intact BoNT/A protein which does not seem to insert itself as effectively in the membrane as its L and H chains (based on their ability to permeabilize liposomes for calcein release, 44,45) adsorbs to the surface of the liposomes and through self association enhances liposome aggregation. It is also possible that BoNT/A adsorbed to the surface could screen surface charges allowing liposomes by themselves to associate and aggregate. A similar mechanism has been proposed for lipid vesicle aggregation mediated by myelin basic protein (51).

While BoNT/A H chain induced nearly the same level of liposome aggregation as the holotoxin, its reversibility was about half that of BoNT/A (**Fig. 8**). The low reversibility could be explained by either irreversible self association of the H chain and liposomes or H chain induced membrane fusion which would obviously be an irreversible process. Evidence of aggregation of the H chain was also observed in temperature-induced unfolding experiments. At pH 4.0, even in the absence of liposomes H chain unfolding exhibited intermediate states (**Fig. 7**) which could arise from non-cooperative unfolding generally observed in oligomeric structures (52). A drastic difference in the unfolding pattern in the presence of liposomes even at pH 7.4 is indicative not only of the existence of oligomeric structures but also of a considerable alteration in the polypeptide folding perhaps arising from binding at the surface of liposomes. Further investigation is needed to dissect the contributions of the different mechanisms in the observed aggregation of liposomes induced by BoNT/A and its active subunit fragments.

The salient features of this study can be summarized as follows: (1) The H chain forms ion channels in planar bilayer membranes. (2) H/L chains induce aggregation/fusion of lipid vesicles at low pH that is believed to occur via L/H chain-induced lipid destabilization. (3) Both H and L chain structures are altered at the acidic pH, suggesting a conformational change in the protein to adapt to the membrane insertion process. (4) The structural reversibility of

conformational changes in the light chain induced by low pH enable it to readapt to the active toxic structure in the cytosol after exposure to low pH in the endosomes.

Further Developments in Improving Techniques

Examination of protein structure, especially under conditions where either proteins tend to aggregate or bind with lipids (which are water insoluble), infrared techniques needed to be developed further. Efforts to further improve infrared methods of protein analysis were carried out during this reporting periods, and have resulted in two manuscripts (**attached in the Appendix**).

Table 1: Secondary structure estimation of BoNT/A, and its subunits, H and L chains under different pH conditions. Results were obtained by analyzing the CD spectra using the JASCO secondary structure estimation program.

	α -helix	β -sheet	Turn	Random coil
BoNT/A				
pH 7.4	36.6 \pm 1.6	24.9 \pm 2.7	12.4 \pm 1.1	26.1 \pm 0.7
pH 4.0	35.2 \pm 1.6	28.1 \pm 2.8	12.2 \pm 0.8	24.6 \pm 0.5
HC				
pH 7.4	32.6 \pm 1.8	21.5 \pm 3.8	17.5 \pm 1.1	28.5 \pm 2.1
pH 4.0	33.6 \pm 3.3	21.4 \pm 6.7	16.1 \pm 2.3	28.9 \pm 3.1
LC				
pH 7.4	44.8 \pm 3.1	22.2 \pm 5.2	11.8 \pm 1.8	21.3 \pm 1.8
pH 4.0	31.2 \pm 3.1	32.8 \pm 8	18.8 \pm 10.1	23.8 \pm 5.3
pH 7.4*	48.8 \pm 4.7	16.1 \pm 2.1	17.0 \pm 2.1	18.2 \pm 0.3

*Denotes the buffer condition was back titrated from pH 4.0 to pH 7.4.

Table 2: Degree of aggregation of liposomes induced by BoNT/A, H chain (HC) and L chain (LC) as monitored by the OD reading at 465nm under different pH conditions.

	pH 7.4	pH 4.0	pH 7.4*	% Reversibility
Liposomes	0.03±0.01	0.045±0.00	0.04±0.01	22
BoNT/A	0.04±0.00	0.56±0.06	0.33±0.07	41
HC	0.06±0.02	0.50±0.01	0.39±0.06	22
LC	0.04±0.03	0.19±0.04	0.14±0.06	27

* Denotes the buffer back titrated from pH 4.0 to pH 7.4.

References (Project B)

8. Singh BR (1996) *Adv. Exp. Med. Biol.*, 391, 63-84.
9. Singh, B. R. (2000) *Nature Struct. Biol.* 7, 617-619.
10. Simpson, L. L. (1981) *Pharmacol Rev.* 33, 155-188.
11. Simpson, L. L. (1989) *In: Botulinum Neurotoxin and Tetanus Toxin* (Simpson L. L., ed., San Diego Academic Press, 1989), pp. 154-178.
12. Lebeda, F. J. and Singh, B. R. (1999) *Toxin Reviews*, 18, 45-76.
13. Montal, M. S., Blewitt, R., Tomich, J. M. and Montal, M. (1992) *FEBS Lett.* 313, 12-18.
14. Oblatt-Montal, M., Yamazaki, M., Nelson, R. and Montal, M. (1995) *Protein Science* 4, 11490-1497.
15. Binz, T., Kurazono, H., Popoff, M. W., Frevert, J., Wernars, K. and Niemann, H. (1990) *J. Biol. Chem.* 265, 9153-9158.
16. Be, X., Fu, F.-N. and Singh, B. R. (1994) *J. Natural Toxins* 3, 49-68.
17. Doyle, J. and Singh, B. R. (1993) *In: Botulinum and Tetanus Neurotoxins: Neurotransmission and Biomedical Aspects* (DasGupta, B. R., ed). Plenum Press. pp. 231-235.
18. Singh, B. R. and Be, X. (1992) *In: Techniques in protein chemistry III* (Angeletti, R. H., ed), Academic Press, Orlando, FL. pp. 373-383.

19. Hoch, D. H., Romero-Mira, M., Ehrlich, B. E., Finkelstein, A., DasGupta, B. R. and Simpson, L. L. (1985) *Proc. Natl. Acad. Sci. USA* 82,1692-1696.
20. Donovan, J. J. and Middlebrook, J. L. (1986) *Biochemistry*. 25, 2872-2876.
21. Shone, C. C., Hambleton, P. and Melling, J. (1987) *Eur. J. Biochem.* 167,175-180.
22. Menestrina, G., Forti, S.,and Gambale, F. (1989) *Biophys J.* 55, 393-405.
23. Simpson, L. L. (1983) *J. Pharmacol Exp. Ther.* 225, 546-552.
24. Sheridan, R. E. (1993) *Soc. Neurosci Abstra.* 19, 1125.
25. Adler, M., Deshpande, S. S., Sheridan, R. E. and Lebeda, F. J. (1994) *In: Therapy with botulinum toxin* (Jankovic, J. and Hallet, M., eds) Dekker, New York. pp 63-70.
26. Simpson, L. L., Coffield, J. A. and Bakry, N. (1994) *J. Pharmacol Exp. Ther.* 269, 256-262.
27. Blaustein, R. O., Germann, W. J., Finkelstein, A. and DasGupta, B. R. (1987) *FEBS Lett.* 226, 115-120.
28. Fu, F.-N., Sharma, S. K. and Singh, B. R. (1998) *J. Prot. Chem.* 17, 17, 53-60.
29. Sathymoorthy, V. and DasGupta, B. R. (1985) *J. Biol. Chem.* 260, 10461-10466.
30. Busath, D. and Szabo, G. (1988) *Biophys. J.* 53, 689-695.
31. Fu, F. -N. and Singh, B. R. (1999) *J. Protein Chem.* 18, 701-707.
32. Fu, F.-N., DeOliveira, D. B., Trumble, W. R., Sarkar, H. K. and Singh, B. R. (1994) *Appl. Spectrosc.* 48,1432-1441.
33. Fu, F. -N., Lomneth, R. B., Cai, S. and Singh, B. R. (1998) *Biochemistry* 37, 5267-5278.
34. Yang, J. T., Wu, C. S. and Martinez, H. M. (1986) *Meth. Enzymol.* 130, 208-269.
35. Bateniany, M. M., Mizukami, H. and Salhany, J. M. (1993) *Biochemistry* 32, 663-668.
36. Singh, B. R. and DasGupta, B. R. (1989) *Biophysical Chem.* 34, 259-267.
37. Strickland, E. H. (1974) *CRC. Crit. Rev. Biochem.* 3, 113-175.
38. Woody, R. W. and Duker, A. K. (1996) *In: Circular dichroism and conformational analysis of biomolecules* (Fasman, G. D., ed.) Plenum Press, New York. pp. 109-157.
39. Boquet, P. and Duflo, E. (1982) *Proc. Natl. Acad. Sci. USA* 79, 7614-7618.
40. Idziorek, T., FitzGerald, D. and Pastan, I. (1990) *Infect. Immun.* 58, 1415-1420.

41. de Fillippis, V., Vangelista, L., Schiavo, G., Tonello, F. and Monetucucco, C. (1995) *Eur. J. Biochem.* 229, 61-69.
42. Blasi, J., Chapman, E. R., Link, E., Binz, T., Yamasaki, S., DeCamilli, P., Sudhof, T., Niemann, H. and Jahn, R. (1993) *Nature* 365, 160-163.
43. Li, L. and Singh, B. R. (2000) *Biochemistry* 39, 6466-6474.
44. Kamata, Y., and Kozaki, S. (1994) *Biochem. Biophys. Res. Commun.* 205, 751-757.
45. Fu, F.-N. and Singh, B. R. (1999) *J. Protein Chem.* 18, 701-707.
46. Montecucco, C., Schiavo, G. and DasGupta, B. R. (1989) *Biochem. J.* 259, 47-53.
47. Singh, B. R. and Fuller, M. P. (1991) *Applied Spectrosc.* 45, 1017-1021.
48. Singh, B. R., Fuller, M. P. and Schiavo, G. (1990) *Biophysical Chem.* 36, 155-166.
49. Cai, S. and Singh, B. R. (2001) *Biochemistry* 40, 4693-4702.
50. Lacy, D. B., Tepp, W., Cohen, A. C., DasGupta, B. R., Stevens, R. C. (1998) *Nat. Struct. Biol.* 5, 898-902
51. Bogg, J. M., Yip, P. M., Rangaraj, G. and Jo, E. (1997) *Biochemistry* 36, 5065-5071.
52. Mei, G., Di Venere, A., Buzanza, M., Vecchini, P., Rosato, N., and Finazzi-Agro, A. (1997) *Biochemistry* 36, 10917-10922.

Project C (Published in Protein Expression and Purification 34, 8-16, 2002)

Cloning, High-Level Expression, Purification, and Characterization of Recombinant Type B Botulinum Neurotoxin Heavy Chain Binding Domain

Purpose of this project was to obtain recombinant form of the binding domain of type B botulinum neurotoxin. Such reagent will be helpful in identifying the BoNT receptor, and in testing the idea of this domain being used as an antidote against botulinum neurotoxin challenge.

ABSTRACT

BoNT is a ~150 kDa protein, consisting of a binding/translocating heavy chain (HC; 100 kDa) and a toxifying light chain (LC; 50 kDa) linked through a disulfide bond. A DNA fragment

encoding type B *Clostridium botulinum* heavy chain binding domain (BoNT/B HC BD) was amplified by polymerase chain reaction with the primers designed with additional GGGCCCC overhang. The DNA fragment was constructed into the expression vector pET 15 b, and the plasmid was transformed into *Escherichia coli*. The high-level expressed recombinant BoNT/B HC BD was isolated from *E. coli* inclusion body, purified by Ni²⁺ column, and characterized by spectroscopic methods.

EXPERIMENTAL PROCEDURE

Materials

All oligonucleotides were synthesized by Integrated DNA Technologies Inc. (Coralville, IA). Genomic DNA isolation kit from Premega (Madison, WI). Restriction endonucleases and Vent DNA polymerase from New England BioLabs Inc. (Beverly, MA). Thermal cycler for PCR (Eppendorf -Netheler – Hinz GmbH, Hamburg, Germany). TA cloning kit and S.N.A.P. Miniprep kit for isolation of plasmids from Invitrogen (Carlsbad, CA). The plasmid pET 15 b was from Novagen (Novagen Inc., Madison, WI). His-Select Nickel affinity gel and CelLytic B II Bacterial Cell Lysis extraction Reagent were obtained from Sigma (St. Louis, MO). Anti-His antibody was from Amersham Pharmacia Bioth (Piscataway, NJ).

Culture and chromosomal DNA isolation of *Clostridium botulinum* type B cells (strain Okra)

Clostridium botulinum type B cells (strain Okra) in a 1.5 ml microcentrifuge tube kept in -80°C was added to a 10 ml cooked meat medium (Difco Laboratories, Becton Dickinson, MD) and cultured at 30 °C for 18 to 20 hours. The *C. botulinum* type B cells in the cooked meat medium was inoculated in 500 ml of toxin production medium (1% N-Z amine type B (Quest International, NY), 2% proteose peptone and 1% yeast extract ((Difco Laboratories, Becton

Dickinson, MD), 0.05% sodium thioglycollate and 1% glucose (Sigma, St. Louis, MO) and incubated at 30 °C for 22 hours.

Chromosomal DNA from *C. botulinum* type B cells was isolated by using Wizard Genomic DNA Purification Kit (Promega, Madison, WI) according to its manufacturer's protocol. Briefly, *C. botulinum* type B cells were pelleted by centrifuging and resuspended in 50 mM EDTA. 10 mg/ml lysozyme was added to the resuspended cell pellet and the sample was incubated at 37 °C for 60 min. Then nuclei lysate was added to the solution and the solution was incubated at 80 °C for 5 min to lyse the cells. RNase solution was added to the cell lysate after the sample cooled to room temperature, and the solution was incubated at 37 °C for 60 min. The supernatant containing the DNA after protein precipitation was transferred to a clean tube containing isopropanol to precipitate the DNA. DNA pellet was obtained by centrifuging, and washed by 70% ethanol. TE buffer (10 mM Tris-Cl, 1 mM EDTA, pH 8.0) was added to the DNA pellet. The DNA sample for PCR was stored at -20 °C.

Primer design and polymerase chain reaction (PCR)

According to BoNT/B sequence in GenBank database under accession number M81186 (53), primers for heavy chain binding domain DNA fragment were designed. Both *Nde* I and *Bam*H I restriction sites were incorporated into the 5' end of the forward sequence and reverse sequence primers, respectively. Because of the high AT content in the *C. botulinum* genome, GGGCCCC overhang was created into the 5' end of each restriction sites.

PCR for the amplification of BoNT/B HC binding domain DNA fragment was performed in 1 X buffer (20 mM Tris-HCl, pH 8.8, 2 mM MgSO₄, 10 mM KCl, 10 mM (NH₄)₂SO₄, 0.1% Triton X-100), a total volume of 50 µl containing 200 ng of chromosomal DNA as template DNA, 100 ng of each primer, 200 µM concentration of each dNTP (deoxynucleosid triphosphate), 1 unit of Vent DNA polymerase (New England BioLabs). The reaction was

carried out using the following reaction cycles in a programmable thermocycler (Eppendorf - Netheler – Hinz GmbH, Hamburg, Germany): initial denaturation at 93 °C for 2 min followed by 30 consecutive cycles consisting of denaturation at 93 °C for 1 min, annealing for 2 min at 59 °C, and extension at 73 °C for 3 min, then final extension at 73 °C for 10 min was followed.

Ten microliter of each reaction product was monitored visually after separation on a 1.0 % (w/v) agarose gel (Molecular Research Center Inc., Cincinnati, OH) run in 0.5 X TBE (45 mM Tris-borate, 1 mM EDTA) buffer, stained with ethidium bromide and viewed under UV illumination. The size of BoNT/B HC binding domain DNA fragment was 2 kb.

Gene construction

The PCR product was treated with Tag polymerase (QIAGEN, Chatsworth, CA) at 72 °C for 10 min to add one Adenine on each side of the DNA fragment. The DNA fragment was purified by agarose gel electrophoresis using Gel Extraction kit (QIAGEN), and ligated into the pCR 2.1 TA cloning vector (Invitrogen, Carlsbad, CA). After overnight incubation at 14 °C, each ligation mixture was transformed into *E. coli* strain INV α F' competent cells and transformants were screened by blue-white color screening technique using X-gal as a β -galactosidase substrate. Twelve recombinant plasmids were isolated by using S.N.A.P. Miniprep kit (Invitrogen, Carlsbad, CA), and digested by *EcoR* I restriction enzyme (New England Biolabs) to check the size of inserts.

One recombinant plasmid containing the insert in expected size was sequenced by the dideoxy chain termination method to confirm the correct DNA sequence by comparing its sequence with BoNT/B sequence in GenBank database under accession number M81186. The identity of the two DNA sequences were analyzed using the Baylor College of Medicine (BCM) Search Launcher and ExPASy Proteomics tools through the internet on computer. The recombinant plasmid was cleaved with *Nde* I and *Bam*H I and then electrophoresed on a 1.0 %

agarose gel. The *Nde* I-*Bam*H I fragment was purified from the agarose gel using Gel Extraction kit (QIAGEN) and then ligated to the *Nde* I-*Bam*H I digested and CIP-treated vector pET-15 b (Novagen Inc., Madison, WI). A typical ligation reaction mixture contained 50 ng of the vector and 300 ng of the insert in a volume of 20 μ l of ligation buffer (20 mM Tris-HCl pH 7.6, 10 mM MgCl₂, 25 μ g/ml acetylated BSA) contained 7.5 mM DTT, 0.75 mM ATP, and 10 U T4 DNA ligase. After overnight incubation at 16 °C, the ligation product was transformed into *E. coli* strain NovaBlue competent cells (Novagen Inc., Madison, WI). The cells were plated on Luria-Bertani agar medium supplemented with ampicillin (50 μ g/ml), and grown at 37 °C overnight. Clones were screened by digestion of a miniprep plasmid DNA (Invitrogen, Carlsbad, CA) with *Nde* I and *Bam*H I. Confirmation that the amplified fragment encoded BoNT/B HC binding domain was obtained by DNA sequencing of a representative plasmid recombinant (designated pET-BoNT/B HC BD). DNA sequencing was by the dideoxy chain termination method.

Expression of the recombinant BoNT/B HC binding domain

The BoNT/B HC BD DNA fragment from *C. botulinum* neurotoxin type B was cloned with the histine tag at the C-terminal end and expressed under the control of the T7 promoter. The pET-BoNT/B HC BD recombinant plasmid was transformed into *E. coli* strain BL21-CodonPlus (DE3)-RIL contained pACYC plasmid (Stratagene, La Jolla, CA). The *E. coli* cells were plated on LB-ampicillin (50 μ g/ml) agar plates and expression of BoNT/B HC BD of several colonies under the control of IPTG-inducible promoters were tested on an analytical scale (1 ml of induced culture).

The clone with most highly expressed BoNT/B HC BD was used to inoculate 50 or 100 ml of 2YT medium (1.6% tryptone, 1% teasy extract, 0.5% NaCl) supplemented with 50 μ g/ml ampicillin and with 50 μ g/ml chloramphenicol (Sigma, St. Louis, MO) at 37 °C overnight. The next morning, the 50 ml culture was added to 1 L medium in a 4-L flask, and the culture was

grown at 37 °C to $OD_{600} = 0.6-0.8$. IPTG was then added to a final concentration of 1 mM, and the induction was carried out at 30 °C for 5 hours.

Purification

E. coli cells were harvested by centrifugation at 5,000 X g for 10 min at 4 °C. All subsequent procedures were performed at 4 °C. Cell pellet was stored at -80 °C. The frozen cell pellet was thawed and resuspended in a lysis buffer (20 mM Tris-Cl, pH 7.5, and a mild nonionic detergent, CellLytic B II Bacterial Cell Lysis Extraction Reagent, Sigma, St. Louis, MO) at the ratio of 5 ml of the lysis buffer per gram of wet cell paste. After the cells were completely resuspended, 5 µg/ml deoxyribonuclease I for reducing the viscosity and a protease inhibitor cocktail for purification of histidine-tagged proteins at the ratio of one ml for 20 g wet weight cell paste (Sigma, St. Louis, MO) were added to the suspension. The extraction suspension was incubated at room temperature for 15 min to fully extract the cells and centrifuged at 25,000 X g for 15 min to pellet the insoluble material. After the supernatant was carefully removed, the supernatant was loaded onto His-Select Nickel affinity gel column (Sigma, St. Louis, MO), and performed the chromatography at the same way as described in the His-Select Nickel affinity gel column chromatography of the inclusion body extract. The cell debris was used to purify the inclusion body and was resuspended in the same lysis buffer at the same ratio. The final concentration of 0.4 mg/ml lysozyme was added to the suspension. The mixture was incubated at room temperature for 15 min, and 20 ml of 20 times diluted lysis buffer with deionized water (Sigma, St. Louis, MO) was added to the extract. The extract was mixed and centrifuged at 25,000 X g for 15 min to collect the inclusion bodies, and the supernatant was carefully removed from the inclusion body. The inclusion body was resuspended in 40 ml of 1:20 diluted lysis buffer, and the extract was centrifuged at 25,000 X g for 15 min, and the

procedure was repeated two more times to further wash the inclusion body, then the inclusion body was stored at -80 °C. The frozen inclusion body from 1 L of the culture was thawed and resuspended in 20 ml of 0.1 M sodium phosphate buffer, pH 8.0 contained 6 M guanidine chloride, 0.4 M sodium chloride, 10 mM beta-mercaptoethanol and sonicated on ice using a macroprobe at 30% output, 4 times for total 2 min (30 sec burst, and 30 sec cooling cycle). The guanidine extract was incubated on a rotating platform for 1 h at room temperature, then clarified by centrifugation at 100,000 X g for 1 h. The supernatant was diluted with 20 ml of 0.1 M sodium phosphate buffer, pH 8.0 contained 8 M urea, 0.4 M sodium chloride, 10 mM beta-mercaptoethanol, and 5 mM imidazole, and applied onto a His-Select Nickel affinity gel (Sigma, St. Louis, MO) column (2 ml bed volume), which was previously equilibrated in the same buffer that was used to dilute the guanidine extract. The column was first washed with 20 ml of equilibration buffer, then with 20 ml of the buffer contained 20 mM imidazole, with 8 M urea, and without beta-mercaptoethanol. The column was gradually washed with 20 ml of 0.1 M sodium phosphate buffer, pH 8.0 contained 0.4 M sodium chloride, 0.1% dodecylphosphocholine (DPC, Avanti Polar Lipids), without urea, and gradual concentration of 20, 40, 60, 80, 100 mM imidazole. Pure BoNT/B HC BD was eluted with 100 mM imidazole.

BoNT/B HC BD fraction was dialyzed overnight against 50 mM sodium phosphate buffer, pH 8.00 contained 0.1 M sodium chloride. The purified BoNT/B HC BD was stored in 20% glycerol solution at -80 °C.

SDS-PAGE (Sodium Dodecyl Sulfate – Polyacrylamide Gel Electrophoresis)

Sodium dodecyl sulfate-polyacrylamide gel electrophoresis was carried out to estimate protein expression under different conditions and to check the purity of the isolated BoNT/B HC BD. The electrophoresis was carried out on a Mini Protein II System (Bio-Rad, Hercules, CA) using a 7.5% polyacrylamide gel.

To monitor the induction of BoNT/B HC BD, culture of every hour after induction was sampled. The cells were centrifuged (5000 X g, 10min) and resuspended in part of the supernatant to have the approximately same turbidity in each suspension sample. Five hundred micro liter of each sample was sonicated for 10 sec on ice using a macroprobe at 30% output. Thirty micro liter of each sonicated sample was added to 30 μ l 2 X reducing SDS sample buffer (0.1 M Tris, pH 6.8, 200 mM dithiothreitol, 4% SDS, 20% glycerol, 0.2% bromophenol blue). After heating at 100 °C for 3 min and 50 μ l of the sample was subjected to SDS-PAGE, and the proteins were detected by Coomassie blue staining. Purified BoNT/B HC BD (mg/ml) and molecular markers were separately mixed with 2 X reducing SDS sample buffer and heated at 100 °C for 3 min. These samples (10 μ l) were applied to the SDS-PAGE gels. After electrophoresis, protein bands were detected by Coomassie blue staining.

To estimate the percentage of total cellular protein represented by the recombinant BoNT/B HC BD, Coomassie blue-stained 7.5% SDS-PAGE gels resolving the total *E. coli* lysate proteins were scanned on an *itti* Imager, plotted, and integrated for density using an *itti* Imager (*itti*, I.c., Petersburg, FL). The BoNT/B HC BD band was integrated for density in each lane and compared with the total integrated density of all proteins in the same lane to obtain the percentage of BoNT/B HC BD of total *E. coli* protein.

Western blot (Anti-His antibody)

Mouse anti-his antibody (Amersham Pharmacia Biotech) as first antibody, and anti-mouse IgG as second antibody AP conjugate (Novagen) were used in the Western blot analysis.

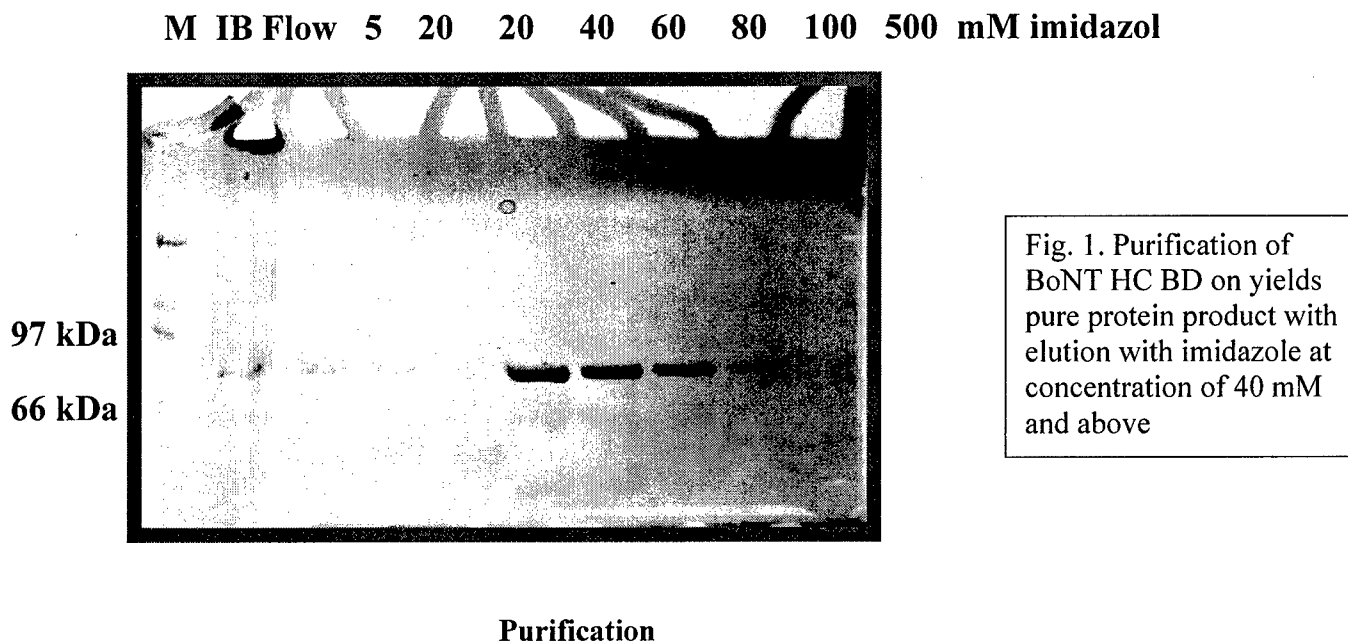
Isoelectric focusing

Isoelectric focusing (IEF) was carried out using the Mini Protein II system from Bio-Rad (Hercules, CA). Briefly, an aliquot of BoNT/B HC BD (mg/ml) was mixed with the same

volume of sample buffer (6% Ampholytes, pH 3.5-10). The electrode buffers used were 0.02 M acetic acid anolyte and 0.02 M NaOH catholyte. After prerunning the gel (5.5% Ampholytes, pH 3.5-10, 5% acrylamide, and 10 % glycerol) at 300 V for 30 min, 50 µl of mixture was applied to the gel. Electrophoresis was performed at 300 V at 8 °C. The gel was fixed in 20% trichloroacetic acid for 5 min and then in destaining solution (30% methanol, 10% acetic acid) for 2 min. The gel was then stained with 0.02% PhastGel Blue R (Pharmacia Biotech) in the destaining solution contained 0.1% CuSO₄ to decrease the background staining, and destained until the background was clear.

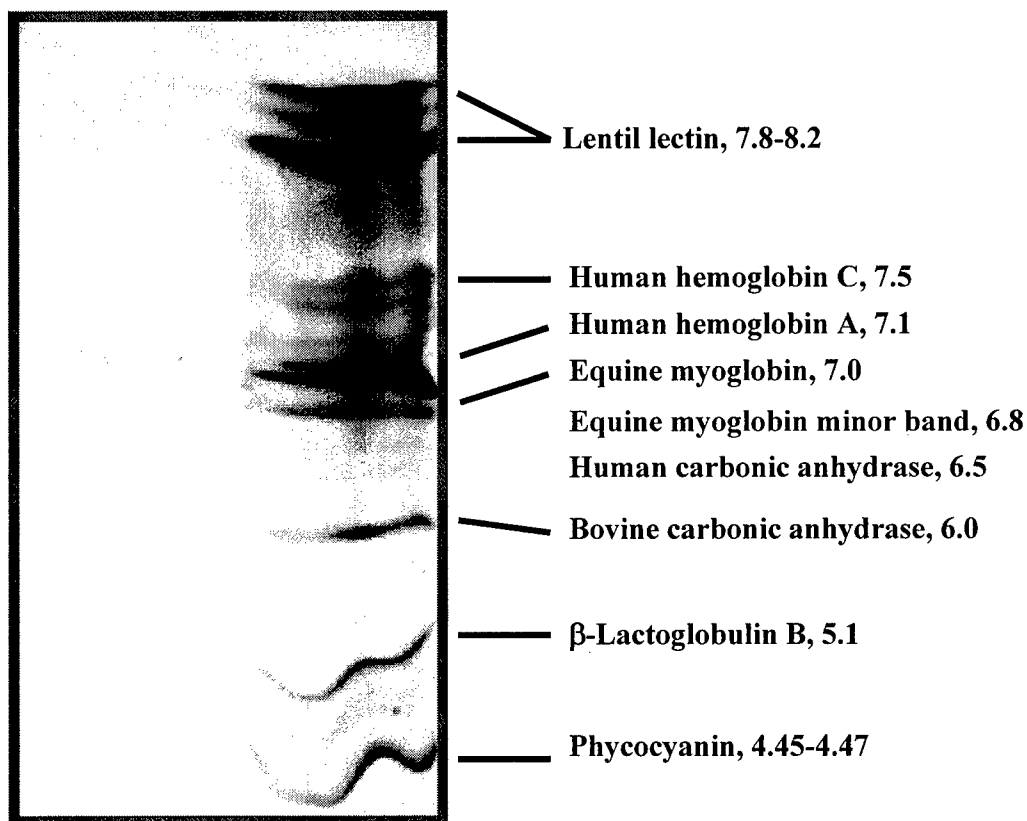
RESULTS

Expression of the cloned gene product in *E. coli* was successful, and the purified product was obtained from the Ni²⁺ affinity column with the elution with imidazole (Fig. 1).



Isoelectric focusing of the recombinant BoNT/B HC BD (Fig. 2) indicated a pI of about 7.1

Fig. 2. Isoelectric focusing of BoNT/B HC BD (left lane), along with standards.



pI of BoNT/B HC BD

Structural analysis of the recombinant was carried out with FT-IR and CD spectroscopies (Figs. 3-5). Curve-fitting and correlation analysis revealed that BoNT/B HC BD is a β -sheet dominated

protein (Table 1). Temperature denaturation analysis (Figs. 6&7) of this domain indicated that there are perhaps two domains of the protein, which undergo independent unfolding processes.

Fig. 3. FT-IR of BoNT/B HC BD

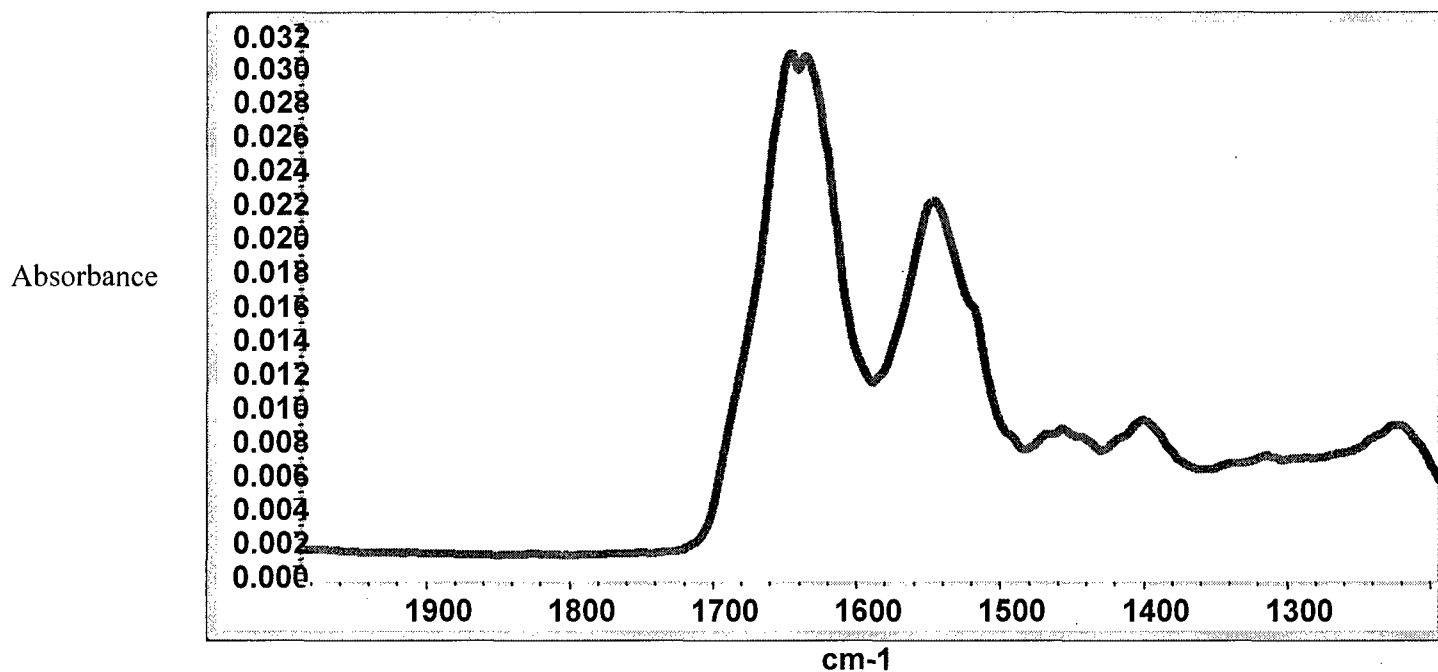
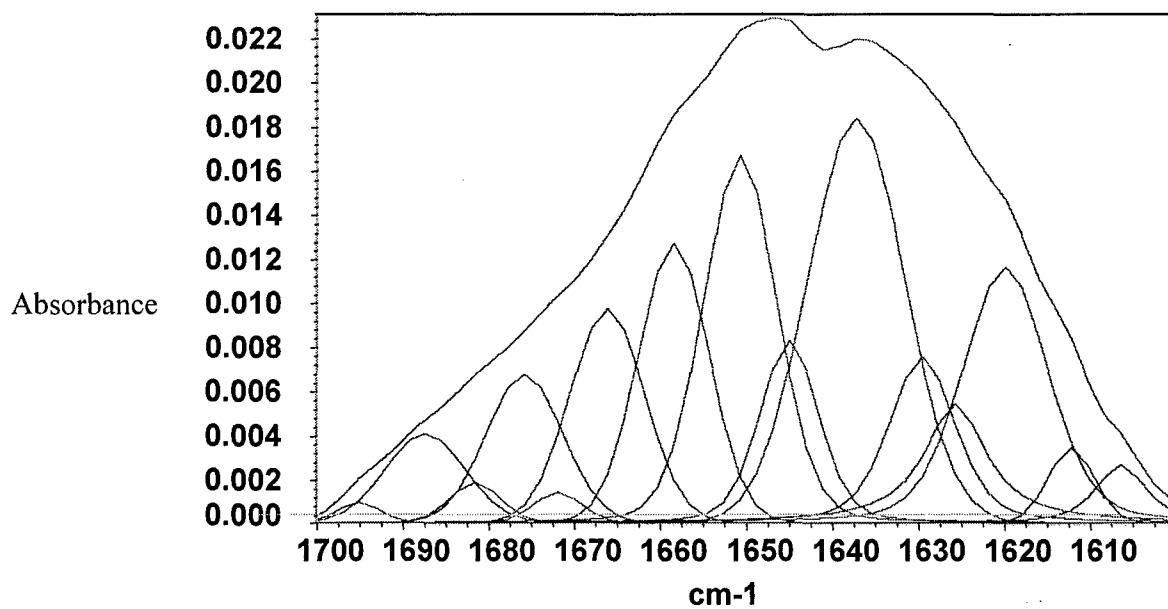


Fig. 4. Curved-fitted IR spectrum of BoNT/B HC BD in Amide I Region



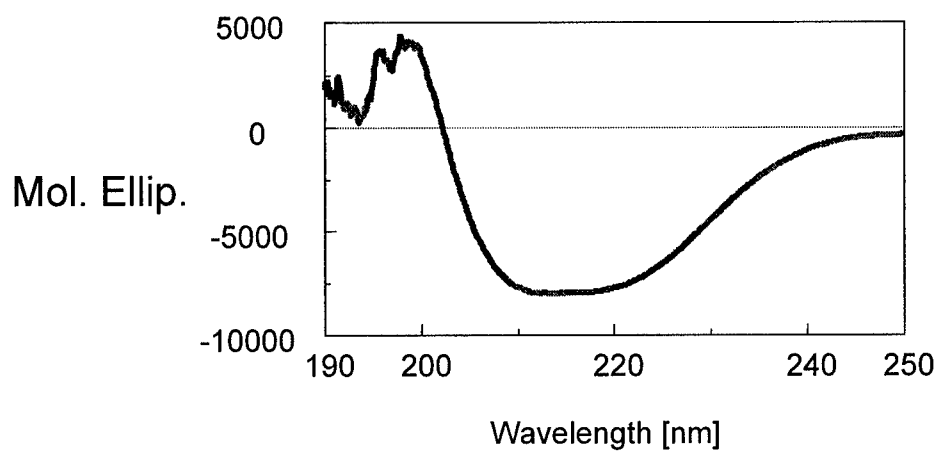


Fig. 5. Circular Dichroism Spectra of BoNT/B HC BD in the Far UV Region

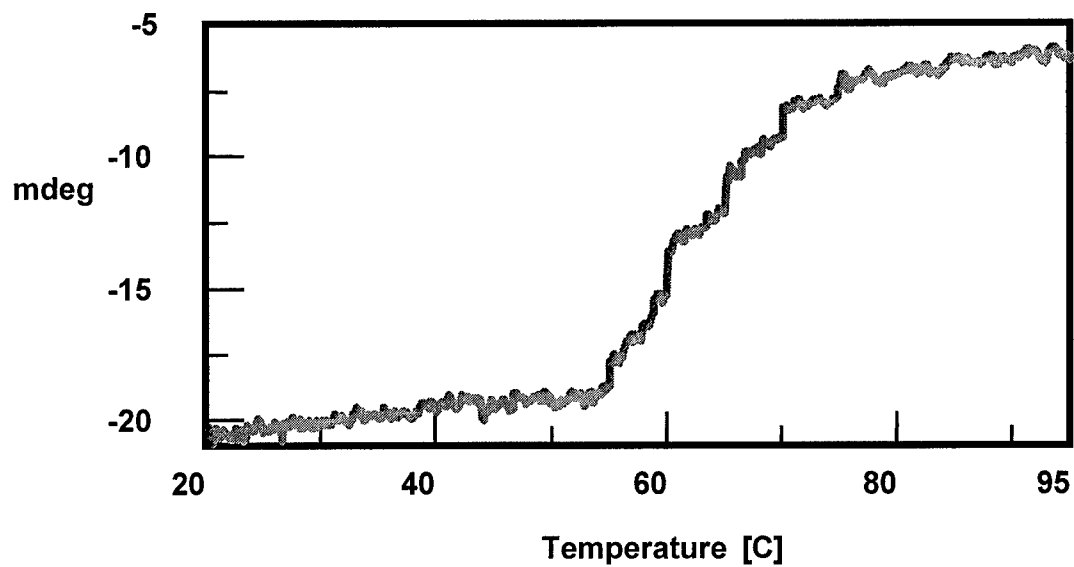


Fig. 6. Temperature Denaturation of BoNT/B HC BD
The signal was monitored at 222 nm

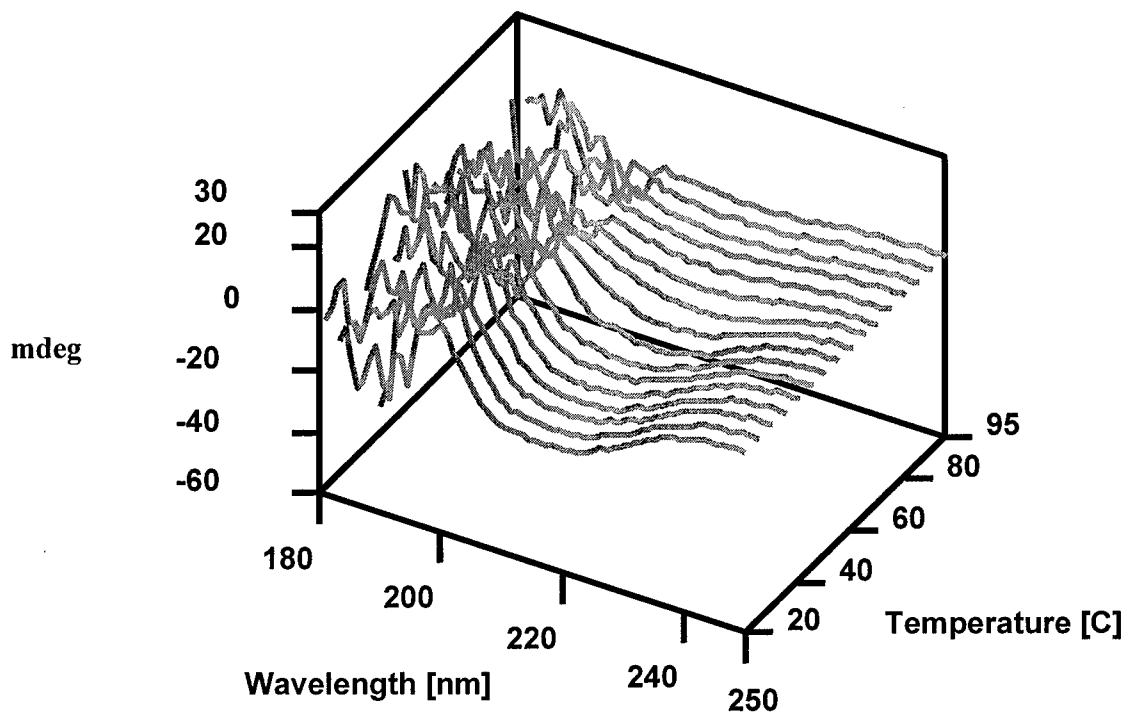


Fig. 7. Far UV CD Analysis of BoNT/B HC BD at Different Temperatures

Table 1: Secondary Structure Estimation of Recombinant BoNT/B HC BD

Methods	% α -helix	% β -sheet	% turn	% random coil
FT-IR Amide I	18	46	30	7
CD	13	36	23	29

These data suggest that we have successfully have expressed and purified BoNT/B HC BD, which is structurally well folded, and is expected to compete well in binding with the receptor.

References (Project C)

53. Whelan, S. M., Elmore, M. J., Bodsworth, N. J., Brehm, J. K., Atkinson, T. and Minton N. P. (1992) *Appl. Environ. Microbiol.* 58, 2345-2354.

Project D (Unpublished data)

Comparative Binding of Synaptotagmin II with BoNT/A and BoNT/ B

Abstract

In view of a recent report (Dong et al., 2003) suggesting that only BoNT/B, and not BoNT/A or /E, binds to synaptotagmin, we have analyzed comparative binding of BoNT/A and BoNT/B with GST-synaptotagmin fusion protein to clarify this latest observation from our findings published earlier (Li and Singh, 1998). In an experimental design similar to Dong et al. (2003), we observed that BoNT/A binds to the synaptotagmin II similar to BoNT/B, albeit at about 10-fold higher concentration. Moreover, the binding of BoNT/B is enhanced by ganglioside whereas BoNT/A binding to synaptotagmin remains unaffected by ganglioside, GT1b.

Immuno-Pull-down assays

To assay for direct Syt II-Hn-33 interaction, GST-synaptotagmin II was used as an affinity matrix to pull down Hn-33 in the presence and absence of gangliosides (GT1b). We also performed direct Syt II-BoNT/A and B interactions.

GST-synaptotagmin II (60 μ g) was immobilized on glutathione-Sepharose beads (200 μ l). Immobilized protein was mixed with Hn-33 (0.6 mg/ml), BoNT/A (0.8 mg/ml), or BoNT/B (0.1 mg/ml), either with (+; 25 μ g/ml) or without (-) ganglioside (GT1b) in 200 μ l PBS (pH 7.4) for 1 h at 4°C. Beads were washed four times with PBS, bound proteins were solubilized by boiling in SDS sample buffer and subjected to SDS-PAGE, and were visualized by staining with Coomassie blue.

Results

Under identical conditions, we observed that at lower concentration of 0.1 mg/ml, only BoNT/B binds to Syt II, at concentration of 0.6 mg/ml (8.7 μ M dimeric Hn-33) and 0.8 mg/ml (2.7 μ M dimeric BoNT/A) bind to Syt II, and the interaction is not dependent on ganglioside.

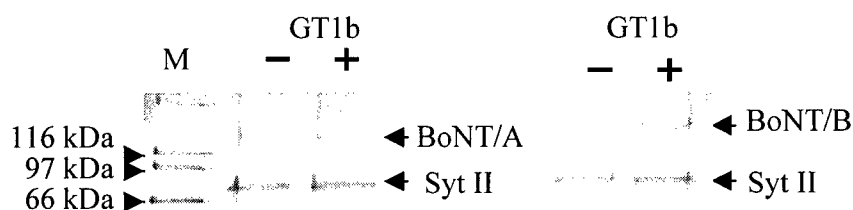


Fig. 1. SDS-PAGE analysis of pull-down assay for the binding of synaptotagmin II (Syt II) with BoNT/A (**left panel**) and BoNT/B (**right panel**) in the presence and absence of ganglioside, GT1b. M: molecular weight standards, the number on the left indicates molecular mass of markers in kDa. Syt II: GST-synaptotagmin II.

References

Dong, M., Richards, D. A., Goodnough, M. C., Tepp, W. H., Johnson, E. A. and Chapman, E. R. (2003) Synaptotagmins I and II mediate entry of botulinum neurotoxin B into cells. *J. Cell Biology*, 162, 1293-1303.

Li L., Singh B.R. (1998) Isolation of synaptotagmin as a receptor for type A and E botulinum neurotoxin and analysis of their comparative binding using a new microtiter plate assay, J. Nat. Toxins 7: 215-226.

Project E (Published in FEBS Journal FEBS Journal, 272, 2717-2726, 2005)

Association of Hemagglutinin-33 of Type A Botulinum Neurotoxin Complex with Synaptotagmin II, a Receptor for Botulinum Neurotoxin

ABSTRACT

Botulinum neurotoxin type A (BoNT/A), the most toxic substance known to the mankind, is produced by *Clostridium botulinum* type A as a complex with a group of neurotoxin-associated proteins (NAPs), possibly through a polycistronic expression of a clustered group of genes. NAPs are known to protect BoNT against adverse environmental conditions and proteolytic digestion. A 33 kDa hemagglutinin (Hn-33), one of the subcomponent of NAPs, is resistant to protease digestion, a feature likely to be involved in the protection of the botulinum neurotoxin from proteolysis. However, it is not known whether Hn-33 plays any other role other than protection of BoNT. We have now discovered that Hn-33 binds to synaptotagmin II (Syt II), the putative receptor of botulinum neurotoxin. Competitive ELISA (enzyme-linked immunosorbent assay) indicated that the Hn-33 inhibits the binding BoNT/A to Syt II, suggesting that it shares binding site with BoNT/A.

INTRODUCTION

Botulinum neurotoxins (BoNTs) are among the most potent toxins known to the humankind (~100 billion times more toxic than cyanide) (Singh, 2000). BoNTs are the causative agents of food-borne, infant, and wound botulism (Tacket and Rogawski, 1989). Because of its extreme toxicity, BoNT is also considered a dreaded biological weapon (Arnon et al., 2001).

Different stains of *C. botulinum* produce seven immunological serotypes of distinct botulinum neurotoxins (BoNT, EC 3.4.24.69), named as A to G. Each of the BoNTs is synthesized as single polypeptide chain of about 150 kDa, which is cleaved endogenously or exogenously resulting into a 100 kDa heavy chain (HC) and a 50 kDa light chain (LC) linked through a disulfide bond (Singh, 2000). BoNT's mode of action involves four steps: extracellular binding to presynaptic membrane, internalization, membrane translocation, and intracellular substrate cleavage through its endopeptidase activity. In the first step, BoNT attaches to nerve membranes through the C-terminus of HC binding to gangliosides and a protein receptor on presynaptic membranes. Polysialylated gangliosides like GT1b were shown to be involved in BoNT/A neurotoxicity (Simpson and Rapport, 1971). Synaptotagmin II (syt II) of rat brain has been identified as the receptor for BoNT/ B (Nishiki et al, 1994; 1996), and also for BoNT/A and E (Li and Singh, 1998; Yowler et al., 2002). In the second step, the neurotoxin is internalized through endocytosis. In the third step, as the pH inside the endosome is lowered with a proton pump (Lebeda and Singh, 1999), and the N-terminal domain of the HC is inserted into the membrane lipid bilayer to form a pore for translocating the LC across the membrane into the cytosol (Lebeda and Singh, 1999; Koriazova and Montal, 2003). Finally, once in the cytosol, the LC acts as a zinc-endopeptidase and cleaves one of the three SNARE (soluble N-ethylmaleimide-sensitive factor attachment protein receptor) proteins. The LCs of BoNT/A and /E cleave SNAP-25 (synaptosome-associated protein of 25 kDa), the BoNT/C LC cleaves syntaxin and SNAP-25, and the LCs of BoNT/B, D, F, G cleave VAMP (vesicle-associated membrane protein) (Singh, 2000). The cleavage of anyone of the SNARE proteins results in blockage of acetylcholine release at the neuromuscular junctions, resulting in flaccid muscle paralysis.

BoNTs are expressed in *C. botulinum* in the form of BoNT cluster genes, which consist of BoNT and a group of neurotoxin associated proteins (NAPs), and a regulatory gene botR

(Marvaud et al., 1998a; 1998b; Li et al., 1998; Dineen et al., 2003) (**Figure 1**). NAPs (also referred to as complexing protein or hemagglutinins) are well known to play critical role in food poisoning by not only protecting the BoNT from low pH and proteases in the gastrointestinal tract but also by assisting BoNT translocation across the intestinal mucosal layer (Sakaguchi, 1983; Fujinaga et al., 1997; Sharma and Singh, 1998; Simpson, 2004). BoNT complex (also referred to as progenitor toxin) consisting of NAPs and BoNT is the native form of the toxin secreted by *C. botulinum*. NAPs have also been recently shown to dramatically enhance the endopeptidase activity of BoNT/A (Cai et al, 1999; Sharma and Singh, 2004).

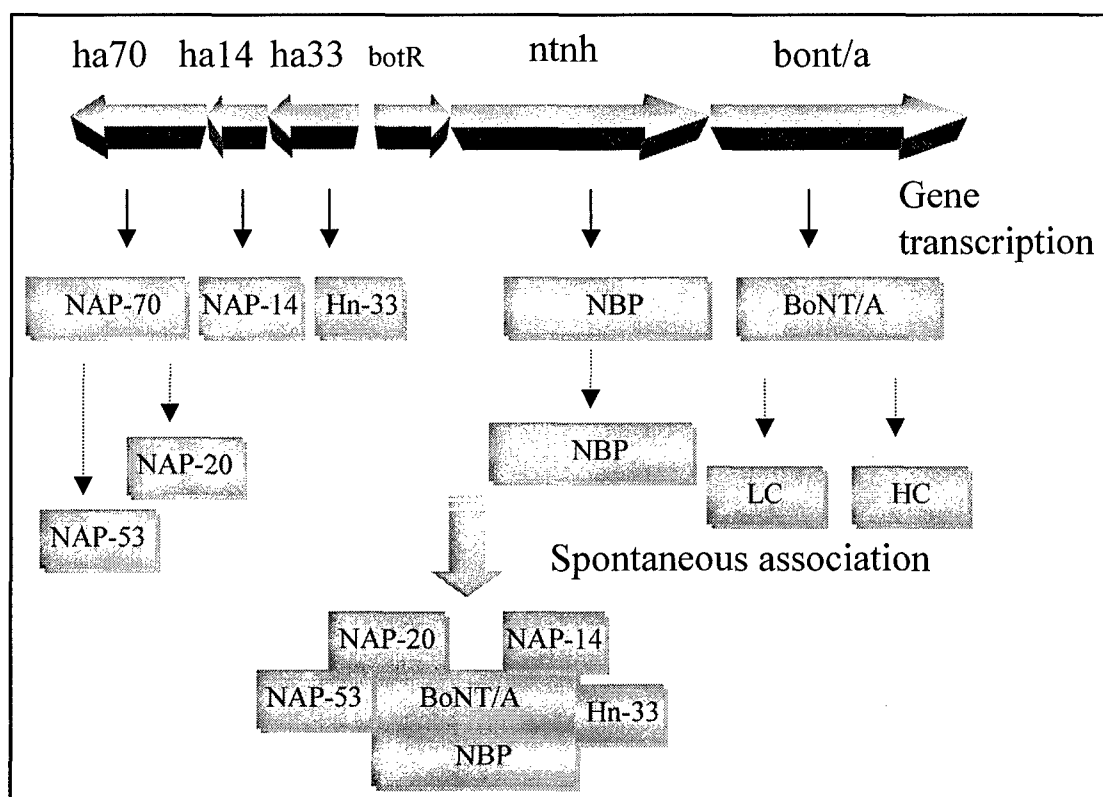


Figure 1. Genetic organization of BoNT/A complex genes and their expressed proteins in forming the BoNT/A complex. The *ha* represents hemagglutinin, and the numbers of following *ha* refer to the molecular masses of the protein expressed by these genes. The NAP-70 gene product is a precursor of NAP-53 and NAP-20. The *botR* is known to regulate BoNT gene expression, *ntnh* represents non-toxin-non hemagglutinin, and encodes for NBP. The *bont/a* encodes for BoNT/A.

Hemagglutinin-33 (Hn-33) is a 33-kDa component of the NAPs, and shows hemagglutination activity (Fu et al., 1998b). The purified Hn-33 is found to be resistant to protease digestion such as trypsin, chymotrypsin, pepsin, and subtilisin, and is presumed to bind intestinal epithelial cells and help in the absorption and translocation of BoNT across small intestinal wall (Fujinaga et al., 1997; Inoue et al., 2001). In addition, Hn-33 is shown to enhance the endopeptidase activity of BoNT/A and BoNT/E (Sharma and Singh, 2004). These observations suggest the possibility of multiple role of Hn-33 in the intoxication process of botulinum neurotoxins.

In this report, we describe an unexpected finding of Hn-33 binding to synaptotagmin II, the putative receptor of purified BoNT. Hn-33 binds to synaptotagmin competitively with BoNT/A, *in vitro* and in synaptosomes, suggesting its possible role in anchoring BoNT complex to nerve terminals.

EXPERIMENTAL PROCEDURE

Materials

The Hn-33, BoNT/A, and BoNT/A complex were purified from *Clostridium botulinum* type A (strain Hall) grown in N-Z amine medium (DasGupta and Sathyamoorthy, 1984) using a series of chromatographic columns as described by Fu et al. (1998a, 1998b). The purified Hn-33, BoNT/A and BoNT/A complex were precipitated with 0.39 g/ml ammonium sulfate and stored at 4°C until use. The precipitate was centrifuged at 10,000 X g for 10 min and dissolved in a desired buffer as needed for experiments.

Synaptosomes were prepared from frozen rat brains (RJO Biologicals Inc., Kansas City, MO) and solubilized according to a previously published procedure (Li and Singh, 1998).

Recombinant glutathione *S*-transferase-fused-synaptotagmin II (GST-Syt II) was isolated as described by Zhou and Singh (2004).

Rabbit anti-Hn-33 antibody was obtained from BBTech (Dartmouth, MA) and sheep anti-rabbit IgG conjugated with FITC was purchased from Sigma (St. Louis, MO). Mouse anti-Syt antibody and goat anti-mouse IgG alkaline phosphatase conjugate were purchased from StressGen Biotechnologies (Victoria, BC, Canada) and Novagen (Madison, WI), respectively.

Isolation and identification of Hn-33 binding proteins in synaptosomes

Hn-33 affinity column was prepared by coupling the purified Hn-33 to Affi-Gel 15 (Bio-Rad, Richmond, CA), an N-hydroxysuccinimide ester of cross-linked agarose. Affi-Gel 15 (1.5 ml) was washed 4 times each with 3 bed volumes of cold deionized water by centrifugation at 600 rpm for 30 sec at 4°C. The Hn-33 (1.5 mg) was dissolved in 1.5 ml coupling buffer (0.1 M bicarbonate buffer pH 8.3), and added to the washed Affi-Gel 15. After mixing them the mixture was incubated on rotating platform at room temperature (25°C) for 1 h. One milliliter of 0.1 M ethanolamine, pH 8.0, was added into the mixture in order to block any remaining reactive groups, and the mixing continued for additional 1 h under the same conditions. The Hn-33-conjugated gel was poured into a 1 x 10 cm glass column.

Following experiments were performed at 4°C. The Hn-33 affinity column was washed with 10 bed volumes of coupling buffer, and then 5 bed volumes of 10 mM HEPES buffer, pH 7.3, until absorbance at 280 nm became zero. The solubilized synaptosomal proteins (Li and Singh, 1998) were applied to the column. Each sample was cycled through the affinity column five times to ensure maximum binding. The column was washed extensively with 10 mM HEPES buffer, pH 7.3 to remove non-specifically adsorbed proteins until absorbance at 280 nm became zero. The column was eluted with 0.1 M NaCl in 10 mM HEPES buffer, pH 7.3, and then with 0.5 M NaCl in the same buffer, at flow rate of 1 ml/min and 1.5 ml fractions were collected. Absorbance at 280 nm was measured for each fraction, each fraction was analyzed with 4-20%

SDS-PAGE after being mixed with SDS-PAGE sample buffer containing 200 mM dithiothreitol (DTT) to obtain reducing condition. Fractions of 0.1 M NaCl eluate and 0.5 M NaCl eluate were analyzed using Western blot described as previous report (Zhou and Singh, 2004).

Similar experiment was carried out with GST-Syt II as well as a control protein (GST, Sigma, St. Louis, MO) by applying them to the Hn-33 affinity column, separately. These experiments provided data to compare to specific binding of Syt II to Hn-33.

Characterization of binding Hn-33 to synaptotagmin

ELISA analysis of binding of Syt II to Hn-33

ELISA was performed according to the procedure described previously (Zhou and Singh, 2004). Briefly, 60 μ l of 0.1 mg/ml Hn-33 in coupling buffer (0.1 M bicarbonate, pH 8.3), and a control protein, GST (60 μ l of 0.1 mg/ml) were coated onto the wells of a polystyrene flat-bottomed 96-well microtite plate (Corning Glass Works, Corning, NY) and incubated at 4°C overnight. After blocking the plate with 1 % (w/v) bovine serum albumin (BSA, St. Louis, MO), 60 μ l of the purified Syt II (0.1 mg/ml) were added to the wells. Mouse anti-Syt antibody (StressGen Biotechnologies, Victoria, BC, Canada) and goat anti-mouse IgG alkaline phosphatase conjugate (Novagen, Madison, WI) were used as primary and secondary antibodies. The absorbance was measured using a microplate reader (GMI, Inc., Albertville, Minnesota) and Softmax software (Molecular Devices, Menlo Park, CA).

Similar experiments were carried out with GST alone, in place of GST-Syt II, to determine its nonspecific binding. Goat anti-GST antibody (Amersham Pharmacia Biotch, Piscataway, NJ) and rabbit anti-goat IgG alkaline phosphatase conjugate (Sigma, St. Louis, MO) were used as primary and secondary antibodies, respectively.

Concentration-dependent binding of Syt II to Hn-33

Binding of different concentrations of Syt II was performed in ELISA format described in the section above. Syt II at different concentrations of 0.1, 0.2, 0.4, and 0.6 μ M in PBS, pH 7.4

was added to the wells, which were coated with 0.1 mg/ml Hn-33, or BSA or GST as control proteins.

Effect of ganglioside on and comparison of the binding of Syt II to Hn-33, BoNT/A, and BoNT/A complex

Binding of the purified Syt II with or without ganglioside (GT1b) to Hn-33, BoNT/A, or BoNT/A complex was carried out using ELISA format described above. For the binding without GT1b, the purified Syt II alone was added to the wells, whereas for the binding with GT1b, the purified 0.1 mg/ml Syt II was mixed with 0.1 mg/ml GT1b (a molar ratio of 1:18), the mixture was incubated at 4°C for 30 min, and then added to the wells coated with Hn-33, BoNT/A, or BoNT/A complex.

Competitive binding of Hn-33 and BoNT/A to Syt II

The purified Syt II (0.1 mg/ml) was mixed with 0.1 mg/ml Hn-33 or 0.1 mg/ml BoNT/A at molar ratio of 2:1, 1:1, 1:2, 1:4, the mixtures were incubated with at 4°C for 1 h, and then added to the wells coated with 0.1 mg/ml BoNT/A or 0.1 mg/ml Hn-33, followed by the ELISA procedure described above.

Immunofluorescence staining

Immunofluorescence staining was carried out either on non-permeabilized or permeabilized synaptosomes using standard methods (Rothberg, 1992). This experiment was performed at room temperature (RT), all the antibodies were diluted in PBS containing 3% BSA, and all washes were 5 times with PBST. The isolated synaptosomes were fixed on glass slides for 30 min with 4% paraformaldehyde (PFA) in PBS and permeabilised with 0.2% Triton X-100 for 15 min. The slides were washed, incubated with 3% BSA in PBS for 30 min, followed by incubation with 0.1 mg/ml Hn-33 for 1 h. After washing, the slides were incubated with rabbit anti-Hn-33 antibody (BBTech, Dartmouth, MA) for 30 min, washed, and then incubated with sheep anti-rabbit IgG conjugated with FITC. The slides were washed and coverslips were

mounted on them with a drop of Fluoromount-G (Southern Biotechnology Associates, Inc., Birmingham, AL), according to the manufacturer's instructions. Fluorescence images were acquired with a Nikon Eclipse E600 MVI microscope with equipped a digital camera controlled by software "SPOT" (Diagnostic Instruments, Inc., Sterling Heights, MI). Two sets of control experiments were carried out. One set of control experiments was carried out without incubating the synaptosomes with Hn-33, but incubating the synaptosomes directly with just buffer alone, or 3%BSA only, or anti-Hn-33 antibody only after blocking with 3%BSA, or anti-rabbit IgG conjugated with FITC only after blocking with 3%BSA. Another set of control experiments was carried out by incubating the synaptosomes with Hn-33, then followed by incubation with 3%BSA only, or anti-Hn-33 antibody only after blocking with 3%BSA, or anti-rabbit IgG conjugated with FITC only after blocking with 3%BSA.

Estimation of protein on gels

For estimating protein bands of SDS-PAGE gels, the gels were scanned on a GEL LOGIC 100 Imager system (Kodak, Rochester, NY), plotted, and integrated for density using a KODAK 1D v.3.6.1 software (Kodak, Rochester, NY).

Determination of protein concentration

The concentration of proteins used in the experiments was determined spectrophotometrically by measuring absorbance at 280 nm and 235 nm using the formula: concentration of protein mg/ml = $(A_{235\text{ nm}} - A_{280\text{ nm}})/2.51$ (Whitaker and Granum, 1980).

RESULTS

Isolation of putative receptor/acceptor of Hn-33 from synaptosomes

In order to identify and isolate protein receptor for Hn-33 on nerve cells, we prepared affinity column of Hn-33 to which MEGA 9 extract of rat brain synaptosomes was applied.

Figure 2 shows a representative elution profile of rat brain synaptosomal membrane proteins on

a Hn-33 affinity column. Non-specifically adsorbed proteins and unbound rat brain synaptosomal membrane proteins were washed out with HEPES buffer in fractions 3 ~ 5. Low affinity proteins

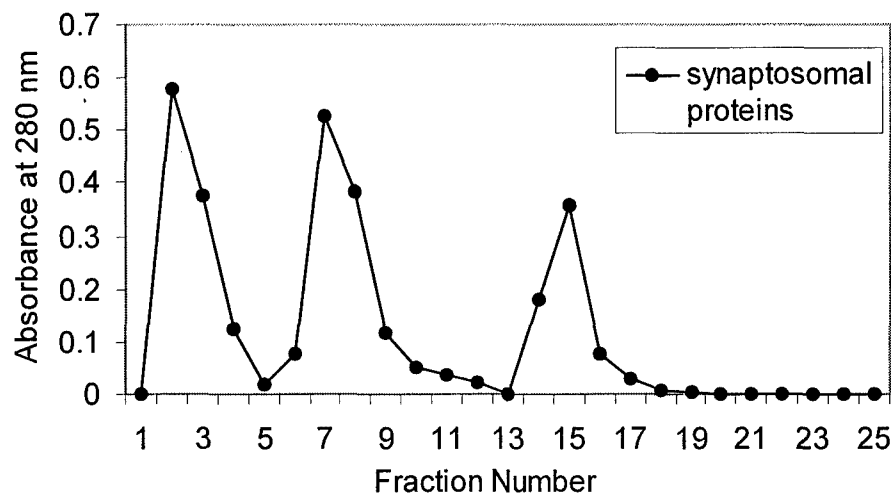


Figure 2. Elution profile of solubilized synaptosomal proteins on Hn-33 affinity column. Protein content is indicated by absorbance at 280 nm. Arrows indicate application of the elution buffer. Each fraction collected was 1.5 ml.

bound to the Hn-33 affinity column were eluted with HEPES buffer containing 0.1 M NaCl in fractions 7, 8, and 9. Proteins with strong affinity for the Hn-33 affinity column were eluted with HEPES buffer containing 0.5 M NaCl in fractions 14, 15, and 16. Analysis of 0.1 M NaCl eluate on SDS-PAGE followed by Coomassie blue staining revealed 5 bands at about 180, 66, 50, 45, and 31 kDa under reducing conditions (**Figure 3A**). Analysis of the 0.5 M NaCl eluate on SDS-PAGE revealed 4 at about 90, 55, 50 and 45 kDa under reducing conditions (**Figure 3A**).

Western blot analysis using anti-synaptotagmin as primary antibody revealed that one band at 65 kDa of 0.1 M NaCl eluate (lane 3) is synaptotagmin in comparing with the positive control of rat brain tissue extract (lane RBTE) and synaptosomal protein extract (lane 1, **Figure 3B**).

In order to identify the nature of synaptotagmin to Hn-33, we prepared affinity column of Hn-33 to which recombinant GST-Syt II was applied. A control experiment was carried out with GST alone as a ligand applied to the Hn-33 affinity column. Affinity column chromatography

was carried out in the same way as the one described for synaptosome extract described above. The elution profile obtained for GST-Syt II (**Figure 4A**) shows only one elution peak with 0.5 M NaCl in Hepes buffer, whereas the control protein GST did not bind to the Hn-33 column (**Figure 4B**). The binding of Syt II to Hn-33 was further confirmed using 4-20% SDS-PAGE (**Figure 5A**) and Western blot (**Figure 5B**). SDS-PAGE analysis showed a protein band at about 90 kDa in the 0.5 M NaCl eluate, which corresponds to the molecular size of recombinant GST-synaptotagmin. Western blot analysis using anti-synaptotagmin as primary antibody revealed that the 0.5 M NaCl eluate of GST-Syt II is positively synaptotagmin II.

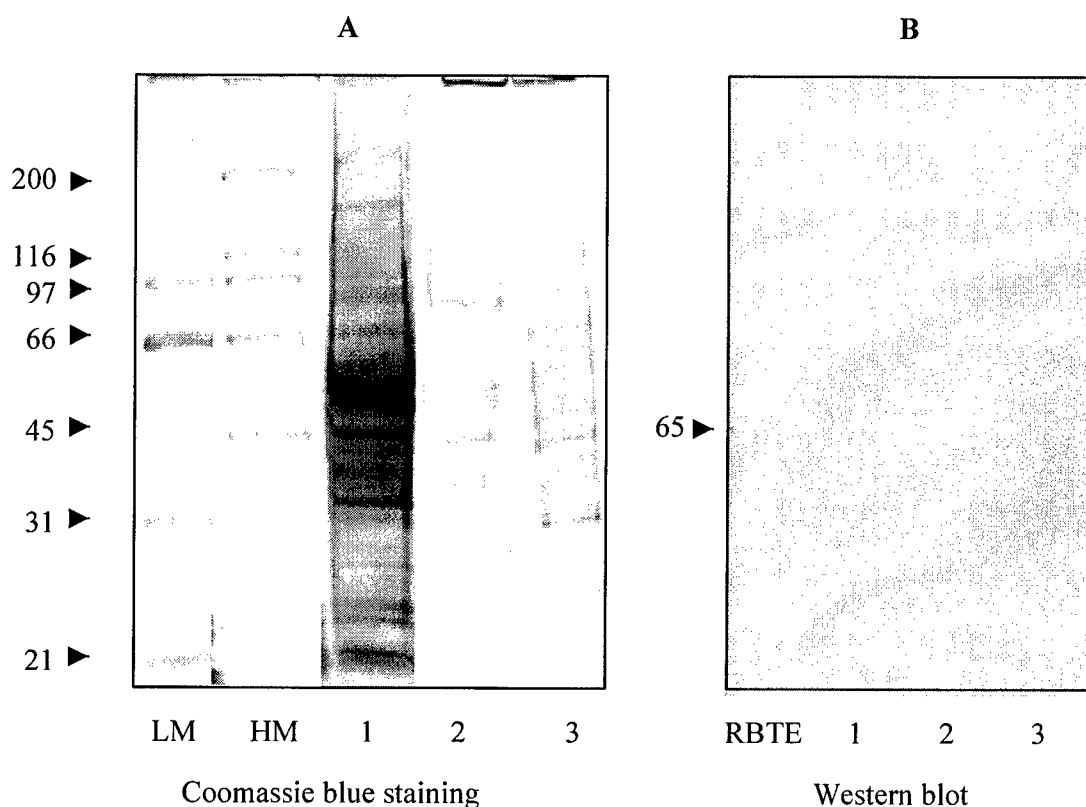


Figure 3. SDS-PAGE analysis of elution peaks from the Hn-33 affinity column (A) and identification by anti-rat synaptotagmin (B). Lanes 1: solubilized synaptosomal proteins land 2: 0.5 M NaCl eluate (fraction 15) from the column, lane 3: 0.1 M NaCl eluate (fraction 9) from the column, lane LM: low molecular weight standards (97, 66, 45, 31, and 21.5 kDa, Bio-Rad), lane HM: high molecular weight standards (200, 116, 97, 66, and 45 kDa, Bio-Rad), lane RBTE: rat brain tissue exacts (a positive control, StressGen Biotechnologies, Victoria, BC, Canada). The number on the left indicates molecular mass of markers in kDa.

Binding properties of Syt II to Hn-33

Binding of Syt II to Hn-33 was carried out in an ELISA format by coating Hn-33 in the wells, and adding purified Syt II to each well, then incubating the plate at RT. The ELISA analysis showed that Syt II binds to Hn-33 overwhelmingly (**Figure 6**). The Syt II did not bind to the wells coated with GST as a control (**Figure 6**). In a parallel study, it was shown that GST did not bind to Hn-33 coated with plate (**Figure 6**).

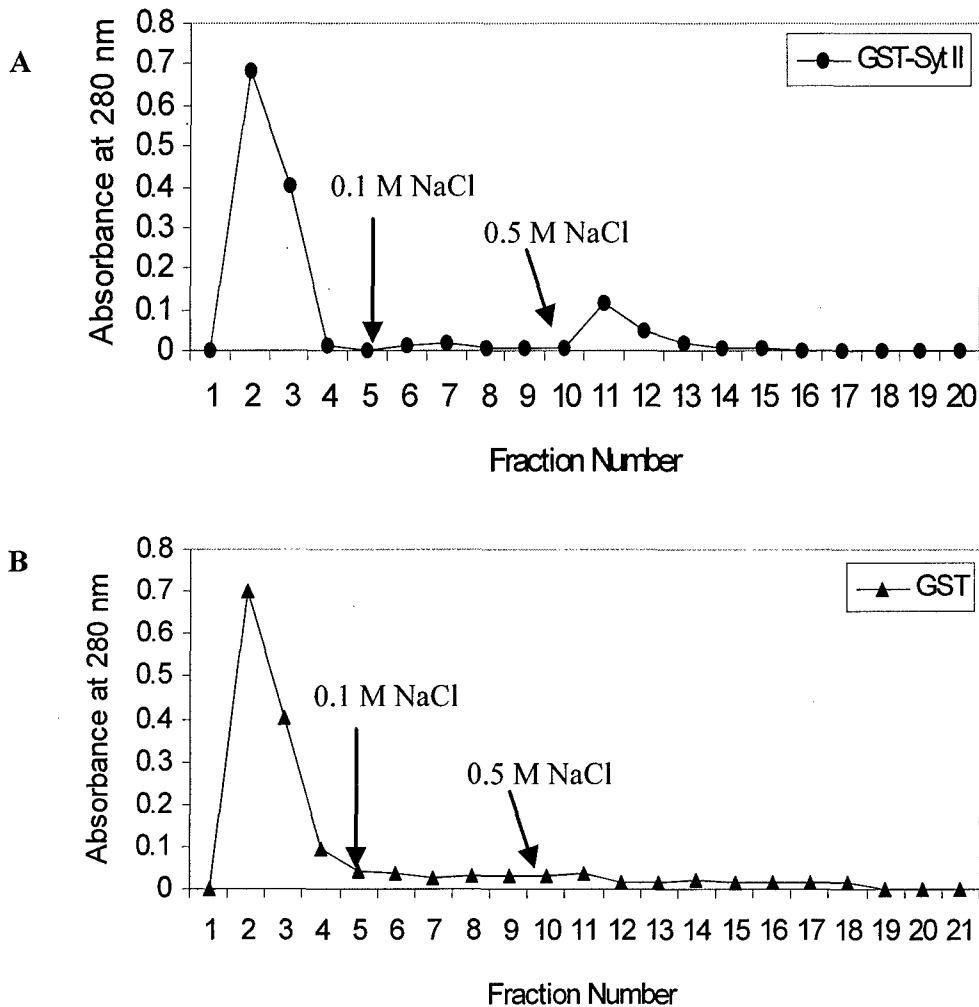


Figure 4. Elution profile of GST-Syt II (A) and GST (B) on Hn-33 affinity column. Protein content is indicated by absorbance at 280 nm. Arrows indicate application of the elution buffer. Each fraction collected was 1.5 ml.

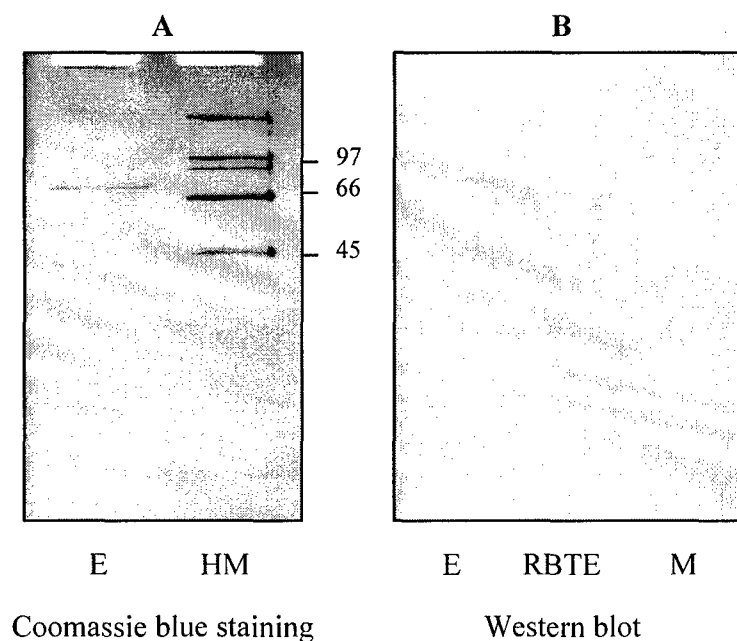


Figure 5. SDS-PAGE (A) and Western blot (B, with rat anti-synaptotagmin) analysis of elution peaks from the Hn-33 affinity column. Lane E: 0.5 M NaCl eluate (fraction 11) after loading purified Syt II onto Hn-33 affinity column, lane RBTE: rat brain tissue extracts (a positive control, StressGen Biotechnologies, Victoria, BC, Canada), lane HM: high molecular weight standards (200, 116, 97, 66, and 45 kDa, Bio-Rad), lane M: Kaleidoscope molecular weight standards (216, 132, 78, 45.7, 32.5, 18.4, 7.6 kDa, Bio-Rad). The numbers in the middle indicate molecular mass of markers in kDa.

Concentration-dependence of Syt II binding to Hn-33 is shown in **Figure 7**. The binding of Syt II to Hn-33 was linear within the concentration range of Hn-33 used (0.1 – 0.6 μM). Linear regression of the binding curve yielded a dissociation constant of 37 nM, suggesting a very strong binding of Syt II to Hn-33.

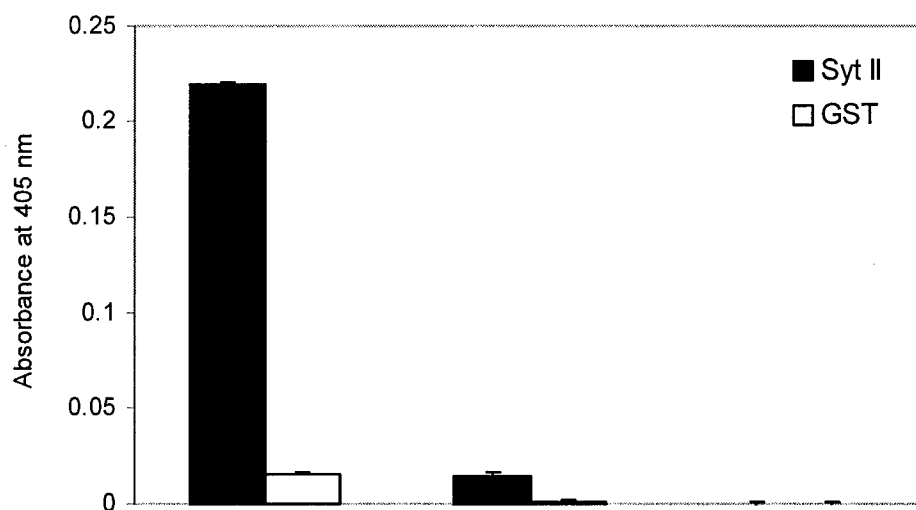


Figure 6. Binding of Syt II to Hn-33 analyzed by ELISA. The purified type A Hn-33, GST, coupling buffer were coated to each well of flat-bottomed 96-well plate at 4°C overnight. After the plate was blocked by 1% BSA, the purified Syt II or GST alone was added to each well. The plate was incubated for 1.5 h at RT on a rocker, and then washed. After incubation with primary and secondary antibodies, the colorimetric detection was followed, and the absorbance at 405 nm of each well was measured using a microplate reader. The result is the mean of three separate experiments, each performed in triplicate; error bars represent the standard deviations.

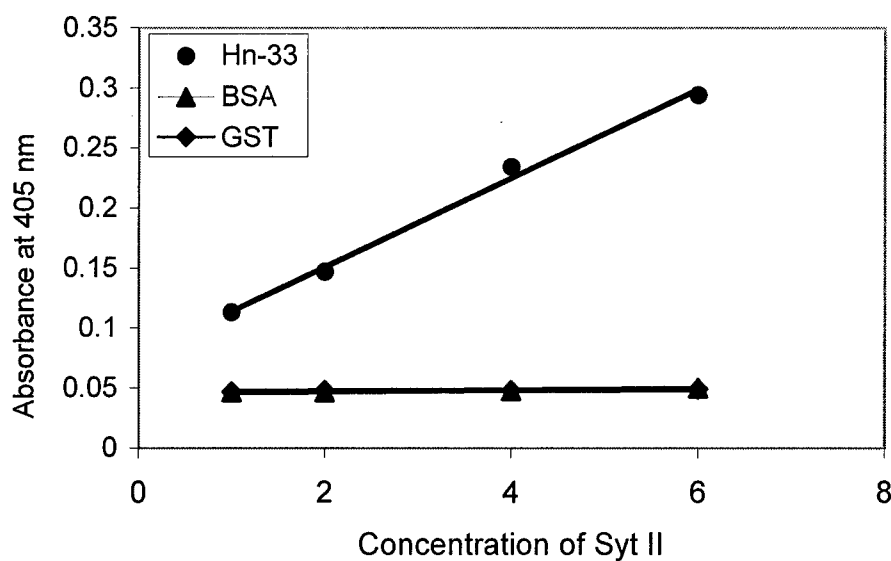


Figure 7. Binding of Syt II at different concentrations to type A Hn-33. Syt II at different concentrations (0.1, 0.2, 0.4, and 0.6 μM) was added to the wells, which were precoated with type A Hn-33, or BSA or GST as control proteins. Binding was detected in ELISA format as described in the ‘Experiment Procedure’ section. The results shown are mean of three separate experiments, each performed in triplicate; error bars represent the standard deviations. The correlation coefficient, R^2 , of linear regression analysis of the binding curve of Syt II to Hn-33 was 0.994.

Effect of ganglioside on and comparison of binding of Syt II to Hn-33, BoNT/A, and BoNT/A complex

Comparison of binding of Syt II to Hn-33, BoNT/A, and BoNT/A complex was carried out in two conditions, one condition was incubation of Syt II with GT1b, another condition was without incubation of Syt II with GT1b. Without incubation with GT1b, Syt II equally binds to Hn-33 and BoNT/A (Figure 8). However, it binds to BoNT/A complex 3-fold higher than Hn-33 and BoNT/A (Figure 8). After incubation with GT1b, Syt II binding to Hn-33, BoNT/A, and BoNT/A complex were significantly reduced. The most dramatic reduction in binding of Syt II due to preincubation with GT1b was observed for purified BoNT/A (~80%). Syt II binding to Hn-33 and BoNT/A complex were reduced by 37% and 18%, respectively, due to preincubation with GT1b (Figure 8). Syt II binding to the control protein (GST) was only negligible and was not affected by GT1b preincubation (Figure 8).

Competitive binding of Hn-33 and BoNT/A to Syt II

The competitive binding of BoNT/A to Syt II was reduced by Hn-33, 1.5-fold, 2.1-fold, 2.8-fold, and 6.6-fold at 2:1, 1:1, 1:2, and 1:4 molar ratio of Syt II:Hn-33, respectively (Figure 9A). Interestingly, the binding of Hn-33 to Syt II was not reduced by BoNT/A (Figure 9B).

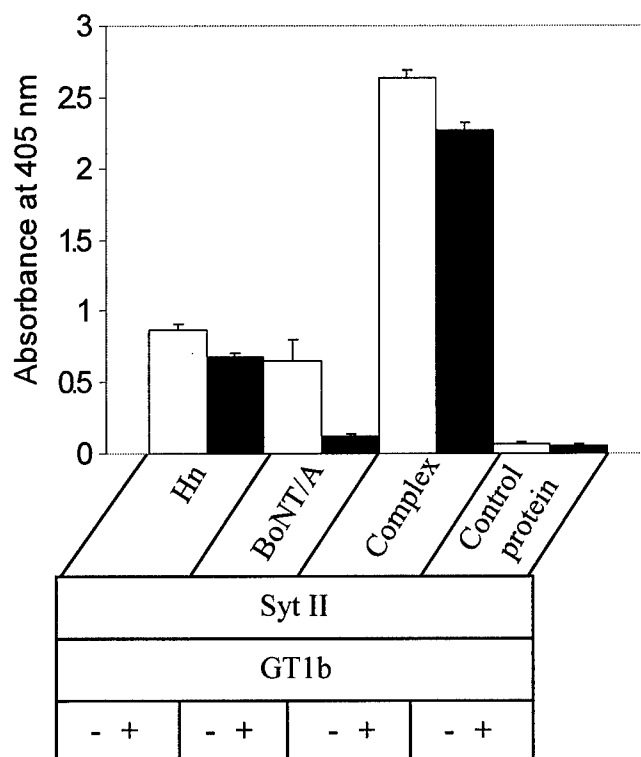


Figure 8. Comparison of binding of Syt II to Hn-33, BoNT/A, and BoNT/A complex. The purified Hn-33, BoNT/A, BoNT/A complex, and GST were separately coated to wells of flat bottomed 96-well plate at 4°C overnight. After the plate was blocked by 1% BSA, the purified Syt II without incubation with GT1b (-) or with incubation with GT1b (+) was added to each well. Binding was detected in ELISA format as described in the 'Experiment Procedure' section. The results are mean of three separate experiments, each performed in triplicate; error bars represent the standard deviations.

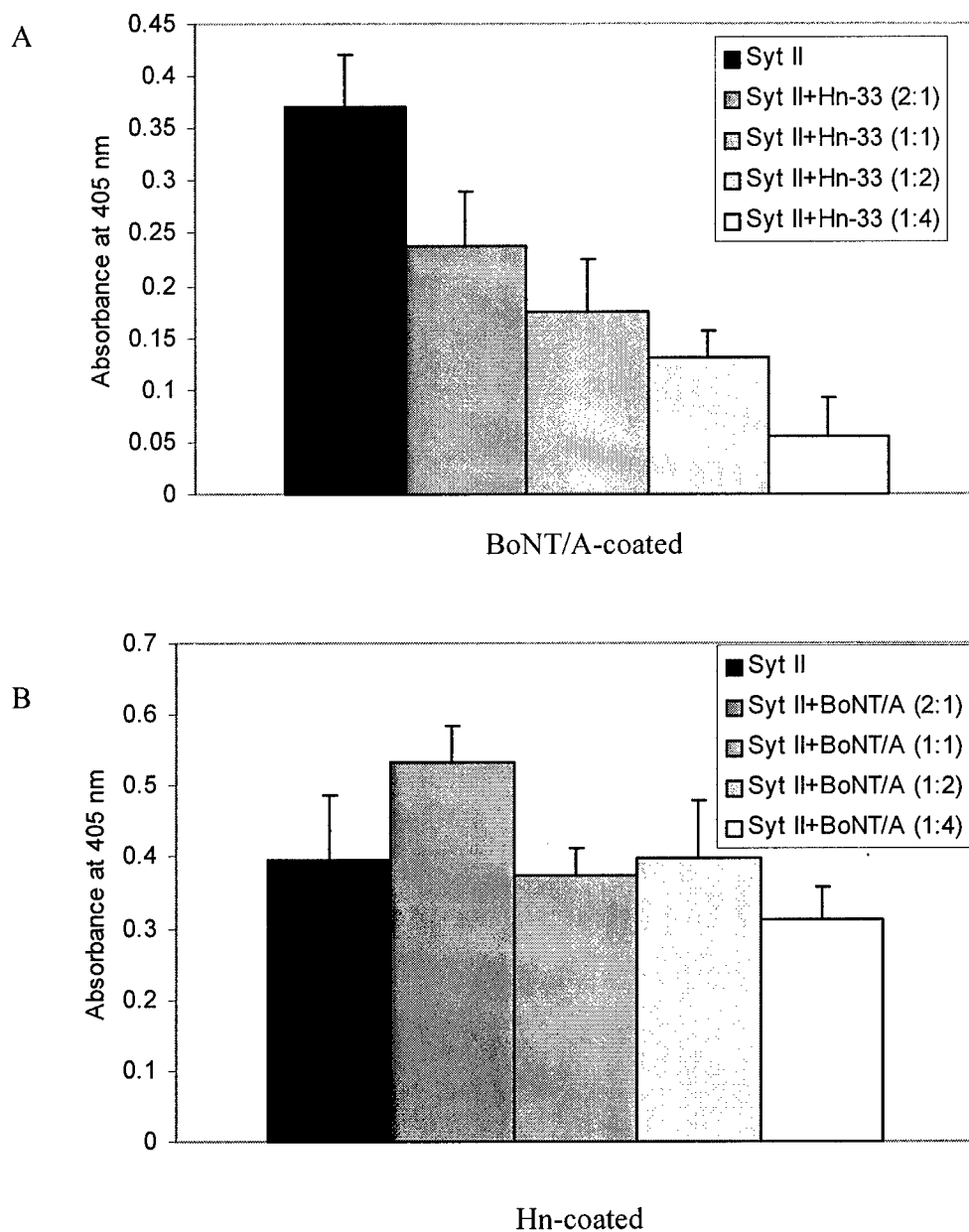


Figure 9. Competitive binding of Hn-33 and BoNT/A to Syt II. The purified Hn-33 or BoNT/A in coupling buffer was coated separately to the wells of flat bottomed 96-well plate at 4°C overnight. Purified Syt II incubated with Hn-33 or BoNT/A at 4°C for 1 h was added to the wells coated with BoNT/A or the wells coated with Hn-33. The result is mean of three separate experiments, each performed in triplicate, error bars represent the standard deviations.

Immunofluorescence staining

Binding of Hn-33 to synaptosomes was analyzed by rabbit anti-Hn-33 antibody, and detecting the latter with FITC-labeled sheep anti-rabbit IgG. As shown in **Figure 10**, only the synaptosomes incubated with type A Hn-33 were recognized by the primary antibody, rabbit anti-Hn-33 and the secondary antibody, anti-rabbit IgG-FITC, showing the fluorescence signal (**Figure 10A**). One set of control experiments carried out without incubating the synaptosomes with Hn-33, but incubating the synaptosomes directly with just buffer (**Figure 10B**), with only 3%BSA (**Figure 10C**), with only primary antibody, rabbit anti-Hn-33 antibody after blocking with 3%BSA (**Figure 10D**), with only anti-rabbit IgG conjugated with FITC after blocking with 3%BSA (**Figure 10E**), did not show any fluorescence signal. Another set of control experiments carried out by incubating the synaptosomes with Hn-33, then followed by incubation with 3%BSA only (**Figure 10F**), or anti-Hn-33 antibody only after blocking with 3%BSA (**Figure 10G**), or anti-rabbit IgG conjugated with FITC only after blocking with 3%BSA (**Figure 10H**), did not show any fluorescence signal.

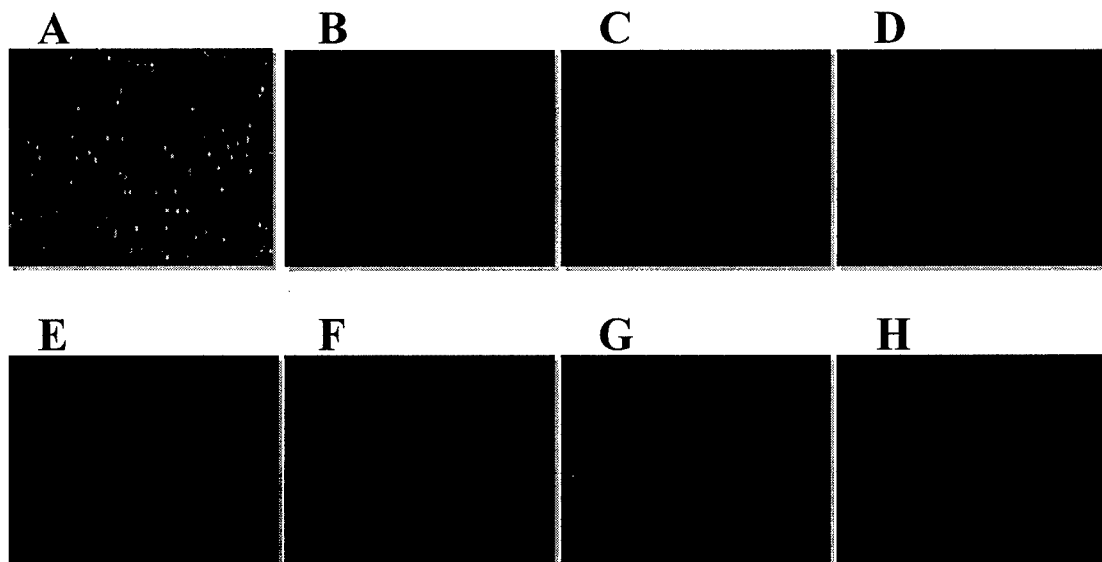


Figure 10. Immunofluorescence detection of Hn-33 binding to synaptosomes.

The synaptosomes were fixed and permeabilized as described in the Experimental Procedures. The synaptosomes incubated with 0.1 mg/ml Hn-33 for 1 h at RT after blocking with 3% BSA, further incubated with both rabbit anti-Hn-33 and anti-rabbit IgG-FITC (A); without incubating the synaptosomes with Hn-33, but incubating the synaptosomes directly with just buffer (B), with only 3%BSA (C), with only primary antibody, rabbit anti-Hn-33 antibody after blocking with 3%BSA (D), with only anti-rabbit IgG conjugated with FITC after blocking with 3%BSA (E); with incubating the synaptosomes with Hn-33, then followed by incubation with 3%BSA only (F), or anti-Hn-33 antibody only after blocking with 3%BSA (G), or anti-rabbit IgG conjugated with FITC only after blocking with 3%BSA (H).

DISCUSSION

The genetic organization of BoNT/A complex genes and their expressed proteins in forming the BoNT/A complex was schematically shown in Figure 1 (Marvaud et al., 1998; Cai et al., 1999; Fujinaga et al, 2000; Dineen et al, 2003; Zhang et al., 2003). Hn-33 is present in proportionally the highest amount of all NAPs in the BoNT/A complex (Cai et al., 1999; Sharma et al., 2003). Therefore we carried out the binding assay of Hn-33 to synaptosomal proteins in order to find the relevance of component of botulinum neurotoxin associated proteins in the neuronal entry.

Results from immunoaffinity chromatography revealed that Hn-33 binds synaptosomal proteins at 180, 66, 50, 45, and 31 kDa (**Figure 3A**), and the protein at 66 kDa was identified as synaptotagmin from Western blot analysis using anti-synaptotagmin as primary antibody (**Figure 3B**). In addition, Hn-33 strongly binds to synaptosomal proteins at about 90, 55, 50 and 45 kDa (**Figure 3A**). The protein at about 90 kDa was identified as heat shock protein from the N-terminal sequencing (PEETQTQDQPM) and the proteins at about 55 and 50 kDa were identified as tubulin from the N-terminal sequencing (MREIVHIQAGQCG).

To confirm the binding of Syt II to Hn-33, we carried out chromatography of Syt II on Hn-33 affinity column, and one band from the elution peak (**Figure 4A**) of the Syt II was observed on the SDS-PAGE gel (**Figure 5A**) and Western blot (**Figure 5B**). On the other hand, chromatography of GST alone on Hn-33 affinity column did not show elution peak (**Figure 4B**). Thus, it was identified that Syt II binds to Hn-33.

To characterize the binding properties of Syt II to Hn-33, we carried out a series of binding experiments in ELISA format. One set of ELISA revealed that Syt II but not GST binds to Hn-33 (Figure 6), indicating that the interaction is probably not at the junction between the GST and Hn-33. These data strongly support the aforementioned view. Moreover, Syt II in higher concentration strongly binds to Hn-33, the binding of Syt II to Hn-33 is 3-fold higher in concentration of 0.6 μ M than 0.1 μ M (Figure 7). Under our experimental conditions, to Hn-33 higher binding of Syt II without incubation with GT1b than incubation with GT1b was shown (Figure 8). Therefore gangliosides GT1b may not be necessarily required for the binding of Syt II to Hn-33.

The competitive binding analysis of Hn-33 and BoNT/A to Syt II revealed that Hn-33 inhibits the binding of Syt II to BoNT/A, however, BoNT/A did not inhibit the binding of Syt II to Hn-33 (Figure 9). This result implies that Hn-33 might have more than one binding site with Syt II, and one of them is sharing binding site with BoNT/A. BoNT/A might have only one binding site with Syt II that is shared with Hn-33. The binding of Syt II to Hn-33 was also identified in synaptosome using fluorescence microscopy (Figure 10).

We have hypothesized on a possible mechanism of the binding of Syt II to Hn-33 and BoNT/A (Figure 11), especially to explain why the synaptotagmin once bound to the Hn-33 coated at the plate is not being competed out by BoNT/A whereas the opposite is not true. As shown in Figure 9, Syt II alone is able to bind to either Hn-33 or BoNT/A, as shown in the upper cartoons of Figure 11. According to our hypothesis, when Syt II is mixed with BoNT/A, and incubated with Hn-33 coated on the plate, the Syt II binds to BoNT/A and BoNT/A in turn binds to Hn-33 through a different site. Thus Syt II ends up binding to Hn-33 through BoNT/A (Figure 11 lower left cartoon). However, when Syt II is mixed with Hn-33, and incubated with BoNT/A coated on the plate, Syt II binding to Hn-33 blocks the latter's binding site to BoNT/A was, resulting in the inhibition of Syt II binding to BoNT/A in the presence of Hn-33.

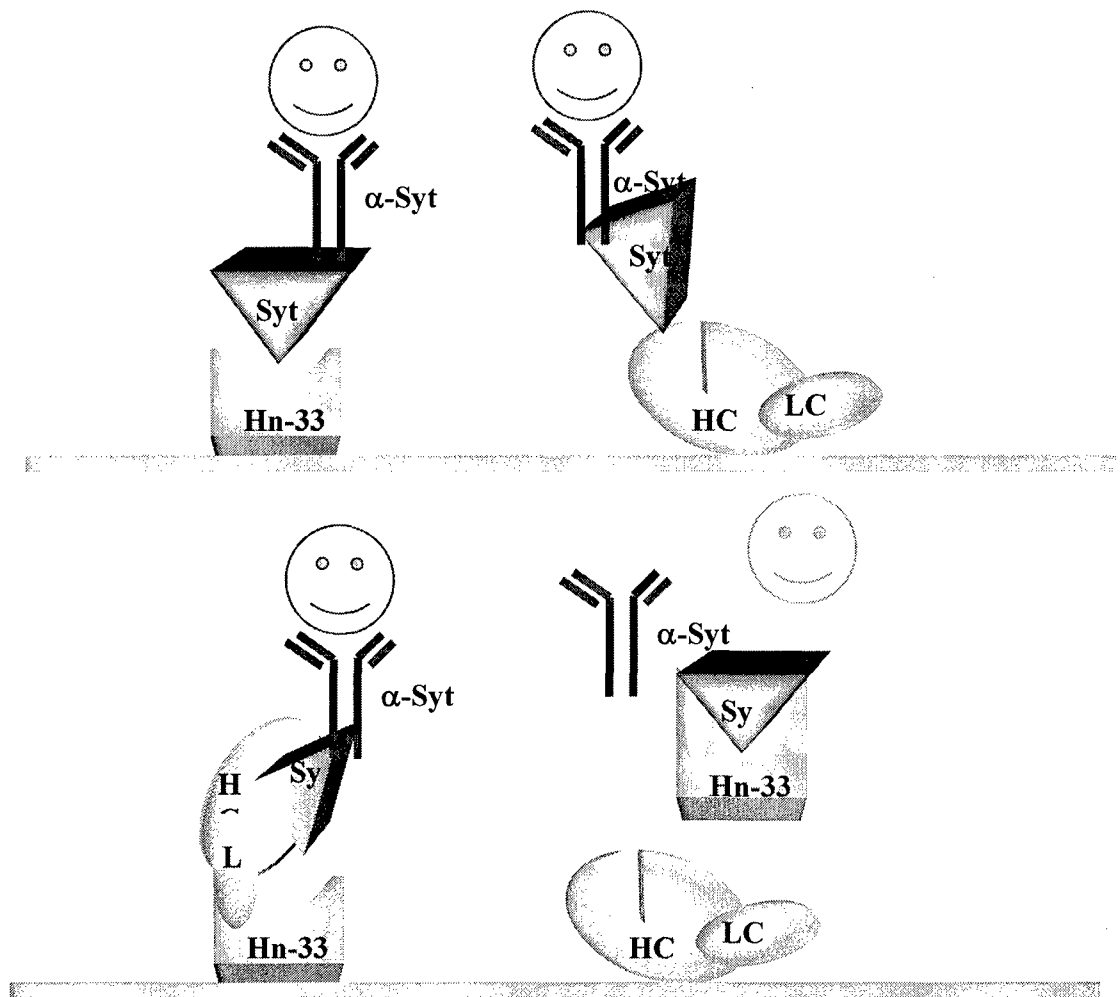


Figure 11. Schematic drawings our hypothesis showing the binding of synaptotagmin II (Syt) to Hn-33 and BoNT/A, coated separately on a microplate (**Upper panels**), and detected by antibody against synaptotagmin II (α -Syt). The binding of to Syt to Hn-33 in the presence of BoNT/A is mediated through a domain of the BoNT/A (**Lower left panel**), whereas Syt binding to BoNT/A in the presence of Hn-33 is blocked by Hn-33, and its own binding site to the BoNT/A is blocked by syt binding (**Lower right panel**).

Hsp90 is a specialized chaperone that is best recognized for its role in stabilizing intermediates of client molecules (Sakisaka, et al., 2002), and is essential for translocation of the binary *C. botulinum* C2 toxin into the cytosol (Haug et al., 2003). It was reported that cytoskeletal protein tubulin directly and stoichiometrically is bound to synaptotagmin I (Honda, et al., 2002). Our results lead us to suggest a novel mechanism of BoNT complex in the

neuronal entry, which synaptotagmin, Hsp90-containing chaperone system, and cytoskeletal protein tubulin might be involved in the neuronal entry of BoNT complex.

In summary, we have demonstrated for the first time the association of Hn-33, the one subcomponent of BoNT/A complex with Syt II. Our results suggest that the Hn-33 not only protects the neurotoxin from proteolysis but also involved in the binding of receptor of the cells at the first step of BoNT actions. This study also contributes to our understanding of the mechanism of botulinum neurotoxin complex actions. The finding of Hn-33 inhibiting the binding of BoNT/A to Syt II provides important information relevant to the design of novel anti-botulism therapeutic agents targeted on blocking the receptor of botulinum neurotoxin.

REFERENCES

- Arnon S.S., Schechter R., Inglesby T.V., Henderson D.A., Bartlett J.G., Ascher M.S., Eitzen E., Fine A.D., Hauer J., Layton M., Lillibridge S., Osterholm M.T., O'Toole T., Parker G., Perl T.M., Russell P.K., Swerdlow D.L., Tonat K. (2001) Botulinum toxin as a biological weapon: medical and public health management. *J. the American Medical Association* 285: 1059-1070.
- Cai S., Sarkar H. K., Singh B.R. (1999) Enhancement of the endopeptidase activity of botulinum neurotoxin by its associated proteins and dithiothreitol. *Biochemistry* 38: 6903-6910.
- DasGupta BR, Sathyamoorthy V (1984) Purification and amino acid composition of type A botulinum neurotoxin. *Toxicon*. 22: 415-24
- Dineen S.S., Bradshaw M., Johnson E.A.. (2003) Neurotoxin gene clusters in *Clostridium* botulinum type A strains: sequence comparison and evolutionary implications. *Curr Microbiol*. 46:345-52.
- Fu F., Lomneth R. B., Cai S., Singh B.R. (1998a) Role of zinc in the structure and toxic activity of botulinum neurotoxin. *Biochemistry* 37: 5267-5278.

- Fu F., Sharma S. K., Singh B.R. (1998b) A protease-resistant novel hemagglutinin purified from type A *Clostridium botulinum*. *J. Protein Chemistry* 7: 53-60.
- Fujinaga Y., Inouea K., Nomurab T., Sasakib J., Marvaudc J. C., Popoff M. R., Kozakid S., Oguma K. (2000) Identification and characterization of functional subunits of *Clostridium botulinum* type A progenitor toxin involved in binding to intestinal microvilli and erythrocytes. *FEBS Letters* 467: 179-183.
- Fujinaga Y., Inoue K., Watanabe S., Yokota K., Hirai Y., Nagamachi E., Oguma K. (1997) The haemagglutinin of *Clostridium botulinum* type C progenitor toxin plays an essential role in binding of toxin to the epithelial cells of guinea pig small intestine, leading to the efficient absorption of the toxin. *Microbiology*, 143: 3841–3847.
- Haug G., Leemhuis J., Tiemann D., Meyer D. K., Aktories K., and Barth H. (2003) The host cell chaperone Hsp90 is essential for translocation of the binary *Clostridium botulinum* C2 toxin into the cytosol. *J. Biolo. Chem.* 278: 32266–32274.
- Honda A., Yamada M., Saisu H., Takahashi H., Mori K. J., and Abe T. (2002) Direct, Ca^{2+} -dependent Interaction between Tubulin and Synaptotagmin I. *J. Biolo. Chem* 277: 20234–20242
- Inoue K., Fujinaga Y., Honke K., Arimitsu H., Mahmut N., Sakaguchi Y., Ohyama T., Watanabe T., Inoue K., Oguma K. (2001) *Clostridium botulinum* type A haemagglutininpositive progenitor toxin (HAM-PTX) binds to oligosaccharides containing Galb1-4GlcNAc through one subcomponent of haemagglutinin (HA1). *Microbiology*, 147: 811–819.
- Koriazova L.K., Montal M. (2003) Translocation of botulinum neurotoxin light chain protease through the heavy chain channel. *Nat Struct Biol.* 10:13-8.
- Lebeda F.J., Singh B.R. (1999) Membrane channel activity and translocation of tetanus and botulinum neurotoxins, *J. Toxicol.-Toxin Reviews* 18: 45-76.

- Li B, Qian X, Sarkar HK, Singh BR (1998) Molecular characterization of type E Clostridium botulinum and comparison to other types of Clostridium botulinum. Biochim Biophys Acta. 1395: 21-27.
- Li L., Singh B.R. (1998) Isolation of synaptotagmin as a receptor for type A and E botulinum neurotoxin and analysis of their comparative binding using a new microtiter plate assay, J. Nat. Toxins 7: 215-226.
- Marvaud JC, Gibert M, Inoue K, Fujinaga Y, Oguma K, Popoff MR (1998a) botR/A is a positive regulator of botulinum neurotoxin and associated non-toxin protein genes in Clostridium botulinum A. Mol Microbiol. 29: 1009-1018.
- Marvaud JC, Eisel U, Binz T, Niemann H, Popoff MR (1998b) TetR is a positive regulator of the tetanus toxin gene in Clostridium tetani and is homologous to botR. Infect Immun. 66: 5698-5702.
- Nishiki T., Kamata Y., Nemoto Y., Omori A., Ito T., Takahashi M., Kozaki S. (1994) Identification of protein receptor for *Clostridium botulinum* type B neurotoxin in rat brain synaptosomes, J. Biol. Chem. 269: 10498-10503.
- Nishiki T., Tokuyama Y., Kamata Y., Nemoto Y., Yoshida A., Sato K., Sekiguchi M., Takahashi M., Kozaki S. (1996) The high-affinity binding of *Clostridium botulinum* type B neurotoxin to synaptotagmin II associated with gangliosides GT1b/GD1a, FEBS Lett. 378: 253-257.
- Rothberg K.G., Heuser J.E., Donzell W.C., Ying Y.S., Glenney J.R., Anderson R.G. (1992) Caveolin, a protein component of caveolae membrane coats. Cell 68: 673-82.
- Sakaguchi, G. (1983) Clostridium botulinum toxin. Pharmac. Ther. 19, 165-194.
- Sakisaka T., Meerlo T., Matteson J., Plutner H. and Balch W. E. (2002) Rab- α GDI activity is regulated by a Hsp90 chaperone complex. The EMBO J. 21: 6125-6135
- Sharma S.K., Ramzan M.A., Singh B.R. (2003) Separation of the components of type A botulinum neurotoxin complex by electrophoresis. Toxicon. 41:321-31.

- Sharma S.K. and Singh B.R. (2004) Enhancement of the Endopeptidase Activity of Purified Botulinum Neurotoxins A and E by an Isolated Component of the Native Neurotoxin Associated Proteins. *Biochem.*
- Sharma S.K., Singh B.R. (1998) Hemagglutinin binding mediated protection of botulinum neurotoxin from proteolysis. *J. Natural Toxins* 7: 239-253.
- Simpson L.L, Rapport M.M. (1971) The binding of botulinum toxin to membrane lipids: sphingolipids, steroids and fatty acids. *J Neurochem.* 18: 1751-9.
- Simpson L.L., Rapport M.M. (1971) Ganglioside inactivation of botulinum toxin. *J Neurochem.* 18: 1341-3.
- Simpson LL (2004) Identification of the major steps in botulinum toxin action *Annu Rev Pharmacol Toxicol.* 44:167-193.
- Singh B.R. (2000) Intimate detail of the most poisonous poison, *Nature Structural Biology* 7: 617-619.
- Tacket CO and Rogawski MA (1989) Botulism. In: Simpson LL (ed), *Botulinum neurotoxin and tetanus toxin.* Academic Press, Inc., San Diego, CA, pp. 351-378.
- Whitaker J.R., Granum P.E. (1980) An absolute method for protein determination based on difference in absorbance at 235 and 280 nm, *Analytical Biochemistry* 109: 156-159.
- Yowler B.C., Kensinger R.D., and Schengrund C.L (2002) Botulinum neurotoxin A activity is dependent upon the presence of specific gangliosides in neuroblastoma cells expressing synaptotagmin I. *J. Bio. Chem.* 277: 32815-32819.
- Zhang L., Lin W., Li S., Aoki K. R. (2003) Complete DNA sequences of the botulinum neurotoxin complex of *Clostridium botulinum* type A-Hall (Allergan) strain. *Gene* 315:21-32.

Zhou Y., Singh B. R. (2004) Cloning, High-Level Expression, Single-Step Purification, and Binding Activity of His₆-Tagged Recombinant Type B Botulinum Neurotoxin Heavy Chain Transmembrane and Binding Domain. *Protein Expression and Purification* 34 (1): 8-16.

Project F (Unpublished)

Comparative Membrane Channel Activity of Botulinum Neurotoxins A and E.

Abstract

In an effort to compare the molecular basis of differential toxic activity of BoNT/A and /E, we have analyzed their membrane channel activity by measuring calcein release from liposomes. Both BoNT/A and /E showed a same level of membrane channel activity that was specifically blocked by IgG specific to the neurotoxins. With the use of fluorescein-labeled dextran, we determined that the size of the channel is appropriate for the translocation of a protein of 50 kDa (the light chain of BoNT).

Introduction

BoNT binds to presynaptic membranes of the neuromuscular junction, and blocks the release of acetylcholine causing flaccid muscle paralysis. BoNTs have been classified into seven serotypes, A to G, and they target presynaptic sites of a neuron.

The action of BoNT involves three steps: 1) Extracellular binding and internalization, 2) Membrane translocation and 3) Intracellular blocking acetylcholine release. BoNT utilizes the process of cellular endocytosis for its own internalization into target cells (**Kitamura et al., 1990**). It binds to a receptor on the synaptic membrane before being internalized into endosomes. Endosomal membrane protein pumps protons to lower the inner pH of endosomes that allows translocation of at least the light chain into the cytosol where it expresses its toxicity

(enzymatic activity) on target substrates and inhibits exocytosis of neurotransmitter from the synaptic vesicle (**Mochida et al., 1989; Montecucco and Schiavo, 1993**).

The Neurotoxin is a protein molecule with a molecular mass of 150 kDa which is composed of two subunits, a heavy (H) chain (100 kDa) and a light (L) chain (50 kDa), that are linked through a disulfide bond (Simpson, 1986). The L chain is the toxic domain which contains a zinc binding motif and has proteolytic effect. Hence, it is called Zn endoprotease (**Montecucco and Schiavo, 1993**).

The Neurotoxin is a water-soluble protein with sufficient numbers of transmembrane or amphiphilic polypeptide segments which are compatible for interaction with the membrane. The C-terminal half of the H chain binds to the nerve membrane leading to internalization of the neurotoxin in the nerve cell through endocytosis (**Montecucco, 1986**). Subsequently, the pH of the endosome is lowered causing the H chain to get integrated in the membrane through the N-terminal half of the H chain for the membrane channel formation which is likely to be very efficient process for the high potency of the neurotoxin (**Blaustein et al., 1987**). Three amphipathic α -helical regions were predicted to be transmembrane from a portion of the N-terminal half of the BoNT/A H chain, responsible for the channel formation (**Lebeda, 1995**). The whole neurotoxin or a part (L chain) is translocated through the membrane channel formed at low pH. Based on image reconstruction from electrons micrographs (**Schmid et al., 1993**), the heavy chain is suggested to form a tetramer in the vesicle membrane. Oligomer formed by the H chain forms a channel size of 8 Å in diameter, which does not seem adequate for the presumed translocation of the L chain. In this study, we have analyzed the membrane channel activity of BoNT/A and BoNT/E to understand the molecular basis of the membrane translocation of the neurotoxin using liposomes as an artificial membrane. The technique to detect the channel size in our experiment is such that the neurotoxin acts from outside, rather

than from inside as is the case in the endosome. The dye inside the liposome passes through the channel formed by the toxin, and is detected by an increase in the fluorescence signal.

Materials and Methods

Botulinum neurotoxins A and E were isolated from *Clostridium botulinum* strains Hall and Alaska, respectively, according to procedures published previously (Singh et al., 1995; Cai et al., 1999). Horse serum against BoNT/A (horse serum 43) and BoNT/E (horse serum 41) was provided by USAMRIID. Rabbit serum containing BoNT/A specific antibody (lot # 6067) was supplied by Dr. Lee, USDA. DEAE-Sephadex A-50, CM-Sepharose and DEAE-Sepharcel were obtained from Pharmacia Biotech, Inc., Piscataway, N.J.

Isolation of specific antibodies against BoNT/A and BoNT/E.

Specific antibodies against BoNT/A and BoNT/E were isolated from horse and rabbit sera using toxin affinity column chromatography. Each of the BoNT/A and BoNT/E affinity columns was prepared by coupling the neurotoxin to Affi-Gel-15 (Bio-Rad, Richmond, CA), an N-hydroxyl succinimide ester of cross-linked agarose, as described previously (Ogert et al., 1992; Li and Singh, 1998). 1.5 mg of BoNT/A or BoNT/E was loaded on a Affi-Gel-15 column (1 ml), which was equilibrated with 0.1 M sodium bicarbonate buffer, pH 9.0 (washing buffer). The affinity column was agitated thoroughly for 1 hour at room temperature (25 °C) and then slowly agitated at 4 °C for 3 hours on a rocker, where complete coupling was allowed to take place. 0.1 ml of 1.0 M ethanolamine (Sigma Chemical Co., St. Louis, MO) was applied to the column for one hour to block any remaining reactive groups. The affinity column was washed with the washing buffer until the uncoupled ligand was eluted i.e. until the absorbance of the eluant read zero at 280 nm. At this point the affinity column of BoNT/A or BoNT/E was ready for purification of specific Immunoglobulin (IgG).

In order to isolate IgG fractions of rabbit and horse sera against BoNT/A and BoNT/E, each serum was applied to a protein G-agarose column (Sigma Chemical Co., Louis, MO). The serum was incubated with protein G column for 30 min, washed with 0.1 M sodium bicarbonate buffer, pH 9.0, and the IgG was eluted with 0.5 M ammonium acetate, pH 3.0. IgGs were dialyzed overnight with 0.15 M phosphate buffer saline (PBS) buffer, pH 7.4. Respective IgG (2 mg) fraction was applied to the BoNT/A and BoNT/E affinity column, which were equilibrated with 0.15 M PBS (phosphate buffered saline) buffer, pH 7.4, and incubated for 2 hours at 25 °C. Columns were further washed with 0.15 M PBS buffer, pH 7.4, to remove all the unbound IgG. BoNT specific IgG was eluted with 0.1 M glycine buffer, pH 2.5. Specific IgG fraction was pooled and dialyzed overnight with 0.1 M PBS, pH 7.4.

Analysis of binding of specific IgG to BoNT/A and BoNT/E using Enzyme Linked Immunosorbent Assay (ELISA)

100 µl of 20 µg/ml of BoNT/A or BoNT/E was added in each well of the microtiter plate and incubated at 4 °C overnight. The wells were washed twice with 0.1% TWEEN 20 in PBS using a microplatter washer (Molecular Devices, Sunnyvale, CA). In order to prevent the non-specific binding of the primary and secondary antibody to the microtiter plate, 300 µl of 3% BSA (bovine serum albumin) solution was added to each well as a blocking agent and incubated at 37 °C for 1 hour. Wells were subsequently washed five times with the washing buffer. Five-fold serial dilution of specific primary antibody (i.e. the one isolated from the affinity column) were made in PBS-BSA solution, applied to the plate, incubated for 2 hours at 37 °C and washed five times. Enzyme-linked secondary antibody, goat anti-rabbit antibody with labeled peroxidase, dilution titer of 1:28,000 (Sigma Chemical Co., St. Louis, MO) against BoNT/A IgG, and rabbit anti-horse antibody with labeled peroxidase, dilution titer of 1:20,000 (Sigma Chemical Co., St. Louis, MO) against BoNT/E IgG were applied to respective plates and incubated for 1 hour at 37 °C. Enzymatic substrate solution for the detection of binding was 0.04% o-phenylenediamine dihydrochloride and 0.012% H₂O₂ (Sigma Chemical Co., St. Louis, MO) in phosphate-citrate

buffer, pH 5.0. 100 μ l of this solution was added to each well. incubated for 15-30 min at room temperature and the reaction was stopped by adding 50 μ l of 2M H₂SO₄. The amount of reaction product, an indication of bound BoNT IgG, was estimated by measuring absorbance at 492 nm using a microplatter reader (Molecular Devices, Sunnyvale, CA. Model No. Vmax)

Preparation of liposomes and release of fluorescent dye from liposomes

Preparation of liposomes

Asolectin from soybean (Sigma Chemical Co., St. Louis, MO), with 20% of phosphatidylcholine and the remaining 80% other lipids including phosphatidylethanolamine, cholesterol and triolein, was used for liposome preparation. The lipids were dissolved at a final concentration of 4 μ mole/ml phosphatidylcholine in 2 ml of HPLC (high performance liquid chromatography) grade chloroform (Fisher Scientific, Pittsburgh, PA). This was treated with nitrogen gas for 2-3 min followed by overnight vacuum drying. The yellow layer of lipid was redissolved in a buffer solution of a dye. The buffer used for dye solution had 10 mM sodium phosphate, 10 mM sodium citrate, 125 mM NaCl and 1.5 mM EDTA, pH 7.4. This is the liposome buffer (**Kamata and Kozaki, 1994**). Dyes used were calcein (10 mM) FITC (fluorescein isothiocyanate)-dextran (20 mM) (Sigma Chemical Co., St. Louis, MO) and they undergo self-quenching by formation of non-fluorescent dimers (excimers) at these high concentrations (**Oku et al., 1982; Kurtzhals et al., 1989**). The lipid suspension was mixed using a vortex for 1 min and subsequently sonicated for 3-4 min till the solution became clear. Size of the liposomes obtained by this method was in the range of 100-500 nm as determined by a dynamic light scattering technique. This technique measures the hydrodynamic diameter of the vesicles through the time behavior of the fluctuations in scattered light intensity (**Day et al., 1977**). This is the recommended size for large unilamellar vesicles (**Szoka and Papahadjopoulos, 1978**).

Free dye (Calcein/FITC-dextran) was separated from liposomes containing dye by a gel filtration method using Sephadex G-75 (calcein) and G-100 (FITC-dextran) columns. The concentration of the liposomes was determined from the turbidity (absorbance) at 334 nm using UV spectrophotometer. Liposomes containing dye were obtained in the first peak whereas the free dye eluted in the second peak.

Fluorimetric analysis of BoNT induced dye release from liposomes

BoNT-mediated dye release from liposomes was monitored by measuring fluorescence signal of calcein or FITC-dextran (excitation at 468 nm and emission at 518 nm) according to the procedure described previously (Fu and Singh, 1999). 20 ml of calcein and FITC-dextran encapsulated liposomes were separately prepared in liposome buffer, pH 7.4. For each set of six experiments 600 μ l of the above liposome solution were taken. Six sets of experiments were carried out as described below.

1) 600 μ l of the liposome solution were placed in a cuvette and the fluorescence signal was recorded at the fixed excitation and emission wavelength for 5 min, i.e. until it gave a stable fluorescence signal. The pH was then lowered to 4.4 using 1.5 N HCl, and the fluorescence was again recorded for 5 min. There was a decrease in fluorescence signal, because calcein fluorescence is quenched at lower pH. The amount of HCl or NaOH needed for achieving pH 4.4 or 7.4, respectively, was estimated by titrating 20 ml of the liposome solution with 1.5 N HCl to pH 4.4, and then back titrating it with 1 N NaOH to pH 7.4. This calculation was used to estimate the amount of 1.5 N HCl and 1 N NaOH for 600 μ l of the liposome solution obtain the pH of 4.4 and 7.4, respectively. In order to compare the low pH mediated release of dye, the fluorescence signal at pH 4.4 was estimated by back titrating the solution to pH 7.4 by 1 N NaOH. To estimate total dye content in the liposomes, the latter were treated with 0.7 mM (final concentration) Triton-X-100 (Pierce, Rockford, IL) and the fluorescence signal of the released dye was recorded.

2) Stock solution of horse IgG against BoNT/E was added to 600 μ l of the liposome solution at pH 7.4. The final concentration of added IgG was 15 μ g/ml. The pH was lowered to 4.4 using 1.5 N HCl, followed by back titration, and finally 100% dye release was calculated using 0.7 mM Triton X-100. The fluorescence signal at each step was recorded for 5 min as in the case of set 1.

3) BoNT/A at a final concentration of 15 μ g/ml was added to liposome solution and all the steps in set 2 were repeated. These steps are shown schematically in Fig. 18.

4) BoNT/E at a final concentration 15 μ g/ml was added to liposome solution and all the steps of set 2 were repeated.

5) BoNT/A was incubated with its specific IgG at 37 °C for 2 hours (ratio and amount of the specific IgG described in the Results and Discussion section). The final concentration of BoNT/A in the mixture was 15 μ g/ml, which was added to the liposome solution and all the steps of set 2 were repeated.

6) BoNT/E was incubated with its specific IgG at 37 °C for 2 hours (ratio and amount of the specific IgG described in the Results and Discussion section). The final concentration of BoNT/E was 15 μ g/ml in the liposomes solution and all the steps of set 2 were repeated.

Identical steps were followed in the case of liposomes filled with FITC-dextran.

Results and Discussion

Binding activity of the botulinum neurotoxin to the IgG

The specific antibodies obtained from the affinity column were tested for binding with their respective antigens. The binding of BoNT/A IgG to BoNT/A was detected at 0.16 μ g/ml of the IgG concentration and that of BoNT/E IgG to BoNT/E at 0.032 μ g/ml of the IgG concentration (Fig. 1). The difference in reactivity between BoNT/A IgG and BoNT/E IgG to their respective

antigens is, therefore, five-fold. Hence we can say that BoNT/E IgG showed a five-fold stronger binding ability to its antigen than did to BoNT/A IgG as observed by the ELISA (Fig. 1). In Fig. 1 we can also see that maximum binding of the BoNT/A and BoNT/E IgGs to their respective antigens takes place between 20 $\mu\text{g}/\text{ml}$ and 100 $\mu\text{g}/\text{ml}$. We therefore chose 50 $\mu\text{g}/\text{ml}$ of IgG for 20 $\mu\text{g}/\text{ml}$ of their antigens for testing their effect on biological function (membrane channel activity) of BoNT/A and BoNT/E.. Hence, for the maximum binding activity which could affect the biological function of the neurotoxin, the ratio of IgG to neurotoxin was set at 2.5:1.

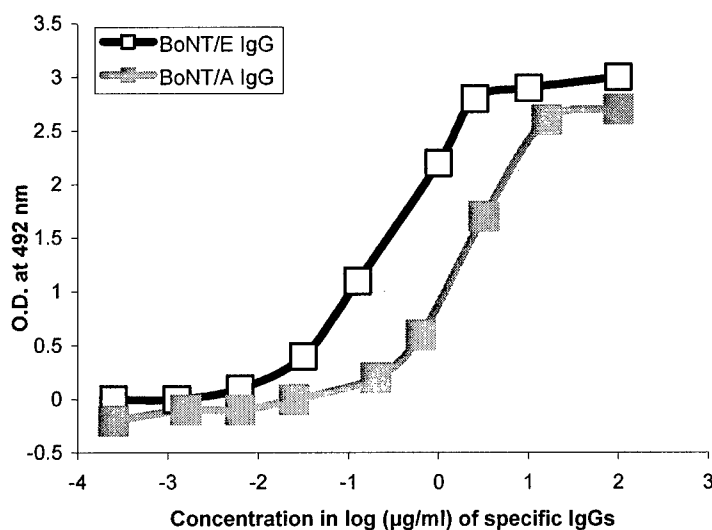


Fig.1. ELISA analysis of the binding of BoNT/E and BoNT/A to their respective IgG antibodies. BoNT/E and BoNT/A at a constant concentration of 20 mg/ml were coated to microplate wells, and five-fold serial dilutions of the specific antibodies dissolved in 0.1 M PBS buffer, pH 7.4, were added to each well.

The neurotoxins were incubated with their respective IgG at 37 $^{\circ}\text{C}$ for 2 hours. This experiment was carried out to observe the decrease in the biological activity of the neurotoxin due to binding of antibody to its antigen. The binding of antibody to the antigen was used for examining the channel forming activity of the two serotypes of botulinum neurotoxin, i.e. BoNT/A and BoNT/E. The antibody effect could result either from its binding to the

polypeptides of the neurotoxin involved in a specific function or from its binding-induced structural change in the neurotoxin.

Cross-reactivity was investigated between the specific IgG of one serotype of botulinum neurotoxin to the serotype of other botulinum neurotoxin. Binding of BoNT/E IgG to BoNT/A starts at 0.8 $\mu\text{g/ml}$ of the IgG concentration, whereas BoNT/A IgG to BoNT/A starts at 0.16 $\mu\text{g/ml}$ of the IgG concentration (**Fig. 2**). The difference between the binding of BoNT/E IgG to BoNT/A and BoNT/A IgG to BoNT/A is ten-fold with respect to their concentration. Hence we estimate that BoNT/A IgG had a 10-fold higher binding ability to BoNT/A than the binding of BoNT/E IgG to BoNT/A (**Fig. 2**). On the other hand, BoNT/A IgG shows almost no binding to BoNT/E (**Fig. 3**). Therefore, experiments were not conducted to observe the cross-reactivity effect on the channel formation.

Channel formation in liposomes

Liposomes obtained after passing through the size exclusion column were treated with nitrogen gas for 2-3 min for maximum stabilization against oxygen. Lipids have double bonds and are easily oxidized in the presence of oxygen. The size of the liposomes was between 100-500 nm estimated by the dynamic light scattering technique (data not shown). It is the recommended size for unilamellar vesicles (**Day et al., 1977**). The liposome preparations have some fluorescence signal recorded at pH 7.5 (**Table 1**), indicating dye release even in the absence of any added molecules.. The reason for such an observation could be (a) not all the dye of the dyes sticking outside the liposomes, and (b) light scattering from liposomes. The signal could not be from the dye inside the liposomes because it is kept at a high self-quenching concentration. The pH of the liposome sample was reduced from 7.4 to 4.4 using 1.5 N HCl to observe the effect of low pH on the liposome membrane. The actual increase in the fluorescence signal at low pH was calculated after back titration to pH 7.4 as described in the Materials and Methods section. In the case of calcein containing liposomes (without addition of any

neurotoxins), there was a slight increase in the signal when the liposomes were back titrated to pH 7.4 (the control pH for this set of experiments). This increase could be because the low pH might disturb the liposome membrane allowing the leakage of small number of calcein molecules (molecular weight = 625 g/mole). Each fluorescence recording was conducted for 5-10 min to obtain a stable value of the fluorescence signal. Each set of experiments was repeated three times to obtain an average for the calcein release.

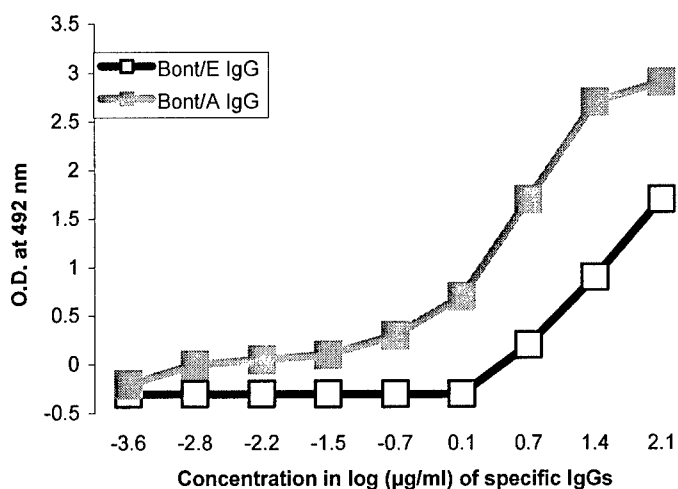


Fig. 2. ELISA analysis of the binding of BoNT/A to IgG raised against BoNT/E and BoNT/A. BoNT/A was kept at a constant concentration of 20 mg/ml for coating the microplate wells, and five-fold serial dilutions of the specific antibodies dissolved in 0.1 M PBS buffer, pH 7.4, was added to each well.

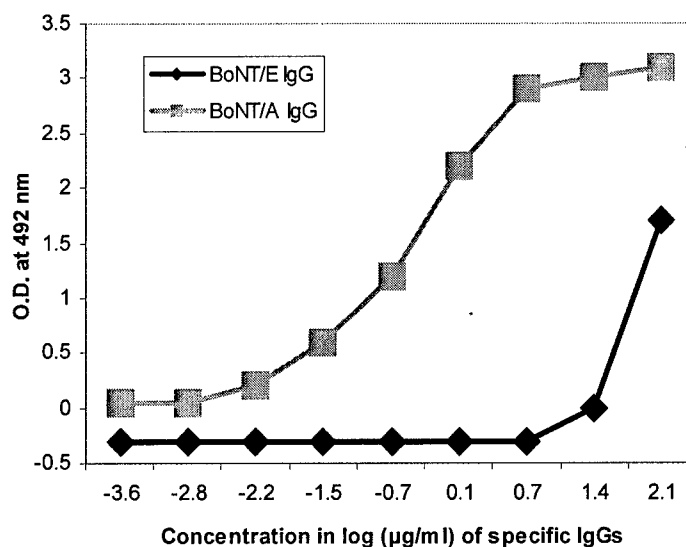


Fig. 3. ELISA analysis of the binding of BoNT/E to IgG raised against BoNT/E and BoNT/A. BoNT/E was kept at a constant concentration of 20 mg/ml for coating the microplate wells, and five-fold serial dilutions of the specific antibodies was added to each well.

Table 1. Experimental data showing increase in fluorescence signal of calcein after its release from liposomes when induced by BoNT/A and BoNT/E. The value represents the average of 2 independent sets of experiments conducted in triplicates. The control and the experiment results are statistically significantly different by t-test ($0.01 > p > 0.001$).

(a) Increase in fluorescence signal at pH 4.4 was calculated by subtracting the liposome signal at pH 7.5 from the fluorescence signal obtained after back titration at pH 7.5 (refer to Materials and Methods section for more detail), (b) Total fluorescence signal was calculated by subtracting the liposome signal at pH 7.5 from the fluorescence signal after Triton X 100 was added, and (c) % calcein release was calculated by dividing (a) / (b) multiplying into 100.

	pH 7.5	pH 4.0	pH 7.5 (back titration)	Triton X-100	Increase in fluorescence at pH 4.4 (a)	Total Fluorescence signal (b)	% calcein release (c) \pm S.D.
Liposome	28.7	24.1	30.8	44.2	2.1	15.5	13.5 \pm 0.3
Liposome + IgG	27.6	23.1	30.4	43	2.8	15.4	18.0 \pm 0.2
Liposome + BoNT/E	28.1	18.8	35.3	44.5	7.2	16.4	43.6 \pm 1.1
Liposome + BoNT/E + IgG	28.9	22.8	31	44.5	2.1	15.6	13.6 \pm 4.3
Liposome + BoNT/A	28.5	19.7	34.9	44.8	6.4	16.3	39.5 \pm 0.2
Liposome + BoNT/A + IgG	28	17.4	32.5	43.5	4.5	15.5	29.0 \pm 4.7

For FITC-dextran release experiments, there was no effect of low pH on the liposome in the absence of any added BoNT samples (control) (**Table 2**). Treatment with Triton-X-100 dissolved the membrane, and one could detect the signal obtained from all the dye encapsulated in the liposomes which indicated total increase in the fluorescence. Rabbit IgG was used as a control to study the specificity of just the neurotoxin for inducing the dye release (channel formation) in liposomes. IgG had no significant effect by itself on the liposome even at low pH (**Tables 1 and 2**).

Table 2. Experimental data showing increase in fluorescence signal of FITC-dextran after its release from liposomes when induced by BoNT/A and BoNT/E. The value represents the average of 2 sets of independent experiments conducted in triplicates. The control and the experiment results are statistically significantly different by t-test ($0.01 > p > 0.001$). (a) Increase in fluorescence signal at pH 4.4 was calculated by subtracting the liposome signal at pH 7.5 from the fluorescence signal obtained after back titration at pH 7.5 (refer to Materials and Methods for more detail), (b) Total fluorescence signal was calculated by subtracting the liposome signal at pH 7.5 from the fluorescence signal after Triton X 100 was added, and (c) % FITC-dextran release was calculate by dividing (a) / (b) and multiplying into 100.

	pH 7.5	pH 4.0	pH 7.5 (back titration)	Triton X- 100	Increase in fluorescence at pH 4.4 (a)	Total Fluorescence signal (b)	% FITC- dextran release (c) \pm S.D.
Liposome	49	23.5	48.9	53.8	0.1	4.8	0.0 \pm 1.0
Liposome +IgG	41.5	20	41.4	48.9	0.1	7.4	5 \pm 0.4
Liposome + BoNT/E	43.3	19.3	47.6	50.8	4.3	7.5	45 \pm 5
Liposome + BoNT/E + IgG	48.09	23.9	48.5	55.7	0.5	7.7	12 \pm 2.9
Liposome + BoNT/A	44.1	23	47.3	50	3.2	5.9	44.8 \pm 4.4
Liposome + BoNT/A + IgG	40.1	18	42.5	48.1	2.4	8	37.0 \pm 4

Addition of either BoNT/A or BoNT/E at low pH showed a considerable increase in the fluorescence signal. Treatment with 0.1 μ M BoNT/E induced 44% of calcein release at pH 4.4 whereas treatment with 0.1 μ M BoNT/A induced 40% of calcein release (**Table 1**). When liposomes were filled with FITC-dextran, BoNT/A and BoNT/E induced 45% and 44.8% of FITC-dextran release, respectively (**Table 2**). The 4% difference in their ability to induce calcein release is not significant enough to explain the difference in their toxicity (100-fold) of their channel forming ability. Hence we can say that BoNT/A and BoNT/E have the same channel forming activity. This suggests that the difference in their toxicity perhaps has a basis in differential effectiveness at other steps (binding and enzymatic activity) of BoNT/A and BoNT/E mode of action. The effect of low pH could be explained by a possible conformational change in the heavy chain at low pH, which could expose its transmembrane domain for insertion into the lipid bilayer (Fu et al., 2002). The dye comes out presumably through a transmembrane pore formed by the heavy chains of respective BoNT serotypes. One of the main aims of this study was to estimate a minimum size of the membrane channel formed by BoNT/A and BoNT/E.

The effect of specific IgG on the channel forming ability of the neurotoxin was significant in the fluorescence experiment. Treatment of liposomes with BoNT/E bound to BoNT/E IgG,

induced only about 14% of the calcein to be released whereas treatment of liposomes with BoNT/A bound to BoNT/A IgG induced the release of about 29% of the calcein (**Table 1**). When liposomes were filled with FITC-dextran, BoNT/E and BoNT/A bound to their respective IgGs induced 12% and 37% of FITC-dextran release, respectively. The data of **Tables 1 and 2** are the averages of 3 readings for two independent experimental sets, and each set is representative of two different preparations of liposomes, neurotoxin, and specific IgG. The small standard deviations (S.D.) measured for % dye release in each case, points to the consistency in our results. Graphical representations of the % release of the dyes are shown in **Figs. 4 and 5**.

The results showed a remarkable decrease in the fluorescence signal when neurotoxins were treated with their specific antibodies. BoNT/E IgG decreases the amount of dye released (FITC-dextran/calcein respectively) by 65% to 73% and BoNT/A IgG decreases the amount released (FITC-dextran/calcein respectively) by 18% to 25%. BoNT/E IgG inhibits channel formation by BoNT/E by 3-4 fold more than BoNT/A IgG inhibits channel formation by BoNT/A. The data from ELISA (**Fig. 1**) has a similar result where BoNT/E IgG has five-fold higher binding activity than BoNT/A IgG to their respective antigens. The antibody could change the structure of the antigen or inhibit its specific function by blocking the respective functional domain. In our experiments, we did not study any structural changes in the antigen, therefore we cannot distinguish between these two mechanisms. BoNT/E IgG might be binding to the transmembrane domain actually involved in the channel formation.

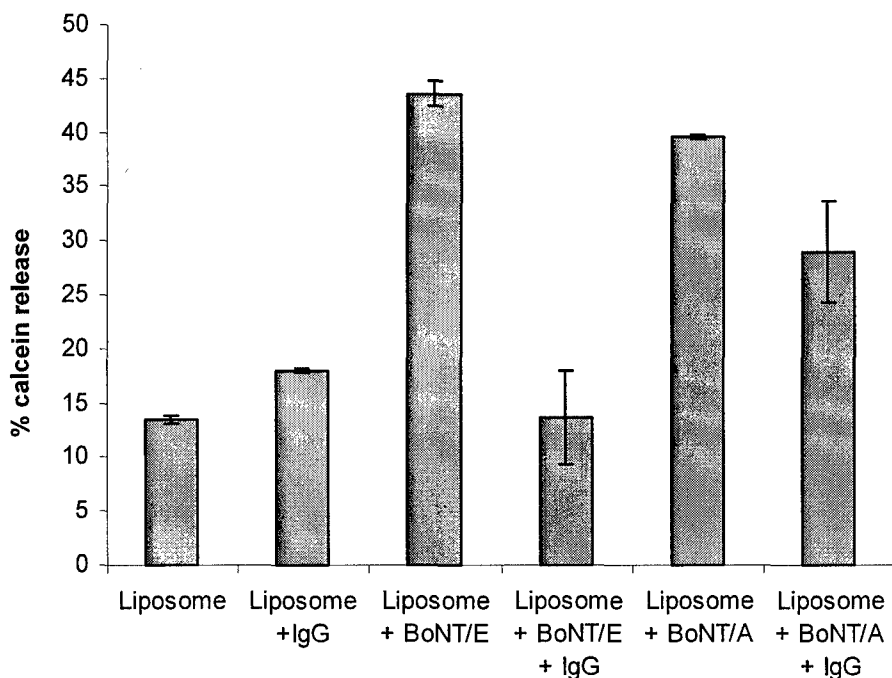


Fig. 4. Graphical representation of the percent release of calcein from the liposomes in the presence of botulinum neurotoxin (BoNT). The bars indicate standard deviations in experimental measurements.

The diameter of the dye in Å is directly correlated with its molecular weight. The maximum size of a membrane channel which allows a particle up to 4000 g/mole in size to pass through (FITC-dextran used in this study) is 24.2 Å in diameter, as the Stokes' radius of this dye is 24.2 Å (Sauer, 1991). The heavy chain is suggested to form a channel of 8 Å in diameter (Finkelstein, 1990), but it does not seem adequate for presumed translocation of the light (L) chain. Also a sequence analysis has shown a 23-residue stretch in the N-terminal domain of the BoNT/A heavy chain with a propensity to form an amphipathic helical bundle in a hydrophobic environment. However, perhaps the size of such channels of about 2.5 - 4 Å (Montal et al., 1992) is not sufficient for the translocation of a 50-kDa L chain. From our results, we conclude that the membrane channel size is much larger than that suggested by other researchers for 50-kDa light chain to pass through. Recent observation by Koriazova and Montal (2003) of the translocation of L chain through H chain channel provides further evidence for larger pore

formed by the H chain in membrane bilayer. Our results on channel formation by BoNT/E in artificial membranes are the first such reports.

We conclude that the channel forming activity of the two serotypes of botulinum neurotoxin is almost identical at least in liposomes, hence the difference in their toxicity under *in vivo* conditions might be due to a difference in their enzymatic activities against the neuronal substrate, difference in their receptor binding activities, or differences in translocation rate mediated by putative proteins in nerve cells.

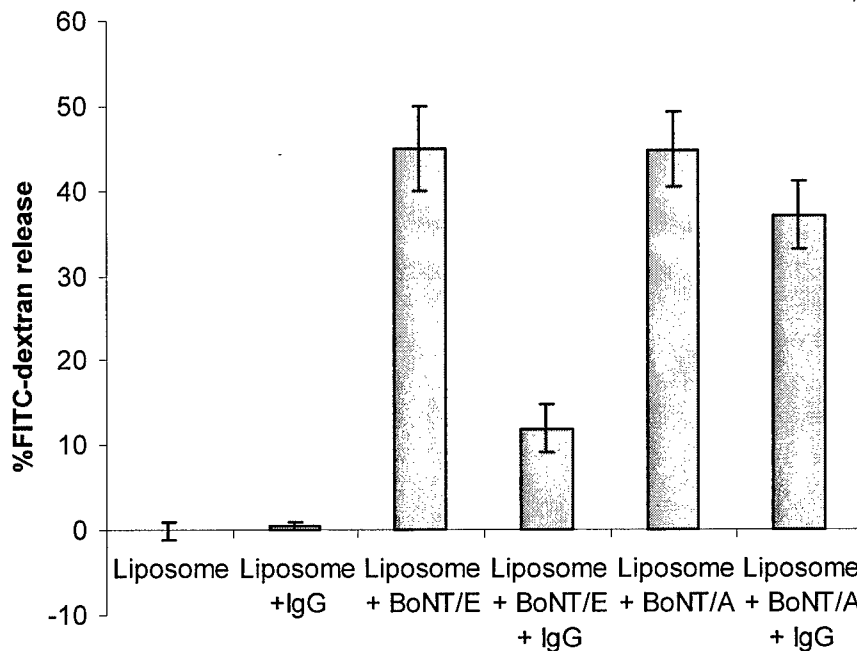


Fig. 5. Graphical representation of percent release of FITC-dextran from liposomes in the presence of botulinum neurotoxin. The bars indicate standard deviations in experimental measurements.

It is notable that in a recent article, Keller et al. (2004) reported from their studies with primary neuronal cell culture and BoNT/A and BoNT/E that rate of translocation of BoNT/E was dramatically faster than that of BoNT/A. This observation suggest contrasts with our observation of similar membrane channel activity by BoNT/A and BoNT/E. These two sets of results can be reconciled if one of the following holds true. (1) In nerve cells, proteins present in the membrane, including possibly the BoNT receptor, helps facilitate the translocation of the L

chain. BoNT/E interaction with such protein is more favorable than that of BoNT/A. (2) The L chain translocation within the channel is faster than that of BoNT/A L chain, suggesting intimate interplay involved in the translocation process. In such case the calcein release assay performed in our experiment is only relevant to the general membrane integration, and pore formation, and not the L chain translocation. L chain translocation is a specific process between the H chain membrane transporter and the L chain.

References

Blaustein, R. O., Germann, W. J., Finkelstein, A. and DasGupta, B. R. (1987) The N-terminal half of the heavy chain of botulinum type A neurotoxin forms channels in planar phospholipid bilayers. *FEBS Letters*, 226, 115-120.

Cai, S., Sarkar, H. K. and Singh, B. R. (1999) Enhancement of the endopeptidase activity of botulinum neurotoxin by its associated proteins and dithiothreitol. *Biochemistry*, 38, 6903-6910.

Day, E. P., Ho, J. T., Kurnez, R. K. and Sun S. T. (1977) Dynamic light scattering study of calcium-induced fusion in phospholipid vesicles. *Biochim. Biophys. Acta*, 470, 503-508.

Finkelstein, A. (1990) Channels formed in phospholipid bilayer membrane by diphtheria, tetanus, botulinum and anthra toxin. *J. Physiol.*, 84, 188-190.

Fu, F.-N. and Singh, B. R. (1999) Calcein permeability of liposomes mediated by type A botulinum neurotoxin and its light and heavy chains. *J. Protein Chem.* 18, 701-707.

Fu, F.-N., Busath, D. D. and Singh, B. R. (2002) Spectroscopic Analysis of Low pH and Lipid induced structural changes in Type A Botulinum Neurotoxin Relevant to Membrane Channel Formation and Translocation. *Biophysical Chemistry* 99, 17-29.

Kamata, Y. and Kozaki, S. (1994) The light chain of botulinum neurotoxin forms channels in a lipid membrane. *Biochem. Biophys. Res. Commun.*, 205, 751-757.

Keller, J. E., Cai, F. and Neale, E. (2004) Uptake of botulinum neurotoxin into culture neurons. *Biochemistry* 43, 526-532.

Kitamura, M., Iwasmori, M. and Nagai, Y. (1990) Interaction between *Clostridium botulinum* neurotoxin and gangliosides. *Biochim. Biophys. Acta*, 628, 328-335.

Koriazova, L. K. and Montal, M. (2003) Translocation of botulinum neurotoxin light chain protease through the heavy chain channel. *Nat Struct. Biol.* 10, 13-18.

- Kurtzhals, P., Larsen, C. and Johansen, M. (1989) High performance size-exclusion chromatographic procedure for the determination of fluoresceinyl isothiocyanate dextrans of various molecular masses in biological media. *J. Chromatog.*, 491, 117-127.
- Lebeda, F. J. (1995) Structural predictions of the channel forming region of botulinum neurotoxin. *Toxicon*, 33, 559-567.
- Li, Li and Singh, B. R. (1995) Isolation and Characterization of a protein receptor for type E botulinum neurotoxin. *Protein Sci.(Supplement # 2)*, 94.
- Mochida, S., Poulain, B., Weller, U., Habermann, E. and Tauc, L. (1989) Light chain of tetanus toxin intracellularly inhibits acetylcholine release at neuromuscular synapses, and its internalization is mediated by heavy chain. *FEBS Lett.*, 253, 47-51.
- Montal, M. S., Blewitt, R., Tomich, J. M. and Montal, M. (1992). Identification of an ion channel-formation motif in the primary structure of tetanus and botulinum neurotoxins. *FEBS Lett.*, 313, 12-18.
- Montecucco, C. (1986) How do tetanus and botulinum toxins bind to neuronal membrane? *Trends Biochem. Sci.*, 11, 314-317.
- Montecucco, C. and Schiavo, G. (1993) Tetanus and botulism neurotoxins: a new group of zinc proteases. *TIBS*, 18, 324-327.
- Oku, N., Kendall, D. A. and MacDonald R.C. (1982) A simple procedure for the determination of the trapped volume of liposomes. *Biochim. Biophys. Acta*, 691, 332-340.
- Sauer, H., Pratsch, L., Tshopp, J., Bhakdi, S. and Peter, R. (1991) Functional size of complement and perforin pores compared by confocal laser scanning microscopy and fluorescence microphotolysis. *Biochim. Biophys. Acta*, 1063, 919-924.
- Schmid M. F., Robinson T. P. and DasGupta B. R. (1993) Direct visualization of botulinum neurotoxin-induced channels in phospholipid vesicles. *Nature*, 364, 827-830.
- Singh, B. R., Foley, J. and Lafontaine, C. (1995) Physico-chemical characterization of the botulinum binding protein from type E botulinum producing *Clostridium botulinum*. *J. Prot. Chem.* 14: 7-18.
- Szoka, F. Jr. and Papahadjopoulos, D. (1978) Procedure for the preparation of liposomes with large internal aqueous space and high capture by reverse-phase evaporation. *Proc. Natl. Acad. Sci., U.S.A.* 75, 4194-4198.

Project G (Published Biochemistry, 43, 4791-4798, 2004)

Enhancement of the Endopeptidase Activity of Purified Botulinum Neurotoxins A and E by an Isolated Component of the Native Neurotoxin Associated Proteins

Abstract

In botulism disease, neurotransmitter release is blocked by a group of structurally related neurotoxin proteins produced by *Clostridium botulinum*. Botulinum neurotoxins (BoNT, A-G), enter nerve terminals and irreversibly inhibit exocytosis via their endopeptidase activities against synaptic proteins SNAP-25, VAMP and Syntaxin. Type A *C. botulinum* secretes the neurotoxin along with 5 other proteins called Neurotoxin Associated Proteins (NAPs). Here we report that Hn-33, one of the NAP components, enhances the endopeptidase activity of not only BoNT/A but also that of BoNT/E, both under *in vitro* conditions and in rat synaptosomes. BoNT/A endopeptidase activity *in vitro* is about twice as high as that of BoNT/E under disulfide reduced conditions. Addition of Hn-33 separately to non-reduced BoNT/A and BoNT/E (which otherwise have only residual endopeptidase activity) enhanced their *in vitro* endopeptidase activity by 21- and 25-fold, respectively. Cleavage of rat brain synaptosome SNAP-25 by BoNTs was used to assay endopeptidase activity *under nerve cell conditions*. Reduced BoNT/A and BoNT/E cleaved synaptosomal SNAP-25 by 20 % and 15 %, respectively. Addition of Hn-33 separately to non-reduced BoNT/A and BoNT/E enhanced their endopeptidase activities by 13-fold for the cleavage of SNAP-25 in synaptosomes, suggesting a possible functional role of Hn-33 in association with BoNTs. We believe that Hn-33 could be used as an activator in the formulation of the neurotoxin for therapeutic use.

Introduction

Botulinum neurotoxins (seven serotypes, A-G) are a group of large proteins with mutually exclusive immunological properties but shared pharmacological characteristics that

cause flaccid muscle paralysis in the botulism disease (1). Botulinum neurotoxins (BoNTs) are extremely toxic proteins (mouse LD₅₀, 10⁸/mg/Kg for type A) of 150 kDa, and consist of a 100 kDa heavy chain and a 50 kDa light chain linked through a disulfide bond (2). Type A botulinum neurotoxin is produced along with 6 neurotoxin associated proteins (NAPs) to form a complex. NAPs are known to protect BoNT from the acidity and proteases of the GI tract (3,4,5), and thus make BoNT one of the most dreaded food poisoning agents (3,6). In addition, due to the extreme toxicity and stability of BoNT in the presence of NAPs, BoNT complexes are considered as a group to be of the most dangerous biological warfare agents (7,8). Sadly, despite their critical role in food poisoning and biological weapons, little is understood as to how these non-toxic accessory proteins (i.e., NAPs) play a critical role in the toxico-infection process of botulism.

Recent discovery that BoNTs are Zn²⁺-endopeptidases (2,9,10) has led to the identification of several target proteins, which are critical for the docking and fusion of synaptic vesicles to the plasma membrane in the neurotransmitter release process. Cellubrevin, SNAP-25 (synaptosomal associated protein of 25 kDa) and syntaxin form the SNARE complex during docking of synaptic vesicles to the plasma membrane. Different BoNT types proteolytically cleave cellubrevin (BoNT/B, BoNT/C, BoNT/D and BoNT/F), SNAP-25 (BoNT/A, BoNT/C and BoNT/E) and syntaxin (BoNT/C) as part of their mode of action to block neurotransmitter release (2). Because of their specificity to inhibit neurotransmitter release at neuromuscular junctions, BoNT is increasingly being used to treat various neuromuscular disorders such as strabismus, torticollis and blepharospasm (11). Interestingly, BoNT only in its complex form with NAPs (present in all BoNT serotypes) is used as a therapeutic agent, which is a more effective drug in this form than the pure BoNT (12). Again, the molecular basis of the superior therapeutic efficacy of BoNT complex is not known. Stabilization of BoNT/A by NAPs has

been proposed as one possible explanation for the higher efficacy of BoNT/A complex compared to the pure BoNT/A (11,12).

The endopeptidase activity of pure BoNT/A is expressed only after its interchain disulfide bond is reduced (2,9,10). We have previously reported (13) that the BoNT/A complex, in contrast to pure BoNT/A, is enzymatically active even under non-reducing conditions, and the endopeptidase activity of BoNT/A complex is 17-fold higher than that of the pure BoNT/A. Under reducing conditions, the BoNT/A complex is significantly (about 15%) more active than the pure BoNT/A, and reduced purified BoNT/A has similar endopeptidase activity to the non-reduced BoNT/A in complex with NAPs (13). The higher endopeptidase activity of BoNT/A complex is due to the presence of NAPs, suggesting a more than accessory role, *such as protection against proteases in the GI tract*, in the toxico-infection process of botulism. The dramatically higher endopeptidase activity of BoNT/A complex raises several questions: 1) Is the reduction of BoNT's disulfide bond the only process that activates endopeptidase activity? 2) Is the higher therapeutic efficacy of BoNT/A complex due to the enhanced endopeptidase activity? 3) Is the cumulative effect of all the NAPs required for the BoNT/A complex to be enzymatically more active? 4) Can the NAPs-mediated activation of endopeptidase activity be observed with cross-serotypes of BoNT?

In this report, we present experimental evidence to suggest that the hemagglutinin-33 (Hn-33; *also referred as HA-35 by some researchers*) component of BoNT/A NAPs can activate BoNT/A equivalent to the cumulative effect of BoNT/A complex. Further, Hn-33 is also able to activate the endopeptidase activity of BoNT/E.

Material and Methods:

Purification of BoNT/A and BoNT/E

BoNT/A from *C. botulinum* (strain Hall) and BoNT/E from *C. botulinum* (strain Alaska) were purified as described previously (5,14). Purified neurotoxins were precipitated with 0.39 g/ml of ammonium sulfate and stored at 4 °C until used. The precipitate was centrifuged at 10,000 x g for 10 min and the pellet was dissolved in a desired assay buffer, followed by dialysis to remove any residual ammonium sulfate.

Production and Purification of hemagglutinin-33

Hn-33 was isolated according to the procedure described by Fu et al. (14) with the use of a DEAE-Sephadex A-50 and a Sephadex G-100 column chromatography.

Concentrations of neurotoxin and Hn-33 were determined according to the extinction coefficients, ϵ mg/ml (278 nm) of 1.63 and 1.74, respectively (14,15).

Expression and purification of GST/SNAP-25

SNAP-25 was expressed and purified according to Cai et al. (13). Cells expressing GST-SNAP-25 fusion protein were collected by centrifugation and resuspended in 10 mM phosphate buffered saline (PBS), pH 7.4, containing 1 mM phenylmethylsulfonyl fluoride (PMSF). Cells were lysed by sonication for 2 min., treated with 1% Triton X-100, and centrifuged to remove cell debris. The supernatant was applied to glutathione-agarose beads (Sigma Chemical Co., St. Louis, MO), washed with PBS buffer to remove other cellular proteins, and GST-SNAP-25 fusion protein was eluted with 10 mM glutathione in 50 mM Tris-HCl buffer, pH 8.0. The fusion protein was precipitated with ammonium sulfate, redissolved in desired assay buffer (50 mM Tris-HCl, 10 mM sodium phosphate, 300 mM NaCl, 2 mM MgCl₂, 0.3 mM CaCl₂, 1 mM mercaptoethanol, 0.1% NaN₃, pH 7.6), and dialyzed against the same buffer, before being used for experiments.

Isolation of rat brain synaptosomes and cleavage of SNAP-25

Frozen rat brains were purchased from RJO Biologicals, Inc. (Kansas City, MO) and were stored at -80 °C. Synaptosomes were prepared as described by Li and Singh (16). The synaptosomes were first washed with HEPES buffer, pH 7.4, containing 140 mM NaCl, 5 mM KCl, 20 mM HEPES, 5 mM NaHCO₃, 1 mM MgCl₂, 1.2 mM Na₂HPO₄, and 10 mM glucose, and were then resuspended in 2 ml of the same buffer. All the procedures were carried out at 4 °C. Synaptosomes (50 µl) in HEPES buffer were incubated with 200 nM (final concentration) nonreduced or reduced (treatment with 20 mM DTT at 37 °C for 30 min) BoNT/A or BoNT/E with 1:1 molar ratio (BoNT/A: Hn-33; BoNT/E: Hn-33) and 1:2 molar ratio (BoNT/A:Hn-33) at 37 °C for 4 h. The samples were then separated on a 12% SDS-PAGE gel, and were immunoblotted using anti-SNAP-25 antibody raised against the 12 amino acid C-terminal residues in rabbit (Stressgen Biotechnologies Corp., Victoria, Canada).

In vitro cleavage of SNAP-25: Western blot

The endopeptidase activity of BoNT was assayed according to a Western blot method established previously (13). GST-SNAP-25 fusion protein (5 µM) was incubated with 200 nM of BoNT/A or BoNT/E in the presence or absence of 200 nM of Hn-33 at 37 °C for 15 min in an assay buffer (50 mM Tris, 10 mM sodium phosphate, 300 mM NaCl, 2 mM MgCl₂, 0.3 mM CaCl₂, 0.1 % NaN₃), pH 7.6, under reducing and non-reducing conditions. For reducing conditions, the BoNT/A and BoNT/E were prepared by pretreatment with 20 mM DTT for 30 min at 37 °C. To investigate the effect of Hn-33, BoNT/A and BoNT/E were preincubated with Hn-33. Hn-33, non-reduced BoNT/A or BoNT/E and reduced BoNT/A or BoNT/E were each separately dissolved in 0.05 M citrate buffer, pH 5.5 and were filtered through a 0.45 µm filter paper. Non-reduced BoNT/A or BoNT/E, were mixed with Hn-33 (molar ratio 1: 1) in a reaction volume of 3 ml. Similarly, reduced BoNT/A or BoNT/E, were mixed with Hn-33 (molar ratio 1:1) in a reaction volume of 3 ml. The reaction mixture was incubated up to 15 min at room temperature (25 °C) because at 30-min incubation time, a complete cleavage of SNAP-

25 was observed (data not shown). Samples were then separated on a 12 % SDS-PAGE gel, and were analyzed by Western blot using a polyclonal antibody raised against the 12 C-terminal amino acid residues of SNAP-25 (Stressgen Biotechnologies Corp., Victoria, Canada) as described previously (13).

The amount of uncleaved SNAP-25 was estimated by scanning the Western blot band using an Image Analyzer (ITTI, St. Petersburg, FL) and Multiscan-R program, and the percent cleavage was calculated by comparing the density of the uncleaved band to that of the control SNAP-25.

Enzyme Linked Immunosorbant Assay (ELISA)

The cleavage of SNAP-25 was also determined by ELISA with the aim to determine the minimum concentration of BoNT/A and BoNT/E required to cleave the SNAP-25. Flat bottom microtiter plates were coated (100 µl/well) with 10 µg/ml of SNAP-25 fusion protein dissolved in 0.01 M phosphate buffer, pH 7.2. Plates were incubated at 4 °C overnight. The plates were then washed 5 times with 0.01 M phosphate buffer, pH 7.2. Serially diluted 200 nM of BoNT/A and BoNT/E, with or without 200 nM of Hn-33, were added into the plates to a total volume of 100 µl. After incubation at 37 °C for 30 min, plates were washed with 0.01 M phosphate buffer, pH 7.2 containing 0.05 % Tween-20, and were subsequently blocked by 3% bovine serum albumin dissolved in 0.01 M phosphate buffer, pH 7.2. Rabbit anti-SNAP-25 antibody (Stressgen Biotechnologies Corp., Victoria, Canada), 3 ng/ml, (100 µl/well) was used as primary antibody to bind with the SNAP-25 remaining in the plates followed by incubation at 37 °C for 30 min. The peroxidase labeled anti-rabbit antibody, 1: 10,000, was added secondary antibody into the plates, and the plates were incubated at 37 °C for 30 min. A substrate solution containing 0.04 % OPD (o-phenylenediamine dihydrochloride) and 0.012 % hydrogen peroxide in citrate phosphate buffer, pH 5.0, was added into the wells, and the plates were incubated for 15 min at room temperature (25 °C). The reaction was subsequently quenched with 50 µl of 2 M sulfuric acid

and the color was monitored by measuring absorbance at 490 nm. Unless otherwise stated, the plates were washed 5 times with 0.01 M phosphate buffer, pH 7.2, containing 0.05 % Tween-20 between the steps. The percent cleavage was calculated by comparing the absorbance of the uncleaved to that of the control SNAP-25.

For kinetic experiments, the ELISA method was used, as described above with the following modifications: after preincubation of Hn-33 with BoNT/A or BoNT/E separately, the BoNT/A or BoNT/E were added to the plate for different time intervals (0 - 40 min). The temperature of the plate was maintained at 37 °C during the addition of samples. After incubation at 37 °C for 40 min, plates were washed with 0.01 M phosphate buffer, pH 7.2, containing 0.05 % Tween-20 and subsequently blocked by 3% bovine serum albumin dissolved in 0.01M phosphate buffer, pH 7.2. Primary and secondary antibodies were used as described above to estimate uncleaved SNAP-25.

Isothermal Titration Calorimetric Analysis of Hn-33 interaction with BoNT/A

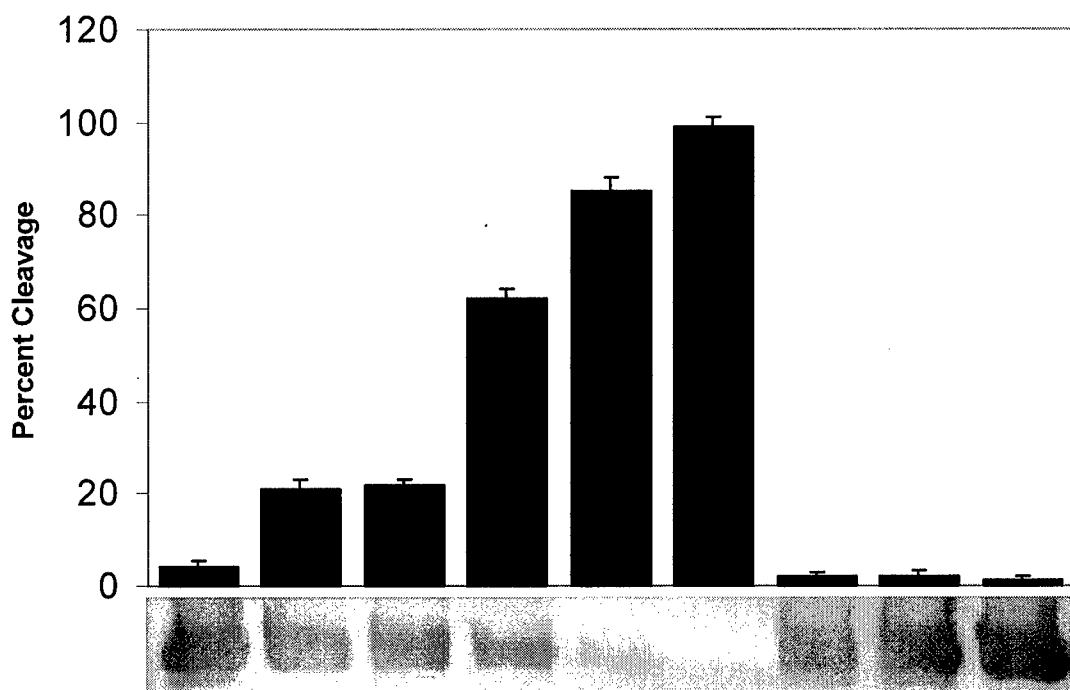
The binding isotherm of Hn-33 to the BoNT/A was generated employing CSC Isothermal Titration Calorimeter (Calorimetric Sciences Corp., Provo, UT). The binding was measured at 25 °C in a 10 mM phosphate buffer, pH 7.4. BoNT/A (0.7 μM) in a total volume of 1.3 mL was placed in the reaction cell. After temperature equilibration, the 0.7 μM of BoNT/A was titrated with 30 μM Hn-33 ligand. The 20 μL injections of Hn-33 ligand was mixed with BoNT/A at 400 second intervals in a reaction cell. The observed heat change accompanying titration was measured after each injection. The total observed heat effects were corrected for the heat of dilution of ligand by performing control titrations in the buffer used for dissolving the protein. The resulting titration curve was deconvoluted for the best –fit model using Titration BindWork in the ITC software package (CSC, Provo, UT) to obtain the affinity constant and the number of binding sites.

Results

Hn-33 induced endopeptidase activity of BoNT/A and BoNT/E in vitro

As SNAP-25 is the substrate for both BoNT/A and BoNT/E (9,17, 18), endopeptidase activities of BoNT/A and BoNT/E were analyzed for their ability to proteolytically cleave recombinant glutathione-S-transferase-SNAP-25 (GST-SNAP-25) fusion protein. The activity was determined by estimating the uncleaved SNAP-25 by Western blot analysis with a polyclonal antibody raised against the C-terminal 12 amino acid residue of SNAP-25. Under non-reducing conditions, 200 nM of pure BoNT/A exhibited negligible residual endopeptidase activity (4 ± 1 % cleavage, $n=3$) whereas BoNT/A, when reduced with 20 mM dithiothreitol (DTT), exhibited a 5.5-fold increase in its endopeptidase activity (22 ± 2 % cleavage, $n=3$). Preincubation of non-reduced BoNT/A with Hn-33 enhanced the endopeptidase activity by 21-fold (85 ± 2 %, $n=3$), while preincubation of reduced BoNT/A separately with Hn-33 enhanced its endopeptidase activity by 25-fold (99 ± 1 %, $n=3$) within 15 min of reaction time at 37°C (Fig. 1, Table 1).

Similar to BoNT/A, under non-reducing conditions, 200 nM of pure BoNT/E exhibited minimal residual endopeptidase activity (2 ± 1 % cleavage, $n=3$) whereas, when reduced with 20 mM dithiothreitol (DTT), it exhibited substantial (5-fold) increase in the endopeptidase activity (10 ± 1 % cleavage, $n=3$) against SNAP-25. (Fig. 2, Table 2). Preincubation of non-reduced BoNT/E with Hn-33 enhanced the endopeptidase activity by 25-fold (50 ± 1 % cleavage, $n=3$), while preincubation of reduced BoNT/E with Hn-33 enhanced the endopeptidase activity by 43-fold (85 ± 2 % cleavage, $n=3$) within 15 min of reaction time at 37 °C.



GST-SNAP-25	+	+	+	+	+	+	+	+	+
BoNT/A	+	+	+	+	+	+	-	-	-
Hn-33	-	-	+	+	+	+	+	-	-
DTT	-	+	-	-	-	+	-	-	+
Incubation, min	30	30	5	10	15	15	30	30	30

Fig.1. Comparative analysis of endopeptidase activity of BoNT/A in the presence or absence of Hn-33. GST-SNAP-25 fusion protein (5 μ M) was incubated with pure BoNT/A (200 nM) in the presence or absence of Hn-33 (1:1 molar ratio) for 30 min at 37 $^{\circ}$ C in assay buffer. Samples were then separated by 12% sodium dodecyl sulfate polyacrylamide gel electrophoresis (SDS-PAGE) and analyzed by Western blot using a polyclonal antibody raised against the C-terminal 12 amino acid residues of SNAP-25 (Stressgen Biotechnologies Corp., Victoria, Canada) as detailed under methods. The results were plotted by averaging the percentage of GST-SNAP-25 cleaved in three independent sets of experiments

We performed a series of control experiments to exclude the possibility SNAP-25 cleavage by Hn-33 itself. When Hn-33 itself was incubated with SNAP-25, no cleavage of the latter was observed. Two other proteins isolated from type E *C. botulinum*, a 120 kDa neurotoxin binding protein (5) and a 70 kDa protein (19) were used in place of Hn-33 to validate the assay of BoNT endopeptidase activity through the ELISA method used in this study. No

endopeptidase activity (cleavage of SNAP-25) was observed in these control experiments. Also, DTT by itself did not induce any cleavage of SNAP-25 (**Fig. 1**).

Table 1: Comparison of SNAP-25 cleavage by BoNT/A or BoNT/E with and without Hn-33 under non-reduced and reduced conditions. The percent cleavage was monitored by two methods, Western blot and ELISA, and represents the average of three individual independent experiments (*data derived from Figs 1-3*).

<i>Neurotoxin</i>	Percent Cleavage							
	Non-reduced BoNT		Non-reduced BoNT + Hn-33		Reduced BoNT		Reduced BoNT + Hn-33	
	Western Blot	ELISA	Western Blot	ELISA	Western Blot	ELISA	Western Blot	ELISA
BoNT/A	4 ± 1	5 ± 2	85 ± 2	92 ± 2	22 ± 2	25 ± 1	99 ± 1	97 ± 4
BoNT/E	2 ± 1	4 ± 3	50 ± 2	52 ± 1	10 ± 1	15 ± 1	85 ± 1	89 ± 2

In order to confirm above cleavage results, the SNAP-25 cleavage by a range of BoNT/A or BoNT/E concentrations was determined by an ELISA method using SNAP-25 C-terminal polyclonal antibody, as described in the “Method” section. Under non-reducing condition, 200 nM of pure BoNT/A exhibited negligible residual endopeptidase activity (5 ± 2 % cleavage, $n = 3$) whereas under reducing conditions it exhibited a 5-fold increase in its endopeptidase activity (25 ± 1 % cleavage, $n = 3$). Preincubation of non-reduced BoNT/A with Hn-33 enhanced the endopeptidase activity by 18-fold (92 ± 2 % cleavage, $n = 3$), while preincubation of reduced BoNT/A with Hn-33 enhanced its endopeptidase activity by 19-fold (97 ± 4 % cleavage, $n = 3$) (**Fig. 3 A and B; Table 1**).

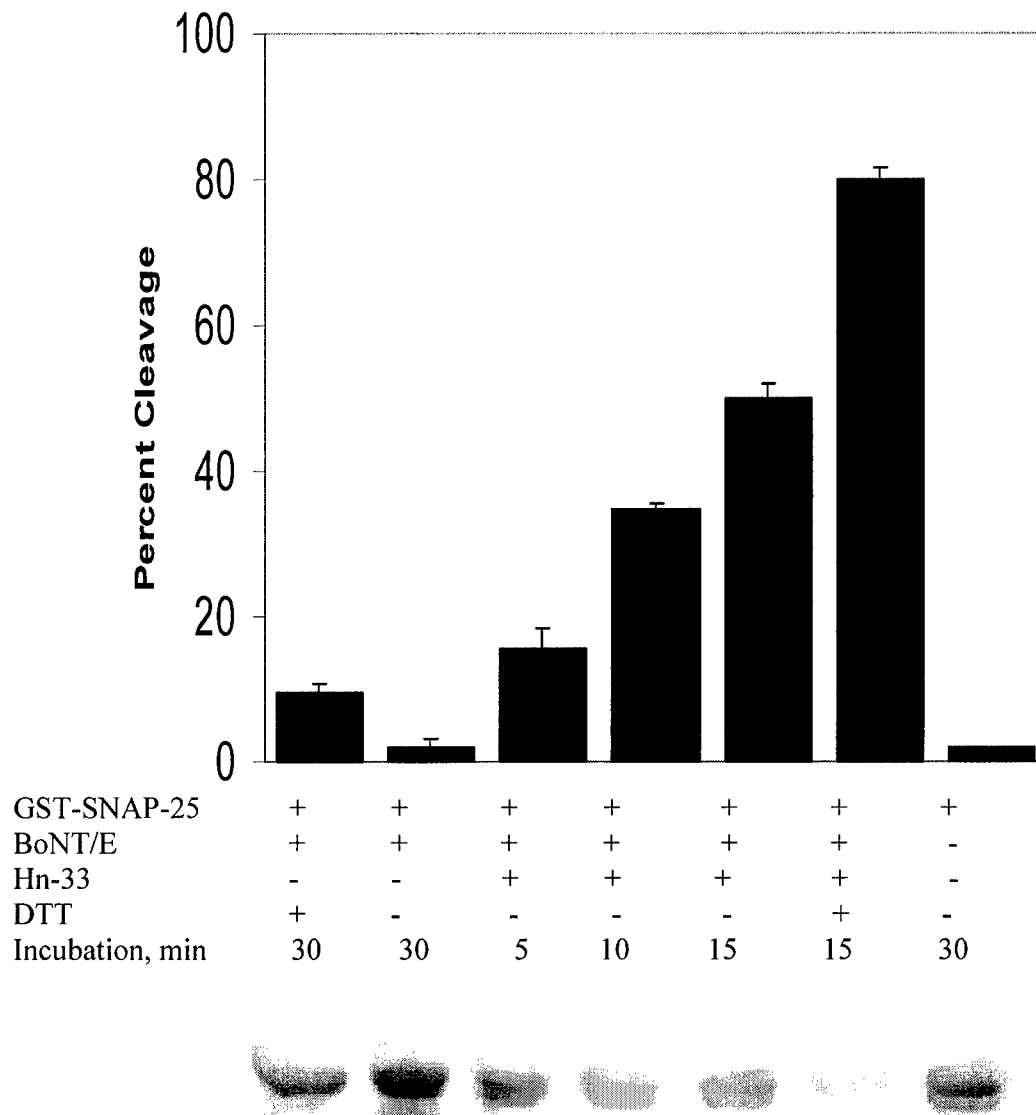


Fig. 2. Comparative analysis of endopeptidase activity of BoNT/E in the presence or absence of Hn-33. GST-SNAP-25 fusion protein (5 μ M) was incubated either with pure BoNT/E (200 nM) in the presence or absence of Hn-33 (1:1 molar ratio) for 30 min at 37 $^{\circ}$ C in assay buffer. Other experimental details were same as those in Fig. 1.

In case of BoNT/E, under non-reducing condition, 200 nM of pure BoNT/E exhibited negligible residual endopeptidase activity (4 ± 3 % cleavage, $n=3$) whereas BoNT/E, when reduced with 20 mM DTT exhibited a 4-fold increase in its endopeptidase activity (15 ± 2 % cleavage, $n=3$). Preincubation of non-reduced BoNT/E with Hn-33 enhanced the endopeptidase

activity by 14-fold (52 ± 1 % cleavage, $n=3$), while preincubation of reduced BoNT/E with Hn-33 enhanced its endopeptidase activity by 25-fold (89 ± 2 % cleavage, $n=3$) (Fig. 3C and D, Table 1).

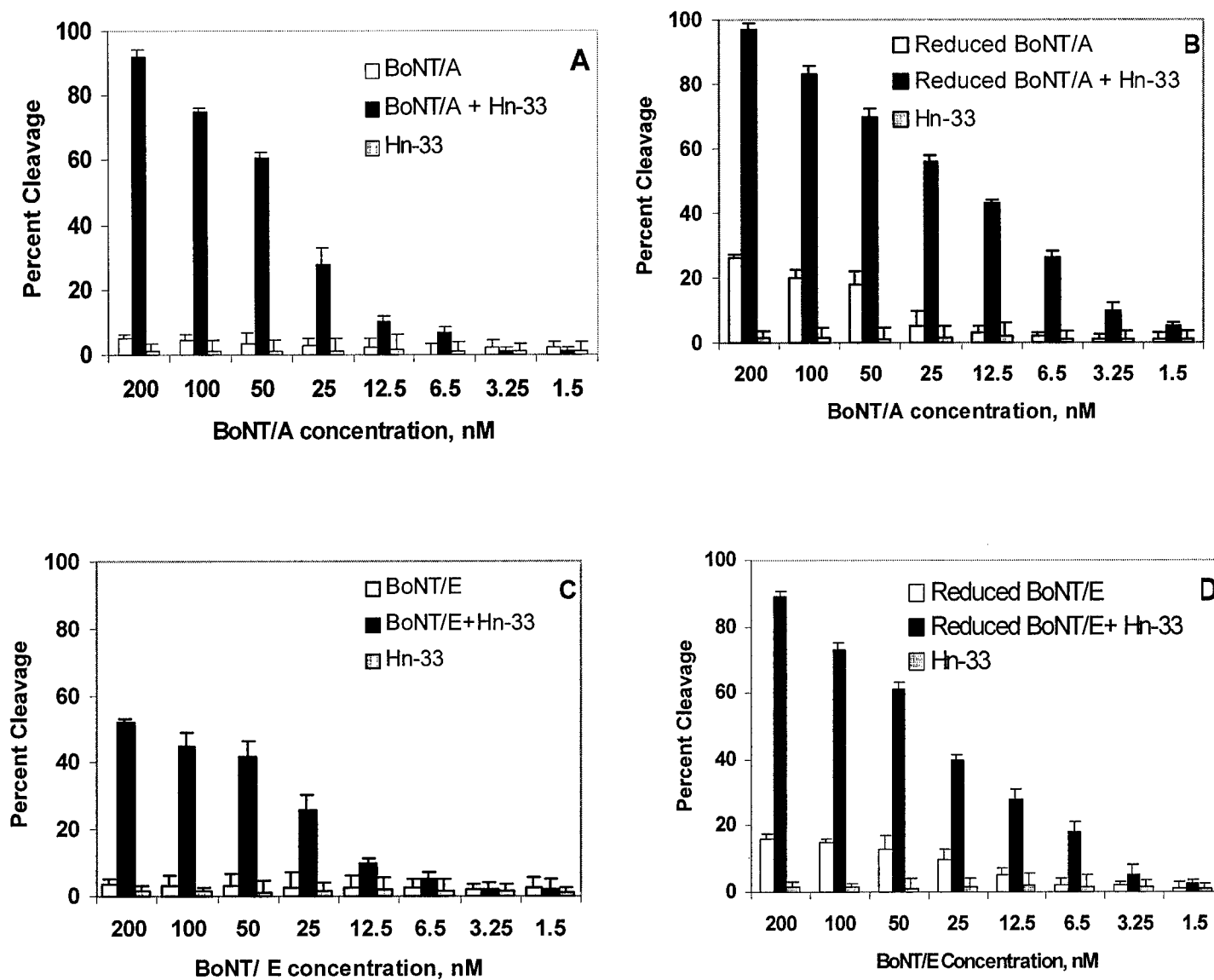


Fig 3. Cleavage of GST-SNAP-25 by non-reduced BoNT/A (A), reduced BoNT/A (B), non-reduced BoNT/E (C) and reduced BoNT/E (D) as analyzed by ELISA. Plates were coated with $10 \mu\text{g/ml}$ of GST-SNAP-25, and were incubated overnight at 4°C . Non-reduced BoNT/A or BoNT/E was pre-incubated with or without Hn-33 (1:1 molar ratio) for 30 min at 37°C before addition to the plates. Anti-SNAP-25 rabbit antibody, 3 ng/ml , was added to the plates. Peroxidase labeled anti-rabbit antibody was used as a secondary antibody as described in methods.

While comparison is made at 200 nM BoNT concentrations, similar cleavage results were observed throughout the concentration range of BoNT used (**Fig. 3; Table 1**). The ELISA results agree with Western blot results.

Hn-33 induced endopeptidase activity of BoNT/A and BoNT/E in synaptosomes

In order to evaluate the physiological significance of BoNT endopeptidase activity enhanced by Hn-33, we compared the Hn-33-induced endopeptidase activity of BoNT/A and BoNT/E against SNAP-25 using rat brain synaptosomes. Under non-reducing conditions, 200 nM of BoNT/A and BoNT/E each cleaved 6 ± 4 , ($n=3$) and 4 ± 2 , ($n=3$), respectively, of SNAP-25 at 37 °C after 4 h reaction time. Reduced BoNT/A (200 nM) cleaved $20 \pm 5\%$, ($n=3$) of SNAP-25 under reaction conditions identical to those listed above. Preincubation of non-reduced BoNT/A with Hn-33 at equimolar concentrations (BoNT/A:Hn-33, 1:1) enhanced the endopeptidase activity of BoNT/A over 13-fold ($78 \pm 5\%$, $n=3$) (**Fig. 4**). Incubation of BoNT/A with Hn-33 at higher molar ratio (BoNT/A: Hn-33, 1:2) did not have any significant additional effect on the endopeptidase activity ($79 \pm 3\%$ SNAP-25 cleavage, $n=3$) compared to the effect of the equimolar concentration of Hn-33 on BoNT/A (**Fig. 4**). Reduction of disulfide bond of BoNT/E (200 nM) enhanced its endopeptidase activity substantially (4-fold) as indicated by $15 \pm 7\%$ cleavage of SNAP-25 ($n=3$) at 37 °C after 4 h reaction time. Preincubation of non-reduced BoNT/E with Hn-33 at equimolar concentrations (BoNT/E:Hn-33, 1:1) enhanced the endopeptidase activity of BoNT/E by over 13-fold ($53 \pm 8\%$ cleavage, $n=3$). (**Fig. 4**).

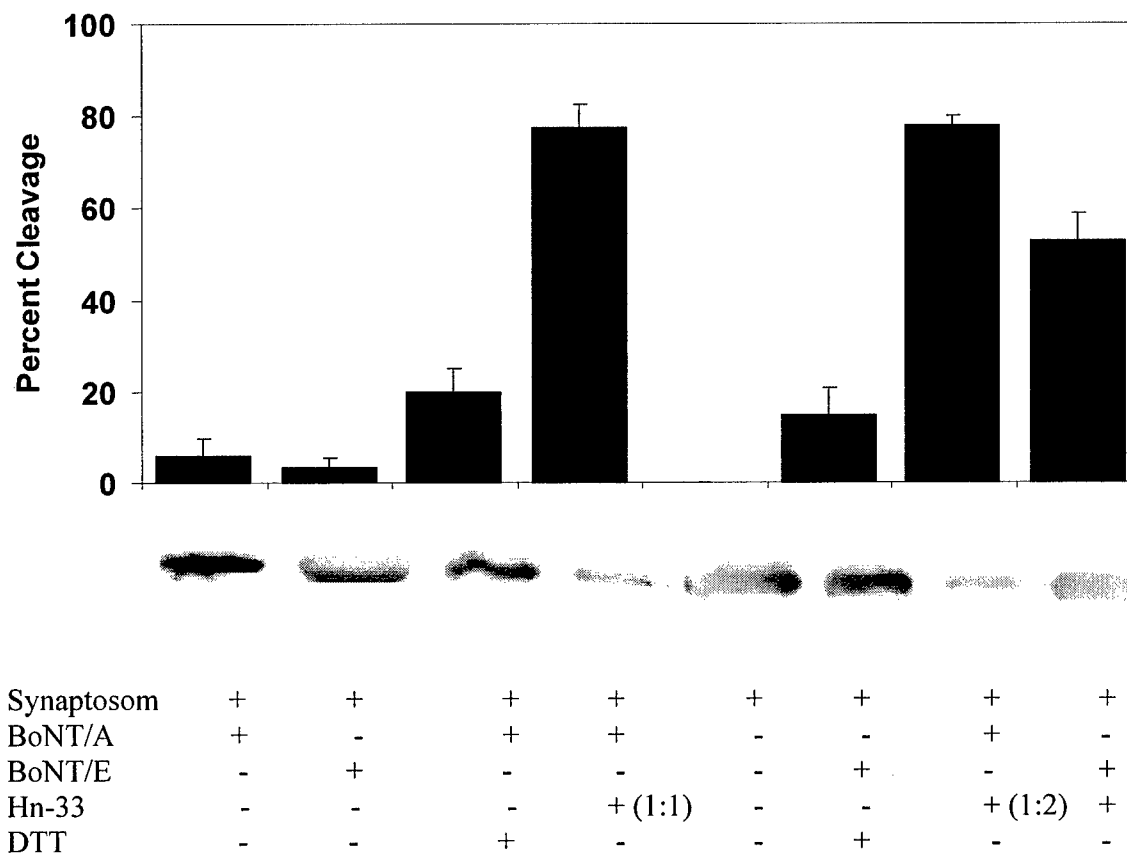


Fig. 4. Comparative analysis of endopeptidase activity of BoNT/A or BoNT/E in the presence and absence of Hn-33 on the level of SNAP-25 of rat brain synaptosomes under non-reducing conditions. Synaptosomes (50 μ l) in Hepes buffer were incubated with 200 nM (final concentration) nonreduced BoNT/A with 1:1 or 1:2 (BoNT/A: Hn-33) or BoNT/E 1:1 (BoNT/E: Hn-33) at 37 °C for 4 h. The samples were then analyzed by 12% SDS-PAGE and were immunoblotted using anti-SNAP-25 antibody as described in method section. The results were plotted by averaging the percentage of SNAP-25 cleaved in three independent sets of experiments.

In a preliminary effort to evaluate the influence of Hn-33 on the kinetics of BoNT endopeptidase activity, initial rates of the endopeptidase activity of BoNT/A and BoNT/E, were determined by estimating the percent cleavage of SNAP-25 at different time intervals. The time course of SNAP-25 cleavage, obtained with ELISA method, showed plateau within 30 min of the reaction time (**Fig. 5**). However, linearity of the curve was observed only for the first 4-min

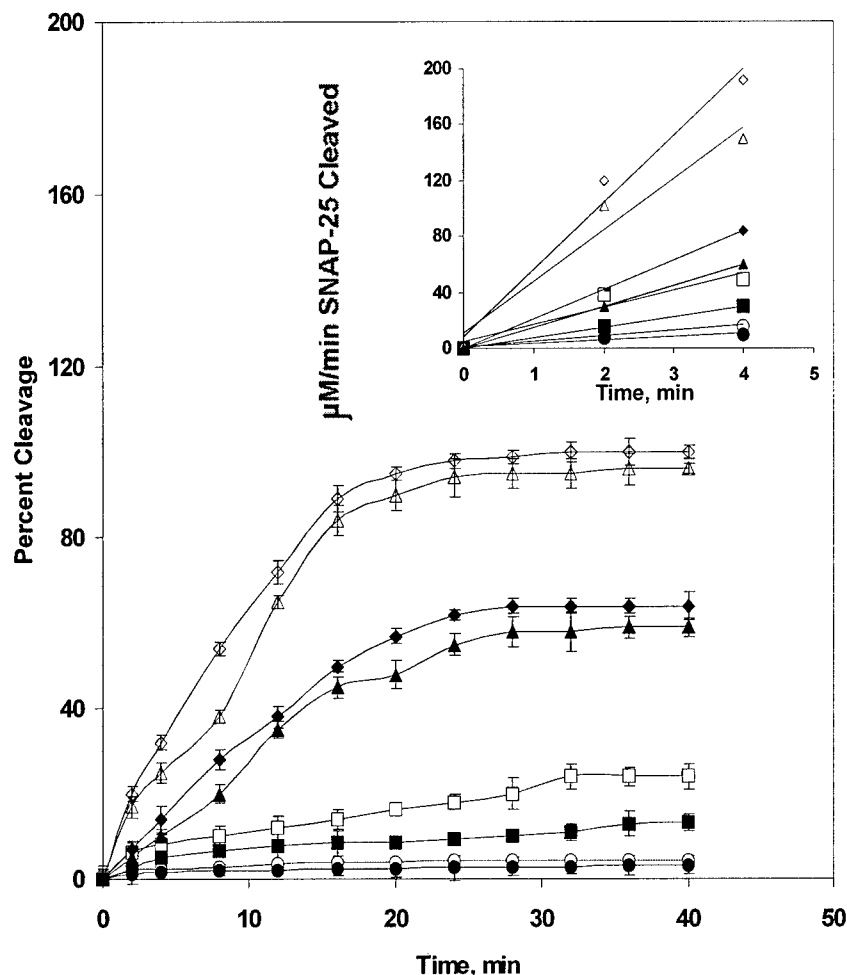


Fig. 5. Time course of SNAP-25 cleavage by BoNT/A or BoNT/E in the presence or absence of Hn-33 analyzed by ELISA. Plates were coated with $10 \mu\text{g/ml}$ of GST-SNAP-25, and incubated overnight at 4°C . Non-reduced BoNT/A or BoNT/E was preincubated with or without Hn-33 (1:1 molar ratio) for 30 min at 37°C prior to addition to the plates. Non-reduced BoNT/A (○) Non-reduced BoNT/E (●), Reduced BoNT/A (□), Reduced BoNT/E (■), Non-reduced BoNT/A when preincubated with Hn-33 (△), Non-reduced BoNT/E when preincubated with Hn-33 (▲), Reduced BoNT/A when preincubated with Hn-33 (◇), Reduced BoNT/E when preincubated with Hn-33 (◆) (For reducing conditions, BoNT/A and BoNT/E were prepared by pretreatment with 20 mM DTT for 30 min at 37°C . Peroxidase labeled anti-rabbit antibody was used as a secondary antibody as described in method section.

reaction time, especially for reactions where no Hn-33 was added. We, therefore, used the slope of the linear portion of the curve within the first 4-min reaction time to estimate initial reaction rates catalyzed by BoNT endopeptidase. Under non-reducing conditions, BoNT/A and BoNT/E showed initial reaction rates of 3.9 and 2.4 $\mu\text{M/min}$, respectively. Under reducing conditions, initial reaction rates for the endopeptidase activity of BoNT/A and BoNT/E were 12.3 and 7.5

$\mu\text{M}/\text{min}$, respectively. Preincubation of non-reduced BoNT/A and BoNT/E separately with Hn-33 at equimolar concentration (BoNT:Hn-33, 1:1) enhanced the rates of their endopeptidase activity by 9.4-fold and 6.3-fold, respectively, with cleavage rates of $37 \mu\text{M}/\text{min}$ (BoNT/A) and $15 \mu\text{M}/\text{min}$ (BoNT/E). Preincubation of reduced BoNT/A or BoNT/E with Hn-33 at equimolar concentration (BoNT:Hn-33, 1:1) enhanced the rates of their endopeptidase activity by 12.2-fold and 8.7-fold, respectively, with cleavage rates of $47.8 \mu\text{M}/\text{min}$ (BoNT/A) and $21 \mu\text{M}/\text{min}$ (BoNT/E), (**Fig. 5, Table 2**).

Table 2: Initial reaction rates of SNAP-25 cleavage by non-reduced and reduced BoNT/A and BoNT/E with and without Hn-33. The initial reaction rate ($\mu\text{M}/\text{min}$) was determined from the slope of the linear portion (4-min) of the SNAP-25 cleavage vs. time plots (Fig. 5).

Neurotoxin	Initial reaction rate, $\mu\text{M}/\text{min}$ SNAP-25 cleaved			
	Non-reduced BoNT	Non-reduced BoNT + Hn-33	Reduced BoNT	Reduced BoNT + Hn-33
BoNT/A	3.9	37.0	12.3	47.8
BoNT/E	2.4	15.0	7.5	21.0

Physical interaction of Hn-33 with BoNT/A

Interaction of Hn-33 with BoNT/A was examined with isothermal calorimetry by measuring heat changes upon titration of BoNT/A solution with Hn-33, both dissolved in 10 mM phosphate buffer, pH 7.4. **Figure 6** shows a typical titration curve. The concentration range chosen provided a very smooth curve of steady heat change with every injection until the injection 15, after which it reached a saturation level (**Fig. 6A**). The saturation level was reached at a molar ratio of 10:1 (Hn-33:BoNT/A). Considering that Hn-33 is known to exist as a dimer (20), this set of data suggests five Hn-33 dimeric molecules bound to one BoNT/A. Interestingly, the molar ratio of Hn-33 to BoNT/A in the BoNT/A complex was found to be 8 based on SDS-

PAGE analysis (21). It is possible that in the absence of other NAPs Hn-33 is able to have more freedom to bind to BoNT/A thus leading to a ratio of 10. The number of binding sites estimated from the curve was 1.0, suggesting that the binding sites belong to a class of similar affinity.

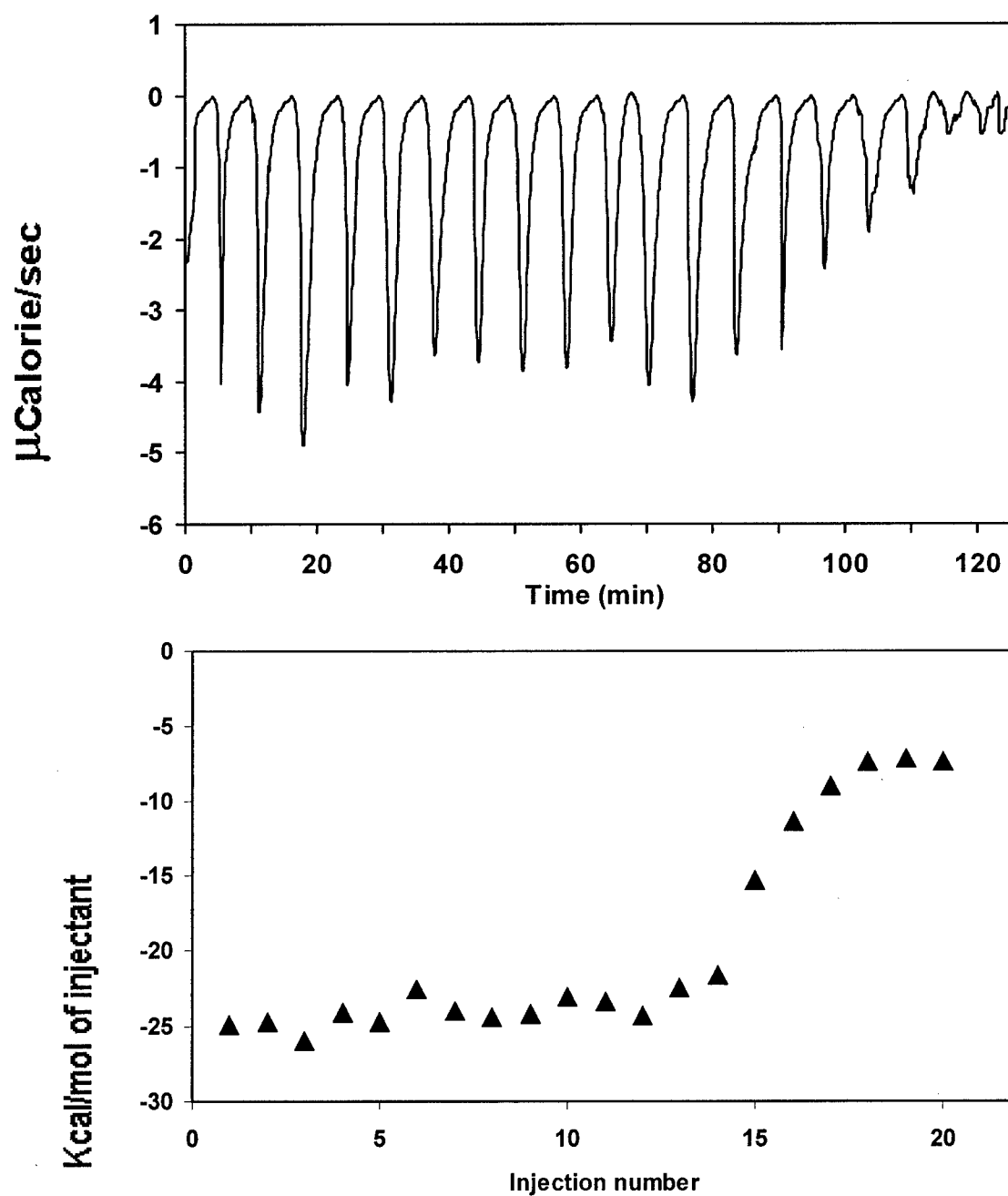


Fig. 6. A typical isothermal calorimetric titration curve for BoNT/A with Hn-33. Sequential injections of 20 μL Hn-33 ligand (concentration, 30 μM) was mixed with 1.3 ml of 0.7 μM BoNT/A at 400 second intervals in a reaction cell. The titration was performed at 25°C in a 10 mM phosphate buffer, pH 7.4. (A) Total heat released is plotted in terms of $\mu\text{cal/sec}$ versus time. The area underneath each injection peak is equal to the total heat released for that injection. (B)

Integrated areas of the heat release peaks in (A) plotted against the injection number. The solid line corresponds to the best-fit curve obtained by a nonlinear regression.

The interaction between Hn-33 and BoNT/A is exothermic (**Fig. 6A**), and ΔH estimated at -120 kJ mol^{-1} from the binding curve (**Fig. 6B**) is within the typical range of strong protein-protein interactions (22, 23). The binding constant was estimated to be $4.32 \times 10^{-5} \text{ M}^{-1}$, which is within the range of interaction between specific proteins (24).

Discussion

Although the discovery of endopeptidase activity of BoNT in 1992 (10) has opened up many avenues to the understanding of the biochemical mechanism of its toxic action, the endopeptidase activity itself has remained a subject of intense research to understand its unique characteristics (2,25,26). Among its unique features, it has been reported that reduction of the disulfide bond between the light and heavy chain is required for the endopeptidase activity (9,10). The active Zn^{2+} plays both catalytic and structural role (27). In the presence of NAPs there is no requirement of disulfide reduction for the endopeptidase activity (13) and dimeric form of the BoNT has lower enzymatic activity than monomeric form (28). Furthermore, except for BoNT/C1, the seven serotypes of BoNT recognize only one specific protein substrate and selective cleavage site (2,29).

It is important to examine the structural basis of unique characteristics of BoNT endopeptidases. Understanding the molecular basis of the unique endopeptidase activity of BoNT is not only likely to provide clues to the mechanistics of the enzyme activity, but the information could lead to the development of antidotes to the most poisonous poison.

A significantly enhanced endopeptidase activity of BoNT/A in the presence of Hn-33 isolated from BoNT/A complex was observed (Table 1) even under conditions where the disulfide bond between the light and heavy chains of BoNT was not reduced. Hn-33 does not reduce the interchain disulfide bond between light and heavy chains of BoNT/A (20). BoNT/A

complex itself is known to have drastically enhanced endopeptidase activity against the SNAP-25 in the solution without reducing the interchain disulfide bond of BoNT/A (13). Interestingly, the enhanced endopeptidase activity of BoNT/A in the presence of Hn-33 is virtually the same as the whole BoNT/A complex, both quantitatively and qualitatively. In qualitative terms, the Hn-33-enhanced endopeptidase activity of BoNT/A did not require reduction of the disulfide bond, (Fig.1, Table 1), just like the BoNT/A complex (13). It may be noted here the disulfide bond of BoNT/A remains intact in the native complex form as well as in a complex with Hn-33 (4,13). Quantitatively, Hn-33 enhanced the endopeptidase activity of non-reduced BoNT/A by 21-fold for 15 min reaction period whereas BoNT/A complex is reported to exhibit endopeptidase activity 17-fold higher than non-reduced pure BoNT/A for a 10 min reaction period (13). Thus, Hn-33 seems to be able to imitate the presence of all the NAPs in BoNT/A complex with respect to the enhancement of the endopeptidase activity.

In BoNT/A complex, there are five NAPs including Hn-33 (13); Hn-33 makes the largest fraction (25%) of the NAPs (20) in the BoNT/A complex. Furthermore, Hn-33 strongly protects BoNT/A against proteases such as trypsin, α -chymotrypsin, subtilisin, etc. (4). These observations are consistent with the effect of Hn-33 on the BoNT/A endopeptidase activity, and strongly suggest that Hn-33 directly interacts with the BoNT/A in the BoNT/A complex.

Although the mechanism by which Hn-33 may enhance the BoNT/A endopeptidase activity is not discernible from current data, possible explanation derived from the known X-ray crystallographic structure of BoNT/A is as follows: The active site of BoNT/A is known to be buried in a crevice of about 24 Å deep, which is occluded by a 56-amino acid residue (residues 490-545) belt (30,31). It has been suggested that disulfide reduction opens up the belt and exposes the active site to the surface of the protein for its binding with the substrate peptide groups (31). We believe that the interaction of Hn-33 exposes the enzyme active site without any need to open up the belt. However, reduction of the disulfide bond and thus opening of the belt

can further expose the active site to the substrate, as indicated by about 17 % additional increase in the endopeptidase activity of BoNT/A (Table 1). Exposure of the active site upon interaction with Hn-33 becomes more plausible in view of a recent report (32) suggesting the enzymatically active structure of BoNT/A in the form of a molten-globule. Molten-globule folded structure is significantly more flexible than native folded structure (33,34).

Interestingly, although Hn-33 was isolated from the BoNT/A complex (14), its effect appears common to all the BoNT serotypes. This was demonstrated by a similar experiment of the endopeptidase activity of BoNT/E and BoNT/A by Hn-33 (Table 1). Hn-33 effect on BoNT/E is especially noteworthy, as the latter does not have a comparative NAP in its complex form (19). Therefore, a similar effect of Hn-33 on the two serotypes of BoNT suggests a common mechanism involved in the accessibility of the active site of BoNTs to their respective substrates. Moreover, there must be common structure motifs of the surface of the BoNT/A and BoNT/E molecules. While 3-dimensional structure of BoNT/E is not yet solved, common structural motifs are well known for BoNT/A and BoNT/B (35,36,37). Future work with crystal structure of Hn-33 and BoNT complex would be required to confirm the common structural motif on BoNT surface for interaction with Hn-33.

Molecular basis of Hn-33-enhanced BoNT endopeptidase activity can be discerned from an additional set of published data, related to the Hn-33 protection of BoNT/A from proteases (4). Hn-33 can completely protect BoNT/A from pepsin, trypsin, α -chymotrypsin, and subtilisin, suggesting Hn-33 either surrounds the protease cleavage sites on BoNT/A, or introduces refolding in BoNT/A so that the cleavage sites become inaccessible. The dissociation constant of 0.4 μ M derived from isothermal calorimetry experiments of BoNT/A and Hn-33 indicates a strong binding between the two proteins capable of introducing polypeptide refolding in BoNT/A. This is especially likely given a single binding site ($n=1.0$) obtained from the titration the isothermal titration curve (Fig. 6). While it is possible that only one binding site is involved

between BoNT/A and Hn-33, more than one binding sites could also lead to $n = 1$, as long as different binding sites have similar binding affinities. More than one binding sites are also likely considering two dimers of Hn-33 bind to BoNT/A (14,20, 21).

Each of the seven serotypes of BoNT has a group of associated NAPs, whose biological roles are not clearly understood. NAPs are known to protect the toxin from adversarial environmental conditions such as temperature, and acidity and proteases of gastric juice (3,38,39). It is notable that Hn-33 represents the largest fraction of BoNT/A NAPs (14) and accounts for most of the hemagglutinin activity of BoNT/A complex (28). Hn-33 by itself can protect BoNT/A from proteases (4). Thus the influence of Hn-33 on the endopeptidase activity of BoNT/A and BoNT/E is consistent with the Hn-33 effect on other biological and physical features of BoNT/A and its complex with the NAPs. Hn-33 seems to imitate the role of all NAPs in BoNT/A complex.

Comparison of SNAP-25 cleavage by BoNT/A and BoNT/E in the presence and absence of Hn-33 in synaptosomes representing nerve cell conditions (Fig. 4) indicated the following: (a) SNAP-25 cleavage by both BoNT/A and BoNT/E is less in synaptosomes compared to the *in vitro* conditions (Table 1, Fig. 4). (b) Hn-33 enhanced the endopeptidase activity of both BoNT/A and BoNT/E even in synaptosomes, albeit to a lesser degree (Table 1, Fig. 4). These results suggest that the neurotoxin complex with Hn-33 enters the synaptosome and the lower cleavage of SNAP-25 (in comparison to *in vitro* conditions) is likely to result from the inaccessibility of SNAP-25 in synaptosome. We have recently made an observation (Y. Zhou and B. R. Singh, unpublished data) that Hn-33 binds to synaptosomes through synaptotagmin, which will further support the possibility of Hn-33 entry into synaptosomes. These results are particularly significant to the possibility of the use of BoNT complex with Hn-33 as a therapeutic agent. The entrance of Hn-33 and BoNT as a complex will have enhanced and stable endopeptidase activity inside the neuronal cell. Stable endopeptidase activity inside the neuronal

is a critical phenomenon for the long lasting effects of botulinum either as a toxin or as a therapeutic agent (40,41).

In summary, our results show that (i) the Hn-33 component of BoNT/A NAPs is able to imitate the effect of all the NAPs in enhancing the endopeptidase activity of BoNT/A; (ii) the Hn-33 of BoNT/A complex is also able to enhance endopeptidase activity of BoNT/E, suggesting a common structural motif BoNT serotypes for Hn-33; and (iii) Hn-33 bound to BoNT/A and /E enhanced the endopeptidase activity in synaptosomes, suggesting a possible entry of Hn-33 and BoNT inside the synaptosome.

References

1. Simpson, L. L. (1989) Peripheral action of the botulinum toxin. In: *Botulinum Neurotoxin and Tetanus Toxins*, (L. L. Simpson ed.), pp 153-178, San Diego: Academic Press.
2. Li, L. and Singh, B. R. (1999) Structure-function relationship of clostridial neurotoxins, *J. Toxicol-Toxin reviews* 18, 95-112.
3. Sakaguchi, G. (1983) Clostridium botulinum neurotoxins, *Pharmac. Ther.* 19, 165-194.
4. Sharma, S.K. and Singh B.R. (1998) Hemagglutinin binding mediated protection of botulinum neurotoxin from proteolysis, *J. Natural Toxin* 7, 239-253.
5. Singh, B. R., Foley, J. and Lafontaine, C. (1995) Physicochemical and immunological characterization of the type E botulinum neurotoxin binding protein purified from Clostridium botulinum, *J. Prot. Chem.* 14, 7-18.
6. Middlebrook, J. L. (1989) Cell surface receptors for protein toxins. In: *Botulinum Neurotoxin and Tetanus Toxin* (Simpson, L. L., Ed.), pp 95-119, Academic Press, San Diego.

7. Zilinskas, R. A. (1997) Iraq's biological weapons. The past as future? *J. Am. Med. Assoc.* 278, 418-424.
8. Singh, B. R., Li, B. and Read, D. (1995) Botulinum versus tetanus neurotoxins: why is botulinum neurotoxin but not tetanus neurotoxin a food poison? *Toxicon* 33, 1541-1547.
9. Blasi, J, Chapman, E. R., Link, E., Binz, T., Yamasaki, S., DeCamilli, P., Sudhof, T., Niemann, H. and Jahn, R. (1993). Botulinum neurotoxin A selectively cleaves the synaptic protein SNAP-25, *Nature* 365, 160-163.
10. Schiavo, G., Benfenati, F., Poulain, B., Rossetto, O., de Laureto, P., DasGupta, B. R. and Montecucco, C. (1992). Tetanus and botulinum B neurotoxins block neurotransmitter release by proteolytic cleavage of synaptobrevin, *Nature* 359, 832-835.
11. Johnson E. A. (1999). Clostridial toxins as therapeutic agents: benefits of nature's most toxic proteins, *Annu Rev Microbiol.* 53, 551-75.
12. Schantz, E. J, Johnson, E. A. (1992). Properties and use of botulinum toxin and other microbial neurotoxins in medicine, *Microbiol Rev.* 56, 80-99.
13. Cai, S., Sarker, H. K. and Singh, B. R. (1999) Enhancement of the endopeptidase activity of botulinum neurotoxin by its associated proteins and dithiothreitol, *Biochemistry* 38, 6903-6910.
14. Fu, F.-N., Sharma, S. K. and Singh, B. R. (1998) A protease-resistant novel hemagglutinin purified from type A *Clostridium botulinum*, *J. Prot. Chem.* 17, 53-60.
15. Dasgupta, B. R. and Sathyamoorthy, V. (1984) Purification and amino acid composition of type A botulinum neurotoxin, *Toxicon* 22, 415-424.
16. Li, L. and Singh, B. R. (1999) In vitro translation of type A *Clostridium botulinum* neurotoxin heavy chain and analysis of its binding to rat synaptosomes, *J. Protein Chem.*, 18, 89-95.

17. Schiavo, G., Rossetto, O., Catsicas, S., Polverino de Laureto, P., DasGupta, B. R., Benfenati, F., Montecucco, C. (1993) Identification of the nerve terminal targets of botulinum neurotoxin serotypes A, D, and E, *J Biol Chem.* 268, 23784-7.
18. Schiavo, G., Santucci, A., Dasgupta, B. R., Mehta, P. P., Jontes, J., Benfenati, F., Wilson, M. C., Montecucco, C. (1993), Botulinum neurotoxin serotypes A and E cleave SNAP-25 at distinct COOH-terminal peptide bond, *FEBS Lett.* 335, 99-103.
19. Zhang, Z. and Singh, B. R. (1995) A novel complex of type E *Clostridium botulinum* *Protein Sci.* 4 (suppl 2), 110.
20. Sharma, S. K., Fu, F. N., Singh, B. R. (1999) Molecular properties of a hemagglutinin purified from type A *Clostridium botulinum*, *J. Protein. Chem.* 18, 29-38.
21. Inoue, K., Fujinaga, Y., Watanabe, T., Ohyama, T., Takeshi, K., Moriishi, K., Nakajima, H., Inoue, K., Oguma, K. (1996) Molecular composition of clostridium botulinum type A progenitor toxins, *Infect. Immun.* 64, 1589-1594.
22. Hibbits, K. A., Gill, D. S., Willson, R. C. (1994) Isothermal titration calorimetric study of the association of hen egg lysozyme and the anti-lysozyme antibody HyHEL-5, *Biochemistry* 33, 3584-3590.
23. Pierce, M. M., Raman, C. S. and Nall, B. T. (1999) Isothermal titration calorimetry of protein-protein interactions, *Methods* 19, 213-221.
24. Li, J. and Weis, R. M. (1996) Measurements of protein - protein interaction by isothermal titration calorimetry with applications to the bacterial chemotaxis system. In: *Techniques in Protein Chemistry*, Vol VII (D. Marshak, E.), pp 33-44, Academic Press.
25. Montecucco, C., Schiavo, G. (1993) Tetanus and botulism neurotoxins: a new group of zinc proteases, *Trends Biochem Sci.* 18, 324-327.

26. Singh, B. R. (2002) Molecular basis of the unique endopeptidase activity of botulinum neurotoxin . In: *Scientific and Therapeutic Aspects of Botulinum Toxin* (M. F. Brin, J. Jankovic, and M. Hallett, eds.), 75-88. Lippincott and Wilkins, Philadelphia.
27. Fu, F. N., Lomneth, R. B., Cai, S., and Singh, B. R. (1998) Role of zinc in the structure and toxic activity of botulinum neurotoxin, *Biochemistry* 37, 5267-5278.
28. Cai, S. and Singh, B.R. (2001) A correlation between differential structural features and the degree of endopeptidase activity of type A botulinum neurotoxin in aqueous solution, *Biochemistry* 40, 4693-4702.
29. Blasi, J., Chapman, E. R., Yamasaki, S., Binz, T., Niemann, H., Jahn, R. (1993) Botulinum neurotoxin C1 blocks neurotransmitter release by means of cleaving HPC-1/syntaxin, *EMBO J.* 12,4821-8.
30. Lacy, D. B., Tepp, W., Cohen, A. C., DasGupta, B. R., Stevens, R.C. (1998) Crystal structure of botulinum neurotoxin type A and implications for toxicity, *Nat Struct Biol.* 10, 898-902.
31. Lacy, D. B. and Stevens, R.C. (1999) Sequence homology and structural analysis of the clostridial neurotoxins, *J. Mol. Biol.* 291, 1091-104.
32. Cai, S. and Singh, B.R. (2001) Role of the disulfide cleavage induced molten globule state of type a botulinum neurotoxin in its endopeptidase activity, *Biochemistry.* 40, 15327-33.
33. Christensen, H., Pain, R. H. (1991)) Molten globule intermediates and protein folding, *Eur Biophys J.* 19, 221-9.
34. Nakagawa, S. H., Tager, H. S. (1993) Importance of main-chain flexibility and the insulin fold in insulin-receptor interactions, *Biochemistry* 32, 7237-7243.

35. Swaminathan, S. and Eswaremoorthy, S. (2000) Structural analysis of the catalytic and binding sites of *Clostridium botulinum* neurotoxin B, *Nat Struct Biol* 7, 693-699
36. Hanson, M. A. and Stevens, R. C. (2000) Cocystal structure of synaptobrevin-II bound to botulinum neurotoxin type B at 2.0 A resolution, *Nature Struct. Biol.* 7, 687-690.
37. Singh, B. R. (2000) Intimate details of the most poisonous poison, *Nature Struct. Biol.* 7, 617-619.
38. Inoue K., Fujinaga, Y., Honke, K., Yokota, K., Ikeda, T., Ohyama, T., Takeshi, K., Watanabe, T., Inoue, K., Oguma, K. (1999) Characterization of haemagglutinin activity of *Clostridium botulinum* type C and D 16S toxins, and one subcomponent of haemagglutinin (HA1), *Microbiology.* 145, 2533-42.
39. Fujinaga, Y., Inoue, K., Nomura, T., Sasaki, J., Marvaud, J. C., Popoff, M. R., Kozaki, S., Oguma, K. (2000) Identification and characterization of functional subunits of *Clostridium botulinum* type A progenitor toxin involved in binding to intestinal microvilli and erythrocytes, *FEBS Lett* 467, 179-183.
40. Keller, J. E., Neale, E.A., Oyler, G. and Adler, M. (1999) Persistence of botulinum neurotoxin action in cultured spinal cord cells, *FEBS Lett.* 456, 137-142.
41. Foran, P. G., Mohammed, N., Lisk, G. O., Nagwaney, S., Lawrence, G. W., Johnson, E., Smith, L., Aoki, K. R. and Dolly, J. O. (2003) Evaluation of the therapeutic usefulness of botulinum neurotoxin B, C1, E, and F compared with the long lasting type A. Basis for distinct durations of inhibition of exocytosis in central neurons, *J. Biol. Chem.* 278, 1363-1371.

Project H (Unpublished)

Discovery of a Novel Type E Botulinum Neurotoxin Complex

Abstract

A new form of complex for type E botulinum neurotoxin has been discovered with wide implications for its stability and biological activity. The complex consists of the neurotoxin and five other neurotoxin associated proteins (NAPs) which enhance its stability against proteases and heat, and activate the neurotoxin's endopeptidase activity.

Introduction

Previous studies have shown (Fuji et al. 1993, East et al. 1994, Haiser et al., 1994, Singh et al., 1995; Johnson's latest reference) that BoNT gene is perhaps co-expressed along with at least one other protein, a neurotoxin binding protein (NBP) that remains associated with BoNT in the bacterial culture. Each of the types A-D BoNT is associated with several other proteins, which have hemagglutinin activity (Inoue et al., 1996, Singh et al., 1996, Li et al., 1998; Johnson's review, 2003; other refs. on B-D and C), to form large (L) complexes. Types E and F have so far been known to associate only with NBP and exist as medium (M) complexes. The complex form of BoNT is critical for its food poisoning and biological warfare potentials as only the complex form can survive adverse environmental conditions such as exposure to acidity, proteases and heat. Current usage of botulinum neurotoxin as a therapeutic agent is also limited to the complex form (Johnson and Schantz, 1992). Genes for NBP and neurotoxin associated proteins (NAPs) that associate with the BoNT to form a complex are located closely on the genomic map. All the serotypes of BoNT except types E and F are known to exist as large complexes with 5-6 different NAPs and NBP.

In this report, we for the first time report the existence of a large complex of type E BoNT that consists of BoNT, NBP and 4 other neurotoxin associated proteins (NAPs) with molecular mass of 80 kDa, 60 kDa, 40 kDa and 18 kDa. The molecular size of the complex was estimated to be 600 kDa.

The genomic organization of BoNT locus has revealed that NAPs genes are present in the direct vicinity of the BoNT gene, suggesting the possibility of concerted gene expression. Functional activity of the neurotoxin (blockage of neurotransmitter release) was retained in the complex both at room temperature as well as after heating to the denaturing temperature of the purified BoNTs, suggesting a protective role of NAPs to the neurotoxin. NAPs also protected against proteolysis of the BoNT by α -chymotrypsin and pepsin.

Results and Discussion

To analyze for the existence of a BoNT/E complex similar to other serotypes, we employed chromatographic methods and isolated a protein complex in *Clostridium botulinum* (strain, Alaska) cultures. Proteins in the cell culture extract were precipitated with ammonium sulfate, and the precipitate was re-dissolved in 50 mM citrate-phosphate buffer, pH 5.5. Chromatographic separation of the re-dissolved protein fraction on an ion-exchange column (DEAE-Sephadex A-50) resulted in an eluted fraction containing six major protein bands on a sodium dodecyl sulfate-polyacrylamide electrophoresis (SDS-PAGE) gel (Fig. 1). The molecular weights of the eluted proteins ranged between 18-150 kDa (Fig. 1).

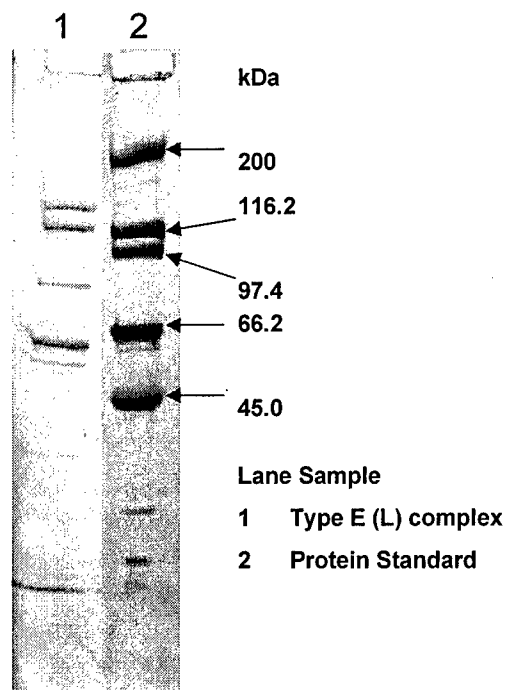


Fig. 1. SDS-PAGE analysis of newly discovered BoNT/E complex

After confirming the complex nature of the BoNT/E NAPs using gel filtration chromatography and dynamic light scattering, we determined the sequence of the N-terminal 10 amino acid residues to compare with the known sequences of BoNT/A, BoNT/B and BoNT/C NAPs. The N-terminal sequence of BoNT/E NAPs are unique in comparison to the NAPs of other BoNTs.

The biological function of newly discovered BoNT/E NAPs in the complex was investigated by examining their protection of BoNT/E against proteolysis and heat denaturation. In proteolysis experiment, incubations of BoNT/E complex with either α -chymotrypsin (5:1, w/w, BoNT/E complex: α -chymotrypsin) at pH 7.5 or pepsin (5:1, w/w) at pH 2.0 did not cause breakdown of BoNT/E or its NAPs (Fig. 2). A comparative set of experiments was carried out with BoNT/A complex (Fig. 3), which has been established in the past to resist against proteolysis. The resistance of BoNT/E complex to proteolysis by α -chymotrypsin and pepsin was similar to that of BoNT/A complex, supporting our

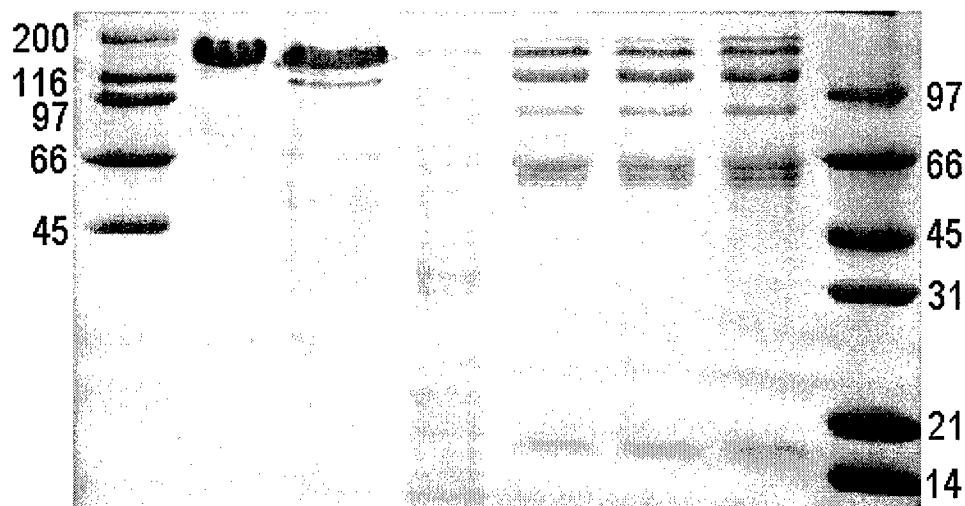


Fig. 2. Proteolysis of BoNT/E neurotoxin complex with Pepsin and α -chymotrypsin. **Lane 1:** High molecular weight markers. **Lane 2:** BoNT/E neurotoxin control. **Lane 3:** BoNT/E neurotoxin-treated with pepsin for 20 min. **Lane 4:** BoNT/E neurotoxin treated with α -chymotrypsin for 20 min. **Lane 5:** BoNT/E neurotoxin complex control. **Lane 6:** BoNT/E neurotoxin complex treated with pepsin for 1h. **Lane 7:** BoNT/E neurotoxin complex treated with α -chymotrypsin for 1 h. **Lane 8:** Low molecular weight markers.

conclusion that BoNT/E NAPs protect BoNT/E similar to BoNT/A NAPs' protection of BoNT/A.

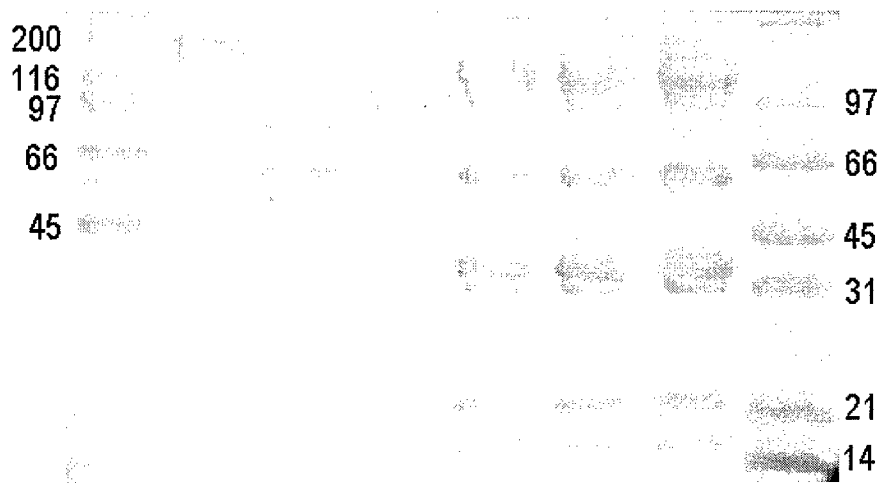


Fig. 3. Proteolysis of BoNT/A neurotoxin complex with Pepsin and α -chymotrypsin. **Lane 1:** High molecular weight markers. **Lane 2:** BoNT/A neurotoxin control. **Lane 3:** BoNT/A neurotoxin treated with pepsin for 20 min. **Lane 4:** BoNT/A neurotoxin treated with α -chymotrypsin for 20 min. **Lane 5:** BoNT/A neurotoxin complex control. **Lane 6:** BoNT/A neurotoxin complex treated with pepsin for 1 h. **Lane 7:** BoNT/A neurotoxin complex treated with α -chymotrypsin for 1 h. **Lane 8:** Low molecular weight markers.

The role of BoNT/E NAPs in heat resistance was examined by testing BoNT/E complex's ability to block norepinephrine release from PC12 cells, a system commonly used to assay BoNT-mediated blockage of neurotransmitter release (Lomneth et al., 1991, Banerjee et al., 1996; Fu et al., 1998). Pure BoNT/E in its native form (unheated) reduced the norepinephrine release from 58 % to 21%, whereas pure BoNT/E at 58 °C for 15 min blocked norepinephrine release to only 53 %. Unheated BoNT/E complex blocked the norepinephrine release from 58 to 20 %. More interestingly, BoNT/E complex heated at 58 °C for 15 min was still able to block norepinephrine release to 33 %, clearly suggesting a protective role of BoNT/E NAPs against heat denaturation of BoNT/E. The protection of BoNT/E by NAPs against heat could be mediated either by resistance against temperature-induced unfolding of BoNT/E or by promoting the refolding of the unfolded BoNT/E. We examined this issue

with recording temperature-induced unfolding of BoNT/E and BoNT/E complex by monitoring circular dichroism (CD) signal at 222 nm (**Fig. 4**). The mid point unfolding temperature for pure BoNT/E was 52 °C whereas for BoNT/E complex, it was 68 °C. At 58 °C, the temperature used for heating BoNT/E and BoNT/E complex to test the effect of heat-induced denaturation on their ability to block norepinephrine release in PC12 cells, BoNT/E complex barely showed any indication of unfolding (**Fig. 4**). However, there was some loss in BoNT/E complex's neurotransmitter blockage ability (~45%) after being heated at 58 °C. Such a loss could result from tertiary structural alterations of BoNT/E not detectable by 222 nm CD signal. It is notable though that irrespective of the molecular mechanism of protection BoNT/E appears to a large extent functionally stable even at 58 °C.

An intriguing observation was made during our experiments of BoNT/E and BoNT/E complex mediated blockage of norepinephrine release from PC 12 cells. BoNT/E complex was either equally or slightly more effective in blocking the neurotransmitter release (21 % vs. 20 % at a total protein concentration of 5 µg/ml. Noting that only 20% of BoNT/E complex consists of BoNT/E, it would amount to a five-fold enhanced activity of BoNT/E in its complex form. Since the BoNT/E concentration present in BoNT/E complex used was below saturation dose level (**Lomneth et al., 1991**), our conclusion of a 5-fold difference in the effectiveness of BoNT/E in its pure and complex form seems appropriate.

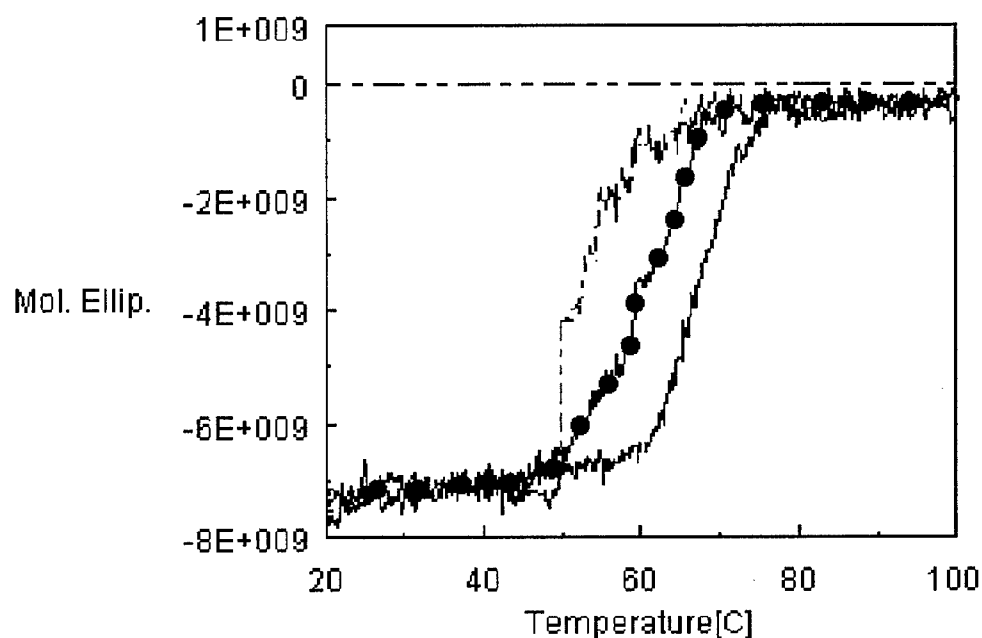


Fig. 4. Temperature denaturation analysis of BoNT/E neurotoxin L complex, BoNT/E neurotoxin M complex, BoNT/E neurotoxin. Protein concentration used for spectral recording was 0.2 mg/. The sample was heated from 20 to 100 °C at the rate of 2 °C/min. BoNT/E neurotoxin L complex (—), BoNT/E neurotoxin M complex (-●-), BoNT/E.

This observation suggests a role for BoNT/E NAPs beyond stabilization and protection of BoNT/E. The NAPs play an active role in enhancing the biological activity of BoNT/E. In PC12 cell system, BoNT/E or BoNT/E complex are introduced inside the cell by mechanical cracking (Lomneth et al., 1991).

Therefore, the higher effectiveness of BoNT/E complex in blocking the neurotransmitter release could arise at the level of its enzymatic cleavage of SNAP-25. We tested this hypothesis by analyzing the endopeptidase activity of BoNT/E and BoNT/E complex against SNAP-25, the known neuronal substrate of BoNT/E (schiavo et al; 1994). The endopeptidase activity was tested against a glutathione-s-transferase (GST)-SNAP-25 fusion protein. As shown in Fig. 5, BoNT/E complex was able to cleave >90% of SNAP-25 whereas pure BoNT/E catalyzed virtually no cleavage when it was not reduced by dithiothreitol (DTT). Even after reduction, pure BoNT/E cleaved significantly less amount of SNAP-25 than the BoNT/E complex. These results of BoNT/E NAPs-enhanced endopeptidase activity of BoNT/E are identical to BoNT/A NAPs-enhanced endopeptidase activity of BoNT/A (Cai et al., 1999). Such a similarity in NAPs-based enhancement in the endopeptidase activity of BoNT/E and BoNT/A support our conclusion that a specific large complex of BoNT/E and its NAPs exists similar to that of BoNT/A complex.

Analysis of the genomic organization of the BoNT/E gene with respect to the genes for BoNT/E NAPs was carried out by designing primers based on the N-terminal amino acid sequences of BoNT/E NAPs including the NBP (Li et al., 1998), a protein whose genes are located next to the BoNT/E gene in the upstream region. So far, we have located the genes for 18 kDa and 80 kDa protein along with the direction of their transcription (Fig. 6). During this process, we also discovered the presence of a 48 kDa protein gene upstream to the NBP gene, with a gap of 18 bp (Li et al., 1998). The partial genomic

organization of BoNT/E, NBP and other BoNT/E NAPs is similar to the genomic organization of other BoNTs and their NAPs (East et al; 1994; Hauser et al., 1994; Li et al., 1998). Although we have not located the genes for the 60 and 40 kDa protein as yet we suspect that they are located next to the 80 kDa protein gene.

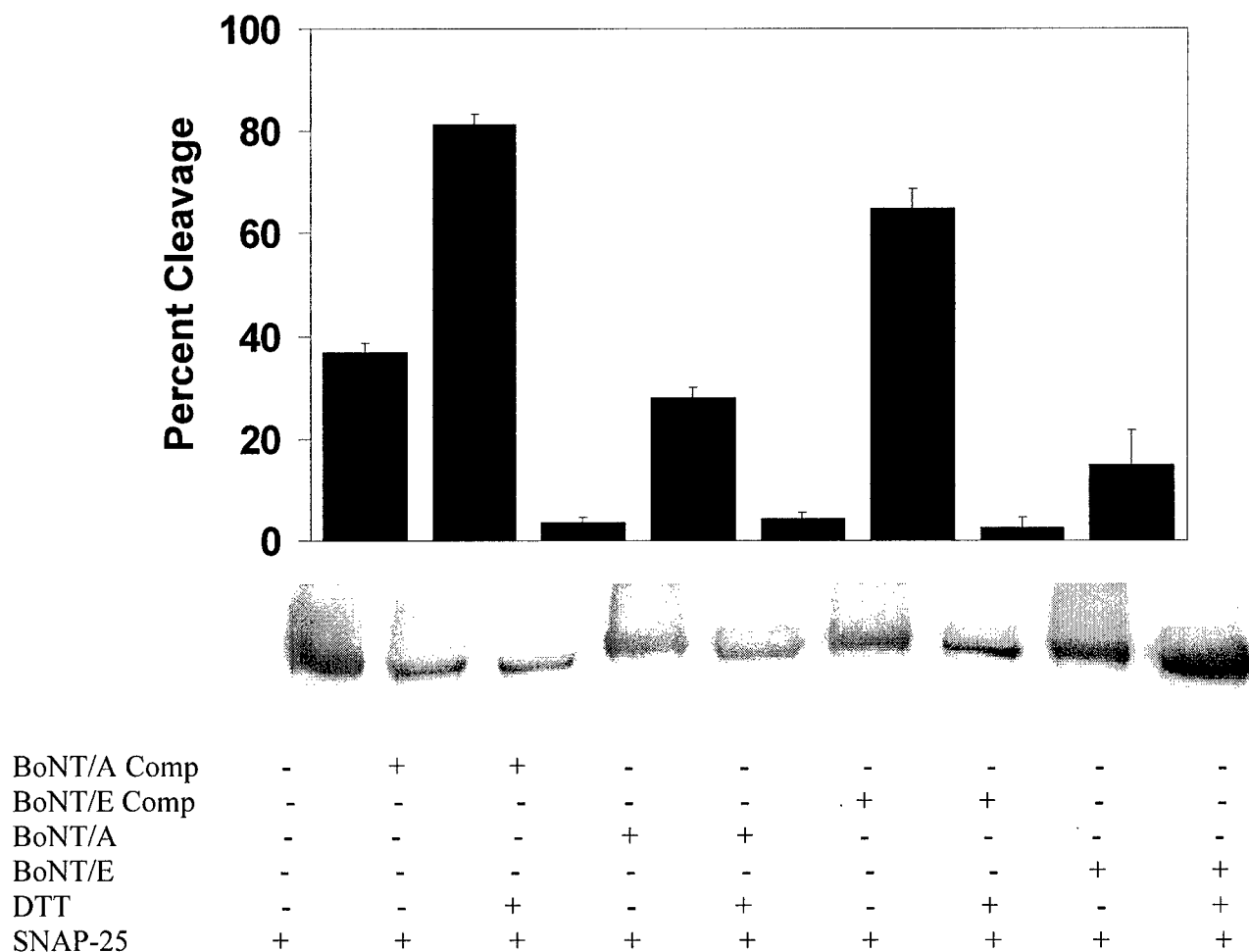


Fig. 5. Comparative analysis of endopeptidase activity of BoNT/A neurotoxin complex and BoNT/E neurotoxin complex. GST-SNAP-25 fusion protein (6 μ M) was incubated either with pure BoNT/A neurotoxin complex (200 nM) or BoNT/E neurotoxin complex (200 nM) for 30 min. at 37 $^{\circ}$ C in assay buffer. Samples were then separated by 12% sodium dodecyl sulfate polyacrylamide gel electrophoresis (SDS-PAGE) and were analyzed by Western blot using a polyclonal antibody raised against the C-terminal 12 amino acid residues of SNAP-25 (Stressgen Biotechnologies Corp., Victoria, Canada) as detailed under methods.

The genomic organization of BoNT and its NAPs present at least three intriguing features. (a) Genes of a BoNT and its NAPs are clustered in the same region of the chromosomal segment (b) Genes for NAPs

are present upstream to the BoNT genes. (c) Genes of BoNT and some of the NAPs are so closely located that they could be transcribed as a polycistronic message. Clustering of genes of BoNT and NAPs could also suggest a closely regulated expression of these genes to form the complex. An upstream location of NAP genes could indicate expression of these genes prior to the BoNT gene. An early expression of NAP genes will be expected if they were to play any role in the proper folding of the BoNT during its biosynthesis and the complex formation. The likely polycistronic nature of BoNT and NAP genes provides perhaps one of the strongest evidence of close biological relationship between BoNT and NAPs. BoNT/E and its NAPs appear to exist genetically similar to other serotypes of *Clostridium botulinum*. In summary, the existence of a unique BoNT/E complex is supported by (1) its isolation from the bacterial culture, (2) the molecular size determined by size exclusion chromatography and dynamic light scattering, which roughly corresponds to cumulative molecular weights of the different components of the complex, (3) functional role of NAPs in protecting the BoNT/E against proteases and heat denaturation, (4) dramatic activation of BoNT/E endopeptidase activity by its NAPs, and (5) genomic organization of BoNT/E and BoNT/E NAPs.

Implications of the existence of 'large' BoNT/E complex similar to the complexes of BoNT/A and other BoNT serotypes extends beyond the mere presence of NAPs in BoNT/E complex. It augers perhaps the beginning of an exploration to understand the role and mode of NAPs in the toxicogenesis of the botulism disease. One of the major reasons for why in the past implications of NAPs in *C. botulinum* have been ignored was the perceived absence of such proteins in strains producing type E and type F botulinum neurotoxins. The complex form of BoNT is critically important for its food poisoning manifestation as the ingestion of only the complex form retains the toxic activity of BoNT (Sakaguchi, 1983). Previous analysis of BoNT/E complex structure had revealed only a 'M' (medium) complex containing the BoNT/E and its NBP (Sakaguchi, 1983; Singh et al., 1995). The oral toxicity of the 'M' complex although higher than pure BoNT/E was much less than that of the L complexes of other BoNT serotypes.

of the BoNT, design of deterrence against *Clostridium botulinum* agents based on BoNT NAPs will also be possible.

Finally, neurobiological research to understand the mechanism of exocytosis has greatly benefitted from BoNT's specificity and accuracy in targeting intracellular neuronal proteins involved in docking and fusions of synaptic vesicles with plasma membrane. The availability of BoNT/E complex with its NAPs-mediated enhanced endopeptidase activity is likely to provide an extra tool of discovery in neuronal exocytosis process. BoNTs are the only known toxins which act on the intracellular targets of presynaptic end of a neuronal cell.

Project I (Unpublished)

Effect of Ganglioside on the Polypeptide Folding of Botulinum Neurotoxin Type E, Its Complex, and Light Chain as Probed by Proteolytic Degradation

At present it is widely accepted that while botulinum neurotoxins find their way to get in plasma membranes, they may first approach lipid receptors on the membrane, upon which their conformation is modified, enabling them to subsequently bind to the protein receptor(s) and finally enter into the membrane to become toxic. However, what kind of role lipid receptors play exactly in this process remains unclear. Thorough understanding of the mechanism is useful for blocking the entry of botulinum toxins into nerve cells, which probably leads to the development of effective vaccines.

The idea of this research is that, if there is any interaction between the toxin and lipid receptors, as per the forementioned presumption, the polypeptide folding of the former is most probably altered. As a result, some embedded amino acids may become exposed and vice versa. When subjected to proteases, the availability of different cleavage sites may vary due to the change of conformation, giving rise to altered cleavage profile. To test this idea, *Clostridium botulinum* neurotoxin E (BoNT/E) and its complex were exposed to trypsin, a protease that is commonly seen in gastrointestinal (GI) tract. Type E neurotoxin complex (TENC) differs from

BoNT/E in that the former consists of not only BoNT/E but also five neurotoxin associated proteins (NAPs) that protect the toxin from harsh environment (**Please see section E of this report**). Cleavage profiles were obtained from SDS-PAGE. Comparison between the cleavage profiles of BoNT/E and TENC helps to understand the function of NAPs during the entry of toxin into the plasma membrane. Ganglioside G_{T1b} was used as a representative of the lipid receptors at nerve cell membrane. Two different levels of ganglioside (toxin/complex:ganglioside=1:1 and 1:100) was applied to investigate if they have any influence on the cleavage profile of BoNT/E and TENC. The effect of different incubation conditions with ganglioside, i.e., incubation temperature (room temperature or 37°C) and time (1 hr or overnight), on trypsin cleavage was also studied.

Cleavage of BoNT/E and TENC by trypsin

The cleavage profiles of BoNT/E and TENC are shown in **Fig. 1**. A band at 150 kDa is observed for BoNT/E. Within 30 min of the addition of trypsin (25:1, w/w), two very thin bands were observed at about 100 and 50 kDa, respectively. The two bands became very solid in 90 min of the proteolytic reaction, demonstrating that BoNT/E was cleaved by trypsin into 2 subunits of approximately 100 and 50 kDa.

As expected, more bands were seen for TENC due to the existence of NAPs (neurotoxin associated proteins; **Fig. 1; Singh et al., 2004**). The bands almost remained the same within 60 min, indicating that the toxin associated by other proteins was hardly cleaved by the trypsin. This confirms that NAPs are able to protect botulinum toxins from the digestion of GI tract proteases.

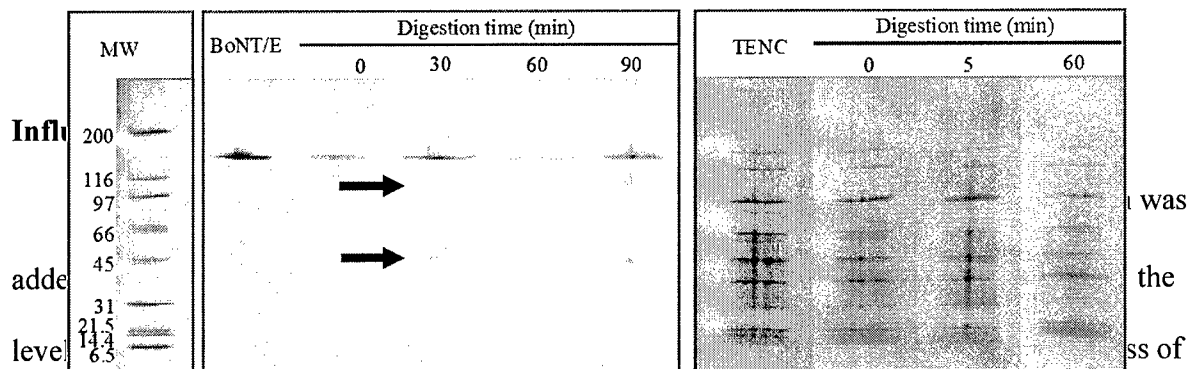


Fig. 1. Cleavage of BoNT/E and TENC by trypsin at room temperature. MW, molecular weight; BoNT/E, botulinum neurotoxin type E and TENC, type E neurotoxin complex.

the bands of subunits increased with the amount of ganglioside applied and the time of incubation. After overnight incubation with G_{T1b} at a 1:100 ratio, the band of BoNT/E was hardly visible (Fig. 2, lower panel). The cleavage by trypsin (25:1, w/w) resulted in the formation of additional bands.

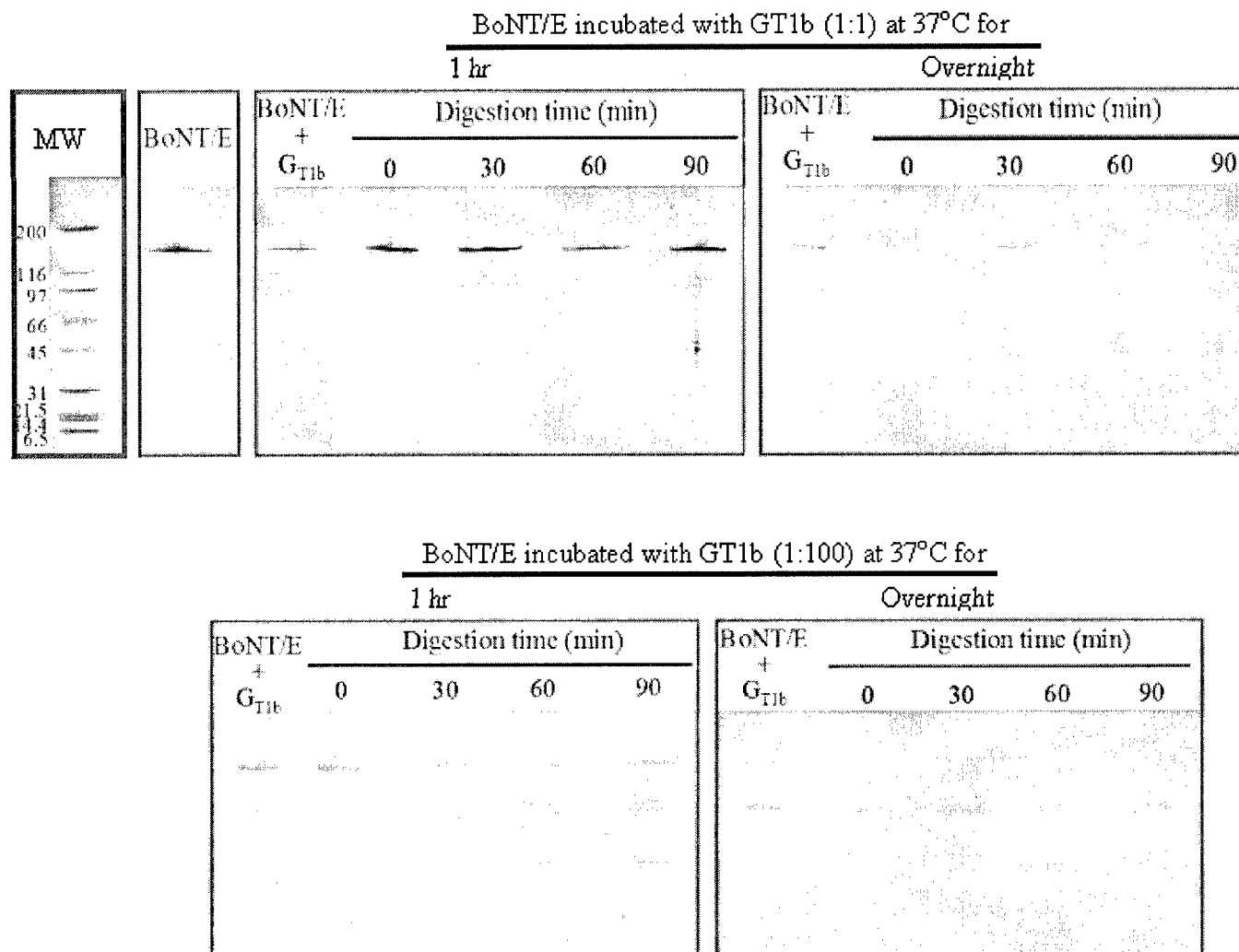


Fig. 2. Cleavage of BoNT/E incubated with ganglioside G_{T1b} at ratios of 1:1 and 1:100.

Comparing **Figs. 1 and 2**, it is obvious that the cleavage pattern of BoNT/E by trypsin was altered with the presence of ganglioside, most probably due to the conformational change.

No significant influence of G_{T1b} was observed on the digestion of TENC, regardless of the concentration of G_{T1b} (**Fig. 3**). Experiments were also carried out at room temperature for 1 hr or overnight (results not shown). However, none of these incubation conditions seemed to change the cleavage pattern of TENC.

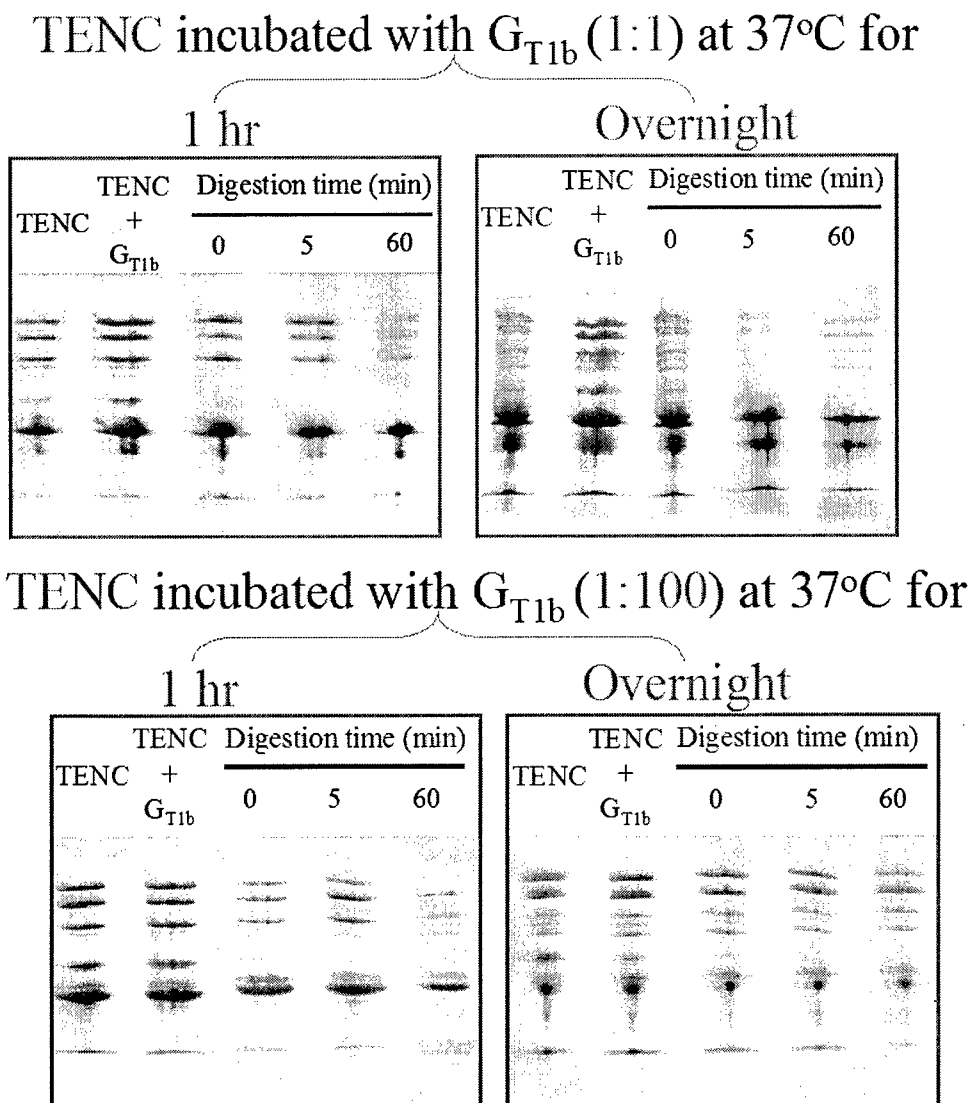


Fig. 3. Cleavage of TENC by trypsin (25:1, w/w) with and without incubation with G_{T1b} (either for 1 h or overnight) before treatment with the trypsin.

Cleavage of light chain E (LCE)

As can be seen in **Fig. 4**, LCE forms a major band at 46 kDa, with minor bands are 30, 26, and 13 kDa. Its cleavage by trypsin occurred within 30 min as indicated by the appearance of more bands at 41, 32, and 23 kDa. The bands at 46 and 13 kDa are dramatically reduced (**Fig. 4**). The incubation of LCE with G_{T1b} at a ratio of 1:1 at 37°C for 1 hr seems to result in bands of slightly different molecular weight. However, this is just a preliminary data, and further work is necessary to confirm these observations.

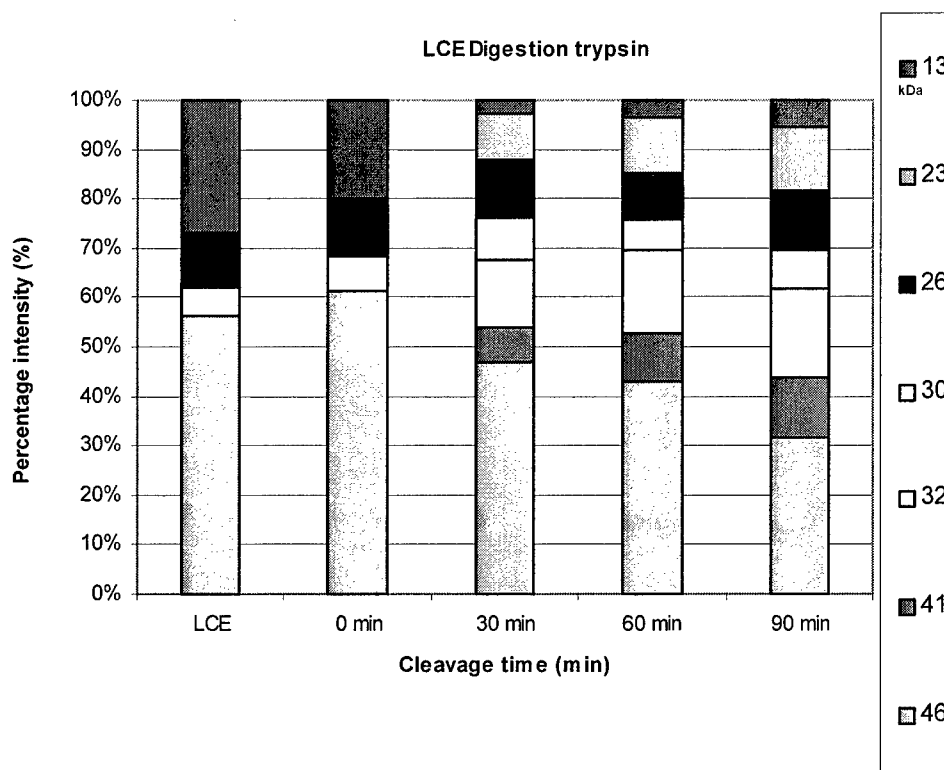


Fig. 4. Polypeptide bands of BoNT/E light chain (LCE) analyzed on SDS-PAGE before and after proteolytic cleavage by trypsin for different periods of time.

Incubation of LCE with $GT1b$ for one hour introduced substantial changes, as monitored by altered proteolytic patterns. Incubation of LCE with $GT1b$ in itself resulted additional polypeptide fragments at 33 and 21 kDa (**Fig. 5**). Incubation with trypsin (25:1, w/w) resulted in additional bands at 42, 33 and 24 kDa, which are similar to those observed upon trypsinization of

LCE alone (**Fig. 4**). In contrast to LCE alone, however, trypsinization of LCE after incubation with GT1b, digested the 46 kDa band completely within 90 min, and the band observed at 42 kDa at 30 and 60 min was also digested at 90 min. Furthermore, the band at 17 kDa (which we believe is the same as the 13 kDa band in **Fig. 4**) was largely retained even after 90 min of digestion.

The above observations of differential proteolytic fragmentation of LCE with trypsin in the presence and absence of GT1b incubation suggest that L chain of BoNT might be directly interacting with the lipids, including the secondary putative receptor, GT1b. L chains have been previously shown to directly interact with lipids (**Montecucco et al., 1988; Kamata and Kozaki, 1994; Fu et al., 2002**), and a direct interaction with the GT1b may be relevant for the binding and translocation of BoNT into nerve cells.

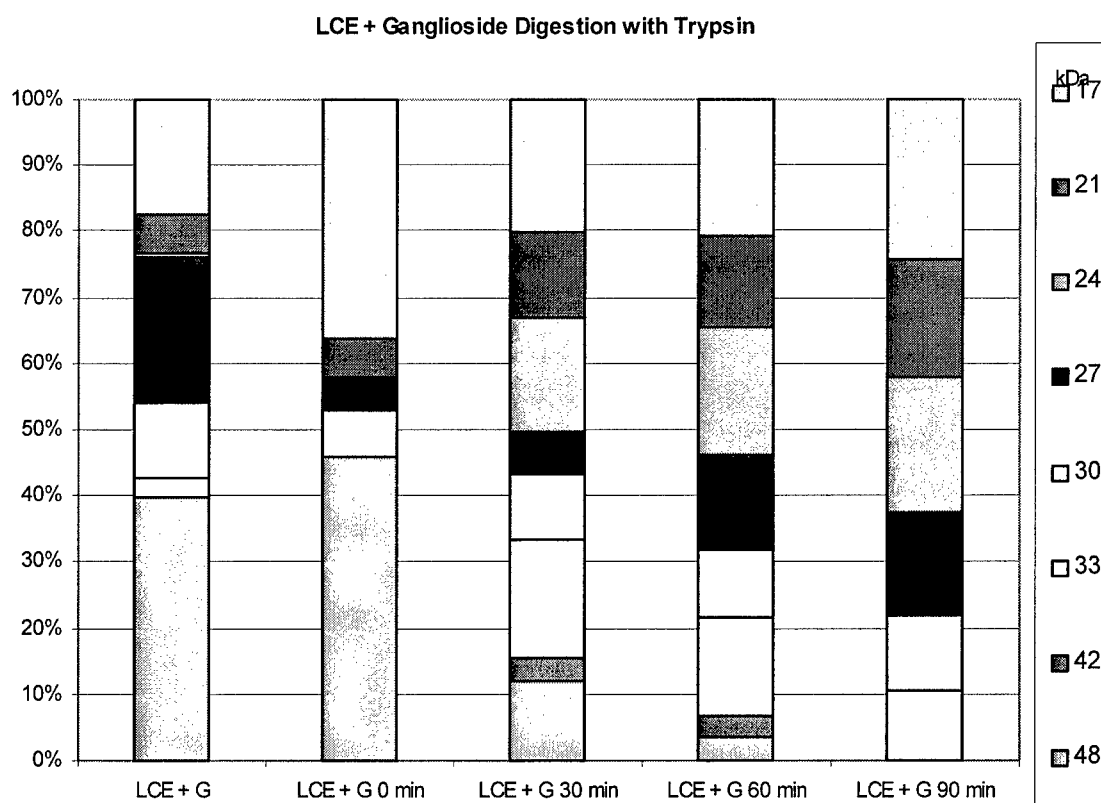


Fig. 5. Polypeptide bands of BoNT/E light chain (LCE) before and after incubation with 1:1 (mole:mole) GT1b for 1 hour at 37 °C. The bands were analyzed on SDS-PAGE before and after proteolytic cleavage by trypsin for different periods of time.

Conclusions and Future work

Current results show the cleavage pattern of BoNT/E was affected by the presence of ganglioside as compared with negative control. Similar effect of ganglioside also seems to apply to LCE, the confirmation of which is needed in future work. These observations provide evidence in regard to the interaction between botulinum neurotoxin and ganglioside, which probably occur while the toxin binds to plasma membrane. To further the understanding of the binding process, different proteases with diverse cleavage sites should be included. Various speciality of different types of proteases may help narrow the regions where conformational changes take place in the toxin molecules. Since the heavy chain of botulinum neurotoxin is generally considered as the binding site when the toxin docks on the membrane, attempts would also be made to compare the cleavage pattern of heavy chain with that of toxin and light chain. This information obtained will be of great importance in finding out the binding site and mechanism of botulinum neurotoxin on neural cell membrane, thus enable the protection of neural cells from botulinum toxin.

References

- Fu, F.-N., Busath, D. D. and Singh, B. R. (2002) Spectroscopic Analysis of Low pH and Lipid induced structural changes in Type A Botulinum Neurotoxin Relevant to Membrane Channel Formation and Translocation. *Biophysical Chemistry* 99, 17-29.
- Kamata, Y., and Kozaki, S. (1994) The light chain of botulinum neurotoxin forms channels in a lipid membrane *Biochem. Biophys. Res. Commun.* 205, 751-757.
- Montecucco, C., Schiavo, G. Gao, Z., Banerlein, E., Bouquet, P. and Dasgupta, B. R. (1988) Interaction of botulinum and tetanus neurotoxins with the lipid bilayer surface. *Biochem. J.*, 259, 47-53.

Project J (Accepted for publication in Protein Expression and Purification, 2005)

Cloning, Expression and Purification of C-quarter of the Heavy Chain (HCQ) of Botulinum Neurotoxin Type A (BoNT /A)

Abstract

Botulinum neurotoxins (BoNTs) are highly potent toxins that inhibit neurotransmitter release from peripheral cholinergic synapses. BoNTs consist of a toxifying light chain (LC; 50 kDa) and

a binding/translocating heavy chain (HC; 100 kDa) linked through a disulfide bond. The complete sequence of BoNT/A consists of 1,296 amino acid residues. The β -trefoil domain for BoNT/A to which gangliosides bind starts at Ser 1092 and this fragment represents the C-half of the C-terminus of the heavy chain (C-quarter HC or HCQ). The recombinant HCQ DNA was successfully cloned into an expression vector (pET15b) which was used to transform *Escherichia coli* strain BL21-StarTM (DE3) for expression. Expression of HCQ was obtained by an extended post-induction time of 15 h at 30 °C. The recombinant histidine tagged HCQ protein was isolated and purified by Nickel affinity gel column chromatography and its molecular weight was verified by gel electrophoresis. The HCQ was positively identified by antibodies raised against BoNT/A employing immunological dot-blot and Western blot assays. HCQ was shown to bind with synaptotagmin (a known BoNT/A receptor) and gangliosides, indicating that the expressed and purified HCQ protein retains a functionally active conformation.

Introduction

Botulinum neurotoxins (BoNTs) are a family of seven structurally and pharmacologically similar but antigenically different proteins produced by different strains of *Clostridium botulinum* (1-3). These proteins are the most toxic substances known, and are the cause of flaccid paralysis in botulism. BoNTs are produced as 150 kDa single-chain polypeptides which are nicked into a 100 kDa heavy chain and a 50 kDa light chain each, linked through a disulfide bond. The heavy chain (HC) is mainly involved in the cell-binding, internalization, and translocation of the BoNT into nerve cells, whereas the light chain (LC) exhibits the intracellular toxic activity (4). The carboxyl terminal portion of the HC is responsible for binding with nerve cell receptors (5). Following binding to the cell surface, the neurotoxin is brought into the endosomal compartment by internalization via receptor mediated endocytosis. The LC gets partially unfolded at low endosomal pH to get across the membrane into cytosol, where it acts as an endopeptidase against one or more of the three SNARE (soluble NSF attachment protein

receptor) proteins: SNAP-25 (synaptosomal associated protein of 25 kDa), syntaxin or VAMP/synaptobrevin (6,7). The cleavage of any of the SNARE proteins prevents the fusion of synaptic vesicles containing acetylcholine, thus blocking the neurotransmitter release (8) that results in the flaccid muscle paralysis.

The carboxyl-terminal domain, referred to as the H_C-fragment, mediates the highly specific binding of clostridial neurotoxins to nerve terminals at the neuromuscular junction through gangliosides and a protein receptor(s) (9). The N-terminal domain of H_C (H_{CN}) has been speculated to bind with a protein receptor (10-12) whereas the C-terminal domain of H_C (H_{CC}) or HCQ domain has been shown to provide sites for binding with gangliosides (13). The amino terminal half of HC (H_N-domain) provides the translocation apparatus for the delivery of the LC from the endosome into the cytosol. According to the crystal structure analysis of the BoNT/A, the H_C clearly consists of two distinct domains (H_{CN} and H_{CC}) (14). The H_{CC} domain (HCQ) starts at Ser 1092 and theoretically its molecular weight is a quarter of the HC (15, 16). The HCQ fragment in its isolated purified form can enable one to study its interactions with receptors of BoNT/A, and to design binding inhibitors to prevent the neurotoxic action.

Receptor-binding domains of clostridial neurotoxins are receiving more attention in recent years for the development of a number of applications including neuronal targeting. Such molecules clearly have a potential application in the treatment of a range of neurologic conditions (17, 18). The binding domain of the HC, which is a nontoxic fragment, can also be used as a potential candidate for the development of therapeutics and diagnostics. In fact, the HCQ fragment of BoNTs seems to be a promising tool in the search for potential vaccines and immunogens (19-22).

In this study, we present results of cloning, expression and purification of the HCQ fragment in order to study its binding characteristics that might enable identification of the

receptors for BoNT/A. The purified HCQ reacted positively with antibodies raised against BoNT /A and also bound to gangliosides and synaptotagmin.

Materials and Methods

Restriction endonucleases and DNA modifying enzymes were purchased from New England Biolabs Inc. (Beverly, MA). All oligonucleotides were synthesized by Integrated DNA Technologies Inc. (Coralville, IA). Eppendorf-Netheler-Hinz GmbH (Hamburg, Germany) thermal cycler (Model-Mastercycler personal) was used for polymerase chain reaction (PCR) experiments. The recombinant plasmid DNA pET 15b encoding the heavy chain of BoNT/A (pET 15b-HCA) was obtained as described previously by Li and Singh (23). The reagents used in all the experiments were of analytical grade. Nuclease free water was used from Ambion Inc. (Austin, TX).

Plasmid DNA Preparation

The plasmid DNA was isolated using S.N.A.P (Simple Nucleic Acid Prep) – a Miniprep Kit supplied by Invitrogen Life Tech (Carlsbad, CA) from *E.coli* strain BL21-Codon Plus (DE3)-RIL (Stratagene, La Jolla, CA). The *E. coli* strain containing two plasmids pACYC and pET15b-HCA (encoding the heavy chain of BoNT/A) was prepared as described previously (23). The heavy chain fragment (pET15b-HCA) was cleaved using restriction enzymes Nde I and BamH I, and then electrophoresed on a 1.0% agarose gel. The DNA of plasmid pET-15b contained the heavy chain insert (Nde I-Bam HI fragment) which was extracted using QIAquick Gel Extraction Kit (Qiagen Inc, Chatsworth, CA) and used as a template for PCR.

Primer design and Polymerase Chain Reaction

Polymerase Chain Reaction was performed to generate a DNA fragment encoding the C-half of the C-terminus of the Heavy chain of BoNT/A. Both Nde I and Bam HI restriction sites were incorporated into the 5' end of the forward sequence and reverse sequence primers,

respectively. PCR reactions were performed in a total volume of 50 μ L containing 200 ng of template DNA, 100 ng of each primer, 200 μ M of each dNTP (deoxy-nucleoside triphosphate), 1 U Vent polymerase (New England Biolabs, Beverly, MA) and nuclease free water to adjust the total volume. The reaction mixture was denatured for 2 min at 93 $^{\circ}$ C, then subjected to 30 consecutive cycles consisting of denaturation (1 min at 93 $^{\circ}$ C), annealing (1 min at 60 $^{\circ}$ C) and polymerization (1 min at 73 $^{\circ}$ C).

According to BoNT/A sequence in GenBank data-base under accession no. M30196 (15), primers for heavy chain binding domain were designed. 5'-GGGCCCC CAT↓ATG TCA AAT TCA GG-3' was the sense primer for BoNT/A HCQ. The antisense primer sequence used was 5'- GGGCCCC GGA↓TCC TTA CAG TGG CCT TTC T-3'. An expected size (615 bp) band was purified by agarose gel electrophoresis, digested with restriction enzymes Bam HI and Nde I and ligated with predigested (restriction enzymes Bam HI and Nde I treated) vector pET15b. An aliquot of the ligation mixture was used to transform *E. coli* strain BL21-StarTM (DE3). The *E. coli* cells were plated on LB-ampicillin (50 μ g/mL) agar plates and the transformants were verified to contain the HCQ by Plasmid DNA isolation and agarose gel electrophoresis.

DNA Sequencing

The recombinant plasmid DNA containing the HCQ gene was sequenced with a 3730xl DNA Analyzer (Genewiz Inc, North Brunswick, NJ) using Big Dye Terminator v3.1 cycle sequencing kit, provided by Applied Biosystems (Foster, CA).

Expression of Recombinant BoNT /A HCQ

The HCQ fragment of BoNT/A was cloned with the His₆ – tag at the N-terminal and expressed under the control of the T7 promoter. The pET15b–HCQ recombinant plasmid was transformed into *E. coli* strain BL21-Star (DE3) and inoculated into a 50-mL aliquot of 2YT medium. The culture was grown under agitation overnight at 37 $^{\circ}$ C, and was stored as a glycerol stock in aliquots at -80 $^{\circ}$ C. Frozen glycerol stock (1.0 mL) was used to inoculate 100 mL of 2YT

medium containing 50 µg/mL ampicillin (RPI Corp, Mount Prospect, IL) at 37 °C. When the optical density (O.D) at 600 nm was approximately 0.6, the 100-mL culture was transferred into 1L 2YT medium containing 50 µg/mL ampicillin in a 4-L flask, and the culture was grown at 37 °C until the O.D at 600 nm reached 0.8. IPTG (Isopropyl-β-D-Thiogalactopyranoside, RPI Corp, Mount Prospect, IL) was then added to a final concentration of 1.0 mM, and the induction was allowed to proceed at 30 °C for 15 h. The *E. coli* cells were harvested by centrifugation at 8000 x g for 10 min at 4 °C using SLA 1500 rotor and Sorvall RC-5B refrigerated superspeed centrifuge (Du Pont Instruments, Wilmington, DE). The cell pellet was stored at -80 °C till protein isolation.

HCQ Protein Isolation and Purification

The HCQ protein being a component of heavy chain is insoluble and is expressed in the form of inclusion bodies. The protein isolation method consisted of isolation and purification of the inclusion bodies from the cell pellet by following a chemical lysis procedure. The frozen cell pellet was thawed and resuspended in a lysis buffer, CelLytic™ B II (Sigma, St. Louis, MO; 20 mM Tris-HCl, pH 7.5, and a mild nonionic detergent), at the ratio of 5 mL of lysis buffer per gram of wet cell paste. After complete resuspension of cell pellet, 5 µg/mL deoxyribonuclease I and protease inhibitor cocktail (Sigma, St. Louis, MO), containing 4-[2-Aminoethyl]benzenesulfonyl fluoride hydrochloride (AEBSF), aprotinin, leupeptine, bestatin, pepstatin A and trans-Epoxy succinyl-L-Leucylamido-[4-Guanidino]Butane (E-64) was added to the suspension at a ratio of 1 mL for 20 g wet cell paste. The suspension was incubated at 25 °C for 15 min to fully extract the cells, and centrifuged at 25,000 x g using SS-34 rotor in a Sorvall RC-5B refrigerated superspeed centrifuge (Du Pont Instruments, Wilmington, DE) for 15 min to pellet the insoluble material. The supernatant was collected and analysed by sodium dodecyl sulphate- polyacrylamide gel electrophoresis (SDS-PAGE). The pellet was resuspended further in the lysis buffer, and lysozyme with a final concentration of 0.4 mg/mL was added to the

suspension. The mixture was incubated at 25 °C for 15 min, and 20 mL of 1:20 diluted lysis buffer was added. The lysis buffer was diluted using deionised water. The suspension was incubated at 25 °C for 15 min and centrifuged at 25,000 x g for 15 min. The supernatant was removed and the inclusion bodies containing pellet was resuspended in 40 mL of 1:20 diluted lysis buffer, and the extract was centrifuged at 25,000 x g for 15 min. The pellet containing remaining inclusion bodies was processed through two more cycles of resuspension and centrifugation to obtain purified inclusion bodies in the final pellet, which were then stored at -80 °C.

The frozen inclusion bodies extracted from 1L culture were thawed and resuspended in 25 mL of 0.1 M sodium phosphate buffer, pH 8.0, containing 6 M guanidine-HCl, 0.4 M NaCl and 10 mM β -mercaptoethanol. Protease inhibitor cocktail was added to the suspension at a ratio of 1 mL for 20 g wet weight cell paste, and the suspension was kept on a rocker for 1 h at 25 °C. The extract was then centrifuged at 100,000 x g using AH-629 rotor in a Sorvall ultracentrifuge OTD55B (Du Pont Instruments, Wilmington, DE) for 1 h at 4 °C. The supernatant was diluted 1:1 with equilibration buffer (EB, 8 M Urea, 0.4 M NaCl, 5 mM imidazole, 10 mM β -mercaptoethanol in 0.1 M sodium phosphate, pH 8.0). The mixture was then loaded onto a His-Select nickel affinity gel (Sigma, St. Louis, MO) column (dimension 1 x 22 cm; 2 mL bed volume) which was previously equilibrated with EB. The column was washed with 20 mL EB, then with 20 mL of EB containing 20 mM imidazole and 8 M urea without β -mercaptoethanol. The protein was then eluted with step gradient of 20, 30 and 100 mM (5 mL each) imidazole dissolved in 0.1 M sodium phosphate buffer, pH 8.0, containing 0.4 M NaCl, 0.1% dodecylphosphocholine (DPC, Avanti Polar lipids, Alabaster, AL) and urea was subsequently removed in this step.

Isoelectric focusing

Isoelectric focusing (IEF) was performed using the Phast System (Pharmacia Biotech; Piscataway, NJ). Briefly, an aliquot of 5 μ L of HCQ (0.3 mg/mL) was loaded on the IEF gel along with prestained standards (pI 4.5-9.6, BioRad, Hercules, CA). The electrophoresis was carried out at 200 V and 2 mA at 15 $^{\circ}$ C for 15 vh, and the focusing was carried out at 2000 V and 5 mA at 15 $^{\circ}$ C for 410 vh. The gel was fixed with 20% trichloroacetic acid for 5 min and rinsed with the destaining solution (30% methanol, 10% acetic acid) for 2 min. The gel was then stained with 0.02% PhastGel Blue R (Pharmacia Biotech, Piscataway, NJ) in the destaining solution containing 0.1% CuSO₄ to decrease the background staining, and destained until the background became clear. The pI of HCQ was calculated using a calibration curve of standard proteins.

Determination of Protein Concentration

The concentration of proteins used in the experiments were determined spectrophotometrically by measurement of their absorbance at 280 and 235 nm using the formula: concentration of protein (mg/mL) = (A_{235nm}-A_{280nm})/2.51 (24).

Immuno-dot-blot assay of HCQ

Immunological dot-blot assay was employed to confirm the heavy chain fragment affinity and specificity with rabbit antibody (IgG) raised against BoNT/A (BBTech Inc., Dartmouth, MA). BoNT/A complex was purified as described previously (25). Three microlitres of HCQ sample (0.1 mg/mL), BoNT/A complex (0.1 mg/mL), BoNT/A heavy chain (0.1 mg/mL) or BSA (0.1 mg/mL, bovine serum albumin, Sigma) were spotted on a transblot transfer medium pure nitrocellulose membrane (0.45 μ M, BioRad Corp, Hercules, CA). The membrane was dried and incubated in the blocking buffer, with gentle shaking for 1h at 25 $^{\circ}$ C, and then incubated with 1:1000 dilution of rabbit anti BoNT/A IgG (BBTech, Dartmouth, MA). The membrane was washed with PBST (phosphate buffered saline, containing 0.05% Tween 20) three times and then incubated in a 1:30,000 dilution of secondary antibody goat anti-rabbit BoNT/A IgG conjugated with alkaline phosphatase (Sigma, St. Louis, MO), for 1 h at 25 $^{\circ}$ C. The colorimetric detection

was carried out by using BCIP (5-bromo-4-chloro-3-indolyl-phosphate) and NBT (Nitroblue tetrazolium, Sigma) as substrates, after washing the membrane three times with PBST.

Western-blot analysis of HCQ

The identification of the expressed protein was carried out by Western blot analysis. Kaleidoscope prestained standards (BioRad, Hercules, CA) were used as molecular weight marker). Purified HCQ from SDS-PAGE was transferred to nitrocellulose membrane (0.2 μ M, Pierce Biotech, Rockford, IL) by using Trans-Blot semi dry electrophoretic cell (BioRad, Hercules, CA) and transfer buffer (39 mM glycine, 48 mM Tris-base, 0.037% SDS, and 20% methanol). The membrane was incubated in the blocking buffer (3% BSA in phosphate buffered saline or PBS), with gentle shaking for 1h at 25 $^{\circ}$ C, and the remaining procedure was followed exactly as described for immunological dot-blot assay.

Binding Activity

Synaptotagmin Binding

Immunological dot blot assay was also employed to examine the binding activity of the purified BoNT/A HCQ protein to synaptotagmin II, a known receptor for BoNT/A (12). Recombinant synaptotagmin II protein was obtained as described earlier by Zhou and Singh (26). Three microliters each of BoNT/A complex (0.1 mg/mL), HCQ (0.1 mg/mL), or BSA (0.1 mg/mL) were spotted on a trans-blot transfer medium pure nitrocellulose membrane (0.45 μ M). The membrane was incubated with a blocking buffer (3 % BSA in PBS), with gentle shaking for 1 h at 25 $^{\circ}$ C, and then incubated with synaptotagmin II (0.1 mg/mL) in the blocking buffer with gentle shaking for 2 h at 25 $^{\circ}$ C. The membrane was washed three times with PBST and then incubated with a 1:1000 dilution of mouse anti-synaptotagmin antibody (StressGen Biotechnologies, Victoria, BC, Canada), dissolved in the blocking buffer, with gentle shaking for 1 h at 25 $^{\circ}$ C. The membrane was washed again three times with PBST, and incubated with a 1:5000 dilution of goat anti-mouse IgG alkaline phosphatase conjugate (Novagen, Madison, WI)

dissolved in the blocking buffer, with gentle shaking for 1 h at 25 °C. The colorimetric detection was carried out by using BCIP and NBT as substrates after washing the membrane three times with PBST.

Ganglioside Binding

Binding of the purified HCQ to gangliosides was performed following the procedure described by Zhou and Singh (26). Polystyrene-96-well flat-bottomed plate (Corning Glass works, Corning, NY) was used and the binding activity was analyzed by Enzyme Linked Immunosorbent Assay (ELISA). Eighty microliters of 3 mg/mL G_{T1b} (Sigma) dissolved in 20 mM sodium phosphate buffer, pH 8.0, was coated to each well and incubated at 4 °C overnight. The plate was then blocked by 1% BSA in PBS for 1 h at 25 °C, and washed four times with PBST. One hundred microliters of purified BoNT/A complex (0.1 mg/mL), HCQ (0.1 mg/mL), HCQ (0.2 mg/mL), BoNT/A heavy chain (0.1 mg/mL), or BSA (0.1 mg/mL) were added to different wells. The plate was incubated for 1 h at 25 °C on a rocker, and washed four times with PBST. One hundred microliters of 1:1000 dilution of rabbit anti BoNT/A IgG (BBTech, Dartmouth, MA) in 3 % BSA was added to each well and incubated for 1 h at 25 °C. One hundred microliters of 1:30,000 dilution of secondary antibody goat anti-rabbit BoNT/A IgG conjugated with alkaline phosphatase (Sigma) was added to each well after washing the plate four times with PBST, and incubating it for 1 h at 25 °C. The colorimetric detection was carried out using para-nitrophenyl phosphate (pNPP, Sigma), after washing the plate four times with PBST. The absorbance of each well at 405 nm was measured using a microplate reader (Molecular Devices, Sunnyvale, CA).

Results and Discussion

Construction of Recombinant His6-tagged BoNT/A HCQ

The plasmid DNA encoding BoNT /A heavy chain (23) was isolated and treated with restriction enzymes Nde I and BamH I. The digestion of the recombinant plasmid with restriction

enzymes resulted in DNA fragments of varying sizes on an agarose gel (data not shown). The 2.5 kb DNA fragment encoding 100 kDa BoNT/A HC was extracted from the gel and used as a template for PCR. According to the codon usage, high A + T content was found in BoNT/A HC. This resulted in addition of GC overhangs to the 5' ends of both the primers for HCQ after taking into consideration their GC/AT ratio. The amplification of BoNT/A HCQ region resulted in a DNA fragment of 615 bp (data not shown). The recombinant HCQ also contained a cluster of six histidine residues for purification of the recombinant protein by metal affinity chromatography. DNA sequencing result (not shown) confirmed the successful cloning of HCQ without any mutation. The expected molecular mass of HCQ (a quarter of approximately 100 kDa HC) is 23.4 kDa.

Expression and purification of His₆-tagged recombinant BoNT/A HCQ

The pET 15b-HCQ (BoNT/A) was transformed into *E.coli* strain BL21-StarTM (DE3) which has His₆ – tag at the N-terminal. HCQ protein expression was under the control of the T7 promoter and was induced by IPTG. The overexpression of HCQ results in the formation of insoluble proteins, called inclusion bodies. A previously described method by Zhou and Singh (26) was followed to isolate the protein from the inclusion bodies. The protein isolation and purification procedure was carried out at 4 °C to ensure that the protein is isolated with proper folding without any change in its conformation. When the cell pellet containing inclusion bodies was washed with lysis buffer, the first wash resulted in supernatant that contained a mixture of proteins (Fig. 1, lane 1). However, the purity of 25 kDa HCQ obtained in the supernatant at every wash step gradually increased, showing lesser contaminating bands on the gel (Fig. 1, lanes 2 and 3). Finally, pure HCQ protein (1.0 mg/mL) was obtained in the supernatants of the fourth and fifth washing steps (Fig. 1, lanes 4 and 5). The purity of the protein was examined using GEL LOGIC 100 Imager system and a KODAK 1 D v.3.6.1. Analysis system. The purified protein was determined to be 92% pure as assessed by SDS-PAGE. The presence of HCQ

protein in wash solutions suggested that it was expressed partly in soluble form or that inclusion bodies are only softly formed.

The HCQ protein was subsequently isolated from the inclusion bodies after treatment with guanidine-HCL and urea, and purified by affinity gel column chromatography. SDS-PAGE analysis of the eluents revealed the presence of 25 kDa protein as a major band in all the eluted fractions as shown in Figs. 2 and 3. A step gradient elution with 20, 30 and 100 mM imidazole was carried out to obtain pure HCQ protein. Eleven milligrams of His6-tagged HCQ (95% purity) was obtained from 1 L of the *E.coli* culture. The isoelectric focusing analysis of His6-tagged HCQ revealed an isoelectric point of 9.4. The calculated isoelectric point from amino acid sequence of His6-tagged HCQ is 9.49 (EMBL Isoelectric point service) and the calculated Molecular weight (MW) of the recombinant HCQ was found to be 24.2 kDa (Peptide calculator version 1.0, Evanston, IL). The isoelectric point was useful to determine the appropriate pH for the dialysis buffer which is vital to avoid precipitation during dialysis. Recombinant HCQ was dialyzed against 50 mM sodium phosphate buffer, pH 7.4, containing 0.1 M NaCl. The purified HCQ was stored in 20% glycerol solution at -80°C.

Immuno-dot-blot assay carried out with rabbit anti-BoNT/A showed a strong reaction with HCQ, albeit not as strong as with BoNT/A complex and BoNT/A heavy chain (Fig. 4). The negative control (BSA) showed no reaction. Thus the immuno-dot-blot analysis (Fig. 4) confirmed the identity of recombinant HCQ. Lower reaction of HCQ compared to BoNT/A HC and BoNT/A complex may reflect on the availability of higher number of epitopes in BoNT/A HC and BoNT/A complex to the antibody raised against BoNT/A.

The identity of HCQ was further confirmed by Western blot analysis. The 25 kDa HCQ showed positive reaction with rabbit IgG raised against BoNT/A (Fig. 5), confirming its identity with BoNT/A as expected.

Binding activity with synaptotagmin

In an effort to evaluate the functional state of the purified HCQ, binding of HCQ with synaptotagmin was determined by immuno-dot blot assay. Synaptotagmin II has been shown to bind strongly to BoNTs, including BoNT/A and is considered as a BoNT/A receptor at nerve cells (12). The result as shown in Fig. 6 clearly indicates binding of HCQ to synaptotagmin II similar to the positive control, BoNT/A complex. The negative control (BSA) showed no binding to synaptotagmin. These results suggests that the HCQ protein was isolated in its functionally active form and binds strongly to its putative receptor.

Binding activity with gangliosides

Gangliosides, especially G_{T1b} , are considered a component of the double- receptor system of BoNT (16). The first step in BoNT attachment to nerve membranes starts with binding of C-terminus of HC to gangliosides on presynaptic membranes. Ganglioside binding could facilitate interaction between toxin and its protein receptor by bringing them in close proximity, or cause a conformational change at the second receptor binding site (3), and is known to be mediated through the C-terminal end (HCQ) of the HC (6). Thus HCQ binding with G_{T1b} was examined to evaluate if the G_{T1b} binding capacity is retained in the recombinant HCQ purified in this study. The binding activity of gangliosides with HCQ was analyzed by ELISA. The results as shown in Fig. 7 indicate binding of the purified HCQ sample to ganglioside (G_{T1b}) similar to the positive controls, BoNT/A complex and BoNT/A heavy chain. BSA sample did not show any significant binding activity with G_{T1b} , suggesting that the binding of HCQ to gangliosides is specific. In addition, although to only limited extent, the two concentrations of HCQ used in binding with G_{T1b} , showed concentration-dependent binding, thus suggesting a specific binding of HCQ to G_{T1b} . Surprisingly, HCQ binding to G_{T1b} was much less than those of BoNT/A heavy chain and BoNT/A complex, suggesting either the role of other domains of

BoNT in HCQ binding with G_{T1b} , or a less than native folding of the HCQ expressed and purified. These issues need further examination.

Conclusions

Botulinum neurotoxins nerve intoxication mechanism is accomplished through the interplay of three key events, each of which is performed by a separate portion of the neurotoxin molecule. The HCQ portion which is the C-half of the C terminus of the heavy chain is implicated to play an important role in the receptor-specific binding of the toxin to the cholinergic neurons. In this study, we have cloned, expressed and purified the C-quarter of the BoNT /A heavy chain in a functionally active form. The availability of recombinant HCQ provides an effective system to study the biochemical and physical interactions involved during BoNT binding to nerve cells. Further analysis of molecular interactions between HCQ and its receptors will enable to understand the mechanism of BoNT action.

References

1. L. Li, B.R. Singh, Structure-Function Relationship of Clostridial Neurotoxins, *J. Toxicol.* 18 (1999) 95-112.
2. B.R. Singh, Critical Aspects of bacterial protein toxins, *Adv. Exp. Med. Biol.* 391 (1996) 63-84.
3. B.R. Singh, Intimate details of the most poisonous poison, *Nature. Struc. Biol.* 7 (2000) 617-619.
4. C. Montecucco, G. Schiavo, Mechanism of action of tetanus and botulinum neurotoxins, *Microbiology* 13 (1994) 1-8.
5. C. Montecucco, How do tetanus and botulinum toxins bind to neuronal membrane, *Trends Biochem. Sci.* 11 (1986) 314-317.

6. A. Rummel, S. Mahrhold, H. Bigalke, T. Binz, The H_{CC}- domain of botulinum neurotoxins A and B exhibits a singular ganglioside binding site displaying serotype specific carbohydrate interaction, *Mol. Microbiol.* 51 (2004) 631-643.
7. F. Fu, R. Lomneth, S. Cai, B.R. Singh, Role of Zinc in the structure and toxic activity of Botulinum neurotoxin, *Biochemistry* 37 (1998) 5267-5278.
8. G. Schiavo, O. Rossetto, C. Montecucco, Clostridial neurotoxins as tools to investigate the molecular events of neurotransmitter release, *Semin. Cell Biol.* 5 (1994) 221-229.
9. A Rummel, S. Bade, J. Alves, H. Bigalke, T. Binz, Two carbohydrate binding sites in the H_{CC}-domain of tetanus neurotoxin are required for toxicity, *J.Mol.Biol.* 326 (2003) 835-847.
10. M. Kitamura, K. Takamiya, S. Aizawa, K. Furukawa, K. Furukawa, Gangliosides are the binding substances in neural cells for tetanus and botulinum toxins in mice, *Biochim. Biophys. Acta* 1441 (1999) 1-3.
11. S. Kozaki, Y. Kamata, S. Watarai, T. Nishiki, S. Mochida, Ganglioside G_{T1b} as a complementary receptor component for clostridium botulinum neurotoxins, *Microb. Pathog.* 25 (1998) 91-99.
12. L. Li, B.R. Singh, Isolation of synaptotagmin as a receptor for types A and E botulinum neurotoxin and analysis of their comparative binding using a new microtiter plate assay, *J. Nat. Toxins*, 7 (1998) 215-226.
13. K. Ginalski, C. Venclovas, B. Lesyng, K. Fidelis, Structure-based sequence alignment for the beta-trefoil subdomain of the clostridial neurotoxin family provides residue level information about the putative ganglioside binding site, *FEBS Letters*, 482 (2000) 119-124.
14. D.B. Lacy, W. Tepp, A. C. Cohen, B. R. DasGupta, R. C. Stevens, Crystal structure of botulinum neurotoxin type A and implications for toxicity, *Nature Struct. Biol.* 5 (1998) 898-902.

15. T. Binz , H. Kurazono , M. Wille, J. Frevert, K. Wernars, H. Neimann, The Complete Sequence of Botulinum Neurotoxin Type A and Comparison with other Clostridial Neurotoxins, *J. Biol. Chem.* 265 (1990) 9153-9158.
16. P. Emsley, C. Fotinou, I. Black, N. F. Fairweather, I. G. Charles, C. Watts, E. Hewitt, N.W. Isaacs, The structures of the H(C) fragment of tetanus toxin with carbohydrate subunit complexes provide insight into ganglioside binding, *J. Biol. Chem.* 275 (2000) 8889-8894.
17. J. M. Sutton, L. Spaven, N.J. Silman, B. Hallis, O. Chow-Worn, C. C. Shone, The Receptor binding domains of Clostridial Neurotoxins, in: M.F. Brin, J. Jankovic, M. Hallett (Eds.) *Scientific and therapeutic aspects of Botulinum Toxin*, Lippincott Williams & Wilkins, Philadelphia, 2002, pp. 41-48.
18. C. Montecucco, O. Rossetto, G. Schiavo, Presynaptic receptor arrays for clostridial neurotoxins, *Trends in Microbiology* 12 (2004) 442-446.
19. L.A. Smith, M.P. Byrne, Vaccines for preventing Botulism, in: M.F. Brin, J. Jankovic, M. Hallett (Eds.) *Scientific and therapeutic aspects of Botulinum Toxin*, Lippincott Williams & Wilkins, Philadelphia, 2002, pp. 427-437.
20. L.L. Simpson, Identification of the characteristics that underlie botulinum toxin potency: implications for designing novel drugs, *Biochimie* 82 (2000) 943-53.
21. L.A. Smith, Development of recombinant vaccines for botulinum neurotoxin, *Toxicon* 36 (1998) 539-1548.
22. M. Tavallaie, A. Chenal, D. Gillet, Y. Pereira, M. Manich, M. Gibert, S. Raffestin, M.R. Popoff, J.C. Marvaud, Interaction between the two subdomains of the C-terminal part of the botulinum neurotoxin A is essential for the generation of protective antibodies, *FEBS Letters* 572 (2004) 299-306.
23. L. Li, B.R. Singh, In vitro translation of Type A Clostridium Botulinum neurotoxin heavy chain and analysis of its binding to rat synaptosomes, *J. Prot Chem.* 18 (1999) 89-95.

24. J.R. Whitaker, P.E. Granum, An absolute method for protein determination based on difference in absorbance at 235 and 280nm, *Anal. Biochem.* 109 (1980) 156-159.
25. S. Cai, H.K. Sarkar, B.R. Singh, Enhancement of the endopeptidase activity of Botulinum neurotoxin by its associated Proteins and Dithiothreitol, *Biochem.* 38 (1999) 6903-6910.
26. Y. Zhou, B.R. Singh, Cloning, high level expression, single step purification and binding activity of His6-tagged recombinant type B Botulinum neurotoxin heavy chain transmembrane and binding domain, *Protein Express. Purif.* 34 (2004) 8-16.



Figure 1

Figure 1. SDS-PAGE analysis of HCQ obtained in the supernatants of the wash steps during the purification of inclusion bodies. Lanes LM and HM, Low and High Molecular weight markers (kDa), respectively; Lanes 1, 2, 3, 4 and 5, supernatants of first, second, third, fourth, and fifth wash, respectively.

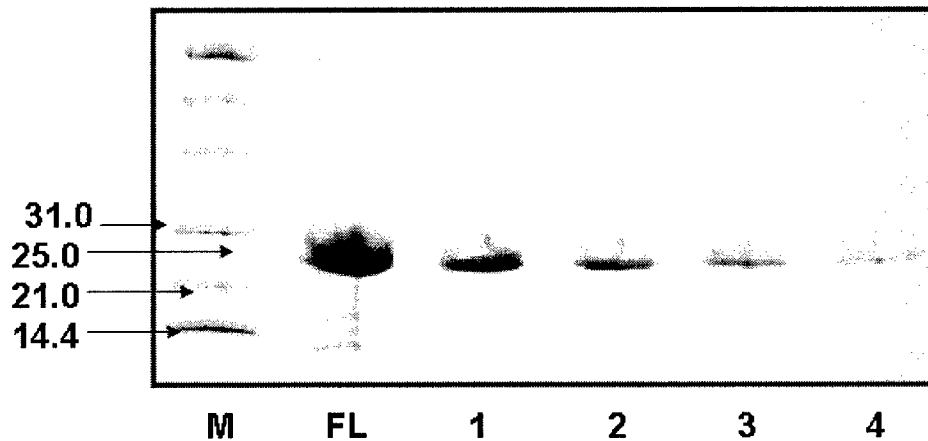


Figure 2

Figure 2. SDS-PAGE analysis of HCQ obtained from His-Nickel affinity column chromatography. Lane M, Low molecular weight marker (kDa); Lane FL, fraction of solubilised inclusion body solution passing through the column after loading onto the column; Lane 1, washing fraction with equilibration buffer, containing β -mercaptoethanol; Lane 2, fraction with equilibration buffer containing, 20 mM imidazole, with no β -mercaptoethanol; Lanes 3 and 4, fractions eluted with 20 and 30 mM imidazole, respectively.

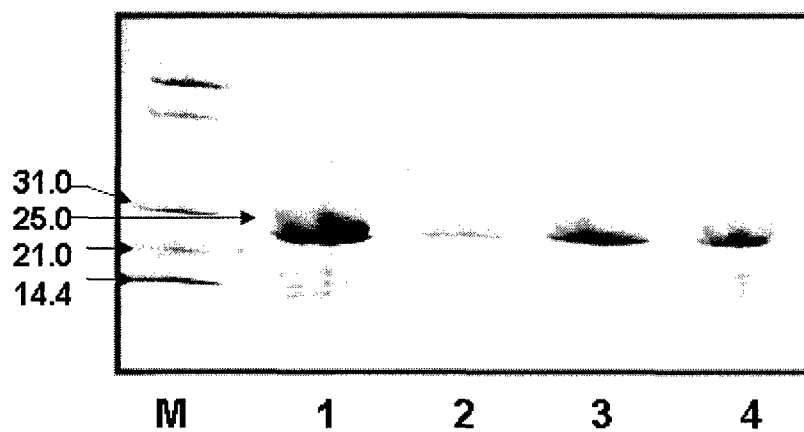


Figure 3

Figure 3. SDS-PAGE Analysis of eluents of His-Nickel Affinity gel column chromatography. Lane M, Low molecular weight marker (kDa); Lanes 1, 2, 3 and 4, 1mL elution fractions of elution buffer containing 100 mM imidazole.

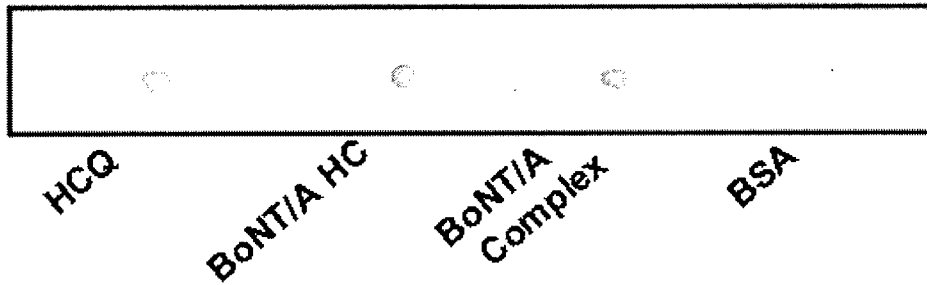


Figure 4

Figure 4. Immuno dot blot assay of HCQ binding with BoNT/A antibodies. The colored spots indicate positive reaction of the sample against rabbit anti-BoNT/A antibody. BoNT/A heavy chain and BoNT/A complex were used as positive controls and BSA was used as a negative control. Concentration of each protein (HCQ, BoNT/A HC, BoNT/A complex and BSA) blotted on the nitrocellulose membrane was 0.1 mg/mL.

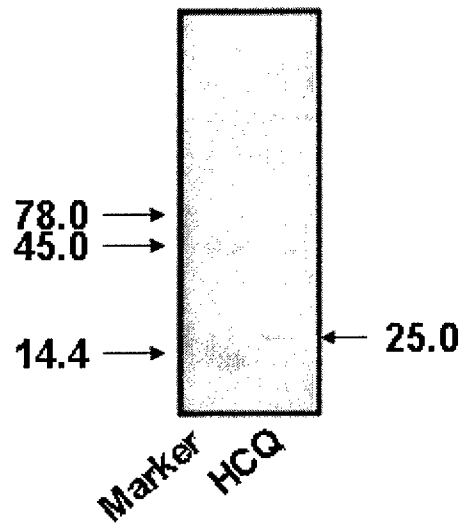


Figure 5

Figure 5. Western blot analysis of recombinant BoNT/A HCQ with antibody raised against BoNT/A toxin. The numbers on the left indicate the molecular mass of markers (kDa).

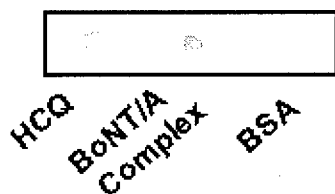


Figure 6

Figure 6. Immuno dot blot assay of HCQ binding with synaptotagmin. The colored spots indicate positive reaction of the sample with synaptotagmin which was monitored with anti-synaptotagmin IgG. BoNT/A complex was used as a positive control and BSA was used as a negative control. Concentration of each protein (HCQ, BoNT/A complex, and BSA) blotted on the nitrocellulose membrane was 0.1 mg/mL.

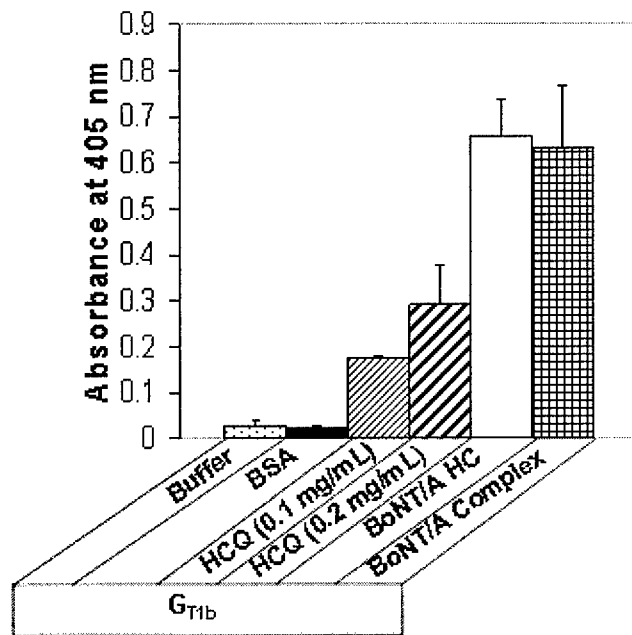


Figure 7

Figure 7. Enzyme-linked immunosorbent assay of binding activity of recombinant HCQ to ganglioside (G_{T1b}). HCQ (0.1 mg/mL), HCQ (0.2 mg/mL), BoNT/A heavy chain (0.1 mg/mL) and BoNT/A complex (0.1 mg/mL) show positive results. Values represent mean from three separate experiments with bars representing standard mean of deviations.

Project K (Unpublished)

Physiological and Biochemical Response of Northern Quahog to Botulinum Neurotoxin

ABSTRACT

Botulinum neurotoxins are the most poisonous poisons and biothreat agents which block acetylcholine release at nerve-muscle junctions causing flaccid muscle paralysis. High doses (more than thousand mouse LD₅₀ units) of type A botulinum neurotoxins were injected in the anterior adductor muscles of northern quahog, *Mercenaria mercenaria*, to test its effect on muscle paralysis and lethality to quahogs. While no muscle paralysis or mortality was observed, the quahogs responded to the toxin injection with ejection of mucus and browning of tissues. Quahogs also responded biochemically in terms of significant reduction (30%) in the activity one of the stress proteins, glutathione-S-transferase. These findings are relevant to developing an invertebrate animal assay model for assay and diagnostics of the botulinum biothreat.

INTRODUCTION

Botulinum neurotoxin (BoNT) is produced by the anaerobic bacterium *Clostridium botulinum* and is generally regarded as the most poisonous of all poisons in nature (Lamanna 1959; Singh, 2000). There are seven serotypes of botulinum toxins, type A-G, exert their paralytic effect by inhibiting acetylcholine release at the neuromuscular junction. The extent of paralysis is dependent on doses, volume and the potency of serotype employed.

Studies of BoNT toxicity revealed remarkable differences in the toxic dose among different species. Biological activity of the toxin is measured in mouse units. Swiss-Webster-mouse LD₅₀, is the amount of toxin required to kill 50% of mice after IP injection. Gill (1982) reported LD₅₀ for mice 0.1-1.0 ng/Kg causing death 6-24 hours after injection. There is no published report for botulinum toxicity from invertebrates. Preliminary toxicity test in our laboratory indicated that quahogs are resistant to BoNT. Invertebrates nerves are known to be relatively insensitive to the Paralytic Shellfish Toxins (PSTs) – a potent neurotoxin produced by several species of marine dinoflagellates (Gubbins 2002). Gubbins et al (2002) observed no mortality in mussels and scallops subjected to Saxitoxin but reported glutathione-S-transferase (GST) activity was induced by high doses of STX (> 100 µg/kg) at 2 – 8 days after exposure in mussel (*Mytilus edulis*). At the same time, no significant difference between control and exposed scallops (*Pecten maximus*).

Glutathione –S-transferases (GST) are a family of multifunctional ubiquitous enzymes found in almost all living organisms (Stenersen et al., 1987; Keeran and Lee, 1987; Lin and Chuang, 1993; Fitzpatrick et al., 1995; Gallagher et al.,1996; Blanchette and Singh, 1999; Vidal and Narbonne, 2000). Multiple forms of GST are known to function in different capacities: intracellular detoxification of drugs, carcinogens and decreasing stress of xenobiotic compounds, intracellular carrier proteins and reduction of hydroxyperoxides and nitrates. Because of its role in the detoxification and removal of xenobiotics, it has been recognized as a biomarker of

pollution and stress (Fitzpatrick et al., 1995, 1997; Akcha et al., 2000; Perez-Lopez et al., 2000; Livingstone et al., 2000; Henson et al., 2001; Blanchette and Singh, 2003; Cheung et al., 2004; Zhang et al., 2004).

The aim of present study is to test the toxicity of BoNT on northern quahog *Mercinaria mercinaria* and to examine if BoNT/A can induce GST activity. Our results show that while the quahogs survive even heavy dose of BoNT/A, the neurotoxin causes significant morphological and physiological changes, including the activity of glutathione-S-transferases.

MATERIALS AND METHODS

Quahogs (clams) were purchased from Captain Frank's seafood. New Bedford, Mass. (Length 80-85 mm; Height 75-80 mm; Weight 145-160 g). They were maintained in laboratory for 2 weeks in seawater and aeration was provided by air bubbling using Spectra/Chrom MP- 1 Pump; room temperature varied from 24 ° – 27 ° C . Clams were not fed, and subjected to natural light cycle.

The clams were divided into two groups. The controls received 200 µL of buffer (20 mM sodium phosphate buffer, pH 7.9) injection into the anterior adductor muscle by inserting a hypodermic needle through a notch filed into the edge of the shell. The experimental group received 20 µg and 96 µg doses (in 200 µL of 20 mM phosphate buffer, pH 7.9) BONT/A complex injection into the anterior adductor muscle using a 1 ml Sub Q (0.45 mm X 16 mm) syringe (BD & CO., Franklin Lakes, NJ). After 3, 6 & 9 days, the shells were removed from the quahogs of control and experimental groups and animals were dissected out quickly in ice to collect the nervous tissue (cerebral, pedal and visceral ganglions and the connecting nerves), anterior adductor muscle, digestive gland, foot and gill were collected and rinsed in 100 mM phosphate buffer, pH 6.8; dried on absorbent paper and then weighed.

The crude extract was prepared according to Blanchette and Singh (1999) by homogenizing the tissues in grinding buffer (100 mM sodium phosphate, 300 mM sucrose, 1 mM ethylenediaminetetraacetic acid or EDTA, pH 6.8 and 6.8 mL of 200 mM phenylmethylsulphonyl fluoride =PMSF; final concentration, ~2mM; in a 1:4 tissue wt:volume ratio of the buffer. The homogenization was carried out at high speed for 60 seconds at 4°C using a Polytron homogenizer (Brinkmann Instruments, Kinematica GmbH, Switzerland). The homogenates were then centrifuged at 16,000 g for 30 min in a Dupont Sorvall SLA – 1500 rotor at 4°C using a Sorvall RC -5B centrifuge. The supernatant was collected for GST activity.

GST activities were measured on Jasco-V-550 Spectrophotometer according to method of Habig et al (1974) by taking 50 µL of 20mM CDNB (1-chloro-2,4-dinitrobenzene) and 50 µL of 20 mM reduced glutathione in 1 mL reaction mixture. The progress of reaction was monitored by measuring the absorbance change at 340 nm.

Protein Assay

Protein concentration of the crude extract was determined by the Bradford (1976) method, with protein assay kit purchased from Bio-Rad (Hercules, CA). Bovine serum albumin (BSA) was used as a standard.

Enzyme Kinetics

The initial rate kinetics of quahog GST with respect to glutathione was examined by measuring the initial rate of conjugation reaction while varying the GSH concentration and keeping the CDNB concentration constant. A control experiment was performed using the same concentration of GSH and CDNB in the absence of GST, and the initial rate in the presence of GST was corrected for the control. Lineweaver-Burk analysis was performed by plotting $1/v$

versus $1/[GSH]$. K_m and V_{max} values were determined from the slope (k_m/V_{max}) and y-intercept ($1/V_{max}$) of the plot.

RESULTS AND DISCUSSION

Toxicity Test

Quahogs were injected with different doses of botulinum neurotoxin- BoNT/A complex, BoNT/B complex and BoNT/F complex for varying time intervals and no mortality was observed even after injecting very high doses (180 μ g BoNT/A complex and 150 μ g BoNT/F). Moreover, there was no visible dysfunction observed in the quahog's ability to shut its shell, indicating no signs of muscle paralysis.

In a similar experiment, Gubbins (2002) had injected *Mytilus edulis* intramuscularly with different doses (10,33,100 and 330 μ g/100 g body weight) of saxitoxin (paralytic shellfish toxin- PST), and observed no mortality in the mussels in 8-day experimental observations.

Morphology

The quahogs administered with 20 μ g and 96 μ g of BoNT/A complex for 3, 6 and 9 days exhibited browning of the body color and an apparent morbidity in the flesh (**Fig.1**). These changes were more pronounced in the quahogs injected with 96 μ g of BoNT/A complex. On the other hand, the controls receiving vehicle (the phosphate buffer) showed cream colored body with more contractile activity in the adductor muscles and foot as compared to BoNT injected quahogs.

Turbidity Test

The first reaction of the BoNT/A complex injected quahogs was that they started ejecting out some milky mucus (within 2-3 hours after injection) from the small pore formed towards

anterior adductor muscles. Due to this activity the color of the sea water becomes milky within the first day after receiving the BoNT injection as compared to controls. The water from containers was checked for absorbance at 600 nm on the spectrophotometer, it exhibits a significant increase in the turbidity in experimental animals (Fig. 2).

The tissue distribution of GST activity towards CDNB has been found to be ubiquitous, in *Mytilus edulis* (Fitzpatrick et al 1997), *Astacus astacus* (Lindstrom-seppa et al., 1983), and *Corbicula fluminea* (Vidal and Narbonne 2000). In quahog (*Mercinaria mercinaria*), it was predominant in the digestive gland and lesser extent in the nervous tissue and gills. Vidal and Narbonne (2000) also reported predominant level of GST in the visceral mass (65%) and to a lesser extent in gill (18%) of *C. fluminea*. Similarly very high level of GST was recorded in digestive glands as compared to gills of Antarctic Scallop by Regoli et al (1997). The digestive gland in mollusca functions analogous to vertebrate liver in which high level of GST activity is encountered. However, in some mussel species, gills possess higher GST activity relative to other organs (e.g. *M. edulis*-Fitzpatrick et al 1997; *Perna viridis*-Cheung et al. 2001).

In present study we examined the level of GST activity in digestive gland (DG), gill and nerve tissues of quahogs before and after administering with 20 µg and 96 µg of BoNT/A complex (Fig. 3). In untreated quahogs, GST specific activity was 1.35 ± 0.75 , 1.72 ± 0.97 , and 0.97 ± 0.11 µmol/min/mg protein in DG, nerve, and gills, respectively, which remained at 10.73 ± 0.87 , 1.70 ± 0.01 , and 1.49 ± 0.11 µmol/min/mg protein 3 days after injection with buffer (Table 2). GST activity measured 3, 6 and 9 days after injection with buffer or BoNT/A complex was exhibits a significant ($p < 0.5$ to < 0.001) decrease (~30%) in GST activity in the digestive gland when compared to controls. The nervous tissue records a minor decrease in GST after 3 days in both (20 and 96 µg injections) the treated groups, thereafter 96 µg injected quahogs show a recovery in GST activity whereas 20 µg injected groups do not exhibit any difference. Gills, on

the other hand, record a significant decrease only after 3 days in BoNT injected quahogs (Fig. 3, Table 2).

Other organisms exposed to Xenobiotic compounds also showed a decrease in GST activity. For example, oral administration of PCB-105 resulted a significant reduction in GST in trout (*O. mykiss*) while in cod (*Gradus morhua*) no significant change was observed (Bernhoft et al 1995). There are reports from several molluscs where GST activity is reduced. For example, Lee (1988) recorded a decrease in GST activity (1-2 folds, 78 nmol/min/mg to 37 nmol/min/mg) upon PCB exposure in *Mytilus edulis*. Michel et al. (1993) also reported depression in GST activity of whole mussel cytosol when exposed to Benzopyrene. Akcha et al. (2000) observed reduced GST activity in *Mytilus galloprovincialis* hepatopancreas from highly polluted site. Vidal et al reported that GST activity in *C. fluminea* towards CDNB and EA (ethyranic acid) remained unaffected by exposure to trichloroethylene, toluene and a complex mixture of polycyclic aromatic hydrocarbons, whereas it displayed a reduced GST activity towards CDNB when exposed to cadmium. On the other hand, the GST activity of hypatopancreas of *Perna viridis* had increased at day 6 and 12 followed by a decrease on day 18 (Cheung et al. 2004). This biphasic response was described as an inhibitory effect due to high concentration of contaminants in mussel tissue or an adaptive response in which the mussel abandoned the GST detoxification pathway in favour of some different pathway.

There are reports suggesting induced GST activity in response to metals and organic contaminants in *Mercenaria mercenaria* (Blanchette and Singh, 2003), *Perna viridis* (Cheung et al., 2004), Rainbow trout (Perez-Lopez et al., 2000), *Amerius nebulosus* (Henson et al., 2001), *Mytilus edulis* and salmon (Gubbins et al., 2002), and *Carassius auratus* (Zhang et al., 2004). Recently, Zhang et al (2004) concluded that a fall in GSH levels may lead to an induction in GST activity of gold fish.

Our experimental findings clearly indicate that the quahogs do not die even at very high dose (180 µg) of BoNT/A, but they undergo some distress showing ejection of mucus as an immediate response and browning of the body color. Decrease in GST activity after receiving 20 µg and 96 µg doses is biochemical response either to the neurotoxin or to the distress caused by the neurotoxin.

Browning of the body color in *Mercenaria mercenaria* has been reported as an immediate response of environmental contamination and a role of red glands is suggested in detoxification by Zaroogian et al. (1989). The responses of quahogs towards BoNT/A, the most poisonous poison (Lamanna, 1959; Singh, 2000) with its toxicity ~100 billion times more toxic than cyanide, may be the result of the general detoxification response. It is very much possible that the doses used (20 µg and 96 µg) may be too high which may have abandoned the GST detoxification mechanism leading to a significant decrease in the digestive gland from day 3 to day 9. However, there is a recovery in the nervous tissue on 6th and 9th day of 96 µg injected quahogs. There is little change in the gill tissue. Gubbins et al. (2002) also observed no mortality in mussel and scallop subjected to another toxin- PST (saxitoxin) at 330 µg and concluded invertebrate nerves are insensitive to PST. However the mussels show an increased GST after PST exposure whereas scallops show no response.

Effect of botulinum neurotoxin on quahog could provide a convenient biological assay system, based on the mucus release and tissue browning. Also, the GST response to botulinum neurotoxin could be used as a biomarker in designing a comprehensive diagnostic system for botulism. However, further investigations are required in order to fully understand how the BoNT acts on the tissue GST response of quahogs.

REFERENCES

1. Akcha F., Izuel, C., Venier, P., Budzinski, H., Burgeot, T. and Narbonne, J.F. (2000) Enzymatic biomarker measurement and study of DNA adduct formation in benzo[a]pyrene - contaminated mussels, *Mytilus galloprovincialis*. *Aquatic Toxicol.* 49, 269-287.
2. Bernhoft, A., Hektoen, H., Skaare, J.U. and Ingerbrihtsen, K. (1995) Distribution and effects on hepatic Xenobiotic metabolizing enzymes by 2,3,3',4,4'-Pentochlorobiphenyl (PCB-105) in cod (*Gadus morhua*) and rainbow trout (*Oncorhynchus mykiss*). *Mar. Env. Res.* 39, 343-348.
3. Blanchette, B.N. and Singh, B.R. (1999) Purification and Characterisation of the Glutathione-S-transferases from the Northern Quahog *Mercenaria mercenaria*. *Mar. Biotechnol.* 1, 74-80.
4. Blanchette, B.N. and Singh, B.R. (2003) Induction of Glutathione-S-transferases in the Quahog *Mercenaria mercenaria* after exposure to the polychlorinated bi-phenyl (PCB) mixture Aroclor 1248. *J. Protein Chem.* 21, 489-494.
5. Bradford, M.M. (1976) A rapid and sensitive method for the quantification of microgram quantities of protein utilizing the principle of protein dye binding. *Anal. Biochem.* 72, 248-254.

6. Cheung, C.C.C., Siu, W.H.L., Richardson, B.J., De Luca-Abott, S.B., and Lam, P.K.S. (2004) Antioxidant responses to benzo[a]pyrene and Aroclor 1254 exposure in green lipped mussel *Perna viridis*. Environ. Pollution. 128, 393-403.
7. Cheung, C.C.C., Zheng, G.J., Li, A.M.Y., Richardson, B.J., and Lam, P.K.S. (2001) Relationship between tissue concentration of polycyclic aromatic hydrocarbons and antioxidative responses of marine mussels *Perna viridis*. Aquatic Toxicol. 52,189-203.
8. Fitzpatrick, P.J., O'Halloran, J., Sheehan, D. and Walsh, A.R. (1997) Assessment of Glutathione-S-transferase and related proteins in the gill and digestive gland of *Mytilus edulis* (L) as potential organic pollution biomarker. Biomarkers 2, 51-56.
9. Fitzpatrick, P.J., Sheehan, D. and Livingstone, D.R. (1995) Studies on isoenzymes of Glutathione-S-transferase in digestive gland of *Mytilus galloprovincialis* with exposure to pollution. Mar. Environ. Res. 39, 241-244.
10. Gallagher, E.P., Stapleton, P.L., Slone, D.H., Schlenk, D., and Eaton, D.L. (1996). Channel catfish glutathione-S-transferase isoenzyme activity toward (\pm)-anti-benzo[a]pyrene-trans-7,8-dihydro-diol-9,10-epoxide. Aquat Toxicol 34, 135-150
11. Gill, D.M., 1982. Bacterial toxins: a table of lethal amounts. Microbial. Rev. 46, 86-94.
12. Gubbins, M.J. (2002) Xenobiotic Metabolizing enzymes in fish and shellfish exposed to paralytic shellfish toxins. Ph.D. Thesis University of Dundee, Aberdeen.

13. Gubbins, M.J., Brian Eddy, F., Gallacher, S. and Stagg, R.M.(2002) Biological effects of paralytic shellfish toxin on Atlantic salmon and bivalve molluscs. Fisheries Research Services (Abstract).
14. Habig, W.H., Pabst, M.J. and Jakoby, W.B. (1974) The first enzymatic step in mercapturic acid formation. J. Biol. Chem. 249, 7130-7139.
15. Henson, K., Stauffer, G. and Gallagher, E.P. (2001) Induction of Glutathione-S-transferase activity and protein expression in brown bullhead (*Ameiurus nebulosus*) liver by ethoxyquin. Toxicol Sci. 62, 54-60.
16. Keeran, W.S. and Lee, R.F. (1987) The purification and characterization of glutathione-s-transferase from hypatopancreas of the blue crab *Callinectes sapidus* . Arch. Biochem. Biophys. 255, 233-243.
17. Lamanna, C. (1959) The most poisonous poison. Science 130, 763-772.
18. Lee, R.F. (1988), Glutathione-S-transferase in marine invertebrates from Langesundjford. Marine Ecol. Prog. Ser. 46, 33-36.
19. Lin, K.S. and Chuang, N.N. (1993) Anionic glutathione-s-transferase in shrimp eyes. Comp. Biochem. Physiol. 105B, 151-156.

20. Lindstrom-seppa, P., Koivusaari and V. Hanninen, O. (1983) Metabolism of foreign compounds in fresh water crayfish (*Astacus astacus* L.) tissues. *Aquatic Toxicol.* 3, 35-46.
21. Livingstone, D.R., Chipman, J.K., Lowe, D.M. (2000) Development of Biomarkers to detect the effect of pollution on aquatic invertebrates: Recent molecular, genotoxic, cellular and immunological studies on the common mussels (*Mytilus edulis* L) and other mytilids. *Int. J. Environ Pollut.* 13, 56-91.
22. Michel,X.R., Suteau, P., Robertson,L.W. and Narbonne, J.F. (1993) Effects of benzo(a)pyrene, 3,3',4,4'-Tetrachlorobiphenyl and 2,2',4,4',5,5'-hexachlorobiphenyl on the xenobiotic metabolising enzymes in the mussel (*Mytilus galoprovincialis*) *Aquatic Toxicol.* 27, 335-344.
23. Perez-Lopez, M., Anglade, P., Bee-Ferte, M.P. (2000) Characterization of hepatic and extra hepatic glutathione-s-transferases in rainbow trout (*Oncorhynchus mykiss*) and there induction by 3,3',4,4'-tetrachlorobiphenyl. *Fish Physiol. Biochem.* 22, 21-32.
24. Regoli, F., Principato, G.B., Bertoli, E., Nigro, M. and Orlando, E. (1997) Biochemical characterization of the anti oxidant system in scallop *Adamussium colbeki* a sentinel organism for monitoring the Antarctic environment. *Polar Biol.* 17, 251-258.
25. Singh,B.R. (2000) Intimate details of the most poisonous poison. *Nature Struct. Biol.* 7, 617-619.

26. Stenersen, J., Kobro, S., Bjerke, M. and Arend, U. (1987) Glutathione transferases in aquatic and terrestrial animals from nine phyla. *Comp. Biochem. Physiol.* 86c, 73-82.
27. Vidal, M.L., Basseres, A. and Narbonne, J. F. (2001) Potential biomarkers of trichloroethylene and toluene exposure in *Corbicula fluminea*. *Environ. Toxicol Pharmacol.* 9, 87-97.
28. Vidal, M.L. and Narbonne, J.F. (2000) Characterization of glutathione-s-transferases activity in the Asiatic clam *Corbicula fluminea*. *Bull. Environ. Contam. Toxicol.* 64, 455-462.
29. Zaroogian, G., Yevich, P., Pavignano, S. (1989) The role of the red gland in *Mercenaria mercenaria* in detoxification. *Mar. Environ. Res.* 28, 447-450.
30. Zhang, J., Shen, H., Wang, X., Wu, J. and Xue, Y. (2004) Effect of chronic exposure of 2,4-dichlorophenol on the antioxidant system in the liver of fresh water fish *Carassius auratus*. *Chemosphere* 55, 167-174.

Table1: Mortality of quahogs upon injection with botulinum neurotoxins.

Neurotoxin Type	Dose	Number of days monitored	Mortality
BoNT/A complex	180 µg	6 days	-
	96 µg	18 days	-
	20 µg	18 days	-
	5.5 µg	18 days	-
BoNT/B complex	30 µg	18 days	-
BoNT/F complex	150 µg	10 days	-
	60 µg	10 days	-

Table2: GST Activity ($\mu\text{mole}/\text{min}/\text{mg}$) in quahog after BoNT administration

Period	Treatment	Digestive Gland	Nerve	Gill
	Untreated Control	10.35 \pm 0.75	1.72 \pm 0.97	0.97 \pm 0.11
3 days	Control	10.73 \pm 0.87	1.70 \pm 0.01	1.49 \pm 0.11
	BoNT-A 20 μg	8.45 \pm 0.45 (p<0.01)	1.47 \pm 0.20	0.57 \pm 0.21 (p<0.001)
	BoNT-A 96 μg	6.46 \pm 0.14 (p<0.001)	1.10 \pm 0.19 (p<0.01)	0.64 \pm 0.12 (p<0.01)
6 days	Control	9.54 \pm 1.25	1.60 \pm 0.04	0.53 \pm 0.04
	BoNT-A 20 μg	6.83 \pm 0.38 (p<0.05)	0.93 \pm 0.34	0.54 \pm 0.05
	BoNT-A 96 μg	6.65 \pm 0.54 (p<0.01)	1.83 \pm 0.07	0.68 \pm 0.18
9 days	Control	9.335 \pm 0.14	1.9 \pm 0.12	0.64 \pm 0.23
	BoNT-A 20 μg	6.85 \pm 0.14 (p<0.001)	0.56 \pm 0.09 (p<0.001)	0.43 \pm 0.02
	BoNT-A 96 μg	7.16 \pm 0.68 (p<0.05)	1.58 \pm 0.35	0.41 \pm 0.07



Fig. 1. *Inner morphology of quahog after injection with BoNT/A complex. (a)* Quahog injected with 96 μ g of BoNT-A complex after 6 days. *(b)* Quahog control injected with vehicle (20 mM phosphate buffer, pH 7.9).

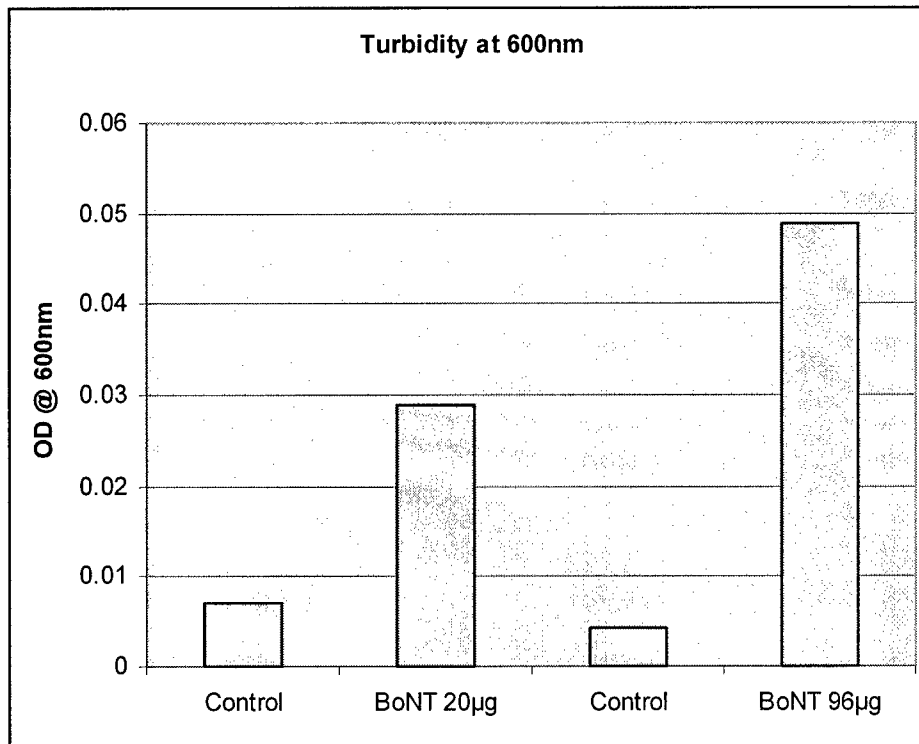
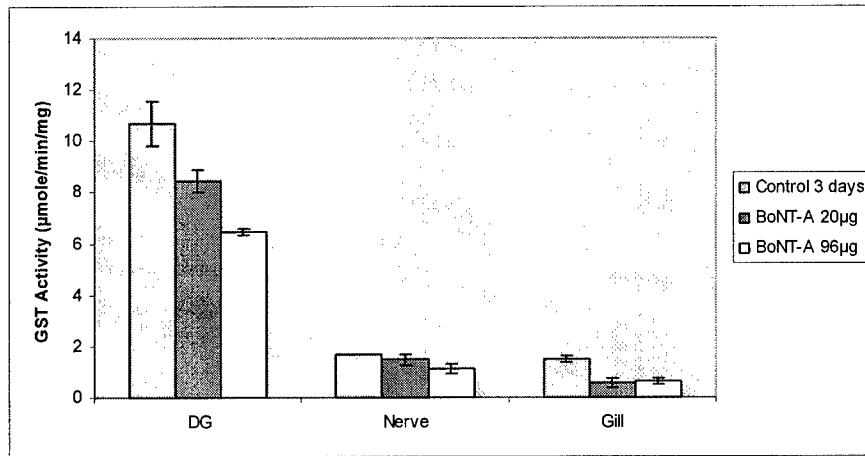
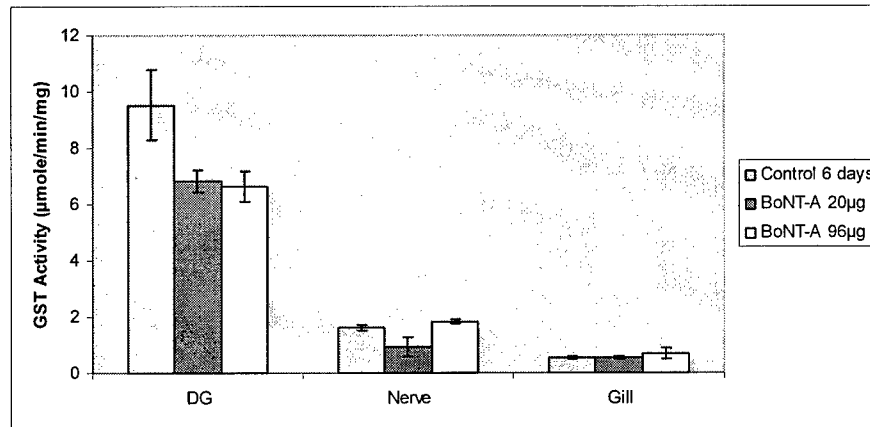


Fig 2. Turbidity of seawater in the surrounding of quahog injected with 96 µg BoNT/A complex.

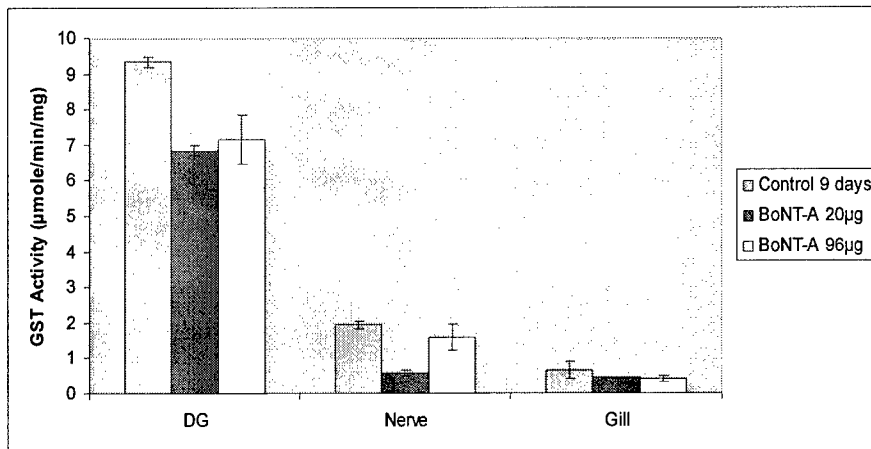
In control experiments, the quahogs were injected with 20 mM phosphate buffer, pH 7.9.



(a) BoNT-A 3 days exposure



(b) BoNT-A 6 days exposure



(c) BoNT-A 9 days exposure

Fig 3. Effect of BoNT/A injection on the glutathione-S-transferase activity in digestive gland, nerve, and gills of quahog.

Key Accomplishments

1. The N-terminal peptide segment of synaptotagmin can be effectively used to examine binding of botulinum neurotoxins with its potential receptor, synaptotagmin.
2. Synaptotagmin binds more than one type of botulinum neurotoxin, suggesting one receptor for all botulinum neurotoxins.
3. Low pH introduces dramatic structural differences in botulinum neurotoxin and its heavy chain which acts as its binding domain to the receptor.
4. Lipid interaction with botulinum neurotoxin at low pH and neutral pH introduces different kind of structural alterations.
5. Receptor binding domain of type B botulinum domain has been successfully cloned, expressed, and purified.
6. BoNT/A binds to synaptotagmin II, but much less compared to BoNT/B. BoNT/B binding to synaptotagmin is enhanced by GT1b but not that of BoNT/A (*Yu Zhou and Bal Ram Singh, unpublished results*).
7. Synaptotagmin II also binds to Hn-33, a major component of BoNT/A complex. Entry of Hn-33 along with BoNT/A L chain might explain long lasting effect of BoNT/A in nerve cells (*Yu Zhou et al., 2005*).
8. Hn-33 of BoNT/A complex dramatically enhances the endopeptidase activity of BoNT/A, including in synaptosome preparations prompting the suggestion that Hn-33 complex of BoNT/A enters the synaptosomes, likely mediated by a receptor protein identified in item (2) (*Sharma and Singh, 2004, Biochemistry 43, 4791-4798*).
9. A new complex of BoNT/E consisting of six proteins has been discovered. This discovery is relevant to the stability and action of the botulinum neurotoxins in general,

as NAPs may play a common role in the pathogenesis (*B. R. Singh, B. Li, P. Lindo, L. Li, Z. Zhang, E. Santos, A. Chang, S. K. Sharma, S. Parikh, R. Lomneth, manuscript in preparation*).

10. Membrane channel activity of BoNT/A and BoNT/E are similar, suggesting the possibility of the role of a receptor in their differential toxic activity (*S. Parikh and B. R. Singh, manuscript submitted*).
11. BoNT/E and its L chain interact with GT1b, and their polypeptide folding is substantially altered. This alteration will be relevant to explain the molecular basis of their translocation inside the nerve cell (*H. Wang and Singh, Unpublished results*).
12. The C-quarter of heavy chain is capable of binding both synaptotagmin and gangliosides. (*Sharma et al., Protein Expression and Purification, in press*).
13. Quahogs are affected by botulinum neurotoxins biochemically and physiologically, but do not die even at very high concentration of the toxin, suggesting that while the toxin binds to the tissues in quahog, it does not paralyze the organism. Further research in this area may lead to identification of antidotes in quahogs. (*Das et al., manuscript submitted*).

Reportable Outcomes

Published articles

1. Fu, F.-N., Busath, D. D. and Singh, B. R. (2002) Spectroscopic Analysis of Low pH and Lipid induced structural changes in Type A Botulinum Neurotoxin Relevant to Membrane Channel Formation and Translocation. *Biophysical Chemistry* 99, 17-29.
2. Singh, B. R. (2002) Molecular basis of the unique endopeptidase activity of botulinum neurotoxin. In: *Scientific and Therapeutic Aspects of Botulinum Toxin* (M. F. Brin, J. Jankovic, and M. Hallet, eds.), Lippincott Williams and Wilkins, Philadelphia. Pp. 75-88.
3. Sharma, S. K. and Singh, B. R. (2004) Enhancement of the Endopeptidase Activity of Purified Botulinum Neurotoxins A and E by an Isolated Component of the Native Neurotoxin Associated Proteins, *Biochemistry*, 43, 4791-4798.
4. Zhou, Y. and Singh, B. R. (2004) Cloning, high-level expression, single-step purification, and binding activity of His(6)-tagged recombinant type B botulinum neurotoxin heavy chain transmembrane and binding domain. *Protein Expr Purif.* 34, 8-16.
5. Cai, S. and Singh, B. R. (2004) A Distinct Utility of Amide III Infrared Band for Secondary Structure Estimation of Aqueous Protein Solutions Using Partial Least Square Methods, *Biochemistry*, 43, 2541-2549.
6. Sharma, S. K. and Singh, B. R. (2004) Botulinum toxin in Neurological diseases. *Saudi Journal of Disability and Rehabilitation*, 10, 111-117.
7. Singh, B. R., Li, B., Sharma, S. K. and Chang, T.W. (2005) *Clostridium botulinum*: the source of bioterror and beauty. In: *Microbes for Biotechnological Applications* (Ed. A. K. Verma), IK International, New Delhi, India.
8. Sharma, S. B., Zhou, Y. and Singh, B. R. (2005) Cloning, Expression and Purification of C-terminal Quarter of the Heavy Chain of Botulinum Neurotoxin Type A. *Protein Expr. Purif.*, in press.

Manuscripts Submitted

9. Das, V.K., Das, S. and Singh, B. R. (2005) Physiological and Biochemical Response of Northern Quahog to Botulinum Neurotoxin. *FEBS Lett.*
10. Parekh. S. and Singh, B. R. (2005) Comparative Membrane Channel Activity of Botulinum Neurotoxins A and E. *Biophys. Biochem. Res. Commun.*

Abstracts

11. Sharma, S. K. and Singh, B. R. (2002) Hn-33 enhances the endopeptidase activity of botulinum neurotoxin A and E against brain synaptosomal SNAP-25. Thirty-ninth Annual Meeting of Interagency Botulism Research Coordinating Committee. October 22-25, Madison, WI.
12. Singh, B. R. (2002) Molecular Steps in Botulinum Action - Known Knowns and Known Unknowns. Thirty-ninth Annual Meeting of Interagency Botulism Research Coordinating Committee. October 22-25, Madison, WI.
13. Sharma, S. K. and Singh, B. R. (2002) Functional and stabilizing roles of neurotoxin associated proteins in type E Clostridium botulinum neurotoxin complex. Second Neuroscience Symposium, University of Massachusetts, Amherst, MA, June 3, 2002.
14. Nunes, R. B. and Singh, B. R. (2002) Understanding the role of zinc in the structure and stability of botulinum neurotoxin type A. Second Neuroscience Symposium, University of Massachusetts, Amherst, MA, June 3, 2002.
15. Zhang, J., Lindo, P. and Singh, B. R. (2002) Botulinum neurotoxin cleavage of synthetic peptide substrate, a segment of SNAP-25, to develop detection system for the toxin. Second Neuroscience Symposium, University of Massachusetts, Amherst, MA, June 3, 2002.
16. Zhang, J., Lindo, P., and Singh, B. R. (2003) "Botulinum Neurotoxin Cleavage of Synthetic Peptide Substrate, a Segment of Snap-25, to Develop a Detection System for the Toxin." Clostridia 03 Pathogenesis, Marine Biology Laboratory Woods Hole, Massachusetts, April 26-30, 2003.
17. Zhou, Y., and Singh, B. R. (2003) "Cloning and Characterization of Recombinant Clostridium Botulinum Neurotoxin Type B Heavy Chain and Binding Domain." Clostridia 03 Pathogenesis, Marine Biology Laboratory Woods Hole, Massachusetts, April 26-30, 2003.
18. Singh, B. R. (2003) "Current and Unsettled Issues in Molecular Steps in Botulinum Action." Clostridia 03 Pathogenesis, Marine Biology Laboratory Woods Hole, Massachusetts, April 26-30, 2003.
19. Sharma, S. K. and Singh, B. R. (2002) Hn-33 enhances the endopeptidase activity of botulinum neurotoxin A and E against brain synaptosomal SNAP-25. Thirty-ninth Annual Meeting of Interagency Botulism Research Coordinating Committee. October 22-25, Madison, WI.
20. Nunes, R. B., and Singh, B. R. (2003) "Probing the Role of Buffer and Salt Concentration in the Structure and Stability of Botulinum Neurotoxin Types A & E." Clostridia 03 Pathogenesis, Marine Biology Laboratory Woods Hole, Massachusetts, April 26-30, 2003.
21. Buck, D. and Singh, B. R. (2003) "Identification of Neuronal Receptor for Botulinum Toxins using Isothermal Calorimetry". Ninth Annual Sigma Xi Research Exhibit. University of Massachusetts Dartmouth, North Dartmouth, MA. May 6-7, 2003.
22. Zhou, Y., Riding, S. J. and Singh B. R. (2003). "Development of New Antidotes for Botulism." Ninth Annual Sigma Xi Research Exhibit. University of Massachusetts Dartmouth, North Dartmouth, MA. May 6-7, 2003.
23. Zhou, Y. Foss, S. and Singh, B. R. (2003) "Isolation of Receptor for Type B Botulinum Neurotoxin Complex and Recombinant Binding Domain for Development of Antidotes for Botulism." Ninth Annual Sigma Xi Research Exhibit. University of Massachusetts Dartmouth, North Dartmouth, MA. May 6-7, 2003.
24. Zhang, J., Lindo, P. and Singh, B. R. (2003) "Development of Diagnostics of Live Botulism Toxins." Ninth Annual Sigma Xi Research Exhibit. University of Massachusetts Dartmouth, North Dartmouth, MA. May 6-7, 2003.
25. Zhang, J., Lindo, P. and Singh, B. R. (2003) "Botulinum Neurotoxin Cleavage of Synthetic Peptide Substrate, A Segment of SNAP-25, to Develop a Detection System for the Toxin." Department of Chemistry and Biochemistry. Ninth Annual Sigma Xi Research Exhibit. University of Massachusetts Dartmouth, North Dartmouth, MA. May 6-7, 2003.

26. Chennamaraju, A. and Singh, B. R. (2003) "Use of Data Mining and Data Warehousing Techniques to Unveil Botulism Science." Ninth Annual Sigma Xi Research Exhibit. University of Massachusetts Dartmouth, North Dartmouth, MA. May 6-7, 2003.
27. Kukreja, R. and Singh, B. R. (2003) "Thermal Stability of Botulinum Neurotoxins Type A and E Complexes using Second Derivative UV Spectroscopy." Ninth Annual Sigma Xi Research Exhibit. University of Massachusetts Dartmouth, North Dartmouth, MA. May 6-7, 2003.
28. Medeiros, S. and Singh, B. R. (2003) "Kinetics of Botulinum Endopeptidase Activity." Ninth Annual Sigma Xi Research Exhibit. University of Massachusetts Dartmouth, North Dartmouth, MA. May 6-7, 2003.
29. Santos, E. L. and Singh, B. R. (2003) "Structural Maneuvering of Botulinum Neurotoxin with pH Changes." Ninth Annual Sigma Xi Research Exhibit. University of Massachusetts Dartmouth, North Dartmouth, MA. May 6-7, 2003.
30. Nunes, R. B. and Singh, B. R. (2003) "Probing the Role of Buffer and salt Concentration in the Structure and Stability of Botulinum Neurotoxin Types A and E." Ninth Annual Sigma Xi Research Exhibit. University of Massachusetts Dartmouth, North Dartmouth, MA. May 6-7, 2003.
31. McNally, E. A. and Singh, B. R. (2003). "The Art of Making the Most Poisonous Poison by Anaerobic Bacteria." Ninth Annual Sigma Xi Research Exhibit. University of Massachusetts Dartmouth, North Dartmouth, MA. May 6-7, 2003.
32. Kukreja, R., Sharma, S., and Singh, B.R. (2004) "Site-Directed mutagenesis of Type A Botulinum Neurotoxin Light Chain identifies the role of Glu-262 in metalloproteolytic activity". Tenth Annual Sigma Xi Research Exhibit, University of Massachusetts Dartmouth, North Dartmouth, MA, April 27-28, 2004.
33. Kukreja, R., and Singh, B.R. (2004) "Role of the Molten Globule Structure in the Botulinum Neurotoxin Endopeptidase Activity". Tenth Annual Sigma Xi Research Exhibit, University of Massachusetts Dartmouth, North Dartmouth, MA, April 27-28, 2004.
34. Foss, S., Zhou, Y. and Singh, B.R. (2004) "Isolation of Receptor for B Botulinum Neurotoxin Complex and Recombinant Binding Domain for Development of Antidotes for Botulism". Tenth Annual Sigma Xi Research Exhibit, University of Massachusetts Dartmouth, North Dartmouth, MA, April 27-28, 2004.
35. Wang, H-H, and Singh, B.R. (2004) "Interaction between Protein and Membrane Lipids and Analyzed Using Fluorescence Spectroscopy". Tenth Annual Sigma Xi Research Exhibit, University of Massachusetts Dartmouth, North Dartmouth, MA, April 27-28, 2004.
36. Zhou, Y. and Singh, B.R. (2004) "Relevance of Component of Botulinum Neurotoxin Associated Proteins in the Neuronal Entry" Tenth Annual Sigma Xi Research Exhibit, University of Massachusetts Dartmouth, North Dartmouth, MA, April 27-28, 2004.
37. Lindo, P., Lingenfelter, P., Callahan, S. and Singh, B.R. (2004) "Purification and comparative structural and functional analysis of hemagglutinin Type B Clostridium HnB-33 and hemagglutinin HnA-33 from Type A Clostridium botulinum". Tenth Annual Sigma Xi Research Exhibit, University of Massachusetts Dartmouth, North Dartmouth, MA, April 27-28, 2004.
38. Ambrin, G., Zhang, J., Bhowmick, S. and Singh, B.R. (2004) "Detection of Botulinum Neurotoxin's Enzymatic Activity of Type A by Fluorescence Microscopy". Tenth Annual Sigma Xi Research Exhibit, University of Massachusetts Dartmouth, North Dartmouth, MA, April 27-28, 2004.
39. Thomas, A. and Singh, B.R. (2004) "The use of Botulinum Neurotoxin Heavy Chain and 33kDa Hemagglutinin as an Oral Vaccine Candidate". Tenth Annual Sigma Xi Research Exhibit, University of Massachusetts Dartmouth, North Dartmouth, MA, April 27-28, 2004.
40. Sharma, S.B., Kukreja, R.V. and Singh, B.R. (2004) "Production of BoNT/A Mutant Light Chain by Site Directed Mutagenesis". Tenth Annual Sigma Xi Research Exhibit, University of Massachusetts Dartmouth, North Dartmouth, MA, April 27-28, 2004.

41. Medeiros, S. and Singh, B.R. (2004) "Structure-Activity Correlation of Botulinum Neurotoxin Endopeptidase". Tenth Annual Sigma Xi Research Exhibit, University of Massachusetts Dartmouth, North Dartmouth, MA, April 27-28, 2004.
42. Chang, T.W. and Singh, B.R. (2004) "Family Secrets of the Most Toxin Proteins: Nucleotide and Protein Sequence Analyses of Neurotoxin Associated Proteins of Clostridium botulinum". Tenth Annual Sigma Xi Research Exhibit, University of Massachusetts Dartmouth, North Dartmouth, MA, April 27-28, 2004.
43. Riding, S., Lindo, P., Biegel, E. and Singh, B.R. (2004) "Comparative Endopeptidase activity of Clostridium botulinum Type B Neurotoxin Complex and Recombinant Type B light chain to explore the role of neurotoxin associated proteins in active enzyme structure". Tenth Annual Sigma Xi Research Exhibit, University of Massachusetts Dartmouth, North Dartmouth, MA, April 27-28, 2004.
44. Santos, E.L. and Singh, B.R. (2004) "Structural response of type A botulinum neurotoxin to the low pH conditions of gastric juice and endosomal compartments monitored using circular dichroism". Tenth Annual Sigma Xi Research Exhibit, University of Massachusetts Dartmouth, North Dartmouth, MA, April 27-28, 2004.
45. BommaReddy, N.R., Michel, H.E. and Singh, B.R. (2004) "Differentiating the Types of Clostridium Botulinum Using Artificial Neural Network". Tenth Annual Sigma Xi Research Exhibit, University of Massachusetts Dartmouth, North Dartmouth, MA, April 27-28, 2004.

Conclusions

Botulinum neurotoxins are likely to have one receptor for all serotypes. Binding segment of the receptor could be developed into an antidote. In the mode of botulinum action, low pH and lipid interaction introduce considerable structural changes in the binding domain of the toxin.

The native form of Botulinum neurotoxins exist in the form of complexes made up of BoNT and 5-6 neurotoxin associated proteins. At least one of the NAPs binds to the same protein receptor as the BoNT, and is likely to assist in the entry of BoNT into nerve cells. Synaptotagmin II, the putative protein receptor of BoNT/B also binds to BoNT/A, albeit much less in amount. The receptor seems to play a role in the translocation rate of BoNT. Finally, GT1b, the second receptor of BoNT interacts with and alters the latter's polypeptide folding, including that of the light chain. This raises the possibility of active interaction of the light chain with lipids during its translocation.

Cloned, expressed, and purified C-quarter domain of BoNT/A H chain binds both synaptotagmin and GT1b, and can become target for developing antidotes.

Finally, we have serendipitously discovered that while BoNT affects quahogs, it does not paralyze the clam, suggesting a possibility of an inhibitory mechanism available in quahog.

Appendix

Published articles

1. Fu, F.-N., Busath, D. D. and Singh, B. R. (2002) Spectroscopic Analysis of Low pH and Lipid induced structural changes in Type A Botulinum Neurotoxin Relevant to Membrane Channel Formation and Translocation. *Biophysical Chemistry* 99, 17-29.
2. Sharma, S. K. and Singh, B. R. (2004) Enhancement of the Endopeptidase Activity of Purified Botulinum Neurotoxins A and E by an Isolated Component of the Native Neurotoxin Associated Proteins, *Biochemistry*, 43, 4791-4798.
3. Zhou, Y. and Singh, B. R. (2004) Cloning, high-level expression, single-step purification, and binding activity of His(6)-tagged recombinant type B botulinum neurotoxin heavy chain transmembrane and binding domain. *Protein Expr Purif.* 34, 8-16.
4. Cai, S. and Singh, B. R. (2004) A Distinct Utility of Amide III Infrared Band for Secondary Structure Estimation of Aqueous Protein Solutions Using Partial Least Square Methods, *Biochemistry*, 43, 2541-2549.
5. Sharma, S. K. and Singh, B. R. (2004) Botulinum toxin in Neurological diseases. *Saudi Journal of Disability and Rehabilitation*, 10, 111-117.
6. Zhou, Y., Foss, S., Lindo, P., Sarkar, H. and Singh, B. R. (2005) Hemagglutinin-33 of type A botulinum neurotoxin complex binds with synaptotagmin II. *FEBS Journal*, 272, 2717-2726.
7. Singh, B. R., Li, B., Sharma, S. K. and Chang, T.W. (2005) Clostridium botulinum: the source of bioterror and beauty. In: *Microbes for Biotechnological Applications* (Ed. A. K. Verma), IK International, New Delhi, India.
8. Sharma, S. B., Zhou, Y. and Singh, B. R. (2005) Cloning, Expression and Purification of C-terminal Quarter of the Heavy Chain of Botulinum Neurotoxin Type A. *Protein Expr. Purif.*, in press.

Manuscripts Submitted

9. Das, V.K., Das, S. and Singh, B. R. (2005) Physiological and Biochemical Response of Northern Quahog to Botulinum Neurotoxin. *FEBS Lett.*
10. Parekh, S. and Singh, B. R. (2005) Comparative Membrane Channel Activity of Botulinum Neurotoxins A and E. *Biophys. Biochem. Res. Commun.*



ELSEVIER

Biophysical Chemistry 99 (2002) 17–29

Biophysical
Chemistry

www.elsevier.com/locate/bpc

Spectroscopic analysis of low pH and lipid-induced structural changes in type A botulinum neurotoxin relevant to membrane channel formation and translocation

Fen-Ni Fu^a, David D. Busath^b, Bal Ram Singh^{a,1,*}^a*Department of Chemistry and Biochemistry, and School of Marine Science and Technology, University of Massachusetts Dartmouth, 285 Old Westport Road, Dartmouth, MA 02747, USA*^b*Zoology Department, Brigham Young University, Provo, UT 84602, USA*

Received 14 March 2002; accepted 1 April 2002

Abstract

Botulinum neurotoxin (BoNT) is an extremely toxic protein to animals and humans. In its mode of action, one of its subunits mediates its translocation by integrating itself into the membrane bilayer. We have examined the membrane channel activity of type A BoNT (BoNT/A) and its heavy (H) chain in planar lipid membrane under various pH conditions to understand the possible role of the channel activity in the translocation of the BoNT/A light (L) chain under physiological conditions. Only BoNT/A H chain, and not the BoNT/A, exhibited membrane channel activity for translocation of ions. The H chain-induced increase in conductance did not require a pH gradient across the lipid membrane, although it was enhanced by a pH gradient. To understand the molecular basis of the membrane channel activity and the translocation of the L chain, the secondary structure of BoNT/A and its H and L chains were analyzed using circular dichroism (CD) and Fourier-transform infrared (FT-IR) spectroscopy at different pH values. BoNT/A showed no structural alternation upon acidifying the buffer pH. However, an increase in β -sheet content of BoNT/A H chain at low pH was noted when examined by FT-IR. The L chain structure significantly changed with decrease in pH, and the change was mostly reversible. In addition, the neurotoxin and its subunit chains induced a partially reversible aggregation of liposomes at low pH, which indicated their integration into the lipid bilayer. Temperature-induced denaturation studies of BoNT/A H chain indicated major structural reorganization upon its interaction with membrane, especially at low pH. © 2002 Elsevier Science B.V. All rights reserved.

Keywords: Botulinum; Circular dichroism; FT-IR; Membrane channel; Neurotoxin; Translocation; Spectroscopy

1. Introduction

Botulinum neurotoxins (BoNTs) are the most toxic substances known to mankind, with strong potential as biological warfare agents; they are lethal to animals within 30 min. Seven serotypes

of BoNT are produced by different strains of *Clostridium botulinum* in the form of a single polypeptide chain. The single chain is nicked endogenously or exogenously by proteases into a 50-kDa light (L) chain and a 100-kDa heavy (H) chain, linked through a disulfide bond [1,2].

The mode of BoNT action is not well understood at the molecular level, especially in terms of its internalization by endocytosis and translocation across the endosomal membrane into the cytoplasm. Based on some experimental evidence and analogies with other dichain toxins, such as diphtheria, cholera and *Pseudomonas* exotoxin A, a working model has been proposed [2,3]. According to this model, the C-terminus half of the BoNT H chain binds to the presynaptic membrane, presumably through gangliosides and a protein receptor. Upon binding, BoNT is internalized into the neuronal cell through endocytosis [1,4,5]. Inside the cell, the pH of the endosome is lowered to 5–6, which leads to the formation of a membrane transporter by the N-terminal half of the H chain. This transporter helps to translocate the whole or a part of BoNT into the cytoplasm. At least the 50-kDa BoNT L chain is transported into the cytoplasm from acidic endocytotic vesicles. Although the transporter is often referred to as the 'H chain channel', we refer to the H chain-based structure that facilitates the L chain transport as the L-chain transporter (LCT), and reserve the term 'channel' for experimentally detected ion channels. The induction of other small molecule permeability is referred to as (small molecules such as calcein) transport.

An understanding of the molecular mechanism of membrane channel or small-molecule transport activity of the neurotoxin could provide knowledge of the translocation process of the neurotoxin and its toxic subunit into the cell. Membrane channel formation by a water-soluble protein is an intriguing phenomenon, because for water solubility, hydrophilic domains are needed on the surface of a protein, whereas for membrane channel formation, adequate hydrophobic segments are required for interaction with a non-polar membrane bilayer. Sequence analysis has revealed a 23-residue stretch in the N-terminal domain of BoNT H chain that would have a propensity to form an amphipathic helix bundle in a hydrophobic environment [6], and the synthetic peptide of the same sequence has been shown to form channels in phospholipid bilayers [7]. However, the diameter of such channels is approximately 2.5 Å, definitely not sufficient for the translocation of a 50-kDa L chain.

Hydrophobicity calculations for BoNT/A have revealed two adjacent peptide segments (H-183–201 and H-205–240, where H refers to the H chain), with strong hydrophobicity compatible for interaction with a lipid bilayer [8]. However, one–two hydrophobic segments of limited length would not be adequate for the membrane channel formation [7]. To explain adequate interaction of BoNT with lipid bilayers, hydrophobic moment characteristics of BoNT/A were analyzed [9–11]. Several polypeptide segments were amphiphilic and could form integral membrane segments or surface segments in conjunction with lipid bilayers. Surface and/or membrane segments were identified in both L and H chains of the neurotoxin. However, it is not clearly understood how these segments are organized to form membrane channels, nor whether there is any relationship between ion channels observed in lipid membranes and the light chain translocation mechanism.

There have been several reports of interactions of clostridial neurotoxins with artificial membranes that lead to the formation of ion-conducting pores, which is generally an acid-dependent process [6,12–15]. These studies were either accomplished with planar lipid bilayers for channel conductance measurement, or were carried out with lipid vesicles for ion permeability. The acid dependence of neurotoxin translocation in intact cells has been inferred from studies in which agents that neutralize or dissipate pH gradients in acidic compartments and block the acidification of the endosomes have been shown to block neurotoxin action [16–19].

Low pH is required for the strong channel formation activity of BoNT and its H chains [12,20]. A pH of 5.0 or lower induces the channel formation. Low pH is likely to affect not only the surface charges of the neurotoxin, but also its conformation [1]. Extensive research work has been carried out with diphtheria toxin to examine low pH-induced structural changes to correlate its membrane channel activity and translocation. However, no information is available on the structural response of BoNT or its subunits to low pH.

In this article, we describe the membrane channel activity of BoNT/A and its H chain in planar lipid membrane under various pH conditions to

elicit the quantitative difference in the channel-forming activity of these proteins. Only BoNT/A H chain, and not the BoNT/A, exhibited ion transport activity (channel). The H chain-induced increase in conductance did not require a pH gradient across the lipid membrane, although it was enhanced by a pH gradient. The secondary structure of BoNT/A and its H and L chains was analyzed using circular dichroism (CD) and Fourier-transform infrared (FT-IR) spectroscopy at different pH values. BoNT/A showed no structural alternation upon acidifying the buffer pH. However, an increase in β -sheet content of the BoNT/A H chain was noted at low pH using FT-IR. The L chain structure significantly changed with decrease in the pH, and such a change was mostly reversible. In addition, the neurotoxin and its subunit chains induced a partially reversible aggregation of liposomes at low pH, which indicated their integration into the lipid bilayer.

2. Material and methods

2.1. Preparation of BoNT/A and its L and H chains

BoNT/A was isolated following the method described in detail by Fu et al. [21]. In order to obtain L and H chains, the pure neurotoxin was applied to a QAE Sephadex A-50 column (2.5 × 40 cm) for chain separation [22]. Following overnight incubation with 0.1 M DTT and 2 M urea containing borate buffer (pH 8.4), the L chain was first eluted with 0.01 M DTT and 2 M urea containing buffer, and the H chain was then eluted with the same buffer (0.01 M DTT, 2 M urea) containing 0.2 M NaCl. Both L and H chains were pooled after analyzing the fractions on SDS-PAGE for their purity.

2.2. Membrane channel activity in planar lipid bilayer experiments

Diphytanoylphosphatidylcholine (DPhPC, Avanti Polar Lipids, Birmingham, AL) was first dissolved in HPLC-grade chloroform and was dried under a nitrogen stream to a thin lipid film, which was resuspended in squalene (Sigma Chemical Co,

St Louis, MO) to a final concentration of 20 mg ml⁻¹. Planar lipid bilayers were formed by painting the lipid solution across the orifice, ~100 μ m in diameter, of a 250- μ l polyethylene pipette tip [23]. The membrane bilayers formed from the DPhPC were found to be more stable for our experiments than those from typical diacylphosphatidyl choline. The salt solution, containing 1 M KCl, 5 mM CaCl₂ and 0.1 mM EDTA, was buffered at pH 4.7 with 5 mM dimethylglutaric acid (DMG; Sigma Chemical Co, St Louis, MO) or with HEPES buffer, pH 7.4. A 100-mV square-wave potential was applied across the bilayer and the current was relayed to a digitizing oscilloscope (Nicolet, Madison, WI) and then to a strip chart recorder. The sign of the potential was recorded according to the potential applied to the *trans* compartment. The bilayer was considered optimally thinned when its resistance approached 50 G Ω and its capacitance, 250 pF. After the membrane was stabilized, heavy chain was added to the front compartment (*cis* side) and mixed into the solution. The *trans* compartment was alkalized (pH > 7.5) by the addition of 0.85% volume of 1 M KOH.

2.3. Effect of BoNT/A and its L and H chains on liposomes aggregation

In this set of experiments, the liposomes were prepared as previously described [24]. In order to monitor the degree of liposome aggregation, the optical density (OD) of liposome suspensions was monitored at 465 nm, a wavelength that is away from the protein absorption spectral region (320–240 nm). The OD was expected to increase upon aggregation of liposomes because large particles scatter more light. The OD was recorded using a UV/Vis spectrophotometer (Uvikon model 9410, Kontron Instruments, San Diego, CA) at room temperature (25 °C). A 1-ml aliquot of liposome suspension with OD of approximately 0.05 at 465 nm was used for each experiment. The liposome suspension was placed in a 1-cm-pathlength quartz cuvette and OD was recorded for 4 min. The solution was then acidified using 2 M HCl (12–15 μ l) to pH 4.0 and the OD signal was recorded for another 4 min. The suspension was again

titrated with 2 M NaOH (14–17 μ l) back to pH 7.5 and the OD recording was continued for an additional 4 min. The OD after every 4-min incubation period was considered to be the steady-state signal and was used to obtain data for histograms. To investigate the effect of BoNT/A and its H/L subunits on liposome aggregation, 0.1 μ M of each protein was separately premixed with liposomes before recording the low pH-induced light scattering changes.

2.4. Circular dichroism spectroscopy

The structures of BoNT/A and its L and H chains were analyzed by CD spectroscopy using a Jasco model J-715 spectropolarimeter equipped with a Peltier temperature controller (model PTC-348W). Samples for CD recording in the far UV spectral region were prepared in 50 mM citrate (pH 4.0) or 50 mM citrate–phosphate (pH 7.0) buffer to a final concentration of 0.5–1.0 mg ml⁻¹. CD spectra were recorded at room temperature (~ 25 °C) using a 0.1-mm-pathlength quartz cell at a spectral resolution of 0.1 nm. Five spectral scans were averaged to obtain a spectrum for each sample. The scan speed was set at 20 nm min⁻¹ with a response time of 8 s. To obtain the actual spectrum of a protein sample, the spectrum recorded for the buffer used for protein solution was mathematically subtracted, and the resulting spectrum was smoothed using a seven-point, third-order smoothing algorithm.

Near-UV CD spectra were recorded between 250 and 320 nm on a Jasco J500 upgrade instrument using a 1-cm-pathlength quartz cuvette at a spectral resolution of 0.2 nm with ~ 0.6 –1.0 mg ml⁻¹ protein solution either in 50 mM citrate–phosphate buffer, pH 7.0, or in 50 mM citrate buffer, pH 4.0. The scan speed used was 20 nm min⁻¹ with a time constant of 4 s. The spectral bandwidth was set at 1 nm, and five scans were recorded at room temperature (25 °C), averaged and smoothed. Actual protein spectra were obtained by subtracting CD signals of buffers used for protein solutions.

2.5. FT-IR spectroscopy

The secondary structure of the heavy chain was also examined by FT-IR spectroscopy using a

Nicolet 8210 FT-IR spectrometer with a zinc selenide attenuated total reflectance (ATR) accessory. The spectral recording conditions were similar to those described by Fu et al. [25,26]. The H chain (~ 0.5 mg ml⁻¹) in different pH buffers (pH 4.0 or 7.0) was introduced to the ATR compartment and the spectra were immediately recorded. The protein spectra at pH 4.0 and 7.0 were obtained by subtracting the respective buffer (pH 4.0 or 7.0) spectra. The secondary structure estimation was carried out by curve-fitting analysis after identifying spectral band positions with Fourier self deconvolution and second-order derivatization, as described by Fu et al. [25,26].

3. Results

3.1. Effect of pH on the channel formation of the BoNT/A and its subunits

In order to investigate the pH effect on the channel activity of BoNT/A, reduced BoNT/A (10 μ g ml⁻¹), or its H chain (5 μ g ml⁻¹) was added to the front of two chambers divided by a 100- μ m-diameter thin lipid bilayer. The pH conditions on the two sides of the bilayer were varied and a measurement of the conductance across the lipid bilayer was carried out as an index of the channel activity of the neurotoxin and its H chain subunit. The L chain of BoNT does not exhibit voltage-gated membrane channel activity [12].

Addition of BoNT/A H chain to one side of the DPhPC membrane separating solutions at a symmetric pH of 7.4 did not induce any significant channel activity, except for a few single-channels that open and close within seconds (Fig. 1). The membrane conductance (G) at a given time was obtained from the relation $G=I/V$, where V is the voltage applied to the *cis* compartment and I is the resulting current. The single channel conductance of the BoNT/A H chain was estimated to be ~ 5 pS under this symmetric, neutral pH (7.4) condition.

At a symmetric pH of 4.7, shortly after (1.6 min) the H chain addition, active single-channel activity began (indicated by the noisy trace) (Fig. 2), which was not observed under symmetric pH 7.4 conditions (Fig. 1). Following this initial

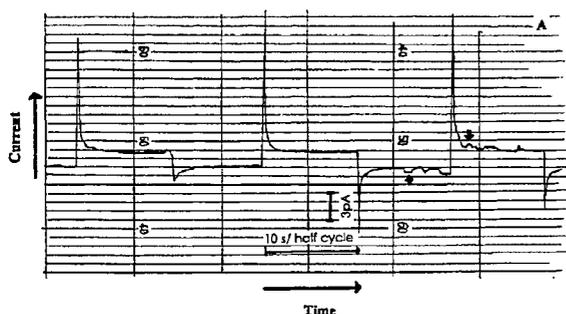


Fig. 1. Single channel currents in a planar lipid bilayer caused by addition of BoNT/A H chain (final concentration 5 $\mu\text{g}/\text{ml}$) at pH 7.4. A 100-mV square-wave potential was applied to a thin DPhPC/squalene bilayer in 0.1 M KCl, 5 mM CaCl_2 , 0.1 mM EDTA at room temperature (25 $^\circ\text{C}$). The arrow indicates single channel activity; 3-pA and 10-s bars indicate the current and time scales, respectively.

channel opening, more channels simultaneously opened (indicated by an abrupt drop within the negative half-cycle), which then led to a steady rise in the macroscopic membrane conductance (indicated by the downward trace in the negative-potential half-cycles) (Fig. 2). From the initial to the macro-opening, the rate of increase in channel activity (to reflect the rate of peptide integration in the membrane) is estimated as 7.5 pS s^{-1} .

When H chain was placed in an asymmetric pH condition (*cis* side 4.7, *trans* alkaline), a rapid increase in the macroscopic membrane conductance was observed following a short time lag after H chain addition (Fig. 3). A rate of increase in channel activity was estimated as 51 pS s^{-1} within the first 10 s.

In Figs. 2 and 3, active channel activity was also observed within the positive half-cycles. However, the channel closing frequency appears to be greater than the opening frequency at the positive potential. Such observations are illustrated more clearly in Fig. 3, as indicated by the asymmetric trace. This phenomenon indicates the voltage-gated channel property of BoNT/A H chain channels, which has also been reported by other researchers [12]. In our membrane bilayer system, membrane conductance was increased when the low pH side was made electrically positive.

The reduced form of BoNT/A was also tested for its channel activity. At symmetric low pH (4.7)

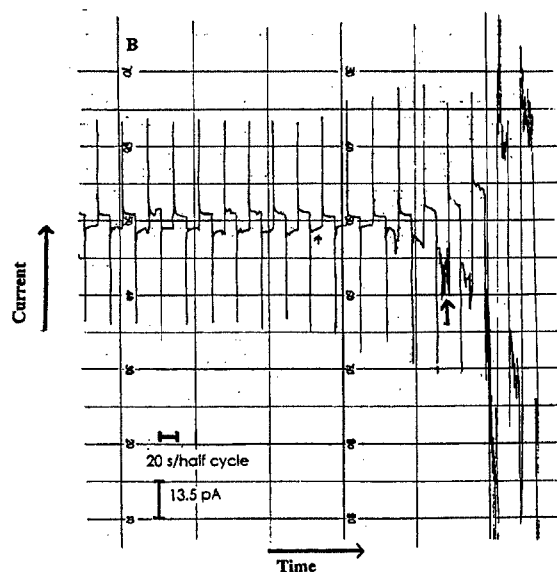


Fig. 2. Channel conductance of a thin DPhPC/squalene bilayer in the presence of 5 $\mu\text{g}/\text{ml}$ of H chain with symmetric pH of 4.7. The short arrow indicates the time of H chain addition, and the long arrow indicates the region of the trace with active channel activity. All other experimental conditions were the same as in Fig. 1.

condition, 10 $\mu\text{g ml}^{-1}$ reduced BoNT/A (treated with 15 mM DTT) either did not exhibit any channel activity or at the maximum evoked 7.5 pS

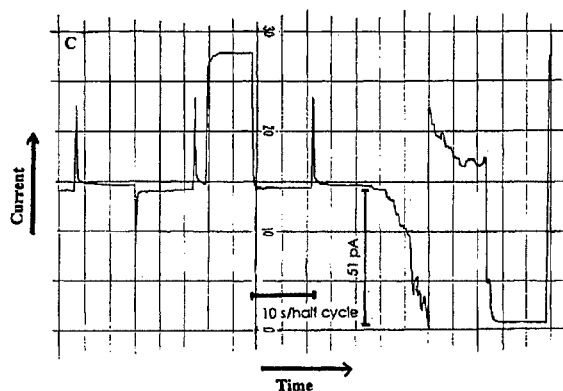


Fig. 3. Channel conductance of DPhPC/squalene bilayer in the presence of 5 $\mu\text{g}/\text{ml}$ H chain at an asymmetric (*cis* 4.7/*trans* alkalized) pH condition. The sample was added before the chart shown here, and other experimental conditions were the same as in Fig. 1.

of conductance over a 25-min period (data not shown). When attempts were made to induce the asymmetric conditions, a higher channel activity was triggered, but the membrane bilayer repeatedly collapsed, suggesting that the reduced protein might destabilize the membrane. A similar observation was made earlier by Blaustein et al. [20], who reported that the membrane channel conductance was noisy when the holo-neurotoxin (reduced) rather than H chain was used. Whether or not this observation could be due to possible interference with the membrane channel activity by the presence of the L chain in the holo-neurotoxin needs to be further investigated.

3.2. Effect of pH on structure of BoNT/A, H and L chains

The conformations of BoNT/A and its subunits were examined with far- and near-UV CD spectroscopy to derive structural information, both at the secondary and tertiary structural level, under low and neutral pH conditions to address the question of molecular responses of these proteins to pH, which could provide a molecular basis for their membrane channel activity and translocation.

3.2.1. Alteration in the secondary structure of H and L chains upon acidification

It has been suggested and observed from the functional activity assays that low pH triggers the membrane channel activity (vide supra), which might be responsible for the translocation of the light chain into the cytosol. The effect of pH on the secondary structure of dichain BoNT/A and its subunits was monitored using far-UV CD. The spectrum recorded for BoNT/A at pH 7.4 (spectrum not shown) showed maximum negative signals at 210 ($-11443^\circ \text{ cm}^2 \text{ d mol}^{-1}$) and 218 nm ($-11220^\circ \text{ cm}^2 \text{ d mol}^{-1}$), and a large positive signal at 193 nm ($16761^\circ \text{ cm}^2 \text{ d mol}^{-1}$), indicating a relatively high α -helical content. Applying a secondary structure estimation method that employs the least-squares combination of standard protein spectra [27] revealed $36.6 \pm 1.6\%$ α -helix, $24.9 \pm 2.6\%$ β -sheet, $12.4 \pm 1.1\%$ turns and $26.2 \pm 0.7\%$ random coil of BoNT/A (Table 1). Changing the pH to 4.0 did not seem to alter the

Table 1
Secondary structure estimation of BoNT/A, and its subunits, H and L chains under different pH conditions

	Secondary structure (%)			
	α -helix	β -sheet	Turn	Random coil
BoNT/A				
pH 7.4	36.6 ± 1.6	24.9 ± 2.7	12.4 ± 1.1	26.1 ± 0.7
pH 4.0	35.2 ± 1.6	28.1 ± 2.8	12.2 ± 0.8	24.6 ± 0.5
HC				
pH 7.4	32.6 ± 1.8	21.5 ± 3.8	17.5 ± 1.1	28.5 ± 2.1
pH 4.0	33.6 ± 3.3	21.4 ± 6.7	16.1 ± 2.3	28.9 ± 3.1
LC				
pH 7.4	44.8 ± 3.1	22.2 ± 5.2	11.8 ± 1.8	21.3 ± 1.8
pH 4.0	31.2 ± 3.1	32.8 ± 8	18.8 ± 10.1	23.8 ± 5.3
pH 7.4 ^a	48.8 ± 4.7	16.1 ± 2.1	17.0 ± 2.1	18.2 ± 0.3

Results were obtained by analyzing the CD spectra using the JASCO secondary structure estimation program.

^a Denotes the buffer condition was back titrated from pH 4.0 to pH 7.4.

secondary structure significantly, except for a slight increase in the β -sheet content (Table 1), which was within the experimental error of estimation.

The far-UV CD spectra were also recorded for the BoNT/A H chain under the same conditions as for BoNT/A. A double minimum signal at 210 and 218 nm (-10074 and $-10218^\circ \text{ cm}^2 \text{ d mol}^{-1}$, respectively, spectrum not shown) was also present in the H-chain spectrum at neutral pH. A positive spectral band was observed at ~ 193 nm ($12947^\circ \text{ cm}^2 \text{ d mol}^{-1}$). Similar to the BoNT/A, the CD spectral shape of BoNT/A H chain basically remained unaltered upon lowering the pH (spectrum not shown). Application of the spectral analysis program [27] revealed no structural difference in BoNT/A H chain at two pH values (pH 7.4 and 4.0; Table 1).

In contrast to insignificant structural alternations observed in BoNT/A and H chain with a decrease in pH, the far-UV CD spectrum of the L chain appeared to indicate drastic structural differences under the two different pH conditions (Fig. 4). The double-well spectral feature of BoNT/A L chain with minima at 218 and 210 nm observed at pH 7.4 changed dramatically to a single minimum centered at 225 nm. The intensity of the CD signal also decreased substantially (33, 57 and 51% change at 218, 210 and 193 nm, respectively).

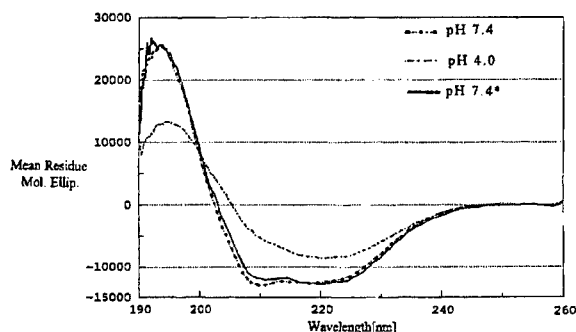


Fig. 4. Far-UV CD spectra of BoNT/A L chain were recorded under different pH conditions: 0.5–1 mg/ml of BoNT/A in a 0.1-mm-pathlength cuvette was scanned from 180 to 260 nm at a scan speed set at 20 nm/min with 8-s response time at room temperature. The spectra presented are the average spectrum from five scans, and the spectral resolution was 0.1 nm.

Changing the pH of BoNT/A L chain, which was previously exposed to pH 4.0 buffer, back to the pH 7.4 buffer fully restored the far-UV CD spectrum to the original BoNT/A L chain spectrum recorded under pH 7.4 buffer conditions (Fig. 4). The double minimum spectral feature of BoNT/A L chain, similar to BoNT/A and H chain, suggested that the L chain was also rich in α -helical polypeptide folding.

Upon exposure to the acidic condition, the changes in the spectral shape and intensity of BoNT/A L chain CD signal suggested a significant decrease in the α -helical content. However, the remnant positive signal between 190 and 200 nm ($\sim 13000^\circ \text{ cm}^2 \text{ dmol}^{-1}$ at the peak) indicated the presence of a substantial amount of the ordered structure under the low pH condition. Secondary structure estimation of BoNT/A L chain at pH 4.0 revealed $31.2 \pm 3.1\%$ α -helix, $32.8 \pm 8\%$ β -sheets, $18.8 \pm 10.1\%$ β -turns and $23.8 \pm 5.3\%$ random coils. (Table 1). Analysis of the reversibility of the low pH-induced structural changes in the L chain revealed a very high degree of secondary structure restoration (44.7 ± 3.1 vs. 47.2 ± 4.7 α -helix, 22.1 ± 5.2 vs. 21.1 ± 7.1 β -sheet, 11.8 ± 1.8 vs. 15 ± 2.1 turns and 21.3 ± 1.8 vs. 18.2 ± 0.3 random coils; Table 1).

The effect of pH on the secondary structure of the H chain was also investigated using the FT-IR/ATR technique. Fig. 5 shows the IR spectra of

the H chain in the amide III spectral region under two pH conditions. At pH 7.0, two major peaks featured at ~ 1235 and 1315 cm^{-1} , representing bands corresponding to β -sheets and α -helix, respectively. The small shoulder at $\sim 1280 \text{ cm}^{-1}$ corresponds to unordered structure [25]. When the H chain was exposed to acidic solution, the band at 1235 cm^{-1} maintained similar intensity, although it was shifted slightly. A shoulder at $\sim 1260 \text{ cm}^{-1}$ appeared, and a general decrease in spectral intensity was observed above 1265 cm^{-1} . Most strikingly, the band at 1324 cm^{-1} corresponding to the α -helical structure of H chain was drastically reduced under the low pH conditions. Estimation of secondary structure by curve-fitting analysis [25,26] revealed a decrease in α -helical content (32 vs. 23%) and increase in β -sheets (32 vs. 45%) after acid exposure of the BoNT/A H chain. The content of other structures (β -turns and random coils) showed only relatively small changes (36 vs. 32%).

3.2.2. Low pH effects on the Tyr topography of BoNT/A H chain

Near-UV CD signals of aromatic amino acid residues are sensitive to topographical and envi-

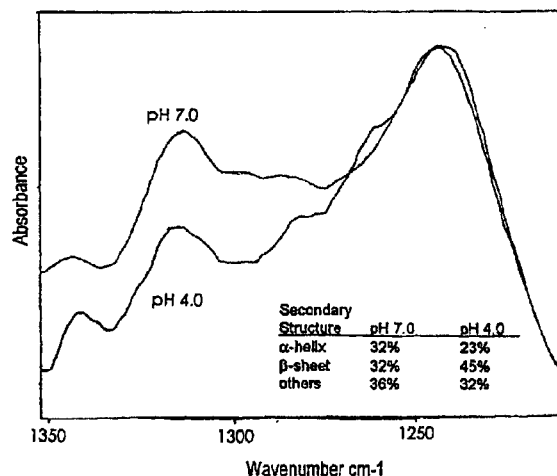


Fig. 5. FT-IR spectrum of BoNT/A H chain in the amide III spectral region under neutral and acidic conditions: 0.5 mg/ml of H chain was applied to a 60° horizontal zinc selenide ATR crystal and 256 scans at 2-cm^{-1} resolution were collected at room temperature (25°C). The average was smoothed and the buffer background was subtracted.

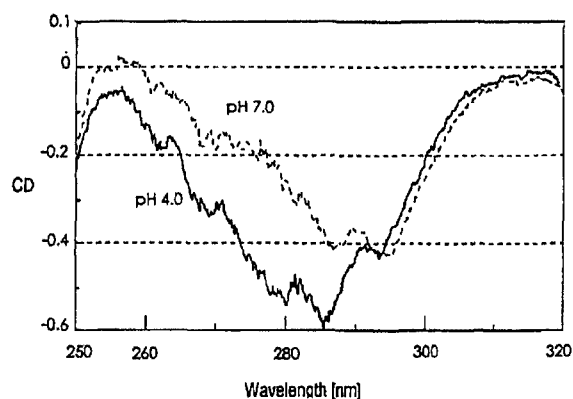


Fig. 6. Near-UV CD spectra of BoNT/A H chain at pH 7.0 and 4.0. Spectra were recorded between 250 and 320 nm at 0.2-nm spectral resolution with a scan speed of 20 nm/min and time constant of 4 s.

ronmental changes in their vicinity [28–31]. At pH 7.0, the H chain spectrum showed two distinctive bands at 295 and 285 nm (Fig. 6), which could be assigned to the 1L_b vibronic state of tryptophan and the 1L_a state of tyrosine, respectively [29]. A relatively featureless spectrum was observed from 280 to 255 nm, with a small shoulder at 270 nm. Upon exposure of the H chain to an acidic environment (pH 4.0), the overall optical activity increased (~ 35 – 50%) at 285 and 280 nm, whereas the band at 295 nm remained unchanged (Fig. 6). Relatively more prominent bands at 264 and 270 nm, known to arise from Phe residues, were observed under pH 4.0 conditions (Fig. 6).

3.2.3. Heavy chain induces the liposome aggregation at low pH

An attempt was made to investigate the impact of liposomes on the folding pattern of the BoNT/A H chain, especially under acidic conditions. However, addition of the H chain to liposome suspension under acidic conditions resulted in a turbid solution that was unsuitable for CD spectral recording for secondary structure analysis. Temperature-induced unfolding of BoNT/A H chain was investigated by monitoring CD signal changes at 222 nm in the presence and absence of liposomes at pH 7.4 and 4.0. The H chain in the absence of the liposomes showed clear optical

activity under both acidic and neutral conditions (vide supra). Heating of the H chain at pH 7.4 appeared to precipitate it quickly once the temperature reached approximately 50°C (Fig. 7). Under low pH conditions, temperature-induced unfolding exhibited a relatively prolonged transition, which appeared to have at least one intermediate state during the transition (Fig. 7). Temperature-induced unfolding of the H chain, when mixed with liposomes under pH 7.4 conditions, exhibited initiation of the unfolding transition at 30°C , which reached a steady-state plateau at 45°C , with clear steady-state intermediates at 37 – 39 and 41 – 42°C . When the pH of the H chain/liposomes mixture was decreased, it resulted in a turbid solution with a total loss of the CD signal. The H chain-mediated enhancement of aggregation (turbidity) was specifically observed only under low pH conditions, which appeared to correlate well with its functional and structural responses analyzed in this study.

In order to investigate further the H chain-induced aggregation of liposomes under different conditions, change in the turbidity was monitored

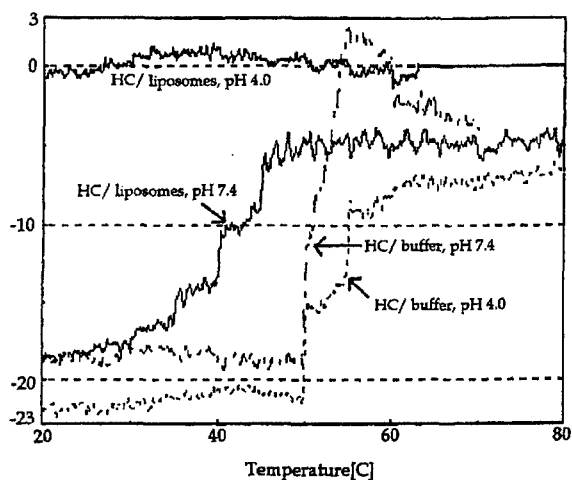


Fig. 7. Temperature-induced unfolding of the BoNT/A H chain (HC) in the presence and absence of liposomes under neutral and acidic pH values: 0.26 mg/ml of the HC was dissolved in pH 7.4 buffer, which was subsequently acidified by adding $3.4\ \mu\text{l}$ of 2 M HCl to pH 4.0. The same concentration of the HC was mixed with liposome suspension ($\text{OD}_{465} = 0.185$) for the liposome effect experiments, and the pH was adjusted by adding $3.4\ \mu\text{l}$ of 2 M HCl.

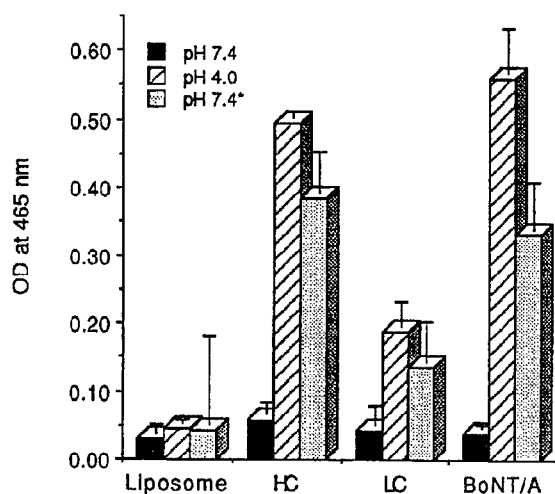


Fig. 8. Degree of liposome aggregation induced by BoNT/A, H chain (HC) and L chain (LC), as measured by optical density (OD) at 465 nm. pH* denotes that the pH has been readjusted from 4.0 back to 7.4 using 2 M NaOH.

by recording changes in OD, as a measure of light scattering, using a UV/Vis spectrophotometer. Steady-state changes in light scattering of the liposome solution, either without or with added protein, were monitored at 465 nm for 4 min at three pH levels, and final OD readings are plotted in Fig. 8.

As shown in Fig. 8, the OD of the liposome suspension in the absence of any added protein was not affected by lowering the pH from 7.4 to 4.0 (the OD only increased from 0.03 to 0.045) (Table 2; Fig. 8), indicating that alteration of the external pH in the absence of BoNT/A or its L and H chains did not induce liposome aggregation. Addition of H chain to the pH 7.4 solution con-

taining liposomes did not induce any change in the OD (Fig. 8). However, a drastic increase in OD occurred after acidifying the solution (OD increased from 0.058 to 0.50). Titration of the low-pH sample back to pH 7.4 partially reduced the OD to 0.39 (a 22% reduction; Table 2). When a similar experiment was performed with BoNT/A L chain, lowering of the pH evoked an OD increase from 0.044 to 0.19, and the back titration to pH 7.4 resulted in the reduction of the OD to 0.137, showing a reversibility of 27% (Fig. 8; Table 2). Lowering the pH of BoNT/A in the presence of liposomes resulted in the largest increase in OD (from 0.039 to 0.56). Back titration of the BoNT/A/liposome mixture reduced the light scattering by approximately 41% (Fig. 8; Table 2).

4. Discussion

Translocation of the BoNT or its L chain across endosomal membrane to the cytosol is a critical step in the mode of BoNT action. Because BoNT is a water-soluble protein, its passage through a non-polar lipid bilayer membrane must require structural adaptation so that peptide segments within the protein having membrane interactive properties (amphiphilic and hydrophobic) could rearrange themselves for integration in the endosomal membrane. One major factor that is known to trigger such structural responses is the low pH occurring physiologically during the endocytosis process. The response of BoNT and its active subunits to low pH and the subsequent behavior of the proteins with planar lipid bilayers and liposomes have been analyzed in this study.

Table 2

Degree of aggregation of liposomes induced by BoNT/A, H chain (HC) and L chain (LC) as monitored by the OD reading at 465 nm under different pH conditions

	Optical density at 465 nm			Reversibility (%)
	pH 7.4	pH 4.0	pH 7.4 ^a	
Liposomes	0.03 ± 0.01	0.045 ± 0.00	0.04 ± 0.01	22
BoNT/A	0.04 ± 0.00	0.56 ± 0.06	0.33 ± 0.07	41
HC	0.06 ± 0.02	0.50 ± 0.01	0.39 ± 0.06	22
LC	0.04 ± 0.03	0.19 ± 0.04	0.14 ± 0.06	27

^a Denotes the buffer back titrated from pH 4.0 to pH 7.4.

The BoNT/A H chain ion-conducting channel in the planar lipid bilayer (Figs. 1–3) [1] is voltage-gated, [2] has low conductance (5 pS) at near-neutral pH values, and [3] has increased propensity of formation under low pH conditions. Based on these observations, low pH seems to stimulate H chain channel activity, and may play a role in inducing the H chain insertion into the lipid bilayer. The role of pH gradient in the membrane channel activity is not very clear as yet. However, in view of the 'voltage-gated' nature of the channel, the pH gradient might play the role of a 'driving force'. In this model, while the applied voltage could trigger a specific structure of H chain membrane channel to an open state, the pH gradient could provide an ionic gradient, allowing stabilization to the open channel state. Such a situation could sustain a deeper opening of the channel, resulting in faster ionic conduction indicated by higher conductance in our experiments (Fig. 3). It is possible that the deepened opening of the membrane channel could be responsible for the translocation of L chain. Hoch et al. [12] demonstrated that under similar conditions BoNT/B H chain membrane channels could translocate cations with the size as large as 12–16 Å. However, in previous studies the symmetric low pH condition was not examined for ion channel activity of BoNT H chain. Our experimental results under symmetric low pH conditions (Fig. 2) suggest that structural changes in BoNT/A H chain introduced by the low pH are not sufficient to induce substantial ion transport. These results therefore suggest the possibility of a new role of the low pH on the *cis* side of the membrane.

Others have also shown that low pH is required for the strong channel formation activity of BoNT and its H chains [12,32]. A pH of 5.0 or lower induces the channel formation. Two possible effects of a low pH are (i) neutralization of negative charges of the protein, and/or (ii) conformational changes in the polypeptide folding due to modulation of backbone hydrogen bonds, either of which could allow exposure of hydrophobic domains and integration of the neurotoxin into the membrane bilayer. It has been observed that low pH increases the surface hydrophobicity of tetanus neurotoxin (TeNT), as demonstrated by labeled

Triton X-100 binding [32]. Similar observations were made for other dichain toxins, such as *Pseudomonas* exotoxin A [33].

The L chain of BoNT, which is the pharmacologically active subunit, is translocated from the endosome to the cytosol to exhibit the toxic activity. How the L chain retains its biological activity after adaptation to low pH and translocation across the membrane is not clearly understood. Based on the observation of the ion-conducting channels formed by BoNT/A and other similar toxins at low pH [6,12–14], it is hypothesized that the L chain undergoes total unfolding and directly traverses the membrane through this ion pore [12] into the cytosol.

The unfolding hypothesis is necessary to explain how a protein the size of the L chain can pass through a pore that has been demonstrated to be only 12–16 Å in diameter [12]. Our experimental results clearly indicate low pH-induced structural changes in BoNT/A L chain as monitored by CD spectroscopy (Fig. 4). The structure reflects a refolded state at pH 4.0. Although our results do not match with results obtained with TeNT L chain [34], where no secondary structure change was observed at pH 5.0, the β -sheets structure promoted below pH 3.0 is similar to our observations at pH 4.0 (Table 1). Most significantly, we have observed that the structural change induced by the low pH in BoNT/A L chain is almost totally reversible, a finding that explains retention of its biological activity as a zinc protease against SNAP-25 at near-neutral pH under both *in vivo* and *in vitro* conditions [35]. It has also been reported that the zinc protease activity of BoNT/A L chain pre-exposed to pH 4.7 is identical to the L chain maintained at pH 7.0 [36].

Because the L chain is not unfolded; *it is rather refolded* under low pH conditions, it is reasonable to consider an alternative mechanism for L chain transport through the H chain ion channel. The L chain might undergo a structural change at low pH, leading to a partially unfolded state, where part of the L chain can interact with the H chain and another part with the lipid bilayer. Such a L/H/lipid multimeric transient complex may only exist at low luminal pH. Once the L chain reaches the cytoplasmic face of the membrane, the com-

plex disassembles in response to the change in pH (back to physiological), where the L chain regains its natural conformation. The fact that L chain is actually capable of interacting with lipid membrane as observed in liposome permeability experiments [37,38] affords evidence in support of such a proposed mechanism. Furthermore, low pH is known to increase L chain interaction with lipids [39] and its surface hydrophobicity [36].

In contrast to the L chain, the secondary structure of H chain as monitored by CD does not change with pH. However, a decrease in the α -helix content is detected by the FT-IR/ATR technique. The discrepancy in results from the two techniques could be either due to higher sensitivity of the FT-IR technique in the amide III region, or to the differential interaction of the protein at two pH values with the ATR crystal. FT-IR spectroscopy is known to be relatively more sensitive to structural change [40,41]. We therefore believe that, irrespective of the cause of sensitivity of the FT-IR, this technique is more likely to elucidate differences in BoNT/A H chain at two different pH values. Results from X-ray crystallographic data are at quite a degree of variance from the estimation of secondary structure of BoNT/A in solution with optical spectroscopy [42]. Therefore, it is not possible to have a reliable independent method to verify estimation of the secondary structure. However, it has recently been reported that the hydrophobic transmembrane segment (650–681), which is predicted to be the channel-forming segment [7,9], is actually a 95-Å straight α -helix according to X-ray crystallography [43]. Taking the thickness of the lipid bilayer (32 Å) into consideration, it is reasonable to predict that this fragment undergoes a conformational change to prevent exposing itself to the hydrophilic (endoplasmic or cytosolic) environment and to accommodate itself within the lipid bilayer. Whether such a change could be triggered by low pH or a lipid environment remains to be elucidated. Our near-UV CD data clearly show a change in the aromatic side-chain arrangement of H chain under acidic (pH 4.0) conditions. A substantial increase in the CD intensity at 285 and 280 nm, possibly arising from Tyr residues, suggests that the micro-environment around Tyr residues becomes more

asymmetric or that the domain containing Tyr residues becomes more rigid under low pH conditions. There are 49 Tyr residues in the H chain and six of them are distributed in the hydrophobic region of the H chain. Y636, Y648 and Y684 are located in the vicinity of the channel-forming region of the BoNT/A H chain, and are therefore likely to be sensitive to any conformational change induced at low pH.

Liposome aggregation experiments reveal that BoNT/A and its individual subunits can induce vesicle aggregation at low pH. Low pH does not cause any significant aggregation of liposomes in the absence of BoNT proteins, suggesting a critical role for proteins in this process. Protein-induced aggregation of lipid vesicles could occur either through charge screening of lipid head groups by the protein or through the association of bound proteins. Proteins could also induce fusion of lipid vesicles by the same mechanisms, leading to larger vesicles that scatter more light. Aggregation of vesicles either through charge screening or through protein association could be reversible, whereas lipid bilayer fusion would probably not be reversible. BoNT/A was the most effective reagent in inducing aggregation and nearly half was reversible, suggesting that the aggregation mediated by the holotoxin does not involve membrane fusion to a large extent. The H chain is nearly as effective in inducing liposome aggregation as the holotoxin, whereas the L chain was only 38% as effective as the H chain (Fig. 8). The sizes of these proteins differ, which is likely to account for some of the differences in their ability to induce liposome aggregation. Reversibility of both L and H chain-mediated aggregation is 22–26%, which is quite significant, but considerably less than the reversibility of holotoxin induced aggregation.

A significant portion of the aggregation reversibility with pH can be explained if we assume that at least part of the aggregation is directly mediated by the oligomeric association of the proteins. Perhaps the intact BoNT/A protein, which does not seem to insert itself as effectively in the membrane as its L and H chains (based on their ability to permeabilize liposomes for calcein release [37,38]), adsorbs to the surface of the liposomes and enhances liposome aggregation

through self-association. It is also possible that BoNT/A adsorbed to the surface could screen surface charges, allowing liposomes by themselves to associate and aggregate. A similar mechanism has been proposed for lipid vesicle aggregation mediated by myelin basic protein [44].

While BoNT/A H chain induced nearly the same level of liposome aggregation as the holotoxin, its reversibility was approximately half that of BoNT/A (Fig. 8). The low reversibility could be explained by either irreversible self-association of the H chain and liposomes, or H chain-induced membrane fusion, which would obviously be an irreversible process. Evidence of aggregation of the H chain was also observed in temperature-induced unfolding experiments. At pH 4.0, even in the absence of liposomes, H chain unfolding exhibited intermediate states (Fig. 7), which could arise from the non-cooperative unfolding generally observed in oligomeric structures [45]. A drastic difference in the unfolding pattern in the presence of liposomes, even at pH 7.4, is indicative not only of the existence of oligomeric structures, but also of considerable alteration in the polypeptide folding, perhaps arising from binding at the surface of liposomes. Further investigation is needed to dissect the contributions of the different mechanisms in the observed aggregation of liposomes induced by BoNT/A and its active subunit fragments.

The salient features of this study can be summarized as follows. (1) The H chain forms ion channels in planar bilayer membranes. (2) H/L chains induce aggregation/fusion of lipid vesicles at low pH that is believed to occur via L/H chain-induced lipid destabilization. (3) Both H and L chain structures are altered at acidic pH, suggesting a conformational change in the protein to adapt to the membrane insertion process. (4) The structural reversibility of conformational changes in the light chain induced by low pH enable it to readapt to the active toxic structure in the cytosol after exposure to low pH in the endosomes.

Acknowledgments

This work was supported by a grant (to BRS) from NIH-National Institute of Neurological Dis-

orders and Stroke (NS33740), from the Camille and Henry Dreyfus Foundation to BRS, and by the US Army Medical Research and Material Command under Contract No DAMD17-02-C-001.

References

- [1] B.R. Singh, *Adv. Exp. Med. Biol.* 391 (1996) 63–84.
- [2] B.R. Singh, *Nat. Struct. Biol.* 7 (2000) 617–619.
- [3] L.L. Simpson, *Pharmacol. Rev.* 33 (1981) 155–188.
- [4] L.L. Simpson, in: L.L. Simpson (Ed.), *Botulinum Neurotoxin and Tetanus Toxin*, Academic Press, San Diego, 1989, pp. 154–178.
- [5] F.J. Lebeda, B.R. Singh, *Toxin Rev.* 18 (1999) 45–76.
- [6] M.S. Montal, R. Blewitt, J.M. Tomich, M. Montal, *FEBS Lett.* 313 (1992) 12–18.
- [7] M. Oblatt-Montal, M. Yamazaki, R. Nelson, M. Montal, *Protein Sci.* 4 (1995) 11490–11497.
- [8] T. Binz, H. Kurazono, M.W. Popoff, J. Frevert, K. Wernars, H. Niemann, *J. Biol. Chem.* 265 (1990) 9153–9158.
- [9] X. Be, F.-N. Fu, B.R. Singh, *J. Nat. Toxins* 3 (1994) 49–68.
- [10] J. Doyle, B.R. Singh, in: B.R. DasGupta (Ed.), *Botulinum and Tetanus Neurotoxins: Neurotransmission and Biomedical Aspects*, Plenum Press, 1993, pp. 231–235.
- [11] B.R. Singh, X. Be, in: R.H. Angeletti (Ed.), *Techniques in Protein Chemistry III*, Academic Press, Orlando, FL, 1992, pp. 373–383.
- [12] D.H. Hoch, M. Romero-Mira, B.E. Ehrlich, A. Finkelstein, B.R. DasGupta, L.L. Simpson, *Proc. Natl. Acad. Sci. USA* 82 (1985) 1692–1696.
- [13] J.J. Donovan, J.L. Middlebrook, *Biochemistry* 25 (1986) 2872–2876.
- [14] C.C. Shone, P. Hambleton, J. Melling, *Eur. J. Biochem.* 167 (1987) 175–180.
- [15] G. Menestrina, S. Forti, F. Gambale, *Biophys. J.* 55 (1989) 393–405.
- [16] L.L. Simpson, *J. Pharmacol. Exp. Ther.* 225 (1983) 546–552.
- [17] R.E. Sheridan, *Soc. Neurosci. Abstr.* 19 (1993) 1125.
- [18] M. Adler, S.S. Deshpande, R.E. Sheridan, F.J. Lebeda, in: J. Jankovic, M. Hallet (Eds.), *Therapy with Botulinum Toxin*, Dekker, New York, 1994, pp. 63–70.
- [19] L.L. Simpson, J.A. Coffield, N. Bakry, *J. Pharmacol. Exp. Ther.* 269 (1994) 256–262.
- [20] R.O. Blaustein, W.J. Germann, A. Finkelstein, B.R. DasGupta, *FEBS Lett.* 226 (1987) 115–120.
- [21] F.-N. Fu, S.K. Sharma, B.R. Singh, *J. Protein Chem.* 17 (1998) 53–60.
- [22] V. Sathymoorthy, B.R. DasGupta, *J. Biol. Chem.* 260 (1985) 10461–10466.
- [23] D. Busath, G. Szabo, *Biophys. J.* 53 (1988) 689–695.
- [24] F.-N. Fu, B.R. Singh, *J. Protein Chem.* 18 (1999) 701–707.

- [25] F.-N. Fu, D.B. DeOliveira, W.R. Trumble, H.K. Sarkar, B.R. Singh, *Appl. Spectrosc.* 48 (1994) 1432–1441.
- [26] F.-N. Fu, R.B. Lomneth, S. Cai, B.R. Singh, *Biochemistry* 37 (1998) 5267–5278.
- [27] J.T. Yang, C.S. Wu, H.M. Martinez, *Methods Enzymol.* 130 (1986) 208–269.
- [28] M.M. Bateniany, H. Mizukami, J.M. Salhany, *Biochemistry* 32 (1993) 663–668.
- [29] B.R. Singh, B.R. DasGupta, *Biophys. Chem.* 34 (1989) 259–267.
- [30] E.H. Strickland, *CRC Crit. Rev. Biochem.* 3 (1974) 113–175.
- [31] R.W. Woody, A.K. Duker, in: G.D. Fasman (Ed.), *Circular Dichroism and Conformational Analysis of Biomolecules*, Plenum Press, New York, 1996, pp. 109–157.
- [32] P. Boquet, E. Duflo, *Proc. Natl. Acad. Sci. USA* 79 (1982) 7614–7618.
- [33] T. Idziorek, D. FitzGerald, I. Pastan, *Infect. Immun.* 58 (1990) 1415–1420.
- [34] V. de Fillippis, L. Vangelista, G. Schiavo, F. Tonello, C. Monetucucco, *Eur. J. Biochem.* 229 (1995) 61–69.
- [35] J. Blasi, E.R. Chapman, E. Link, et al., *Nature* 365 (1993) 160–163.
- [36] L. Li, B.R. Singh, *Biochemistry* 39 (2000) 6466–6474.
- [37] Y. Kamata, S. Kozaki, *Biochem. Biophys. Res. Commun.* 205 (1994) 751–757.
- [38] F.-N. Fu, B.R. Singh, *J. Protein Chem.* 18 (1999) 701–707.
- [39] C. Montecucco, G. Schiavo, B.R. DasGupta, *Biochem. J.* 259 (1989) 47–53.
- [40] B.R. Singh, M.P. Fuller, *Appl. Spectrosc.* 45 (1991) 1017–1021.
- [41] B.R. Singh, M.P. Fuller, G. Schiavo, *Biophys. Chem.* 36 (1990) 155–166.
- [42] S. Cai, B.R. Singh, *Biochemistry* 40 (2001) 4693–4702.
- [43] D.B. Lacy, W. Tepp, A.C. Cohen, B.R. DasGupta, R.C. Stevens, *Nat. Struct. Biol.* 5 (1998) 898–902.
- [44] J.M. Bogg, P.M. Yip, G. Rangaraj, E. Jo, *Biochemistry* 36 (1997) 5065–5071.
- [45] G. Mei, A. Di Venere, M. Buganza, P. Vecchini, N. Rosato, A. Finazzi-Agro, *Biochemistry* 36 (1997) 10917–10922.

**Enhancement of the Endopeptidase
Activity of Purified Botulinum Neurotoxins
A and E by an Isolated Component of the
Native Neurotoxin Associated Proteins**

Shashi Kant Sharma and B. R. Singh

Department of Chemistry and Biochemistry, and Center for Marine
Science and Technology, University of Massachusetts Dartmouth,
Dartmouth, Massachusetts 02747

Biochemistry[®]

Reprinted from
Volume 43, Number 16, Pages 4791-4798

www.sciencedirect.com

Enhancement of the Endopeptidase Activity of Purified Botulinum Neurotoxins A and E by an Isolated Component of the Native Neurotoxin Associated Proteins

Shashi Kant Sharma[‡] and B. R. Singh*

Department of Chemistry and Biochemistry, and Center for Marine Science and Technology,
University of Massachusetts Dartmouth, Dartmouth, Massachusetts 02747

Received August 29, 2003; Revised Manuscript Received February 23, 2004

ABSTRACT: In botulism disease, neurotransmitter release is blocked by a group of structurally related neurotoxin proteins produced by *Clostridium botulinum*. Botulinum neurotoxins (BoNT, A–G) enter nerve terminals and irreversibly inhibit exocytosis via their endopeptidase activities against synaptic proteins SNAP-25, VAMP, and Syntaxin. Type A *C. botulinum* secretes the neurotoxin along with 5 other proteins called neurotoxin associated proteins (NAPs). Here, we report that hemagglutinin-33 (Hn-33), one of the NAP components, enhances the endopeptidase activity of not only BoNT/A but also that of BoNT/E, both under in vitro conditions and in rat synaptosomes. BoNT/A endopeptidase activity in vitro is about twice as high as that of BoNT/E under disulfide-reduced conditions. Addition of Hn-33 separately to nonreduced BoNT/A and BoNT/E (which otherwise have only residual endopeptidase activity) enhanced their in vitro endopeptidase activity by 21- and 25-fold, respectively. Cleavage of rat-brain synaptosome SNAP-25 by BoNTs was used to assay endopeptidase activity under nerve-cell conditions. Reduced BoNT/A and BoNT/E cleaved synaptosomal SNAP-25 by 20% and 15%, respectively. Addition of Hn-33 separately to nonreduced BoNT/A and BoNT/E enhanced their endopeptidase activities by 13-fold for the cleavage of SNAP-25 in synaptosomes, suggesting a possible functional role of Hn-33 in association with BoNTs. We believe that Hn-33 could be used as an activator in the formulation of the neurotoxin for therapeutic use.

Botulinum neurotoxins (seven serotypes, A–G) are a group of large proteins with mutually exclusive immunological properties but share pharmacological characteristics that cause flaccid muscle paralysis in the botulism disease (1). Botulinum neurotoxins (BoNTs)¹ are extremely toxic proteins (mouse LD₅₀, 10⁸ mg⁻¹ kg⁻¹ for type A) of 150 kDa and consist of a 100 kDa heavy chain and a 50 kDa light chain linked through a disulfide bond (2). Type A BoNT is produced along with 6 neurotoxin associated proteins (NAPs) to form a complex. NAPs are known to protect BoNT from the acidity and proteases of the GI tract (3–5), and thus make BoNT one of the most dreaded food poisoning agents (3, 6). In addition, because of the extreme toxicity and stability of BoNT in the presence of NAPs, BoNT complexes are considered as a group of the most dangerous biological warfare agents (7, 8). Sadly, despite their critical role in food poisoning and biological weapons, little is understood as to how these nontoxic accessory proteins (i.e., NAPs) play a critical role in the toxicoinfection process of botulism.

* To whom correspondence should be addressed: Department of Chemistry and Biochemistry, University of Massachusetts Dartmouth, 285 Old Westport Road, Dartmouth, MA 02747. Phone: 508-999-8588. Fax: 508-999-8451. E-mail: bsingh@umassd.edu.

[‡] Present address: Center for Food Safety and Applied Nutrition, Food and Drug Administration, 5100 Paint Branch Pkwy, HFS-300, College Park, MD 20740-3835.

¹ Abbreviations: BoNT, botulinum neurotoxin; NAP, neurotoxin associated protein; SNAP-25, synaptosomal associated protein of 25 kDa; DTT, dithiothreitol; GST, glutathione-S-transferase; SDS-PAGE, sodium dodecyl sulfate polyacrylamide gel electrophoresis; ELISA, enzyme-linked immunosorbent assay; Hn-33, hemagglutinin-33.

Recent discovery that BoNTs are Zn²⁺-endopeptidases (2, 9, 10) has led to the identification of several target proteins, which are critical for the docking and fusion of synaptic vesicles to the plasma membrane in the neurotransmitter release process. Cellubrevin, SNAP-25 (synaptosomal associated protein of 25 kDa), and syntaxin form the SNARE complex during docking of synaptic vesicles to the plasma membrane. Different BoNT types proteolytically cleave cellubrevin (BoNT/B, BoNT/C, BoNT/D, and BoNT/F), SNAP-25 (BoNT/A, BoNT/C, and BoNT/E), and syntaxin (BoNT/C) as part of their mode of action to block neurotransmitter release (2). Because of their specificity to inhibit neurotransmitter release at neuromuscular junctions, BoNT is increasingly being used to treat various neuromuscular disorders such as strabismus, torticollis, and blepharospasm (11). Interestingly, BoNT only in its complex form with NAPs (present in all BoNT serotypes) is used as a therapeutic agent, which is a more effective drug in this form than the pure BoNT (12). Again, the molecular basis of the superior therapeutic efficacy of BoNT complex is not known. Stabilization of BoNT/A by NAPs has been proposed as one possible explanation for the higher efficacy of the BoNT/A complex compared to the pure BoNT/A (11, 12).

The endopeptidase activity of pure BoNT/A is expressed only after its interchain disulfide bond is reduced (2, 9, 10). We have previously reported (13) that the BoNT/A complex, in contrast to pure BoNT/A, is enzymatically active even under nonreducing conditions and the endopeptidase activity of BoNT/A complex is 17-fold higher than that of the pure

BoNT/A. Under reducing conditions, the BoNT/A complex is significantly (about 15%) more active than the pure BoNT/A, and reduced purified BoNT/A has similar endopeptidase activity to the nonreduced BoNT/A in complex with NAPs (13). The higher endopeptidase activity of the BoNT/A complex is due to the presence of NAPs, suggesting a more than accessory role, such as protection against proteases in the GI tract, in the toxicoinfection process of botulism. The dramatically higher endopeptidase activity of the BoNT/A complex raises several questions: (1) Is the reduction of the disulfide bond of BoNT the only process that activates endopeptidase activity? (2) Is the higher therapeutic efficacy of the BoNT/A complex because of the enhanced endopeptidase activity? (3) Is the cumulative effect of all of the NAPs required for the BoNT/A complex to be enzymatically more active? (4) Can the NAPs-mediated activation of endopeptidase activity be observed with cross serotypes of BoNT?

In this paper, we present experimental evidence to suggest that the hemagglutinin-33 (Hn-33, also referred as HA-35 by some researchers) component of BoNT/A NAPs can activate BoNT/A equivalent to the cumulative effect of the BoNT/A complex. Further, Hn-33 is also able to activate the endopeptidase activity of BoNT/E.

MATERIALS AND METHODS

Purification of BoNT/A and BoNT/E. BoNT/A from *C. botulinum* (strain Hall) and BoNT/E from *C. botulinum* (strain Alaska) were purified as described previously (5, 14). Purified neurotoxins were precipitated with 0.39 g/mL of ammonium sulfate and stored at 4 °C until used. The precipitate was centrifuged at 10000g for 10 min, and the pellet was dissolved in a desired assay buffer, followed by dialysis to remove any residual ammonium sulfate.

Production and Purification of Hn-33. Hn-33 was isolated according to the procedure described by Fu et al. (14) with the use of a DEAE-Sephadex A-50 and a Sephadex G-100 column chromatography.

Concentrations of neurotoxin and Hn-33 were determined according to the extinction coefficients, ϵ mg/mL (278 nm) of 1.63 and 1.74, respectively (14, 15).

Expression and Purification of Glutathione-S-Transferase (GST)/SNAP-25. SNAP-25 was expressed and purified according to Cai et al. (13). Cells expressing GST/SNAP-25 fusion protein were collected by centrifugation and resuspended in 10 mM phosphate-buffered saline (PBS) at pH 7.4, containing 1 mM phenylmethanesulfonyl fluoride (PMSF). Cells were lysed by sonication for 2 min, treated with 1% Triton X-100, and centrifuged to remove cell debris. The supernatant was applied to glutathione-agarose beads (Sigma Chemical Co., St. Louis, MO) and washed with PBS buffer to remove other cellular proteins, and GST/SNAP-25 fusion protein was eluted with 10 mM glutathione in 50 mM Tris-HCl buffer at pH 8.0. The fusion protein was precipitated with ammonium sulfate, redissolved in the desired assay buffer (50 mM Tris-HCl, 10 mM sodium phosphate, 300 mM NaCl, 2 mM MgCl₂, 0.3 mM CaCl₂, 1 mM mercaptoethanol, and 0.1% NaN₃ at pH 7.6), and dialyzed against the same buffer, before being used for experiments.

Isolation of Rat-Brain Synaptosomes and Cleavage of SNAP-25. Frozen rat brains were purchased from RJO

Biologicals, Inc. (Kansas City, MO) and were stored at -80 °C. Synaptosomes were prepared as described by Li and Singh (16). The synaptosomes were first washed with HEPES buffer at pH 7.4, containing 140 mM NaCl, 5 mM KCl, 20 mM HEPES, 5 mM NaHCO₃, 1 mM MgCl₂, 1.2 mM Na₂HPO₄, and 10 mM glucose, and were then resuspended in 2 mL of the same buffer. All of the procedures were carried out at 4 °C. Synaptosomes (50 μ L) in HEPES buffer were incubated with 200 nM (final concentration) nonreduced or reduced [treatment with 20 mM dithiothreitol (DTT) at 37 °C for 30 min] BoNT/A or BoNT/E with a 1:1 molar ratio (BoNT/A:Hn-33, BoNT/E:Hn-33) and a 1:2 molar ratio (BoNT/A:Hn-33) at 37 °C for 4 h. The samples were then separated on a 12% sodium dodecyl sulfate polyacrylamide gel electrophoresis (SDS-PAGE) gel and were immunoblotted using anti-SNAP-25 antibody raised against the 12 amino acid C-terminal residues in a rabbit (Stressgen Biotechnologies Corp., Victoria, Canada).

In vitro Cleavage of SNAP-25: Western Blot. The endopeptidase activity of BoNT was assayed according to a Western blot method established previously (13). GST/SNAP-25 fusion protein (5 μ M) was incubated with 200 nM of BoNT/A or BoNT/E in the presence or absence of 200 nM of Hn-33 at 37 °C for 15 min in an assay buffer (50 mM Tris, 10 mM sodium phosphate, 300 mM NaCl, 2 mM MgCl₂, 0.3 mM CaCl₂, and 0.1% NaN₃) at pH 7.6, under reducing and nonreducing conditions. For reducing conditions, the BoNT/A and BoNT/E were prepared by pretreatment with 20 mM DTT for 30 min at 37 °C. To investigate the effect of Hn-33, BoNT/A and BoNT/E were preincubated with Hn-33. Hn-33, nonreduced BoNT/A or BoNT/E, and reduced BoNT/A or BoNT/E were each separately dissolved in 0.05 M citrate buffer at pH 5.5 and were filtered through a 0.45 μ m filter paper. Nonreduced BoNT/A or BoNT/E were mixed with Hn-33 (molar ratio 1:1) in a reaction volume of 3 mL. Similarly, reduced BoNT/A or BoNT/E were mixed with Hn-33 (molar ratio 1:1) in a reaction volume of 3 mL. The reaction mixture was incubated up to 15 min at room temperature (25 °C) because, at a 30-min incubation time, a complete cleavage of SNAP-25 was observed (data not shown). Samples were then separated on a 12% SDS-PAGE gel and were analyzed by Western blot using a polyclonal antibody raised against the 12 C-terminal amino acid residues of SNAP-25 (Stressgen Biotechnologies Corp.) as described previously (13).

The amount of uncleaved SNAP-25 was estimated by scanning the Western blot band using an Image Analyzer (ITTI, St. Petersburg, FL) and a Multiscan-R, and the percent cleavage was calculated by comparing the density of the uncleaved band to that of the control SNAP-25.

Enzyme-Linked Immunosorbent Assay (ELISA). The cleavage of SNAP-25 was also determined by ELISA with the aim to determine the minimum concentration of BoNT/A and BoNT/E required to cleave the SNAP-25. Flat-bottom microtiter plates were coated (100 μ L/well) with 10 μ g/mL of SNAP-25 fusion protein dissolved in a 0.01 M phosphate buffer at pH 7.2. Plates were incubated at 4 °C overnight. The plates were then washed 5 times with 0.01 M phosphate buffer at pH 7.2. Serially diluted 200 nM of BoNT/A and BoNT/E, with or without 200 nM of Hn-33, were added into the plates to a total volume of 100 μ L. After incubation at 37 °C for 30 min, plates were washed with 0.01 M phosphate

buffer at pH 7.2 containing 0.05% Tween-20 and were subsequently blocked by 3% bovine serum albumin dissolved in a 0.01 M phosphate buffer at pH 7.2. Rabbit anti-SNAP-25 antibody (Stressgen Biotechnologies Corp.), 3 ng/mL, (100 μ L/well) was used as the primary antibody to bind with the SNAP-25 remaining in the plates followed by incubation at 37 °C for 30 min. The peroxidase-labeled anti-rabbit antibody, 1:10 000, was added as a secondary antibody onto the plates, and the plates were incubated at 37 °C for 30 min. A substrate solution containing 0.04% OPD (*o*-phenylenediamine dihydrochloride) and 0.012% hydrogen peroxide in a citrate phosphate buffer at pH 5.0 was added into the wells, and the plates were incubated for 15 min at room temperature (25 °C). The reaction was subsequently quenched with 50 μ L of 2 M sulfuric acid, and the color was monitored by measuring the absorbance at 490 nm. Unless otherwise stated, the plates were washed 5 times with 0.01 M phosphate buffer at pH 7.2, containing 0.05% Tween-20, between the steps. The percent cleavage was calculated by comparing the absorbance of the uncleaved to that of the control SNAP-25.

For kinetic experiments, the ELISA method was used, as described above with the following modifications: after preincubation of Hn-33 with BoNT/A or BoNT/E separately, the BoNT/A or BoNT/E was added to the plate for different time intervals (0–40 min). The temperature of the plate was maintained at 37 °C during the addition of the samples. After incubation at 37 °C for 40 min, plates were washed with 0.01 M phosphate buffer at pH 7.2, containing 0.05% Tween-20, and subsequently blocked by 3% bovine serum albumin dissolved in 0.01 M phosphate buffer at pH 7.2. Primary and secondary antibodies were used as described above to estimate uncleaved SNAP-25.

Isothermal Titration Calorimetric Analysis of Hn-33 Interaction with BoNT/A. The binding isotherm of Hn-33 to the BoNT/A was generated employing the CSC isothermal titration calorimeter (Calorimetric Sciences Corp., Provo, UT). The binding was measured at 25 °C in a 10 mM phosphate buffer at pH 7.4. BoNT/A (0.7 μ M) in a total volume of 1.3 mL was placed in the reaction cell. After temperature equilibration, the 0.7 μ M of BoNT/A was titrated with 30 μ M Hn-33 ligand. The 20 μ L injections of Hn-33 ligand was mixed with BoNT/A at 400-s intervals in a reaction cell. The observed heat change accompanying titration was measured after each injection. The total observed heat effects were corrected for the heat of dilution of the ligand by performing control titrations in the buffer used for dissolving the protein. The resulting titration curve was deconvoluted for the best-fit model using Titration BindWork in the ITC (CSC) to obtain the affinity constant and the number of binding sites.

RESULTS

Hn-33 Induced Endopeptidase Activity of BoNT/A and BoNT/E in Vitro. Because SNAP-25 is the substrate for both BoNT/A and BoNT/E (9, 17, 18), endopeptidase activities of BoNT/A and BoNT/E were analyzed for their ability to proteolytically cleave recombinant GST/SNAP-25 fusion protein. The activity was determined by estimating the uncleaved SNAP-25 by Western blot analysis with a polyclonal antibody raised against the C-terminal 12 amino acid

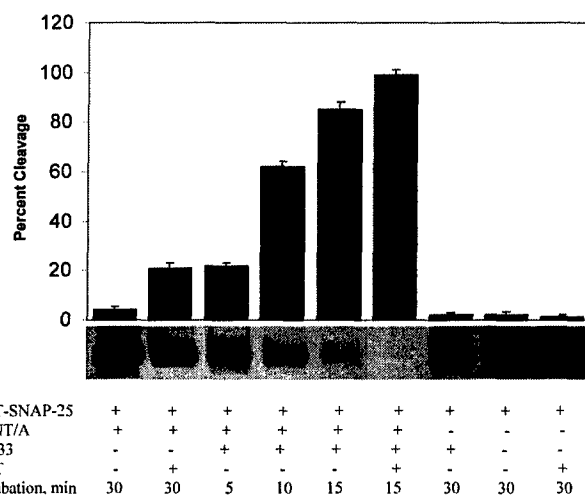


FIGURE 1: Comparative analysis of the endopeptidase activity of BoNT/A in the presence or absence of Hn-33. GST/SNAP-25 fusion protein (5 μ M) was incubated with pure BoNT/A (200 nM) in the presence or absence of Hn-33 (1:1 molar ratio) for 30 min at 37 °C in an assay buffer. Samples were then separated by 12% SDS-PAGE and analyzed by Western blot using a polyclonal antibody raised against the C-terminal 12 amino acid residues of SNAP-25 (Stressgen Biotechnologies Corp.) as detailed in the Materials and Methods. The results were plotted by averaging the percentage of GST/SNAP-25 cleaved in three independent sets of experiments.

residue of SNAP-25. Under nonreducing conditions, 200 nM of pure BoNT/A exhibited negligible residual endopeptidase activity ($4 \pm 1\%$ cleavage, $n = 3$), whereas BoNT/A, when reduced with 20 mM DTT, exhibited a 5.5-fold increase in its endopeptidase activity ($22 \pm 2\%$ cleavage, $n = 3$). Preincubation of nonreduced BoNT/A with Hn-33 enhanced the endopeptidase activity by 21-fold ($85 \pm 2\%$, $n = 3$), while preincubation of reduced BoNT/A separately with Hn-33 enhanced its endopeptidase activity by 25-fold ($99 \pm 1\%$, $n = 3$) within 15 min of the reaction time at 37 °C (Figure 1, Table 1).

Similar to BoNT/A, under nonreducing conditions, 200 nM of pure BoNT/E exhibited minimal residual endopeptidase activity ($2 \pm 1\%$ cleavage, $n = 3$), whereas, when reduced with 20 mM DTT, it exhibited a substantial (5-fold) increase in the endopeptidase activity ($10 \pm 1\%$ cleavage, $n = 3$) against SNAP-25. (Figure 2, Table 2). Preincubation of nonreduced BoNT/E with Hn-33 enhanced the endopeptidase activity by 25-fold ($50 \pm 1\%$ cleavage, $n = 3$), while preincubation of reduced BoNT/E with Hn-33 enhanced the endopeptidase activity by 43-fold ($85 \pm 2\%$ cleavage, $n = 3$) within 15 min of the reaction time at 37 °C.

We performed a series of control experiments to exclude the possibility of SNAP-25 cleavage by Hn-33 itself. When Hn-33 itself was incubated with SNAP-25, no cleavage of the latter was observed. Two other proteins isolated from type E *C. botulinum*, a 120 kDa neurotoxin binding protein (5) and a 70 kDa protein (19), were used in place of Hn-33 to validate the assay of BoNT endopeptidase activity through the ELISA method used in this paper. No endopeptidase activity (cleavage of SNAP-25) was observed in these control experiments. Also, DTT by itself did not induce any cleavage of SNAP-25 (Figure 1).

To confirm the above cleavage results, the SNAP-25 cleavage by a range of BoNT/A or BoNT/E concentrations

Table 1: Comparison of SNAP-25 Cleavage by BoNT/A or BoNT/E with and without Hn-33 under Nonreduced and Reduced Conditions^a

neurotoxin	percent cleavage							
	nonreduced BoNT		nonreduced BoNT + Hn-33		reduced BoNT		reduced BoNT + Hn-33	
	Western blot	ELISA	Western blot	ELISA	Western blot	ELISA	Western blot	ELISA
BoNT/A	4 ± 1	5 ± 2	85 ± 2	92 ± 2	22 ± 2	25 ± 1	99 ± 1	97 ± 4
BoNT/E	2 ± 1	4 ± 3	50 ± 2	52 ± 1	10 ± 1	15 ± 1	85 ± 1	89 ± 2

^a The percent cleavage was monitored by two methods, Western blot and ELISA, and represents the average of three individual independent experiments (data derived from Figures 1–3).

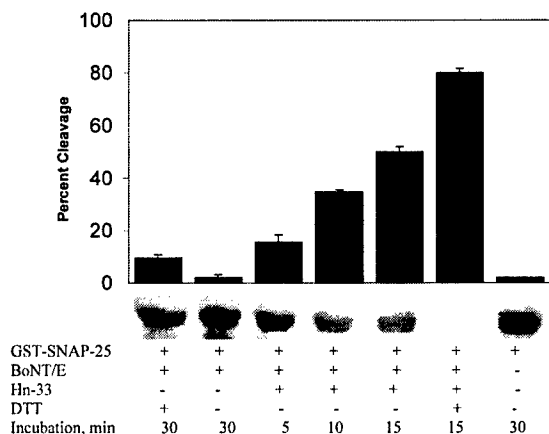


FIGURE 2: Comparative analysis of the endopeptidase activity of BoNT/E in the presence or absence of Hn-33. GST/SNAP-25 fusion protein (5 μ M) was incubated either with pure BoNT/E (200 nM) in the presence or absence of Hn-33 (1:1 molar ratio) for 30 min at 37 °C in an assay buffer. Other experimental details were the same as those in Figure 1.

Table 2: Initial Reaction Rates of SNAP-25 Cleavage by Nonreduced and Reduced BoNT/A and BoNT/E with and without Hn-33^a

neurotoxin	initial reaction rate (μ M/min) of SNAP-25 cleaved			
	nonreduced BoNT	nonreduced BoNT + Hn-33	reduced BoNT	reduced BoNT + Hn-33
BoNT/A	3.9	37.0	12.3	47.8
BoNT/E	2.4	15.0	7.5	21.0

^a The initial reaction rate (μ M/min) was determined from the slope of the linear portion (4 min) of the SNAP-25 cleavage versus the time plots (Figure 5).

was determined by an ELISA method using SNAP-25 C-terminal polyclonal antibody, as described in the Materials and Methods section. Under a nonreducing condition, 200 nM of pure BoNT/A exhibited negligible residual endopeptidase activity (5 ± 2% cleavage, $n = 3$), whereas under reducing conditions it exhibited a 5-fold increase in its endopeptidase activity (25 ± 1% cleavage, $n = 3$). Preincubation of nonreduced BoNT/A with Hn-33 enhanced the endopeptidase activity by 18-fold (92 ± 2% cleavage, $n = 3$), while preincubation of reduced BoNT/A with Hn-33 enhanced its endopeptidase activity by 19-fold (97 ± 4% cleavage, $n = 3$) (parts A and B of Figure 3, Table 1).

In case of BoNT/E, under nonreducing condition, 200 nM of pure BoNT/E exhibited negligible residual endopeptidase activity (4 ± 3% cleavage, $n = 3$), whereas BoNT/E, when reduced with 20 mM DTT, exhibited a 4-fold increase in its endopeptidase activity (15 ± 2% cleavage, $n = 3$). Preincubation of nonreduced BoNT/E with Hn-33 enhanced the endopeptidase activity by 14-fold (52 ± 1% cleavage, $n = 3$), while preincubation of reduced BoNT/E with Hn-33

enhanced its endopeptidase activity by 25-fold (89 ± 2% cleavage, $n = 3$) (parts C and D of Figure 3, Table 1).

While the comparison is made at 200 nM BoNT concentrations, similar cleavage results were observed throughout the concentration range of BoNT used (Figure 3; Table 1). The ELISA results agree with the Western blot results.

Hn-33 Induced Endopeptidase Activity of BoNT/A and BoNT/E in Synaptosomes. To evaluate the physiological significance of BoNT endopeptidase activity enhanced by Hn-33, we compared the Hn-33-induced endopeptidase activity of BoNT/A and BoNT/E against SNAP-25 using rat-brain synaptosomes. Under nonreducing conditions, 200 nM of BoNT/A and BoNT/E each cleaved 6 ± 4% ($n = 3$) and 4 ± 2% ($n = 3$), respectively, of SNAP-25 at 37 °C after a 4-h reaction time. Reduced BoNT/A (200 nM) cleaved 20 ± 5% ($n = 3$) of SNAP-25 under reaction conditions identical to those listed above. Preincubation of nonreduced BoNT/A with Hn-33 at equimolar concentrations (BoNT/A:Hn-33, 1:1) enhanced the endopeptidase activity of BoNT/A over 13-fold (78 ± 5%, $n = 3$) (Figure 4). Incubation of BoNT/A with Hn-33 at a higher molar ratio (BoNT/A:Hn-33, 1:2) did not have any significant additional effect on the endopeptidase activity (79 ± 3% SNAP-25 cleavage, $n = 3$) compared to the effect of the equimolar concentration of Hn-33 on BoNT/A (Figure 4). Reduction of the disulfide bond of BoNT/E (200 nM) enhanced its endopeptidase activity substantially (4-fold) as indicated by 15 ± 7% cleavage of SNAP-25 ($n = 3$) at 37 °C after a 4-h reaction time. Preincubation of nonreduced BoNT/E with Hn-33 at equimolar concentrations (BoNT/E:Hn-33, 1:1) enhanced the endopeptidase activity of BoNT/E by over 13-fold (53 ± 8% cleavage, $n = 3$) (Figure 4).

In a preliminary effort to evaluate the influence of Hn-33 on the kinetics of BoNT endopeptidase activity, initial rates of the endopeptidase activity of BoNT/A and BoNT/E were determined by estimating the percent cleavage of SNAP-25 at different time intervals. The time course of SNAP-25 cleavage, obtained with the ELISA method, showed a plateau within 30 min of the reaction time (Figure 5). However, linearity of the curve was observed only for the first 4 min of the reaction time, especially for reactions where no Hn-33 was added. We, therefore, used the slope of the linear portion of the curve within the first 4 min of the reaction time to estimate the initial reaction rates catalyzed by BoNT endopeptidase. Under nonreducing conditions, BoNT/A and BoNT/E showed initial reaction rates of 3.9 and 2.4 μ M/min, respectively. Under reducing conditions, initial reaction rates for the endopeptidase activity of BoNT/A and BoNT/E were 12.3 and 7.5 μ M/min, respectively. Preincubation of nonreduced BoNT/A and BoNT/E separately with Hn-33 at an equimolar concentration (BoNT:Hn-33, 1:1) enhanced the rates of their endopeptidase activity by

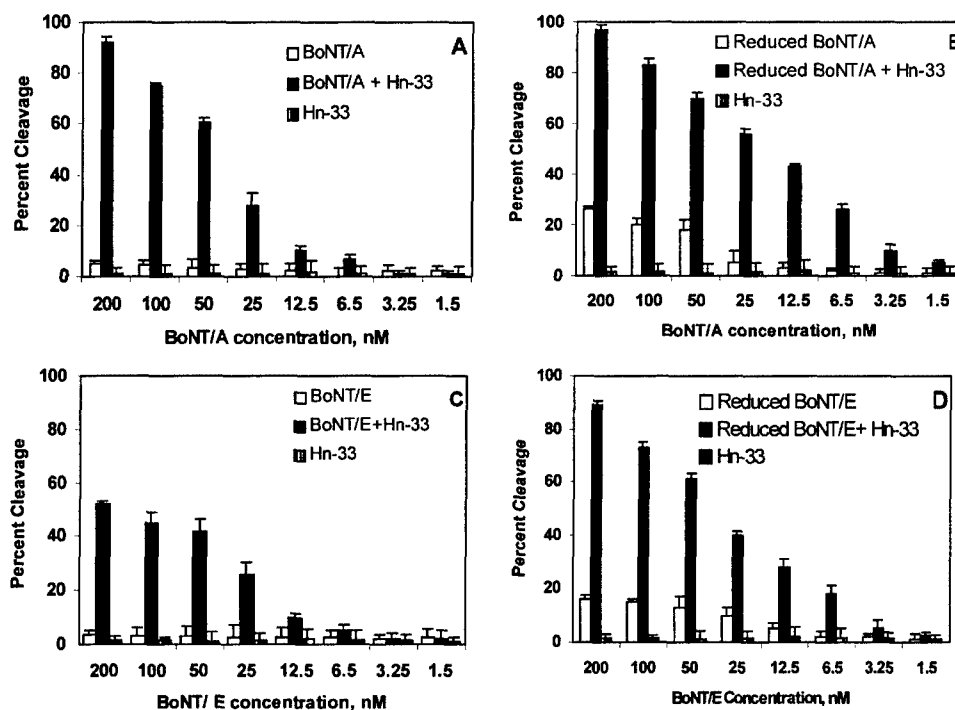


FIGURE 3: Cleavage of GST/SNAP-25 by nonreduced BoNT/A (A), reduced BoNT/A (B), nonreduced BoNT/E (C), and reduced BoNT/E (D) as analyzed by ELISA. Plates were coated with 10 $\mu\text{g}/\text{mL}$ of GST/SNAP-25 and were incubated overnight at 4 $^{\circ}\text{C}$. Nonreduced BoNT/A or BoNT/E was preincubated with or without Hn-33 (1:1 molar ratio) for 30 min at 37 $^{\circ}\text{C}$ before addition to the plates. Anti-SNAP-25 rabbit antibody (3 ng/mL) was added to the plates. Peroxidase-labeled anti-rabbit antibody was used as a secondary antibody as described in the Materials and Methods.

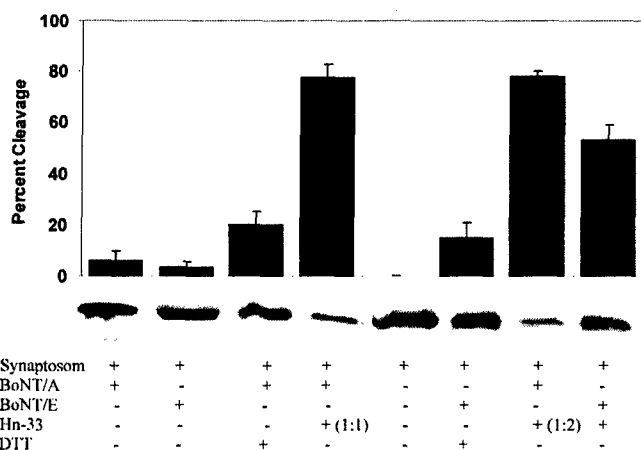


FIGURE 4: Comparative analysis of the endopeptidase activity of BoNT/A or BoNT/E in the presence and absence of Hn-33 on the level of SNAP-25 of rat-brain synaptosomes under nonreducing conditions. Synaptosomes (50 μL) in Hepes buffer were incubated with 200 nM (final concentration) nonreduced BoNT/A with 1:1 or 1:2 (BoNT/A–Hn-33) or BoNT/E with 1:1 (BoNT/E–Hn-33) at 37 $^{\circ}\text{C}$ for 4 h. The samples were then analyzed by 12% SDS–PAGE and were immunoblotted using anti-SNAP-25 antibody as described in the Materials and Methods. The results were plotted by averaging the percentage of SNAP-25 cleaved in three independent sets of experiments.

9.4- and 6.3-fold, respectively, with cleavage rates of 37 (BoNT/A) and 15 $\mu\text{M}/\text{min}$ (BoNT/E). Preincubation of reduced BoNT/A or BoNT/E with Hn-33 at an equimolar concentration (BoNT:Hn-33, 1:1) enhanced the rates of their endopeptidase activity by 12.2- and 8.7-fold, respectively, with cleavage rates of 47.8 (BoNT/A) and 21 $\mu\text{M}/\text{min}$ (BoNT/E) (Figure 5, Table 2).

Physical Interaction of Hn-33 with BoNT/A. Interaction of Hn-33 with BoNT/A was examined with isothermal

calorimetry by measuring heat changes upon titration of the BoNT/A solution with Hn-33, both dissolved in a 10 mM phosphate buffer at pH 7.4. Figure 6 shows a typical titration curve. The concentration range chosen provided a very smooth curve of steady heat change with every injection until injection 15, after which it reached a saturation level (Figure 6A). The saturation level was reached at a molar ratio of 10:1 (Hn-33–BoNT/A). Considering that Hn-33 is known to exist as a dimer (20), this set of data suggests five Hn-33 dimeric molecules bound to one BoNT/A. Interestingly, the molar ratio of Hn-33 to BoNT/A in the BoNT/A complex was found to be 8:1 based on SDS–PAGE analysis (21). It is possible that in the absence of other NAPs Hn-33 is able to have more freedom to bind to BoNT/A thus leading to a ratio of 10:1. The number of binding sites estimated from the curve was 1.0, suggesting that the binding sites belong to a class of similar affinity.

The interaction between Hn-33 and BoNT/A is exothermic (Figure 6A), and ΔH estimated at -120 kJ mol^{-1} from the binding curve (Figure 6B) is within the typical range of strong protein–protein interactions (22, 23). The binding constant was estimated to be $4.32 \times 10^{-5} \text{ M}^{-1}$, which is within the range of interactions between specific proteins (24).

DISCUSSION

Although the discovery of endopeptidase activity of BoNT in 1992 (10) has opened up many avenues to the understanding of the biochemical mechanism of its toxic action, the endopeptidase activity itself has remained a subject of intense research to understand its unique characteristics (2, 25, 26). Among its unique features, it has been reported that reduction of the disulfide bond between the light and heavy chain is required for the endopeptidase activity (9, 10). The active

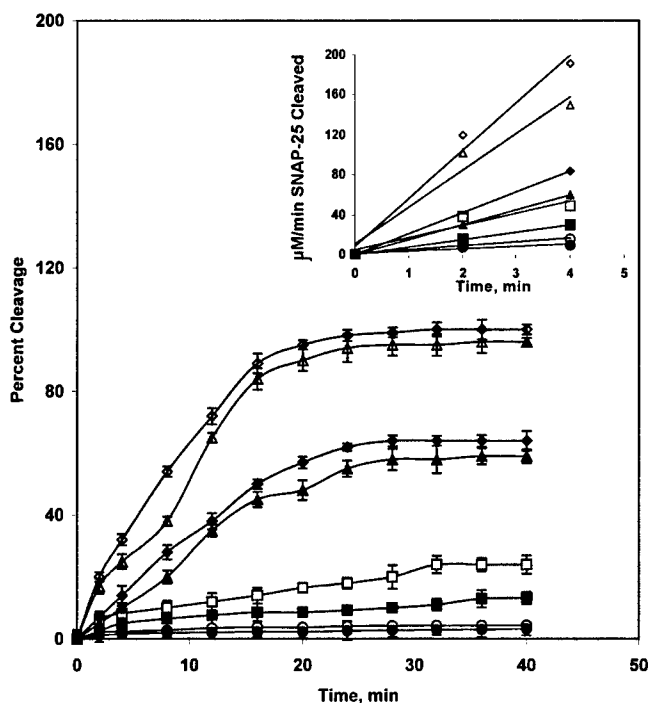


FIGURE 5: Time course of SNAP-25 cleavage by BoNT/A or BoNT/E in the presence or absence of Hn-33 analyzed by ELISA. Plates were coated with 10 $\mu\text{g}/\text{mL}$ of GST/SNAP-25 and incubated overnight at 4 $^{\circ}\text{C}$. Nonreduced BoNT/A or BoNT/E was preincubated with or without Hn-33 (1:1 molar ratio) for 30 min at 37 $^{\circ}\text{C}$ prior to addition to the plates. Nonreduced BoNT/A (O) Nonreduced BoNT/E (●), Reduced BoNT/A (□), Reduced BoNT/E (■), Nonreduced BoNT/A when preincubated with Hn-33 (Δ), Nonreduced BoNT/E when preincubated with Hn-33 (\blacktriangle), Reduced BoNT/A when preincubated with Hn-33 (\diamond), Reduced BoNT/E when preincubated with Hn-33 (\blacklozenge). For reducing conditions, BoNT/A and BoNT/E were prepared by pretreatment with 20 mM DTT for 30 min at 37 $^{\circ}\text{C}$. Peroxidase-labeled anti-rabbit antibody was used as a secondary antibody as described in the Materials and Methods.

Zn^{2+} plays both a catalytic and structural role (27). In the presence of NAPs, there is no requirement of disulfide reduction for the endopeptidase activity (13) and the dimeric form of the BoNT has a lower enzymatic activity than the monomeric form (28). Furthermore, except for BoNT/C1, the seven serotypes of BoNT recognize only one specific protein substrate and selective cleavage site (2, 29).

It is important to examine the structural basis of unique characteristics of BoNT endopeptidases. Understanding the molecular basis of the unique endopeptidase activity of BoNT is not only likely to provide clues to the mechanistic of the enzyme activity, but the information could lead to the development of antidotes to the most poisonous poison.

A significantly enhanced endopeptidase activity of BoNT/A in the presence of Hn-33 isolated from the BoNT/A complex was observed (Table 1) even under conditions where the disulfide bond between the light and heavy chains of BoNT was not reduced. Hn-33 does not reduce the interchain disulfide bond between light and heavy chains of BoNT/A (20). The BoNT/A complex itself is known to have a drastically enhanced endopeptidase activity against SNAP-25 in solution without reducing the interchain disulfide bond of BoNT/A (13). Interestingly, the enhanced endopeptidase activity of BoNT/A in the presence of Hn-33 is virtually the same as the whole BoNT/A complex, both quantitatively and qualitatively. In qualitative terms, the Hn-33-enhanced en-

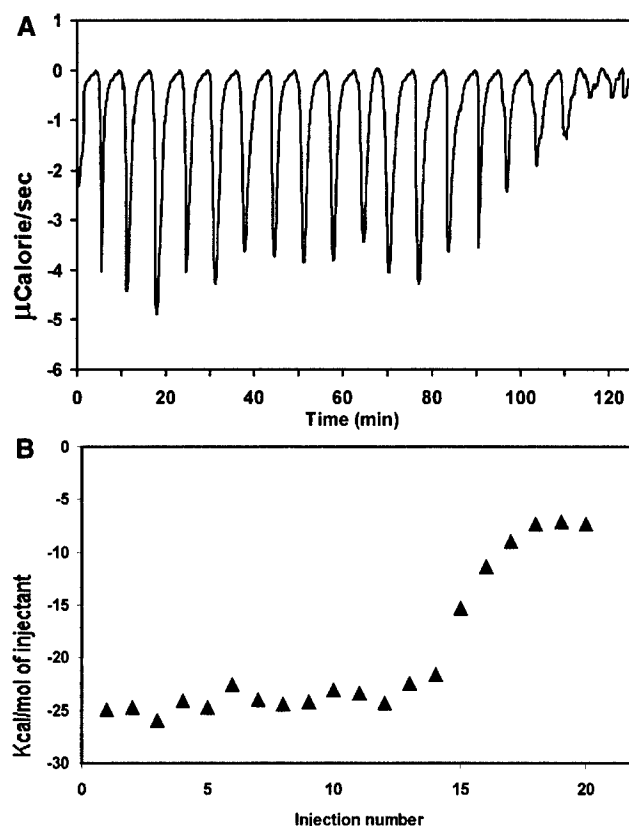


FIGURE 6: Typical isothermal calorimetric titration curve for BoNT/A with Hn-33. Sequential injections of 20 μL of Hn-33 ligand (concentration = 30 μM) was mixed with 1.3 mL of 0.7 μM BoNT/A at 400-s intervals in a reaction cell. The titration was performed at 25 $^{\circ}\text{C}$ in a 10 mM phosphate buffer at pH 7.4. (A) Total heat released is plotted in terms of microcalories per second versus time. The area underneath each injection peak is equal to the total heat released for that injection. (B) Integrated areas of the heat-release peaks in A plotted against the injection number. The solid line corresponds to the best-fit curve obtained by a nonlinear regression.

dopeptidase activity of BoNT/A did not require reduction of the disulfide bond (Figure 1, Table 1), just like the BoNT/A complex (13). It may be noted here that the disulfide bond of BoNT/A remains intact in the native complex form as well as in a complex with Hn-33 (4, 13). Quantitatively, Hn-33 enhanced the endopeptidase activity of nonreduced BoNT/A by 21-fold for a 15-min reaction period, whereas BoNT/A complex is reported to exhibit endopeptidase activity 17-fold higher than nonreduced pure BoNT/A for a 10-min reaction period (13). Thus, Hn-33 seems to be able to imitate the presence of all of the NAPs in the BoNT/A complex with respect to the enhancement of the endopeptidase activity.

In the BoNT/A complex, there are five NAPs including Hn-33 (13); Hn-33 makes up the largest fraction (25%) of the NAPs (20) in the BoNT/A complex. Furthermore, Hn-33 strongly protects BoNT/A against proteases such as trypsin, α -chymotrypsin, subtilisin, etc. (4). These observations are consistent with the effect of Hn-33 on the BoNT/A endopeptidase activity and strongly suggest that Hn-33 directly interacts with BoNT/A in the BoNT/A complex.

Although the mechanism by which Hn-33 may enhance the BoNT/A endopeptidase activity is not discernible from the current data, a possible explanation derived from the known X-ray crystallographic structure of BoNT/A is as

follows: The active site of BoNT/A is known to be buried in a crevice about 24-Å deep, which is occluded by a 56 amino acid residue (residues 490–545) belt (30, 31). It has been suggested that disulfide reduction opens up the belt and exposes the active site to the surface of the protein for its binding with the substrate peptide groups (31). We believe that the interaction of Hn-33 exposes the enzyme active site without any need to open up the belt. However, reduction of the disulfide bond and thus opening of the belt can further expose the active site to the substrate, as indicated by an approximately 17% additional increase in the endopeptidase activity of BoNT/A (Table 1). Exposure of the active site upon interaction with Hn-33 becomes more plausible in view of a recent report (32) suggesting the enzymatically active structure of BoNT/A in the form of a molten globule. A molten-globule-folded structure is significantly more flexible than a native-folded structure (33, 34).

Interestingly, although Hn-33 was isolated from the BoNT/A complex (14), its effect appears common to all of the BoNT serotypes. This was demonstrated by a similar experiment of the endopeptidase activity of BoNT/E and BoNT/A by Hn-33 (Table 1). The Hn-33 effect on BoNT/E is especially noteworthy, because the latter does not have a comparative NAP in its complex form (19). Therefore, a similar effect of Hn-33 on the two serotypes of BoNT suggests a common mechanism involved in the accessibility of the active site of BoNTs to their respective substrates. Moreover, there must be common structure motifs of the surface of the BoNT/A and BoNT/E molecules. While the three-dimensional structure of BoNT/E is not yet solved, common structural motifs are well-known for BoNT/A and BoNT/B (35–37). Future work with the crystal structure of Hn-33 and the BoNT complex would be required to confirm the common structural motif on the BoNT surface for the interaction with Hn-33.

Molecular basis of Hn-33-enhanced BoNT endopeptidase activity can be discerned from an additional set of published data, related to the Hn-33 protection of BoNT/A from proteases (4). Hn-33 can completely protect BoNT/A from pepsin, trypsin, α -chymotrypsin, and subtilisin, suggesting Hn-33 either surrounds the protease cleavage sites on BoNT/A or introduces refolding in BoNT/A so that the cleavage sites become inaccessible. The dissociation constant of 0.4 μ M derived from isothermal calorimetry experiments of BoNT/A and Hn-33 indicates a strong binding between the two proteins capable of introducing polypeptide refolding in BoNT/A. This is especially likely given a single binding site ($n = 1.0$) obtained from the isothermal titration curve (Figure 6). While it is possible that only one binding site is involved between BoNT/A and Hn-33, more than one binding sites could also lead to $n = 1$, as long as different binding sites have similar binding affinities. More than one binding site is also likely considering two dimers of Hn-33 bind to BoNT/A (14, 20, 21).

Each of the seven serotypes of BoNT has a group of associated NAPs, whose biological roles are not clearly understood. NAPs are known to protect the toxin from adversarial environmental conditions such as temperature, acidity, and proteases of the gastric juice (3, 38, 39). It is notable that Hn-33 represents the largest fraction of BoNT/A NAPs (14) and accounts for most of the hemagglutinin activity of the BoNT/A complex (28). Hn-33 by itself can

protect BoNT/A from proteases (4). Thus, the influence of Hn-33 on the endopeptidase activity of BoNT/A and BoNT/E is consistent with the Hn-33 effect on other biological and physical features of BoNT/A and its complex with the NAPs. Hn-33 seems to imitate the role of all NAPs in the BoNT/A complex.

Comparison of SNAP-25 cleavage by BoNT/A and BoNT/E in the presence and absence of Hn-33 in synaptosomes representing nerve cell conditions (Figure 4) indicated the following: (a) SNAP-25 cleavage by both BoNT/A and BoNT/E is less in synaptosomes compared to the in vitro conditions (Table 1, Figure 4). (b) Hn-33 enhanced the endopeptidase activity of both BoNT/A and BoNT/E even in synaptosomes, albeit to a lesser degree (Table 1, Figure 4). These results suggest that the neurotoxin complex with Hn-33 enters the synaptosome and the lower cleavage of SNAP-25 (in comparison to in vitro conditions) is likely to result from the inaccessibility of SNAP-25 in the synaptosome. We have recently made an observation (Y. Zhou and B. R. Singh, unpublished data) that Hn-33 binds to synaptosomes through synaptotagmin, which will further support the possibility of Hn-33 entry into synaptosomes. These results are particularly significant to the possibility of the use of the BoNT complex with Hn-33 as a therapeutic agent. The entrance of Hn-33 and BoNT as a complex will enhance and stabilize the endopeptidase activity inside the neuronal cell. Stable endopeptidase activity inside the neuronal is a critical phenomenon for the long lasting effects of botulinum either as a toxin or as a therapeutic agent (40, 41).

In summary, our results show that (i) the Hn-33 component of BoNT/A NAPs is able to imitate the effect of all of the NAPs in enhancing the endopeptidase activity of BoNT/A; (ii) the Hn-33 of the BoNT/A complex is also able to enhance the endopeptidase activity of BoNT/E, suggesting a common structural motif of BoNT serotypes for Hn-33; and (iii) Hn-33 bound to BoNT/A and BoNT/E enhanced the endopeptidase activity in synaptosomes, suggesting a possible entry of Hn-33 and BoNT inside the synaptosome.

ACKNOWLEDGMENT

This work was in part supported by a U.S. Army Medical Research and Materiel Command under Contract No. DAMD17-02-C-001 and by National Institutes of Health through New England Center of Excellence for Biodefense (AI057159-01).

REFERENCES

1. Simpson, L. L. (1989) in *Botulinum Neurotoxin and Tetanus Toxins* (Simpson, L. L., Ed.) pp 153–178, Academic Press, San Diego, CA.
2. Li, L., and Singh, B. R. (1999) *J. Toxicol., Toxin Rev.* 18, 95–112.
3. Sakaguchi, G. (1983) *Pharmacol. Ther.* 19, 165–194.
4. Sharma, S. K., and Singh, B. R. (1998) *J. Nat. Toxins* 7, 239–253.
5. Singh, B. R., Foley, J., and Lafontaine, C. (1995) *J. Protein Chem.* 14, 7–18.
6. Middlebrook, J. L. (1989) in *Botulinum Neurotoxin and Tetanus Toxin* (Simpson, L. L., Ed.) pp 95–119, Academic Press, San Diego, CA.
7. Zilinskas, R. A. (1997) *J. Am. Med. Assoc.* 278, 418–424.
8. Singh, B. R., Li, B., and Read, D. (1995) *Toxicon* 33, 1541–1547.

9. Blasi, J., Chapman, E. R., Link, E., Binz, T., Yamasaki, S., DeCamilli, P., Sudhof, T., Niemann, H., and Jahn, R. (1993) *Nature* 365, 160–163.
10. Schiavo, G., Benfenati, F., Poulain, B., Rossetto, O., de Laureto, P., DasGupta, B. R., and Montecucco, C. (1992) *Nature* 359, 832–835.
11. Johnson, E. A. (1999) *Annu. Rev. Microbiol.* 53, 551–75.
12. Schantz, E. J., and Johnson, E. A. (1992) *Microbiol. Rev.* 56, 80–99.
13. Cai, S., Sarker, H. K., and Singh, B. R. (1999) *Biochemistry* 38, 6903–6910.
14. Fu, F.-N., Sharma, S. K., and Singh, B. R. (1998) *J. Protein Chem.* 17, 53–60.
15. Dasgupta, B. R., and Sathyamoorthy, V. (1984) *Toxicon* 22, 415–424.
16. Li, L., and Singh, B. R. (1999) *J. Protein Chem.* 18, 89–95.
17. Schiavo, G., Rossetto, O., Catsicas, S., de Laureto, P., P., DasGupta, B. R., Benfenati, F., and Montecucco, C. (1993) *J. Biol. Chem.* 268, 23784–23787.
18. Schiavo, G., Santucci, A., Dasgupta, B. R., Mehta, P. P., Jontes, J., Benfenati, F., Wilson, M. C., and Montecucco, C. (1993) *FEBS Lett.* 335, 99–103.
19. Zhang, Z., and Singh, B. R. (1995) *Protein Sci.* 4 (suppl 2), 110.
20. Sharma, S. K., Fu, F. N., and Singh, B. R. (1999) *J. Protein Chem.* 18, 29–38.
21. Inoue, K., Fujinaga, Y., Watanabe, T., Ohyama, T., Takeshi, K., Moriishi, K., Nakajima, H., Inoue, K., and Oguma, K. (1996) *Infect. Immun.* 64, 1589–1594.
22. Hibbits, K. A., Gill, D. S., and Willson, R. C. (1994) *Biochemistry* 33, 3584–3590.
23. Pierce, M. M., Raman, C. S., and Nall, B. T. (1999) *Methods* 19, 213–221.
24. Li, J., and Weis, R. M. (1996) in *Techniques in Protein Chemistry* (Marshak, D., Ed.) Vol. 7, pp 33–44, Academic Press.
25. Montecucco, C., and Schiavo, G. (1993) *Trends Biochem. Sci.* 9, 324–327.
26. Singh, B. R. (2002) in *Scientific and Therapeutic Aspects of Botulinum Toxin* (Brin, M. F., Jankovic, J., and Hallett, M., Eds.) pp 75–88, Lippincott and Wilkins, Philadelphia, PA.
27. Fu, F. N., Lomneth, R. B., Cai, S., and Singh, B. R. (1998) *Biochemistry* 37, 5267–5278.
28. Cai, S., and Singh, B. R. (2001) *Biochemistry* 40, 4693–4702.
29. Blasi, J., Chapman, E. R., Yamasaki, S., Binz, T., Niemann, H., and Jahn, R. (1993). *EMBO J.* 12, 4821–4828.
30. Lacy, D. B., Tepp, W., Cohen, A. C., DasGupta, B. R., and Stevens, R. C. (1998) *Nat. Struct. Biol.* 10, 898–902.
31. Lacy, D. B., and Stevens, R. C. (1999) *J. Mol. Biol.* 291, 1091–1104.
32. Cai, S., and Singh, B. R. (2001) *Biochemistry* 40, 15327–15333.
33. Christensen, H., and Pain, R. H. (1991) *Eur. Biophys. J.* 19, 221–229.
34. Nakagawa, S. H., and Tager, H. S. (1993) *Biochemistry* 32, 7237–7243.
35. Swaminathan, S., and Eswaramoorthy, S. (2000) *Nat. Struct. Biol.* 7, 693–699.
36. Hanson, M. A., and Stevens, R. C. (2000) *Nat. Struct. Biol.* 7, 687–690.
37. Singh, B. R. (2000) *Nat. Struct. Biol.* 7, 617–619.
38. Inoue, K., Fujinaga, Y., Honke, K., Yokota, K., Ikeda, T., Ohyama, T., Takeshi, K., Watanabe, T., Inoue, K., and Oguma, K. (1999) *Microbiology* 145, 2533–2542.
39. Fujinaga, Y., Inoue, K., Nomura, T., Sasaki, J., Marvaud, J. C., Popoff, M. R., Kozaki, S., and Oguma, K. (2000) *FEBS Lett.* 467, 179–183.
40. Keller, J. E., Neale, E. A., Oyler, G., and Adler, M. (1999) *FEBS Lett.* 456, 137–142.
41. Foran, P. G., Mohammed, N., Lisk, G. O., Nagwaney, S., Lawrence, G. W., Johnson, E., Smith, L., Aoki, K. R., and Dolly, J. O. (2003) *J. Biol. Chem.* 278, 1363–1371.

BI0355544



Cloning, high-level expression, single-step purification, and binding activity of His₆-tagged recombinant type B botulinum neurotoxin heavy chain transmembrane and binding domain

Yu Zhou and Bal Ram Singh^{*,1}

Department of Chemistry and Biochemistry, and The School for Marine Science and Technology, University of Massachusetts Dartmouth, North Dartmouth, MA 02747, USA

Received 1 July 2003, and in revised form 6 October 2003

Abstract

Botulinum neurotoxins (BoNTs) are highly potent toxins that inhibit neurotransmitter release from peripheral cholinergic synapses and associate with infant botulism. BoNT is a ~150 kDa protein, consisting of a binding/translocating heavy chain (HC; 100 kDa) and a toxifying light chain (LC; 50 kDa) linked through a disulfide bond. C-terminal half of the heavy chain is binding domain, and N-terminal half of the heavy chain is translocation domain that includes transmembrane domain. A functional botulinum neurotoxin type B heavy chain transmembrane and binding domain (Ile 624–Glu 1291) has been cloned into a bacterial expression vector pET 15b and produced as an N-terminally six-histidine-tagged fusion protein (BoNT/B HC TBD). (His₆)-BoNT/B HC TBD was highly expressed in *Escherichia coli* BL21-CodonPlus (DE3)-RIL and isolated from the *E. coli* inclusion bodies. After solubilizing the purified inclusion bodies with 6 M guanidine-HCl in the presence of 10 mM β-mercaptoethanol, the protein was purified and refolded in a single step on Ni²⁺ affinity column by removing β-mercaptoethanol first, followed by the removal of urea. The purified protein was determined to be 98% pure as assessed by SDS-polyacrylamide gel. (His₆)-BoNT/B HC TBD retained binding to synaptotagmin II, the receptor of BoNT/B, which was confirmed by immunological dot blot assay, also to ganglioside, which was investigated using enzyme-linked immunosorbent assay.

© 2003 Elsevier Inc. All rights reserved.

Keywords: Botulinum neurotoxin; *Clostridium*; Dot blot; ELISA; Synaptotagmin; Synaptosomes

Botulinum neurotoxins (BoNT, EC 3.4.24.69) produced by *Clostridium botulinum* are among the most potent toxins known to human (~100 billion times more toxic than cyanide), and the agent responsible for the deadly food poisoning disease is known as botulism [1]. Because of its extreme toxicity, BoNT is considered a major dreaded biological weapon [2].

Clostridium botulinum cells produce seven serotypes of BoNTs, named as A to G. BoNTs are released as single polypeptide chain of about 150 kDa each, which are cleaved endogenously or exogenously resulting into a 100 kDa heavy chain (HC) and a 50 kDa light chain (LC) linked through a disulfide bond [1]. C-terminal half

of the heavy chain is binding domain, and N-terminal half of the heavy chain is the translocation domain in which transmembrane domain was contained.

The BoNT's mode of action involves three steps: extracellular binding and internalization, membrane translocation, and intracellular substrate cleavage and blockage of acetylcholine release. The heavy chain plays dual role in the toxic action of BoNTs, cell surface binding (binding domain), and translocation across membranes (translocation domain), while the light chain is responsible for the intracellular toxic activity. In the first step, the neurotoxin via the C-terminal fragment of its HC binds to nerve membrane through a protein receptor and is internalized through endocytosis. Synaptotagmin, an integral membrane protein of synaptic vesicles of rat brain, has been identified as the receptor for BoNT/B [3,4]. Synaptotagmin has also been shown

* Corresponding author. Fax: 1-508-99-8451.

E-mail address: bsingh@umassd.edu (B.R. Singh).

¹ The Henry Dreyfus Teacher-Scholar.

to bind to BoNT/A and E [5]. In the second step, as the pH inside endosome is lowered with proton pumps [6], the N-terminal domain of the HC is inserted into the membrane bilayer and assists in translocating the LC across the membrane of endosome. Finally, once in the cytoplasm, the LC cleaves one of the three SNARE proteins (soluble NSF attachment protein receptor): VAMP/synaptobrevin, SNAP-25 (synaptosomal-associated protein of 25 kDa), and syntaxin. The cleavage of any of the SNARE proteins results in blockage of acetylcholine release at the neuromuscular junctions, resulting in flaccid muscle paralysis.

BoNT/B is a polypeptide of 1291 amino acids [7], which is made of ~50 kDa light chain (Pro 1 through Lys 440) and ~100 kDa heavy chain (Ala 441 through Glu 1291). The heavy chain can be further cleaved by papain into two fragments, the C-terminal domain binds to the target cell surface and the N-terminal domain is involved in translocating the toxin across the membrane [8]. The transmembrane region within the N-terminal domain consists of residues 637–659 [9]. Development of protocols to obtain recombinant heavy chain binding domain along with the transmembrane domain will not only allow availability of the heavy chain binding domain containing transmembrane domain without the need to grow culture of *C. botulinum* requiring serious biosafety precautions, but also will help researchers to carry out experiments requiring large amounts of heavy chain binding domain containing the transmembrane segment. An understanding of mechanism and factors affecting transmembrane segment interaction with membrane and BoNT binding at the molecular level will allow design and development of convenient chemical antidotes against BoNT agents.

An antidote to botulism poisoning currently exists in the form of antibody that is produced in horse serum. However, its supply and shelf life are limited. The antibody antidote works by capturing the toxin in the bloodstream, which requires timely intervention of antibodies. Development of nontoxic fragments of BoNT as immunogens and recombinant vaccines for BoNT has been reported [10,11]. It was reported that recombinant tetanus and BoNT binding domains cause a significant delay in the paralysis induced by the corresponding holotoxins on the mouse phrenic nerve-hemidiaphragm preparation [12]. Question arises as to why the BoNT binding domains cannot block the paralysis? Could the BoNT binding domain containing transmembrane domain block the paralysis?

In this study, a DNA fragment encoding type B *C. botulinum* heavy chain binding domain containing transmembrane segment (BoNT/B HC TBD) was amplified by polymerase chain reaction (PCR). The DNA fragment was constructed into an expression vector pET 15b and the plasmid was transformed into *Escherichia coli* BL21-CodonPlus (DE3)-RIL. The high-level

expressed recombinant BoNT/B HC TBD was isolated from *E. coli* inclusion body, purified, and refolded in a single step by Ni²⁺ affinity chromatography. The binding activity of the purified recombinant BoNT/B HC TBD to synaptotagmin II, the receptor of BoNT/B, was confirmed by immunological dot blot assay. And the binding of the purified recombinant BoNT/B HC TBD to ganglioside was confirmed by ELISA.

Experimental procedure

Materials

All oligonucleotides were synthesized by Integrated DNA Technologies (Coralville, IA). Genomic DNA isolation kit was from Promega (Madison, WI). Restriction endonucleases, alkaline phosphatase, calf intestinal (CIP), and Vent DNA polymerase were from New England BioLabs (Beverly, MA). Thermal cycler for PCR was from Eppendorf-Netheler-Hinz GmbH (Hamburg, Germany). TA cloning kit and S.N.A.P. Miniprep kit for isolation of plasmids were from Invitrogen (Carlsbad, CA). The plasmid pET 15b was from Novagen (Novagen, Madison, WI). His-Select nickel affinity gel and CelLytic B II Bacterial Cell Lysis extraction reagent were obtained from Sigma (St. Louis, MO). Anti-His antibody was from Amersham Pharmacia Biotech (Piscataway, NJ).

Culture and chromosomal DNA isolation of *Clostridium botulinum* type B cells (strain Okra)

Clostridium botulinum type B cells (strain Okra) in a 1.5 ml microcentrifuge tube kept at -80 °C was added to a 10 ml cooked meat medium (Difco Laboratories, Sparks, MD) and cultured at 30 °C for 18–20 h. The *C. botulinum* type B cells in the cooked meat medium were inoculated in 500 ml of toxin production medium (1% N-Z amine type B (Quest International, Norwich, NY), 2% proteose peptone and 1% yeast extract (Difco Laboratories, Becton–Dickinson, Sparks, MD), 0.05% sodium thioglycollate, and 1% glucose (Sigma, St. Louis, MO) and incubated at 30 °C for 22 h.

Chromosomal DNA from *C. botulinum* type B cells was isolated by using Wizard Genomic DNA Purification Kit (Promega, Madison, WI) according to manufacturer's protocol. Briefly, *C. botulinum* type B cells were pelleted by centrifugation and resuspended in 50 mM EDTA, and suspension was incubated at 37 °C for 60 min after addition of 10 mg/ml lysozyme in the suspension. Then nuclei lysis buffer was added to the suspension and the suspension was incubated at 80 °C for 5 min to lyse the cells. RNase solution was added to the cell lysate after the sample cooled to room temperature and the solution was incubated at 37 °C for

60 min. The supernatant containing the DNA after protein precipitation was transferred to a clean tube containing isopropanol to precipitate the DNA. DNA pellet was obtained by centrifuging and washed by 70% ethanol. TE buffer (10 mM Tris-Cl, 1 mM EDTA, pH 8.0) was added to the DNA pellet. The DNA sample for PCR was stored at -20°C .

Primer design and polymerase chain reaction

According to BoNT/B sequence in GenBank database under Accession No. M81186 [13], primers for heavy chain binding domain containing transmembrane domain DNA fragment were designed as shown in Fig. 1. Both of *Nde*I and *Bam*HI restriction sites were incorporated into the 5' end of the forward sequence and reverse sequence primers, respectively. Because of the high AT content in the *C. botulinum* genome, GGGCCCC overhang was created into the 5' end of each restriction site.

PCR for the amplification of BoNT/B HC transmembrane and binding domain DNA fragment was performed in $1\times$ buffer (20 mM Tris-HCl, pH 8.8, 2 mM MgSO_4 , 10 mM KCl, 10 mM $(\text{NH}_4)_2\text{SO}_4$, and 0.1% Triton X-100), a total volume of 50 μl containing 200 ng of chromosomal DNA as template DNA, 100 ng of each primer, 200 μM concentration of each dNTP (deoxynucleoside triphosphate), and 1 U Vent DNA polymerase (New England BioLabs, Beverly, MA). The reaction was carried out using the following reaction cycles in a programmable thermocycler (Eppendorf-Netheler-Hinz GmbH, Hamburg, Germany): initial denaturation at 93°C for 2 min followed by 30 consecutive cycles consisting of denaturation at 93°C for 1 min, annealing for 2 min at 59°C , and extension at 73°C for 3 min, then final extension at 73°C for 10 min followed. The size of

BoNT/B HC transmembrane and binding domain DNA fragment as monitored on 1.0% agarose gel was 2 kb.

Gene construction

The PCR product was treated with Tag polymerase (Qiagen, Chatsworth, CA) at 72°C for 10 min to add one adenine on each side of the BoNT/B HC transmembrane and binding DNA fragment. The DNA fragment was purified by agarose gel electrophoresis using Gel extraction kit (Qiagen) and ligated into the pCR 2.1 TA cloning vector (Invitrogen, Carlsbad, CA). One recombinant plasmid containing the expected size insert was sequenced by the dideoxy chain termination method to confirm the correct DNA sequence by comparing its sequence with the BoNT/B sequence in GenBank database under Accession No. M81186. The identity of the two DNA sequences was analyzed using the Baylor College of Medicine (BCM) Search Launcher, and Expert Protein Analysis System (Exp-ASy) Molecular Biology Server through the Internet on a computer. The recombinant plasmid was cleaved with *Nde*I and *Bam*HI, the *Nde*I-*Bam*HI fragment was purified from the agarose gel, and then ligated to the *Nde*I-*Bam*HI digested and CIP-treated vector pET-15b (Novagen, Madison, WI). Clones were screened by digestion of a miniprep plasmid DNA (Invitrogen, Carlsbad, CA) with *Nde*I and *Bam*HI. Confirmation of the open reading frame (ORF) of the recombinant plasmid that the insert DNA fragment encoded BoNT/B HC transmembrane and binding domain was carried out by DNA sequencing of a representative plasmid recombinant (designated pET-BoNT/B HC TBD).

Expression, refolding, and purification of the recombinant BoNT/B HC transmembrane and binding domain

The BoNT/B HC TBD DNA fragment was cloned with the His_6 -tag at the N-terminal end and expressed under the control of the T7 promoter. The pET-BoNT/B HC TBD recombinant plasmid was transformed into *E. coli* strain BL21-CodonPlus (DE3)-RIL contained pACYC plasmid (Stratagene, La Jolla, CA). The *E. coli* cells were plated on LB-ampicillin (50 $\mu\text{g}/\text{ml}$) agar plates and expression of BoNT/B HC TBD of several colonies under the control of isopropyl- β -D-thiogalactopyranoside (IPTG)-inducible promoters were tested on an analytical scale (1 ml of induced culture). Each of the culture sample was tested for the expression of protein on a sodium dodecyl sulfate-polyacrylamide gel (7.5%) electrophoresis (SDS-PAGE).

To monitor the induction of BoNT/B HC TBD, the clone with the most highly expressed BoNT/B HC TBD was used to inoculate 50 ml of 2YT medium (1.6% tryptone, 1% yeast extract, and 0.5% NaCl), supplemented with 50 $\mu\text{g}/\text{ml}$ ampicillin and 50 $\mu\text{g}/\text{ml}$

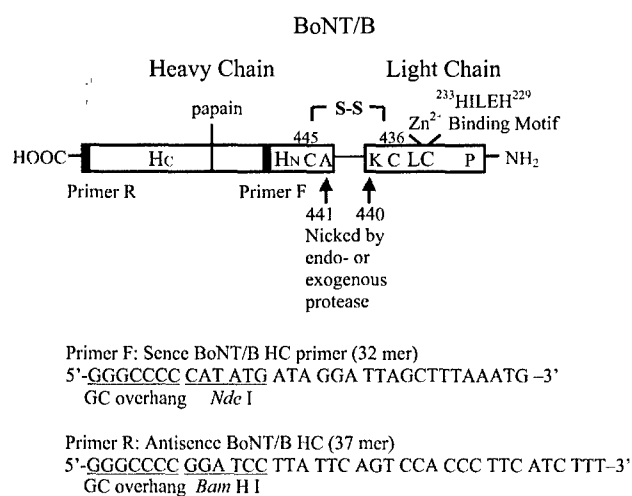


Fig. 1. Structural model of BoNT/B and DNA sequences of primers utilized in the construction of the pET-BoNT/B HC TBD plasmid.

chloramphenicol (Sigma, St. Louis, MO), and the culture was incubated at 37°C overnight. The next morning, the 50 ml culture was added to 1 L of 2YT medium in a 4-L PYREX flask, and the culture was grown at 37°C to $OD_{600} = 0.6–0.8$. IPTG was then added to a final concentration of 1 mM, and 2 ml of culture was sampled every hour after induction. Cells were centrifuged (5000g, 10 min) and resuspended in part of the supernatant to have approximately same turbidity in each suspension sample. Each sample was analyzed by SDS-PAGE after sonication.

For isolation and purification of the BoNT/B HC TBD, the *E. coli* clone with highest expressed BoNT/B HC TBD was grown for 5 h at 37°C under IPTG induction as described above. The cells were harvested by centrifugation at 5000g for 10 min at 4°C and cell pellet was stored at -80°C. The frozen cell pellet was thawed and resuspended in a lysis buffer, CelLytic B II bacterial cell lysis extraction reagent (Sigma, St. Louis, MO), containing 20 mM Tris-HCl, pH 7.5, and a mild non-ionic detergent, at the ratio of 5 ml of the lysis buffer per gram of wet cell paste. After the cells were completely resuspended, 5 µg/ml deoxyribonuclease I was added to digest any associated DNA. This step helped us to reduce viscosity of the extract. Also a protease inhibitor cocktail containing AEBSF, phosphoramidon, pepstatinA, bestatin, and E-64 (Sigma, St. Louis, MO) was added to the suspension at the ratio of 1 ml for 20 g wet weight cell paste to prevent proteolysis during the purification of histidine-tagged proteins. The suspension was incubated at room temperature for 15 min to fully extract the cells and centrifuged at 25,000g for 15 min to pellet the insoluble material. The supernatant was loaded onto His-Select nickel affinity gel column (Sigma, St. Louis, MO), and the chromatography was performed as described for the His-Select nickel affinity gel column chromatography of the inclusion body extract (see below).

The cell debris was used to purify the inclusion body and resuspended in the same lysis buffer at the same ratio described above. The final concentration of 0.4 mg/ml lysozyme was added to the suspension. The mixture was incubated at room temperature (25°C) for 15 min, and 20 ml of 1:20 diluted lysis buffer with deionized water (Sigma, St. Louis, MO) was added to the extract. The extract was mixed and centrifuged at 25,000g for 15 min to collect the inclusion bodies as pellets, and the supernatant was carefully removed from the inclusion bodies. The inclusion body pellet was resuspended in 40 ml of 1:20 diluted lysis buffer, and the extract was centrifuged at 25,000g for 15 min, and the procedure was repeated two more times to further wash the inclusion bodies, which were then stored at -80°C.

The frozen inclusion bodies from 1 L of the culture were thawed and resuspended in 20 ml of 0.1 M sodium phosphate buffer, pH 8.0, containing 6 M guanidine-

HCl, 0.4 M NaCl, and 10 mM β-mercaptoethanol, and sonicated on ice using a microprobe at 30% output, 4 times for a total of 2 min (30 s burst and 30 s cooling cycle). The guanidine-HCl extract was incubated on a rotating platform for 1 h at room temperature (25°C) and then clarified by centrifugation at 100,000g for 1 h at 4°C. The supernatant was diluted with 20 ml of column equilibration buffer (0.1 M sodium phosphate buffer, pH 8.0, containing 8 M urea, 0.4 M NaCl, 10 mM β-mercaptoethanol, and 5 mM imidazole), and applied onto a His-Select nickel affinity gel (Sigma, St. Louis, MO) (2 ml bed volume), which was previously equilibrated with the equilibration buffer. The column chromatography was performed at 4°C. The column was first washed with 20 ml of equilibration buffer, then with 20 ml of the buffer, containing 20 mM imidazole and 8 M urea, with no β-mercaptoethanol. The protein was eluted with step concentration gradient of 20, 40, 60, 80, and 100 mM imidazole dissolved in 0.1 M sodium phosphate buffer, pH 8.0, containing 0.4 M NaCl, 0.1% dodecylphosphocholine (DPC, Avanti Polar Lipids, Alabaster, AL). Urea was removed at this step.

BoNT/B HC TBD fraction was dialyzed overnight against 50 mM sodium phosphate buffer, pH 8.0, containing 0.1 M NaCl. The purified BoNT/B HC TBD was stored in 20% glycerol solution at -80°C after freezing in liquid nitrogen.

Estimation of protein

SDS-PAGE gels were scanned on a GEL LOGIC 100 Imager system, plotted, and integrated for density using a KODAK 1 D v.3.6.1 (Kodak). The BoNT/B HC TBD band was integrated for density in each lane and compared with the total integrated density of all proteins in the same lane to obtain the percentage of BoNT/B HC TBD of total protein.

Western blot analysis

To confirm that BoNT/B HC TBD is a His₆-tagged fusion protein, Western blot analysis was carried out using anti-His antibody as the primary antibody. The purified BoNT/B HC TBD from SDS-PAGE was transferred to Immun-Blot PVDF (polyvinylidene fluoride) membrane (0.2 µM, Bio-Rad) by using Bio-Rad Mini Protein II System and transfer buffer (39 mM glycine, 48 mM Tris-base, 0.037% SDS, and 20% methanol). The membrane was incubated in the blocking buffer of 3% bovine serum albumin (BSA, Sigma)/phosphate-buffered saline (PBS, 137 mM NaCl, 2.7 mM KCl, and 4.3 mM Na₂HPO₄ · 7 H₂O, pH 7.3), with gentle shaking for 1 h at room temperature (RT, 25°C). After decanting and discarding the blocking buffer, the membrane was incubated in a 1:3000 dilution of mouse anti-His antibody (Amersham Pharmacia Biotech,

Piscataway, NJ) in the blocking buffer, with gentle shaking for 1 h at RT. After washing the membrane with PBST (PBS containing 0.05% Tween) for three times, each time for 5 min, the membrane was incubated in a 1:5000 dilution of goat anti-mouse IgG alkaline phosphatase conjugate (Novagen, Madison, WI) as secondary antibody with the blocking buffer, with gentle shaking for 1 h at RT. The colorimetric detection was carried out by using 5-bromo-4-chloro-3-indolyl-phosphate *p*-toluidine salt (BCIP) and nitro-blue tetrazolium chloride (NBT) (Novagen) as substrate, after the membrane was washed with PBST for three times. Manufacturers' instructions were followed throughout.

Binding activity

Immunological dot blot assay was employed to confirm the binding activity of the purified BoNT/B HC TBD to synaptosome or synaptotagmin II, the receptor of BoNT/B. Synaptosomal protein extracts were isolated from rat brains (RJO Biologicals, Kansas City, MO) according to a previously published procedure [5]. Recombinant glutathione *S*-transferase (GST)-synaptotagmin fusion protein was prepared by inserting the entire synaptotagmin II (GenBank Accession No. M64488) obtained by PCR (chromosomal DNA from rat brain was used as template DNA, a *Bam*HI and an *Eco*RI restriction site were incorporated into the 5' end of the forward sequence and reverse sequence primers, respectively) into the *Bam*HI/*Eco*RI sites of the expression vector pGEX-2T (Amersham Pharmacia Biotech, Piscataway, NJ), and isolated from *E. coli* strain BL21 and purified by glutathione-Sepharose 4B column chromatography (Amersham Pharmacia Biotech, Piscataway, NJ). BoNT/B complex was purified as described by DasGupta and Sugiyama [14]. Three microliters of synaptosomal protein extracts or synaptotagmin II, BoNT/B complex, BoNT/B HC TBD, and 50 mg/ml BSA were spotted on a Trans-Blot transfer medium pure nitrocellulose membrane (0.45 μ M, Bio-Rad). The concentration of synaptosomal protein extracts, synaptotagmin II, BoNT/B complex, and BoNT/B HC TBD was 0.1 mg/ml each. The membrane was incubated in the blocking buffer of 3% BSA in PBS, with gentle shaking for 1 h at RT, and then incubated with synaptosomal protein extract or synaptotagmin II solution in the blocking buffer, with gentle shaking for 2 h at RT. The membrane was washed with PBST for three times and then incubated in a 1:1000 dilution of mouse anti-synaptotagmin antibody (StressGen Biotechnologies, Victoria, BC, Canada) as primary antibody in the blocking buffer, with gentle shaking for 1 h at RT. After washing three times with PBST, the membrane was incubated in a 1:5000 dilution of goat anti-mouse IgG alkaline phosphatase conjugate (Novagen) as the secondary antibody in the blocking buffer, with gentle

shaking for 1 h at RT. The colorimetric detection was carried out by using BCIP and NBT (Novagen) as substrates, after washing the membrane with PBST for three times.

Binding of the purified BoNT/B HC TBD to ganglioside was performed using polystyrene-96-well flat-bottomed plate (Corning Glass Works, Corning, NY) by ELISA. Eighty microliters of 3 mg/ml G_{T1b} (Sigma, St. Louis, MO) dissolved in 20 mM sodium phosphate buffer, pH 8.0, was coated to each well at 4 °C overnight. The plate was then blocked by 1% BSA in PBS for 2 h at RT and washed 4 times with PBST. Sixty microliters of the purified BoNT/B HC TBD (0.1 mg/ml) and 0.1 mg/ml BoNT/A LC (recombinant type A botulinum neurotoxin light chain with histidine tag at the C-terminal end) purified as described by Li and Singh [15] were added to each well. The plate was incubated for 1.5 h at RT on a rocker, and then washed 4 times with PBST. To each well 60 μ l of anti-His antibody (Amersham Pharmacia Biotech, Piscataway, NJ) in 3% BSA was added and incubated for 1 h at RT. After washing the plate, 60 μ l of goat anti-mouse IgG alkaline phosphatase conjugate (Novagen, Madison, WI) was added to each well and incubated for 1 h at RT. The colorimetric detection was carried out using BCIP and NBT (Novagen), after washing the plate with PBST for five times. The absorbance at 490 nm of each well was measured using a microplate reader (GMI, Albertville, Minnesota).

Isoelectric focusing

Isoelectric focusing (IEF) was carried out using the Mini Protein II system from Bio-Rad (Hercules, CA). Briefly, an aliquot (20 μ l) of BoNT/B HC TBD (0.1 mg/ml) was mixed with the same volume of sample buffer (6% ampholytes, pH 3.5–10). The electrode buffers used were 0.02 M acetic acid anolyte and 0.02 M NaOH catholyte. After pre-running the gel (5.5% ampholytes, pH 3.5–10, 5% acrylamide, and 10% glycerol) at 300 V for 30 min, 40 μ l of mixture was applied to the gel. Electrophoresis was performed at 300 V at 8 °C for 3 h. The gel was fixed with 20% trichloroacetic acid for 5 min and rinsed with the destaining solution (30% methanol, 10% acetic acid) for 2 min. The gel was then stained with 0.02% PhastGel Blue R (Pharmacia Biotech, Piscataway, NJ) in the destaining solution containing 0.1% CuSO₄ to decrease the background staining and destained until the background was clear.

Determination of protein concentration

The concentration of proteins used in the experiments was determined spectrophotometrically by measurement of their absorbance at 280 and 235 nm using the formula: concentration of protein mg/ml = $(A_{235} \text{ nm} - A_{280} \text{ nm}) / 2.51$ [16].

Results and discussion

The C- and N-terminal regions of botulinum neurotoxin heavy chain are responsible for toxin binding to the nerve cell and its translocation into the cytosol, respectively. However, molecular mechanism of BoNT binding and translocation is not well understood. Purification of native BoNT HC from whole toxin is a difficult process because it involves its efficient separation from BoNT LC, and a chance to have some intact BoNT contamination in the preparation. In addition, working with large quantities of botulinum neurotoxin poses a health risk. To avoid these problems and to more economically obtain high yields of pure HC binding domain along with the transmembrane domain, alternative strategies are required as described before.

Construction of the recombinant plasmid for overproduction of His₆-tagged BoNT/B HC binding domain along with the transmembrane domain protein in *E. coli*

The coding sequence of BoNT/B HC binding domain along with the transmembrane domain DNA fragment was PCR amplified from genomic DNA of *C. botulinum* type B and cloned into pET 15b vector, thus obtaining the recombinant BoNT/B HC TBD plasmid. Restriction sites *Nde*I and *Bam*HI were introduced at 5' and 3' ends of the BoNT/B HC TBD coding region, respectively, by means of primers tailored with added-on adaptor sequences using PCR (Fig. 1). GC overhangs were added to the 5' ends of both primers to assist in their annealing to the template, and the addition of the GC overhangs at the 5' ends of both primers was an important step towards successful cloning and expression of BoNT/B HC TBD. The high AT content in the *C. botulinum* genome (over 70%) is a major obstacle in the expression of HC in *E. coli*. Cloning and expression of the binding domain using synthetic gene, and of recombinant translocation domain, and the entire BoNT/A HC using normal gene cloning have been reported [17–19]. However, cloning and expression of BoNT/B HC binding domain containing transmembrane domain has not been performed, although there were several reports of cloning of BoNT/B genes [12,13,20–22].

The PCR product was purified from the agarose gel after electrophoresis, cloned into pCR 2.1, excised with *Nde*I and *Bam*HI, and then ligated into the *Nde*I–*Bam*HI digested and CIP-treated vector pET-15b. The pET-BoNT/B HC TBD recombinant plasmid was digested with restriction enzymes *Nde*I and *Bam*HI, *Nde*I only, or *Bam*HI only and compared with the uncut recombinant plasmid to confirm the ligation. DNA sequencing and amino acid sequencing revealed that an open reading frame (ORF) encoding the BoNT/B HC binding domain along with the transmembrane domain region (Ile 624–Glu 1291) contains additional 20 amino

acid residues at N-terminus (GSSHHHHHHSSGLVPRGSHM), including a cluster of six histidine residues for purification of the recombinant protein by metal-affinity chromatography.

Expression and purification of His₆-tagged recombinant BoNT/B HC TBD

The pET-BoNT/B HC TBD was transformed into *E. coli* strain BL21-CodonPlus (DE3)-RIL. The resulting *E. coli* BL21-CodonPlus (DE3)-RIL (pET-BoNT/B HC TBD) strain overproduced His₆-tagged recombinant BoNT/B HC TBD, driven by the T7 promoter with IPTG-inducer. A band corresponding to an 81 kDa His₆-tagged BoNT/B HC TBD was observed in SDS-PAGE of total lysate of *E. coli* BL21-CodonPlus (DE3)-RIL (pET-BoNT/B HC TBD) culture after IPTG induction (Fig. 2, 1–24 h). This band was absent in the control total lysate of *E. coli* BL21-CodonPlus (DE3)-RIL (pET-BoNT/B HC TBD) culture (Fig. 2, 0 h). The clone with highest expressed BoNT/B HC TBD was used to carry out the time course of the BoNT/B HC TBD expression after several colonies under the control of IPTG-inducible promoters was tested on an analytical scale. It was observed that higher level of the BoNT/B HC TBD was expressed with less nonspecific proteins at 5 h of induction (Fig. 2). The cells used to produce the recombinant BoNT/B HC TBD at large scale were cultured for 5 h after induction.

Our attempt to obtain the BoNT/B HC TBD from the supernatant after centrifugation of sonicated *E. coli*

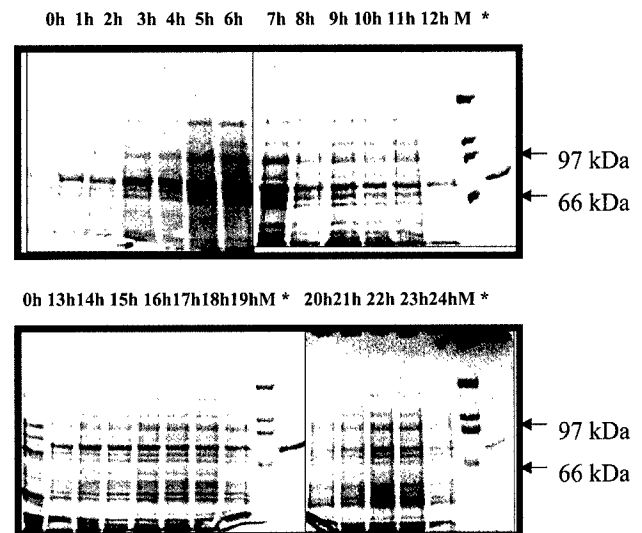


Fig. 2. SDS-PAGE analysis of the recombinant BoNT/B HC TBD expression at different times after IPTG induction. The electrophoresis was carried out on a Mini Protein II System (Bio-Rad, Hercules, CA) and the proteins were detected by Coomassie blue staining. Lanes 0–24 h indicate the hours after IPTG added. Lane M is molecular markers. Asterisks indicate the purified BoNT/B HC TBD. The number on the right indicates molecular mass of markers in kDa.

cells was not successful as no protein was obtained after performing the His-Select nickel affinity gel column chromatography (data not shown). We then tried to isolate the inclusion bodies and successfully obtained the BoNT/B HC TBD from the *E. coli* inclusion bodies.

A half-gram of inclusion body was purified from the frozen cell pellet of 1 L culture (4 g bacterial pellet). We attempted the dialysis method using CelLytic IB (Sigma, St. Louis, MO) to refold the solubilized (His)₆-BoNT/B HC TBD, and manufacturers' instruction was followed throughout, but most of the (His)₆-BoNT/B HC TBD formed precipitates. We therefore designed an approach to perform refolding of (His)₆-BoNT/B HC TBD in conjunction with its purification on the Ni²⁺-affinity column. The frozen inclusion bodies were solubilized in the buffer, 0.1 M sodium phosphate buffer, pH 8.0, containing 6 M guanidine-HCl, 10 mM β-mercaptoethanol, and 0.4 M NaOH. The column was first equilibrated with the equilibration buffer that contained 5 mM imidazole, 8 M urea, and 10 mM β-mercaptoethanol. After loading the protein on the column, it was washed with the equilibration buffer containing urea and β-mercaptoethanol to ensure its solubility. In the next step, the protein bound to the affinity column was washed with the same equilibration buffer, except it contained no β-mercaptoethanol, and it contained 20 mM imidazole instead of 5 mM imidazole. Higher concentration of imidazole was used to remove any nonspecific proteins bound to the Ni²⁺-affinity column.

Refolding of the protein was further facilitated in the next step by washing the column bound BoNT/B HC TBD with the same equilibration buffer containing 20 mM instead of 5 mM imidazole, but lacking both β-mercaptoethanol and urea. Removal of urea was aimed at establishing native H-bonds among various amino acid groups of the BoNT/B HC TBD. In the following steps, the protein was eluted with step concentration gradient of 20, 40, 60, 80, and 100 mM imidazole in the elution buffer containing 0.1% DPC. Purity of the protein was examined by SDS-PAGE (Fig. 3) and using GEL LOGIC 100 Imager system and a KODAK 1 D v.3.6.1. Analysis system. The protein eluted with 60 and 80 mM imidazole was determined to be 90% pure (Fig. 3, lanes 5 and 6), and pure BoNT/B HC TBD was eluted with 100 mM imidazole (Fig. 3, lane 7). The purified protein was determined to be 98% pure as assessed by the SDS-polyacrylamide gel. Ten milligrams of His₆-tagged BoNT/B HC TBD was obtained from 1 L of the *E. coli* culture. A concentration of 0.25 mg/ml was possible to prepare without any precipitation even at 4 °C.

To identify the expressed protein, we used anti-His antibody that recognizes continuous four, or over four, histidines. The Western blot analysis indicated that the

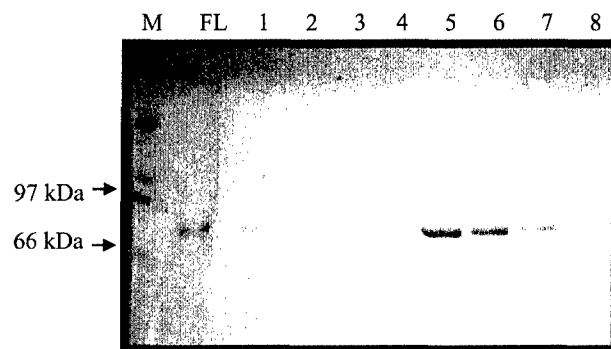


Fig. 3. SDS-PAGE analysis of eluents of Ni²⁺ affinity gel column chromatography used for purification of BoNT/B HC TBD. The number on the left indicates molecular mass of markers in kDa. Lane M is molecular markers. Lane FL presents the fraction of solubilized inclusion body solution through the column after loading onto the column. Lane 1 is the washing fraction with equilibration buffer. Lane 2 is the fraction with equilibration buffer containing 20 mM imidazole, with no β-mercaptoethanol. Lane 3 is the fraction with equilibration buffer containing 20 mM imidazole, with no urea. Fractions eluted with 40 mM (lanes 4), 60 mM (lanes 5), 80 mM (lanes 6), 100 mM (lanes 7), and 200 mM (lanes 8) imidazole are shown.

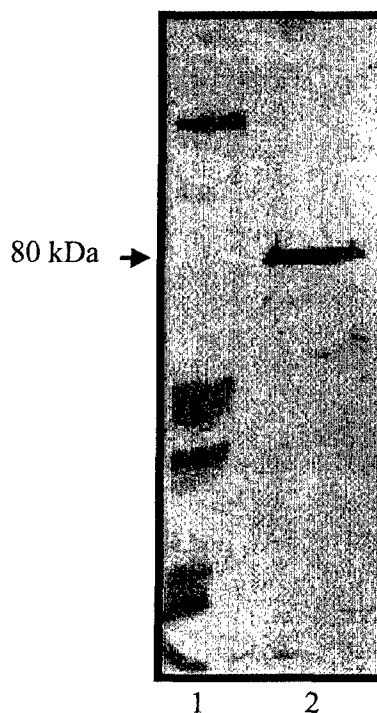


Fig. 4. Western blot analysis of histidine-tagged fusion protein of the BoNT/B HC TBD. Purified BoNT/B HC TBD from SDS-PAGE after electrophoresis using a 7.5% polyacrylamide gel was transferred to Immun-Blot PVDF membrane. The membrane was incubated in 3% BSA and then incubated in 1:3000 dilution of mouse anti-His antibody in the blocking buffer. After washing, the membrane was incubated in 1:5000 dilution of goat anti-mouse IgG alkaline phosphatase conjugate in the blocking buffer. The colorimetric detection was carried out by using BCIP and NBT. The number on the left indicates the molecular mass of markers in kDa. Lane 1 is molecular markers. Lane 2 is purified BoNT/B HC TBD.

recombinant BoNT/B HC TBD is a positive His-tagged fusion protein (Fig. 4) since there are no other four continuous histidines in the amino acid sequence of the BoNT/B HC TBD.

The isoelectric focusing analysis of the His₆-tagged BoNT/B HC TBD revealed an isoelectric point of 7.0. The calculated theoretical isoelectric point of His₆-tagged BoNT/B HC TBD is 6.3, with calculated MW for the recombinant BoNT/B HC TBD being 81.2 kDa (ExpASY Compute pI/Mw tool). The information of isoelectric point allowed us to use a dialysis buffer with appropriate pH to avoid the precipitation during the dialysis. BoNT/B HC TBD fraction was successfully dialyzed against 50 mM sodium phosphate buffer, pH 8.0, containing 0.1 M NaCl. It was found that dialysis of the recombinant BoNT/B HC TBD without salt resulted in precipitation inside of dialysis membrane. The purified BoNT/B HC TBD was stored in 20% glycerol solution at -80°C.

Binding with potential receptor with immuno-dot-blot assay

The dot blot assay revealed the binding of the purified BoNT/B HC TBD to synaptosomal protein extracts (Fig. 5A) and synaptotagmin II (Fig. 5B), the putative receptor of BoNT/B. The assay indicated the binding of BoNT/B HC TBD as strong as the binding of the BoNT/B complex (a positive control). However, there was no binding of BSA (as a negative control) to synaptosomal protein extracts or the synaptotagmin II even when high concentration of BSA was used (Fig. 5).

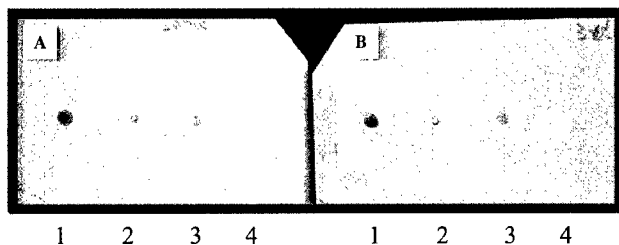


Fig. 5. Dot blot assay of binding activity of the recombinant BoNT/B HC TBD to synaptosomal protein extracts (A) or synaptotagmin II (B). Three microliters of 0.1 mg/ml synaptosomal protein extracts (A) or synaptotagmin II (B), 0.1 mg/ml BoNT/B complex, 0.1 mg/ml BoNT/B HC TBD, and 50 mg/ml BSA were spotted on the pure nitrocellulose membrane. (A) 1—synaptosomal protein extracts, 2—BoNT/B complex, 3—BoNT/B HC TBD, and 4—BSA. (B) 1—synaptotagmin II, 2—BoNT/B complex, 3—BoNT/B HC TBD, and 4—BSA. The membrane was incubated with synaptosomal protein extracts (A) and synaptotagmin II (B) solution in blocking buffer after blocking with 3% BSA. The membrane was then incubated in 1:1000 dilution of mouse anti-synaptotagmin antibody then followed in 1:5000 dilution of goat anti-mouse IgG alkaline phosphatase conjugate after washing three times with PBST. The colorimetric detection was carried out using BCIP and NBT.

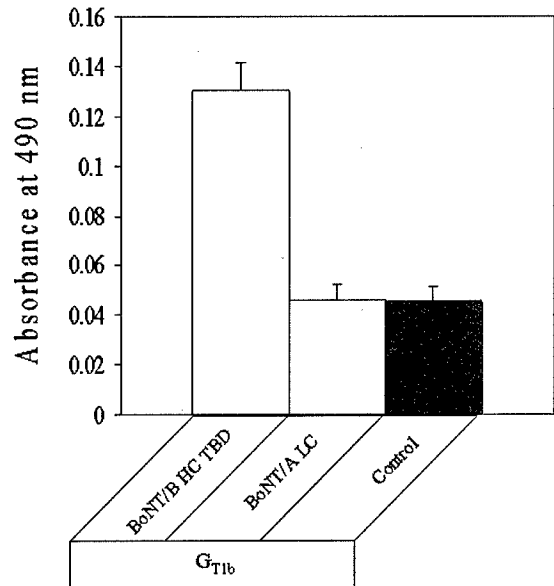


Fig. 6. Enzyme-linked immunosorbent assay of binding activity of the recombinant BoNT/B HC TBD to ganglioside (G_{T1b}). Wells were coated with ganglioside (G_{T1b}), and incubated with BoNT/B HC TBD (white column), or incubated with BoNT/A LC (gray column), and incubated with blocking buffer (black column). Mouse anti-His antibody and goat anti-mouse IgG alkaline phosphatase conjugate were used as primary and secondary antibodies. Values are means from three replications with standard error bars.

Binding with ganglioside using ELISA

The first step in BoNT attachment to nerve membranes starts with C-terminus of HC binding to gangliosides on presynaptic membranes. Ganglioside binding could either bring the toxin and the protein receptor into close proximity, or cause a conformational change at the second receptor binding site to enhance interactions [1]. ELISA-based analysis of BoNT/B HC TBD binding with G_{T1b} indicated a substantial binding of the purified BoNT/B HC TBD to ganglioside (G_{T1b}) (Fig. 6). However, the BoNT/A LC did not show binding activity with G_{T1b} (Fig. 6), suggesting that BoNT/B HC TBD to gangliosides is specific.

In summary, for the first time we have successfully cloned and developed a procedure to purify (10 mg/L culture) the highly expressed recombinant BoNT/B HC binding domain along with the transmembrane domain in a functionally active form.

Acknowledgments

This work was supported by a grant from the Sandia National Laboratories, and US Army Medical Research and Materiel Command under Contract No. DAMD17-02-C-0001. The authors thank Mr. Sean Foss and Mr. Stephen J. Riding for their assistance.

References

- [1] B.R. Singh, Intimate detail of the most poisonous poison, *Nat. Struct. Biol.* 7 (2000) 617–619.
- [2] S.S. Arnon, R. Schechter, T.V. Inglesby, D.A. Henderson, J.G. Bartlett, M.S. Ascher, E. Eitzen, A.D. Fine, J. Hauer, M. Layton, S. Lillibridge, M.T. Osterholm, T. O'Toole, G. Parker, T.M. Perl, P.K. Russell, D.L. Swerdlow, K. Tonat, Botulinum toxin as a biological weapon: medical and public health management, *J. Am. Med. Assoc.* 285 (2001) 1059–1070.
- [3] T. Nishiki, Y. Kamata, Y. Nemoto, A. Omori, T. Ito, M. Takahashi, S. Kozaki, Identification of protein receptor for *Clostridium botulinum* type B neurotoxin in rat brain synaptosomes, *J. Biol. Chem.* 269 (1994) 10498–10503.
- [4] T. Nishiki, Y. Tokuyama, Y. Kamata, Y. Nemoto, A. Yoshida, K. Sato, M. Sekiguchi, M. Takahashi, S. Kozaki, The high-affinity binding of *Clostridium botulinum* type B neurotoxin to synaptotagmin II associated with gangliosides GT1b/GD1a, *FEBS Lett.* 378 (1996) 253–257.
- [5] L. Li, B.R. Singh, Isolation of synaptotagmin as a receptor for type A and E botulinum neurotoxin and analysis of their comparative binding using a new microtiter plate assay, *J. Nat. Toxins* 7 (1998) 215–226.
- [6] F.J. Lebeda, B.R. Singh, Membrane channel activity and translocation of tetanus and botulinum neurotoxins, *J. Toxicol.-Toxin Rev.* 18 (1999) 45–76.
- [7] S. Prabakaran, W. Tepp, B.R. DasGupta, Botulinum neurotoxin types B and E: purification, limited proteolysis by endoproteinase Glu-C and pepsin, and comparison of their identified cleaved sites relative to the three-dimensional structure of type A neurotoxin, *Toxicon* 39 (2001) 1515–1531.
- [8] S. Swaminathan, S. Eswaramoorthy, Crystal structure of *Clostridium botulinum* neurotoxin serotype B, in: M.F. Brin, M. Hallett, J. Jankovic (Eds.) *Scientific and Therapeutic Aspects of Botulinum Toxin*, Lippincott Williams & Wilkins, Philadelphia, PA, 2002, pp. 29–39.
- [9] B. Persson, P. Argos, Topology prediction of membrane proteins, *Protein Sci.* 5 (1996) 363–371.
- [10] H.F. LaPenotiere, M.A. Clayton, J.L. Middlebrook, Expression of a large, nontoxic fragment of botulinum neurotoxin serotype A and its use as an immunogen, *Toxicon* 33 (1995) 1383–1386.
- [11] L.A. Smith, Development of recombinant vaccines for botulinum neurotoxin, *Toxicon* 36 (1998) 1539–1548.
- [12] G. Lalli, J. Herreros, S.L. Osborne, C. Montecucco, O. Rossetto, G. Schiavo, Functional characterisation of tetanus and botulinum neurotoxins binding domains, *J. Cell Sci.* 112 (1999) 2715–2724.
- [13] S.M. Whelan, M.J. Elmore, N.J. Bodsworth, J.K. Brehm, T. Atkinson, N.P. Minton, Molecular cloning of the *Clostridium botulinum* structural gene encoding the type B and determination of its entire nucleotide sequence, *Appl. Environ. Microbiol.* 58 (1992) 2345–2354.
- [14] B.R. DasGupta, H. Sugiyama, Molecular forms of neurotoxins in proteolytic *Clostridium botulinum* type B cultures, *Infect. Immun.* 14 (1976) 680–686.
- [15] L. Li, B.R. Singh, High-level expression, purification, and characterization of recombinant type A botulinum neurotoxin light chain, *Protein Expr. Purif.* 17 (1999) 339–344.
- [16] J.R. Whitaker, P.E. Granum, An absolute method for protein determination based on difference in absorbance at 235 and 280 nm, *Anal. Biochem.* 109 (1980) 156–159.
- [17] M.A. Clayton, J.M. Clayton, D.R. Brown, J.L. Middlebrook, Protective vaccination with a recombinant fragment of *Clostridium botulinum* neurotoxin serotype A expressed from a synthetic gene *Escherichia coli*, *Infect. Immun.* 63 (1996) 2738–2742.
- [18] D.B. Lacy, R.C. Stevens, Recombinant expression and purification of the botulinum neurotoxin type A translocation domain, *Protein Expr. Purif.* 11 (1997) 195–200.
- [19] L. Li, B.R. Singh, In Vitro translation of type A *Clostridium botulinum* neurotoxin heavy chain and analysis of its binding to rat synaptosomes, *J. Protein Chem.* 18 (1999) 89–95.
- [20] G.H. Yang, S.D. Rhee, H.H. Jung, O.H. Jhee, K.H. Yang, Cloning and characterization of the upstream region of *Clostridium botulinum* type B neurotoxin gene, *Biochem. Mol. Biol. Int.* 45 (1998) 401–407.
- [21] R.A. Hutson, M.D. Collins, A.K. East, D.E. Thompson, Nucleotide sequence of the gene coding for non-proteolytic *Clostridium botulinum* type B neurotoxin: comparison with other clostridial neurotoxins, *Curr. Microbiol.* 28 (1994) 101–110.
- [22] H. Ihara, T. Kohda, F. Morimoto, K. Tsukamoto, T. Karasawa, S. Nakamura, M. Mukamoto, S. Kozaki, Sequence of the gene for *Clostridium botulinum* type B neurotoxin associated with infant botulism, expression of the C-terminal half of heavy chain and its binding activity, *Biochem. Biophys. Acta* 1625 (2003) 19–26.

A Distinct Utility of the Amide III Infrared Band for Secondary Structure Estimation of Aqueous Protein Solutions Using Partial Least Squares Methods

Shouwei Cai and Bal Ram Singh

Department of Chemistry and Biochemistry, University of Massachusetts Dartmouth, Dartmouth, Massachusetts 02747

A Distinct Utility of the Amide III Infrared Band for Secondary Structure Estimation of Aqueous Protein Solutions Using Partial Least Squares Methods

Biochemistry[®]

Reprinted from
Volume 43, Number 9, Pages 2541-2549

A Distinct Utility of the Amide III Infrared Band for Secondary Structure Estimation of Aqueous Protein Solutions Using Partial Least Squares Methods[†]

Shuwei Cai and Bal Ram Singh*

Department of Chemistry and Biochemistry, University of Massachusetts Dartmouth, Dartmouth, Massachusetts 02747

Received June 13, 2003; Revised Manuscript Received December 5, 2003

ABSTRACT: Fourier transform infrared spectroscopy is becoming an increasingly important method to study protein secondary structure. The amide I region of the protein infrared spectrum is the widely used region, whereas the amide III region has been comparatively neglected due to its low signal. Since there is no water interference in the amide III region and, more importantly, the different secondary structures of proteins have more resolved differences in their amide III spectra, it is quite promising to use the amide III region to determine protein secondary structure. In our current study, a partial least squares (PLS) method was used to predict protein secondary structures from the protein IR spectra. The IR spectra of aqueous solutions of 16 different proteins of known crystal structure have been recorded, and the amide I, the amide III, and the amide I combined with the amide III region of these proteins were used to set up the calibration set for the PLS algorithm. Our results correlate quite well with the data from X-ray studies, and the prediction from the amide III region is better than that from amide I or combined amide I and amide III regions.

The three-dimensional structures of biological macromolecules and their physiological functions are intimately related. Proteins are thought to be the “second part of the genetic code”, and they play a pivotal role in living cells. Their functions are responsible for a large number of biological processes, including the facilitation of metabolism, communication, transport, and maintenance of structural integrity. The diversity of the functions of proteins is only matched by the diversity of protein structure. The importance of understanding the structure–function relationship of proteins has underscored the need for a rapid, reliable, and sensitive probe of the molecular conformation of proteins. Such a method should allow study in aqueous media and also be suitable for use in measuring the effects of environmental factors, ligand binding, and other perturbations on molecular conformation. A variety of techniques have been applied to the elucidation of the three-dimensional structure of proteins, ranging from computer-aided prediction based on the sequence of the constituent amino acids and energetic consideration (1) to precise methods for identification of their molecular coordinates, such as NMR spectroscopy (2) and X-ray diffraction (3).

Fourier transform infrared (FTIR)¹ spectroscopy has emerged as a useful tool for the characterization of protein secondary structure with a precision lying between that of the purely predictive and the molecular coordinate ap-

proaches (4). One of the strengths of infrared spectroscopy is that it is amenable to a variety of sample forms including solid films or powder, solutions, liquid crystals, and so forth. Protein crystals are not necessary nor are external molecular probes required, which would supply information only about the surrounding microenvironment. Infrared spectroscopy not only provides information about protein structure in the native environment, but it can also provide insight into conformational alternations associated with changing environmental conditions, such as pH, temperature, pressure, and solvent. This advantage renders FTIR spectroscopy especially useful for probing membrane-associated proteins that are difficult to be probed by other spectroscopic techniques.

Methods currently being used to extract information on protein secondary structure from infrared spectra are based on empirical correlation between the frequencies of certain vibrational modes and types of secondary structure of polypeptide chains such as α -helix, β -sheet, β -turn, and random coil. The mode most often used and by far best characterized in this respect is the so-called amide I mode. It represents primarily the C=O stretching vibrations of amide groups and gives rise to infrared band(s) in the region between 1600 and 1700 cm^{-1} . Due to the strong absorption of water between 1640 and 1650 cm^{-1} , most structure determinations by amide I mode are performed in D_2O solutions. However, uncertainty in the NH/ND exchange process may cause a certain degree of ambiguity (5). Also, serious overlapping of the random coil and the α -helix bands in the amide I region makes it difficult to accurately predict α -helix contents in proteins. Attempts have also been made to exploit other vibrational modes, particularly the amide II and amide III bands. Unfortunately, even though the intensity of the amide II region is relatively strong, it is not very sensitive to the secondary structure changes of proteins.

[†] This study was supported in part by a grant (NS33740) from the National Institute of Neurological Disorders and Strokes, National Institutes of Health. B.R.S. is a Henry Dreyfus Teacher–Scholar.

* To whom correspondence should be addressed. Telephone: 508-999-8588. Fax: 508-999-8451. E-mail: bsingh@umassd.edu.

¹ Abbreviations: FTIR, Fourier transform infrared spectroscopy; PLS, partial least squares; CLS, classic least squares; ATR, attenuated total reflectance; SEP, standard error of prediction; PCC, Pearson correlation coefficient.

Furthermore, the amide II bands are strongly overlapped by bands originating from amino acid side chain vibrations (6). On the other hand, the amide III bands, which are predominantly due to the in-phase combination of N–H in-plane bending and C–N stretching vibrations, are highly sensitive to the secondary structure folding (7, 8). In addition, there is no H₂O interference in this region. Therefore, even though the signal of the amide III bands is ~5–10-fold weaker than that of the amide I bands, the amide III region is still very promising to estimate protein secondary structure content.

In recent years, several researchers have used the amide III region to study protein structures (9–15). Since both the amide I and amide III regions are broad bands, it is not possible to resolve individual bands corresponding to different secondary structure elements from the original spectra. Even though spectral resolution in the amide III region is higher than that in the amide I region, the resolution enhancement methods, such as second derivatization, are still needed to appropriately curve fit the spectra for estimating secondary structures of proteins (7–15). The most common method used to solve this problem is to employ resolution enhancement or band-narrowing methods (4). However, there is a certain degree of subjectivity associated with methods based on the band-narrowing approach such as the initial choice of input parameters and the assignment of secondary structures in boundary frequency regions.

Chemometric methods have been developed to resolve the individual species in a multicomponents system (16). Since such a method is based on full spectral analysis, it involves the use of a calibration matrix of the IR spectra of proteins with known X-ray structure and therefore avoids the need to deconvolve the spectra and assign the bands. Thus, such a method can avoid most of the subjectivity associated with the band assignment process. The PLS method is one of these methods, which is commonly used in analytical chemistry (17). Previously, the PLS method has been applied to amide I and amide II regions of protein IR spectra to predict protein secondary structure (18). In this paper, we describe application of the PLS method in the amide III region of protein IR spectra to predict the protein secondary structures. We used 16 different proteins, whose structures have already been resolved by X-ray crystallography, to set up the calibration matrix, and we employed the amide I, amide III, and a combination of amide I and amide III as the spectral region for estimating protein secondary structure. The results indicate better than 90% prediction accuracy for α -helix, β -sheet, and β -turns and 74% prediction accuracy for random coils.

MATERIALS AND METHODS

Proteins and Infrared Spectroscopic Measurement. The following proteins were purchased from Sigma Chemical Co. (St. Louis, MO) and used without further purification: alcohol dehydrogenase, carbonic anhydrase, α -chymotrypsinogen, α -chymotrypsin, concanavalin A, cytochrome *c*, hemoglobin, immunoglobulin G, lactate dehydrogenase, lysozyme, ovalbumin, myoglobin, papain, ribonuclease A, trypsin, and trypsin inhibitor. These proteins were chosen because their secondary structures have already been known from X-ray crystallography. The protein solutions were prepared in 20 mM sodium phosphate buffer, pH 7.2, except

for α -chymotrypsinogen (pH 4.5, 20 mM sodium acetate buffer), α -chymotrypsin (pH 3.8, water with trace hydrochloric acid), ribonuclease A (pH 3.8, water with trace hydrochloric acid), concanavalin A (pH 5.0, 20 mM sodium acetate buffer), lysozyme (pH 4.5, 20 mM sodium acetate buffer), and trypsin (pH 8.0, 20 mM sodium phosphate buffer). The pH values were chosen in order to match the X-ray crystallography condition and to compare the structure of proteins between solution and crystal. We used pH 7.2 conditions for recording of other proteins whose crystal structures were solved in the pH range of 6.7–7.8. It is recognized that the conditions for crystal structures (salts, organic solvents, etc.) were not identical to the solution conditions used in this study for recording IR spectra. However, assuming the ordered crystal structures of proteins as true representatives of the structure in aqueous solution, even at slightly different pHs, we believe it is appropriate to use X-ray crystallographic data to predict secondary structures of proteins based on IR spectral recordings. Similar approaches have been successfully used in the past for using X-ray crystallographic data for estimating protein secondary structure from IR spectra (19). The concentration of these proteins used in our experiments was 1 mg/mL.

A Nicolet Model 8210 FTIR spectrometer, equipped with a zinc selenide attenuated total reflectance (ATR) accessory and DTGS detector, was used for spectral recordings at room temperature. The spectrometer was purged with CO₂-free dry air for at least 24 h before spectra were recorded. For each spectrum, a 256-scan interferogram was collected at a resolution of 4 cm⁻¹. In every case, the single beam spectrum of the buffer and the protein solutions were divided by the background single beam spectrum and then converted to the absorbance spectra. To obtain the protein spectra, the buffer spectra were subtracted. The following criteria were used to judge the water subtraction: a flat baseline between 2000 and 1700 cm⁻¹ and no negative lobe between this range (20, 21). All spectra were smoothed with a nine-point Savitsky–Golay function to remove the possible noise before further data analysis.

Partial Least Squares Method (PLS). The basis of all quantitative analysis using spectroscopy is Beer's law. The multicomponent analyses are based on the additivity of Beer's law; i.e., the absorbance at a specific wavenumber (wavelength) is the sum of the absorbance of all sample components that absorb at that wavenumber (wavelength). If the absorbance at different wavenumbers is collected, Beer's law can be written in the form:

$$A = \sum(KLC + E_a) \quad (1)$$

where **A** = the vector of absorbances, **K** = the matrix of absorptivities, **L** = the vector of path lengths, **C** = the vector of concentration, and **E_a** = the matrix of the spectral error.

The classic least squares method (CLS) belongs to this kind of method and is most widely used. For the CLS method, it is assumed that protein spectra are linear combinations of *l* pure structure spectra, i.e., α -helix, β -sheet, β -turn, and random coil. Supposing there are *m* calibration proteins measured at *n* wavenumbers, then

$$A = CK + E_a \quad (2)$$

where \mathbf{A} is an $m \times n$ matrix of the spectra of the m calibration proteins, \mathbf{C} is an $m \times l$ matrix of the concentration, and \mathbf{K} is an $l \times n$ matrix in which rows are the pure structure spectra.

The \mathbf{K} matrix can be obtained from the calibration set as follows:

$$\mathbf{K} = \mathbf{A}\mathbf{C}^T(\mathbf{C}\mathbf{C}^T)^{-1} \quad (3)$$

where \mathbf{C}^T is the transpose of matrix \mathbf{C} and superscript -1 stands for the inverse of a matrix.

The \mathbf{K} matrix contains the absorptivity coefficients for each of the l components at the n selected wavenumbers.

Once the \mathbf{K} matrix is known, the unknown concentration can be calculated as follows:

$$\mathbf{c} = (\mathbf{K}\mathbf{K}^T)^{-1}\mathbf{K}\mathbf{A} \quad (4)$$

where \mathbf{A} is the spectrum of the protein to be analyzed. Since the resolving \mathbf{K} matrix is the central part of CLS, CLS is also called the \mathbf{K} matrix.

The CLS method is used widely because the mathematical steps are straightforward, and many standards and wavenumbers can be used in the calibration to obtain an averaging effect (therefore, the CLS method actually is a full-spectrum method). A major disadvantage of the CLS method is that all interfering chemical components in the spectral region of interest need to be known and included in the calibration. This is not an easy task for complex spectra like those of proteins. In addition, the two matrix inversions required by this method are a major source of errors.

The partial least squares method (PLS) is a factor analysis method, which has many of the full-spectrum advantages of the CLS method (17). In the PLS method, the calibration spectra can be represented as follows:

$$\mathbf{A} = \mathbf{T}\mathbf{B} + \mathbf{E}_a \quad (5)$$

where \mathbf{B} is an $h \times n$ matrix with the rows of \mathbf{B} being the new PLS basis set of h full-spectrum vectors, called loading vectors or loading spectra, \mathbf{T} is an $m \times h$ matrix of intensities (or scores) in the new coordinate system of the h PLS loading vectors (also called factors) for the calibration spectra, and \mathbf{E}_a is an $m \times n$ matrix of spectral residuals not fitted by the PLS model.

The analogy between the PLS model and the CLS model is quite clear since both equations involve the decomposition of \mathbf{A} into the product of two smaller matrices. However, rather than basis vectors being the pure component spectra in the CLS, they are the loading vectors generated by the PLS algorithm. The intensities in the new coordinate system are no longer the concentrations that they were in CLS; instead, they are linearly related to the concentrations. The new basis set of full-spectrum loading vectors is composed of linear combinations of the original calibration spectra. The amount (i.e., intensities) of each of the loading vectors that are required to reconstruct each calibration spectrum is the score. In general, only a small number of the full-spectrum basis vector is required to represent the calibration spectra (\mathbf{A}). Therefore, the PLS algorithm reduces the number of intensities (n) of each spectrum in the spectra matrix \mathbf{A} to a small number of intensities (h) in the new coordinate system of the loading vectors. The data compression step also

reduces the noise, as noise is distributed throughout all loading vectors, while the true spectral variation is generally concentrated in the early loading vectors.

The \mathbf{c} vector of size m , containing the concentration, can be related to the spectral intensities (\mathbf{T}) in the new coordinate system by solving the following set of equations:

$$\mathbf{c} = \mathbf{T}\mathbf{v} + \mathbf{e}_c \quad (6)$$

where \mathbf{v} is the $h \times 1$ vector of coefficients relating the scores (intensities) to the conformation fractions, \mathbf{T} is the matrix of scores (intensities) from the PLS spectral decomposition, and \mathbf{e}_c is the vector of concentration errors. During calibration, the least squares solution of eq 6 is

$$\mathbf{v} = [\mathbf{T}^T\mathbf{T}]^{-1}\mathbf{T}^T\mathbf{c} \quad (7)$$

During prediction, the unknown concentration is obtained by solving the equation:

$$\mathbf{c} = \mathbf{t}\mathbf{v} \quad (8)$$

where \mathbf{t} is the vector of size h of the intensities of the PLS loading data in the new coordinate system for the spectrum of the unknown sample.

The advantages of the PLS method are that it is insensitive to the presence of impurities and makes full use of all the spectral data. In addition, this method eliminates the problem of calculating the two matrix inversions in the CLS method. Since columns of \mathbf{T} are orthogonal in the PLS algorithm, the least squares solution to \mathbf{v} involves a trivial inversion of the diagonal ($\mathbf{T}^T\mathbf{T}$) matrix.

The cross-validation was used to determine the optimum number of factors for the PLS algorithm. The standard error of prediction (SEP) was used to evaluate the prediction accuracy (17, 18):

$$\text{SEP} = [(\sum(x_i - y_i)^2)/(N - 1)]^{1/2}$$

where x_i is the result from the PLS method, y_i is the result from X-ray studies, and N is the number of proteins used.

To carry out the cross-validation (17), one of the samples is left out of the calibration set. The rest of the samples are used to perform the decomposition for one factor (loading factor) and to calculate the calibration matrix. The calibration matrix is used to predict the concentration of the sample left out. Subsequently, the next sample is left out, and the above prediction is repeated, until all samples are predicted. The SEP for this factor is calculated. The above procedure is repeated using two factors. The process is continued in this fashion up to the maximum number of factors (most of the time, the maximum number of factors is half of the sample numbers in the calibration set).

For this study, we used the PLSplus program created by Galactic Industries Corp. (Salem, NH) to calibrate and predict the secondary structure of proteins.

The spectral regions we used are amide I (1700–1600 cm^{-1}), amide III (1350–1200 cm^{-1}), and the combination of amide I and amide III. Before calibration and prediction, the spectra were normalized to a total intensity of one in each region. This step helped to remove the protein concentration effect. To predict the secondary structure of unknown proteins, a series of calibration spectra whose secondary structures are already known must be set up. After these

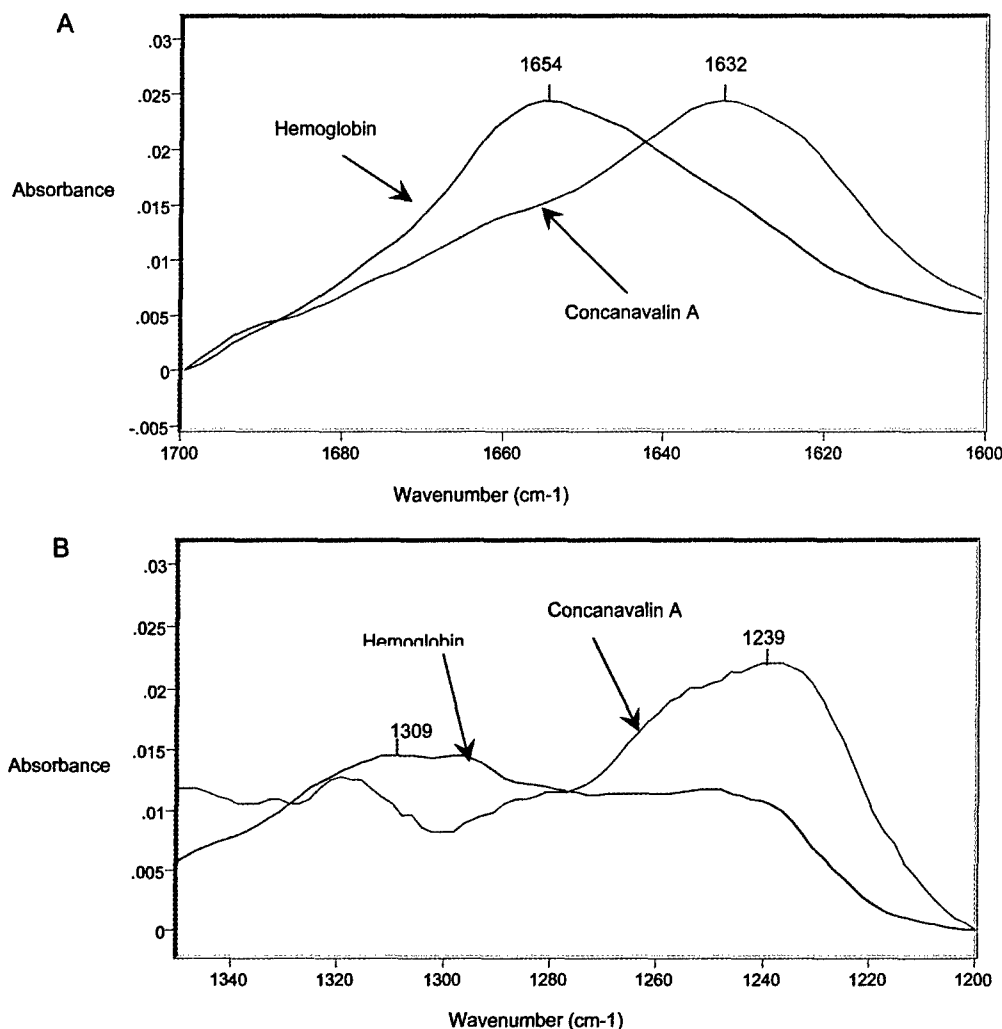


FIGURE 1: Comparison of FTIR spectra of the α -helix protein (hemoglobin) and β -sheet protein (concanavalin A). Panels: (A) amide I region and (B) amide III region.

spectra are loaded into a calibration file and the contents of each structure are input, the calibration file is ready to be used to predict the protein with an unknown structure. To predict the secondary structure of a protein, the protein is eliminated from the calibration file, and its structure is predicted by using the other 15 proteins as the calibration set.

RESULTS

Amide I and amide III regions of the infrared spectra of proteins are the two regions that are very sensitive to their secondary structure. For example, Figure 1 shows the spectra of aqueous solutions of hemoglobin and concanavalin A, which are two proteins with completely different conformations. Hemoglobin is a high α -helix protein (86% helix) with no β -sheet, and concanavalin A is a high β -sheet protein (65% β -sheet) with 3% α -helix. These significant differences in shape and frequency render the amide I and amide III regions particularly useful for predicting the conformation of proteins in an aqueous solution from their infrared spectra.

The amide III region was first analyzed using the CLS method. By doing so, we resolved the pure spectra of different secondary structures in protein on the basis of the assumption that amide III infrared bands are only contributed by four types of protein structures (Figure 2). The maximum

absorbance of pure spectra for α -helix is around 1300 cm^{-1} , the maximum absorbance for β -sheet is around 1235 cm^{-1} , and the β -turn bands are located around $1260\text{--}1280\text{ cm}^{-1}$, while the random coil is located around $1240\text{--}1260\text{ cm}^{-1}$. Those pure spectra of four types of protein structure are approximately matched to the results of an earlier study using resolution enhancement analysis of the amide III band (22), suggesting that the most contribution of amide III infrared bands is from protein amide bonds, especially for α -helix and β -sheet. The pure spectra of β -turn and random coil resolved from the CLS method showed a more complicated pattern. The β -turn spectrum showed a peak at 1265 cm^{-1} and a shoulder at 1235 cm^{-1} , with some negative absorption at $1320\text{--}1330\text{ cm}^{-1}$ (Figure 2). The pure spectrum of random coil has shown two bands at 1245 and 1285 cm^{-1} , with significant negative absorption beyond 1290 cm^{-1} (Figure 2). The β -sheet, on the other hand, showed some positive peaks above 1290 cm^{-1} (Figure 2). Both β -turn and random coil structures are not expected to have any spectral contribution above 1300 cm^{-1} . Therefore, the peaks (both positive and negative) seen in β -turn and random coil spectra are likely to arise from contributions of other vibrational modes. The protein amide III region not only involves vibrational modes of the peptide group but also includes the side chain vibrations as well as other nondefined modes of vibration.

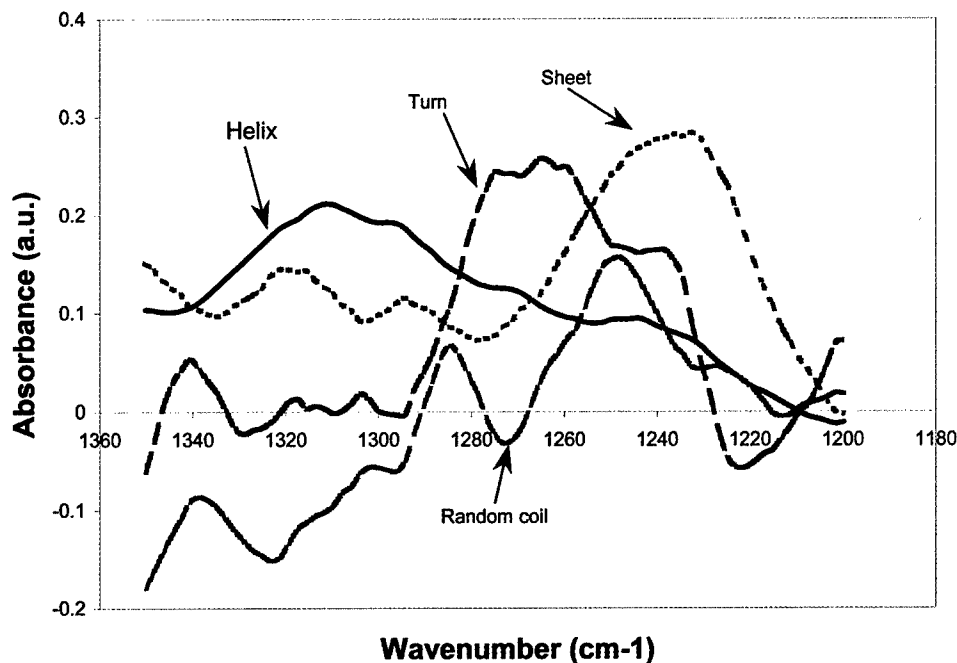


FIGURE 2: Infrared spectra calculated by the classical least squares method for the α -helix, β -sheet, β -turn, and random coil.

Since vibrational contributions other than those from protein secondary structures are not defined in the calibration file, the CLS algorithm mixes nondefined spectral contributions to those structures in the defined calibration file on the basis of least squares minimization. This approach obviously adds error in the prediction of the secondary structure content. Thus the complicated features of the amide III region make it very difficult to use CLS for resolving the protein secondary structures. That is the reason for the complicated spectral features shown in random coil and β -turn spectra (Figure 2). Those observations also suggested that the side chain and other interference have more effect on the random coil and β -turn spectral region.

To alleviate the limitations of the CLS method described above, we employed the PLS analysis to obtain accurate prediction of the secondary structure of proteins. The PLS algorithm is used to analyze both the amide I and amide III infrared bands of proteins. To determine the optimum number of factors used in the PLS algorithm, a cross-validation calculation for all the samples in the training set has been performed. The prediction depends on the number of loading factors as shown in Figure 3. The number of factors (components) involved in different secondary structures is higher in amide III alone or in the combined regions of amide I and III compared to the amide I region alone, suggesting that the amide III bands of the protein are more complex than the amide I bands. The number of factors corresponding to the minimum SEP is chosen for the construction of the calibration model.

The PLS algorithm was applied to amide I and amide III spectra to predict the protein's secondary structure. The results are listed in Table 1 and are compared with data from the X-ray studies (23).

We also performed the statistical tests to assess correlation between secondary structure estimation based on IR spectra and secondary structure estimated from X-ray crystallography. Protein secondary structures estimated from the PLS method were compared with data from X-ray crystal-

lography by computing the Pearson correlation coefficients (PCC) (25) and SEP:

$$\text{PCC} = \frac{(N \sum x_i y_i - \sum x_i \sum y_i)}{\{[N \sum x_i^2 - (\sum x_i)^2]^{1/2} [N \sum y_i^2 - (\sum y_i)^2]^{1/2}\}}$$

where x_i is the result from the PLS method and y_i is the result from X-ray studies. The statistical test results are listed in Table 2. For a perfect correlation, a PCC of 1.0 and a SEP of 0 are expected. For totally noncorrelated spectra, the PCC will be 0.

As can be derived from Table 2, β -turn and random coil structures predicted from amide III spectra were better correlated with X-ray crystallographic structures than those obtained from either amide I or amide I plus amide III spectra. The correlation analysis between the PLS result and X-ray data also showed that the α -helix and β -sheets were highly correlated with the X-ray data (PCC above 0.900). The β -turn or the random coil, especially the random coil (PCC was 0.771 when using amide III spectra and only 0.351 when using amide I spectra), on the other hand, were not well correlated.

For α -helix, the Pearson correlation coefficient (PCC) between X-ray data and amide III IR spectra was 0.950, which was reduced to 0.925 when amide I region was used alone. When amide I plus amide III was used, the PCC increased to 0.958. For β -sheets, the PCC for combined regions of amide III and amide I was the highest observed at 0.970, while it was reduced to 0.963 and 0.950 when using amide III spectra and amide I spectra, respectively.

DISCUSSION

The band-narrowing techniques and curve-fitting procedures have been applied to extract quantitative information of protein secondary structures from the infrared spectra. However, the lack of uniqueness in band assignments and elements of subjectivity in the initial choice of input

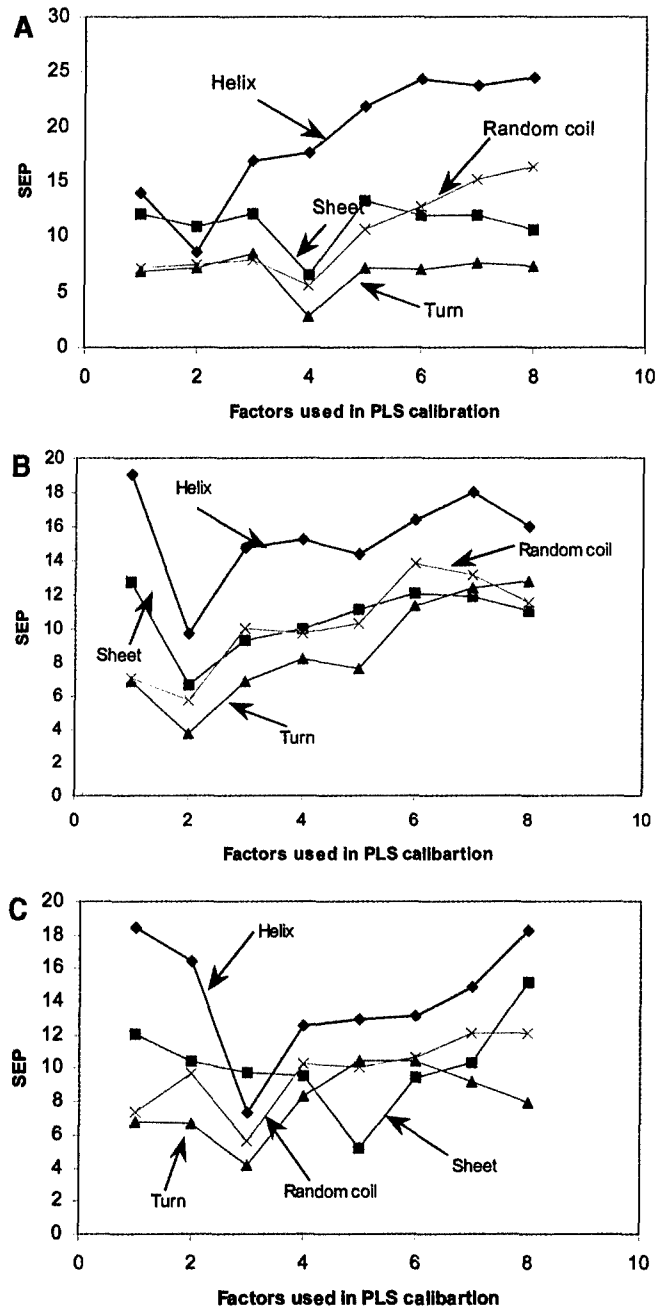


FIGURE 3: Dependence of α -helix, β -sheet, β -turn, and random coil SEP values for PLS from the number of factors used. Panels: (A) using the amide III region; (B) using the amide I region; (C) using the combined regions of amide I and amide III.

parameters for the deconvolution and curve-fitting step raise doubts about the general validity of this procedure (26). Chemometric methods can avoid spectral deconvolution and band assignments. Since the chemometric methods are based on the pattern recognition, the pretreatment of the data can be kept to the minimum. Therefore, it is possible to set up a spectral database for proteins of known structure, which can be used to predict the unknown structures of proteins. These methods were first applied to circular dichroism (CD) spectroscopy (27, 28), but they are equally applicable to vibrational spectroscopy (18, 29, 30). The PLS algorithm belongs to these chemometric methods.

Our results indicate that the amide III region gives a better prediction for four types of secondary structures of protein than either the amide I region or amide I plus amide III region

(Table 2 and Figure 4). This is because different secondary structures reflect a larger spectral difference in the amide III region than in the amide I region (see Figure 1). According to eq 1, if two spectra are very similar, the equation will become mortal, and the error of the prediction will become larger. For some special cases, if the two spectra are the same, no prediction can be obtained. Therefore, the greater the difference present in the spectra of the species in the system, the less the possibility to get the mortal equation and, thus, the greater the accuracy of the result obtained. The α -helix and random coil are overlapped in the amide I region, which makes it a higher risk to be collinear. Therefore, most studies did not differentiate those two structures when using chemometric-based methods in the amide I region (18, 29, 31). When we separate the two structures in the current study, the random coil prediction becomes significantly deviated from the X-ray study with just the PCC of 0.385 (Table 2). Since the amide I region of protein IR spectra has a higher risk to get collinear spectra for different secondary structures, the amide III region is a better region for use in the PLS algorithm.

The interference from the side chain of the peptide is a major concern in the use of the amide III region. By analysis of the loading factors (components) for each type of secondary structure of a protein, the amide I region clearly shows a simpler spectral character, with the minimum SEP when the factor reaches 2. This suggests that only two factors contributed to each type of structure in the amide I region; adding more factors will only add more "noise" vectors in the calibration model, leading to a higher SEP. In the amide III region, on the other hand, the SEP reaches its minimum at factors of 2, 4, 4, and 4 for α -helix, β -sheet, β -turn, and random coil, respectively. This means that there are structures other than the protein secondary structure contributing to this spectral region. When amide I and amide III spectral regions were combined, the SEP reaches a minimum at factors of 3, 5, 3, and 3 for α -helix, β -sheet, β -turn, and random coil, respectively. The complicated feature of the combined region is apparently from the amide III region. Those complicated spectral features are due to both side chain contribution and the other less well defined vibration mode. Due to the complicated feature of the amide region of a protein, it will be very difficult to use the CLS method to resolve the protein structure. We have analyzed the protein secondary structure from amide III bands using the CLS method and compared the results obtained from the PLS algorithm. As seen from Table 3, when amide III bands are used, the PLS algorithm showed better prediction results than the CLS algorithm. This point is supported by the data presented in Figure 2. While the maximum absorbance of α -helix and β -sheet is close to the reported values from the curve-fitting method (22), the β -turn and random coil structures are different from the reported values (22). This is due to the unknown species existing in the calibration set. The PLS method can tolerate some unknown species in the system by including those as the loading vectors in the calibration set. This advantage makes the PLS method less sensitive to those less well defined vibration modes than both the CLS and curve-fitting methods. As shown in Table 3, the prediction for β -turn and random coil from amide III bands is much better when the PLS algorithm is used.

Table 1: Comparison of Protein Secondary Structures Determined by PLS and X-ray Crystallography

protein	α -helix	β -sheet	β -turn	random coil	method
ovalbumin	35	35	18	12	X-ray (24)
	46	29	16	9	PLS amide III
	28	33	22	17	PLS amide I
	36	31	19	14	PLS amides I and III
alcohol dehydrogenase	29	40	19	12	X-ray (23)
	22	43	19	16	PLS amide III
	31	39	16	13	PLS amide I
	32	40	14	14	PLS amides I and III
carbonic anhydrase	16	45	25	14	X-ray (23)
	12	50	24	14	PLS amide III
	9	52	24	15	PLS amide I
	9	52	22	16	PLS amides I and III
α -chymotrypsin	11	50	25	15	X-ray (23)
	20	41	21	18	PLS amide III
	4	60	23	13	PLS amide I
	13	50	21	17	PLS amides I and III
chymotrypsinogen	12	49	23	16	X-ray (23)
	4	56	25	15	PLS amide III
	14	52	20	15	PLS amide I
	4	55	20	21	PLS amides I and III
concanavalin A	3	65	22	10	X-ray (23)
	6	67	18	9	PLS amide III
	3	66	23	8	PLS amide I
	4	67	24	5	PLS amides I and III
cytochrome c	49	11	18	22	X-ray (23)
	60	10	18	12	PLS amide III
	64	7	13	16	PLS amide I
	56	12	17	15	PLS amides I and III
hemoglobin	86	0	8	6	X-ray (23)
	68	10	10	12	PLS amide III
	67	9	10	14	PLS amide I
	66	10	10	14	PLS amides I and III
IgG	3	67	18	12	X-ray (23)
	1	65	21	12	PLS amide III
	15	56	19	10	PLS amide I
	10	60	19	10	PLS amides I and III
lactate dehydrogenase	42	26	5	27	X-ray (23)
	46	27	1	26	PLS amide III
	60	14	11	15	PLS amide I
	54	17	10	19	PLS amides I and III
lysozyme	45	19	23	13	X-ray (23)
	50	17	23	10	PLS amide III
	43	22	18	17	PLS amide I
	47	20	19	13	PLS amides I and III
myoglobin	85	0	8	7	X-ray (23)
	79	0	10	11	PLS amide III
	75	7	6	12	PLS amide I
	87	0	5	9	PLS amides I and III
papain	28	29	18	25	X-ray (23)
	27	38	19	21	PLS amide III
	32	32	20	16	PLS amide I
	30	31	22	18	PLS amides I and III
ribonuclease A	23	46	21	10	X-ray (23)
	31	39	20	10	PLS amide III
	27	41	15	17	PLS amide I
	25	40	20	15	PLS amides I and III
trypsin inhibitor	26	45	16	13	X-ray (23)
	21	51	15	13	PLS amide III
	18	48	20	14	PLS amide I
	23	43	20	14	PLS amides I and III
trypsin	9	56	24	11	X-ray (23)
	10	53	25	12	PLS amide III
	11	52	23	14	PLS amide I
	7	55	26	12	PLS amides I and III

Table 2: Correlation Analysis of Protein Secondary Structures between the PLS Method and X-ray Data

statistical parameter	α -helix	β -sheet	β -turn	random coil	spectral region
PCC	0.950	0.963	0.935	0.771	amide III
SEP	8.3	5.8	2.3	3.9	amide III
PCC	0.925	0.950	0.828	0.351	amide I
SEP	10.0	6.8	3.6	5.7	amide I
PCC	0.958	0.970	0.874	0.622	amides I and III
SEP	7.5	5.2	3.1	4.8	amides I and III

Przybycien et al. (31) have tried to decompose the protein structure into the baseline background (including the residues from buffer and water), the vibrational peaks in the frequency range analyzed that are not correlated with protein secondary structure, and the amide I and/or amide III bands only contributed to protein secondary structure. By using the nonlinear and multiple linear regressions, they isolated the "ideal" reference spectra in the amide I and amide III regions, corresponding only to protein secondary structures. By analyzing those ideal reference spectra of proteins with known X-ray structures, they could predict the structure of unknown proteins. While this method is better than the traditional CLS method, it may over- or underestimate the contributions from noise by setting the function minimum. The PLS method, on the other hand, uses the loading factors to correct the unknown species in the calibration set. When the cross-validation is performed, the optimized number of loading factors can be determined for each structural type of protein. This step will avoid any possibility of either overestimation or underestimation of the spectral contributions from nondefined vibrational modes.

The prediction accuracy of PLS depends on the size of the data and the proteins in the sample set. We have compared the results from this paper with our preliminary results from a set of nine proteins (Table 4) (32). The prediction accuracy for random coil and β -turn improved in our current study. The prediction of α -helix and β -sheet is similar to the earlier study despite the increased sample set. The PLS algorithm has encountered difficulties in those cases where the spectral properties of the unknown protein lie outside the properties of the spectra within the calibration set. We have three proteins (lactate dehydrogenase, cytochrome *c*, and papain) in this sample set, where the random coil is over 20% from X-ray crystallography, whereas only one protein's random coil is over 20% (cytochrome *c*) in the previous study (32). This suggests that the proteins in the sample set should cover most types of structure in a wide range. This is difficult to achieve for certain types of structure, such as random coil, since this structure is very low in most proteins.

The ATR sampling technique also raises some concern, since binding of proteins on the ATR crystal may change the protein structure. However, several researchers (13, 14, 33, 34) suggest that binding of the protein on the crystal does not change protein structure significantly. The comparison of protein infrared spectra collected from ATR and transmission also has been studied (35, 36), and no significant differences have been observed between these two sampling techniques (35, 36). The result from our current work also supports this statement.

Two assumptions were made for the development of the PLS method: first, the secondary structure of proteins in

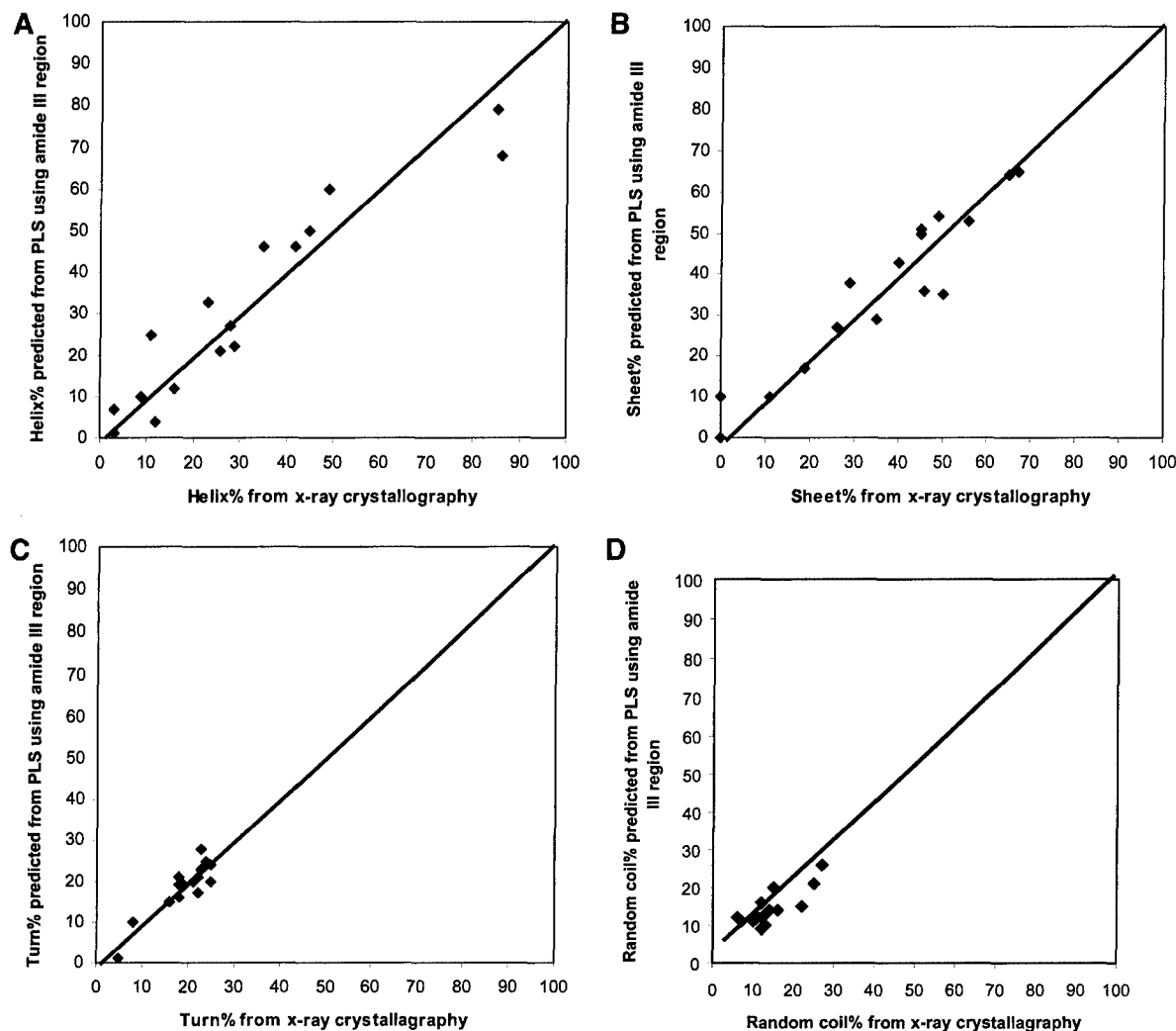


FIGURE 4: Correlation of secondary structure determined by the PLS method from amide III with values determined from X-ray crystallography (20). Panels: (A) α -helix; (B) β -sheet; (C) β -turn; (D) random coil.

Table 3: Comparison of Prediction Accuracy in the Amide III Region Using Different Algorithms

statistical parameter	prediction algorithm	α -helix	β -sheet	β -turn	random coil
PCC	PLS	0.950	0.963	0.935	0.771
SEP		8.3	5.8	2.3	3.9
PCC	CLS	0.916	0.940	0.751	0.402
SEP		11.4	7.8	6.3	13.0

Table 4: Effect of Sample Size on the Prediction Accuracy in the Amide III Region

statistical parameter	sample size	α -helix	β -sheet	β -turn	random coil
PCC	16 (this study)	0.950	0.963	0.935	0.771
SEP		8.3	5.8	2.3	3.9
PCC	9 (29)	0.943	0.968	0.821	0.412
SEP		11.0	6.8	4.0	5.1

solution is considered to be the same as that determined by X-ray diffraction in the crystalline form; second, the normalization procedure assumes equal absorptivity of amide bands irrespective of secondary structure variation.

The most definitive comparisons of solution versus crystal structure are provided by multidimensional NMR studies, which can yield solution structures for small proteins (<50 kDa) (37), comparable to those from X-ray diffraction. One review (37) concluded that, in most cases, the solution and

crystal structures are very similar, allowing for some differences in the local conformation and dynamics of surface residues. Thus, the practice of using crystal structures to calibrate spectroscopic methods for determining solution structures is generally satisfactory, but anomalous cases may be encountered (10).

When the spectra in the amide I and amide III regions were normalized so that the sum of the absorbances in each region is equal to unity, the assumption was made that the integrated area in each region (amide I or amide III) is nearly constant for different proteins. Therefore, it was also assumed that there are equal molar absorptivities of amide bands regardless of the type of secondary structure (as in the case of the band-narrowing analysis). The correlation study done by Susi and Byler (4) suggested that this may be a reasonable assumption. However, studies on poly(L-lysine) have shown that the molar absorptivities of different secondary structures are significantly different (38).

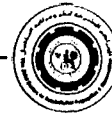
The combination of amide I and amide III regions showed a better prediction for α -helix and β -sheet than using the amide III alone but a worse prediction for β -turn and random coil. This is possibly due to the fact that the amide I region signal is much higher than the amide III signal, and the amide I region is not very sensitive to β -turn and random coil, especially so for the latter (Table 2).

CONCLUDING REMARKS

On the basis of all our experimental results, we believe that the PLS method is a very promising method for predicting the protein secondary structure; it will make prediction more objective than curve-fitting-based methods. The amide III region showed a much better prediction than the amide I region. Although there is a concern that there is more contribution of less well defined structures in the amide III region, the PLS method can tolerate those unknown species.

REFERENCES

- Fasman, G. D. (1989) Protein conformational prediction, *Trends Biochem. Sci.* 14, 295–299.
- Braun, W. (1987) Distance geometry and related methods for protein structure determination from NMR data, *Q. Rev. Biophys.* 19, 115–157.
- Wlodawer, A., Bott, R., and Sjolín, L. (1982) The refined crystal structure of ribonuclease A at 2.0 Å resolution, *J. Biol. Chem.* 257, 1325–1332.
- Susi, H., and Byler, D. M. (1986) Resolution-enhanced Fourier transform infrared spectroscopy of enzymes, *Methods Enzymol.* 130, 290–311.
- Englander, S. W., Downer, N. W., and Teitelbaum, H. (1972) Hydrogen exchange, *Annu. Rev. Biochem.* 41, 903–924.
- Chirgadze, Y. N., Fedorov, O. V., and Trushina, N. P. (1975) Estimation of amino acid residue side-chain absorption in the infrared spectra of protein solutions in heavy water, *Biopolymers* 14, 679–694.
- Anderle, G., and Mendelsohn, R. (1987) Thermal denaturation of globular proteins. Fourier transform-infrared studies of the amide III spectral region, *Biophys. J.* 52, 69–74.
- Kaiden, K., Matsui, T., and Tanaka, S. (1987) A study of the amide III band by FT-IR spectroscopy of the secondary structure of albumin, myoglobin, and γ -globin, *Appl. Spectrosc.* 41, 861–865.
- Singh, B. R., Fuller, M. P., and Schiavo, G. (1990) Molecular structure of tetanus neurotoxin as revealed by Fourier transform infrared and circular dichroic spectroscopy, *Biophys. Chem.* 46, 155–166.
- Singh, B. R., Fu, F.-N., and Ledoux, D. N. (1994) Crystal and solution structures of superantigenic staphylococcal enterotoxins compared, *Nat. Struct. Biol.* 1, 358–360.
- Griebenow, K., and Klibanov, A. M. (1995) Lyophilization-induced reversible changes in the secondary structure of proteins, *Proc. Natl. Acad. Sci. U.S.A.* 92, 10966–10976.
- Costantino, H. R., Griebenow, K., Mishra, P., Langer, R., and Klibanov, A. M. (1995) Fourier transform infrared spectroscopic investigation of protein stability in the lyophilized form, *Biochim. Biophys. Acta* 1253, 69–74.
- Griebenow, K., and Klibanov, A. M. (1996) On protein denaturation in aqueous-organic mixtures but not in pure organic solvents, *J. Am. Chem. Soc.* 118, 11695–11700.
- Bramanti, E., Benedetti, E., Sagripanti, A., Papineschi, F., and Benedetti, E. (1997) Determination of secondary structure of normal fibrin from human peripheral blood, *Biopolymers* 41, 545–553.
- Fu, F.-N., DeOliveira, D. B., Trumble, W., Sarkar, H. K., and Singh, B. R. (1994) Secondary structure estimation of proteins using the amide III region of Fourier transform infrared spectroscopy: application to analyze calcium-binding-induced structural changes in calsequestrin, *Appl. Spectrosc.* 48, 1432–1441.
- Lober, A., and Kowalski, B. R. (1988) Effect of interferences and calibration design on accuracy: implications for sensor and sample selection, *J. Chemom.* 2, 67–79.
- Haaland, D. M., and Thomas, E. V. (1988) Partial least-squares methods for spectral analysis. 1. Relation to other quantitative calibration methods and extraction of qualitative information, *Anal. Chem.* 60, 1193–1202.
- Dousseau, F., and Pezolet, M. (1990) Determination of the secondary structure content of proteins in aqueous solutions from their amide I and amide II infrared bands. Comparison between classical and partial least-squares methods, *Biochemistry* 29, 8771–8779.
- Dong A., Huang, P., and Caughey, W. S. (1990) Protein structures in water from second-derivative amide I infrared spectra, *Biochemistry* 29, 3303–3308.
- Haris, P. I., Lee, D. C., and Chapman, D. A. (1986) Fourier transform infrared investigation of the structural differences between ribonuclease A and ribonuclease S, *Biochim. Biophys. Acta* 847, 255–265.
- Mitchell, R. C., Haris, P. I., Fallowfield, C., Keeling, D. J., and Chapman, D. (1988) Fourier transform infrared spectroscopic studies on gastric H^+/K^+ -ATPase, *Biochim. Biophys. Acta* 941, 31–38.
- Cai, S., and Singh, B. R. (1999) Identification of beta-turn and random coil amide III infrared bands for secondary structure estimation of proteins, *Biophys. Chem.* 80, 7–20.
- Levitt, M., and Greer, J. (1977) Automatic identification of secondary structure in globular proteins, *J. Mol. Biol.* 114, 181–239.
- Stein P. E., Leslie, A. G., Finch, J. T., and Carrell, R. W. (1991) Crystal structure of uncleaved ovalbumin at 1.95 Å resolution, *J. Mol. Biol.* 221, 941–959.
- Kalnín, N. N., Baikalov, I. A., and Venyaminov, S. Y. (1990) Quantitative IR spectrophotometry of peptide compounds in water (H₂O) solutions. III. Estimation of the protein secondary structure, *Biopolymers* 30, 1273–1280.
- Surewicz, W. K., Mantsch, H. H., and Chapman, D. (1993) Determination of protein secondary structure by Fourier transform infrared spectroscopy: a critical assessment, *Biochemistry* 32, 389–394.
- Yang, J. T., and Wu, C. S. (1986) Martinez HM. Calculation of protein conformation from circular dichroism, *Methods Enzymol.* 130, 208–269.
- Manavalan, P., and Johnson, W. C., Jr. (1987) Variable selection method improves the prediction of protein secondary structure from circular dichroism spectra, *Anal. Biochem.* 167, 76–85.
- Lee, D. C., Haris, P. I., Chapman, D., and Mitchell, R. C. (1990) Determination of protein secondary structure using factor analysis of infrared spectra, *Biochemistry* 29, 9185–9193.
- Compton, L. A., and Johnson, W. C. (1986) Analysis of protein circular dichroism spectra for secondary structure using a simple matrix multiplication, *Anal. Biochem.* 155, 155–167.
- Vedantham, G., Sparks, H. G., Sane, S. U., Tzannis, S., and Przybycien, T. M. (2000) A holistic approach for protein secondary structure estimation from infrared spectra in H₂O solutions, *Anal. Biochem.* 285, 33–49.
- Cai, S., and Singh, B. R. (2000) Determination of the secondary structure of proteins from amide I and amide III infrared bands using partial least-square method, in *Infrared analysis of peptides and proteins* (Singh, B. R., Ed.) pp 117–129, American Chemical Society, Washington, DC.
- Jakobsen, R. J., and Wasacz, F. M. (1990) Infrared spectra-structure correlations and adsorption behavior for helix proteins, *Appl. Spectrosc.* 44, 1478–1482.
- Boncheva, M., and Vogel, H. (1997) Formation of stable polypeptide monolayers at interfaces: controlling molecular conformation and orientation, *Biophys. J.* 73, 1056–1072.
- Singh, B. R., and Fuller, M. P. (1991) FT-IR in combination with the attenuated total reflectance technique: A very sensitive method for the structural analysis of polypeptides, *Appl. Spectrosc.* 45, 1017–1021.
- Oberg, K. A., and Fink, A. L. (1998) A new attenuated total reflectance Fourier transform infrared spectroscopy method for the study of proteins in solution, *Anal. Biochem.* 256, 92–106.
- Wagner, G. (1997) An account of NMR in structural biology, *Nat. Struct. Biol.* 4, 841–844.
- Jackson, M., Haris, P. I., and Chapman, D. (1989) Fourier transform infrared spectroscopic studies of lipids, polypeptides and proteins, *J. Mol. Struct.* 214, 329–355.



BOTULINUM TOXIN IN NEUROLOGICAL DISEASES

Shashi Kant Sharma* and Bal Ram Singh†

يتم انتاج التوكسين العصبي بوتولينيوم بواسطة بكتيريا لاهوائية كلوستريديوم بونولينيوم. وتعتبر المادة البيولوجية الأشد سمية من المواد المعروفة. قد تؤدي كمية قليلة جدا من البوتولينيوم إلى التسمم، شلل بهيبت من الأعلى إلى الأسفل مع أعراض بصلية دائمة مؤثرا على الجهاز العصبي التلقائي اللاإرادي غالبا وبعد أن عرف سابقا كمسبب لشلل خطير قد يكون قاتلا جراء هضم الطعام الملوث، أصبح التوكسين يستخدم حديثا لأغراض علاجية وتجميلية. يسبب التوكسين الشلل بإعاقه تحرير الأسيتيلكولين قبل نقطة الإشتباك عند الرباط العضلي العصبي. تكسين البوتولينيوم أ كان الأول الموافق عليه من إدارة الأدوية والغذية الأمريكية في عام ١٩٨٩ لعلاج اعتلالين في عضلات العين (تشنج جفن العين والحوال) وفي العام ٢٠٠٠ لعلاج اضطراب التوتر العنقي وهو اعتلال عصبي للحركة يسبب انقباضات وتقلصات شديدة في الكتف والرقبة. انتشر استخدام تكسين البوتولينيوم وأصبح يستخدم الآن كوسيلة آمنة وفعالة لعلاج اضطرابات عضلية متعددة ولتخفيف تجاعيد الوجه بدون جراحة. الأبحاث في طريقها لإستخدام تكسين البوتولينيوم لتحرير الأدوية، الشقيقة، الزهايمر وعلاج السرطان. فعالية التوكسين في علاج العديد من الأمراض العصبية العضلية واستخداماته العلاجية المتعددة وضعته في قمة قائمة تطور الأدوية.

Botulinum neurotoxin is produced by the anaerobic bacterium *Clostridium botulinum*. It is the most poisonous biological substance known. Very small amounts of botulinum toxin can lead to botulism, a descending paralysis with prominent bulbar symptoms and often affecting the autonomic nervous system. Previously known only as a cause of a serious and often fatal paralysis acquired through ingestion of contaminated food, the toxin recently has been used for medicinal and cosmetic purpose. The toxin causes paralysis by blocking the presynaptic release of acetylcholine at the neuromuscular junction. Botulinum toxin A was first approved by US Food and Drug Administration in the year 1989, to treat two eye muscle disorders (blepharospasm and strabismus) and in the year 2000 to treat cervical dystonia, a neurological movement disorder causing severe neck and shoulder contractions. The use of botulinum toxin has further expanded and now it is being used as a safe and effective way to treat several neuromuscular disorders and to reduce facial wrinkles without surgery. Research is underway to use botulinum toxin for drug delivery, migraine, Alzheimer and treatment of cancer. Its effectiveness in the treatment of various neuromuscular diseases and its multi therapeutic uses has placed the toxin on top of new drug development list.

Key Words: Botulinum toxin, Botox®, Dysport®, MYOBLOC®, NEUROBLOC®, Blepharospasm, synaptobrevin, SANP-25, Chronic headache, Neurotransmitter

INTRODUCTION

Although botulism occurs rarely, it is a dangerous because of its high fatality rate. Clinical descriptions of botulism possibly reach as far back in history as ancient Rome and Greece. However, the relationship between contaminated food and botulism was not defined until the late 1700s. In 1793, the German physician, Justinus

Kerner, deduced that a substance in spoiled sausages, which he called wurstgift (German for sausage poison), caused botulism. The toxin's origin and identity remained elusive until Emile von Ermengem, a Belgian professor, isolated *Clostridium botulinum* in 1895 and identified it as the source of the deadliest poison known¹.

Botulinum toxins (BoNTs) are the most toxic compounds known, with an estimated toxic dose (serotype A) of only 0.001 micrograms/kg of body weight; botulinum toxin is 15,000 times more toxic than the nerve agent VX and 100,000 times more toxic than sarin. On a molar basis, they are 300-fold more lethal than diphtheria toxin, 3×10^4 more toxic than ricin, 1×10^9 more toxic than curare and 1×10^{11} more toxic than NaCN².

From the *Center for Food Safety Applied Nutrition, US Department of Food and Drug Administration, College Park, MD 20740, and †Department of Chemistry and Biochemistry, University of Massachusetts Dartmouth, Dartmouth, MA 02747, USA.

Address reprint requests to: Bal Ram Singh, Department of Chemistry and Biochemistry, University of Massachusetts Dartmouth, 285 Old Westport Road, Dartmouth, MA 02747, USA. Tel: 508-999-8388, Fax: 508-999-8451, Email: bsingh@umassd.edu

The extreme toxicity and its exclusive action on neuromuscular junctions led to the investigation of its medicinal use for neuromuscular disorders. Researches have envisioned the use of the deadliest toxin for therapeutic purpose. The first preparation of crystalline forms of BoNT/A toxin was dated during World War II when an American researcher named Dr. Edward Schantz isolated the crude form of the toxin. Purification of the crude form (900 kDa) of botulinum type A complex was carried out in the 1940 to 1960 at Fort Detrick by Dr. Edward Schantz and his colleagues^{3,4}. The use of botulinum toxin type A as an injectable selective muscle-weakening agent was investigated experimentally in monkey in the 1960s and late 1970s and in human in the late 1970s⁵⁻⁹. Subsequently, in the 1980s, BoNT/A was used for blepharospasm and other focal dystonias⁹. The United States Food and Drug Administration approved BoNT/A (BOTOX®, Allergan, Inc.) in the management of strabismus, blepharospasm and related facial spasms in 1989 and cervical dystonias in 2000. Botulinum toxin type B first became available commercially in the USA in 2000, and was approved for cervical dystonia, but not for blepharospasm or strabismus. Botulinum toxin A is manufactured under the trade name BOTOX® (Allergan, Inc.) in the United States and DYSPORT® (Ipsen, Inc.) in Europe. In the last few years, BoNT/A has also been produced in China. The Chinese toxin (Lanzhou Biological Products Institute, China) is being marketed in Asia as BTX-A. Botulinum toxin B is available in the U.S. as MYOBLOC® and in Europe as NEUROBLOC®¹⁰⁻¹².

Still, there is much we do not know about botulinum neurotoxin, and we are in the phase where its use as a diagnostic and therapeutic agent is in great demand. An effort is being made to understand some of the less well-known biochemical aspects of botulinum toxin. Areas of investigation include long-term effects, optimal treatment regimens, and reasons for treatment failure. Nevertheless, many efforts have been made to understand its structure, function and biochemical properties and pharmacological actions to improve its therapeutic uses for various neuromuscular disorders.

Structure and Function

Botulinum neurotoxins (BoNTs) are produced by various strains of the anaerobic spore-forming bacilli *Clostridium botulinum*, *C. butyricum* and *C. baratii*¹³⁻¹⁵. There are seven serotypes, A-G¹⁶. BoNTs produced

in fluid culture or in food are complexes of one or more neurotoxin associated proteins (NAPs), resulting in molecular sizes of 12, 16 and 19S¹⁷⁻¹⁹. The 16S complex is referred to as 'large' or L toxin and 19S is referred as 'extra large' or LL toxin. The pure BoNT itself has been referred to as small or 7S toxin¹⁸. BoNT/A complex can exist in three forms: M, L or LL²⁰. BoNT/B, /C, /D and /E complexes exist in two forms: L and M^{18,21,22}. So far, BoNT/F complex is known to exist only in M form, and BoNT/G complex exists only in L form²³. The M complex consists of the BoNT and the neurotoxin binding protein (NBP)²⁴, which is also commonly referred to as non-toxic non-hemagglutinin (NTNH). The L complex consists of BoNT, NBP, and five other NAPs. Genes of these proteins are topographically located in close proximity to each other, and their expression is regulated in a coordinated manner^{25,26}.

Each neurotoxin consists of a heavy chain (M_r ~100000) and a light chain (M_r ~50000), covalently linked by a single disulfide bond (Figure 1). The heavy chain includes domains for binding to peripheral motor neurons and toxin internalization, while the light chain is a zinc metalloprotease, specific for proteins involved in acetylcholine release. BoNTs A, C, and E cleave synaptosomal-associated protein of M_r 25,000 (SNAP-25), while synaptobrevin is the target of B, D, F, and G. In addition to SNAP-25, BoNT C also cleaves syntaxin (Figure 2). Each neurotoxin hydrolyzes only a single bond in its substrate, but this is sufficient to prevent exocytosis of neurotransmitter^{27,28}.

The mode of action of BoNT can be divided into

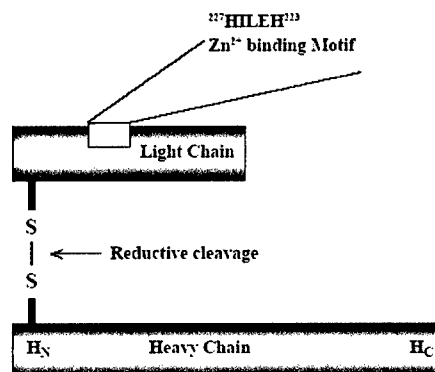


Figure 1. Schematic structure of BoNT/A showing common structural features of clostridial toxins.

four steps: ingestion and intestinal absorption, binding to neuronal membranes, internalization, and blockage of neurotransmitter release²⁹. Since it is the preformed BoNT, rather than the organism, that is the pathogenic agent, the first step in the toxico-infection process is the ingestion and absorption of the BoNT at the intestinal wall. NAPs play a critical role in protecting the BoNT from the acidity and proteases of the GI-tract³⁰. NAPs have also been proposed to help BoNT anchor to the intestinal wall and translocate it across the mucosal layer.

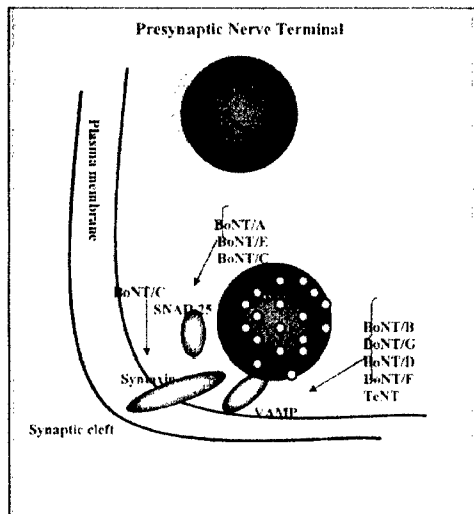


Figure 2. Exclusive substrates for botulinum neurotoxins and their mechanism of action in neuronal cell. The VAMP, SNAP-25 and Syntaxin (SNARE proteins) form a complex with the help of ATPase and NSF (N-ethylmaleimide-Sensitive Factor). The botulinum toxin cleaves these proteins before they form a complex. The SNARE protein complex is involved in the trafficking of the synaptic vesicle containing neurotransmitter.

Medicinal Use

Botulinum toxin A

Botulinum toxin A has been successfully used for the treatment of many disorders related to excessive muscle contraction, such as strabismus, blepharospasm, hemifacial spasm and cervical dystonia⁵. BoNT-A also significantly reduces pain associated with craniocervical dystonia - an effect that has long been considered secondary to its muscle relaxant action^{31,32}. Botulinum toxin A also has been used successfully to treat

several different types of headaches, including tension type headaches^{33,34}, cervicogenic headaches^{35,36} and migraine^{31,37,38}. Botulinum toxin is now widely considered as a pharmaceutical agent with multiple uses, and has propelled into the public eye after it was widely reported to act as an anti-wrinkle drug for facial cosmetic enhancement. This has established its new image as a glamour drug. Botulinum toxin is reported to be useful in more than 50 conditions, with indications spanning many specialties^{39,40}. In the late 1980s, a group of physicians at Columbia University noticed that patients who received injections for nerve disorders also experienced cosmetic improvement. They pursued this investigation and soon developed the botulinum toxin therapy in common use today.

The manufacturing of botulinum toxins for therapeutics involves a series of complex and specialized chromatographic protein purification steps. Two preparations of botulinum toxin A are commercially available. The one is BOTOX[®] from Allergan, Inc. and the other is DYSPORT[®] from Ipsen, Ltd. that are commercially available. These two preparations are widely used for treatment and cosmetic use. They differ based on their preparation and potency. In these two preparations adding either sodium chloride (BOTOX[®], Allergan, Inc.) or lactose (DYSPORT[®], Ipsen, Ltd.) protects the steric conformation of BoNT¹⁰. Human serum albumin is also added to prevent loss from surface adsorption. The toxin is then dried either with freezing (DYSPORT[®], Ipsen, Inc.) or without freezing (BOTOX[®], Allergan, Inc.)¹⁰. Numerous factors influence the clinical potency of the two preparations and hence, units of each product are not clinically equivalent or interchangeable. However, it is clear from the literature and from clinical experience that the units used to quantify the toxin activity of the two products are not equivalent. This apparent difference in the potency of the two products causes difficulties when comparing the results of studies using different preparations, and when changing from one preparation to the other. It is likely that any difference between the two products is the result of the different assay methods used to quantify the activity of the products^{41,42}. Different experimental paradigms have been used to find an appropriate conversion factor in dystonic patients, but the results are conflicting. (the ratio Botox:Dysport found being between 1:3 and 1:6)⁴³⁻⁴⁷. Using a 4:1 conversion ratio for Dysport and Botox, similar results were obtained for the

two treatments in an appropriately powered study, suggesting that this conversion factor is a good estimate of their comparative clinical potencies^{47,48}.

Comparative studies between other botulinum preparations have not yet been published except the toxin preparation produced in China¹². In a case study with 785 patients, there were no significant differences found in the clinical effects of two preparations (BOTOX and CBTX-A), including the latency of response, maximal benefit, and duration of improvement. The patients' subjective assessments were similar. But the requested dose of the Chinese preparation which produced the similar effects, was statistically higher than that of Botox. Side effects included a skin rash appearing within a few days after injections in 3 cases of CBTX-A group, but none from the Botox group. No statistical differences were noted in the other adverse reaction between them. The injections of two kinds of preparation both were simple and effective for the patients with cervical dystonia. Chinese preparation is a little less powerful but much cheaper than Botox¹².

Injections with botulinum toxin are generally well tolerated. After injection the toxin diffuses into the muscles and adjacent tissues. Its effect diminishes with increasing distance from the injection site, but spread to nearby muscles is enhanced when higher volumes of the toxin are injected⁴⁹. Although the use of botulinum toxin is safe, the most frequent adverse reactions are dysphagia, pain, soreness and bruising at the injection site, local weakness, symptomatic general weakness, malaise and nausea. Adverse reactions usually occur within the first week following injection of botulinum toxin and, while generally transient, these reactions may last several months. Localized pain, tenderness and/or bruising may be associated with the injection.

Botulinum toxin B

On December 11, 2000, a botulinum toxin type B product (MyoblocTM) was approved by the FDA in the United States as a treatment for patients with cervical dystonia. MyoblocTM is the U.S. trade name for Elan Biopharmaceuticals' botulinum toxin type B product. Since that time, it has been used effectively to reduce facial wrinkles. Myobloc is particularly suggested for relaxing muscles used in frowning and squinting, if for no other reasons then for its name.

Botulinum toxin type B (BTX-B; Myobloc) is

Table: Recent medicinal use of botulinum neurotoxin

Disorders	Dysfunction
1. Chronic headache	Tension-type headache ⁵⁶
2. Overactive bladder (OAB)	Spastically contraction of detrusor bladder muscles ⁵¹
3. Laryngeal dystonia	Vocal cord dystonia ⁵²
4. Temporomandibular joint dislocation	Dysfunction of the joint, muscles of the jaw ⁵³
5. Dysuria or urinary retention	Non-relaxing urethral sphincter ⁵⁴
6. Tourette's syndrome	Involuntary, rapid, sudden movements of muscles ⁵⁵
7. Focal hyperhidrosis	Excessive sweating ⁵⁴

approved for general use in the treatment of cervical dystonia (CD). In two large pivotal trials, it was found to be safe and effective in decreasing the movements, pain, and disability associated with CD^{57,58}. Being the newest botulinum toxin based product, it is still being evaluated for various neuromuscular conditions. However, it is being tested with promise against upper and lower-limb spasticity^{59,60}, and piriformis syndrome⁶¹.

Although BTX-B is generally considered safe, recent case reports by Dressler and Benecke⁶² indicate that side effects include visual disturbances, dry eyes, and dry mouth which suggest systemic diffusion of physiologically active quantities of toxin from the sites of injection. This interpretation is limited, however, by the small number of cases⁶³. One thing has clearly been observed that there is more antibody response to BTX-B based drugs because of the requirement of dramatically higher dose (about 100-fold higher compared to BTX-based drug)⁶⁴. Therefore, while BTX-B may be an alternative to BTX-A non-responders, it could be useful for long-term treatment.

Botulinum toxin type B differs from botulinum toxin type A in several ways. It is provided in a liquid form as opposed to a lyophilized powder that requires reconstitution in saline. Botulinum toxin type B has shown stability for months when stored appropriately at 2°C to 8°C, whereas botulinum toxin type A must be stored at -5°C as a powder and must be used within hours once reconstituted according to the manufacturer's recommendation⁶⁵. In practice, botulinum toxin type A may be stable for much longer. Also, because

they are antigenically distinct. botulinum toxin type A nonresponders may respond to botulinum toxin type B and *vice versa*⁶⁶.

Botulinum neurotoxin serotypes have similar structures and basic mechanisms of action. However, there are biochemical differences between them. For example, BoNTs produced in fluid culture or in food are complexes of one or more neurotoxin associated proteins (NAPs), resulting in molecular sizes of 12, 16 and 19S¹⁷⁻¹⁹. BoNTs A, C, and E cleave synaptosomal-associated protein of M_r 25,000 (SNAP-25), while synaptobrevin is the target of B, D, F, and G. In addition to SNAP-25, BoNT C also cleaves syntaxin. Therefore, biochemical differences between botulinum toxin serotypes may confer unique *in vivo* biological properties. In some cases, botulinum B was found to be more effective than botulinum A. For example, Flynn and Clark⁶⁷ compared the rate of diffusion of botulinum toxin types A and B in the forehead and found that toxin type B had a slightly faster action than type A. All patients responded to type B quickly, whereas some had a delayed response to type A. The study is based on case reports of monitored diffusion of toxin. The biochemical aspect of such faster diffusion is still unknown.

CONCLUSIONS

Generally, neurotoxins are considered lethal to humans when used in high doses either by deliberate or accident. Botulinum toxin is a rare example of potentially lethal biological agent that can be used as a medicine for several neuromuscular disorders. It has many unique characteristics including exclusive substrate specificity and localized action. Research is underway to use botulinum toxin as a drug delivery vehicle. Despite its extreme toxicity it has been widely used as a wrinkle remover which is perhaps the single most popular use. While its use as a therapeutic agent is relatively safe, care must be taken as it can interact with other antibiotics, especially those which interfere with neurotransmission. Caution should also be exercised when botulinum toxin type A is utilized for treatment of patients with myasthenia gravis, Eaton Lambert Syndrome, or other disorders that produce a depletion of acetylcholine. Although it is considered the most toxic substance known to mankind, researches are turning this killer into cure.

ACKNOWLEDGEMENTS

This work was in part supported by a U.S. Army Medical Research and Materiel Command under Contract No. DAMD17-02-C-001, and by National Institutes of Health through New England Center of Excellence for Biodefense (AI057159-01).

REFERENCES

1. Van Ermengen E: Uber einen neuen anaeroben Bacillus und seine Beziehungen zum Botulismus. *Z Hyg infektionskrankh* 1897;26:1-56.
2. Middlebrook JL: Cell surface receptors for protein toxins. In: Simpson LL (Eds.). *Botulinum neurotoxin and tetanus toxin*. New York: Academic Press 1989, 95-119.
3. Scott AB, Suzuki D: Systemic toxicity of botulinum toxin by intramuscular injection in the monkey. *Mov. Disord* 1988;3:333-35.
4. Shapiro RE, Specht CD, Collins BE, et al: Identification of a ganglioside recognition domain of tetanus toxin using a novel ganglioside photoaffinity label. *J Biol. Chem* 1997;48:30380-30386.
5. Johnson EA: CLOSTRIDIAL TOXINS AS THERAPEUTIC AGENTS: Benefits of Nature's Most Toxic Proteins. *Annu Rev Microbiol* 1999;53:551-575.
6. Schantz EJ, Johnson EA: Botulinum toxin: the story of its development for the treatment of human disease. *Perspect Biol Med* 1997;40:317-327.
7. Schantz EJ, Johnson EA: Properties and use of botulinum toxin and other microbial neurotoxins in medicine. *Microbiol. Rev* 1992;56:80-99.
8. Schantz EJ: Historical perspective: Jankovic J, Hallett M (eds): *Therapy with Botulinum Toxin*. xxiii-vi. New York: Marcel-Dekker 1994, 608.
9. Scott AB: Botulinum toxin injection of eye muscles to correct strabismus. *Trans Am Ophthalmol Soc* 1981;79:734-770.
10. Muthane U, Panikar D: Botulinum toxins: Pharmacology and its current therapeutic evidence for use. *Neurology India* 2003;51:455-460.
11. Jankovic J, Brin MF: Botulinum toxin: historical perspective and potential new indications. *Muscle And Nerve* 1997;20:S129-145.
12. Tang, X, Wan X: Comparison of botox with a chinese type a botulinum toxin. *Chin Med J (Engl)* 2000;113:794-798.
13. Simpson LL: Molecular pharmacology of botulinum toxin and tetanus toxin *Annu. Rev. Pharmacol. Toxicol* 1986;26:427-453.
14. Hall JD, McCroskey LM, Pincomb BJ, et al: Isolation of an organism resembling *Clostridium barati* which produces type F botulinum toxin from an infant with botulism. *J. Clin. Microbiol* 1985;21:654-655.
15. Aureli P, Fenicia L, Pasolini B, et al: Two cases of type E infant botulism caused by neurotoxicogenic *Clostridium butyricum* in Italy. *J. Infect. Dis* 1986;154:207-211.
16. Schiavo G, Matteoli M, Montecucco C: Neurotoxins affecting neuroexocytosis. *Physiol. Rev* 2000;80:717-766.
17. Schantz EJ, Spero L: Molecular size of Cl. Botulinum toxins. Ingram M, Roberts TA (eds). Chapman and Hall, London. 1967, 296-301.

18. Sakaguchi G: Clostridium botulinum toxins. *Pharmac. Ther* 1983;19:165-194.
19. Sugii S, Sakaguchi G: Botulogenic properties of vegetables with special reference to the molecular size of the toxin in them. *J. Food Safety* 1977;1:53-65.
20. Sagane Y, Watanabe T, Kouguchi H, et al: Spontaneous nicking in the nontoxic-nonhemagglutinin component of the Clostridium botulinum toxin complex. *Biochem. Biophys. Res. Commun* 2002;292:434-440.
21. Zhang Z, Singh BR: A novel complex of type E Clostridium botulinum. *Protein Sci* 1995;4(Suppl. 2):110.
22. Li BL, Parikh SN, Lomenth RB, et al: A novel type E Clostridium botulinum neurotoxin progenitor complex. *Protein Sci* 1997;6(Suppl. 2):139 T.
23. Fujita R, Fujinaga K, Inoue H, et al: Molecular characterization of two forms of nontoxic-nonhemagglutinin components of Clostridium botulinum type A progenitor toxins. *FEBS Lett* 1995;376:41-44.
24. Singh BR, Li B. Read: Botulinum versus tetanus neurotoxins: why is botulinum neurotoxin a food poison but not tetanus? *Toxicon* 1995;33:1541-1547.
25. East AK, Bhandari M, Stacey JM, et al: Organization and phylogenetic interrelationships of genes encoding components of the botulinum toxin complex in proteolytic Clostridium botulinum types A, B, and F: evidence of chimeric sequences in the gene encoding the nontoxic nonhemagglutinin component. *Int. J. Syst. Bacteriol* 1996;46:1105-1112.
26. Marvaud JC, Gilbert M, Inoue K, et al: botR is a positive regulator of botulinum neurotoxin and associated nontoxic protein genes in Clostridium botulinum A. *Mol. Microbiol* 1998;29:1009-1018.
27. Humeau Y, Doussau F, Grant NJ, et al: How botulinum and tetanus neurotoxins block neurotransmitter release *Biochimie* 2000;82:427-446.
28. Schiavo G, Matteoli M, Montecucco C: Neurotoxins affecting neuroexocytosis. *Physiol. Rev* 2000;80:717-766.
29. Eswaramoorthy S, Kumaran D, Swaminathan S: A novel mechanism for Clostridium botulinum neurotoxin inhibition. *Biochemistry* 2002;41(31):9795-802.
30. Sharma, SK, Singh BR: Hemagglutinin binding mediated protection of botulinum neurotoxin from proteolysis. *J. Natural Toxin* 1997;7:239-253.
31. Brin MF, Swope DM, O'Brien C, et al: Botox for migraine: double-blind, placebo-controlled, region-specific evaluation. *Cephalgia* 2000;20:421-422.
32. Gobel H, Heinze A, Heinze-Kuhn K, et al: Botulinum toxin A in the treatment of headache syndromes and pericranial pain syndromes. *Pain* 2001;91:195-199.
33. Wheeler AH: Botulinum toxin A, adjunctive therapy for refractory headaches associated with pericranial muscle tension. *Headache* 1998;38:468-471.
34. Schulte-Mattler WJ, Wieser T, Zierz S: Treatment of tension-type headache with botulinum toxin: a pilot study. *Eur J Med Res* 1999;4:183-186.
35. Hobson DE, Gladish DF: Botulinum toxin injection for cervicogenic headache. *Headache* 1997;37:253-255.
36. Freund BJ, Schwartz M: Treatment of chronic cervical-associated headache with botulinum toxin A: a pilot study. *Headache* 2000;40:231-236.
37. Binder WJ, Brin MF, Blitzer A, et al: Botulinum toxin type A (BOTOX) for treatment of migraine headaches: an open-label study. *Otolaryngol Head Neck Surg* 2000;123:669-676
38. Silberstein S, Mathew N, Saper J, et al: Botulinum toxin type A as a migraine preventive treatment. For the BOTOX Migraine Clinical Research Group *Headache* 2000;40:445-450
39. Misra, VJ: Editorial: The changed image of botulinum toxin. *Bio Med. J* 2002;325:1188.
40. Jost WH, Kohl A: Botulinum toxin: evidencebased criteria in rare indications. *J Neurol* 2001;248 suppl1:3944.
41. Odegren T, Hjaltason H, Kaakkola S, et al: A double blind, randomized, parallel group study to investigate the dose equivalence of Dysport® and Botox® in the treatment of cervical dystonia. *J Neurol Neurosurg Psychiatry* 1998;64:6-12.
42. Hambleton P, Pickett AM: Potency equivalence of botulinum toxin preparations. *J R Soc Med* 1994;87:719-724.
43. Ranoux D, Gury C, Fondarai J, et al: Respective potencies of Botox and Dysport: a double blind, randomized, crossover study in cervical dystonia. *J Neurol Neurosurg Psychiatry* 2002;72:459-62.
44. Durif F: Clinical bioequivalence of the current commercial preparations of botulinum toxin. *Eur Neurol* 1995;2:17-18.
45. Marion MH, Sheehy M, Sangla S, et al: Dose standardization of botulinum toxin. *J Neurol Neurosurg Psychiatry* 1995;59:102-103.
46. Whurr R, Brooks G, Barnes C: Comparison of dosage effects between the American and British botulinum toxin A products in the treatment of spasmodic dysphonia [abstract]. *Mov Disord* 1995;10:387.
47. Sampaio C, Ferreira JJ, Simoes F, et al: DYSBOT: a single-blind, randomized parallel study to determine whether any differences can be detected in the efficacy and tolerability of two formulations of botulinum toxin type A-Dysport and Botox-assuming a ratio of 4:1. *Mov Disord* 1997;12:1013-1018.
48. Sampaio C, Costa, J, Ferreira, JJ: Clinical compatibility of marketed formulations of botulinum toxin. *Mov Disord* 2004;19:S129-S136.
49. Munchau A, K P Bhatia KP: Uses of botulinum toxin injection in medicine today(Clinical Review). *BMJ* 2000;320:161-165.
50. Wilhelm JSM, Krack P: Treatment of chronic tension-type headache with botulinum toxin A: a randomized, double-blind, placebo-controlled multicenter study. *Pain* 2004. In Press.
51. Wein AJ: Diagnosis and treatment of the overactive bladder. *Urology* 2003;62:20-27.

Hemagglutinin-33 of type A botulinum neurotoxin complex binds with synaptotagmin II

Yu Zhou, Sean Foss, Paul Lindo, Hemanta Sarkar and Bal Ram Singh

Department of Chemistry and Biochemistry, and the Botulinum Research Center, University of Massachusetts Dartmouth, MA, USA

Keywords

botulinum neurotoxin; *Clostridium*; hemagglutinin; synaptotagmin; synaptosomes

Correspondence

B. R. Singh, Department of Chemistry and Biochemistry, and Botulinum Research Center, University of Massachusetts Dartmouth, 285 Old Westport Road, North Dartmouth, MA 02747, USA
Fax: +1 508 999 8451
Tel: +1 508 999 8588
E-mail: bsingh@umassd.edu

(Received 23 November 2004, revised 18 February 2005, accepted 28 March 2005)

doi:10.1111/j.1742-4658.2005.04688.x

Botulinum neurotoxins (BoNTs) are among the most potent toxins known (approximately 100 billion times more toxic than cyanide) [1]. BoNTs are the causative agents of food-borne, infant and wound botulism [2]. Because of its extreme toxicity, BoNT is also considered a dreaded biological weapon [3].

Different strains of *Clostridium botulinum* produce seven distinct serotypes of botulinum neurotoxins (EC 3.4.24.69), named A to G. Each of the BoNTs is synthesized as a single polypeptide chain of about 150 kDa, which is cleaved endogenously or exogenously resulting in a 100 kDa heavy chain and a 50 kDa light chain, linked through a disulfide bond [1]. The mode of action of BoNT involves four steps: extracellular binding to the presynaptic membrane, internalization, membrane translocation, and intracellular substrate cleavage through its endopeptidase activity. In the first step, BoNT attaches to nerve membranes

Botulinum neurotoxin type A (BoNT/A), the most toxic substance known to mankind, is produced by *Clostridium botulinum* type A as a complex with a group of neurotoxin-associated proteins (NAPs) through polycistronic expression of a clustered group of genes. NAPs are known to protect BoNT against adverse environmental conditions and proteolytic digestion. Hemagglutinin-33 (Hn-33) is a 33 kDa subcomponent of NAPs that is resistant to protease digestion, a feature likely to be involved in the protection of the botulinum neurotoxin from proteolysis. However, it is not known whether Hn-33 plays any role other than the protection of BoNT. Using immunoaffinity column chromatography and pull-down assays, we have now discovered that Hn-33 binds to synaptotagmin II, the putative receptor of botulinum neurotoxin. This finding provides important information relevant to the design of novel antibotulism therapeutic agents targeted to block the entry of botulinum neurotoxin into nerve cells.

through the C-terminus of the heavy chain, binding to gangliosides and a protein receptor on presynaptic membranes [4]. Synaptotagmin II (Syt II) from rat brain has been identified as the receptor for BoNT/B [5,6], and also for BoNT/A and E [7]. The second step involves the internalization of the neurotoxin through endocytosis. In the third step, as the pH inside the endosome is lowered with a proton pump [8], the N-terminal domain of the heavy chain is inserted into the membrane lipid bilayer to form a pore for translocating the light chain across the membrane into the cytosol [8,9]. Finally, once in the cytosol, the light chain acts as a zinc-endopeptidase and cleaves one of the three soluble *N*-ethylmaleimide-sensitive factor attachment protein receptor (SNARE) proteins. The light chains of BoNT/A and E cleave a synaptosome-associated protein of 25 kDa (SNAP-25), the BoNT/C light chain cleaves syntaxin and SNAP-25, and the

Abbreviations

BoNT/A, Botulinum neurotoxin type A; FITC, fluorescein-5-isothiocyanate; GST, glutathione *S*-transferase; Hn-33, hemagglutinin-33; NAP, neurotoxin-associated protein; SNAP-25, 25 kDa synaptosome-associated protein; SNARE, soluble *N*-ethylmaleimide-sensitive factor attachment protein receptor; Syt II, synaptotagmin II; VAMP, vesicle-associated membrane protein.

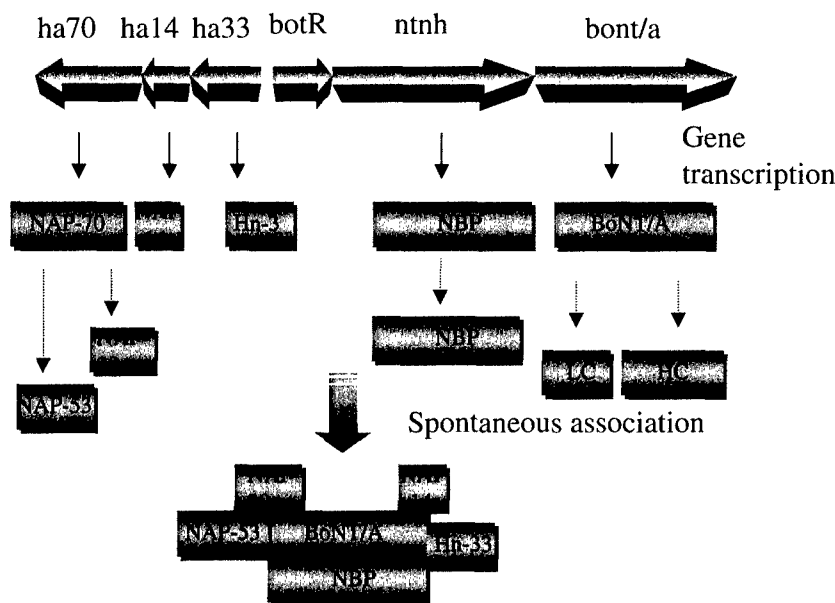


Fig. 1. Genetic organization of the BoNT/A complex genes and their expressed proteins in forming the BoNT/A complex. ha represents hemagglutinin, and the numbers refer to the molecular masses of the protein expressed by these genes. The NAP-70 gene product is a precursor of NAP-53 and NAP-20. botR is known to regulate BoNT gene expression, and ntnh represents nontoxin-nonhemagglutinin and encodes NBP. bont/a encodes BoNT/A.

light chains of BoNT/B, D, F and G cleave the vesicle-associated membrane protein (VAMP) [1]. The cleavage of any one of the SNARE proteins results in the blockage of acetylcholine release at the neuromuscular junctions, resulting in flaccid muscle paralysis.

BoNTs are expressed in *C. botulinum* in the form of BoNT cluster genes, which consist of genes for BoNT, a group of neurotoxin associated proteins (NAPs), and a regulatory gene botR [10–13] (Fig. 1). NAPs (also referred to as complexing protein or hemagglutinins) are well known to play a critical role in food poisoning by not only protecting the BoNT from low pH and proteases in the gastrointestinal tract but also by assisting BoNT translocation across the intestinal mucosal layer [14–18]. The BoNT complex (also referred to as progenitor toxin), consisting of NAPs and BoNT, is the native form of the toxin secreted by *C. botulinum*. NAPs have also been shown recently to dramatically enhance the endopeptidase activity of BoNT/A [19,20].

BoNTs are also being used as therapeutic agents against numerous neuromuscular disorders, as well as cosmetic agents [20,21]. Therapeutic and cosmetic formulation consists of BoNT and NAPs. Hemagglutinin-33 (Hn-33) is a 33 kDa component of the NAPs, and it shows hemagglutination activity [22]. The purified Hn-33 is found to be resistant to digestion by proteases such as trypsin, chymotrypsin, pepsin and subtilisin [15]. It also presumed to bind intestinal epithelial cells and help in the absorption and translocation of BoNT across small intestinal wall [16,23]. In addition, Hn-33 is shown to enhance the endopeptidase activity of BoNT/A and BoNT/E [20]. These observations

suggest the possibility of multiple roles of Hn-33 in the intoxication process of botulinum neurotoxins.

In this report, we describe an unexpected finding of Hn-33 binding to synaptotagmin II, the putative receptor of purified BoNT. Hn-33 binds to synaptotagmin *in vitro* and in synaptosomes, suggesting its possible role in the attachment of the BoNT complex to nerve terminals.

Results

Isolation of a putative receptor of Hn-33 from synaptosomes

To identify and isolate the protein receptor for Hn-33 from nerve cells, we prepared an affinity column of Hn-33, to which rat brain synaptosomal protein extract was applied. Figure 2 shows a representative

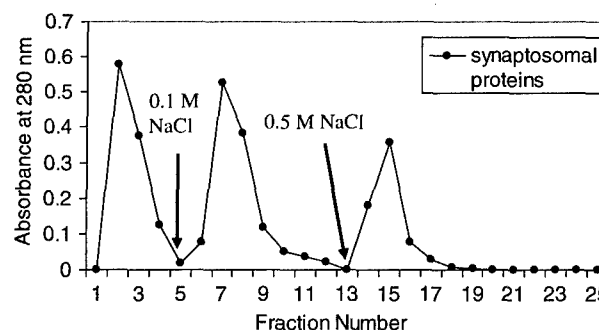


Fig. 2. Elution profile of solubilized synaptosomal proteins on the Hn-33 affinity column. Protein content is indicated by absorbance at 280 nm, while arrows indicate the application of the elution buffer. Each fraction collected was 1.5 mL.

elution profile of rat brain synaptosomal membrane proteins on an Hn-33 affinity column. Nonspecifically adsorbed proteins and unbound rat brain synaptosomal membrane proteins were washed out with 10 mM Hepes buffer, pH 7.3, in fractions 3–5. Proteins bound to the Hn-33 affinity column were eluted with 10 mM Hepes buffer, pH 7.3, containing 0.1 M NaCl in fractions 7, 8 and 9, and containing 0.5 M NaCl in fractions 14, 15 and 16. Analysis of the 0.1 M NaCl eluate on SDS/PAGE followed by Coomassie blue staining revealed five bands at approximately 180, 66, 50, 45 and 31 kDa under reducing conditions. Similar analysis of the 0.5 M NaCl eluate revealed four protein bands with molecular masses of approximately 90, 55, 50 and 45 kDa. Western blot analysis using anti-synaptotagmin as the primary antibody revealed that one 65 kDa band from the 0.1 M NaCl eluate is synaptotagmin, as indicated by comparison with a positive control of rat brain tissue extract and synaptosomal protein extract (data not shown). Anti-synaptotagmin IgG did not react with any of the proteins eluted using 10 mM Hepes buffer, pH 7.3, containing 0.5 M NaCl.

Binding of synaptotagmin to an Hn-33 affinity column

The binding nature of synaptotagmin to Hn-33 was analyzed further by preparing an affinity column of Hn-33 to which recombinant glutathione *S*-transferase (GST)–Syt II was applied. A control experiment was carried out with GST alone as a ligand applied to the Hn-33 affinity column. Affinity column chromatography was carried out in the same way as that described for the synaptosome extract. The elution profile obtained for GST–Syt II (Fig. 3A) shows only one elution peak with 0.5 M NaCl in 10 mM Hepes buffer, pH 7.3, whereas the control protein GST did not bind to the Hn-33 column (Fig. 3A). Syt II binding to Hn-33 column was further confirmed by analyzing the eluate with 4–20% SDS/PAGE (Fig. 3B) and western blotting (Fig. 3C). SDS/PAGE analysis showed a single protein band at about 90 kDa in the 0.5 M NaCl eluate, which corresponds to the molecular size of recombinant GST–synaptotagmin. Western blot analysis using anti-synaptotagmin as the primary antibody revealed that the 0.5 M NaCl eluate of GST–Syt II is synaptotagmin II.

Binding of Hn-33 to synaptotagmin

The interaction of Hn-33 with synaptotagmin was confirmed further by immobilizing GST–Syt II on glutathione–Sepharose beads, and incubating the beads

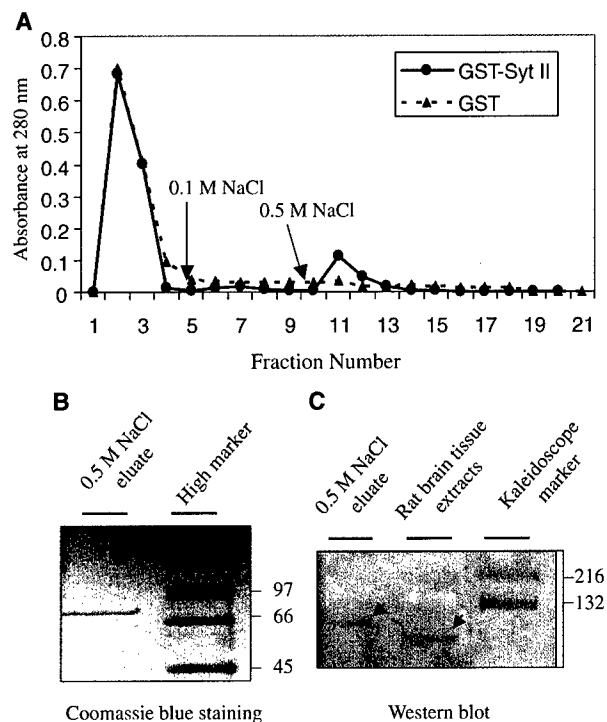


Fig. 3. Elution profile of GST–Syt II and GST on the Hn-33 affinity column (A). Protein content is indicated by absorbance at 280 nm, while arrows indicate the application of the elution buffer. Each fraction collected was 1.5 mL. SDS/PAGE (B) and western blot with rat anti-synaptotagmin IgG (C) analyses of elution peaks from the Hn-33 affinity column. Arrows indicate the positive bands, and the numbers indicate molecular mass markers in kDa.

with Hn-33 in NaCl/P_i buffer, pH 7.4. After thorough washing, the bound materials were eluted with 15 mM reduced glutathione in 50 mM Tris/HCl (pH 8.0) and subjected to SDS/PAGE analysis. The GST–Syt II at 90 kDa and Hn-33 at 33 kDa were found in the eluate of bound material (Fig. 4A).

In a similar experiment, GST–Syt II immobilized on glutathione–Sepharose beads was used to pull down Hn-33 (Fig. 4B) and BoNT/A (Fig. 4C) from solution. The results of the pull-down assay, as examined by the SDS/PAGE, revealed that under identical conditions Hn-33 at a concentration of 18.0 μ M and BoNT/A at 5.3 μ M bound substantially to Syt II, and these binding activities were independent of ganglioside (Fig. 4B,C).

ELISA analysis of concentration dependent Syt II binding to Hn-33

The binding of Syt II to Hn-33 was carried out in an ELISA format by coating Hn-33 in the wells, adding purified Syt II to each well, and then incubating the

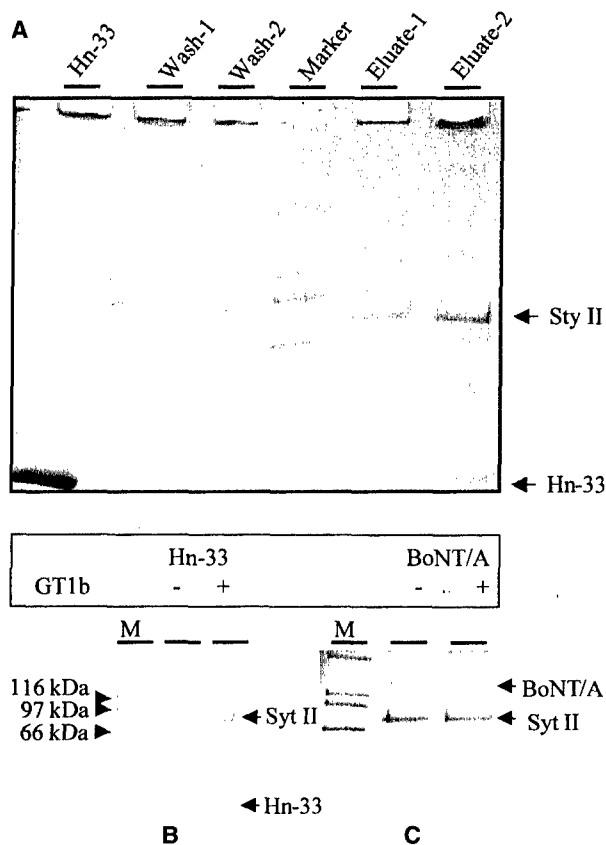


Fig. 4. SDS/PAGE analysis of eluate from the GST-Syt II-Sepharose affinity column (A). The glutathione-Sepharose beads immobilized with GST-Syt II were mixed with Hn-33 for 2 h at 4 °C. The mixture was then applied to a glass column (1.2 cm × 8 cm), which was thoroughly washed (Wash-1, Wash-2) with NaCl/P_i and then eluted with 15 mM reduced glutathione in 50 mM Tris/HCl, pH 8.0 (Eluate-1, Eluate-2). Binding of GST-Syt II with Hn-33 (B) and BoNT/A (C) as analyzed by the pull-down assay. The glutathione-Sepharose beads immobilized with GST-Syt II were mixed with Hn-33 (18.0 μM), or BoNT/A (5.3 μM) in the absence (-) or presence (+) of GT1b (12.5 μM) for 1 h at 4 °C. Beads were washed four times with NaCl/P_i, bound proteins were solubilized by boiling in SDS sample buffer, and analyzed by SDS/PAGE with Coomassie blue staining. M, molecular mass markers, with sizes in kDa.

plate at room temperature (25 °C). The ELISA analysis with anti-Syt II IgG showed substantial binding of Syt II to Hn-33 (Fig. 5A). Syt II did not bind to the wells coated with GST as a control (Fig. 5A). In a parallel study, it was shown that GST did not bind to an Hn-33-coated plate (Fig. 5A).

Concentration-dependence of Syt II binding to Hn-33 is shown in Fig. 5B. This binding was linear within the concentration range of Hn-33 used (0.1–0.6 μM). Linear regression of the binding curve yielded a slope of 0.27 μM⁻¹, suggesting moderate binding of Syt II to Hn-33. Further experiments need

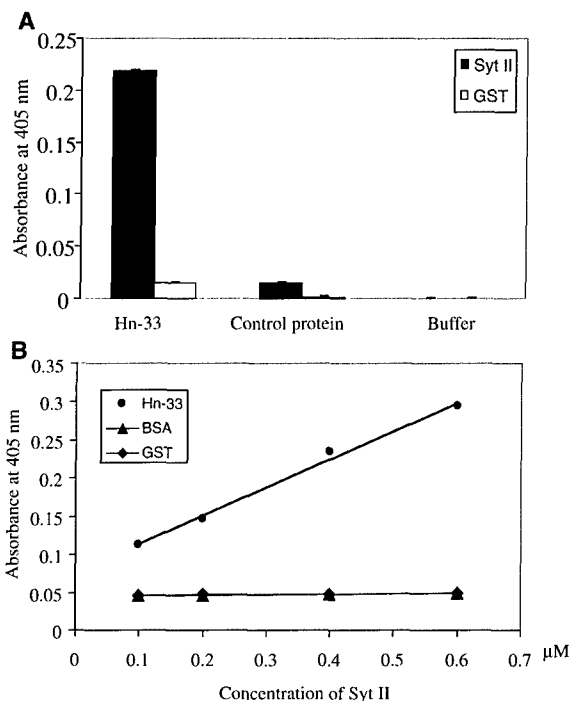


Fig. 5. ELISA analysis of binding of Syt II to Hn-33. (A) Purified type A Hn-33, GST (control protein) and coupling buffer were coated to each well of a flat-bottomed 96-well plate and incubated at 4 °C overnight. After the plate was blocked with 1% (w/v) BSA, the purified Syt II or GST alone was added to each well. The plate was incubated for 1.5 h at room temperature (25 °C) on a rocker and then washed. After incubation with primary and secondary antibodies, the colorimetric detection was followed, and the absorbance at 405 nm of each well was measured using a microplate reader. (B) Syt II at different concentrations was added to the wells, which were precoated with type A Hn-33, or BSA or GST as control proteins. The correlation coefficient, R^2 , of linear regression analysis ($y = 0.037x + 0.0767$) of the binding curve of Syt II to Hn-33 was 0.994. The results shown are the mean of three separate experiments, each performed in triplicate; error bars represent the standard deviations.

to be carried out to determine the dissociation constant.

Immunofluorescence staining

The binding of Hn-33 directly to synaptosomes was analyzed by rabbit anti-(Hn-33) IgG, detecting the latter with fluorescein-5-isothiocyanate (FITC)-labeled sheep anti-rabbit IgG. As shown in Fig. 6, only the synaptosomes incubated with Hn-33 were recognized by the primary and secondary antibodies, detected by the fluorescence signal (Fig. 6A). Negligible fluorescence signals appeared in those synaptosomes incubated without Hn-33, and with only FITC-conjugated anti-rabbit IgG, after blocking with 3% (w/v) BSA (Fig. 6B).

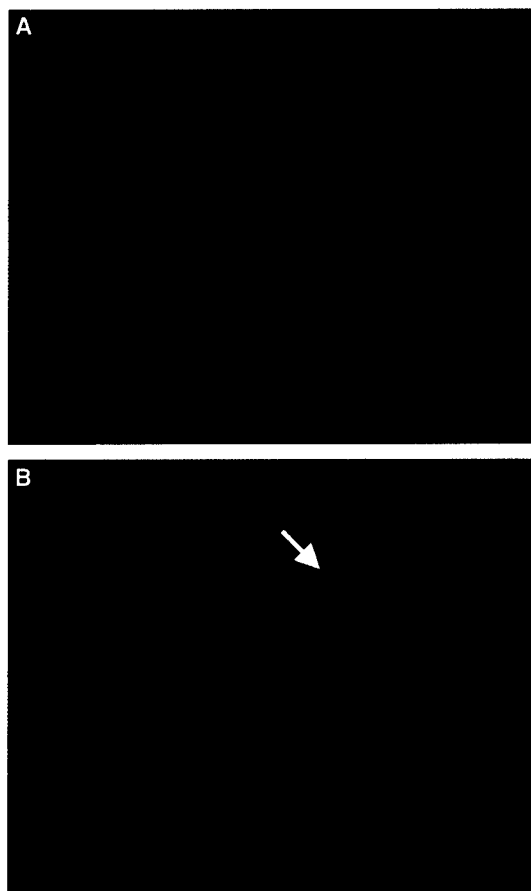


Fig. 6. Immunofluorescence detection of Hn-33 binding to synaptosomes. The synaptosomes were fixed and permeabilized as described in the Experimental Procedures. The synaptosomes incubated with $3.03 \mu\text{M}$ Hn-33 for 1 h at room temperature (25°C) after blocking with 3% (w/v) BSA, then further incubated with both rabbit anti-(Hn-33) and anti-rabbit IgG-FITC (A). Synaptosomes incubated only with anti-rabbit IgG-FITC (not with Hn-33) after blocking with 3% (w/v) BSA (B).

Synaptosomes incubated with FITC-labeled Hn-33 showed a strong signal even after five washes. However, preincubation of synaptosomes incubated with unlabeled Hn-33, even at 1 : 1 molar ratio, blocked the binding of FITC-Hn-33, showing no fluorescence signal (data not shown).

Discussion

The impact of the complex structure and mode of action of botulinum neurotoxin on human health is serious and manifold. One of the most intriguing features of BoNTs is their existence as complexes with a set of NAPs [19,20].

The genetic organization of BoNT/A complex genes and their expressed proteins in forming the BoNT/A

complex is shown schematically in Fig. 1 [10,13, 19,24,25]. The complex form of BoNT/A is the native form produced by *C. botulinum* consisting of the toxin and five NAPs [19].

Notably, BoNT/A in its complex form is used as the therapeutic agent in two commercial products, BoToxTM [25] and DysportTM [26]. Entry of the complex may have relevance to the effectiveness of those therapeutic agents. Hn-33 is present in proportionally the highest amount of all NAPs in the BoNT/A complex [19,27], and has been shown to affect the structure and function of BoNT/A, including the endopeptidase activity [20]. In a previous study, Sharma and Singh [20] showed that Hn-33 was able to enhance the endopeptidase activity of BoNT/A against SNAP-25 inside the synaptosome, indicating that Hn-33 enters into the synaptosome. Binding of Hn-33 to the synaptosome membrane through specific proteins is likely to precede its entry. Therefore, we carried out the binding assay of Hn-33 to synaptosomal proteins in order to find the relevance of this component of NAPs in neuronal entry.

Affinity chromatography on an Hn-33 column revealed that synaptotagmin, a protein identified as a potential receptor of BoNT/A, B, E and G [6,7,28,29], binds to Hn-33. Other proteins eluted with 0.1 M NaCl were of 180, 50, 45 and 31 kDa molecular mass. Their identity remains to be elucidated. Synaptotagmin binding to Hn-33 column appears weak as it was possible to elute it with 0.1 M NaCl. However, elution of ligands with 0.1 M NaCl is considered to indicate specific binding [30].

To examine the binding of Hn-33 to synaptotagmin further, we carried out chromatography of Syt II on an Hn-33 affinity column. Interestingly, Syt II was not dislodged with 0.1 M NaCl; rather it was eluted with 0.5 M NaCl (Fig. 3) as a single elution band. The eluted Syt II was analyzed by western blotting and compared with Syt II in rat brain tissue extract (Fig. 3C), showing compatibility between recombinant Syt II and the native Syt II present in the brain extract. The western blot band seen at 90 kDa is due to the fusion protein obtained from GST (25 kDa) and synaptotagmin (65 kDa). Hn-33 does not bind to GST itself (Fig. 3A). A control experiment was performed using casein, as a protein different from Hn-33. A casein affinity column was prepared by coupling casein to Affi-Gel 15, and purified synaptotagmin was applied to the casein affinity column. It was shown that GST-Syt II did not bind to casein (data not shown), and no nonspecific binding of Syt II to the matrix and specific binding of Syt II to Hn-33 were observed.

To compare synaptotagmin binding to Hn-33 with former's binding with BoNT, we employed a pull-down assay used by other researchers to examine the binding of two proteins, including BoNT binding to synaptotagmin [28,29]. The pull-down assay provides a better way to examine the binding between Syt II and Hn-33, as both Syt II and Hn-33 are free to interact with each other because GST is used to anchor Syt II to the beads. BoNT/A and E have been shown to bind to synaptotagmin on an affinity column [7]. The pull-down assay showed that Syt II binds with Hn-33 and BoNT/A (Fig. 4B,C). The binding of Syt II to Hn-33 is similar to that of its binding to BoNT/A (Fig. 4B,C).

GT1b, a ganglioside well known to affect synaptotagmin binding to BoNT/B [6], did not appear to affect Syt II binding with Hn-33 or BoNT/A in this experiment (Fig. 4B,C). The finding is consistent with the earlier observation of the noninfluence of GT1b on synaptotagmin binding with BoNT/A and BoNT/E [7]. The difference in the effect of GT1b on BoNT/B binding to Syt reported by Nishiki *et al.* [6] and Dong *et al.* [28] could be due to full-length Syt being used by the former, whereas a truncated Syt was used by the latter.

To characterize the binding properties of Syt II to Hn-33, we carried out binding experiments in the ELISA format. One set of ELISA results revealed that Syt II, not GST, binds to Hn-33 (Fig. 5A), indicating that the interaction is not at the junction between GST and Hn-33. In comparison to Syt II binding to a control protein (GST), its binding to Hn-33 is about 10-fold higher (Fig. 5A). These data strongly support the aforementioned view, and suggest specificity of Syt II binding with Hn-33. Moreover, ELISA analysis of concentration-dependent binding of Syt II to Hn-33 clearly suggests specific interaction between Syt II and Hn-33 with a slope of $2.7 \times 10^5 \text{ M}^{-1}$ (Fig. 5B). The binding affinity of Hn-33 to Syt II is considerably less than its affinity to BoNT/B [5], whereas it appears comparable with Syt II binding to BoNT/A (Fig. 4B,C). While the K_a of Hn-33 and Syt II is low, it is still comparable to the binding of substrates such as NAD^+ and its enzymes, such as aldolase ($0.7 \times 10^4 \text{ M}^{-1}$ [31]) and glutamate dehydrogenase ($1.4 \times 10^3 \text{ M}^{-1}$ [32]).

The specific binding of Hn-33 to Syt II *in vitro* and its binding to the synaptosome (Fig. 6) could have significant implications not only on the mode of BoNT/A entry into nerve cells, but also the longevity of the toxin inside the cell. BoNT/A endopeptidase activity is known to persist for months inside the nerve cell [33–38]. We surmise that if Hn-33 also enters the cell

with BoNT/A, it could protect the latter against the proteolytic enzymes of nerve cells.

In summary, we have demonstrated for the first time the association of Hn-33, one subcomponent of the BoNT/A complex, with Syt II *in vitro*. The binding of Syt II to Hn-33 was also identified on synaptosomes using fluorescence microscopy (Fig. 6). Our results suggest that Hn-33 not only protects the neurotoxin from proteolysis but is also involved in binding to nerve cell receptors during the first step of BoNT action.

Experimental procedures

Materials

Hn-33, BoNT/A and the BoNT/A complex were purified from *C. botulinum* type A (strain Hall) grown in N-Z amine medium [39] using a series of chromatographic columns as described by Fu *et al.* [22,40]. Purified Hn-33, BoNT/A and BoNT/A complex were precipitated with 0.39 g mL^{-1} ammonium sulfate and stored at 4°C until use. The precipitate was centrifuged at $10\,000 \text{ g}$ for 10 min and dissolved in a desired buffer as needed for experiments.

Synaptosomes were prepared from frozen rat brains (RJO Biologicals Inc., Kansas City, MO, USA) and solubilized with the addition of nonanoyl-*N*-methylglucamide (MEGA-9), which is nonionic detergent, transparent in the UV region, and ideal for use as a membrane protein solubilizer in the buffer, according to a previously published procedure [7].

Recombinant glutathione *S*-transferase fused to full length synaptotagmin II (GST-Syt II) was isolated as described by Zhou and Singh [41].

Rabbit anti-(Hn-33) IgG was obtained from BBTech (Dartmouth, MA, USA), and sheep anti-rabbit IgG conjugated with FITC was purchased from Sigma (St. Louis, MO, USA). Mouse anti-Syt IgG and goat anti-mouse IgG alkaline phosphatase conjugate were purchased from Stress-Gen Biotechnologies (Victoria, BC, Canada) and Novagen (Madison, WI, USA), respectively.

Isolation and identification of Hn-33 binding proteins in synaptosomes

The Hn-33 affinity column was prepared by coupling purified Hn-33 to Affi-Gel 15 (Bio-Rad, Richmond, CA, USA), an *N*-hydroxysuccinimide ester of crosslinked agarose. Affi-Gel 15 (1.5 mL) was washed four times each with three bed volumes of cold deionized water by centrifugation at 55 g for 30 s at 4°C . Hn-33 (1.5 mg) was dissolved in 1.5 mL coupling buffer (0.1 M bicarbonate buffer, pH 8.3) and added to the washed Affi-Gel 15. After mixing, this was incubated on a rotating platform at room temperature

(25 °C) for 1 h. One milliliter of 0.1 M ethanolamine, pH 8.0, was added to the mixture to block any remaining reactive groups, and the mixing continued for additional 1 h under the same conditions. The Hn-33-conjugated gel was poured into a 1 × 10 cm glass column.

The following experiments were performed at 4 °C. The Hn-33 affinity column was washed with 10 bed volumes of coupling buffer, then five bed volumes of 10 mM Hepes buffer, pH 7.3, until the absorbance at 280 nm was zero. The solubilized synaptosomal proteins [7] were applied to the column. Each sample was cycled through the affinity column five times to ensure maximum binding. The column was washed extensively with 10 mM Hepes buffer, pH 7.3, to remove nonspecifically adsorbed proteins until absorbance at 280 nm became zero. Because the presence of detergent (MEGA-9) in washing buffer did not affect protein elution from the affinity column, the detergent was excluded from the wash buffer to avoid its interference in further assays of the eluted synaptotagmin. The column was eluted with 0.1 M NaCl in 10 mM Hepes buffer, pH 7.3, then with 0.5 M NaCl in the same buffer, at flow rate of 1 mL·min⁻¹. Fractions of 1.5 mL were collected and the absorbance at 280 nm was measured. Each fraction was analyzed with 4–20% SDS/PAGE after being mixed with SDS/PAGE sample buffer [100 mM Tris/HCl, pH 6.8, 200 mM dithiothreitol, 4% (w/v) SDS (electrophoresis grade), 0.2% (w/v) bromophenol blue, 20% (v/v) glycerol] to obtain reducing conditions. Fractions of 0.1 M NaCl eluate and 0.5 M NaCl eluate were analyzed using western blotting as described previously [41].

Synaptotagmin II binding to column-immobilized Hn-33

A similar experiment was carried out with full length GST-Syt II and a control protein (GST from Sigma) by applying them to the Hn-33-agarose affinity column, separately. These experiments provided data to compare to the specific binding of Syt II to Hn-33. Fraction of 0.5 M NaCl eluate was analyzed using a western blot as described previously [41].

Hn-33 binding to column-immobilized GST-synaptotagmin

GST-Syt II immobilized on glutathione-Sepharose beads (1 mL; Amersham Pharmacia Biotech, Piscataway, NJ, USA) was incubated with 1 mL of Hn-33 (30.3 µM) in NaCl/P_i buffer for 2 h at 4 °C with gentle shaking. The mixture was then poured into a glass column (1.2 cm × 8 cm). The column was washed with 10 bed volumes of NaCl/P_i, then eluted with five bed volumes of 50 mM Tris/HCl (pH 8.0) containing 15 mM reduced glutathione (Sigma). The eluates were analyzed using SDS/PAGE and were visualized by staining with Coomassie blue.

Hn-33 binding to Syt analyzed by pull-down assays

A pull-down assay was designed according to the procedure described previously [27,28] to confirm the binding of Hn-33 to synaptotagmin while using BoNT/A as a positive control. GST-Syt II was immobilized on glutathione-Sepharose beads (200 µL). The beads were then mixed with Hn-33 (18.0 µM) or BoNT/A (5.3 µM) in the absence (–) or presence (+ 12.5 µM) of ganglioside (GT1b) in 200 µL NaCl/P_i (pH 7.4) for 1 h at 4 °C. Subsequently, beads were washed four times with NaCl/P_i, until the absorbance at 280 nm was zero. Bound proteins were solubilized by boiling in SDS sample buffer and analyzed by SDS/PAGE and Coomassie blue staining.

Concentration-dependent binding of Syt II to Hn-33 analyzed by ELISA

ELISA was performed according to the procedure described previously [41]. Briefly, 60 µL of 3.03 µM Hn-33 in coupling buffer (0.1 M bicarbonate, pH 8.3) and a control protein, GST (60 µL of 4.0 µM), were coated onto the wells of a polystyrene flat-bottomed 96-well microtiter plate (Corning Glass Works, Corning, NY, USA) and incubated at 4 °C overnight. After blocking the plate with 1% (w/v) bovine serum albumin (BSA; Sigma), 60 µL of the purified Syt II (1.1 µM) were added to the wells. Mouse anti-Syt IgG (StressGen Biotechnologies) and goat anti-mouse IgG alkaline phosphatase conjugate (Novagen, Madison, WI, USA) were used as primary and secondary antibodies. The absorbance was measured using a microplate reader (GMI, Inc., Albertville, Minnesota, USA) and SOFTMAX software (Molecular Devices, Menlo Park, CA, USA).

Similar experiments were carried out with GST alone, in place of GST-Syt II, to determine its nonspecific binding. Goat anti-GST IgG (Amersham Pharmacia Biotech) and rabbit anti-goat IgG alkaline phosphatase conjugate (Sigma) were used as the primary and secondary antibodies, respectively.

Binding of different concentrations of Syt II was performed in the ELISA format described above. Syt II at different concentrations of 0.1, 0.2, 0.4 and 0.6 µM in NaCl/P_i, pH 7.4 was added to the wells, which were coated with 3.03 µM Hn-33, 1.5 µM BSA or 4.0 µM GST as control proteins.

Immunofluorescence staining

Immunofluorescence staining was carried out on permeabilized synaptosomes using standard methods [42]. This experiment was performed at room temperature (25 °C), all antibodies were diluted in NaCl/P_i containing 3%

(w/v) BSA and all washes were five times with PBST. The isolated synaptosomes were fixed on glass slides for 30 min with 4% (w/v) paraformaldehyde in NaCl/P_i and permeabilized with 0.2% (v/v) Triton X-100 for 15 min. The slides were washed and incubated with 3% (w/v) BSA in NaCl/P_i for 30 min, followed by incubation with 3.03 μ M Hn-33 for 1 h. After washing, the slides were incubated with rabbit anti-(Hn-33) serum (BBTech) for 30 min, washed, and then incubated with sheep anti-rabbit IgG conjugated with FITC. The slides were washed and coverslips were mounted on them with a drop of Fluoromount-G (Southern Biotechnology Associates, Inc., Birmingham, AL, USA), according to the manufacturer's instructions. Fluorescence images were acquired with a Nikon Eclipse E600 MVI microscope equipped with a digital camera controlled by SPOT software (Diagnostic Instruments, Inc., Sterling Heights, MI, USA). One control experiment was carried out without incubating the synaptosomes with Hn-33, but incubating the synaptosomes directly with anti-rabbit IgG conjugated with FITC after blocking with 3% (w/v) BSA.

Hn-33 was labeled with FITC using the FluoroTag FITC Conjugation Kit (Sigma-Aldrich), and inhibition of binding to synaptosomes of FITC-labeled Hn-33 by unlabeled Hn-33 was carried out similar to the procedure described above. Briefly, after blocking of the synaptosomes fixed on the glass slides with 3% (w/v) BSA followed by incubation with 18.0 μ M Hn-33 for 30 min, the synaptosomes were then incubated with 18.0 μ M, 9.0 μ M and 4.5 μ M FITC-labeled Hn-33 for 1 h. The slides were washed five times, coverslips were mounted and fluorescence images were observed using fluorescence microscopy. The synaptosomes incubated separately with unlabeled Hn-33 and FITC-labeled Hn-33 were also carried out in parallel.

Estimation of protein on gels

For estimating protein bands using SDS/PAGE, the gels were scanned on a GEL LOGIC 100 Imager system (Kodak, Rochester, NY, USA), plotted and integrated for density using KODAK 1D v.3.6.1 software.

Determination of protein concentration

The concentration of proteins used in the experiments was determined spectrophotometrically by measuring A_{280} and A_{235} and using the formula: concentration of protein ($\text{mg}\cdot\text{mL}^{-1}$) = $(A_{235} - A_{280})/2.51$ [43].

Acknowledgements

This work was supported by a grant from the U.S. Army Medical Research and Materiel Command

under Contract No. DAMD17-02-C-001 and by the National Institutes of Health through New England Center of Excellence for Biodefense (AI057159-01).

References

- 1 Singh BR (2000) Intimate detail of the most poisonous poison. *Nat Struct Biol* **7**, 617–619.
- 2 Cherington M (2004) Botulism: update and review. *Semin Neurol* **24**, 155–163.
- 3 Arnon SS, Schechter R, Inglesby TV, Henderson DA, Bartlett JG, Ascher MS, Eitzen E, Fine AD, Hauer J, Layton M, et al. (2001) Botulinum toxin as a biological weapon: medical and public health management. *J Am Med Assoc* **285**, 1059–1070.
- 4 Montecucco C, Rossetto O & Schiavo G (2004) Presynaptic receptor arrays for clostridial neurotoxins. *Trends Microbiol* **12**, 442–446.
- 5 Nishiki T, Kamata Y, Nemoto Y, Omori A, Ito T, Takahashi M & Kozaki S (1994) Identification of protein receptor for *Clostridium botulinum* type B neurotoxin in rat brain synaptosomes. *J Biol Chem* **269**, 10498–10503.
- 6 Nishiki T, Tokuyama Y, Kamata Y, Nemoto Y, Yoshida A, Sato K, Sekiguchi M, Takahashi M & Kozaki S (1996) The high-affinity binding of *Clostridium botulinum* type B neurotoxin to synaptotagmin II associated with gangliosides GT1b/GD1a. *FEBS Lett* **378**, 253–257.
- 7 Li L & Singh BR (1998) Isolation of synaptotagmin as a receptor for type A and E botulinum neurotoxin and analysis of their comparative binding using a new microtiter plate assay. *J Nat Toxins* **7**, 215–226.
- 8 Lebeda FJ & Singh BR (1999) Membrane channel activity and translocation of tetanus and botulinum neurotoxins. *J Toxicol - Toxin Rev* **18**, 45–76.
- 9 Koriazova LK & Montal M (2003) Translocation of botulinum neurotoxin light chain protease through the heavy chain channel. *Nat Struct Biol* **10**, 13–18.
- 10 Marvaud JC, Gibert M, Inoue K, Fujinaga Y, Oguma K & Popoff MR (1998) botR/A is a positive regulator of botulinum neurotoxin and associated non-toxin protein genes in *Clostridium botulinum* A. *Mol Microbiol* **29**, 1009–1018.
- 11 Marvaud JC, Eisel U, Binz T, Niemann H & Popoff MR (1998) TetR is a positive regulator of the tetanus toxin gene in *Clostridium tetani* and is homologous to botR. *Infect Immun* **66**, 5698–5702.
- 12 Li B, Qian X, Sarkar HK & Singh BR (1998) Molecular characterization of type E *Clostridium botulinum* and comparison to other types of *Clostridium botulinum*. *Biochim Biophys Acta* **1395**, 21–27.
- 13 Dineen SS, Bradshaw M & Johnson EA (2003) Neurotoxin gene clusters in *Clostridium botulinum* type A strains: sequence comparison and evolutionary implications. *Curr Microbiol* **46**, 345–352.

- 14 Sakaguchi G (1983) *Clostridium botulinum* toxin. *Pharmac Ther* **19**, 165–194.
- 15 Sharma SK & Singh BR (1998) Hemagglutinin binding mediated protection of botulinum neurotoxin from proteolysis. *J Natural Toxins* **7**, 239–253.
- 16 Fujinaga Y, Inoue K, Watanabe S, Yokota K, Hirai Y, Nagamachi E & Oguma K (1997) The haemagglutinin of *Clostridium botulinum* type C progenitor toxin plays an essential role in binding of toxin to the epithelial cells of guinea pig small intestine, leading to the efficient absorption of the toxin. *Microbiology* **143**, 3841–3847.
- 17 Fujinaga Y (2004) Interactions of botulinum and cholera toxin with host intestinal epithelial cells. *Nippon Saikingu Zasshi* **59**, 395–401.
- 18 Fujinaga Y, Inoue K, Watarai S, Sakaguchi Y, Arimitsu H, Lee JC, Jin Y, Matsumura T, Kabumoto Y, Watanabe T, Ohyama T, et al. (2004) Molecular characterization of binding subcomponents of *Clostridium botulinum* type C progenitor toxin for intestinal epithelial cells and erythrocytes. *Microbiology* **150**, 1529–1538.
- 19 Cai S, Sarkar HK & Singh BR (1999) Enhancement of the endopeptidase activity of botulinum neurotoxin by its associated proteins and dithiothreitol. *Biochem* **38**, 6903–6910.
- 20 Sharma SK & Singh BR (2004) Enhancement of the endopeptidase activity of purified botulinum neurotoxins A and E by an isolated component of the native neurotoxin associated proteins. *Biochem* **43**, 4791–4798.
- 21 Chaddock JA, Purkiss JR, Alexander FC, Doward S, Fooks SJ, Friis LM, Hall YH, Kirby ER, Leeds N, Mouldsdale HJ, et al. (2004) Retargeted clostridial endopeptidases: inhibition of nociceptive neurotransmitter release in vitro, and antinociceptive activity in *in vivo* models of pain. *Mov Disord* **8**, S42–S47.
- 22 Fu F, Sharma SK & Singh BR (1998) A protease-resistant novel hemagglutinin purified from type A *Clostridium botulinum*. *J Protein Chem* **7**, 53–60.
- 23 Inoue K, Fujinaga Y, Honke K, Arimitsu H, Mahmut N, Sakaguchi Y, Ohyama T, Watanabe T, Inoue K & Oguma K (2001) *Clostridium botulinum* type A haemagglutinin-positive progenitor toxin (HAM-PTX) binds to oligosaccharides containing Galb1–4GlcNAc through one subcomponent of haemagglutinin (HA1). *Microbiology* **147**, 811–819.
- 24 Fujinaga Y, Inoue K, Nomura T, Sasakib J, Marvaud JC, Popoff MR, Kozakid S & Oguma K (2000) Identification and characterization of functional subunits of *Clostridium botulinum* type A progenitor toxin involved in binding to intestinal microvilli and erythrocytes. *FEBS Lett* **467**, 179–183.
- 25 Zhang L, Lin W, Li S & Aoki KR (2003) Complete DNA sequences of the botulinum neurotoxin complex of *Clostridium botulinum* type A-Hall (Allergan) strain. *Gene* **315**, 21–32.
- 26 Markey AC (2004) Dysport. *Dermatol Clin* **22**, 213–219.
- 27 Sharma SK, Ramzan MA & Singh BR (2003) Separation of the components of type A botulinum neurotoxin complex by electrophoresis. *Toxicon* **41**, 321–331.
- 28 Dong M, Richards DA, Goodnough MC, Tepp WH, Johnson EA & Chapman ER (2003) Synaptotagmins I and II mediate entry of botulinum neurotoxin B into cells. *J Cell Biol* **162**, 1293–1303.
- 29 Rummel A, Karnath T, Henke T, Bigalke H & Binz T (2004) Synaptotagmins I and II act as nerve cell receptors for botulinum neurotoxin G. *J Biol Chem* **279**, 30865–30870.
- 30 Singh BR, Choi JK, Kim IS & Song PS (1989) Binding of 124-kilodalton oat phytochrome to liposomes and chloroplasts. *Physiologia Plantarum* **76**, 319–325.
- 31 Chumachenko YV, Sytnik AI & Demchenko AP (1990) The interaction of rabbit aldolase with NADH. *Biochim Biophys Acta* **1038**, 274–276.
- 32 Brown SB (1980) Circular dichroism and optical rotation. In *An Introduction to Spectroscopy for Biochemists* (Brown SB, ed), pp. 148–234. Academic Press, London, New York.
- 33 Keller JE, Neale EA, Oyler G & Adler M (1999) Persistence of botulinum neurotoxin action in cultured spinal cord cells. *FEBS Lett* **456**, 137–142.
- 34 Foran PG, Mohammed N, Lisk GO, Nagwaney S, Lawrence GW, Johnson E, Smith L, Aoki KR & Dolly JO (2003) Evaluation of the therapeutic usefulness of botulinum neurotoxin B, C1, E, and F compared with the long lasting type A. Basis for distinct durations of inhibition of exocytosis in central neurons. *J Biol Chem* **278**, 1363–1371.
- 35 Meunier FA, Lisk G, Sesardic D & Dolly JO (2003) Dynamics of motor nerve terminal remodeling unveiled using SNARE-cleaving botulinum toxins: the extent and duration are dictated by the sites of SNAP-25 truncation. *Mol Cell Neurosci* **22**, 454–466.
- 36 Adler M, Keller JE, Sheridan RE & Deshpande SS (2001) Persistence of botulinum neurotoxin A demonstrated by sequential administration of serotypes A and E in rat EDL muscle. *Toxicon* **39**, 233–243.
- 37 Fernandez-Salas E, Ho H, Garay P, Steward LE & Aoki KR (2004) Is the light chain subcellular localization an important factor in botulinum toxin duration of action? *Mov Disord* **19** (Suppl. 8), S23–S34.
- 38 Fernandez-Salas E, Steward LE, Ho H, Garay PE, Sun SW, Gilmore MA, Ordas JV, Wang J, Francis J & Aoki KR (2004) Plasma membrane localization signals in the light chain of botulinum neurotoxin. *Proc Natl Acad Sci USA* **101**, 3208–3213.
- 39 DasGupta BR & Sathyamoorthy V (1984) Purification and amino acid composition of type A botulinum neurotoxin. *Toxicon* **22**, 415–424.
- 40 Fu F, Lomneth RB, Cai S & Singh BR (1998) Role of zinc in the structure and toxic activity of botulinum neurotoxin. *Biochemistry* **37**, 5267–5278.

- 41 Zhou Y & Singh BR (2004) Cloning, high-level expression, single-step purification, and binding activity of His₆-tagged recombinant type B botulinum neurotoxin heavy chain transmembrane and binding domain. *Protein Expression Purification* **34**, 8–16.
- 42 Rothberg KG, Heuser JE, Donzell WC, Ying YS, Glenney JR & Anderson RG (1992) Caveolin, a protein component of caveolae membrane coats. *Cell* **68**, 673–682.
- 43 Whitaker JR & Granum PE (1980) An absolute method for protein determination based on difference in absorbance at 235 and 280 nm. *Anal Biochem* **109**, 156–159.

Clostridium botulinum: the source of bioterror and beauty

Bal Ram Singh¹, Bilian Li¹, Shashi K. Sharma² and Tzoo-Wang Chang¹

¹Department of Chemistry and Biochemistry, and Botulinum Research Center, University of Massachusetts Dartmouth, 285 Old Westport Road, Dartmouth, MA 02747; ²Center for Food Safety Applied Nutrition, US Department of Food and Drug Administration, College Park, MD 20740

Botulinum neurotoxins (BoNTs) are a very unique group of proteins, with extreme biological activities as toxins, therapeutics, and cosmetics. There are only about a couple of hundred cases of botulism globally. However, because of the extreme toxicity of the agent (about 100 billion times more toxic than cyanide, based on mouse lethal dose), it is estimated to one of the most expensive food poisoning diseases (Todd, 1989).

Currently, there are seven serotypes of BoNTs (A-G) known to be produced by different strains of anaerobic bacteria, *Clostridium botulinum*. Although there is little immuno-cross-reactivity, and there are only less than 50% sequence homologies among various serotypes of BoNTs, their site of action, mode of action, and target of action is remarkably similar, if not identical. Each of the BoNTs binds to the presynaptic region of nerve membrane at nerve-muscle junctions, translocates whole or a part of the toxin inside the nerve cells, and blocks the release acetylcholine, resulting in a flaccid muscle paralysis (Li and Singh, 1999; Arnon et al., 2001; Singh, 2000; 2002)

Combination of extreme toxicity, nerve as the site of action, and resulting physiologically action of muscular paralysis has made botulinum neurotoxin a molecule of elevated anxiety and curiosity. It has been attempted as a bioterror agent, a fully developed biological weapon for military use, and also as a therapeutic agent against numerous neuromuscular disorders, such as strabismus, blepharospasm, and torticollis, involving excessive release of neurotransmitter. More curiously, therapeutic botulinum

neurotoxin preparations are being used for cosmetic purposes to remove frown lines and facial wrinkles.

Clostridium botulinum, therefore, has become a source of bioterror and beauty, both being pursued simultaneously for scientific development to counter the former while promoting the latter.

Clostridium botulinum

C. botulinum, which was first isolated from a contaminated ham and from the spleen of a patient by van Ermengem in Belgium in 1895 (Foster, 1993; van Ermengem, 1897), is a Gram positive, spore-forming bacterium which grows anaerobically at 37 °C or 30 °C under pH 6.5-7.0 conditions.

Most of *C. botulinum* as well as *C. butyricum* and *C. baratii* can produce botulinum neurotoxins (BoNTs). Strains of *C. botulinum* are classified into seven types, A to G, according to the antigenic properties of neurotoxins they produce. Generally, one strain of *C. botulinum* can only produce one type of neurotoxin, but several strains that produce more than one type of neurotoxin have been recognized over the years. One type C strain (C6813) was found to produce the mosaic neurotoxin, of which had one-third of the C-terminal region was similar to that of type D neurotoxin (Moriishi et al., 1996). One type A strain, called type AB now, was shown to produce both type A and type B neurotoxins (Fujinaga et al., 1995). *C. botulinum* type G, the organism differs phenotypically from other *C. botulinum* types, is now designated as *C. argentinense* (Campbell et al., 1993a). *Clostridium butyricum* and *Clostridium baratii* were found producing type E and type F neurotoxins, respectively (Fujii et al., 1993c, Thompson et al., 1993).

Strains of *C. botulinum* can also be divided into four distinct phenotypic groups (I to IV) based on biochemical properties and nucleic acid hybridization studies. Group I includes type A, proteolytic strains of types B and F. Group II includes type E, non-proteolytic strains of types B and F. Group III is types C and D and Group IV is type G (Campbell et al., 1993b). Rinner, Stackebrandt (1994) and Campbell et al. (1993b) proved from a very high level of 23S rRNA sequence similarity that Groups I, II, III and IV *C. botulinum* represent a single genetic unit phylogenetically remote from each other and that the marked genotypic variation within the species does not correlate with the neurotoxins produced. *C. baratii* belonged to a new group, group V. The Same conclusions were drawn from 16S rRNA sequence similarities (Hutson et al., 1993). However, the genetic relationship inferred from the BoNT sequences differs markedly from above conclusions and there is clearly established now that all three types of BoNT/F (proteolytic, non-proteolytic and *C. baratii* type F) are genealogically highly related (Elmore et al., 1995).

The spores of proteolytic *C. botulinum* are heat resistant and do not multiply at temperatures below 10 °C, but the spores of non-proteolytic *C. botulinum*, which are less heat resistant, can germinate relatively rapidly at temperatures in the range of 2 to 10 °C (Lund and Peck., 1994). Type A *C. botulinum* has 0.39 hour generation time and reaches its exponential growth after 5 hours of anaerobic incubation of spores (Call et al., 1995).

The bacterial growth curve of type A *C. botulinum* (strain Hall) shows a lag period of 4 hours, and log phase at 10 hours before reaching the stationary phase (Shukla and Singh, 2000).

The studies with a monoclonal antitoxin conjugated with colloidal gold demonstrated that the BoNT was synthesized in the cell cytoplasm at late-exponential phase (17 hours) and reached its maximum concentration at stationary phase (24-25 hours). The BoNT was translocated across the cytoplasmic membrane and then exported to the extracellular medium via cell wall exfoliation. The greatest proportion of BoNT was located within the cell wall at 45 hours (Call et al., 1995).

The spores of *C. botulinum* are widely distributed in soil, mud and surface waters over much of the globe, but different types of *C. botulinum* prevail in different geographical locations. In the western United States, Brazil, Argentina and China, type A spores predominate, while proteolytic type B spores tend to predominate in soils of the eastern United States, and non-proteolytic type B in Britain and Europe. Type E is often associated with freshwater and marine sediments, and northern regions such as northern Canada and Japan (McClure et al., 1994). Initially, the strains of *C. botulinum* type A were divided into two groups, infant type A and type A, based on the cases of infant botulism in Japan and the classical food-borne botulism (Sakaguchi et al., 1990). But studies of Cordoba et al. (1994) revealed that the strains of *C. botulinum* type A could be divided into two groups, A1 and A2, based on different geographical locations isolated and did not correlate with their origins as both from the cases of infant botulism and from classical food-borne botulism. Strains isolated from infant botulism in Japan and several

strains isolated from classical food-borne botulism in United Kingdom and in Mauritius fell into group A2 while all strains examined from the USA and two strains from UK, from both infant and food-borne botulism fell into group A1. Group A1 is typical *C. botulinum* type A containing hemagglutinin genes and shows hemagglutinin activity. Several group A1 strains contain an unexpressed type B neurotoxin gene. Group A2 lack the hemagglutinin gene and possess no hemagglutinin activity. The type A neurotoxin genes from group A1 and A2 are different. Recently, a third isotype of type A botulinum neurotoxin (A3) has been identified, which differs significantly with types A1 and A2 in its amino acid sequence (Marks, 2004).

Botulism

Historically, botulism – derived from botulinus meaning sausage, was discovered long before the name appeared in the literature. Earliest reference to possible botulism related disease is found in an edict by Emperor Leo VI of Byzantium (886-911) in which manufacturing of blood sausages was forbidden (Erbguth, 2004). However, the first systematic study of ‘sausage poisoning’ was carried out in 1815 by a health officer in the town of Herrenberg of Wurttemberg (Germany) by the name of J. G. Steinbuch, and later independently by Justinus Kerner, another medical officer in the town of Welzheim in Wurtemberg (Erbguth, 2004). Kerner’s work was published in journals and monographs in early 1800s. In 1822, Kerner described his observations and experiments with sausage toxin, also referred as fat poison, in a monograph. Kerner wrote “The nerve conduction is brought by the toxin into a condition in which its influence on the chemical process of life is interrupted. The capacity of nerve conduction is interrupted by the toxin in the same way as in an

electrical conductor by rust". Interestingly, Kerner had also hypothesized on the idea of sausage toxin being used as a therapeutic agent (Erbguth, 1998).

Botulism is a severe disease characterized by flaccid paralysis and caused by botulism neurotoxins, extremely potent food poisons with a mouse lethal dose of 0.1ng/kg (Montecucco and Schiavo, 1993). Three types of botulism have been observed, so far. Classical food borne botulism is caused by ingestion of food where the bacteria have produced the neurotoxin. Infant botulism result due to the production of neurotoxin in the intestine after germination and outgrowth of ingested spores. Wound botulism maybe due to the outgrowth of bacteria in the wound or due to unknown origin (Hatheway and Ferreira, 1996; Cordoba et al, 1994). Classical food borne botulism in humans is caused mainly by *C. botulinum* types A, B, E and rarely by type F neurotoxins. Classical food borne botulism in animals is always caused by *C. botulinum* types C1 and D neurotoxins (Cordoba et al., 1994, Fach et al., 1993). In contrast, the causative agents for infant botulism can be *C. botulinum* types A or B neurotoxins or *Clostridium butyricum* type E and *Clostridium baratii* type F neurotoxins. The wound botulism is rare in humans and the causative agents are either type A or type B from group I (Hatheway, 1993), but is increasingly significantly in recent years among drug users (Merrison et al., 2002). Neurotoxins can also be used in the therapy of a variety of human muscle disorders such as strabismus, hemifacial spasm and blepharospasm (Schantz and Johnson, 1992; Eleopra et al., 2004).

Various animal models are used to examine mechanism of botulism in animals and humans. Different serotypes of BoNT are known to selectively cause the disease in

different animals. For example, BoNT/C is mostly associated with avian botulism, BoNT/C and BoNT/D with cattle, sheep and horse, and BoNT/A, BoNT/B and BoNT/E are associated with human, cattle and horse botulism, while BoNT/E is particularly associated with fish botulism (Huss and Eskildsen, 1974; Burns and Williams, 1975; Ala-Huikko et al., 1977; Fernandez et al., 1989; Baldassi et al., 1991; Haagsma, 1991; Jeffrey et al., 1994; Ashie et al., 1996; Ortolani et al., 1997). It is believed that botulism by a selective serotype of BoNT in a given animal is in part related to the presence of a high affinity receptor for that serotype in the host animal system (Fig. 1).

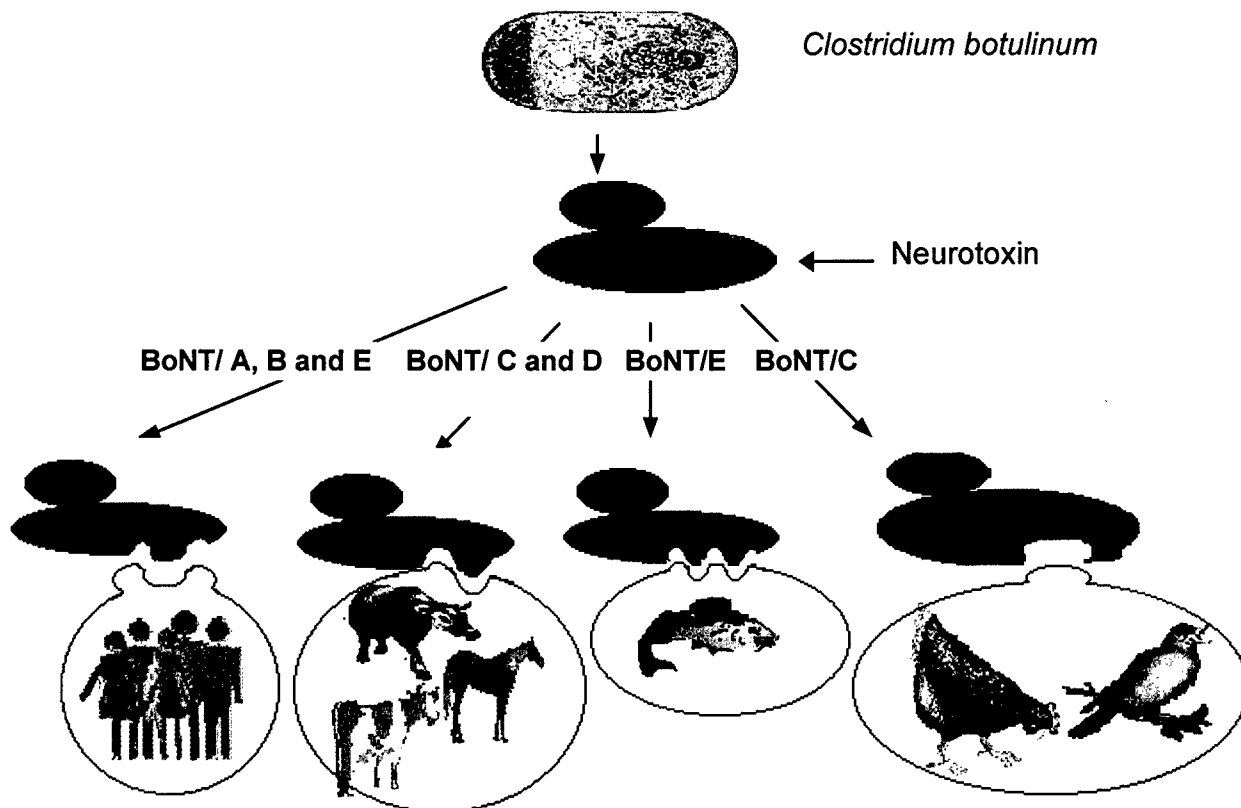


Fig. 1. Schematic representation of different binding topography of various serotypes of BoNT for their interactions with unique protein receptors in different animals.

Botulinum neurotoxins

Botulism neurotoxins are large proteins (150 kDa, 7S). They remain inactive as a single chain after synthesis and are activated by protease nicking to form a dichain molecule (a 50 kDa light chain and a 100 kDa heavy chain) linked together by a disulfide bond. The proteolytic strains of *C. botulinum* produce endogenous proteases, but non-proteolytic strains of *C. botulinum* require exogenous proteases, such as trypsin in the intestinal tract (Call et al, 1995). The light chain or heavy chain individually are nontoxic and play different roles in the pathway of intoxication. The light chains of neurotoxins are in fact zinc endopeptidases, which catalyze the hydrolysis of synaptic vesicle docking and fusion complex and block the release of acetylcholine (Ahnert-hilger and Bigalke, 1995). The heavy chains may fold into a conformation that protects the neurotoxins against the proteolytic cleavage (Schantz and Johnson, 1992). The C-terminal part of heavy chains (H_C) is responsible for cell surface binding and the N-terminal part of heavy chains (H_N) is involved in channel formation. The H_C domain is also divided (Fig. 2) into two structural, and possibly functional domains (H_{C1} and H_{C2}) with their specific binding to protein and lipid receptors.

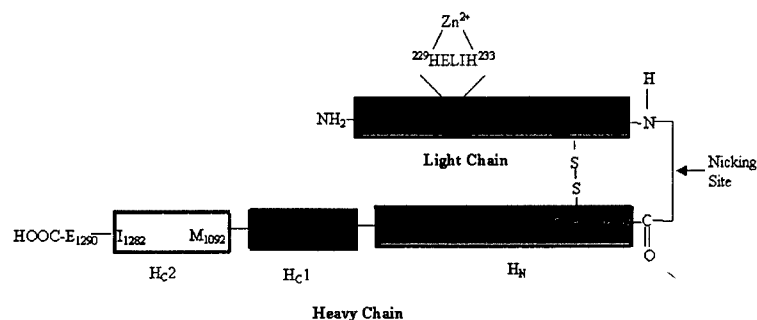


Figure 2: . Schematic diagram of BoNT showing its L and H chains. The two different domains of the H chain shaded with different patterns indicate the N-terminal and C-terminal halves (about 50 kDa each).

The botulinum neurotoxin is produced in three progenitor toxin forms: M, L and LL forms. The M form consists of neurotoxin (150 kDa) and a nontoxic protein component (120 kDa) which is called neurotoxin binding protein (NBP) (Singh et al., 1995) or nontoxic nonhemagglutinin component (NTNH) (East and Collins, 1994) with 12S molecular size (the molecular size of complex forms is expressed as sedimentation equilibrium values). The L form has molecular weight of about 500 kDa and a molecular size of 16S. The LL form is about 900 kDa and 19S. The L and LL complexes consist of several hemagglutinin components besides the BoNT and NBP, and exhibit hemagglutinin activity (Fujii, 1995; Somers and DasGupta, 1991). In 1998, Singh research group named the proteins other than the neurotoxin present in botulinum neurotoxin complex as neurotoxin associated proteins or NAPs (Fu et al., 1998). BoNT/A complex can exist in three forms: M, L or LL. BoNT/B, /C and /D complexes involve in two forms: L and M. BoNT/E and /F complexes are known to exist only in M form, and BoNT/G complex exists only in L form (Fujita et al., 1995). Some of types A and B neurotoxins which cause the infant botulism, also exist in M form (Cordoba et al., 1994).

The size of the complex formed in BoNT/A and BoNT/B depends on the medium for bacterial growth. The addition of iron or manganese to the growth medium results in a higher concentration of M and L forms of neurotoxin complexes (Schantz and Johnson, 1992). In addition, some

foods such as vegetables have high botulinogenic properties. *C. Botulinum* types A and B are found to produce the stable L and LL forms of neurotoxin complexes in vegetables, whereas they produce the less stable M complex in tuna and pork (Schantz and Johnson, 1992).

The nontoxic components of progenitor neurotoxin (NAPs) appear to play a critical role in the toxico-infection by neurotoxin. They are presumed to protect neurotoxins against the digestive proteases and stomach acidity when the progenitor neurotoxins pass through the gastrointestinal tract (Ahnert-Hilger and Bigalke, 1995; Schantz and Johnson, 1992; Somer and DasGupta, 1991). Such protection is important in the food poisoning activity of the neurotoxin. For example, if NAPs are removed, the oral toxicity of the purified type A neurotoxin goes down by 43,000 fold (Singh et al., 1995). Tetanus neurotoxin (TeNT) which was produced by anaerobic *Clostridium tetani* is not a food poison and is in fact inactive by the oral route because of the absence of NAPs (Singh et al., 1995). The oral toxicity increases with incremental association of the neurotoxins with the protective proteins. In BoNT/A and BoNT/B, the larger forms of progenitor neurotoxins (19S and 16S) are more toxic by the oral route and more resistant to acid and pepsin than the smaller form (12S) of progenitor neurotoxins (Schantz and Johnson, 1992; Fu et al., 1998; Sharma and Singh, 1998; Sharma et al., 1999). The progenitor neurotoxins believed to dissociate into the neurotoxins and NAPs in the small intestine or in an alkaline condition and the components of NAPs might also play a

role in the adhesion of progenitor neurotoxins to the intestinal tissue before the dissociation of the progenitor neurotoxins (Sakaguchi, 1983; Fujinaga et al., 1994; 1997; 2000). Certain carbohydrate groups which help the NAPs to anchor to the intestinal wall have been identified (Inoue et al., 2001; Nishikawa et al., 2004).

The neurotoxins and nontoxic components can reassociate spontaneously when the pH is lowered (Hambleton, 1992). An ordered interaction between neurotoxins and their NAPs was suggested by the observation that the L and LL forms of type A neurotoxin form crystals (Schantz and Johnson, 1992).

***C. botulinum* genomic organization**

C. botulinum (Type A, strain Hall A, ATCC 3502) genomes have an average GC content of about 28.2% (Sanger web, 2003), which is lower than that of other bacteria (Hatheway, 1993). Most *C. botulinum* strains and related nontoxigenic species were believed to carry plasmids. Type A *C. botulinum* (strain Hall A, ATCC3502) contains a 16,344 bp plasmid (Sanger web, 2003) and *C. tetani* (strain E88) contains a very large plasmid in the size of 74,082 bp (Holger et al., 2003). All of the proteolytic type F strains tested by Strom et al. (1984) contain a single 11.5 Mdal (17.48Kb, 1Kb of dsDNA = 660KDa) (Brinkmann web, 2004) plasmid, but only some of the nonproteolytic type F strains harbor a single 2.2 Mdal plasmid. Codon usage in the botulinum gene was similar to that for the tetanus toxin gene, but it is different from that for *E. coli* genes (Makeoff et al., 1989). 90.3% of the degenerated codons from botulinum and tetanus toxin genes end in A or U and AUG and UAA are translational initiation

and termination codons (Schantz and Johnson, 1992). A number of codons from neurotoxin genes are rarely used in *E. coli* genes. This is an important factor that will lead to a poor expression of neurotoxin gene in *E. coli* (Clayton et al., 1995).

The genomic organizations of BoNTs and their associated proteins were suggested by researchers (Hauser et al. 1994; East et al. 1994; Fujita et al. 1995), which are summarized in Figure 3. No characteristic signal peptide sequences are observed in any of the progenitor neurotoxin genes. The genes of progenitor neurotoxins are closely grouped as operons on the chromosome, phage or plasmid. NBP gene is located only 26 bp (type A, strain 667Ab or NCTC2916 or CDC3281) (Santos-Buelga et al., 1998; Hutson et al., 1996; Rodriguez et al., 1998) or 44bp (type A, strain ATCC 3502) (Sanger, 2003) or 15 bp (type C, strain C-6814 or C-Yoichi) (Sagane et al., 2000; 2001) or 15 bp (type D, strain D-4947) (Kouguchi et al., 2002) or 11 bp (type F, Langeland) (East et al., 1998) or 12 bp (type F, strain F202) (East et al., 1994) or 14 bp (type F, *C. baratii*, strain ATCC 43256) (East et al., 1998) or 85 bp (type G, strain ATCC 27322) (Bhandari et al., 1997) upstream of the BoNT gene. There are two promoter regions for neurotoxin genes. One overlaps the C-terminal end of NBP genes and the other is shared with the NBP genes, controlling co-transcription of the two genes. The neurotoxin genes are either transcribed alone or along with NBP genes via a polycistronic mRNA, and thus these two genes form an operon. HA gene clusters form another operon transcribed in the opposite directions from the BoNT and NBP genes. HA gene clusters are located 262 bp (in type C, strain C-6814 or C-Yoichi) (Sagane et al., 2000; 2001) or 261 bp (type D, strain D-4947) (Kouguchi et al., 2002) or 925 bp (in type A, strain Hall A-hyper) (Dineen et al., 2003) or 698 bp (type A, ATCC 3502) or 811 bp (type

A(B), NCTC 2916)(Rodriguez et al., 1998) upstream of the NBP gene, respectively. Each HA gene contains its own transcription terminator which is predicted to form a stem-and loop structure in the mRNA.

***C. botulinum* neurotoxin genes**

The genes of all seven types of neurotoxins have been sequenced and the polypeptide chain lengths deduced from the nucleotide sequences are approximately the same, ranging from 1251 (BoNT/E, strain Beluga) to 1315 (TeNT, strain E88 Massachusetts) amino acid residues (Elmore et al., 1995; Hutson et al., 1994; Campbell et al, 1993a; Thompson et al., 1990, 1993; East et al., 1992; Whelan et al., 1992; Binz et al, 1990a, 1990b; Fujii et al., 1990). However, the gene localization of different serotypes of BoNT is different. BoNT/A, B and E genes are located in chromosome, BoNT/C1, D in phage and BoNT/G and BuNT/E in plasmids (Hauser et al., 1995; Ahnert-Hilger and Bigalke, 1995). The neurotoxin gene (*tetX*) and its transcription factor (*tetR*) are also clusterly located in the 74kb plasmid in *C.tetani* (Holger et al., 2003) . Whether the BoNT/F genes are located in chromosome or in plasmid is not clear yet (Hauser et al., 1995, Strom et al., 1984). The homology among all types of BoNT genes ranges from 55.2% to 98.2% and is listed in Table 1. The homology of tetanus gene to other BoNT genes ranges from 55.3% to 62.1%, which is lower than that among BoNT genes. In table 1, BoNT/NpB is non-proteolytic type B neurotoxin, BuNT/E is neurotoxin produced by *C. butyricum* type E and BaNT/F is neurotoxin produced by *C. baratii*.

Table 1. Comparison of clostridial neurotoxins showing percent identity (lower left) and percent similarity (upper right) (from Hauser et al., 1995).

	TeTx	BoNT A	BoNT B	BoNT NpB	BoNT C1	BoNT D	BoNT E	BuNT E	BoNT F	BaNT F	BoNT G
TeTx		55.3	61.8	62.1	56.2	55.3	57.8	58.0	59.0	57.9	60.8
BoNT/A	35.4		60.0	60.2	55.2	55.2	61.0	60.5	61.8	63.2	58.8
BoNT/B	42.4	44.1		96.0	59.1	57.3	61.6	61.3	61.7	62.5	74.9
BoNT/NpB	42.7	40.7	92.8		58.4	56.6	61.9	61.3	61.8	62.8	74.2
BoNT/C1	35.1	33.9	36.0	35.0		69.1	55.9	56.0	56.3	56.4	57.4
BoNT/D	34.1	34.3	36.6	36.4	53.8		57.1	57.1	57.1	56.8	57.6
BoNT/E	37.9	41.3	40.0	40.2	34.3	35.6		98.2	77.3	77.2	60.0
BuNT/E	37.9	41.5	40.0	40.1	34.8	35.4	96.9		77.1	76.8	60.0
BoNT/F	38.5	41.4	41.0	41.7	34.6	36.4	62.2	62.1		80.7	58.6
BaNT/F	40.5	44.1	42.8	43.3	35.1	35.5	63.9	63.6	70.5		59.5
BoNT/G	41.6	41.2	58.4	57.7	35.0	37.1	39.5	40.6	39.3	40.7	

Several strains of *Clostridium botulinum* or *Clostridium butyrium* do not possess BoNT genes (non-toxic *Clostridium* strains) (Zhou et al., 1993). The following evidences from the studies of BoNT and TeTx genes suggest that BoNT and TeTx genes derive from a common ancestor and that the variation of BoNT genes probably result from BoNT gene transfer among *Clostridium* species and subsequent DNA evolution (Elmore et al., 1995; Hauser et al., 1995). The non-toxic *Clostridium* strains may have evolved after loss of the neurotoxin genes (Rinner and Stackebrandt, 1994).

- The G+C content of BoNT (26.31%) and TeTx genes (27.83%) is similar, as is that of *C. botulinum* genomes (28.2%) (Fairweather et al., 1986 ;Holger et al., 2003; Willis, 1990).

- The percent identity among BoNTs and TeNT at the amino acid level range from 34.1 to 96.9% (Table 1) and are unrelated to other known protein sequences.
- The BoNT genes could localize at chromosome, phage or plasmids.
- BoNT/E and BuNT/E are produced by two very different *Clostridium* strains, *C. botulinum* and *C. butyricum*, respectively yet they share 97% identity at the amino acid level, which is much higher than the average identity between different BoNT genes produced by *C. botulinum* (43%). The similar high identity (90%) is observed between BoNT/Bp (proteolytic type B) and BoNT/Bnp (non-proteolytic type B). The identity between BoNT/F and BaNT/F (produced by *C. baratii*) is also high (70.5%) (Table 1).
- Nucleic acid sequences of BoNT/A genes from *C. botulinum* type A strains 62 A and NCTC2916 are identical but there are totally unrelated after the 97 nucleotides downstream from the 3' nucleotide regions of the BoNT/A genes (Binz et al., 1990a; Thompson et al., 1990).
- The neurotoxin genes of *C. botulinum* type C strains could be transformed into *C. novyei* type A strains with appropriate vectors (Rinner and Stackebrandt, 1994). Evidences show (Zhou et al., 1993) that the neurotoxin genes can be transferred from *Clostridium butyricum* to a nontoxic *Clostridium botulinum* type E-like strains with a helper strain (nontoxic *C. butyricum*).
- The fact that some *C. botulinum* strains contain more than one type of neurotoxin genes (A(B), A(F), or BF) supports the gene transfer hypothesis and suggest that an additional genetic events (mutation, deletion, recombination, etc) have occurred. This hypothesis is also

proved by the results (Hutson et al, 1996) that some of type A strains contain silent type B gene. The type B neurotoxin gene is unexpressed because the deletion and substitution of some nucleotides result in multiple stop signals due to the reading frame shift.

- The gene transfers among *Clostridium* strains probably involve a mobile DNA element on the chromosome or the mobilization of a large plasmid harboring the BoNT gene (Hauser et al., 1995).

***C. botulinum* neurotoxin binding protein (NBP) genes**

The nucleic acid sequences of *C. botulinum* types A, B, C1, D, E, F and *C. butyricum* type E NBP genes have been determined (Hutson et al., 1996; Fujita et al., 1995; Hauser et al., 1994; East and Collins, 1994b; Fujii et al., 1993a, 1993b, 1993c). All of the NBP genes are approximately 3.5kb in length, similar the BoNT genes. Several experimental results demonstrate that the expression of NBP genes are very important to the BoNTs. First, each NBP gene is located at the N-terminal of BoNT gene with very little space between them (46bp in type A, 14bp in type C, 27bp in type E from both *C. botulinum* and *C. butyricum*, 14bp in type F). Second, the transcription of the NBP gene is always in association with the BoNT gene, and only the BoNT gene, not the NBP gene can be transcribed alone. Third, all types of *C. botulinum* contain a NBP gene.

The homology of NBPs is higher than that of BoNT genes (Table 2), which suggested that the NBP genes are more conserved than the BoNT gene. The close identities between NBP/E and NBP/EBu (98%) (Fujii et al., 1993C), and between BoNT/E and BuNT/E (97%) are the strong evidence that the NBP and BoNT genes transfer among the genus *Clostridium*. It is very surprising that the identity of the BoNT/C and

BoNT/D genes (53.8%) is much lower than that of the corresponding NBP genes (93.0%). However, this result corresponds to the fact that both types C and D are responsible for animal botulism, but cleave the different substrates, Hpc-1/syntaxin and VAMP/synaptobrevin, respectively.

Table 2. Percent amino acid identities (lower left-hand triangle) and similarities (upper right-hand triangle) of NBP.

	A	B	C	D	E	F	G
A		90.5	83.0	83.0	79.0	81.5	86.0
B	81.5		81.5	81.5	76.0	78.0	87.0
C	65.4	66.5		95.0	73.0	75.5	82.0
D	65.4	66.5	93.0		72.0	73.5	80.0
E	65.8	59.0	54.0	53.0		77.0	69.0
F	74.0	61.5	56.5	55.5	65.0		73.0
G	72.0	75.0	65.0	64.0	54.0	58.0	

There is a short (14 residues) repeat in the amino acid sequence of the NBPs which could show as L-L/N-S-L-I/M/V-S/T-T/S-A/T-I-P-F-P/L-Y/F-G from 97 to 111 and from 136 to 150. The second repeat may play an important role in distinguishing the M complex from other types of progenitor neurotoxins as evidences from the following observation. First, the amino acid residues from 99 to 149, which include the second repeat from 136-150, was deleted in NBPs from M complex (NBP/E, NBP/F and NBP/EBu). Second, NBPs from M forms of A, C and D progenitor neurotoxins were cleaved in the second repeat region to yield approximately 13 kDa and 106 kDa components (Fujita et al., 1995).

NBP have also sequence homology to both BoNT (all types) and TeNT in light chain area. This area is also the conserved domain named peptidase_M27 area. NBP has

not been found any peptidase activity yet but did contain the protein sequence similarity with a known Zn dependent peptidase.

***C. botulinum* hemagglutinin genes**

The hemagglutinin genes HA33, HA17 and HA70 from type C *C. botulinum* were sequenced by Hauser et al. (1994). The three genes, which are closely linked and form an operon, are transcribed alone or together in the opposite direction to that of NBP and BoNT genes. The HA17 gene encoding 146 amino acids is located between the HA33 and HA70 genes. Homology among the HA33 genes is shown in Table 3.

Table 3. Percent amino acid identities (lower left-hand triangle) and similarities (upper right-hand triangle) of HA 33

	HA33/A	HA33/Bnp	HA33/Bp	HA33/C	HA33/D
HA33/A		93.0	88.5	58.0	58.0
HA33/Bnp*	89.0		89.0	58.0	58.0
HA33/Bp**	83.5	82.0		58.0	57.0
HA33/C	38.5	41.0	39.0		78.0
HA33/D	38.5	40.0	35.0	65.0	

* Bnp: non-proteolytic type B neurotoxin

** Bp: proteolytic type B neurotoxin

The high homology between HA/A and HA/B and low homology between HA/A, HA/B, HA/C and HA/D may reflect similarity in specificity and activity of type A and type B, both of which cause human botulism (East et al., 1994a).

The HA70 is cleaved to a predicted 22 kDa protein and a 48 kDa protein after translation, which correspond to the HA20-23 and HA53-57 bands from type A and C on SDS-PAGE (Fujita et al., 1995; Tsuzuki et al., 1992). Homology among the HA70 genes is shown in Table 4.

The HA70/C has been found to share 27.6% identity and 46.4% similarity with the 259 N-terminal amino acids of *C. perfringens* type A enterotoxin, a protein which binds to a cell membrane receptor and leads to change in plasma membrane permeability. Moreover, a tripeptide cell attachment sequence (Arg-Gly-Asp) was found at amino acid 30-32 of HA22. These data suggest that HA70 might play a role in adhesion of the progenitor neurotoxins to the intestinal tissue before the progenitor toxins dissociate into neurotoxins and nontoxic components in the small intestine (Fujinaga et al., 1994).

Table 4. Percent amino acid identities (lower left-hand triangle) and similarities (upper right-hand triangle) of HA70.

	A	B	C	D	G
A		98.5	82.5	82.5	83.0
B	96.0		85.5	85.0	84.0
C	68.5	71.5		95.5	76.0
D	68.5	71.0	93.5		77.0
G	72.0	73.0	65.0	65.0	

The HA33 and HA53/C have been shown to exhibit hemagglutinin activity, but the HA17, HA57/A and HA57/B purified from SDS-PAGE did not show any hemagglutinin activity (Somers and DasGupta, 1991).

These protein may only exhibit an hemagglutinin activity when associated with other hemagglutinin components.

Sequence analysis results show that *Clostridium tetani* E88 genome does not contain any one of *C. botulinum* NAPs nucleotide and protein sequences. Therefore, the genetic evidence at the molecular level suggests that *Clostridium tetani* (Massachusetts E88) genotypically lack NAPs genes, and thus phenotypically lack the protection from NAP-like proteins. This result greatly supports the hypothesis that NAPs might transform the neurotoxin to be food poison and explains the reason why botulinum is food poison but tetanus is not, as suggested by Singh et al. previously (Singh et al., 1995).

The putative regulation gene, orf 22.

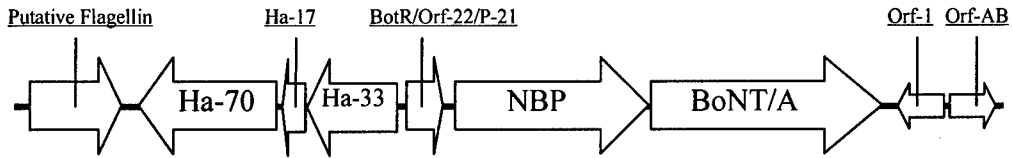
The orf 22 gene encoding 178 amino acids with a calculated Mr of 21.7 kDa, located at downstream of the HA genes in type C and upstream of the HA genes in types A and B, has the same transcriptional direction as that of the NBP and BoNT genes. Although referred with different names (orf 22/ BotR/ P-21) in different types of botulinum serotypes, amino acid sequence homology among different type of orf22 genes as shown in Table 5 ranges between 58 and 97.5%. The amino acid sequences of type A and type C orf22 show 52.0% identity in contrast to 98%, 91%, 90% identity between orf22 of type A and proteolytic type B (Bp), type A and non-proteolytic type B (Bnp), proteolytic and non-proteolytic type B, respectively (East et al, 1994a; Hauser et al, 1994). The orf22 product is postulated to regulate the expression of genes for HA, NBP, and BoNT because it displays the characteristics of DNA binding proteins in terms of basic pI (10.4), and helix-turn-helix motifs (Hauser et al., 1994). Moreover, it shows a 29% identity with the *uviA* gene product, a *C. perfringens* regulatory protein (Hauser et al., 1995, East et al., 1994a).

Table 5. Percent amino acid identities (lower left-hand triangle) and similarities (upper right-hand triangle) of Orf22.

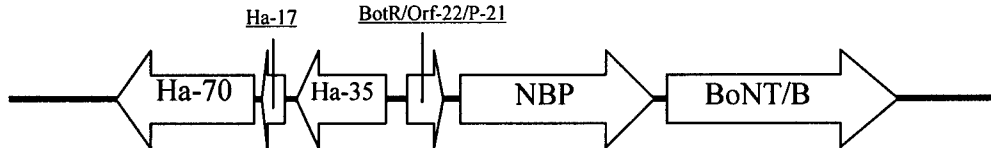
	A	B	C	D	F	G	TetR
A		97.5	72.5	72.0	78.5	83.0	84.5
B	95.5		66.5	66.0	71.0	78.0	79.5
C	52.0	48.0		89.0	58.0	60.0	65.0
D	52.0	48.0	86.0		66.0	68.0	71.0
F	60.5	55.0	45.0	53.0		83.0	81.5
G	59.0	54.0	42.0	44.0	60.0		83.5
TetR	66.5	61.5	48.0	52.0	66.5	65.0	

Fig.3.

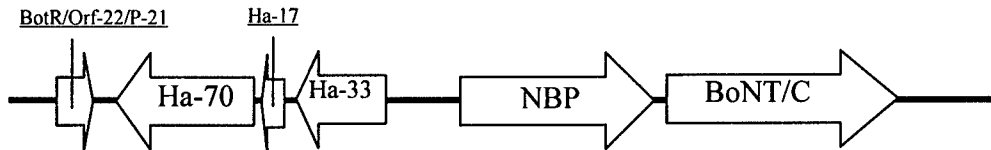
Type A (Strain: Allergan-Hall A, 62A, Hall-A hyper) BoNT Complex



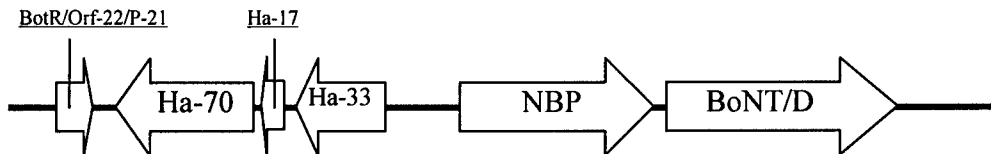
Type B (Strain: Lamannan Korea) BoNT Complex



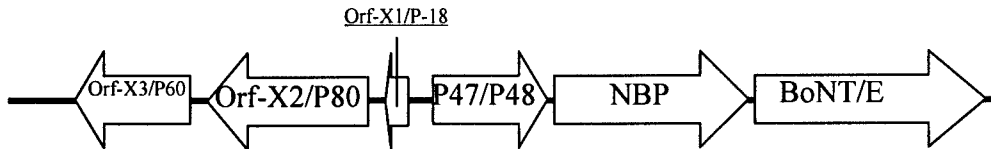
Type C (Strain: C-6814, C-Yoichi) BoNT Complex



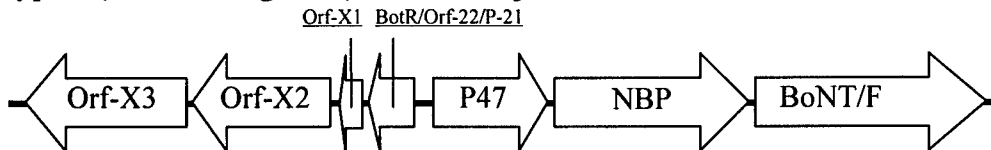
Type D (Strain: D-4947) BoNT Complex



Type E (Strain: Iwanai, Alaska) BoNT Complex



Type F (Strain: Langeland) BoNT Complex



Type G (Strain: ATCC27322) BoNT Complex

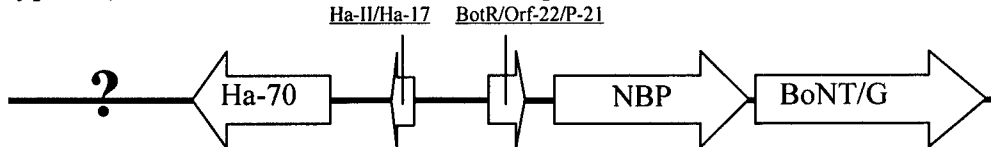


Figure 3. Genomic organization of all 7 types of *C.botulinum*. Proteins corresponding to genes labeled as ORF (types E, F and G) are yet to be identified, although tentative assignment has been made for type E genes. The question mark (?) in type G *C. botulinum* reflect unavailability of the sequence data.

Our BLAST sequence analyses results also showed the botulinum type A, B, C and D are more similar not only because of their NAPs gene loci pattern but also they share more and higher sequence homology with each others. However, the type E and F have different NAPs proteins and interestingly is there is no BotR, which is a transcription regulator, to be found inside the currently discovered gene loci of botulinum type E.

Sequence analyses also suggest that except for Ha-33, most of the NAPs proteins are unique and generally have protein sequence similarity with prokaryotic organism only.

Mode of Action

The mode of action of the BoNT is not well understood at the molecular level. Based on some experimental evidence and analogies with other dichain toxins such as diphtheria, cholera and *Pseudomonas* exotoxin A, a working model involving three steps (Fig. 4) has been proposed (Simpson, (ed.), 1981, 1986, 1989; Singh, 1996).

(i) **Extracellular step** involves binding of the neurotoxin to presynaptic membranes through the C-terminal half of the H chain. The C-terminal half of the H chain has been suggested to bind to gangliosides on the presynaptic membrane (Simpson, (ed.), 1981, 1986). According to a 'double receptor' model (Montecucco, 1986), the C-terminal domain of the neurotoxin binds first with the ganglioside that alters its protein structure and makes it compatible for binding with a protein receptor. Structural changes in botulinum and tetanus neurotoxins upon binding with gangliosides (or detergent) were

experimentally observed (Montecucco, 1986; Lazarovici et al., 1987; Singh et al., 1991). These changes could also be involved in exposing transmembrane and surface-seeking peptide domains. Recently, several reports have appeared suggesting existence of different protein receptors for different serotypes of BoNT and for tetanus neurotoxin (Li and Singh 1998; Nishiki et al., 1993, 1994, 1996; Schengrund et al., 1992; Schiavo et al., 1991, 1999; Kozaki 1999; Thilo, 1993). Latest results have suggested that the receptor for at least BoNT/B is an isoform of synaptotagmin whose binding is modified by gangliosides (Nishiki et al., 1993, 1994 and 1996). Synaptotagmin is involved in the interaction with the synaptic vesicle docking and fusion proteins, and is expected to be exposed on the neuronal surface following exocytotic discharge. It is proposed that gangliosides could prime the structure of the receptor for binding with the neurotoxin.

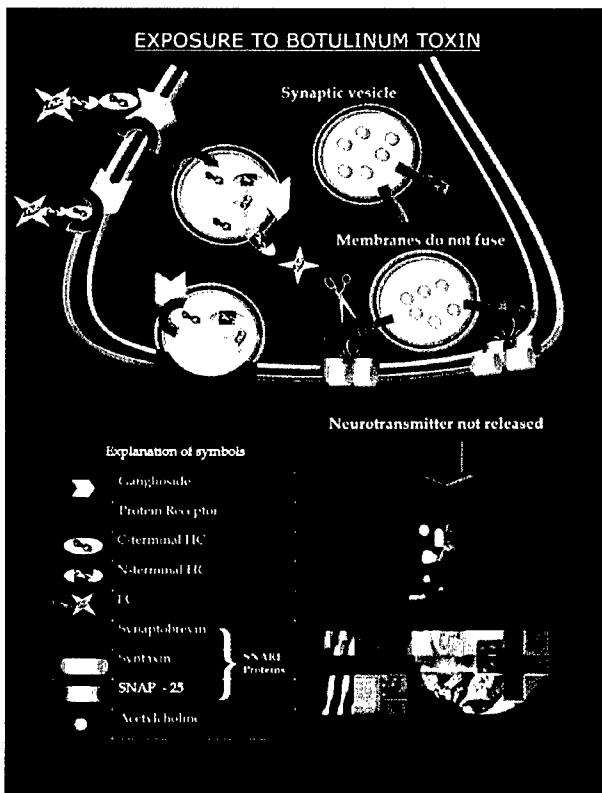


Fig. 4. Schematic representation of the steps involved in the binding, internalization and intracellular activity of BoNTs.

Critical Analysis of the Role of Gangliosides in BoNT Action: According to the 'double receptor' model of BoNT binding to neuronal cells, gangliosides bind to BoNT H chain that facilitates its binding to the receptor (Montecucco, 1986). However, recent studies (e.g., Montecucco, 1986) and some earlier observations (where gangliosides can be used as antidote against BoNT action; Kitamura et al., 1980; Simpson and Rapport, 1971) indicate that binding of gangliosides with BoNT does not actually 'prime' it for binding with the protein receptor. It is becoming increasingly clear that gangliosides are perhaps more important for the activity of the receptor rather than acting as receptor (Nishiki, 1993). One observation in favor of this hypothesis is the fact that gangliosides inhibit BoNTs (Kozaki et al., 1984) which will be contrary to their role as a primary receptor that 'primes' BoNT for its eventual binding with the protein receptor.

Two possible modes of ganglioside involvement in BoNT action are as follows:

- (a) Gangliosides is important for the binding activity of the protein receptor, most likely by altering its structure. However, the presence of gangliosides in the membrane could also influence the membrane organization which could change

the protein receptor's topography in the membrane that may be relevant for its binding to BoNT.

(b) Gangliosides present in abundance in nerve tissue act as low affinity acceptors of BoNT, and bind specifically to BoNT binding domain (c-terminal half of H chain). Even though the affinity is low, only a selective group of gangliosides (GT1b) bind with BoNT (Schengrund et al., 1991, 1992), and such binding is very specific, as shown in the crystal structure (Swaminathan and Eswaramoorthy, 2000) involving **about ten residues in three groups** in case of BoNT/B. Although gangliosides do not meet several basic tenets (e.g., high affinity, scarcity, etc.) of a protein receptor (Middlebrook, 1989), their binding to specific BoNT segments and their abundance at the nerve membrane can overcome the lack of high affinity.

(c) It is possible that gangliosides play both the functions outlined above.

(ii) Internalization and Translocation steps: Upon binding, the neurotoxin is internalized through endocytosis (**Fig. 4**). Inside the cell, pH of the endosome is lowered to 5.5-6.0 (Thilo, 1993), which leads to the formation of a membrane channel by the N-terminal half of the H chain. This channel helps translocate the whole or a part of the neurotoxin into the cytoplasm. At least the 50-kDa BoNT L chain is transported into the cytoplasm from acidic endocytotic vesicles. This transport is dependent upon the 100-kDa H chain (Bandyopadhyay et al., 1987) which has been suggested to form a tetramer in the vesicle membrane as suggested by results of image reconstruction from electron micrographs (Schmid et al., 1993). The H chain incorporates spontaneously into

phospholipid bilayers to form channels that allow ions as well as the L chain to pass through (Finkelstein, 1990; Koriazova and Montal, 2003).

Low pH is required for the strong channel formation activity of botulinum and tetanus neurotoxins and their H chains (Boquet and Duflot, 1982; Hoch et al., 1985). A pH of 5.0 or lower induces the channel formation. Two possible effects of the low pH are (i) neutralization of negative charges of the protein and/or conformational changes in the polypeptide folding which allow the integration of the neurotoxin into the membrane bilayer, and (ii) change in the structure of the BoNT receptor which could either release BoNT's H chain and/or assist in the membrane channel formation. Recent results have suggested that BoNT exists in oligomeric form in aqueous solution (Singh et al., 1993; 1994) as well as perhaps in lipid vesicle (Schmid et al., 1993) that may be relevant to the membrane channel formation by BoNT and its interaction with a receptor.

(iii) Intracellular step of the BoNT action is relatively better understood. It is known that the L chain subunit of the neurotoxin, once inside the nerve cells, is sufficient to block the neurotransmitter release (Bittner et al., 1989; Stecher et al., 1989; Mochida et al., 1989) that results into flaccid muscle paralysis. The neurotoxin does not affect either biosynthesis or packaging of the acetylcholine in the nerve cell (cf. 27: Simpson (ed.), 1989). Recent experimental evidence has suggested that botulinum and tetanus neurotoxins are zinc-proteases, and the substrates for the different serotypes of BoNTs and TeNT are the constitutive components of the secretory machinery (see Huttner, 1993; Montecucco and Schiavo, 1993 and 1994). Cleavage of these substrates blocks the docking and fusion of synaptic vesicles (**Fig. 4**).

Medicinal Use

Even though the crystalline form of type A botulinum neurotoxin (what is now known as BoNT/A complex) was first isolated 1940s (Lamanna et al., 1946), and its medicinal value was not experimented till 1970s (Scott, 1989), the medicinal use of the botulinum neurotoxin, “sausage poison” or fat poison, as it was referred to in early 1800s, was predicted in a monograph by Justinus Kerner in 1822 (Erbguth, 2004). Based on his seven years of studies with sausage poisoning cases and experiments, Kerner concluded that the toxin applied in minimal doses should reduce or block the hyperactivity and hyperexcitability of the motor and the autonomic nervous system. Kerner wrote “The fatty acid or zoonic acid administration in such doses, that its action could be restricted to the sphere of the sympathetic nervous system only, could be of benefit in the many diseases which originate from hyperexcitation of this system”, and “ as an analogy it can be expected that in outbreaks of sweat, perhaps also in mucous hypersecretion, the fatty acid will be of therapeutic value.” Of course, it was just a hypothesis at that time, which was recognized by Dr. Kerner himself: “What is said here about the fatty acid as therapeutic drug belongs to the realm of hypotheses and may be confirmed or disproved by observations in the future” (Erbguth, 2004).

Much work has been done in that direction, confirming the predictions of Kerner. Of the seven serotypes of BoNT discovered , so far, two (types A and B) are currently licensed for medicinal uses, and all the serotypes have potential to be used (Eleopra et al., 2004) against many neuromuscular disorders.

Botulinum neurotoxin A

For about two decades BoNT/A has been successfully used for the treatment of many disorders related to excessive muscle contraction, such as strabismus, blepharospasm, hemifacial spasm and cervical dystonia (Johnson, 1999). BoNT/A also significantly reduces pain associated with craniocervical dystonia—an effect that has long been considered secondary to its muscle relaxant action (Brin et al., 2000; Gobel et al., 2001). BoNT/A also has been used successfully to treat several different types of headaches, including tension type headaches (Wheeler, 1998; Schulte-Mattler et al., 1999) , cervicogenic headaches (Hobson et al., 1997; Freund et al., 2000) and migraine (Brin et al., 2000; Binder et al., 2000; Silberstein et al., 2000) Botulinum neurotoxin is now widely considered as a pharmaceutical agent with multiple uses, and has propelled into the public eye after it was widely reported to act as an anti-wrinkle drug for facial cosmetic enhancement. This has established its new image as a glamour drug. Botulinum neurotoxin is reported to be useful in about 100 conditions, with indications spanning many specialties (Misra, 2002; Jost et al., 2001). In the late 1980s, a group of physicians at Columbia University noticed that patients who received injections for nerve disorders also experienced cosmetic improvement. They pursued this investigation and soon developed the botulinum neurotoxin therapy in common use today. In fact, cosmetic use has become the single most common use of the botulinum neurotoxin-based product.

Clostridium botulinum produces the botulinum neurotoxin in a complex form, consisting of BoNT and NAPs. While there are several laboratories in the world which produce the BoNT complex for research, the manufacturing of botulinum neurotoxins for therapeutics involves a series of complex and specialized chromatographic protein purification steps. Quality control is the key for the therapeutic products. Two

preparations of botulinum toxin A are commercially available. The one is BOTOX® from Allergan, Inc. and the other is DYSPORT® from Ipsen, Ltd. are commercially available. These two preparations are widely used for treatment and cosmetic use. They differ based on their preparation and potency. In these two preparations adding either sodium chloride (BOTOX®, Allergan, Inc.) or lactose (DYSPORT®, Ipsen, Ltd.) protects the steric conformation of BoNT (Muthane et al., 2003) . Human serum albumin is also added to prevent loss from surface adsorption. The toxin is then dried either with freezing (DYSPORT®, Ipsen, Inc.) or without freezing (BOTOX®, Allergan, Inc.) (Muthane et al., 2003) . Numerous factors influence the clinical potency of the two preparations and hence, units of each product are not clinically equivalent or interchangeable. However, it is clear from the literature and from clinical experience that the units used to quantify the toxin activity of the two products are not equivalent. This apparent difference in the potency of the two products causes difficulties when comparing the results of studies using different preparations, and when changing from one preparation to the other. It is likely that any difference between the two products is the result of the different assay methods used to quantify the activity of the products (Odergren et al., 1998; Hambleton et al., 1994) . Different experimental paradigms have been used to find an appropriate conversion factor in dystonic patients, but the results are conflicting, (the ratio Botox:Dysport found being between 1:3 and 1:6) (Ranoux et al., 2002; Durif, 1995; Marion et al., 1995; Whurr et al., 1995; Sampaio et al., 1997) . Using a 4:1 conversion ratio for Dysport and Botox, similar results were obtained for the two treatments in an appropriately powered study, suggesting that this conversion factor is a good estimate of their comparative clinical potencies (Sampaio, et al., 1997; Sampaio et al., 2004) .

Pharmacokinetic measurements in terms of compound muscle action potential (CMAPs) with phrenic nerves also provide a similar (4.2:1) for Dysport and Botox (Wohlfarth et al., 2004).

Comparative clinical studies between other botulinum preparations have not yet been published except the toxin preparation produced in china (Tang et al., 2000) . In a case study with 785 patients, there were no significant differences found in the clinical effects of two preparations (BOTOX and CBTX-A), including the latency of response, maximal benefit, and duration of improvement. The patients' subjective assessments were similar. But the requested dose of the Chinese preparation which produced the similar effects, was statistically higher than that of Botox. Side effects included a skin rash appeared within a few days after injections in 3 cases of CBTX-A group, but none from the Botox group. No statistical differences were noted in the other adverse reaction between them. The injections of two kinds of preparation both were simple and effective for the patients with cervical dystonia. Chinese preparation is a little less powerful but much cheaper than Botox (Tang et al., 2000).

Injections with botulinum neurotoxin prepared for medicinal use are generally well tolerated. After injection the toxin diffuses into the muscles and adjacent tissues. Its effect diminishes with increasing distance from the injection site, but spread to nearby muscles is enhanced when higher volumes of the toxin are injected (Munchau et al., 2000) . Although the use of botulinum toxin is safe, the most frequently adverse reactions are dysphagia, pain, soreness and bruising at the injection site, local weakness, symptomatic general weakness, malaise and nausea. Adverse reactions usually occur within the first week following injection of botulinum toxin and, while generally

transient, these reactions may last several months. Localized pain, tenderness and/or bruising may be associated with the injection.

Table: Recent medicinal use of botulinum neurotoxin.

<i>Disorders</i>	<i>Dysfunction</i>
1. Chronic headache	Tension-type headache (Schulte-Mattler and Krack., 2004)
2. Overactive bladder (OAB)	Spastically contraction of detrusor bladder muscles (Wein, 2003)
3. Laryngeal dystonia	Vocal cord dystonia (Hamano et al., 2004)
4. Temporomandibular joint dislocation	Dysfunction of the joint, muscles of the jaw (Ricardo et al., 2003)
5. Dysuria or urinary retention	Non-relaxing urethral sphincter (Leippold et al., 2003)
6. Tourette's syndrome	Involuntary, rapid, sudden movements of muscles (Porta et al., 2004)
7. Focal hyperhidrosis	Excessive sweating (Naumann et al., 2004)

Botulinum neurotoxin B

On December 11, 2000, a botulinum toxin type B product (Myobloc™) was approved by the FDA in the United States as a treatment for patients with cervical dystonia. Myobloc™ is the U.S. trade name for Elan Biopharmaceuticals' botulinum neurotoxin type B product. Since that time, it has been used effectively to reduce facial wrinkles. Myobloc is particularly suggested for relaxing muscles used in frowning and squinting, if for no other reasons then for its name.

Botulinum neurotoxin type B (BTX-B; Myobloc) is approved for general use in the treatment of cervical dystonia (CD). In two large pivotal trials, it was found to be safe and effective in decreasing the movements, pain, and disability associated with CD (Brin et al., 1999; Brashear et al., 1999) . Being the newest botulinum toxin based product, it is still being evaluated for various neuromuscular conditions. However, it is being tested

with promise against upper and lower-limb spasticity (Bell et al., 2003; Brashear et al., 2003) and piriformis syndrome (Fishman et al., 2004).

Although BTX-B is generally considered safe, recent case reports by Dressler and Benecke (Dressler et al., 2002) indicate that side effects include visual disturbances, dry eyes, and dry mouth which suggest systemic diffusion of physiologically active quantities of toxin from the sites of injection. This interpretation is limited, however, by the small number of cases (Lang, 2003). One thing has clearly been observed that there is more antibody response to BTX-B based drugs because of the requirement of dramatically higher dose (about 100-fold higher compared to BTX-based drug) (Eleopra et al., 2004). Therefore, while BTX-B may be an alternative to BTX-A non-responders, it could be useful for long-term treatment.

The product based on BoNT/B differs from BoNT/A-based products in several ways. It is provided in a liquid form as opposed to a lyophilized powder that requires reconstitution in saline. BoNT/B has shown stability for months when stored appropriately at 2°C to 8°C, whereas BoNT/A must be stored at -5°C as a powder and must be used within hours once reconstituted according to the manufacturer's recommendation (Kim et al., 2003). In practice, BoNT/A may be stable for much longer. Also, because they are antigenically distinct, BoNT/A non-responders may respond to BoNT/B, and *vice versa* (Setler, 2000).

As described earlier, BoNT serotypes have similar structures and basic mechanisms of action. However, there are biochemical differences between them. For example, BoNTs produced in fluid culture or in food are complexes of one or more neurotoxin associated proteins (NAPs), resulting in molecular sizes of 12, 16 and 19S

(Schantz et al., 1967; Sakaguchi, 1983; Sugii et al., 1977) . BoNT/A, /C, and /E cleave synaptosomal-associated protein of M_r 25,000 (SNAP-25), while synaptobrevin is the target of BoNT/B, /D, /F, and /G. In addition to SNAP-25, BoNT/C also cleaves syntaxin. Therefore, biochemical differences between botulinum toxin serotypes may confer unique *in vivo* biological properties. In some cases, BoNT/B was found to be more effective than BoNT/A. For example, Flynn and Clark (Flynn et al., 2003) compared the rate of diffusion of botulinum neurotoxin types A and B in the forehead and found that BoNT/B had a slightly faster action than BoNT/A. All patients responded to BoNT/B quickly, whereas some had a delayed response to BoNT/A. The study is based on case reports of monitored diffusion of toxin. The biochemical aspect of such faster diffusion is still unknown.

Conclusions

Generally, neurotoxins are considered lethal to humans when used in high doses either by deliberate or accident. Botulinum toxin is a rare example of potentially lethal biological agent that can be used as a medicine for several neuromuscular disorders. It has many unique characteristics including exclusive substrate specificity and localized action. Research is underway to use botulinum neurotoxin as a drug delivery vehicle. Despite its extreme toxicity it has been widely used as a wrinkle remover which is perhaps the single most popular use. While its use as a therapeutic agent is relatively safe, care must be taken as it can interact with other antibiotics, especially those which interfere with neurotransmission. Caution should also be exercised when botulinum toxin type A is utilized for treatment of patients with myasthenia gravis, Eaton Lambert Syndrome, or other disorders that produce a depletion of acetylcholine. Although the most toxic

substance known to mankind has been transformed from a killer to cure, safe guards need to be put in place so that the reagents are prepared and used safely. A recent case involving the use of research grade botulinum toxin for therapeutic use has results in severe paralysis of several patients (Wahlberg, 2005).

Acknowledgements

This work was in part supported by a U.S. Army Medical Research and Material Command under Contract No. DAMD17-02-C-001, and by National Institutes of Health through New England Center of Excellence for Biodefense (AI057159-01).

References

- Ahnert-Hilger G and Bigalke H: Molecular aspects of tetanus and botulinum neurotoxin poisoning. *Progr. in Neurobio.* **1995**; 46, 83-96. Review.
- Ala-Huikka K, Nurmi E, Pajulahti H and Raevuori M: The occurrence of *Clostridium botulinum* type E in Finnish trout farms and the prevention of toxin formation in fresh-salted vacuum-packed trout fillets. *Nord. Vet. Med.* **1977**; 29:386-391.
- Arnon SS, Schechter R, Inglesby TV, Henderson DA, Bartlett DA, Scher MS, Eitzen, E., Fine AD, Hauer J, Layton M, Lillibridge S, Osterholm MT, O'Toole T, Parker, G, Perl TM, Russell PK, Swerdlow DL and Tonal K: Botulinum Toxin as a biological weapon: Medical and public health management. *JAMA* **2001**; 285, 1059-1070
- Ashie IN, Smith JP and Simpson BK: Spoilage of shelf-life extension of fresh fish and shellfish. *Crit. Rev. Food Sci. Nutr.* **1996**; 36:87-121.
- Aureli P, Fenicia L, Pasolini B, et al: Two cases of type E infant botulism caused by neurotoxic Clostridium butyricum in Italy. *J. Infect. Dis* **1986**; 154: 207-211.
- Baldassi L, Hipolito M, Portugal MA, Calil EM, Moulin AA and Pires D de C: Bovine botulism: laboratory confirmation of clinical diagnosis in 1986-1989. *Pev. Saude Publica* **1991**; 25:371-374.
- Bandyopadhyay S, Clark AW, DasGupta BR and Sathyamoorthy V: Role of the heavy and light chains of botulinum toxin in neuromuscular paralysis. *J. Biol. Chem.* **1987**; 262:2660-2663.
- Bell KR, Williams, F: Use of botulinum toxin type A and type B for spasticity in upper and lower limbs. *Phys Med Rehabil Clin N Am* **2003**; 14:821-835.
- Bhandari M, Campbell KD, Collins MD, and East AK: Molecular characterization of the clusters of genes encoding the botulinum neurotoxin complex in clostridium botulinum (*Clostridium argentinense*) type G and nonproteolytic Clostridium botulinum type B. *Curr. Microbiol.* **1997**; 35 (4), 207-214.
- Binder WJ, Brin MF, Blitzer A, et al: Botulinum toxin type A (BOTOX) for treatment of migraine headaches: an open-label study. *Otolaryngol Head Neck Surg* **2000**; 123:669-676.
- Binz T, Kurazono H, Wille M, Frevert J, Wermars K and Niemann H: The complete sequence of botulinum neurotoxin type A and comparison with other clostridial neurotoxins. *J. Bio. Chem.* **1990a**; 265:9153-9158.
- Binz T, Kurazono H, Popoff MR, Elkund MW, Sakaguchi G, Kozaki S, Krieglstein K, Henschen A, Gill DM and Niemann H: Nucleotide sequence of the gene encoding *Clostridium botulinum* neurotoxin type D. *Nucleic. Acids Res.* **1990b**; 18:5556-5556.
- Bittner MA, Habig WH and Holz RW: Isolated light chain of tetanus toxin inhibits exocytosis: Studies in digitonin permeabilized cells. *J. Neurochem.* **1989**; 53:966-968.

- Boquet P and Duflot E: Tetanus toxin fragment forms channels in lipid vesicles at low pH. *Proc. Natl. Acad. Sci. USA* **1982**; 79:7614-7618.
- Brashear A, Lew MF, Dykstra DD: Safety and efficacy of NeuroBloc (botulinum toxin type B) in type A-responsive cervical dystonia. *Neurology* **1999**; 53:1439-1446.
- Brashear A, McAfee AL, Kuhn ER, Ambrosius WT: Treatment with botulinum toxin type B for upper-limb spasticity. *Arch Phys Med Rehabil* **2003**; 84:103-107.
- Brinkmann web site for nucleic acid conversions:
http://www.brinkmann.com/support_practical-nuc-conv.asp
- Brin MF, Lew MF, Adler CH: Safety and efficacy of NeuroBloc (botulinum toxin type B) in type A-resistant cervical dystonia. *Neurology* **1999**; 53:1431-1438.
- Brin MF, Swope DM, O'Brien C, et al: Botox for migraine: double-blind, placebo-controlled, region-specific evaluation. *Cephalgia* **2000**; 20:421-422.
- Burns GF and Williams H: Clostridium botulinum in Scottish fish farms and farmed trout. *J. Hyg. (London)* **1975**; 74:1-6.
- Call JE, Cooke PH and Miller AJ: In situ characterization of *Clostridium botulinum* neurotoxin synthesis and export. *J. App. Bact.* **1995**; 79:257-263.
- Campbell KD, Collins MD and East AK: Nucleotide sequence of the gene coding for *Clostridium Botulinum (Clostridium argentinense)* type G neurotoxin: genealogical comparoson with other clostridial neutoxins. *Biochim. Biophys. Acta.* **1993a**; 1216:487-491.
- Campbell KD, East AK, Thompson DE and Collins MD: Studies on the large subunit ribosomal RNA genes and intergenic spacer regions of non-proteolytic *Clostridium Botulinum* types B, E and F. *Res. Microbio.* **1993b**; 144:171-180.
- Campbell KD, Collins MD and East AK: Gene probes for identification of the botulinal neurotoxin gene and specific identification of neurotoxin types B, E, and F. *J. Clini. Microbio.* **1993c**; 31:2255-2262.
- Clayton MA, Clayton JM, Brown DR and Middlebrook JL: Protective vaccinatn with a recombinant fragment of *Clostridium botulinum* neurotoxin serotype A expressed from a synthetic gene in *Escherichia coli*. *Infec. Immun.* **1995**; 63:2738-2742.
- Cordoba JJ, Collins MD and East AK: Studies on the genes encoding botulinum neurotoxin type A of *Clostridium botulinum* from a variety of saurces. *System. Appl. Microbio.* **1994**; 18:13-22.
- Dineen SS, Bradshaw M and Johnson EA: Neurotoxin Gene Clusters in *Clostridium botulinum* Type A Strains: Sequence Comparison and Evolutionary Implications. *Curr. Microbiol.* **2003**; 46 (5), 345-352.
- Dressler D, Benecke R: Initial experiences with clinical use of botulinum toxin type B [German]. *Nervenarzt* **2002**; 73:194-8.
- Durif F. Clinical bioequivalence of the current commercial preparations of botulinum toxin. *Eur Neurol* **1995**; 2:17-18.
- East AK, Bhandari M, Hielm S and Collins MD: Analysis of the botulinum neurotoxin type F gene clusters in proteolytic and nonproteolytic *Clostridium botulinum* and *Clostridium barati*. *Curr. Microbiol.* **1998**; 37 (4), 262-268.
- East AK, Bhandari M, Stacey JM, et al: Organization and phylogenetic interrelationships of genes encoding components of the botulinum toxin complex in proteolytic *Clostridium botulinum* types A, B, and F: evidence of chimeric sequences in the

- gene encoding the nontoxic nonhemagglutinin component. *Int. J. Syst. Bacteriol* **1996**; 46:1105-1112.
- East AK and Collins MD: Conserved structure of genes encoding components of botulinum neurotoxin complex M and the sequence of the gene coding for the nontoxic component in nonproteolytic *Clostridium botulinum* type F. *Curr. Microbiol.* **1994**; 29 (2), 69-77.
- East AK, Stacey JM and Collins MD: Cloning and sequencing of a hemagglutinin component of the botulinum neurotoxin complex encoded by *Clostridium botulinum* types A and B. *System. Appl. Microbio.* **1994a**; 17:306-312.
- East AK and Collins MD: Conserved structure of genes encoding components of the botulinum neurotoxin complex M and the sequence of the gene encoding for the nontoxic component in nonproteolytic *Clostridium botulinum* type F. *Curr. Microbio.* **1994b**; 29:69-77.
- East AK, Richard PT, Allaway D, Collins MD and Thmopson DE: Sequence of the gene encoding type F neurotoxin of *Clostridium botulinum*. *FEMS Microbio. Lett.* **1992**; 96:225-230.
- Eleopra R, Tugnoli V, Quatrone R, Rossetto O, Montecucco C: Different types of botulinum toxin in humans. *Mov Disord* **2004**; 19:S53-S59.
- Elmore MJ, Hutson RA, Collins, MD, Bodsworth NJ, Whelan S and Minton NP: Nucleotide sequence of the gene coding for proteolytic (group I) *Clostridium botulinum* type F neurotoxin: genealogical comparison with other colstridial neurotoxins. *System. Appl. Microbio.* **1995**; 18:23-31.
- Erbguth FJ: Botulinum toxin, a historical note. *Lancet* **1998**; 351:1280.
- Erbguth FJ: Historical notes on botulism, *Clostridium botulinum*, botulinum toxin, and the idea of the therapeutic use of the toxin. *Mov. Disord.* **2004**; 19:S2-S6.
- Eswaramoorthy S, Kumaran D, Swaminathan S: A novel mechanism for *Clostridium botulinum* neurotoxin inhibition. *Biochemistry* **2002**; 41(31):9795-802.
- Fairweather NF and Lyness VA: The complete nucleotide sequence of tetanus toxin. *Nucleic Acids Res.* **1986**; 14 (19), 7809-7812.
- Fach P, Hauser D, Guillou JP and Popoff MR: Polymerase chain reaction for the rapid identification of *Clostridium botulinum* type A strains and detection in food samples. *J. App. Bact.* **1993**; 75:234-239.
- Fernandez RA, Ciccarelli AS, Arenas GN and Gimenez DF: Type D and A *Clostridium botulinum* in necropsy samples from bovines with 'mad de Aguapey'. *Rev. Argent. Microbiol.* **1989**; 21:47-53.
- Finkelstein A: Channels formed in phospholipid bilayer membranes by diphtheria, tetanus, botulinum and anthrax toxin. *J. Physiol.* **1990**; 84:188-190.
- Fishman LM, Konnoth C, Rozner B: Botulinum neurotoxin type B and physical therapy in the treatment of piriformis syndrome: a dose-finding study. *Am J Phys Med Rehabil* **2004**; 83:42-50.
- Flynn TC, Clark RE: Botulinum toxin type B (MYOBLOC) versus botulinum toxin type A (BOTOX) frontalis study: rate of onset and radius of diffusion. *Dermatol Surg* **2003**; 29:519-522.

- Foster EM: Reflections on a half-century of foodborne botulism. in Botulinum and Tetanus Neurotoxins, p505. DasGupta, B. R., Edit. Plenum Press, New, York, 1993.
- Freund BJ, Schwartz M: Treatment of chronic cervical-associated headache with botulinum toxin A: a pilot study. *Headache* **2000**; 40:231-236.
- Fu FN, Sharma SK, Singh BR: A protease-resistant novel hemagglutinin purified from type A *Clostridium botulinum*. *J Protein Chem.* **1998**; 17:53-60.
- Fujii N: Structure and function of botulinum toxin, Hokkaido igaku zasshi-hokkaido J. Med. Sci. **1995**; 70:19-28.
- Fujii N, Kimura K, Tsuzuki K, Yokosawa N, Oguma K: Construction and expression of the genes for neurotoxins and non-toxic components in *C. botulinum* types C and E, in Botulinum and Tetanus Neurotoxins. B. R. DasGupta, ED., Plenum Press, New York, **1993a**; P405-419.
- Fujii N, Kimura K, Yokosawa N, Yashiki T, Tsuzuki K, Oguma K: The complete nucleotide sequence of the gene encoding the nontoxic component of *Clostridium botulinum* type E progenitor toxin. *J. Gen. Microbio.* **1993b**; 139:79-86.
- Fujii N, Kimura K, Yokosawa N, Oguma K, Yashiki T, Takeshi K, Ohyama T, Isogai E, Isogai H: Similarity in nucleotide sequence of the encoding nontoxic *Clostridium butyricum* strain BL 6340 and *Clostridium botulinum* type E strain Mashike. *Micro. Immunol.* **1993c**; 37:395-398.
- Fujii N, Kimura K, Murakami T, Indoh T, Yashiki T, Tzumuki K, Yokosawa N, Oguma K: The nucleotide and deduced amino acid sequences of EcoRI fragment containing the 5'-terminal region of *Clostridium botulinum* type E toxin gene cloned from Mashike, Iwanai and Otaru strains. *Micro. Immunol.* **1990**; 34:1041.
- Fujinaga Y, Inoue K, Nomura T, Sasaki J, Marvaud JC, Popoff MR, Kozaki S, Oguma K: Identification and characterization of functional subunits of *Clostridium botulinum* type A progenitor toxin involved in binding to intestinal microvilli and erythrocytes. *FEBS Lett.* **2000**; 467:179-183.
- Fujinaga Y, Inoue K, Shimazaki S, Tomochika K, Tsuzuki K, Fujii N, Watanabe T, Ohyama T, Takeshi K, Inoue K, Oguma K: Molecular construction of *Clostridium botulinum* type C progenitor toxin and its gene organization. *Biochem. and Biophys. Res. Commun.* **1994**; 205:1291-1298.
- Fujinaga Y, Inoue K, Watanabe S, Yokota K, Hirai Y, Nagamachi E, Oguma K: The haemagglutinin of *Clostridium botulinum* type C progenitor toxin plays an essential role in binding of toxin to the epithelial cells of guinea pig small intestine, leading to the efficient absorption of the toxin. *Microbiology.* **1997**; 143:3841-3847.
- Fujinaga Y, Inoue K, Watarai S, Sakaguchi Y, Arimitsu H, Lee JC, Jin Y, Matsumura T, Kabumoto Y, Watanabe T, Ohyama T, Nishikawa A, Oguma K: Molecular characterization of binding subcomponents of *Clostridium botulinum* type C progenitor toxin for intestinal epithelial cells and erythrocytes. *Microbiology.* **2004**; 150:1529-38.
- Fujinaga Y, Takeshi K, Inoue K, Fujita R, Ohyama T, Moriishi K and Oguma K: Type A and B neurotoxin genes in a *Clostridium botulinum* type AB strain. *Biochem. and Biophys. Res. Commun.* **1995**; 213:737-745.

- Fujita R, Fujinaga K, Inoue H, et al: Molecular characterization of two forms of nontoxic–nonhemagglutinin components of *Clostridium botulinum* type A progenitor toxins. *FEBS Lett* **1995**; 376: 41–44.
- Gobel H, Heinze A, Heinze-Kuhn K, et al: Botulinum toxin A in the treatment of headache syndromes and pericranial pain syndromes. *Pain* **2001**; 91:195–199.
- Haagsma J: Botulism in cattle, a review. *Tijdschr. Diergeneskd.* **1991**; 116:663–669.
- Hall JD, McCroskey LM, Pincomb BJ, et al: Isolation of an organism resembling *Clostridium barati* which produces type F botulinum toxin from an infant with botulism. *J. Clin. Microbiol* **1985**; 21: 654–655.
- Hamano K, Satoko K, Masaharu H, et al: Laryngeal dystonia in a case of severe motor and intellectual disabilities due to Japanese encephalitis sequelae. *Brain and Development* **2004**; 26:335–338.
- Hambleton P: *Clostridium botulinum* toxins: a general review of involvement in disease, structure, mode of action and preparation for clinical use. *J. Neurol.* **1992**; 239:16–20.
- Hambleton P, Pickett AM: Potency equivalence of botulinum toxin preparations. *J R Soc Med* **1994**; 87:719–724.
- Hatheway CL: Bacteriology and pathology of neurotoxic clostridia. in *Botulinum and Tetanus Neurotoxins*, p491. DasGupta, B. R., Edit. Plenum Press, New, York, **1993**.
- Hatheway CL and Ferreira J: Detection and identification of *Clostridium botulinum* neurotoxins. In: *Natural Toxins II: Structure, Mechanism of Action and Detection* (Singh, B. R. and Tu, A., eds.), Plenum Press, New York. **1996**; pp.481–498.
- Hauser D, Eklund MW, Boqueet P and Popoff MR: Botulinum neurotoxin C1 complex, clostridial neurotoxin homology and genetic transfer in *Clostridium botulinum*, *Toxicon* **1995**; 33:515–526.
- Hauser D, Gibert M, Marvaud JC, Eklund MW and Popoff MR: Organization of the botulinum neurotoxin C1 gene and its associated non-toxic protein genes in *Clostridium botulinum* C 468. *Mol. Gen. Genet.* **1994**; 243:631–640.
- Hobson DE, Gladish DF: Botulinum toxin injection for cervicogenic headache. *Headache* **1997**; 37:253–255.
- Hoch DH, Romero-Mira M, Ehrlich BE, Finkelstein A, DasGupta BR and Simpson LL: Channels formed by botulinum, tetanus and diphtheria toxins in planer lipid bilayers: relevance to translocation of proteins across membranes. *Proc. Natl. Acad. Sci. USA* **1985**; 82:1692–1696.
- Holger Bruggemann, Sebastian Baumer, Wolfgang Florian Fricke, Arnim Wiezer, Heiko Liesegang, Iwona Decker, Christina Herzberg, Rosa Martinez-Arias, Rainer Merkl, Anke Henne and Gerhard Gottschalk: The genome sequence of *Clostridium tetani*: the causative agent of tetanus disease. *Proc. Natl. Acad. Sci. USA* **2003**; 100 (3), 1316–1321.
- Humeau Y, Doussau F, Grant NJ, et al: How botulinum and tetanus neurotoxins block neurotransmitter release *Biochimie* **2000**; 82:427–446.
- Huss HH and Eskildsen U: Botulism in farmed trout caused by *Clostridium botulinum* type E; a preliminary report. *Nord. Vet. Med.* **1974**; 26:733–738.

- Hutson RA, Collins MD, East AK and Thompson DE: Nucleotide sequence of the gene coding for non-proteolytic *Clostridium botulinum* type B neurotoxin: Comparison with other colstridial neurotoxins. *Curr. Microbio.* **1994**; 28:101-110.
- Hutson RA, Thompson DE, Lawson PA, Schocken-Itturino RP, Bitter EC and Collins MD: Genetic interrelationships of proteolytic *Clostridium Botulinum* types A, B, and F and other members of the *Clostridium Botulinum* complex as revealed by small-subunit rRNA gene sequences. *Antonie van Leeuwenhoek* **1993**; 64:273.
- Hutson RA, Zhou Y, Collins MD, Johnson EA, Hatheway CL and Sugiyama H: Genetic characterization of *Clostridium botulinum* type A containing silent type B neurotoxin gene sequences. *J. Biol. Chem.* **1996**; 271:10786-10792.
- Huttner WB: Snappy exocytotoxins. *Nature* **1993**; 365:104-105.
- Inoue K, Fujinaga Y, Honke K, Arimitsu H, Mahmut N, Sakaguchi Y, Ohyama T, Watanabe T, Inoue K, Oguma K: *Clostridium botulinum* type A haemagglutinin-positive progenitor toxin (HA(+)-PTX) binds to oligosaccharides containing Gal beta1-4GlcNAc through one subcomponent of haemagglutinin (HA1). *2001; Microbiology.* 147:811-819.
- Jankovic J, Brin MF: Botulinum toxin: historical perspective and potential new indications. *Muscle And Nerve* **1997**; 20:S129-145.
- Jeffrey JS, Galey FD, Meteyer CU, Kinde H and Rezvani M: Type C botulism in turkeys: determination of the median toxic dose. *J. Vet. Diagn. Invest.* **1994**; 6:93-95.
- Johnson EA: CLOSTRIDIAL TOXINS AS THERAPEUTIC AGENTS: Benefits of Nature's Most Toxic Proteins. *Annu Rev Microbiol* **1999**; 53:551-575.
- Jost WH, Kohl A. Botulinum toxin: evidence-based medicine criteria in rare indications. *J Neurol.* **2001**; 248 suppl 1:39-44.
- Kim, Eugene JMD, Ramirez Alexander LMD, Reeck Jay BMD, et al: The Role of Botulinum Toxin Type B (Myobloc) in the Treatment of Hyperkinetic Facial Lines. *Plastic and Reconstructive Surgery*; **2003**; 112: Supplement pp 88S-93S.
- Kitamura M, Iwamori M and Nagai Y: Interaction between *Clostridium botulinum* neurotoxin and gangliosides. *Biochim. Biophys. Acta* **1980**; 628:328-335.
- Koriazoa LK and Montal M: Translocation of botulinum neurotoxin light chain protease through the heavy chain channel. *Nat Struct. Biol.* **2003**; 10; 13-18
- Kouguchi H, Watanabe T, Sagane Y, Sunagawa H and Ohyama T: In vitro reconstitution of the *Clostridium botulinum* type D progenitor toxin. *J. Biol. Chem.* **2002**; 277, 2650-2656.
- Kozaki S: Botulinum toxin receptors. *International Conference 1999: Basic and Therapeutic Aspects of Botulinum and Tetanus Toxins*, Orlando, Fl., November 16-18,, **1999**. Abstract page 28.
- Kozaki S, Sakaguchi G, Nishimura M, Iwamori M and Nagai Y: Inhibitory effect of ganglioside GT1b on the activities of *Clostridium botulinum* toxins. *FEMS Microbiol. Lett.* **1984**; 21:219-223.
- Lamanna C, MacElroy OE and Eklund HW: The purification and crystallization of *Clostridium botulinum* type A toxin. *Science* **1946**; 103, 613-614.
- Lang AM: Botulinum Toxin Type A Therapy in Chronic Pain Disorders. *Arch Phys Med Rehabil* **2003**; 84:S69-S73.

- Lazarovici P, Yanai P and Yavin E: Molecular interactions between micellar polysialogangliosides and affinity purified tetanotoxins in aqueous solution. *J. Biol. Chem.* **1987**; 262:2645-2651.
- Leippold T, Reitz A, Schurch B: Botulinum toxin as a new therapy option for voiding disorders: current state of the art. *Eur Urol* **2003**; 44:165-74.
- Li BL, Parikh SN, Lomenth RB, et al: A novel type E *Clostridium botulinum* neurotoxin progenitor complex. *Protein Sci* **1997**; 6 (Suppl. 2):139T.
- Li L and Singh BR: Isolation of synaptotagmin as a receptor for types A and E botulinum neurotoxin and analysis of their comparative binding using a new microtiter plate assay. *J. Natural Toxins* **1998**; 7:215-226.
- Li L and Singh BR: (1999) Structure-function relationship of clostridial neurotoxins. *Toxin Reviews* 18:95-112.
- Lund BM and Peck MW: Heat resistance and recovery of spores of non-proteolytic *Clostridium botulinum* in relation to refrigerated, processed foods with an extended shelf-life. *J. App. Bact. Sympo. Suppl.* **1994**; 76:115S-128S.
- Makoff AJ, Oxer MD, Romanos MA, Fairweather NF and Ballantine S: Expression of tetanus toxin fragment C in *E. Coli*: high level expression by removing rare codons. *Nucleic Acids Res.* **1989**; 17:10191-10202.
- Marion MH, Sheehy M, Sangla S, et al: Dose standardization of botulinum toxin. *J Neurol Neurosurg Psychiatry* **1995**; 59:102-103.
- Marks JD: Development of botulinum neurotoxin immunotherapy. In: Botulinum Neurotoxin and Ricin Investigators Meeting, Bethesda, MD, October 26, 2004.
- Marvaud JC, Gilbert M, Inoue K, et al: botR is a positive regulator of botulinum neurotoxin and associated nontoxic protein genes in *Clostridium botulinum* A. *Mol. Microbiol* **1998**; 29:1009-1018.
- McClure PJ, Cple MB and Smelt JPP M: Effects of water activity and pH on growth of *Clostridium Botulinum*. *J. App. Bact. Symp. Suppl.* **1994**; 76:105S-114S.
- Merrison AF, Chidley KE, Dunnett J, Sieradzan KA: Wound botulism associated with subcutaneous drug use. *BMJ.* **2002**; 325:1020-1021.
- Middlebrook JL: Cell surface receptors for protein toxins. In: Simpson LL (Eds.). Botulinum neurotoxin and tetanus toxin. New York: Academic Press **1989**; 95-119.
- Misra VJ: Editorial: The changed image of botulinum toxin. *Bio Med. J* **2002**; 325:1188.
- Mochida S, Poulain B, Weller U, Habermann E and Tauc L: Light chain of tetanus toxin intracellularly inhibits acetylcholine release at neuro-muscular synapses, and its internalization is mediated by heavy chain. *FEBS Lett.* **1989**; 253:47-51.
- Montecucco C: How do tetanus and botulinum toxins bind to neuronal membrane? *Trends Biochem. Sci.* **1986**; 11:314-317.
- Montecucco C and Schiavo G: Mechanism of action of tetanus and botulinum neurotoxins. *Mol. Microbio.* **1994**; 13:1-8.
- Montecucco C and Schiavo G: Tetanus and botulism neurotoxins: a new group of zinc proteases. *TiBS* **1993**; 18:324-327.
- Moriishi K, Koura M, Fujii N, Fujinaga Y, Igoue K, Syuto B and Oguma K: Molecular cloning of the gene encoding the mosaic neurotoxin, composed of parts of botulinum neurotoxin types C1 and D, and PCR detection of this gene from

- Clostridium botulinum* type C organisms. *App. Environ. Microbio.* **1996**; 62:662-667.
- Munchau A, K P Bhatia KP: Uses of botulinum toxin injection in medicine today(Clinical Review). *BMJ* **2000**; 320:161 – 165.
- Muthane U, Panikar D: Botulinum toxins: Pharmacology and its current therapeutic evidence for use. *Neurology India* **2003**; 51:455-460.
- Naumann M, Hamm H: High-dose injection of botulinum toxin to treat focal hyperhidrosis: what's wrong with the concept? *J Am Acad Dermatol* **2004**; 50:326-7.
- Nishikawa A, Uotsu N, Arimitsu H, Lee JC, Miura Y, Fujinaga Y, Nakada H, Watanabe T, Ohyama T, Sakano Y, Oguma K: The receptor and transporter for internalization of *Clostridium botulinum* type C progenitor toxin into HT-29 cells. *Biochem Biophys Res Commun.* **2004**; 319(2):327-33.
- Nishiki T, Ogasawara K, Kamata Y and Kozaki S: Solubilization and characterization of the acceptor for *Clostridium botulinum* type B neurotoxin from rat brain synaptic membranes. *Biochim. Biophys. Acta* **1993**; 1158:333-338.
- Nishiki T, Kamata Y, Nemoto Y, Omori Y, Ito T, Takahashi M and Kozaki S: Identification of protein receptor for *Clostridium botulinum* type B neurotoxin in rat brain synaptosomes. *J. Biol. Chem.* **1994**; 269:10498-10503.
- Nishiki T, Tokuyama Y, Kamata Y, Nemoto Y, Yoshida A, Sato K, Sekiguchi M, Takahashi M and Kozaki S: The high-affinity binding of *Clostridium botulinum* type B neurotoxin to synaptotagmin II associated with gangliosides GT1b/GD1a. *FEBS Lett.* **1996**; 378:253-257.
- Odergren T, Hjaltason H, Kaakkola S, et al: A double blind, randomised, parallel group study to investigate the dose equivalence of Dysport® and Botox® in the treatment of cervical dystonia. *J Neurol Neurosurg Psychiatry* **1998**; 64: 6-12.
- Ortolani EL, Brito LA, Mori CS, Schalch U, Pacheco J and Baldacci L: Botulism outbreak associated with poultry litter consumption in three Brazilian cattle herds. *Vet. Hum. Toxicol.* **1997**; 39:89-92.
- Porta M, Maggioni G, Ottaviani F, et al: Treatment of phonic tics in patients with Tourette's syndrome using botulinum toxin type A. *Neurol Sci* **2004**; 24:420-3.
- Ranoux D, Gury C, Fondarai J, et al: Respective potencies of Botox and Dysport: a double blind, randomised, crossover study in cervical dystonia. *J Neurol Neurosurg Psychiatry* **2002**; 72(4):459-62.
- Ricardo GS, Christina MM, Olsson AB, et al: Botulinum toxin type a in the treatment of temporomandibular joint dislocation in an adult with anoxic brain injury: a case report. *Archives of Physical Medicine and Rehabilitation* **2003**; 84, 9, E8.
- Rinner SGE and Stackebrandt E: Further evidence for the genetic heterogeneity of *Clostridium botulinum* as determined by 23S rRNA oligonucleotide probing. *System. Appl. Microbiol.* **1994**; 17:180-188.
- Rodriguez Jovita M, Collins MD and East AK: Gene organization and sequence determination of the two botulinum neurotoxin gene clusters in *Clostridium botulinum* type A(B) strain NCTC 2916. *Curr. Microbiol.* **1998**; 36: 226-231.

- Sagane Y, Kouguchi H, Watanabe T, Sunagawa H, Inoue K, Fujinaga Y, Oguma K and Ohyama T: Role of C-terminal region of HA-33 component of botulinum toxin in hemagglutination. *Biochem. Biophys. Res. Commun.* **2001**; 288: 650-657.
- Sagane Y, Watanabe T, Kouguchi H, et al: Spontaneous nicking in the nontoxic–nonhemagglutinin component of the *Clostridium botulinum* toxin complex. *Biochem. Biophys. Res. Commun* **2002**; 292:434–440.
- Sagane Y, Watanabe T, Kouguchi H, Yamamoto T, Kawabe T, Murakami F, Nakatsuka M and Ohyama T: Organization of Gene Encoding Components of the Botulinum Progenitor Toxin in *Clostridium botulinum* Type C Strain 6814: Evidence of Chimeric Sequence in the Gene Encoding Each Component. Published Only in DataBase (**2000**)
- Sakaguchi G: *Clostridium botulinum* toxins. *Pharmac. Ther* **1983**; 19:165–194.
- Sakaguchi G, Sakaguchi S, Kamata Y, Tabita K, Asao T, Kozaki S: Distinct characters of *Clostridium botulinum* type a strains and their toxin associated with infant botulism in Japan. *Int. J. Food Microbiol.* **1990**; 11:231-242.
- Sampaio C, Costa J, Ferreira JJ: Clinical compatibility of marketed formulations of botulinum toxin. *Mov Disord* **2004**; 19: S129-S136.
- Sampaio C, Ferreira JJ, Simoes F, et al: DYSBOT: a single-blind, randomized parallel study to determine whether any differences can be detected in the efficacy and tolerability of two formulations of botulinum toxin type A—Dysport and Botox—assuming a ratio of 4:1. *Mov Disord* **1997**; 12:1013–1018.
- Sanger FTP site for downloading *C.botulinum* (Hall A ATCC3502) genome data::
<ftp://ftp.sanger.ac.uk/pub/pathogens/cb/>
- Sanger web site for *C.botulinum* (Hall A, ATCC3502) genome data:
http://www.sanger.ac.uk/Projects/C_botulinum/
- Santos-Buelga JA, Collins MD and East AK: Characterization of the genes encoding the botulinum neurotoxin complex in a strain of *Clostridium botulinum* producing type B and F neurotoxins. *Curr. Microbiol.* **1998**; 37 (5), 312-318.
- Schantz EJ: Historical perspective: Jankovic J, Hallett M (eds): *Therapy with Botulinum Toxin*, xxiii-vi. New York: Marcel-Dekker **1994**; 608.
- Schantz EJ, Johnson EA: Botulinum toxin: the story of its development for the treatment of human disease. *Perspect Biol Med* **1997**; 40:317-327.
- Schantz EJ, Johnson EA: Properties and use of botulinum toxin and other microbial neurotoxins in medicine. *Microbiol. Rev* **1992**; 56:80-99.
- Schantz EJ, Spero L: (1967) Molecular size of *Cl. Botulinum* toxins. Ingram M, Roberts TA (eds).Chapman and Hall, London. 296-301.
- Schengrund CL, DasGupta BR, Ringler NJ: Binding of botulinum and tetanus neurotoxins to ganglioside GT1b and derivatives thereof. *J Neurochem.* **1991**; 57:1024-1032.
- Schengrund C-L, Ringler NJ and DasGupta BR: Adherence of botulinum and tetanus neurotoxins to synaptosomal proteins. *Brain Res. Bull.* **1992**; 29:917-924.

- Schiavo G, Rosetto O, Ferrari G and Montecucco C: Tetanus receptor. Specific cross-linking of tetanus toxin to a protein of NGF-differentiated PC 12 cells. *FEBS Lett.* **1991**; 290:227-230.
- Schiavo G: Characterization of tetanus toxin receptors. *International Conference 1999: Basic and Therapeutic Aspects of Botulinum and Tetanus Toxins*, Orlando, FL., November 16-18., **1999**. Abstract page 23.
- Schiavo G, Matteoli M, Montecucco C. Neurotoxins affecting neuroexocytosis. *Physiol. Rev* **2000**; 80: 717-766.
- Schmid MF, Robinson JP, DasGupta BR: Direct visualization of botulinum neurotoxin-induced channels in phospholipid vesicles. *Nature* **1993**; 364:827-830.
- Schulte-Mattler WJ, Krack P; BoNTTH Study Group: Treatment of chronic tension-type headache with botulinum toxin A: a randomized, double-blind, placebo-controlled multicenter study, *Pain* **2004**; 109:110-114.
- Schulte-Mattler WJ, Wieser T, Zierz S: Treatment of tension-type headache with botulinum toxin: a pilot study. *Eur J Med Res* **1999**; 4:183-186.
- Scott AB: Botulinum toxin injection of eye muscles to correct strabismus. *Trans Am Ophthalmol Soc* **1981**; 79:734-770.
- Scott A B: Clostridial toxins as therapeutic agents. In: *Botulinum Neurotoxin and Tetanus Toxin* (L. L. Simpson, ed.), Academic Press, San Diego. **1989**; pp. 399-412.
- Scott AB, Suzuki D: Systemic toxicity of botulinum toxin by intramuscular injection in the monkey. *Mov. Disord* **1988**; 3:333-335.
- Setler P: The biochemistry of botulinum toxin type B. *Neurology*, **2000**; 55: S22-8.
- Shapiro RE, Specht CD, Collins BE, et al: Identification of a ganglioside recognition domain of tetanus toxin using a novel ganglioside photoaffinity label. *J. Biol. Chem.* **1997**; 48:30380-30386.
- Sharma SK and Singh BR: Hemagglutinin binding protection of botulinum neurotoxin from proteolysis. *J. Natural Toxins* **1998**; 7, 239-253.
- Sharma SK, Fu FN and Singh BR: Molecular properties of a hemagglutinin purified from type A botulinum neurotoxin complex. *J. Protein Chem.* **1999**;18: 29-38.
- Silberstein S, Mathew N, Saper J, et al: Botulinum toxin type A as a migraine preventive treatment. For the BOTOX Migraine Clinical Research Group. *Headache* **2000**; 40: 445-450.
- Simpson LL(ed.): *Botulinum toxin and Tetanus Toxin*. Academic Press, San Diego. **1989**.
- Simpson LL: Molecular pharmacology of botulinum toxin and tetanus toxin *Annu. Rev. Pharmacol. Toxicol* **1986**; 26:427-453.
- Simpson LL: The origin, structure and pharmacological properties of botulinum toxin. *Pharmacol. Rev.* **1981**; 33:155-188.
- Simpson LL and Rapport MM: The binding of botulinum toxin to membrane lipids: sphingolipids, steroids, and fatty acids. *J. Neurochem.* **1971**; 18:1341-1343.
- Singh BR: Intimate details of the most poisonous poison. *Nature Struct. Biol.* **2000**; 7, 617-619.

- Singh BR: Molecular basis of the unique endopeptidase activity of botulinum neurotoxin. In: Scientific and Therapeutic Aspects of Botulinum Toxin (M. F. Brin, J. Jankovic, and M. Hallet, eds.), Lippincott Williams and Wilkins, Philadelphia. 2002, Pp. 75-88
- Singh BR, Barcomb-Caddle LA, Fu FN and Li B: Gene probe-based detection of type E botulinum neurotoxin binding protein using polymerase chain reaction. *Toxicon* 1996; 34(7):737-42.
- Singh BR, Fuller MP and DasGupta BR: Botulinum neurotoxin type A: Structure and interaction with micellar concentration of SDS determined by FT-IR spectroscopy. *J. Protein Chem.* 1991; 10:637-649.
- Singh BR, Li B, Read: Botulinum versus tetanus neurotoxins: why is botulinum neurotoxin a food poison but not tetanus?. *Toxicon* 1995; 33:1541-1547.
- Somers E and DasGupta BR: *Clostridium botulinum* types A, B, C1, and E produce proteins with or without hemagglutinating activity: Do they share common amino acid sequences and genes? *J. Prot. Chem.* 1991; 10:415-425.
- Stecher B, Weller U, Habermann E, Gratzl M and Ahnert-Hilger G: The light chain but not the heavy chain of botulinum A toxin inhibits exocytosis from permeabilized adrenal chromaffin cells. *FEBS Lett.* 1989; 255:391-394.
- Strom MS, Elkund MW and Poysky FT: Plasmids in *Clostridium botulinum* and related *Clostridium* species. *App. Environ Microbio.* 1984; 48:956-963.
- Sugii S, Sakaguchi G: Botulogenic properties of vegetables with special reference to the molecular size of the toxin in them. *J. Food Safety* 1977; 1: 53-65.
- Tang X, Wan X: Comparison of botox with a chinese type a botulinum toxin. *Chin Med J (Engl)* 2000; 113:794-798.
- Thilo L: Endosome processing: structural, functional and kinetic interrelations. In: *Proceedings of the International Conference on Botulinum and Tetanus Neurotoxins: Neurotransmission and Biomedical Aspects* (B. R. DasGupta, ed.), Plenum Press. 1993; 165-177.
- Thompson DE, Brehm JK, Oultram JD, Swinfield TJ, Shone CC, Atkinson T, Melling J and Minton NP: The complete amino acid sequence of the *Clostridium botulinum* type A neurotoxin, deduced by nucleotide sequence analysis of the encoding gene. *Eur. J. Biochem.* 1990; 189:73.
- Thompson DE, Hutson RA, East AK, Allaway D, Collins MD and Richardson PT: Nucleotide sequence of the gene coding for *Clostridium barati* type F neurotoxin: Comparison with other colstridial neurotoxins. *FEMS Microbio. Lett.* 1993; 108:175-182.
- Todd EC: Costs of acute bacterial foodborne disease in Canada and the United States. *Int J Food Microbiol.* 1989 9:313-326.
- Tsuzuki K, Kimura K, Fujii N, Yokoszwa N and Oguma K: The complete nucleotide sequence of the gene coding for the nontoxic-non-hemagglutinin component of *Clostridium botulinum* type C progenitor toxin *Biochem. Biophys. Res. Comm.* 1992; 183:1273-1279.

- Van Ermengen E: Uber einen neuen anaeroben Bacillus und seine Beziehungen zum Botulismms. *Z Hyg infektionskrankh* **1897**; 26:1-56.
- Wahlberg D: Fake Botox-injured pair warns others. *Palm Beach Post* 2005, February 5 issue.
- Wein AJ: Diagnosis and treatment of the overactive bladder. *Urology* **2003**; 62:20-27.
- Wheeler AH: Botulinum toxin A, adjunctive therapy for refractory headaches associated with pericranial muscle tension. *Headache* **1998**; 38:468-471.
- Whelan SM, Elmore MJ, Bodsworth NJ, Brehm JK, Atkinson T and Minton NP: Molecular cloning of the *Clostridium botulinum* structural gene encoding the type B neurotoxin and determination of its entire nucleotide sequence. *App. Environ. Microbio.* **1992**; 58:2345-2354.
- Whurr R, Brooks G, Barnes C: Comparison of dosage effects between the American and British botulinum toxin A products in the treatment of spasmodic dysphonia [abstract]. *Mov Disord* **1995**; 10:387.
- Willis AT: *Clostridium: the spore-bearing anaerobes*. Lonton, A.H., Topley W. W. C ed. *Topley Wilson's principles of bacteriology, virology and immunity*. Edward Arnold, London. **1990**; P211-246.
- Wohlfarth K, Kampe K, Bigalke H: Pharmacokinetic properties of different formulations of botulinum neurotoxin type A. *Mov. Disord* **2004**; 19: S65-S67.
- Zhang Z, Singh BR: A novel complex of type E *Clostridium botulinum*. *Protein Sci* **1995**; 4 (Suppl. 2):110.
- Zhou Y, Sugiyama H and Johnson EA: Transfer of neurotoxigenicity from *Clostridium butyricum* to a nontoxigenic *Clostridium botulinum* type E-like strains. *App. Environ. Microbio.* **1993**; 59:3825-3831.

Cloning, Expression and Purification of C-terminal Quarter of the Heavy Chain of Botulinum Neurotoxin Type A

Sapna Sharma, Yu Zhou and Bal Ram Singh^{*,1}

Department of Chemistry and Biochemistry, and The Botulinum Research Center,
University of Massachusetts Dartmouth, North Dartmouth, MA 02747

*To whom correspondence should be addressed.

Bal Ram Singh,

Department of Chemistry and Biochemistry, and The School for Marine Science and
Technology, University of Massachusetts Dartmouth,

285 Old Westport Road, North Dartmouth, MA 02747, USA

Telephone: 508-999-8588; Fax: 508-999-8451; e-mail: bsingh@umassd.edu (B.R. Singh).

¹The Henry Dreyfus Teacher-Scholar

Abstract

Botulinum neurotoxins (BoNTs) are highly potent toxins that inhibit neurotransmitter release from peripheral cholinergic synapses. BoNTs consist of a toxifying light chain (LC; 50 kDa) and a binding/translocating heavy chain (HC; 100 kDa) linked through a disulfide bond. The complete sequence of BoNT/A consists of 1,296 amino acid residues. The β -trefoil domain for BoNT/A to which gangliosides bind starts at Ser 1092 and this fragment represents the C-half of the C-terminus of the heavy chain (C-quarter HC or HCQ). The recombinant HCQ DNA was successfully cloned into an expression vector (pET15b) which was used to transform *Escherichia coli* strain BL21-StarTM (DE3) for expression. Expression of HCQ was obtained by an extended post-induction time of 15 h at 30 °C. The recombinant histidine tagged HCQ protein was isolated and purified by Nickel affinity gel column chromatography and its molecular weight was verified by gel electrophoresis. The HCQ was positively identified by antibodies raised against BoNT/A employing immunological dot-blot and Western blot assays. HCQ was shown to bind with synaptotagmin (a known BoNT/A receptor) and gangliosides, indicating that the expressed and purified HCQ protein retains a functionally active conformation.

Key words: Botulinum; dot-blot; expression; gangliosides; neurotoxin; purification; receptor

Introduction

Botulinum neurotoxins (BoNTs) are a family of seven structurally and pharmacologically similar but antigenically different proteins produced by different strains of *Clostridium botulinum* (1-3). These proteins are the most toxic substances known, and are the cause of flaccid paralysis in botulism. BoNTs are produced as 150 kDa single-chain polypeptides which are nicked into a 100 kDa heavy chain and a 50 kDa light chain each, linked through a disulfide bond. The heavy chain (HC) is mainly involved in the cell-binding, internalization, and translocation of the BoNT into nerve cells, whereas the light chain (LC) exhibits the intracellular toxic activity (4). The carboxyl terminal portion of the HC is responsible for binding with nerve cell receptors (5). Following binding to the cell surface, the neurotoxin is brought into the endosomal compartment by internalization via receptor mediated endocytosis. The LC gets partially unfolded at low endosomal pH to get across the membrane into cytosol, where it acts as an endopeptidase against one or more of the three SNARE (soluble NSF attachment protein receptor) proteins: SNAP-25 (synaptosomal associated protein of 25 kDa), syntaxin or VAMP/synaptobrevin (6,7). The cleavage of any of the SNARE proteins prevents the fusion of synaptic vesicles containing acetylcholine, thus blocking the neurotransmitter release (8) that results in the flaccid muscle paralysis.

The carboxyl-terminal domain, referred to as the H_C-fragment, mediates the highly specific binding of clostridial neurotoxins to nerve terminals at the neuromuscular junction through gangliosides and a protein receptor(s) (9). The N-terminal domain of H_C (H_{CN}) has been speculated to bind with a protein receptor (10-12) whereas the C-terminal domain of H_C (H_{CC}) or HCQ domain has been shown to provide sites for binding with

gangliosides (13). The amino terminal half of HC (H_N -domain) provides the translocation apparatus for the delivery of the LC from the endosome into the cytosol. According to the crystal structure analysis of the BoNT/A, the H_C clearly consists of two distinct domains (H_{CN} and H_{CC}) (14). The H_{CC} domain (HCQ) starts at Ser 1092 and theoretically its molecular weight is a quarter of the HC (15, 16). The HCQ fragment in its isolated purified form can enable one to study its interactions with receptors of BoNT/A, and to design binding inhibitors to prevent the neurotoxic action.

Receptor-binding domains of clostridial neurotoxins are receiving more attention in recent years for the development of a number of applications including neuronal targeting. Such molecules clearly have a potential application in the treatment of a range of neurologic conditions (17, 18). The binding domain of the HC, which is a nontoxic fragment, can also be used as a potential candidate for the development of therapeutics and diagnostics. In fact, the HCQ fragment of BoNTs seems to be a promising tool in the search for potential vaccines and immunogens (19-22).

In this study, we present results of cloning, expression and purification of the HCQ fragment in order to study its binding characteristics that might enable identification of the receptors for BoNT/A. The purified HCQ reacted positively with antibodies raised against BoNT /A and also bound to gangliosides and synaptotagmin.

Materials and Methods

Restriction endonucleases and DNA modifying enzymes were purchased from New England Biolabs Inc. (Beverly, MA). All oligonucleotides were synthesized by Integrated DNA Technologies Inc. (Coralville, IA). Eppendorf-Netheler-Hinz GmbH

(Hamburg, Germany) thermal cycler (Model-Mastercycler personal) was used for polymerase chain reaction (PCR) experiments. The recombinant plasmid DNA pET 15b encoding the heavy chain of BoNT/A (pET 15b-HCA) was obtained as described previously by Li and Singh (23). The reagents used in all the experiments were of analytical grade. Nuclease free water was used from Ambion Inc. (Austin, TX).

Plasmid DNA Preparation

The plasmid DNA was isolated using S.N.A.P (Simple Nucleic Acid Prep) – a Miniprep Kit supplied by Invitrogen Life Tech (Carlsbad, CA) from *E.coli* strain BL21-Codon Plus (DE3)-RIL (Stratagene, La Jolla, CA). The *E. coli* strain containing two plasmids pACYC and pET15b-HCA (encoding the heavy chain of BoNT/A) was prepared as described previously (23). The heavy chain fragment (pET15b-HCA) was cleaved using restriction enzymes Nde I and BamH I, and then electrophoresed on a 1.0% agarose gel. The DNA of plasmid pET-15b contained the heavy chain insert (Nde I-Bam HI fragment) which was extracted using QIAquick Gel Extraction Kit (Qiagen Inc, Chatsworth, CA) and used as a template for PCR.

Primer design and Polymerase Chain Reaction

Polymerase Chain Reaction was performed to generate a DNA fragment encoding the C-half of the C-terminus of the Heavy chain of BoNT/A. Both Nde I and Bam HI restriction sites were incorporated into the 5' end of the forward sequence and reverse sequence primers, respectively. PCR reactions were performed in a total volume of 50 μ L containing 200 ng of template DNA, 100 ng of each primer, 200 μ M of each dNTP

(deoxy-nucleoside triphosphate), 1 U Vent polymerase (New England Biolabs, Beverly, MA) and nuclease free water to adjust the total volume. The reaction mixture was denatured for 2 min at 93 °C, then subjected to 30 consecutive cycles consisting of denaturation (1 min at 93 °C), annealing (1 min at 60 °C) and polymerization (1 min at 73 °C).

According to BoNT/A sequence in GenBank data-base under accession no. **M30196** (15), primers for heavy chain binding domain were designed. 5'-GGGCCCC CAT↓ATG TCA AAT TCA GG-3' was the sense primer for BoNT/A HCQ. The antisense primer sequence used was 5'- GGGCCCC GGA↓TCC TTA CAG TGG CCT TTC T-3'. An expected size (615 bp) band was purified by agarose gel electrophoresis, digested with restriction enzymes Bam HI and Nde I and ligated with predigested (restriction enzymes Bam HI and Nde I treated) vector pET15b. An aliquot of the ligation mixture was used to transform *E. coli* strain BL21-StarTM (DE3). The *E. coli* cells were plated on LB-ampicillin (50 µg/mL) agar plates and the transformants were verified to contain the HCQ by Plasmid DNA isolation and agarose gel electrophoresis.

DNA Sequencing

The recombinant plasmid DNA containing the HCQ gene was sequenced with a 3730xl DNA Analyzer (Genewiz Inc, North Brunswick, NJ) using Big Dye Terminator v3.1 cycle sequencing kit, provided by Applied Biosystems (Foster, CA).

Expression of Recombinant BoNT /A HCQ

The HCQ fragment of BoNT/A was cloned with the His₆ – tag at the N-terminal and expressed under the control of the T7 promoter. The pET15b–HCQ recombinant

plasmid was transformed into *E. coli* strain BL21-Star (DE3) and inoculated into a 50-mL aliquot of 2YT medium. The culture was grown under agitation overnight at 37 °C, and was stored as a glycerol stock in aliquots at -80 °C. Frozen glycerol stock (1.0 mL) was used to inoculate 100 mL of 2YT medium containing 50 µg/mL ampicillin (RPI Corp, Mount Prospect, IL) at 37 °C. When the optical density (O.D) at 600 nm was approximately 0.6, the 100-mL culture was transferred into 1L 2YT medium containing 50 µg/mL ampicillin in a 4-L flask, and the culture was grown at 37 °C until the O.D at 600 nm reached 0.8. IPTG (Isopropyl-β-D-Thiogalactopyranoside, RPI Corp, Mount Prospect, IL) was then added to a final concentration of 1.0 mM, and the induction was allowed to proceed at 30 °C for 15 h. The *E. coli* cells were harvested by centrifugation at 8000 x g for 10 min at 4 °C using SLA 1500 rotor and Sorvall RC-5B refrigerated superspeed centrifuge (Du Pont Instruments, Wilmington, DE). The cell pellet was stored at -80 °C till protein isolation.

HCQ Protein Isolation and Purification

The HCQ protein being a component of heavy chain is insoluble and is expressed in the form of inclusion bodies. The protein isolation method consisted of isolation and purification of the inclusion bodies from the cell pellet by following a chemical lysis procedure. The frozen cell pellet was thawed and resuspended in a lysis buffer, CelLytic™ B II (Sigma, St. Louis, MO; 20 mM Tris-HCl, pH 7.5, and a mild nonionic detergent), at the ratio of 5 mL of lysis buffer per gram of wet cell paste. After complete resuspension of cell pellet, 5 µg/mL deoxyribonuclease I and protease inhibitor cocktail (Sigma, St. Louis, MO), containing 4-[2-Aminoethyl]benzenesulfonyl fluoride

hydrochloride (AEBSF), aprotinin, leupeptine, bestatin, pepstatin A and trans-Epoxy succinyl-L-Leucylamido-[4-Guanidino]Butane (E-64) was added to the suspension at a ratio of 1 mL for 20 g wet cell paste. The suspension was incubated at 25 °C for 15 min to fully extract the cells, and centrifuged at 25,000 x g using SS-34 rotor in a Sorvall RC-5B refrigerated superspeed centrifuge (Du Pont Instruments, Wilmington, DE) for 15 min to pellet the insoluble material. The supernatant was collected and analysed by sodium dodecyl sulfate- polyacrylamide gel electrophoresis (SDS-PAGE). The pellet was resuspended further in the lysis buffer, and lysozyme with a final concentration of 0.4 mg/mL was added to the suspension. The mixture was incubated at 25 °C for 15 min, and 20 mL of 1:20 diluted lysis buffer was added. The lysis buffer was diluted using deionised water. The suspension was incubated at 25 °C for 15 min and centrifuged at 25,000 x g for 15 min. The supernatant was removed and the inclusion bodies containing pellet was resuspended in 40 mL of 1:20 diluted lysis buffer, and the extract was centrifuged at 25,000 x g for 15 min. The pellet containing remaining inclusion bodies was processed through two more cycles of resuspension and centrifugation to obtain purified inclusion bodies in the final pellet, which were then stored at -80 °C.

The frozen inclusion bodies extracted from 1L culture were thawed and resuspended in 25 mL of 0.1 M sodium phosphate buffer, pH 8.0, containing 6 M guanidine-HCl, 0.4 M NaCl and 10 mM β -mercaptoethanol. Protease inhibitor cocktail was added to the suspension at a ratio of 1 mL for 20 g wet weight cell paste, and the suspension was kept on a rocker for 1 h at 25 °C. The extract was then centrifuged at 100,000 x g using AH-629 rotor in a Sorvall ultracentrifuge OTD55B (Du Pont Instruments, Wilmington, DE) for 1 h at 4 °C. The supernatant was diluted 1:1 with

equilibration buffer (EB, 8 M Urea, 0.4 M NaCl, 5 mM imidazole, 10 mM β -mercaptoethanol in 0.1 M sodium phosphate, pH 8.0). The mixture was then loaded onto a His-Select nickel affinity gel (Sigma, St. Louis, MO) column (dimension 1 x 22 cm; 2 mL bed volume) which was previously equilibrated with EB. The column was washed with 20 mL EB, then with 20 mL of EB containing 20 mM imidazole and 8 M urea without β -mercaptoethanol. The protein was then eluted with step gradient of 20, 30 and 100 mM (5 mL each) imidazole dissolved in 0.1 M sodium phosphate buffer, pH 8.0, containing 0.4 M NaCl, 0.1% dodecylphosphocholine (DPC, Avanti Polar lipids, Alabaster, AL) and urea was subsequently removed in this step.

Isoelectric focusing

Isoelectric focusing (IEF) was performed using the Phast System (Pharmacia Biotech; Piscataway, NJ). Briefly, an aliquot of 5 μ L of HCQ (0.3 mg/mL) was loaded on the IEF gel along with prestained standards (pI 4.5-9.6, BioRad, Hercules, CA). The electrophoresis was carried out at 200 V and 2 mA at 15 $^{\circ}$ C for 15 vh, and the focusing was carried out at 2000 V and 5 mA at 15 $^{\circ}$ C for 410 vh. The gel was fixed with 20% trichloroacetic acid for 5 min and rinsed with the destaining solution (30% methanol, 10% acetic acid) for 2 min. The gel was then stained with 0.02% PhastGel Blue R (Pharmacia Biotech, Piscataway, NJ) in the destaining solution containing 0.1% CuSO_4 to decrease the background staining, and destained until the background became clear. The pI of HCQ was calculated using a calibration curve of standard proteins.

Determination of Protein Concentration

The concentration of proteins used in the experiments were determined spectrophotometrically by measurement of their absorbance at 280 and 235 nm using the formula: concentration of protein (mg/mL) = $(A_{235\text{nm}} - A_{280\text{nm}}) / 2.51$ (24).

Immuno-dot-blot assay of HCQ

Immunological dot-blot assay was employed to confirm the heavy chain fragment affinity and specificity with rabbit antibody (IgG) raised against BoNT/A (BBTech Inc., Dartmouth, MA). BoNT/A complex was purified as described previously (25). Three microlitres of HCQ sample (0.1 mg/mL), BoNT/A complex (0.1 mg/mL), BoNT/A heavy chain (0.1 mg/mL) or BSA (0.1 mg/mL, bovine serum albumin, Sigma) were spotted on a transblot transfer medium pure nitrocellulose membrane (0.45 μM , BioRad Corp, Hercules, CA). The membrane was dried and incubated in the blocking buffer, with gentle shaking for 1h at 25 $^{\circ}\text{C}$, and then incubated with 1:1000 dilution of rabbit anti BoNT/A IgG (BBTech, Dartmouth, MA). The membrane was washed with PBST (phosphate buffered saline, containing 0.05% Tween 20) three times and then incubated in a 1:30,000 dilution of secondary antibody goat anti-rabbit BoNT/A IgG conjugated with alkaline phosphatase (Sigma, St. Louis, MO), for 1 h at 25 $^{\circ}\text{C}$. The colorimetric detection was carried out by using BCIP (5-bromo-4-chloro-3-indolyl-phosphate) and NBT (Nitroblue tetrazolium, Sigma) as substrates, after washing the membrane three times with PBST.

Western-blot analysis of HCQ

The identification of the expressed protein was carried out by Western blot analysis. Kaleidoscope prestained standards (BioRad, Hercules, CA) were used as molecular weight marker). Purified HCQ from SDS-PAGE was transferred to nitrocellulose membrane (0.2 μ M, Pierce Biotech, Rockford, IL) by using Trans-Blot semi dry electrophoretic cell (BioRad, Hercules, CA) and transfer buffer (39 mM glycine, 48 mM Tris-base, 0.037% SDS, and 20% methanol). The membrane was incubated in the blocking buffer (3% BSA in phosphate buffered saline or PBS), with gentle shaking for 1h at 25 $^{\circ}$ C, and the remaining procedure was followed exactly as described for immunological dot-blot assay.

Binding Activity

Synaptotagmin Binding

Immunological dot blot assay was also employed to examine the binding activity of the purified BoNT/A HCQ protein to synaptotagmin II, a known receptor for BoNT/A (12). Recombinant synaptotagmin II protein was obtained as described earlier by Zhou and Singh (26). Three microliters each of BoNT/A complex (0.1 mg/mL), HCQ (0.1 mg/mL), or BSA (0.1 mg/mL) were spotted on a trans-blot transfer medium pure nitrocellulose membrane (0.45 μ M). The membrane was incubated with a blocking buffer (3 % BSA in PBS), with gentle shaking for 1 h at 25 $^{\circ}$ C, and then incubated with synaptotagmin II (0.1 mg/mL) in the blocking buffer with gentle shaking for 2 h at 25 $^{\circ}$ C. The membrane was washed three times with PBST and then incubated with a 1:1000 dilution of mouse anti-synaptotagmin antibody (StressGen Biotechnologies, Victoria,

BC, Canada), dissolved in the blocking buffer, with gentle shaking for 1 h at 25 °C. The membrane was washed again three times with PBST, and incubated with a 1:5000 dilution of goat anti-mouse IgG alkaline phosphatase conjugate (Novagen, Madison, WI) dissolved in the blocking buffer, with gentle shaking for 1 h at 25 °C. The colorimetric detection was carried out by using BCIP and NBT as substrates after washing the membrane three times with PBST.

Ganglioside Binding

Binding of the purified HCQ to gangliosides was performed following the procedure described by Zhou and Singh (26). Polystyrene-96-well flat-bottomed plate (Corning Glass works, Corning, NY) was used and the binding activity was analyzed by Enzyme Linked Immunosorbent Assay (ELISA). Eighty microliters of 3 mg/mL G_{T1b} (Sigma) dissolved in 20 mM sodium phosphate buffer, pH 8.0, was coated to each well and incubated at 4 °C overnight. The plate was then blocked by 1% BSA in PBS for 1 h at 25 °C, and washed four times with PBST. One hundred microliters of purified BoNT/A complex (0.1 mg/mL), HCQ (0.1 mg/mL), HCQ (0.2 mg/mL), BoNT/A heavy chain (0.1 mg/mL), or BSA (0.1 mg/mL) were added to different wells. The plate was incubated for 1 h at 25 °C on a rocker, and washed four times with PBST. One hundred microliters of 1:1000 dilution of rabbit anti BoNT/A IgG (BBTech, Dartmouth, MA) in 3 % BSA was added to each well and incubated for 1 h at 25 °C. One hundred microliters of 1:30,000 dilution of secondary antibody goat anti-rabbit BoNT/A IgG conjugated with alkaline phosphatase (Sigma) was added to each well after washing the plate four times with PBST, and incubating it for 1 h at 25 °C. The colorimetric detection was carried out using

para-nitrophenyl phosphate (pNPP, Sigma), after washing the plate four times with PBST. The absorbance of each well at 405 nm was measured using a microplate reader (Molecular Devices, Sunnyvale, CA). *A quantitative binding analysis was carried out using the same procedure with different concentrations - 0.025 mg/mL, 0.05 mg/mL, 0.1 mg/mL, 0.2 mg/mL of HCQ. BoNT/A complex and BSA were used as positive and negative controls, respectively.*

Results and Discussion

Construction of Recombinant His6-tagged BoNT/A HCQ

The plasmid DNA encoding BoNT /A heavy chain (23) was isolated and treated with restriction enzymes Nde I and BamH I. The digestion of the recombinant plasmid with restriction enzymes resulted in DNA fragments of varying sizes on an agarose gel (data not shown). The 2.5 kb DNA fragment encoding 100 kDa BoNT/A HC was extracted from the gel and used as a template for PCR. According to the codon usage, high A + T content was found in BoNT/A HC. This resulted in addition of GC overhangs to the 5' ends of both the primers for HCQ after taking into consideration their GC/AT ratio. The amplification of BoNT/A HCQ region resulted in a DNA fragment of 615 bp (data not shown). The recombinant HCQ also contained a cluster of six histidine residues for purification of the recombinant protein by metal affinity chromatography. DNA sequencing result (not shown) confirmed the successful cloning of HCQ without any mutation. The expected molecular mass of HCQ (a quarter of approximately 100 kDa HC) is 23.4 kDa.

Expression and purification of His6-tagged recombinant BoNT/A HCQ

The pET 15b-HCQ (BoNT/A) was transformed into *E.coli* strain BL21-Star™ (DE3) which has His₆ – tag at the N-terminal. HCQ protein expression was under the control of the T7 promoter and was induced by IPTG. The overexpression of HCQ results in the formation of insoluble proteins, called inclusion bodies. A previously described method by Zhou and Singh (26) was followed to isolate the protein from the inclusion bodies. The protein isolation and purification procedure was carried out at 4 °C to ensure that the protein is isolated with proper folding without any change in its conformation. When the cell pellet containing inclusion bodies was washed with lysis buffer, the first wash resulted in supernatant that contained a mixture of proteins (Fig. 1, lane 1). However, the purity of 25 kDa HCQ obtained in the supernatant at every wash step gradually increased, showing lesser contaminating bands on the gel (Fig. 1, lanes 2 and 3). Finally, pure HCQ protein (1.0 mg/mL) was obtained in the supernatants of the fourth and fifth washing steps (Fig. 1, lanes 4 and 5). The purity of the protein was examined using GEL LOGIC 100 Imager system and a KODAK 1 D v.3.6.1. Analysis system. The purified protein was determined to be 92% pure as assessed by SDS-PAGE. The presence of HCQ protein in wash solutions suggested that it was expressed partly in soluble form or that inclusion bodies are only softly formed.

The HCQ protein was subsequently isolated from the inclusion bodies after treatment with guanidine-HCL and urea, and purified by affinity gel column chromatography. SDS-PAGE analysis of the eluents revealed the presence of 25 kDa protein as a major band in all the eluted fractions as shown in Figs. 2 and 3. A step gradient elution with 20, 30 and 100 mM imidazole was carried out to obtain pure HCQ

protein. Eleven milligrams of His6-tagged HCQ (95% purity) was obtained from 1 L of the *E.coli* culture. The isoelectric focusing analysis of His6-tagged HCQ revealed an isoelectric point of 9.4. The calculated isoelectric point from amino acid sequence of His6-tagged HCQ is 9.49 (EMBL Isoelectric point service) and the calculated Molecular weight (MW) of the recombinant HCQ was found to be 24.2 kDa (Peptide calculator version 1.0, Evanston, IL). The isoelectric point was useful to determine the appropriate pH for the dialysis buffer which is vital to avoid precipitation during dialysis. Recombinant HCQ was dialyzed against 50 mM sodium phosphate buffer, pH 7.4, containing 0.1 M NaCl. The purified HCQ was stored in 20% glycerol solution at -80°C. Immuno-dot-blot assay carried out with rabbit anti-BoNT/A showed a strong reaction with HCQ, albeit not as strong as with BoNT/A complex and BoNT/A heavy chain (Fig. 4). The negative control (BSA) showed no reaction. Thus the immuno-dot-blot analysis (Fig. 4) confirmed the identity of recombinant HCQ. Lower reaction of HCQ compared to BoNT/A HC and BoNT/A complex may reflect on the availability of higher number of epitopes in BoNT/A HC and BoNT/A complex to the antibody raised against BoNT/A.

The identity of HCQ was further confirmed by Western blot analysis. The 25 kDa HCQ showed positive reaction with rabbit IgG raised against BoNT/A (Fig. 5), confirming its identity with BoNT/A as expected.

Binding activity with synaptotagmin

In an effort to evaluate the functional state of the purified HCQ, binding of HCQ with synaptotagmin was determined by immuno-dot blot assay. Synaptotagmin II has been shown to bind strongly to BoNTs, including BoNT/A and is considered as a

BoNT/A receptor at nerve cells (12). The result as shown in Fig. 6 clearly indicates binding of HCQ to synaptotagmin II similar to the positive control, BoNT/A complex. The negative control (BSA) showed no binding to synaptotagmin. These results suggests that the HCQ protein was isolated in its functionally active form and binds strongly to its putative receptor.

Binding activity with gangliosides

Gangliosides, especially G_{T1b} , are considered a component of the double-receptor system of BoNT (16). The first step in BoNT attachment to nerve membranes starts with binding of C-terminus of HC to gangliosides on presynaptic membranes. Ganglioside binding could facilitate interaction between toxin and its protein receptor by bringing them in close proximity, or cause a conformational change at the second receptor binding site (3), and is known to be mediated through the C-terminal end (HCQ) of the HC (6). Thus HCQ binding with G_{T1b} was examined to evaluate if the G_{T1b} binding capacity is retained in the recombinant HCQ purified in this study. The binding activity of gangliosides with HCQ was analyzed by ELISA. The results as shown in Fig. 7A indicate binding of the purified HCQ sample to ganglioside (G_{T1b}) similar to the positive controls, BoNT/A complex and BoNT/A heavy chain. BSA sample (control) did not show any significant binding activity with G_{T1b} , suggesting that the binding of HCQ to gangliosides is specific. *In addition, based on the serial dilution of HCQ to examine concentration dependence of its binding with G_{T1b} , we found the binding incrementally correlated with the increase in HCQ concentration (Fig. 7B), thus suggesting a specific binding of HCQ to G_{T1b} .* Surprisingly, HCQ binding to G_{T1b} was

much less than those of BoNT/A heavy chain (Fig. 7A) and BoNT/A complex (Fig. 7A&B), suggesting either the role of other domains of BoNT in HCQ binding with G_{T1b} , or a less than native folding of the HCQ expressed and purified. These issues need further examination.

Conclusions

Botulinum neurotoxins nerve intoxication mechanism is accomplished through the interplay of three key events, each of which is performed by a separate portion of the neurotoxin molecule. The HCQ portion which is the C-half of the C terminus of the heavy chain is implicated to play an important role in the receptor-specific binding of the toxin to the cholinergic neurons. In this study, we have cloned, expressed and purified the C-quarter of the BoNT /A heavy chain in a functionally active form. The availability of recombinant HCQ provides an effective system to study the biochemical and physical interactions involved during BoNT binding to nerve cells. Further analysis of molecular interactions between HCQ and its receptors will enable to understand the mechanism of BoNT action.

Acknowledgement

This work was supported by U.S Army Medical Research and Material Command under Contract, DAMD17-02-C-001. The authors thank Paul Lindo and Stephen Riding for their assistance.

References

1. L. Li, B.R. Singh, Structure-Function Relationship of Clostridial Neurotoxins, *J. Toxicol.* 18 (1999) 95-112.

2. B.R. Singh, Critical Aspects of bacterial protein toxins, *Adv. Exp. Med. Biol.* 391 (1996) 63-84.
3. B.R. Singh, Intimate details of the most poisonous poison, *Nature. Struc. Biol.* 7 (2000) 617-619.
4. C. Montecucco, G. Schiavo, Mechanism of action of tetanus and botulinum neurotoxins, *Microbiology* 13 (1994) 1-8.
5. C. Montecucco, How do tetanus and botulinum toxins bind to neuronal membrane, *Trends Biochem. Sci.* 11 (1986) 314-317.
6. A. Rummel, S. Mahrhold, H. Bigalke, T. Binz, The H_{CC}- domain of botulinum neurotoxins A and B exhibits a singular ganglioside binding site displaying serotype specific carbohydrate interaction, *Mol. Microbiol.* 51 (2004) 631-643.
7. F. Fu, R. Lomneth, S. Cai, B.R. Singh, Role of Zinc in the structure and toxic activity of Botulinum neurotoxin, *Biochemistry* 37 (1998) 5267-5278.
8. G. Schiavo, O. Rossetto, C. Montecucco, Clostridial neurotoxins as tools to investigate the molecular events of neurotransmitter release, *Semin. Cell Biol.* 5 (1994) 221-229.
9. A Rummel, S. Bade, J. Alves, H. Bigalke, T. Binz, Two carbohydrate binding sites in the H_{CC}-domain of tetanus neurotoxin are required for toxicity, *J.Mol.Biol.* 326 (2003) 835-847.
10. M. Kitamura, K. Takamiya, S. Aizawa, K. Furukawa, K. Furukawa, Gangliosides are the binding substances in neural cells for tetanus and botulinum toxins in mice, *Biochim. Biophys. Acta* 1441 (1999) 1-3.

11. S. Kozaki, Y. Kamata, S. Watarai, T. Nishiki, S. Mochida, Ganglioside G_{T1b} as a complementary receptor component for clostridium botulinum neurotoxins, *Microb. Pathog.* 25 (1998) 91-99.
12. L. Li, B.R. Singh, Isolation of synaptotagmin as a receptor for types A and E botulinum neurotoxin and analysis of their comparative binding using a new microtiter plate assay, *J. Nat. Toxins*, 7 (1998) 215-226.
13. K. Ginalski, C. Venclovas, B. Lesyng, K. Fidelis, Structure-based sequence alignment for the beta-trefoil subdomain of the clostridial neurotoxin family provides residue level information about the putative ganglioside binding site, *FEBS Letters*, 482 (2000) 119-124.
14. D.B. Lacy, W. Tepp, A. C. Cohen, B. R. DasGupta, R. C. Stevens, Crystal structure of botulinum neurotoxin type A and implications for toxicity, *Nature Struct. Biol.* 5 (1998) 898-902.
15. T. Binz , H. Kurazono , M. Wille, J. Frevert, K. Wernars, H. Neimann, The Complete Sequence of Botulinum Neurotoxin Type A and Comparison with other Clostridial Neurotoxins, *J. Biol. Chem.* 265 (1990) 9153-9158.
16. P. Emsley, C. Fotinou, I. Black, N. F. Fairweather, I. G. Charles, C. Watts, E. Hewitt, N.W. Isaacs, The structures of the H(C) fragment of tetanus toxin with carbohydrate subunit complexes provide insight into ganglioside binding, *J. Biol. Chem.* 275 (2000) 8889-8894.
17. J. M. Sutton, L. Spaven, N.J. Silman, B. Hallis, O. Chow-Worn, C. C. Shone, The Receptor binding domains of Clostridial Neurotoxins, in: M.F. Brin, J. Jankovic, M.

Hallett (Eds.) Scientific and therapeutic aspects of Botulinum Toxin, Lippincott Williams & Wilkins, Philadelphia, 2002, pp. 41-48.

18. C. Montecucco, O. Rossetto, G. Schiavo, Presynaptic receptor arrays for clostridial neurotoxins, *Trends in Microbiology* 12 (2004) 442-446.

19. L.A. Smith, M.P. Byrne, Vaccines for preventing Botulism, in: M.F. Brin, J. Jankovic, M. Hallett (Eds.) Scientific and therapeutic aspects of Botulinum Toxin, Lippincott Williams & Wilkins, Philadelphia, 2002, pp. 427-437.

20. L.L. Simpson, Identification of the characteristics that underlie botulinum toxin potency: implications for designing novel drugs, *Biochimie* 82 (2000) 943-53.

21. L.A. Smith, Development of recombinant vaccines for botulinum neurotoxin, *Toxicon* 36 (1998) 539-1548.

22. M. Tavallaie, A. Chenal, D. Gillet, Y. Pereira, M. Manich, M. Gibert, S. Raffestin, M.R. Popoff, J.C. Marvaud, Interaction between the two subdomains of the C-terminal part of the botulinum neurotoxin A is essential for the generation of protective antibodies, *FEBS Letters* 572 (2004) 299-306.

23. L. Li, B.R. Singh, In vitro translation of Type A Clostridium Botulinum neurotoxin heavy chain and analysis of its binding to rat synaptosomes, *J. Prot Chem.* 18 (1999) 89-95.

24. J.R. Whitaker, P.E. Granum, An absolute method for protein determination based on difference in absorbance at 235 and 280nm, *Anal. Biochem.* 109 (1980) 156-159.

25. S. Cai, H.K. Sarkar, B.R. Singh, Enhancement of the endopeptidase activity of Botulinum neurotoxin by its associated Proteins and Dithiothreitol, *Biochem.* 38 (1999) 6903-6910.

26. Y. Zhou, B.R. Singh, Cloning, high level expression, single step purification and binding activity of His6-tagged recombinant type B Botulinum neurotoxin heavy chain transmembrane and binding domain, *Protein Express. Purif.* 34 (2004) 8-16.

Figure Legends:

Figure 1. SDS-PAGE analysis of HCQ obtained in the supernatants of the wash steps during the purification of inclusion bodies. Lanes LM and HM, Low and High Molecular

weight markers (kDa), respectively; Lanes 1, 2, 3, 4 and 5, supernatants of first, second, third, fourth, and fifth wash, respectively.

Figure 2. SDS-PAGE analysis of HCQ obtained from His-Nickel affinity column chromatography. Lane M, Low molecular weight marker (kDa); Lane FL, fraction of solubilised inclusion body solution passing through the column after loading onto the column; Lane 1, washing fraction with equilibration buffer, containing β -mercaptoethanol; Lane 2, fraction with equilibration buffer containing, 20 mM imidazole, with no β -mercaptoethanol; Lanes 3 and 4, fractions eluted with 20 and 30 mM imidazole, respectively.

Figure 3. SDS-PAGE Analysis of eluents of His-Nickel Affinity gel column chromatography. Lane M, Low molecular weight marker (kDa); Lanes 1, 2, 3 and 4, 1mL elution fractions of elution buffer containing 100 mM imidazole.

Figure 4. Immuno dot blot assay of HCQ binding with BoNT/A antibodies. The colored spots indicate positive reaction of the sample against rabbit anti-BoNT/A antibody. BoNT/A heavy chain and BoNT/A complex were used as positive controls and BSA was used as a negative control. Concentration of each protein (HCQ, BoNT/A HC, BoNT/A complex and BSA) blotted on the nitrocellulose membrane was 0.1 mg/mL.

Figure 5. Western blot analysis of recombinant BoNT/A HCQ with antibody raised against BoNT/A toxin. The numbers on the left indicate the molecular mass of markers (kDa).

Figure 6. Immuno dot blot assay of HCQ binding with synaptotagmin. The colored spots indicate positive reaction of the sample with synaptotagmin which was monitored with anti-synaptotagmin IgG. BoNT/A complex was used as a positive control and BSA was used as a negative control. Concentration of each protein (HCQ, BoNT/A complex, and BSA) blotted on the nitrocellulose membrane was 0.1 mg/mL.

Figure 7. **A.** Enzyme-linked immunosorbent assay of binding activity of recombinant HCQ to ganglioside (G_{T1b}). HCQ (0.2 mg/mL), BoNT/A heavy chain (0.1 mg/mL) and BoNT/A complex (0.1 mg/mL) show positive results. **B.** *Concentration dependence of HCQ binding with GT1b as determined by ELISA. BoNT/A complex was used as a positive control, and BSA as a negative control for the HCQ binding. Values represent mean from three separate experiments with bars representing standard mean of deviations.*

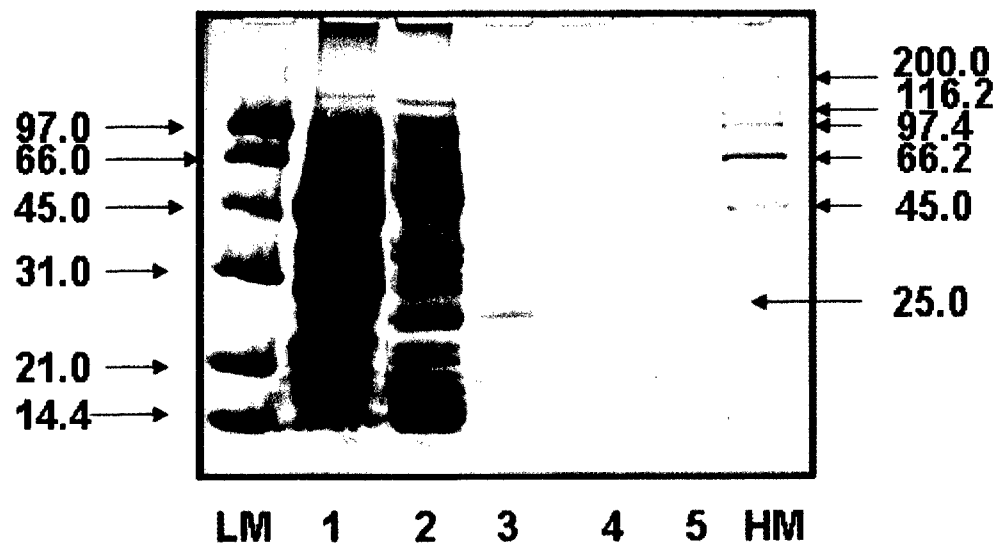


Figure 1

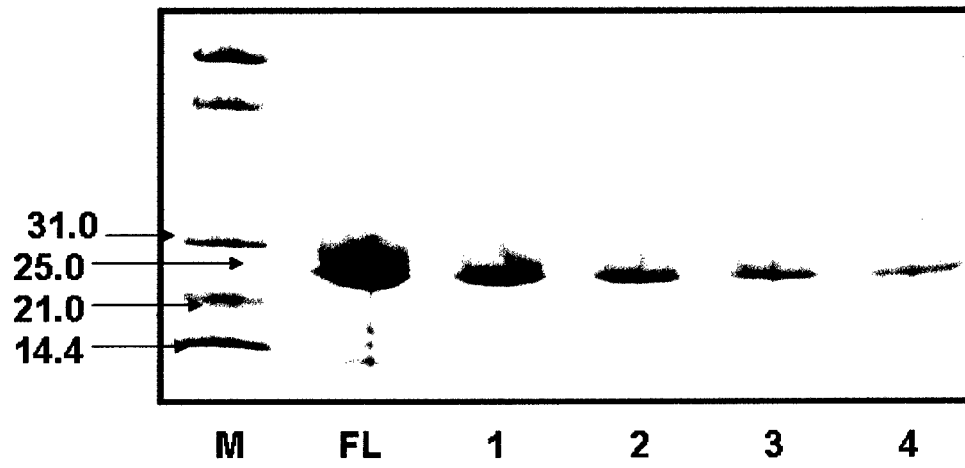


Figure 2

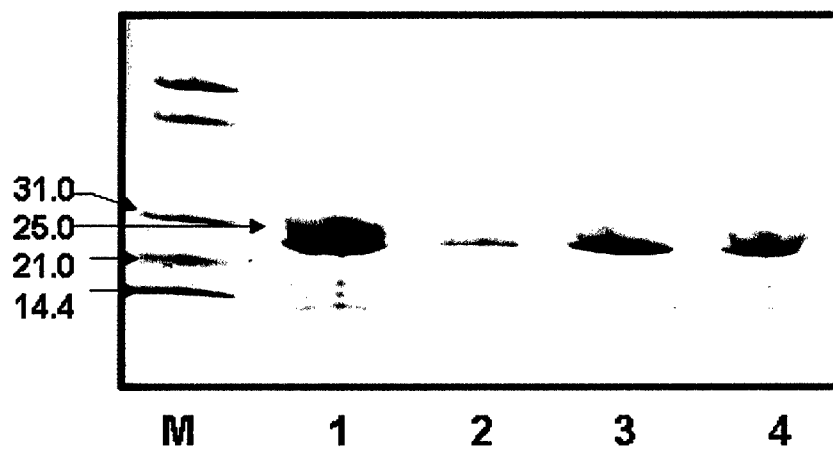


Figure 3

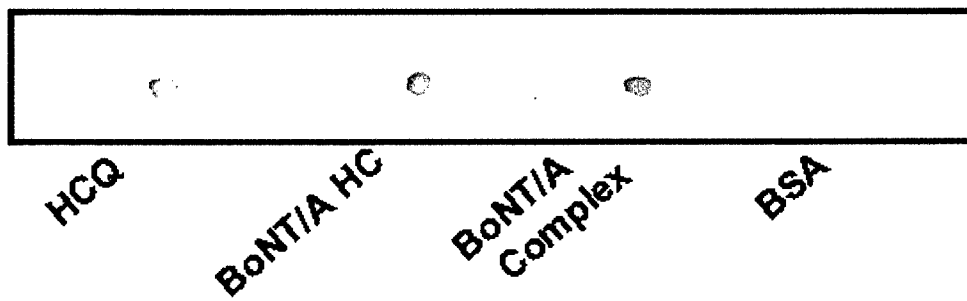


Figure 4

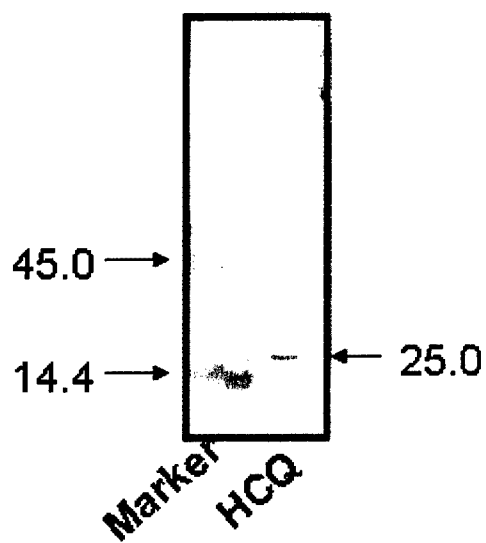


Figure 5

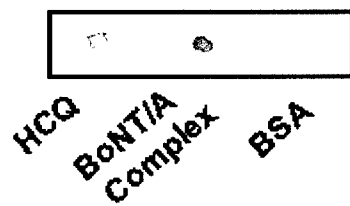


Figure 6

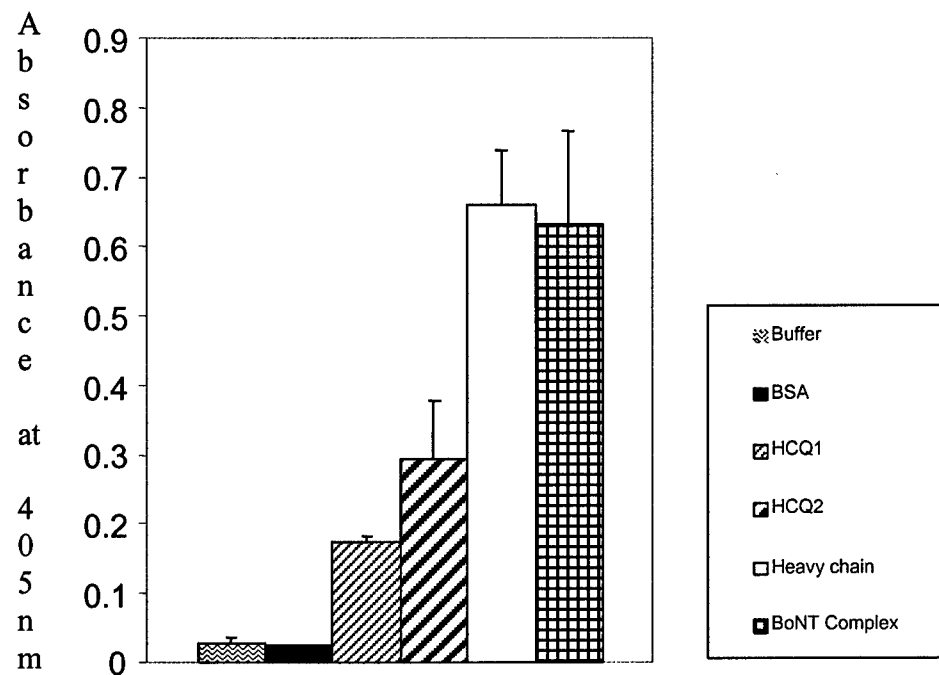


Figure 7A

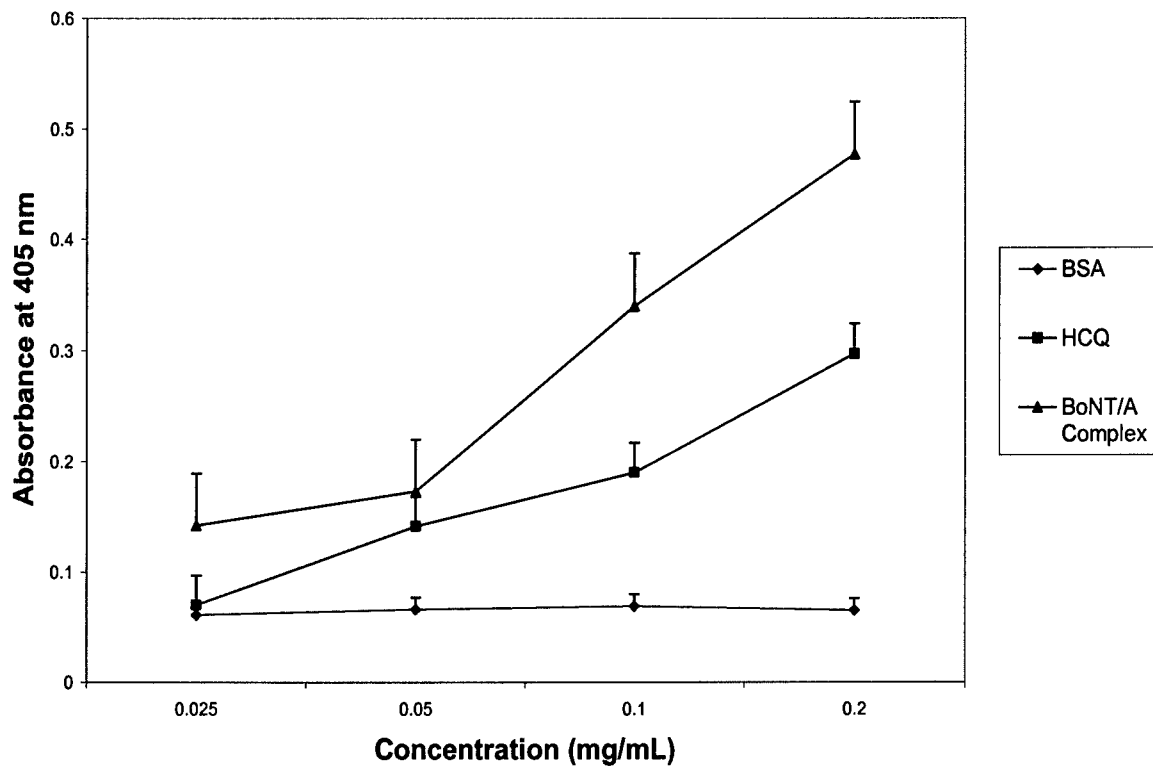


Figure 7B

Unique Physiological and Biochemical Response of Northern Quahog to Botulinum Neurotoxin

VIJAI KRISHNA DAS¹, SHOBHA DAS² and BAL RAM SINGH*
Department of Chemistry and Biochemistry, and Botulinum Research Center,
University of Massachusetts Dartmouth, Dartmouth, MA 02747, USA

Running title: Quahog response to botulinum

Key words: Biothreat, Botulinum, Diagnostics, Mercenaria, Neurotoxin, Quahog Toxicity

*To whom correspondence should be addressed:

Bal Ram Singh
Department of Chemistry and Biochemistry
University of Massachusetts Dartmouth
285 Old Westport Road
Dartmouth, MA 02747, USA

Phone: 508-999-8588

Fax: 508-999-8451

Email: bsingh@umassd.edu

¹Permanent address: Department of Zoology, Kamla Nehru Institute of Physical and Social Sciences, Sultanpur 228118, India

²Permanent address: Department of Zoology, Ganpati Sahai Post Graduate College, Sultanpur 228118, India

ABSTRACT

Botulinum neurotoxins are the most poisonous poisons and biothreat agents which block acetylcholine release at nerve-muscle junctions causing flaccid muscle paralysis. High doses (more than thousand mouse LD₅₀ units) of type A botulinum neurotoxins were injected in the anterior adductor muscles of northern quahog, *Mercenaria mercenaria*, to test its effect on muscle paralysis and lethality to quahogs. While no muscle paralysis or mortality was observed, the quahogs responded to the toxin injection with ejection of mucus and browning of tissues. Quahogs also responded biochemically in terms of significant reduction (30%) in the activity of one of the stress proteins, glutathione-S-transferase. These findings are relevant to developing an invertebrate animal assay model for assay and diagnostics of the botulinum biothreat.

INTRODUCTION

Botulinum neurotoxin (BoNT) is produced by the anaerobic bacterium *Clostridium botulinum* and is generally regarded as the most poisonous of all poisons in nature [1,2]. There are seven serotypes of botulinum toxins, type A-G, exert their paralytic effect by inhibiting acetylcholine release at the neuromuscular junction. The extent of paralysis is dependent on doses, volume and the potency of serotype employed.

Studies of BoNT toxicity revealed remarkable differences in the toxic dose among different species. Biological activity of the toxin is measured in mouse units. Swiss-Webster-mouse LD 50, is the amount of toxin required to kill 50% of mice after IP injection[3], reported LD₅₀ for mice 0.1-1.0 ng/Kg causing death 6-24 hours after injection. There is no published report for botulinum toxicity from invertebrates. Preliminary toxicity test in our laboratory indicated that quahogs are resistant to BoNT. Invertebrates nerves are known to be relatively insensitive to the Paralytic Shellfish Toxins (PSTs) – a potent neurotoxin produced by several species of marine dinoflagellates [4]. Gubbins et al. [5], observed no mortality in mussels and scallops subjected to Saxitoxin but reported glutathione-S-transferase (GST) activity was induced by high doses of STX (> 100 µg/kg) at 2 – 8 days after exposure in mussel (*Mytilus edulis*). At the same time, no significant difference between control and exposed scallops (*Pecten maximus*). Glutathione –S-transferases (GST) are a family of multifunctional ubiquitous enzymes found in almost all living organisms [6, 7, 8, 9, 10, 11, 12]. Multiple forms of GST are known to function in different capacities: intracellular detoxification of drugs, carcinogens and decreasing stress of xenobiotic compounds, intracellular carrier proteins and reduction of hydroperoxides and nitrates. Because of its role in the

detoxification and removal of xenobiotics, it has been recognized as a biomarker of pollution and stress [9, 13, 14, 15, 16, 17, 18, 19, 20].

The aim of present study is to test the toxicity of BoNT on northern quahog *Mercinaria mercinaria* and to examine if BoNT/A can induce GST activity. Our results show that while the quahogs survive even heavy dose of BoNT/A, the neurotoxin causes significant morphological and physiological changes, including the activity of glutathione-S-transferases.

MATERIALS AND METHODS

Quahogs (clams) were purchased from Captain Frank's Seafood, New Bedford, MA. (Length 80-85 mm; Height 75-80 mm; Weight 145-160 g). They were maintained in laboratory for 2 weeks in seawater and aeration was provided by air bubbling using Spectra/Chrom MP- 1 Pump; room temperature varied from 24 ° – 27 ° C . Clams were not fed, and subjected to natural light cycle.

The clams were divided into two groups. The controls received 200 µL of buffer (20 mM sodium phosphate buffer, pH 7.9) injection into the anterior adductor muscle by inserting a hypodermic needle through a notch filed into the edge of the shell. The experimental group received 20 µg and 96 µg doses (in 200 µL of 20 mM phosphate buffer, pH 7.9) BONT/A complex injection into the anterior adductor muscle using a 1 ml Sub Q (0.45 mm X 16 mm) syringe (BD & CO., Franklin Lakes, NJ). After 3, 6 & 9 days, the shells were removed from the quahogs of control and experimental groups and animals were

dissected out quickly in ice to collect the nervous tissue (cerebral, pedal and visceral ganglions and the connecting nerves), anterior adductor muscle, digestive gland, foot and gill were collected and rinsed in 100 mM phosphate buffer, pH 6.8; dried on absorbent paper and then weighed.

The crude extract was prepared according to Blanchette and Singh [11] by homogenizing the tissues in grinding buffer (100 mM sodium phosphate, 300 mM sucrose, 1 mM ethylenediaminetetraacetic acid or EDTA, pH 6.8 and 6.8 mL of 200 mM phenylmethylsulphonyl fluoride = PMSF; final concentration, ~2mM; in a 1:4 tissue wt: volume ratio of the buffer. The homogenization was carried out at high speed for 60 seconds at 4°C using a Polytron homogenizer (Brinkmann Instruments, Kinematica GmbH, Switzerland). The homogenates were then centrifuged at 16,000 g for 30 min in a Dupont Sorvall SLA – 1500 rotor at 4°C using a Sorvall RC -5B centrifuge. The supernatant was collected for GST activity.

GST activities were measured on Jasco-V-550 Spectrophotometer according to method of Habig et al., 1974 [21], by taking 50 µL of 20mM CDNB (1-chloro-2,4-dinitrobenzene) and 50 µL of 20 mM reduced glutathione in 1 mL reaction mixture. The progress of reaction was monitored by measuring the absorbance change at 340 nm.

Protein Assay

Protein concentration of the crude extract was determined by the Bradford [22], method, with protein assay kit purchased from Bio-Rad (Hercules, CA). Bovine serum albumin (BSA) was used as a standard.

Enzyme Kinetics

The initial rate kinetics of quahog GST with respect to glutathione was examined by measuring the initial rate of conjugation reaction while varying the GSH concentration and keeping the CDNB concentration constant. A control experiment was performed using the same concentration of GSH and CDNB in the absence of GST, and the initial rate in the presence of GST was corrected for the control. Lineweaver-Burk analysis was performed by plotting $1/v$ versus $1/[GSH]$. K_m and V_{max} values were determined from the slope (k_m/V_{max}) and y-intercept ($1/V_{max}$) of the plot.

RESULTS AND DISCUSSION

Toxicity Test

Quahogs were injected with different doses of botulinum neurotoxin- BoNT/A complex, BoNT/B complex and BoNT/F complex for varying time intervals and no mortality was observed even after injecting very high doses (180 μg BoNT/A complex and 150 μg BoNT/F). Moreover, there was no visible dysfunction observed in the quahog's ability to shut its shell, indicating no signs of muscle paralysis. In a similar experiment, [4], had injected *Mytilus edulis* intramuscularly with different doses (10,33,100 and 330 $\mu\text{g}/100$ g body weight) of saxitoxin (paralytic shellfish toxin-PST), and observed no mortality in the mussels in 8-day experimental observations.

Morphology

The quahogs administered with 20 µg and 96 µg of BoNT/A complex for 3, 6 and 9 days exhibited browning of the body color and an apparent morbidity in the flesh (Fig.1). These changes were more pronounced in the quahogs injected with 96 µg of BoNT/A complex. On the other hand, the controls receiving vehicle (the phosphate buffer) showed cream colored body with more contractile activity in the adductor muscles and foot as compared to BoNT injected quahogs.

Turbidity Test

The first reaction of the BoNT/A complex injected quahogs was that they started ejecting out some milky mucus (within 2-3 hours after injection) from the small pore formed towards anterior adductor muscles. Due to this activity, the color of the seawater becomes milky within the first day after receiving the BoNT injection as compared to controls. The water from containers was checked for absorbance at 600 nm on the spectrophotometer, it exhibits a significant increase in the turbidity in experimental animals (Fig. 2).

Effect on GST

The tissue distribution of GST activity towards CDNB has been found to be ubiquitous, in *Mytilus edulis*, Fitzpatrick et al, 1997 [13], *Astacus astacu* [23], and *Corbicula fluminea* [12]. In quahog (*Mercinaria mercinaria*), it was predominant in the digestive gland and lesser extent in the nervous tissue and gills [12], also reported predominant level of GST in the visceral mass (65%) and to a lesser extent in gill (18%) of *C. fluminea*. Similarly very high level of GST was recorded in digestive glands as compared to gills of Antarctic Scallop by Regoli et al. [24]. The digestive gland in mollusca

functions analogous to vertebrate liver in which high level of GST activity is encountered. However, in some mussel species, gills possess higher GST activity relative to other organs e.g. *M. edulis* [13], *Perna viridus* [25].

In present study, we examined the level of GST activity in digestive gland (DG), gill and nerve tissues of quahogs before and after administering with 20 µg and 96 µg of BoNT/A complex (**Fig. 3**). In untreated quahogs, GST specific activity was 1.35 ± 0.75 , 1.72 ± 0.97 , and 0.97 ± 0.11 µmol/min/mg protein in DG, nerve, and gills, respectively, which remained at 10.73 ± 0.87 , 1.70 ± 0.01 , and 1.49 ± 0.11 µmol/min/mg protein 3 days after injection with buffer (**Table 2**). GST activity measured 3, 6 and 9 days after injection with buffer or BoNT/A complex was exhibits a significant ($p < 0.5$ to < 0.001) decrease (~30%) in GST activity in the digestive gland when compared to controls. The nervous tissue records a minor decrease in GST after 3 days in both (20 and 96 µg injections) the treated groups, thereafter 96 µg injected quahogs show a recovery in GST activity whereas 20 µg injected groups do not exhibit any difference. Gills, on the other hand, record a significant decrease only after 3 days in BoNT injected quahogs (**Fig. 3, Table 2**).

Other organisms exposed to Xenobiotic compounds also showed a decrease in GST activity. For example, oral administration of PCB-105 resulted a significant reduction in GST in trout (*O. mykiss*) while in cod (*Gradus morhua*) no significant change was observed [26]. There are reports from several mollusks where GST activity is reduced. For example, Lee [27], recorded a decrease in GST activity, 1-2 folds, 78 nmol/min/mg to 37 nmol/min/mg) upon PCB exposure in *Mytilus edulis*. Michel et al [28] also reported

depression in GST activity of whole mussel cytosol when exposed to Benzopyrene. Akcha et al. [14], observed reduced GST activity in *Mytilus galloprovincialis* hepatopancreas from highly polluted site. Vidal et al. [29], reported that GST activity in *C. fluminea* towards CDNB and EA (ethycranic acid) remained unaffected by exposure to trichloroethylene, toluene and a complex mixture of polycyclic aromatic hydrocarbons, whereas it displayed a reduced GST activity towards CDNB when exposed to cadmium. On the other hand, the GST activity of hepatopancreas of *Perna viridis* had increased at day 6 and 12 followed by a decrease on day 18 [19]. This biphasic response was described as an inhibitory effect due to high concentration of contaminants in mussel tissue or an adaptive response in which the mussel abandoned the GST detoxification pathway in favour of some different pathway.

There are reports suggesting induced GST activity in response to metals and organic contaminants in *Mercenaria mercenaria* [18], *Perna viridis*, [19], Rainbow trout [15], *Amerius nebulosus* [17], *Mytilus edulis* and salmon [5], and *Carassius auratus* [20]. Recently, Zhang et al. [20] concluded that a fall in GSH levels may lead to an induction in GST activity of gold fish.

Our experimental findings clearly indicate that the quahogs do not die even at very high dose (180 µg) of BoNT/A, but they undergo some distress showing ejection of mucus as an immediate response and browning of the body color. Decrease in GST activity after receiving 20 µg and 96 µg doses is biochemical response either to the neurotoxin or to the distress caused by the neurotoxin.

Browning of the body color in *Mercenaria mercenaria* has been reported as an immediate response of environmental contamination and a role of red glands is suggested in detoxification by Zarogian et al. [30]. The responses of quahogs towards BoNT/A, the most poisonous poison [1, 2], with its toxicity ~100 billion times more toxic than cyanide, may be the result of the general detoxification response. It is very much possible that the doses used (20 µg and 96 µg) may be too high which may have abandoned the GST detoxification mechanism leading to a significant decrease in the digestive gland from day 3 to day 9. However, there is a recovery in the nervous tissue on 6th and 9th day of 96 µg injected quahogs. There is little change in the gill tissue. Gubbins et al. [4], also observed no mortality in mussel and scallop subjected to another toxin - PST (saxitoxin) at 330 µg and concluded invertebrate nerves are insensitive to PST. However, the mussels show an increased GST after PST exposure whereas scallops show no response.

Effect of botulinum neurotoxin on quahog could provide a convenient biological assay system, based on the mucus release and tissue browning. Also, the GST response to botulinum neurotoxin could be used as a biomarker in designing a comprehensive diagnostic system for botulism. However, further investigations are required in order to fully understand how the BoNT acts on the tissue GST response of quahogs.

ACKNOWLEDGEMENTS

This work was supported by a grant from the U.S. Army Medical Research and Material Command under Contract No. DAMD17-02-C-001 and by the National Institutes of Health through New England Center of Excellence for Biodefense (AI057159-01).

Table1: Mortality of quahogs upon injection with botulinum neurotoxins.

Neurotoxin Type	Dose	Number of days monitored	Mortality
BoNT/A complex	180 µg	6 days	-
	96 µg	18 days	-
	20 µg	18 days	-
	5.5 µg	18 days	-
BoNT/B complex	30 µg	18 days	-
BoNT/F complex	150 µg	10 days	-
	60 µg	10 days	-

Table2: GST Activity ($\mu\text{mole}/\text{min}/\text{mg}$) in quahog after BoNT administration

Period	Treatment	Digestive Gland	Nerve	Gill
	Untreated Control	10.35 \pm 0.75	1.72 \pm 0.97	0.97 \pm 0.11
3 days	Control	10.73 \pm 0.87	1.70 \pm 0.01	1.49 \pm 0.11
	BoNT-A 20μg	8.45 \pm 0.45 (p<0.01)	1.47 \pm 0.20	0.57 \pm 0.21 (p<0.001)
	BoNT-A 96μg	6.46 \pm 0.14 (p<0.001)	1.10 \pm 0.19 (p<0.01)	0.64 \pm 0.12 (p<0.01)
6 days	Control	9.54 \pm 1.25	1.60 \pm 0.04	0.53 \pm 0.04
	BoNT-A 20μg	6.83 \pm 0.38 (p<0.05)	0.93 \pm 0.34	0.54 \pm 0.05
	BoNT-A 96μg	6.65 \pm 0.54 (p<0.01)	1.83 \pm 0.07	0.68 \pm 0.18
9 days	Control	9.335 \pm 0.14	1.9 \pm 0.12	0.64 \pm 0.23
	BoNT-A 20μg	6.85 \pm 0.14 (p<0.001)	0.56 \pm 0.09 (p<0.001)	0.43 \pm 0.02
	BoNT-A 96μg	7.16 \pm 0.68 (p<0.05)	1.58 \pm 0.35	0.41 \pm 0.07

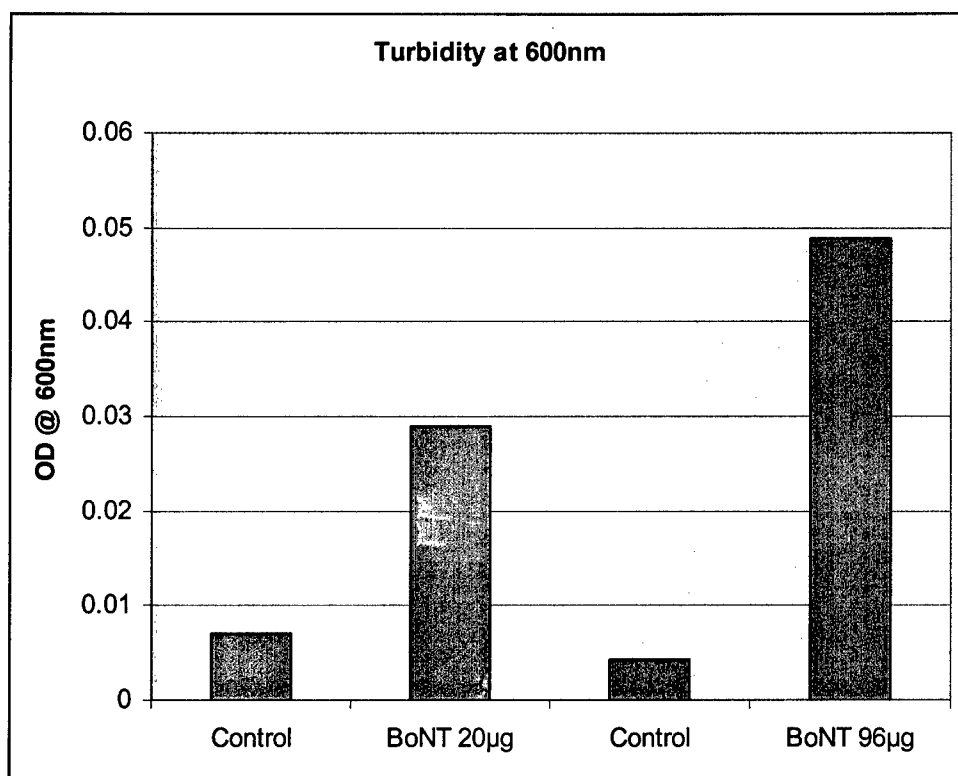
Figure Legends

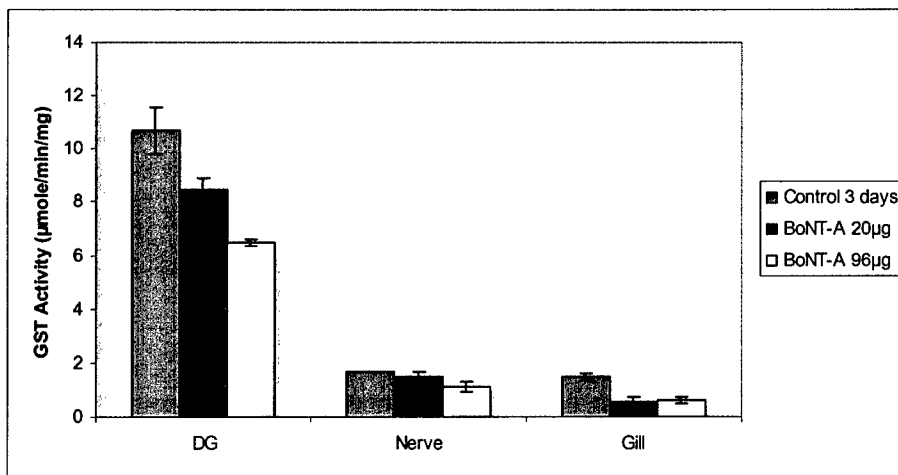
Fig. 1. *Inner morphology of quahog after injection with BoNT/A complex. (a)* Quahog injected with 96 μg of BoNT-A complex after 6 days. **(b)** Quahog control injected with vehicle (20 mM phosphate buffer, pH 7.9).

Fig 2. Turbidity of seawater in the surrounding of quahog injected with 96 μg BoNT/A complex. In control experiments, the quahogs were injected with 20 mM phosphate buffer, pH 7.9.

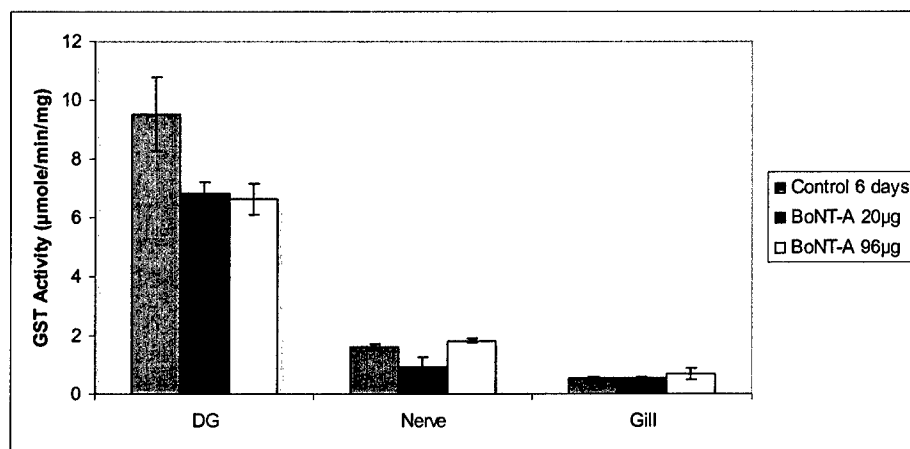
Fig 3. Effect of BoNT/A injection on the glutathione-S-transferase activity in digestive gland, nerve, and gills of quahog.



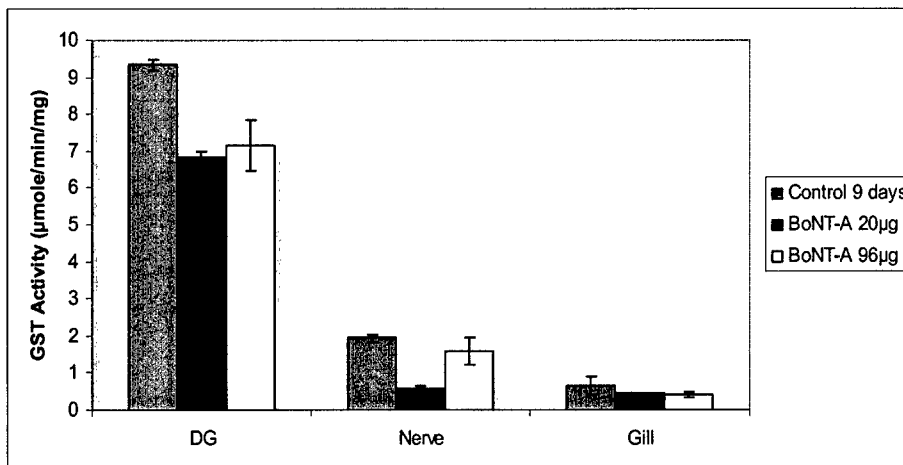




(a) BoNT-A 3 days exposure



(b) BoNT-A 6 days exposure



(c) BoNT-A 9 days exposure

REFERENCES

- [1] Lamanna, C. 1959. The most poisonous poison. *Science* 130: 763-72.
- [2] Singh, B. R. 2000. Intimate details of the most poisonous poison. *Nat Struct Biol* 7, no. 8: 617-9.
- [3] Gill, D. M. 1982. Bacterial toxins: a table of lethal amounts. *Microbiol Rev* 46, no. 1: 86-94.
- [4] Gubbins, M. J. 2002. Xenobiotic metabolising enzymes in fish and shellfish exposed to paralytic shellfish toxins. Ph.D. Thesis. University of Dundee.
- [5] Gubbins, M. J., F. B. Eddy, S. Gallacher, and R. M. Stagg. 2002. Biological Effects of Paralytic Shellfish Toxins on Atlantic Salmon and Bivalve Molluscs. <http://www.marlab.ac.uk/FRS.Web/Uploads/Documents/Biologicalaeffects.pdf>
- [6] Stenersen, J., S. Kobro, M. Bjerke, and U. Arend. 1987. Glutathione transferases in aquatic and terrestrial animals from nine phyla. *Comp Biochem Physiol C* 86, no. 1: 73-82.
- [7] Keeran, W. S., and R. F. Lee. 1987. The purification and characterization of glutathione S-transferase from the hepatopancreas of the blue crab, *Callinectes sapidus*. *Arch Biochem Biophys* 255, no. 2: 233-43.
- [8] Lin, K. S., and N. N. Chuang. 1993. Anionic glutathione S-transferases in shrimp eyes. *Comp Biochem Physiol B* 105, no. 1: 151-6.
- [9] Fitzpatrick, Patrick J., David Sheehan, and David R. Livingstone. 1995. Studies on isoenzymes of glutathione S-transferase in the digestive gland of *Mytilus galloprovincialis* with exposure to pollution. *Mar. Environ. Res.* 39, no. 1-4: 241-44.
- [10] Gallagher, E. P., P. L. Stapleton, D. H. Slone, D. Schlenk, and D. L. Eaton. 1996. Channel catfish glutathione S-transferase isoenzyme activity toward (plus or minus)-anti- benzo[a]pyrene -trans-7,8-dihydrodiol-9,10-epoxide. *Aquat. Toxicol* 34, no. 2: 135-50.
- [11] Blanchette, B. N., and B. R. Singh. 1999. Purification and Characterization of the Glutathione-S-transferases from the Northern Quahog *Mercinaria mercinaria*. *Mar Biotechnol (NY)* 1, no. 1: 74-80.
- [12] Vidal, M. L., and J. F. Narbonne. 2000. Characterization of glutathione S-transferase activity in the Asiatic clam *Corbicula fluminea*. *Bull Environ Contam Toxicol* 64, no. 3: 455-62.
- [13] Fitzpatrick, P. J. O'Halloran J. Sheehan D. and Walsh A. R. 1997. Assessment of a glutathione S-transferase and related proteins in the gill and digestive gland of *Mytilus edulis* (L.), as potential organic pollution biomarkers. *Biomarkers* 2, no. 1: 51-56.

-
- [14] Akcha, F., C. Izuel, P. Venier, H. Budzinski, T. Burgeot, and J. Narbonne. 2000. Enzymatic biomarker measurement and study of DNA adduct formation in benzo. *Aquatic Toxicol* 49, no. 4: 269-87.
- [15] Perez-Lopez, M., P. Anglade, M. P. Bec-Ferte, L. Debrauwer, E. Perdu, J. P. Cravedi, and P. Rouimi. 2000. Characterization of hepatic and extrahepatic glutathione S-transferases in rainbow trout (*Oncorhynchus mykiss*) and their induction by 3,3',4,4'-tetrachlorobiphenyl. *Fish Physiol. Biochem.* 22, no. 1: 21-32.
- [16] Livingstone, D. R., J. K. Chipman, D. M. Lowe, C. Minier, C. L. Mitchelmore, M. N. Moore, L. D. Peters, and R. K. Pipe. 2000. Development of biomarkers to detect the effects of organic pollution on aquatic invertebrates: recent molecular, genotoxic, cellular and immunological studies on the common mussel (*Mytilus edulis* L.) and other mytilids. *Int. J. Environ. Pollut.* 13, no. 1: 56-91.
- [17] Henson, K. L., G. Stauffer, and E. P. Gallagher. 2001. Induction of glutathione S-transferase activity and protein expression in brown bullhead (*Ameiurus nebulosus*) liver by ethoxyquin. *Toxicol Sci* 62, no. 1: 54-60.
- [18] Blanchette, B. N., and B. R. Singh. 2002. Induction of glutathione-S-transferase in the Northern quahog *Mercenaria mercenaria* after exposure to the polychlorinated biphenyl (PCB) mixture Aroclor 1248. *J Protein Chem* 21, no. 8: 489-94.
- [19] Cheung, C. C., W. H. Siu, B. J. Richardson, S. B. De Luca-Abbott, and P. K. Lam. 2004. Antioxidant responses to benzo[a]pyrene and Aroclor 1254 exposure in the green-lipped mussel, *Perna viridis*. *Environ Pollut* 128, no. 3: 393-403.
- [20] Zhang, J., H. Shen, X. Wang, J. Wu, and Y. Xue. 2004. Effects of chronic exposure of 2,4-dichlorophenol on the antioxidant system in liver of freshwater fish *Carassius auratus*. *Chemosphere* 55, no. 2: 167-74.
- [21] Habig, W. H., M. J. Pabst, and W. B. Jakoby. 1974. Glutathione S-transferases. The first enzymatic step in mercapturic acid formation. *J Biol Chem* 249, no. 22: 7130-9.
- [22] Bradford, M. M. 1976. A rapid and sensitive method for the quantitation of microgram quantities of protein utilizing the principle of protein-dye binding. *Anal Biochem* 72: 248-54.
- [23] Lindstrom-Seppa, P., U. Koivusaari, and O. Hanninen. 1983. Metabolism of Foreign Compounds in Fresh Water Crayfish (*Astacus astacus* L.) tissues: Fresh Water Crayfish *Astacus-Astacus* Tissues. *Aquatic Toxicol* 3, no. 1: 35-46.
- [24] Regoli, F., G. B. Principato, E. Bertoli, M. Nigro, and E. Orlando. 1997. Biochemical characterization of the antioxidant system in the scallop *Adamussium colbecki*, a sentinel organism for monitoring the Antarctic environment. *Polar Biol.* 17, no. 3: 251-58.
- [25] Cheung, C. C., G. J. Zheng, A. M. Li, B. J. Richardson, and P. K. Lam. 2001. Relationships between tissue concentrations of polycyclic aromatic hydrocarbons and

antioxidative responses of marine mussels, *Perna viridis*. *Aquat Toxicol* 52, no. 3-4: 189-203.

[26] Bernhoft, A., H. Hektoen, J. U. Skaare, and K. Ingebrigtsen. 1995. Distribution and effects on hepatic xenobiotic metabolizing enzymes of 2,3,3',4,4'-pentachlorobiphenyl (PCB-105) in cod (*Gadus Morhua* and rainbow trout (*Oncorhynchus mykiss*). *Seventh International Symposium on Responses of Marine Organisms to Pollutants (PRIMO 7)*, 343-48.

[27] Lee, RF. 1988. Glutathione S-transferase in marine invertebrates from Langesundfjord: BIOLOGICAL EFFECTS OF POLLUTANTS. RESULTS OF A PRACTICAL WORKSHOP; Practical Workshop on Biological Effects of Pollutants, Oslo (Norway), Aug 1986. *Marine Ecology Progress Series* 46, no. 1-3: 33-36.

[28] Michel, X. R., P. Suteau, L. W. Robertson, and J. F Narbonne. 1993. Effects of benzo(a)pyrene, 3,3',4,4'-tetrachlorobiphenyl and 2,2',4,4',5,5'-hexachlorobiphenyl on the xenobiotic-metabolizing enzymes in the mussel (*Mytilus galloprovincialis*). *Aquatic Toxicol.* 27, no. 3-4: 335-44.

[29] Vidal, M., A. Basseres, and J. Narbonne. 2001. Potential biomarkers of trichloroethylene and toluene exposure in *Corbicula fluminea*. *Environ. Toxicol. Pharmacol.* 9, no. 3: 87-97.

[30] Zaroogian, G., P. Yevich, and S. Pavignano. 1989. The role of the red gland in *Mercenaria mercenaria* in detoxification: RESPONSES OF MARINE ORGANISMS TO POLLUTANTS; 5. Int. Symp. on Responses of Marine Organisms to Pollutants, Plymouth (UK), 12 Apr 1989. *Mar. Environ. Res.* 28, no. 1-4 : 447-50.

**Comparative Membrane Channel Size and Activity of Botulinum
Neurotoxins A and E.**

Sweta Parikh and Bal Ram Singh

Botulinum Research Center, and Department of Chemistry and Biochemistry,
University of Massachusetts Dartmouth, 285 Old Westport Road, Dartmouth, MA
02747

Running Title: Botulinum membrane channel

Keywords: Antibody, Botulinum, Calcein, Channel, Fluorescence, Liposome,
Membrane

To whom correspondence should be addressed:

Bal Ram Singh
Department of Chemistry and Biochemistry
University of Massachusetts Dartmouth
285 Old Westport Road
Dartmouth, MA 02747, USA

Phone: 508-999-8588

Fax: 508-999-8451

Email: bsingh@umassd.edu

ABSTRACT

In an effort to compare the molecular basis of differential toxic activity of botulinum neurotoxin A (BoNT/A) and BoNT/E, we have analyzed their membrane channel activity by measuring calcein release from liposomes. Both BoNT/A and /E showed a same level of membrane channel activity that was specifically blocked by IgG specific to the neurotoxins. With the use of fluorescein-labeled dextran, we determined that the size of the channel is at least 24.2 Å which is appropriate for the translocation of a protein of 50 kDa (the light chain of BoNT). These findings would suggest that the difference in the toxicity level of the two BoNT serotypes might reflect differences in either endopeptidase activity or their binding to receptor(s).

INTRODUCTION

BoNTs are large proteins (150 kDa, synthesized as inactive single polypeptide chain which are activated by endogenous or exogenous protease nicking to form a dichain molecule (a 50 kDa light chain and a 100 kDa heavy chain) linked through a disulfide bond. The proteolytic strains of *C. botulinum* (e.g., type A) produce endogenous proteases [1], but non-proteolytic strains of *C. botulinum* (type E) require exogenous proteases, such as trypsin in the intestinal tract for activation [2]. The light chains (LCs) of neurotoxins are, in fact, zinc-endopeptidases, which cleave several proteins involved in synaptic vesicle docking and fusion complex and block the release of acetylcholine [3, 4]. The heavy chain (HC) plays an accessory role of binding to the target nerve cells and translocating the light chain into the cell cytoplasm.

The mode of BoNT action is not well understood at the molecular level. A working model exists [5], involving three major steps of binding, internalization and translocation, and intracellular enzymatic activity:

Binding of the neurotoxin to presynaptic membranes occurs through the C-terminal half of the H chain. The C-terminal half of the H chain binds to the gangliosides on the presynaptic membrane [6], followed by its subsequent binding to a protein receptor. After binding, the neurotoxin is internalized through endocytosis. The pH of the endosome is lowered to below 5.5 which leads to the integration of the N-terminal half of the H chain to form a membrane channel/transporter [7], through which L chain is translocated into the cytoplasm [8]. It has been shown that the H chain incorporates spontaneously into lipid

bilayers to form channels that allow ions up to 15 Å in minimal dimension to pass through [8-10].

The BoNT translocation mechanism although believed to be similar to other dichain toxins, especially to diphtheria toxin (which is one of the most investigated dichain bacterial toxins [9, 11, 12], there is no clear consensus or understanding of the process. To begin with, BoNT and TeNT (closely related in structure and function with BoNT) have different mechanism involved in the translocation, as the TeNT undergoes retrograde translocation whereas BoNT exits endocytic vesicles in the presynaptic region of the axon [13]. Even among the BoNTs there is clear difference in their translocation. For example, Keller et al. [14], in their experiments with primary neuronal cell culture observed that BoNT/E translocates much faster than BoNT/A.

In this study, we have analyzed the membrane channel activity of BoNT/A and BoNT/E to understand the molecular basis of the membrane translocation of the neurotoxin using liposomes as an artificial membrane. The technique to detect the channel size in our experiment is such that the neurotoxin acts from outside, rather than from inside as is the case in the endosome. The dye inside the liposome passes through the channel formed by the toxin, and is detected by an increase in the fluorescence signal.

Materials and Methods

Botulinum neurotoxins A and E were isolated from *Clostridium botulinum* strains Hall and Alaska, respectively, according to procedures published previously [15, 16]. Horse serum against, BoNT/A (horse serum 43) and BoNT/E

(horse serum 41) was provided by USAMRIID. Rabbit serum containing BoNT/A specific antibody (lot # 6067) was supplied by Dr. Lee, USDA. DEAE-Sephadex A-50, CM-Sepharose and DEAE-Sephacel were obtained from Pharmacia Biotech, Inc., Piscataway, N.J.

Isolation of specific antibodies against BoNT/A and BoNT/E.

Specific antibodies against BoNT/A and BoNT/E were isolated from horse and rabbit sera using toxin affinity column chromatography. Each of the BoNT/A and BoNT/E affinity columns was prepared by coupling the neurotoxin to Affi-Gel-15 (Bio-Rad, Richmond, CA), an N-hydroxyl succinimide ester of cross-linked agarose, as described previously [17, 18]. 1.5 mg of BoNT/A or BoNT/E was loaded on a Affi-Gel-15 column (1 ml), which was equilibrated with 0.1 M sodium bicarbonate buffer, pH 9.0 (washing buffer). The affinity column was agitated thoroughly for 1 hour at room temperature (25 °C) and then slowly agitated at 4 °C for 3 hours on a rocker, where complete coupling was allowed to take place. 0.1 ml of 1.0 M ethanolamine (Sigma Chemical Co., St. Louis, MO) was applied to the column for one hour to block any remaining reactive groups. The affinity column was washed with the washing buffer until the uncoupled ligand was eluted i.e. until the absorbance of the eluant read zero at 280 nm. At this point the affinity column of BoNT/A or BoNT/E was ready for purification of specific Immunoglobulin (IgG).

In order to isolate IgG fractions of rabbit and horse sera against BoNT/A and BoNT/E, each serum was applied to a protein G-agarose column (Sigma Chemical Co., Louis, MO). The serum was incubated with protein G column for

30 min, washed with 0.1 M sodium bicarbonate buffer, pH 9.0, and the IgG was eluted with 0.5 M ammonium acetate, pH 3.0. IgGs were dialyzed overnight with 0.15 M phosphate buffer saline (PBS) buffer, pH 7.4. Respective IgG (2 mg) fraction was applied to the BoNT/A and BoNT/E affinity column, which were equilibrated with 0.15 M PBS (phosphate buffered saline) buffer, pH 7.4, and incubated for 2 hours at 25 °C. Columns were further washed with 0.15 M PBS buffer, pH 7.4, to remove all the unbound IgG. BoNT specific IgG was eluted with 0.1 M glycine buffer, pH 2.5. Specific IgG fraction was pooled and dialyzed overnight with 0.1 M PBS, pH 7.4. Analysis of binding of specific IgG to BoNT/A and BoNT/E using Enzyme Linked Immunosorbent Assay (ELISA)

100 μ l of 20 μ g/ml of BoNT/A or BoNT/E was added in each well of the microtiter plate and incubated at 4 °C overnight. The wells were washed twice with 0.1% TWEEN 20 in PBS using a microplatter washer (Molecular Devices, Sunnyvale, CA). In order to prevent the non-specific binding of the primary and secondary antibody to the microtiter plate, 300 μ l of 3% BSA (bovine serum albumin) solution was added to each well as a blocking agent and incubated at 37 °C for 1 hour. Wells were subsequently washed five times with the washing buffer. Five-fold serial dilution of specific primary antibody (i.e. the one isolated from the affinity column) were made in PBS-BSA solution, applied to the plate, incubated for 2 hours at 37 °C and washed five times. Enzyme-linked secondary antibody, goat anti-rabbit antibody with labeled peroxidase, dilution titer of 1:28,000 (Sigma Chemical Co., St. Louis, MO) against BoNT/A IgG, and rabbit anti-horse antibody with labeled peroxidase, dilution titer of 1:20,000 (Sigma Chemical Co., St. Louis, MO) against BoNT/E IgG were applied to respective

plates and incubated for 1 hour at 37 °C. Enzymatic substrate solution for the detection of binding was 0.04% o-phenylenediamine dihydrochloride and 0.012% H₂O₂ (Sigma Chemical Co., St. Louis, MO) in phosphate-citrate buffer, pH 5.0. 100 µl of this solution was added to each well. incubated for 15-30 min at room temperature and the reaction was stopped by adding 50 µl of 2M H₂SO₄. The amount of reaction product, an indication of bound BoNT IgG, was estimated by measuring absorbance at 492 nm using a microplatter reader (Molecular Devices, Sunnyvale, CA. Model No. Vmax)

Preparation of liposomes and release of fluorescent dye from liposomes

Preparation of liposomes

Asolectin from soybean (Sigma Chemical Co., St. Louis, MO), with 20% of phosphatidylcholine and the remaining 80% other lipids including phosphatidylethanolamine, cholesterol and triolein, was used for liposome preparation. The lipids were dissolved at a final concentration of 4 µmole/ml phosphatidylcholine in 2 ml of HPLC (high performance liquid chromatography) grade chloroform (Fisher Scientific, Pittsburgh, PA). This was treated with nitrogen gas for 2-3 min followed by overnight vacuum drying. The yellow layer of lipid was redissolved in a buffer solution of a dye. The buffer used for dye solution had 10 mM sodium phosphate, 10 mM sodium citrate, 125 mM NaCl and 1.5 mM EDTA, pH 7.4. This was the liposome buffer [19]. Dyes used were calcein (10 mM) FITC (fluorescein isothiocyanate)-dextran (20 mM) (Sigma Chemical Co., St. Louis, MO) and they undergo self-quenching by formation of non-fluorescent dimers (excimers) at these high concentrations [20, 21]. The lipid suspension was mixed using a vortex for 1 min and subsequently sonicated

for 3-4 min till the solution became clear. Size of the liposomes obtained by this method was in the range of 100-500 nm as determined by a dynamic light scattering technique. This technique measures the hydrodynamic diameter of the vesicles through the time behavior of the fluctuations in scattered light intensity [22]. This is the recommended size for large unilamellar vesicles [23].

Free dye (Calcein/FITC-dextran) was separated from liposomes containing dye by a gel filtration method using Sephadex G-75 (calcein) and G-100 (FITC-dextran) columns. The concentration of the liposomes was determined from the turbidity (absorbance) at 334 nm using UV spectrophotometer. Liposomes containing dye were obtained in the first peak whereas the free dye eluted in the second peak.

Fluorimetric analysis of BoNT induced dye release from liposomes

BoNT-mediated dye release from liposomes was monitored by measuring fluorescence signal of calcein or FITC-dextran (excitation at 468 nm and emission at 518 nm) according to the procedure described previously [24]. 20 ml of calcein and FITC-dextran encapsulated liposomes were separately prepared in liposome buffer, pH 7.4. For each set of six experiments, 600 μ l of the above liposome solution were taken. Six sets of experiments were carried out as described below.

In the first set, 600 μ l of the liposome solution were placed in a cuvette and the fluorescence signal was recorded at the fixed excitation and emission

wavelength for 5 min, i.e. until it gave a stable fluorescence signal. The pH was then lowered to 4.4 using 1.5 N HCl, and the fluorescence was again recorded for 5 min. There was a decrease in fluorescence signal, because calcein fluorescence is quenched at lower pH. The amount of HCl or NaOH needed for achieving pH 4.4 or 7.4, respectively, was estimated by titrating 20 ml of the liposome solution with 1.5 N HCl to pH 4.4, and then back titrating it with 1 N NaOH to pH 7.4. This calculation was used to estimate the amount of 1.5 N HCl and 1 N NaOH for 600 μ l of the liposome solution obtain the pH of 4.4 and 7.4, respectively. In order to compare the low pH mediated release of dye, the fluorescence signal at pH 4.4 was estimated by back titrating the solution to pH 7.4 by 1 N NaOH. To estimate total dye content in the liposomes, the latter were treated with 0.7 mM (final concentration) Triton-X-100 (Pierce, Rockford, IL) and the fluorescence signal of the released dye was recorded.

In the second set, stock solution of horse IgG against BoNT/E was added to 600 μ l of the liposome solution at pH 7.4. The final concentration of added IgG was 15 μ g/ml. The pH was lowered to 4.4 using 1.5 N HCl, followed by back titration, and finally 100% dye release was calculated using 0.7 mM Triton X-100. The fluorescence signal at each step was recorded for 5 min as in the case of set 1.

In the third set, BoNT/A at a final concentration of 15 μ g/ml was added to liposome solution and all the steps in set 2 were repeated. In the fourth set, BoNT/E at a final concentration 15 μ g/ml was added to liposome solution and all the steps of set 2 were repeated.

In the fifth set, BoNT/A was incubated with its specific IgG at 37 °C for 2 hours (ratio and amount of the specific IgG described in the Results and Discussion section). The final concentration of BoNT/A in the mixture was 15 µg/ml, which was added to the liposome solution and all the steps of set 2 were repeated.

In the sixth set, BoNT/E was incubated with its specific IgG at 37 °C for 2 hours (ratio and amount of the specific IgG described in the Results and Discussion section). The final concentration of BoNT/E was 15 µg/ml in the liposomes solution and all the steps of set 2 were repeated.

Identical steps were followed in the case of liposomes filled with FITC-dextran.

Results and Discussion

Channel formation in liposomes

Liposomes obtained after passing through the size exclusion column were treated with nitrogen gas for 2-3 min for maximum stabilization against oxygen. Lipids have double bonds and are easily oxidized in the presence of oxygen. The size of the liposomes was between 100-500 nm estimated by the dynamic light scattering technique (data not shown). It is the recommended size for unilamellar vesicles [22]. The liposome preparations have some fluorescence signal recorded at pH 7.5 (**Table 1**), indicating dye release even in the absence of any added molecules. The reason for such an observation could be (a) not all the dye of the dyes sticking outside the liposomes, and (b) light scattering from

liposomes. The signal could not be from the dye inside the liposomes because it is kept at a high self-quenching concentration. The pH of the liposome sample was reduced from 7.4 to 4.4 using 1.5 N HCl to observe the effect of low pH on the liposome membrane. The actual increase in the fluorescence signal at low pH was calculated after back titration to pH 7.4 as described in the Materials and Methods section. In the case of calcein containing liposomes (without addition of any neurotoxins), there was a slight increase in the signal when the liposomes were back titrated to pH 7.4 (the control pH for this set of experiments). This increase could be because the low pH might disturb the liposome membrane allowing the leakage of small number of calcein molecules (molecular weight = 625 g/mole). Each fluorescence recording was conducted for 5-10 min. to obtain a stable value of the fluorescence signal. Each set of experiments was repeated three times to obtain an average for the calcein release.

For FITC-dextran release experiments, there was no effect of low pH on the liposome in the absence of any added BoNT samples (control) (**Table 2**). Treatment with Triton-X-100 dissolved the membrane, and one could detect the signal obtained from all the dye encapsulated in the liposomes, which indicated total increase in the fluorescence. Rabbit IgG was used as a control to study the specificity of just the neurotoxin for inducing the dye release (channel formation) in liposomes. IgG had no significant effect by itself on the liposome even at low pH (**Tables 1 and 2**).

Addition of either BoNT/A or BoNT/E at low pH showed a considerable increase in the fluorescence signal. Treatment with 0.1 μ M BoNT/E induced 44% of calcein release at pH 4.4 whereas treatment with 0.1 μ M BoNT/A induced 40%

of calcein release (**Table 1**). When liposomes were filled with FITC-dextran, BoNT/A and BoNT/E induced 45% and 44.8% of FITC-dextran release, respectively (**Table 2**). The 4% difference in their ability to induce calcein release is not significant enough to explain the difference in their toxicity (100-fold) from their channel forming ability. Hence we can say that BoNT/A and BoNT/E have the same channel forming activity in liposomes. This suggests that the difference in their toxicity perhaps has a basis in differential effectiveness at other steps (binding and enzymatic activity) of BoNT/A and BoNT/E mode of action. The effect of low pH could be explained by a possible conformational change in the heavy chain at low pH, which could expose its transmembrane domain for insertion into the lipid bilayer [25]. The dye comes out presumably through a transmembrane pore formed by the heavy chains of respective BoNT serotypes.

Effect of BoNT antibodies on channel formation

The effect of specific IgG on the channel forming ability of the neurotoxin was significant in the fluorescence experiment. Treatment of liposomes with BoNT/E bound to BoNT/E IgG, induced only about 14% of the calcein to be released whereas treatment of liposomes with BoNT/A bound to BoNT/A IgG induced the release of about 29% of the calcein (**Table 1**). When liposomes were filled with FITC-dextran, BoNT/E and BoNT/A bound to their respective IgGs induced 12% and 37% of FITC-dextran release, respectively. The data of **Tables 1 and 2** are the averages of 3 readings for two independent experimental sets, and each set is representative of two different preparations of liposomes,

neurotoxin, and specific IgG. The small standard deviations (S.D.) measured for % dye release in each case, points to the consistency in our results. Graphical representations of the % release of the dyes are shown in **Figs. 4 and 5**.

The results showed a remarkable decrease in the fluorescence signal when neurotoxins were treated with their specific antibodies. BoNT/E IgG decreases the amount of dye released (FITC-dextran/calcein respectively) by 65% to 73% and BoNT/A IgG decreases the amount released (FITC-dextran/calcein respectively) by 18% to 25%. BoNT/E IgG inhibits channel formation by BoNT/E by 3-4 fold more than BoNT/A IgG inhibits channel formation by BoNT/A. In order to explore basis of differential effect of IgG on the membrane channel activities of BoNT/A and BoNT/E, we examined binding effectiveness of IgGs to their respective antigens.

Binding activity of the botulinum neurotoxin to the IgG

The neurotoxins were incubated with their respective IgG at 37 °C for 2 hours. This experiment was carried out to observe the decrease in the biological activity of the neurotoxin due to binding of antibody to its antigen. The binding of antibody to the antigen was used for examining the channel forming activity of the two serotypes of botulinum neurotoxin, i.e. BoNT/A and BoNT/E. The antibody effect could result either from its binding to the polypeptides of the neurotoxin involved in a specific function or from its binding-induced structural change in the neurotoxin.

The specific antibodies obtained from the affinity column were tested for binding with their respective antigens. The binding of BoNT/A IgG to BoNT/A was

detected at 0.16 $\mu\text{g/ml}$ of the IgG concentration and that of BoNT/E IgG to BoNT/E at 0.032 $\mu\text{g/ml}$ of the IgG concentration (**Fig. 3**). The difference in reactivity between BoNT/A IgG and BoNT/E IgG to their respective antigens is, therefore, five-fold. Hence we concluded that BoNT/E IgG showed a five-fold higher binding effectiveness to its antigen than did to BoNT/A IgG as observed by the ELISA (**Fig. 3**). In **Fig. 3** we can also see that maximum binding of the BoNT/A and BoNT/E IgGs to their respective antigens takes place between 20 $\mu\text{g/ml}$ and 100 $\mu\text{g/ml}$. We therefore chose 50 $\mu\text{g/ml}$ of IgG for 20 $\mu\text{g/ml}$ of their antigens for testing their effect on biological function (membrane channel activity) of BoNT/A and BoNT/E. Hence, for the maximum binding activity, which could affect the biological function of the neurotoxin, the ratio of IgG to neurotoxin was set at 2.5:1.

Cross-reactivity was investigated between the specific IgG of one serotype of botulinum neurotoxin to the serotype of other botulinum neurotoxin. Binding of BoNT/E IgG to BoNT/A starts at 0.8 $\mu\text{g/ml}$ of the IgG concentration, whereas BoNT/A IgG to BoNT/A starts at 0.16 $\mu\text{g/ml}$ of the IgG concentration (**Fig. 4**). The difference between the binding of BoNT/E IgG to BoNT/A and BoNT/A IgG to BoNT/A is ten-fold with respect to their concentration. Hence, we estimate that BoNT/A IgG had a 10-fold higher binding ability to BoNT/A than the binding of BoNT/E IgG to BoNT/A (**Fig. 4**). On the other hand, BoNT/A IgG shows almost no binding to BoNT/E (**Fig. 5**). Therefore, experiments were not conducted to observe the cross-reactivity effect on the channel formation.

The data from ELISA (**Figs 3 and 4**) has a similar result where BoNT/E IgG has five-fold higher binding activity than BoNT/A IgG to their respective

antigens. The antibody could change the structure of the antigen or inhibit its specific function by blocking the respective functional domain. In our experiments, we did not examine any structural changes in the antigen, therefore we cannot distinguish between these two mechanisms. BoNT/E IgG being more effective in blocking the channel activity might be binding to the transmembrane domain actually involved in the channel formation.

Size of the membrane channel

One of the main aims of this study was to estimate a minimum size of the membrane channel formed by BoNT/A and BoNT/E. The diameter of the dye in Å is directly correlated with its molecular weight. The maximum size of a membrane channel which allows a particle up to 4000 g/mole in size to pass through (FITC-dextran used in this study) is 24.2 Å in diameter, as the Stokes' radius of this dye is 24.2 Å [26]. The heavy chain is suggested to form a channel of 8 Å in diameter [10], but it does not seem adequate for presumed translocation of the light (L) chain. Also a sequence analysis has shown a 23-residue stretch in the N-terminal domain of the BoNT/A heavy chain with a propensity to form an amphipathic helical bundle in a hydrophobic environment. However, perhaps the size of such channels of about 2.5 - 4 Å [27], is not sufficient for the translocation of a 50-kDa L chain. Even the 15 Å size of the channel suggested recently requires complete unfolding of L chain at low pH [8], although issue of such a drastic unfolding at low pH is not settled [27]. From our results, we conclude that the membrane channel size is much larger than that suggested by other researchers for 50-kDa light chain to pass through. Recent observation by

Koriazova and Montal [8] of the translocation of L chain through H chain channel provides further evidence for larger pore formed by the H chain in membrane bilayer. Indeed 24.2 Å channel size would be more amenable to the translocation of L chain in its molten globule conformation suggested by Li and Singh [29].

Membrane channel activity and the level of toxicity

Our results on channel formation by BoNT/E in artificial membranes are the first such reports. We conclude that the channel forming activity of the two serotypes of botulinum neurotoxin is almost identical at least in liposomes, hence the difference in their toxicity under *in vivo* conditions might be due to a difference in their enzymatic activities against the neuronal substrate, difference in their receptor binding activities, or differences in translocation rate mediated by putative proteins in nerve cells. A recent report shows that the catalytic efficiency of BoNT/E endopeptidase is in fact significantly higher (10-fold) than the BoNT/A Endopeptidase [29, 30], suggesting that the difference in the toxicity level of BoNT/A and /E can not be correlated with the endopeptidase activity, unless we assume that the endopeptidase activity under *in vivo* conditions is dramatically different for the two serotypes of BoNT.

It is notable that in a recent article Keller et al. [14] reported from their studies with primary neuronal cell culture and BoNT/A and BoNT/E that rate of translocation of BoNT/E was dramatically faster than that of BoNT/A. This observation contrasts with our observation of similar membrane channel activity by BoNT/A and BoNT/E. These two sets of results can be reconciled if one of the following holds true. (1) In nerve cells, proteins present in the membrane,

including possibly the BoNT receptor, helps facilitate the translocation of the L chain. BoNT/E interaction with such protein is more favorable than that of BoNT/A. (2) The BoNT/E L chain translocation within the channel is faster than that of BoNT/A L chain, suggesting intimate interplay involved in the translocation process. In such case the calcein release assay performed in our experiment is only relevant to the general membrane integration, and pore formation, and not the L chain translocation. L chain translocation is a specific process between the H chain membrane transporter and the L chain.

Acknowledgements

This work was in part supported by a U.S. Army Medical Research and Material Command under Contract No. DAMD17-02-C-001, and by National Institutes of Health through New England Center of Excellence for Biodefense (AI057159-01).

References

1. Schantz, E. J. and Johnson, E. A. Properties and use of botulinum toxin and other microbial neurotoxins in medicine. *Microbiol Rev.* 1992 Mar; 56, 80-99.
2. Call, J. E.; Cooke, P. H., and Miller, A. J. In situ characterization of *Clostridium botulinum* neurotoxin synthesis and export. *J Appl Bacteriol.* 1995; 79, 257-263.
3. Ahnert-Hilger, G. and Bigalke, H. Molecular aspects of tetanus and botulinum neurotoxin poisoning. *Prog Neurobiol.* 1995; 46, 83-96.
4. Li, L. and Singh B. R. Structure function relationship of clostridial neurotoxins. *Toxin Rev.* 1999; 18, 95-112.
5. Singh, B. R. Intimate details of the most poisonous poison. *Nat Struct Biol.*; 2000; 7, 617-619.
6. Rummel, A.; Mahrhold, S.; Bigalke, H., and Binz, T. The HCC-domain of botulinum neurotoxins A and B exhibits a singular ganglioside binding site displaying serotype specific carbohydrate interaction. *Mol Microbiol.* 2004; 51, 631-643.
7. Lebeda, F. J. and Singh, B. R. Membrane channel activity and translocation of tetanus and botulinum neurotoxins. *Toxin Rev.* 1999; 18, 45-76.
8. Koriyazova, L. K. and Montal, M. Translocation of botulinum neurotoxin light chain protease through the heavy chain channel. *Nat Struct Biol.* 2003 Jan; 10, 13-18.
9. Hoch, D. H.; Romero-Mira, M.; Ehrlich, B. E.; Finkelstein, A.; DasGupta, B. R., and Simpson, L. L. Channels formed by botulinum, tetanus, and diphtheria toxins in planar lipid bilayers: relevance to translocation of proteins across membranes. *Proc Natl Acad Sci U S A.* 1985; 82, 1692-1696.
10. Finkelstein A. Channels on Phospholipid bilayer membrane by diphtheria, tetanus, botulinum and anthra toxin. *Journal De Physiologie.* 1990; 84, 188-190.
11. Oh, K. J.; Senzel, L.; Collier, R. J., and Finkelstein, A. Translocation of the catalytic domain of diphtheria toxin across phospholipid bilayers by its own T domain . *Proc. Natl. Acad. Sci. USA.* 1999; 96, 8467-8470.
12. Ratts, R.; Zeng, H.; Berg, E. A.; McComb, M. E.; Castello, C. E.; VanderSpek, J. C., and Murphy, J. R. The cytosolic entry of diphtheria toxin catalytic domain requires a host cell cytosolic translocation factor complex . *J. Cell Biol.* 2003; 160, 1139-1150.

13. Lalli, G.; Bohnert, S.; Deinhardt, K.; Verastegui, C., and Schiavo, G. The journey of tetanus and botulinum neurotoxins in neurons. *Trends Microbiol.* 2003; 11, 431-437.
14. Keller, J. E.; Cai, F., and Neale, E. A. Uptake of botulinum neurotoxin into cultured neurons. *Biochemistry.* 2004; 43, 526-532.
15. Singh, B. R.; Foley, J., and Lafontaine, C. Physico-chemical characterization of the botulinum binding protein from type E botulinum producing *Clostridium Botulinum*. *Journal Protein Chemistry.* 1995; 14, 7-18.
16. Cai, S.; , Sarkar H. K., and Singh, B. R. Enhancement of the endopeptidase activity of botulinum neurotoxin by its associated proteins and dithiothreitol. *Biochemistry.* 1999; 38, 6903-6910.
17. Ogert, R. A.; Brown, J. E.; Singh, B. R.; Shriver-Lake, L. C., and Ligler, F. S. Detection of *Clostridium botulinum* toxin A using a fiber optic-based biosensor, *Anal. Biochem.* 1992; 205, 306-312.
18. Li, L. and Singh, B. R. Isolation of synaptotagmin as a receptor for types A and E botulinum neurotoxin and analysis of their comparative binding using a new microtiter plate assay. *J Nat.Toxins.* 1998; 7, 215-226.
19. Kamata, Y. and Kozaki, S. The light chain of botulinum neurotoxin forms channels in a lipid membrane. *Biochem Biophys Res Commun.* 1994; 205, 751-757.
20. Oku, N.; Kendall, D. A., and MacDonald, R. C. A simple procedure for the determination of the trapped volume of liposomes. *Biochim Biophys. Acta.* 1982; 691, 332-340.
21. Kurtzhals, P.; Larsen, C., and Johansen, M. High-performance size-exclusion chromatographic procedure for the determination of fluoresceinyl isothiocyanate dextrans of various molecular masses in biological media. *J Chromatogr.* 1989; 491, 117-127.
22. Day, E. P.; Ho, J. T.; Kunze, R. K. Jr, and Sun, S. T. Dynamic light scattering study of calcium-induced fusion in phospholipid vesicles. *Biochim Biophys Acta.* 1977; 470, 503-508.
23. Szoka, F. Jr. and Papahadjopoulos, D. Procedure for the preparation of liposomes with large internal aqueous space and high capture by reverse-phase evaporation. *Proc. Natl. Acad. Sci., U.S.A.* 1978; 75, 4194-4198.
24. Fu, F. N. and Singh, B. R. Calcein permeability of liposomes mediated by type A botulinum neurotoxin and its light and heavy chains. *J Protein Chem.* 1999; 18, 701-707.

25. Fu, F. N.; Busath, D. D., and Singh, B. R. Spectroscopic analysis of low pH and lipid-induced structural changes in type A botulinum neurotoxin relevant to membrane channel formation and translocation. *Biophys Chem.* 2002; 99, 17-29.
26. Sauer, H.; Pratsch, L.; Tschopp, J.; Bhakdi, S., and Peters, R. Functional size of complement and perforin pores compared by confocal laser scanning microscopy and fluorescence microphotolysis. *Biochim Biophys Acta.* 1991; 1063, 137-146.
27. Montal, M. S. ; Blewitt, R.; Tomich, J. M., and Montal, M. Identification of an ion channel formation motif in the primary structure of tetanus and botulinum neurotoxins. *FEBS Letters.* 1992; 313, 12-18.
28. Spectroscopic analysis of pH-induced changes in the molecular features of type A botulinum neurotoxin light chain. *Biochemistry.* 2000; 39, 6466-6674.
29. Li, L.; Binz, T.; Niemann, H., and Singh, B. R. Probing the mechanistic role of glutamate residue in the zinc-binding motif of type A botulinum neurotoxin light chain. *Biochemistry.* 2000; 39, 2399-2405.
30. Agarwal, R.; Binz, T., and Swaminathan, S. Analysis of Active Site Residues of Botulinum neurotoxin E by mutational, functional, and structural studies: Glu335Gln Is an apoenzyme. *Biochemistry.* 2005; 44, 8291-8302.

Figure legends

Fig.1. ELISA analysis of the binding of BoNT/E and BoNT/A to their respective IgG antibodies. BoNT/E and BoNT/A at a constant concentration of 20 $\mu\text{g/ml}$ were coated to microplate wells, and five-fold serial dilutions of the specific antibodies dissolved in 0.1 M PBS buffer, pH 7.4, were added to each well.

Fig. 2. ELISA analysis of the binding of BoNT/A to IgG raised against BoNT/E and BoNT/A. BoNT/A was kept at a constant concentration of 20 $\mu\text{g/ml}$ for coating the microplate wells, and five-fold serial dilutions of the specific antibodies dissolved in 0.1 M PBS buffer, pH 7.4, was added to each well.

Fig. 3. ELISA analysis of the binding of BoNT/E to IgG raised against BoNT/E and BoNT/A. BoNT/E was kept at a constant concentration of 20 $\mu\text{g/ml}$ for coating the microplate wells, and five-fold serial dilutions of the specific antibodies was added to each well.

Fig. 4. Graphical representation of the percent release of calcein from the liposomes in the presence of botulinum neurotoxin (BoNT). The bars indicate standard deviations in experimental measurements.

Fig. 5. Graphical representation of percent release of FITC-dextran from liposomes in the presence of botulinum neurotoxin. The bars indicate standard deviations in experimental measurements.

Table 1. Experimental data showing increase in fluorescence signal of calcein after its release from liposomes when induced by BoNT/A and BoNT/E. The value represents the average of 2 independent sets of experiments conducted in triplicates. The control and the experiment results are statistically significantly different by t-test ($0.01 > p > 0.001$).

(a) Increase in fluorescence signal at pH 4.4 was calculated by subtracting the liposome signal at pH 7.5 from the fluorescence signal obtained after back titration at pH 7.5 (refer to Materials and Methods section for more detail), (b) Total fluorescence signal was calculated by subtracting the liposome signal at pH 7.5 from the fluorescence signal after Triton X 100 was added, and (c) % calcein release was calculated by dividing (a) / (b) multiplying into 100.

	pH 7.5	pH 4.0	pH 7.5 (back titration)	Triton X-100	Increase in fluorescence at pH 4.4 (a)	Total Fluorescence signal (b)	% calcein release (c) \pm S.D.
Liposome	28.7	24.1	30.8	44.2	2.1	15.5	13.5 \pm 0.3
Liposome +IgG	27.6	23.1	30.4	43	2.8	15.4	18.0 \pm 0.2
Liposome + BoNT/E	28.1	18.8	35.3	44.5	7.2	16.4	43.6 \pm 1.1
Liposome + BoNT/E + IgG	28.9	22.8	31	44.5	2.1	15.6	13.6 \pm 4.3
Liposome + BoNT/A	28.5	19.7	34.9	44.8	6.4	16.3	39.5 \pm 0.2
Liposome + BoNT/A + IgG	28	17.4	32.5	43.5	4.5	15.5	29.0 \pm 4.7

Table 2. Experimental data showing increase in fluorescence signal of FITC-dextran after its release from liposomes when induced by BoNT/A and BoNT/E. The value represents the average of 2 sets of independent experiments conducted in triplicates. The control and the experiment results are statistically significantly different by t-test ($0.01 > p > 0.001$). (a) Increase in fluorescence signal at pH 4.4 was calculated by subtracting the liposome signal at pH 7.5 from the fluorescence signal obtained after back titration at pH 7.5 (refer to Materials and Methods for more detail), (b) Total fluorescence signal was calculated by subtracting the liposome signal at pH 7.5 from the fluorescence signal after Triton X 100 was added, and (c) % FITC-dextran release was calculate by dividing (a) / (b) and multiplying into 100.

	pH 7.5	pH 4.0	pH 7.5 (back titration)	Triton X- 100	Increase in fluorescence at pH 4.4 (a)	Total Fluorescence signal (b)	% FITC- dextran release (c) ± S.D.
Liposome	49	23.5	48.9	53.8	0.1	4.8	0.0 ± 1.0
Liposome +IgG	41.5	20	41.4	48.9	0.1	7.4	.5 ± 0.4
Liposome + BoNT/E	43.3	19.3	47.6	50.8	4.3	7.5	45±5
Liposome + BoNT/E + IgG	48.09	23.9	48.5	55.7	0.5	7.7	12 ± 2.9
Liposome + BoNT/A	44.1	23	47.3	50	3.2	5.9	44.8 ± 4.4
Liposome + BoNT/A + IgG	40.1	18	42.5	48.1	2.4	8	37.0 ± 4

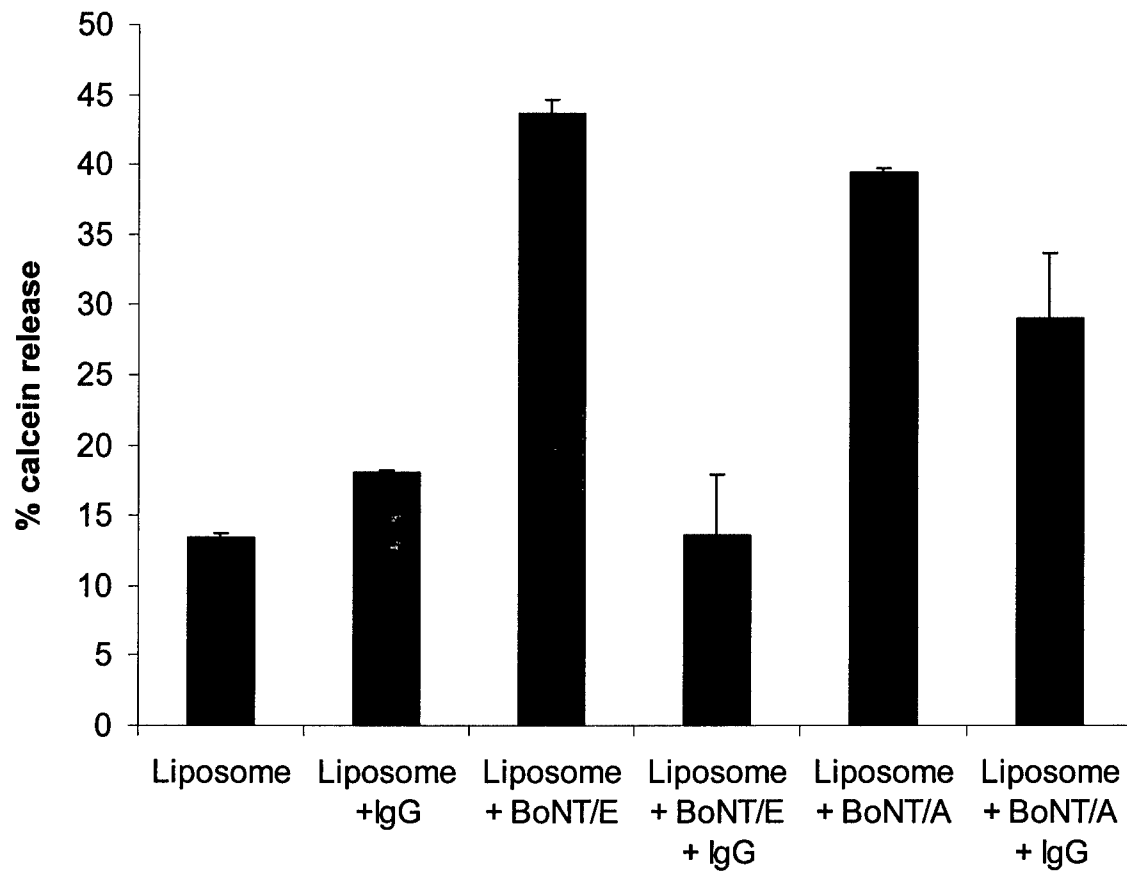


Fig. 1.

Parikh and Singh

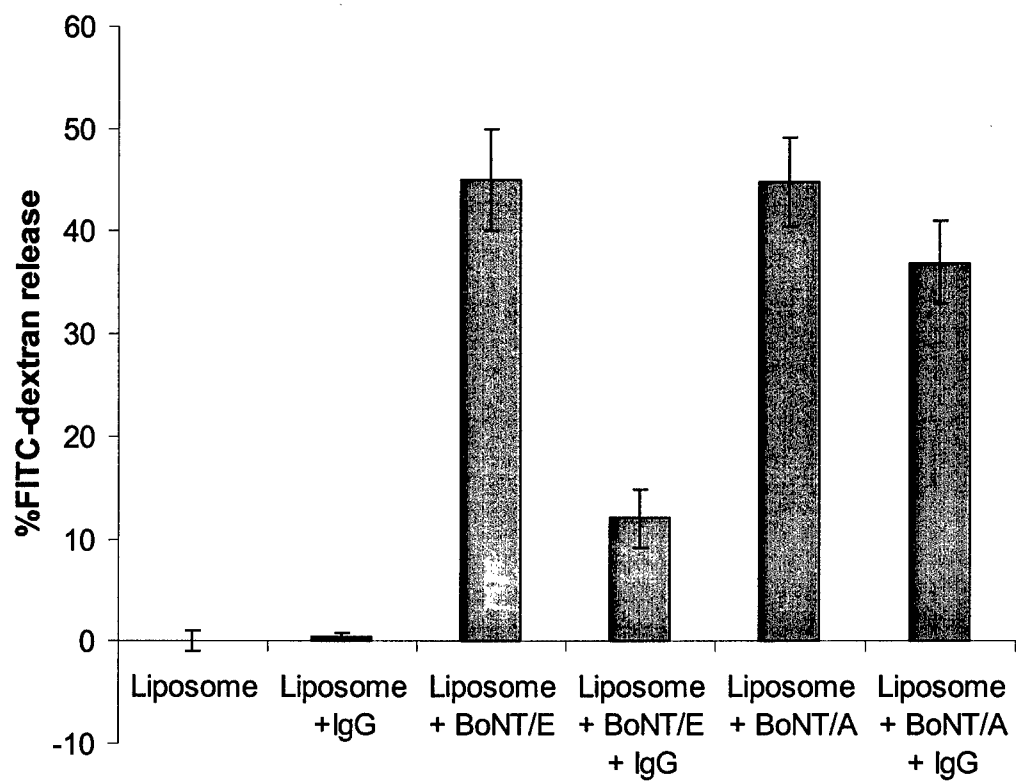


Fig. 2.

Parikh and Singh

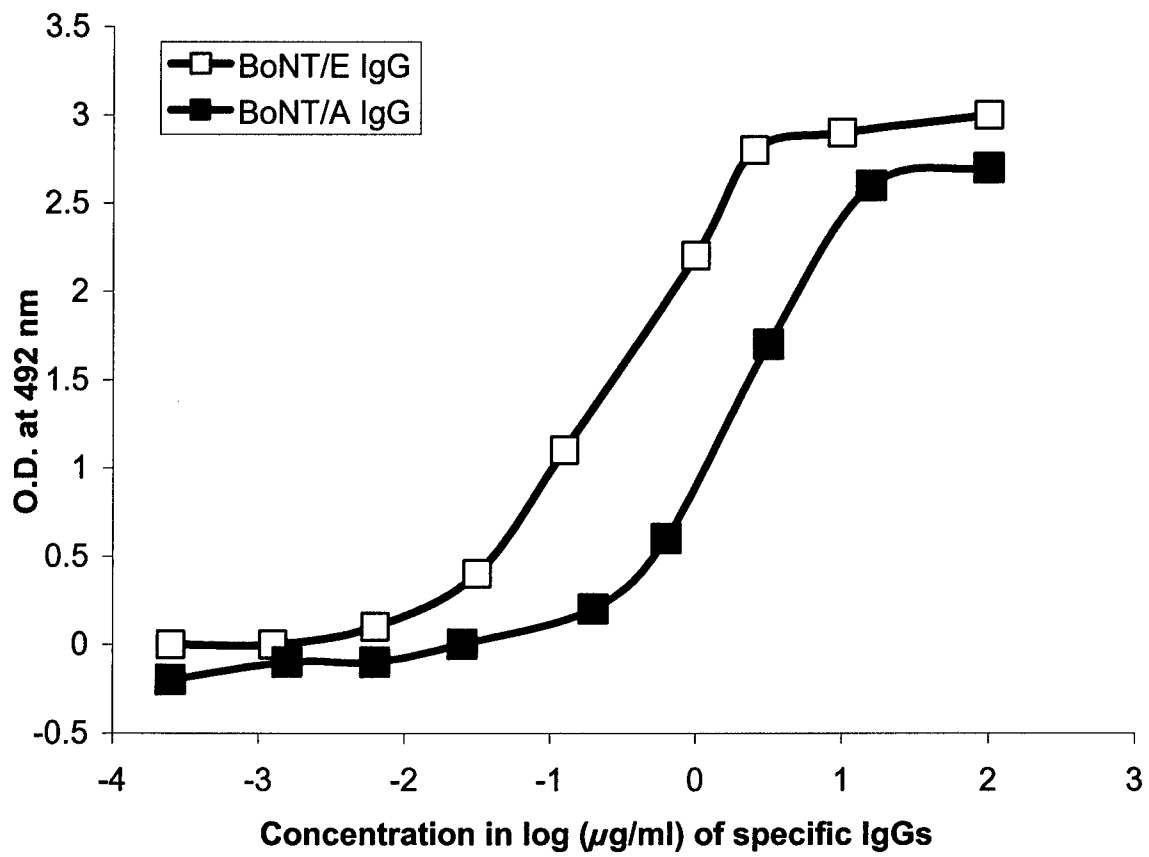
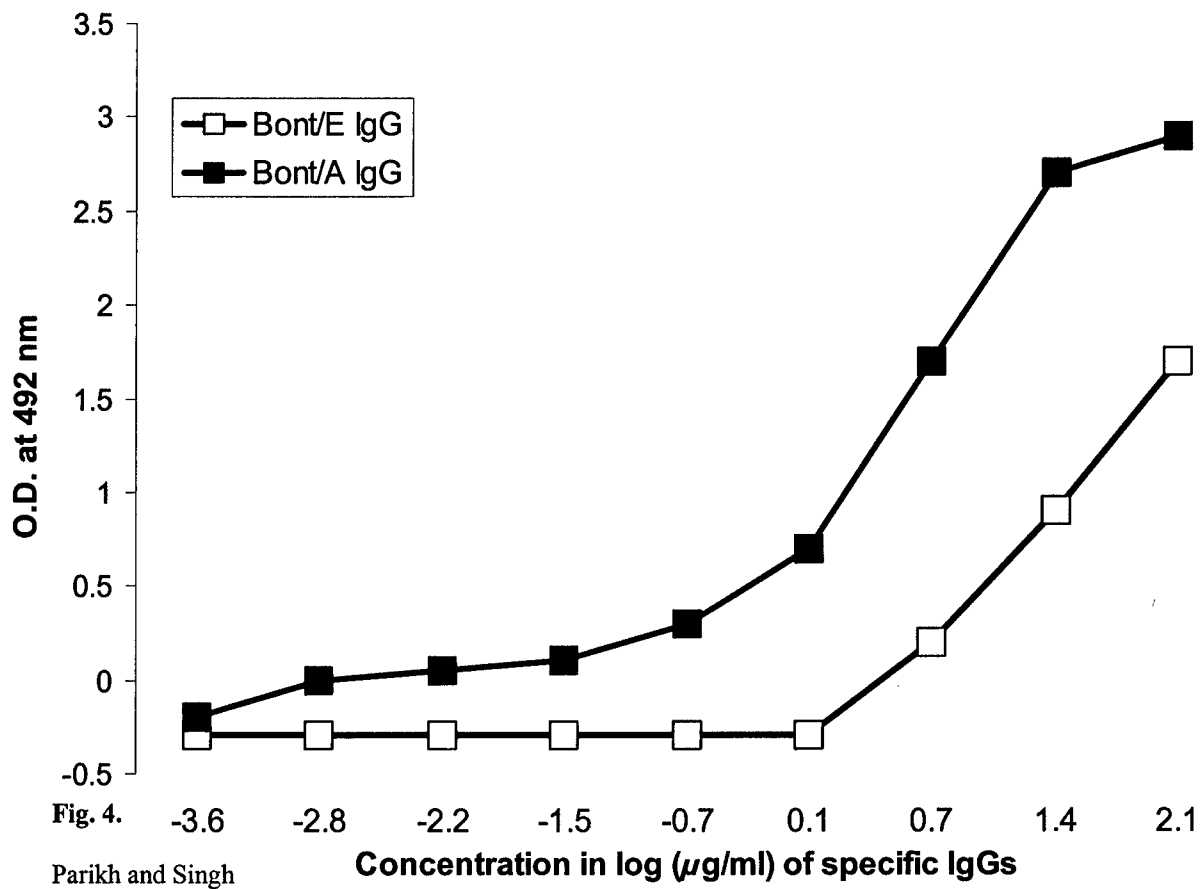


Fig. 3.

Parikh and Singh



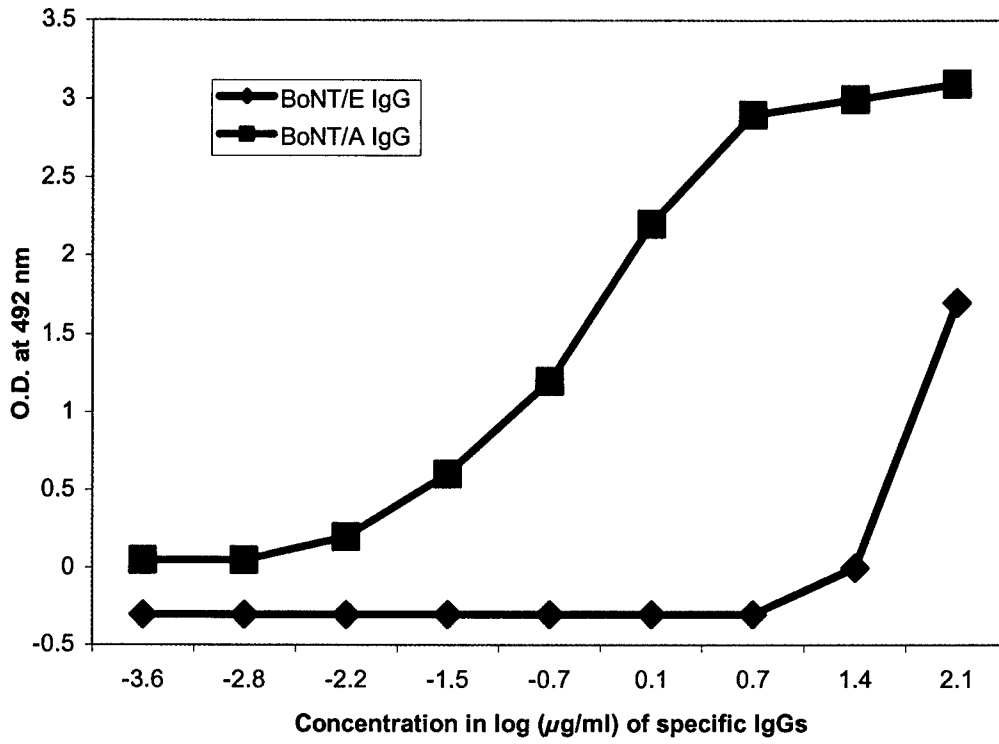


Fig. 5.

Parikh and Singh
